National Heart and Lung Institute

London, W12 0NN

Transcriptomics in Pulmonary Arterial Hypertension

Diagnostics and Pathobiology

Thesis submitted for the degree of

Doctor of Philosophy

Imperial College London

By

Pablo Otero Núñez

2022

Statement of Originality

I declare that this thesis was conducted and written by myself, and all work included is my own unless declared otherwise.

Pablo Otero.

The work here presented includes research conducted by:

Dr. Yukyee Wu
Dr. Lars Harbaum
Dr. Christopher J. Rhodes
Dr. Pavandeep Ghataorhe

Copyright Declaration

Ethics codes

U.K. National Cohort Study of PAH:

- 13/EE/0203

Hammersmith Hospital:

- 11/LO/0395
- 17/LO/0563

List of Publications

The work here presented contributed to the publication of the following:

- Rhodes CJ*, Otero-Núñez P*, Wharton J, et al. ***Whole-Blood RNA Profiles Associated with Pulmonary Arterial Hypertension and Clinical Outcome***. Am J Respir Crit Care Med. 2020 Aug 15;202(4):586-594.

- Ulrich A, Otero-Núñez P, Wharton J, et al**. *Expression Quantitative Trait Locus Mapping in Pulmonary Arterial Hypertension***. Genes (Basel). 2020;11(11):1247. Published 2020 Oct 22. doi:10.3390/genes11111247.

- Harbaum L, Rhodes CJ, Otero-Núñez P, et al. ***The application of 'omics' to pulmonary arterial hypertension***. Br J Pharmacol. 2021;178(1):108-120.

- Kariotis, S., Jammeh, E., Swietlik, E.M. et al. ***Biological heterogeneity in idiopathic pulmonary arterial hypertension identified through unsupervised transcriptomic profiling of whole blood***. Nat Commun 12, 7104 (2021).

Acknowledgements

There is this quote I once heard—unfortunately I cannot recall who was person uttering these words—which went "I have always wanted to have done a PhD". Not TO DO, but rather to HAVE DONE. It is only now, looking back, that I fully understand its meaning.

The scale of a PhD project cannot be conveyed with just words, it truly is a monumental task requiring an infinite source of dedication, motivation and patience. Truth is, however, that we are only humans, and that makes us terribly limited beings. What I have not yet mentioned is the equally monumental enjoyment and satisfaction one experiences when taking a PhD project head-on. It is what makes you look back and be mesmerised by all the things you have done, the experiences you have shared, the successes you have managed to obtain and the failures you have suffered. But, as I said, we are only human, and we are very limited.

It is for that reason that I must give a huge thank you to all the people that have accompanied me along the way and have made possible that I actually reach this stage. There really is not a chance I would have managed to accomplish any of this and thrive throughout the whole process without you.

Chris and Martin, my project supervisors. You probably have ruined research for me, as I am positive I will never be able to encounter better guidance than what you have offered me throughout these years. Your scientific brilliance is only second to the kindness, patience and support you have constantly offered me. I truly thank you.

Eleni, Rachel, Yukyee, Marili, Alex, my dear lab friends. Venting out with you has been the greatest therapeutic experience throughout these years. Your unconditional help and support have helped me weather any storm I have faced—or, in all honesty, created myself—. I really appreciate your patience with this unorthodox scientist! I also wanted to thank all past and present members of the PH group at Imperial for the research environment you have created. It feels great to be a part of this institution.

Mum. For once I cannot put into words the extent of the gratefulness I feel for everything you have done for me. For us. The courage you have always shown me has guided me in my journey. You are my best example and my strongest, unwavering support. I am me thanks to you. I push forward in everything I do because I know you will unconditionally have my back and save me if necessary. Thank you.

To the rest of my family and all my friends. I know. I know I am not easy, and I know this project has also taken a toll on you. I am aware of the price anyone close to me must pay for my dedication towards my work. I appreciate it endlessly. Every amazing moment I have spent with you has been in my mind, fuelling my will to complete my work and spend more time alongside you. Abuela, Aita, María, Diego, Carlos, Ángela, Christina, Alberto, Santos, Elenita, Inés, Daphne, Olalla, Basel, Cam, Brut, Carolina. You know who you are, and I am so happy for having you in my life.

I saved you for last, Abu. I have been waiting for eight years to write you these words. I did it. I really did it. I kept our promise. I wish you could see me. I know you are proud. I wish I could see you. I lead my life based off what you taught me. I think about you a lot. I miss you a lot. Thank you.

This is for you.

Abstract

Pulmonary arterial hypertension (PAH) is a rare disease characterised by remodelling of the pulmonary vasculature and subsequent increase in vascular resistance, leading to right ventricle overexertion and eventual heart failure. Responses to treatment and disease progression vastly differ between PAH patients, while standard clinical phenotypes are not sufficient for accurate patient stratification.

Molecular profiling through multi-omic approaches offers greater granularity for PAH patient characterisation and could improve initial risk stratification, treatment selection and monitoring, as well as providing insights into new biological pathways not yet targeted by current therapies.

Transcriptomic approaches, such as RNA-sequencing (RNAseq), permit comprehensive analyses of gene expression in tissue samples. Whole blood RNA analysis offers an alternative "liquid biopsy" to lung biopsy—which carries a high risk in PAH—and can be performed sequentially. Previous PAH whole blood transcriptomic studies have been limited by cohort numbers and methodologies used—such as the less sensitive and probe-dependent microarrays—, especially when compared with the comprehensive nature of RNAseq.

RNAseq followed by differential expression analysis were utilised to identify PAH-associated transcriptomic profiles in a cohort of 359 PAH patients and 72 age- and sex-matched healthy controls. A LASSO RNA diagnostic model of 25 differentially expressed genes best distinguishing between PAH patients and healthy controls derived from whole blood PAH RNA signature could effectively separate PAH patients in an independent group. RNA model scores were associated with disease severity ($p= 0.008$) and survival ($p= 4.66x10^{-6}$) in patients. These results were validated externally in two different cohorts (including 58 and 156 PAH patients and 25 and 110 healthy controls respectively), which highlighted the potential role in PAH of adenosylmethionine decarboxylase 1 (AMD1) and polyamines. Mendelian randomisation analysis implicated SMAD5 in PAH pathogenesis ($p= 0.028$). A combined diagnostic model of 25 RNAs and 7 metabolites was developed which performed better at distinguishing PAH patients from healthy controls than the 7-metabolite model alone ($p= 0.002$).

A second analysis more sensitive to the specific characteristics of PAH was also conducted. A cohort of 147 PH patients and 45 disease controls was utilised to identify gene expression differences between PAH, other forms of PH and other symptomatic cardiovascular non-PH patients ("disease controls"). LASSO diagnostic models were developed from RNA profiles, and they were able to distinguish between disease controls and both PAH ($p= 0.049$) and all PH ($p= 1.92x10\text{-}5$) patients, but not between PAH and other PH ($p= 0.719$). Comparison of RNA profiles highlighted the potential role of SEC22B, ZNF254, PPA2, CAMKMT, FER and EDEM1 in PAH pathology.

An *in-silico* analysis for compound repurposing, the Connectivity Map (CMap) database, was utilised to predict small molecule compounds which reverse the identified whole blood PAH RNA signature. The protein synthesis inhibitor Homoharringtonine—approved for leukaemia treatment and one of the top six compounds identified by CMap—, was shown to effectively reverse PAH transcriptional changes in isolated PBMCs and hPAECs and induce positive functional changes in hPAECs *in vitro.*

These results emphasise the potential of transcriptomics—and general omics—for PAH research. PAH RNA profiles were identified that associated with disease progression and mortality and several transcripts were implicated in PAH pathology. RNA profiles separating PH patients from other symptomatic patients were also identified. Homoharringtonine showed therapeutic potential in *in vitro* assays using PBMCs and hPAECs and should be investigated further.

Table of Contents

List of Figures

Chapter 2

Chapter 3

Chapter 4

Chapter 5

List of Tables

Chapter 2

Chapter 3

Chapter 4

List of Abbreviations

ACT-β	Actin beta
AIC	Akaike Information Criterion
ALAS2	Aminolevulinate Synthase 2
ALK-1	Activin A Receptor Type II-like Kinase Transcription Factor 1
AMD1	Adenosyl-methionine Decarboxylase 1
AML	Acute Myeloid Leukaemia
APAH	Associated Pulmonary Arterial Hypertension
ATP	Adenosine Triphosphate
AUC	Area Under the Curve
Az	Azithromycin
BCLAF1	B-cell Lymphoma 2-associated Transcription Factor 1
BING	Best Inferred Genes
BMI	Body Mass Index
BMP	Bone Morphogenic Protein
BMPR1	Bone Morphogenic Protein Receptor 1
BMPR2	Bone Morphogenic Protein Receptor 2
BNP	Brain Natriuretic Peptide
CAMKMT	Calmodulin Lysine Methyl Transferase
cAMP	Cyclic Adenosine Monophosphate
CBLN2	Cerebellin 2 Precursor
CCBs	Calcium Channel Blockers
CCL-2	C-C motif chemokine ligand 2
CCND3	Cyclin D3
cGMP	Cyclic Guanosine Monophosphate Class II DP-b Chain
CMap	Connectivity Map
CML	Chronic Myeloid Leukaemia
COL4A1	Collagen Type IV Alpha 1 Chain
COL4A2	Collagen Type IV Alpha 2 Chain
CpG	Cytosine-phosphateguanine
CPT1A	Carnitine Palmitoyltransferase 1 A
CRISPR	Clustered Regularly Interspaced Short Palindromic Repeats
CT	Computed Tomography
CTEPH	Chronic Thromboembolic Pulmonary Hypertension
CXCL10	C-X-C Motif Chemokine Ligand 10
DCs	Disease Controls
DEG	Differentially Expressed Gene
DHEA-S	Dehydroisoandrosterone-sulfate
DMSO	Dimethyl Sulfoxide
DNA	Deoxyribonucleic Acid
DPAH	Drug-Induced Pulmonary Arterial Hypertension
ECs	Endothelial Cells

EDEM1	Endoplasmic Reticulum Degradation-enhancing α-mannosidase-like Protein 1
EDTA	Ethylenediamin Tetra-acetic Acid
eEF1A1	Eukaryotic Translation Elongation Factor 1 Alpha 1
EGM	Endothelial Cell Growth Medium
EGR1	Early Growth Response 1
EndoMT	Endothelial-to-Mesenchymal Transition
ENG	Endoglin
EPAS1	Endothelial PAS Domain Protein 1
EphB4	Erythropoietin-producing Hepatocyte Receptor B4
eQTL	Expression Quantitative Trait Loci
ERAF	Alpha Haemoglobin Stabilizing Protein
ET-1	Endothelin-1
ETA	Endothelin Receptor A
ETB	Endothelin Receptor B
FBLN2	Fibulin 2
FBS	Foetal Bovine Serum
FC	Fold Change
FDR	False Discovery Rate
FER	Feline Sarcoma-related
FIGN	Fidgetin
GAPDH	Glyceraldehyde-3-phosphate Dehydrogenase
GNG2	G Protein Subunit Gamma 2
GOLGA4	Golgin A4
GPCRs	G-protein Coupled Receptors
GRN	Granulin
GWAS	Genome-Wide Association Study
HDL4	Huntington Disease-like 4
HHT	Homoharringtonine
HIF	Hypoxia Inducible Factor
HLA-DPB1	Histocompatibility Complex
HLX	H2.0 Like Homeobox
hMVECs	Human Microvasculature Endothelial Cells
hPAECs	Human Pulmonary Artery Endothelial Cells
HPAH	Heritable Pulmonary Arterial Hypertension
HV	Healthy Volunteers
IFNs	Type I Interferons
IL	Interleukin
IPA	Ingenuity Pathway Analysis
IPAH	Idiopathic Pulmonary Arterial Hypertension
IPF	Idiopathic Pulmonary Fibrosis
JAK	Janus Kinase
JNK	c-Jun N-terminal Kinases
KCNA5	Potassium Voltage-Gated Channel Subfamily A Member 5
KCNK3	Potassium Two Pore Domain Channel Subfamily K Member 3
KLF10	Krüppel-like Factor 10
KLF2	Krüppel-like Factor 2
KO	Knock-out

LASSO	Least Absolute Shrinkage and Selection Operator
LD	Linkage Disequilibrium
lncRNAs	Long non-coding RNAs
LPS	Lipopolysaccharide
lSSc	Limited Systemic Sclerosis
MAPK	Mitogen-activated Protein Kinase
MCT	Monocrotaline
MGI	Mouse Genomics Informatics
MMP	Matrix Metalloproteinases
mPAP	Mean Pulmonary Artery Pressure
mPCWP	Mean Pulmonary Capillary Wedge Pressure
MR	Mendelian Randomisation
mTOR	Rapamycin
MTT	Tetrazolium Dye
ncRNA	non-coding RNA
NO	Nitric Oxide
NOS	Nitric Oxide Synthase
NOTCH	Neurogenic Locus Notch Homolog
NRG1	Neuregulin-1
NT-proBNP	N-terminal pro-BNP
OLFM4	Olfactomedin 4
P2RY5	Lysophosphatidic Acid Receptor
PAH	Pulmonary Arterial Hypertension
PASMCs	Pulmonary Artery Smooth Muscle Cells
PBMCs	Peripheral Blood Mononuclear Cells
PBS	Phosphate-buffered Saline
PCBP1	Poly(RC) Binding Protein 1
PCF11	Polyadenylation and Cleavage Factor Subunit 11
PCP	Planar Cell Polarity
PDE5	Phosphodiesterase Type 5
PF	Pulmonary Fibrosis
PGI2	Prostacyclin
PH	Pulmonary Hypertension
PI3K	Phosphoinositide 3-kinase
PPA2	Inorganic Pyrophosphatase 2
PTP	Protein Tyrosine Phosphatase
PVR	Pulmonary Vascular Resistance
RIN	RNA Integrity Number
RNA	Ribonucleic Acid
RNAseq	RNA Sequencing
ROC	Receiver Operating Characteristic
RPM	Revolutions Per Minute
RPMI	Roswell Park Memorial Institute
RT-qPCR	Real Time Quantitative Reverse Transcription Polymerase Chain Reaction
RV	Right Ventricle
RVSP	Right Ventricular Systolic Pressure
SEC22B	Secretory-22 Homolog B

SESN1	Sestrin-1
sGC	Soluble Guanylate Cyclase
siRNA	Small Interfering RNA
SMAD	Small Mothers Against Decapentaplegic
SNARE	Soluble N-ethylmaleimide-Sensitive Factor Attachment Protein Receptor
SNORD	Small Nucleolar RNA
SNP	Single Nucleotide Polymorphism
SOX17	Sex Determining Region Y-Box
SPAST	Spastin
SRSF2	Serine Arginine Splicing Factor 2
SSc	Systemic Sclerosis
SuHx	Sugen-Hypoxia
TBX4	T-Box Transcription Factor 4
TCA	Tricarboxylic Acid
TF	Transcription Factor
TGF-β	Transforming Growth Factor Beta
TLRs	Toll-like Receptors
TPM	Transcripts Per Million
TRPCs	Transient Receptor Potential Channels
VEGF	Vascular Endothelial Growth Factor
WBC	White Blood Cell
WHO	World Health Organisation
WU	Wood Units
ZNF	Zinc Finger

1 – Introduction

1.1 Pulmonary Vasculature

The pulmonary vasculature is a low-pressure vessel circuit responsible for the transportation of deoxygenated blood from the right heart into the lungs for alveolar gas exchange and blood reoxygenation to occur. It is also responsible for the return of oxygenated blood from the lungs into the left heart for its subsequent distribution into the rest of the body through the systemic circuit. Its large-scale structure comprises the pulmonary artery arising from the conus arteriosus in the right ventricle, which then branches into subsequently smaller vessels in the arterioles and then capillaries, reaching the end of the airways—the alveoli—at the end of bronchioles in the lungs (1). Bronchioles result from the division of larger bronchi arising from the trachea, the main airway connecting the nostrils and mouth to the lungs. These two systems running in parallel allow for gas exchange to occur and for blood to be oxygenated.

Size metrics for the pulmonary vasculature include a vessel diameter ranging from around 30 mm in the case of the larger pulmonary artery, to a much narrower 10 µM in the case of the smallest capillaries reaching the alveoli (2). In terms of pressure levels within the system, it comprises a relatively low mean pulmonary artery systolic pressure of around 14 mmHg (millimetres of mercury) when compared to the normal range for the aortic systolic pressure at around 80-120 mmHg. This drastic difference in normal pressure ranges for the two circuits reflects the different distances blood must flow within each system (much longer in the case of systemic blood) and results in different vessel characteristics as vessel structure adapts to optimise its response to pressure. In the case of systemic vessels, this means a much thicker layer of smooth muscle covering the inner endothelial layer than in the pulmonary vasculature (3).

Arteries within the pulmonary vasculature are comprised of three distinct layers—the tunica intima, media and adventitia—consisting of different cell types and displaying different characteristics and functions. The innermost layer is the tunica intima, where endothelial cells make up a single-cell layer supported by connective tissue and in contact with the blood flow. This pulmonary artery endothelial cell (PAEC) layer makes up the vessel wall separating the blood flow from the rest of the artery, which allows them to function as key signalling mediators for optimal arterial function, identifying and reacting to changes in blood pressure or associated shear stress as vessel luminal area changes, or at arterial branching points (Figure 1.1) (2). Optimal EC function is paramount for vessel stability, so the fate of vascular ECs is tightly regulated to form either arterial, venous or lymphatic vessels as necessary during development. Pathways involved in PAEC differentiation, such as Notch (4), have been implicated in vascular disease processes (see details on Introduction 1.3.4 and Introduction 1.3.6.1).

The tunica intima is separated by an internal elastic lamina from the tunica media, strengthening vessel structural stability (2). The tunica media is the intermediate layer and is mainly comprised of pulmonary artery smooth muscle cells (PASMCs) arranged in a circumferential pattern which allows for vessel contraction and relaxation as required to optimise blood flow control. These PASMCs are surrounded by another external elastic lamina. The final, outermost layer is the tunica adventitia, comprised of fibroblasts, collagen fibres and another elastic lamina, further increasing vessel stability and preventing excessive expansion (Figure 1.1) (3).

Pulmonary artery differences exist within the pulmonary circuit depending on the roles they need to play, their relative location within the circuit and their blood flow features, namely blood pressure and shear stress. Larger, proximal arteries face higher pressures and require increased wall thickness and elasticity to withstand the large blood flow coming from the right heart. They therefore include more collagen fibres to strengthen the vessel wall, as well as several layers of interspersed PASMCs and elastic laminae to increase their distensibility (5). Arteries become progressively less muscularised as their diameter decreases and they are subjected to lower blood pressure, eventually finding non-muscularised vessels—the capillaries—at the most distal parts of the circuit, where a single layer of external elastic lamina separates the PAEC layer from the tunica adventitia. This optimises the gas exchange process by minimising the distance between air in the adjacent alveoli and blood within the vessel (3,6). The network of alveolar capillaries eventually converges into venules and these into sparsely muscularised pulmonary veins transporting reoxygenated blood into the left heart for systemic distribution (2).

1.2 Pulmonary Hypertension

Pulmonary hypertension (PH) is a heterogeneous lung vasculature disorder characterised by pulmonary artery remodelling through over-muscularisation of small vessels, increased stiffness in larger arteries (reducing their ability to adapt to changes in blood pressure through distension) and excessive fibrosis; all of which result in an increase in pulmonary blood pressure. This increase in blood pressure greatly elevates right heart stress and ventricular afterload and eventually leads to severe right heart hypertrophy, disease and failure and premature death (7,8). The prevalence of PH lies at 1% globally within the normal population and goes up to 10% in the 65+ age group (9).

Clinically, PH is characterised by an increase in resting mean pulmonary artery pressure (mPAP) from the normal mPAP average of around 14 mmHg (10) to an mPAP of at least 25 mmHg (11). This scale, however, represents a risk continuum and not an absolute threshold. Intermediate pressures above 19 or 21 mmHg have shown to incur in higher risk than lower pressure levels and, in recent years, have been categorised as borderline PH, showing evidence of worse functional performance (12,13). There have been attempts at resetting the threshold for PH diagnosis, but simply lowering the 25 mmHg pressure threshold could result in an unspecific increased cardiac output phenotype being detected rather than actual disease (14). A combination of an mPAP >20 mmHg and a pulmonary vascular resistance (PVR) above 3 Wood Units has therefore been proposed to optimise diagnosis (15).

The term pulmonary hypertension refers to a spectrum of diseases with different clinical phenotypes, pathophysiology and associated co-morbidities. This results in five different main PH subgroups recognised by international associations, which are subject to future updates based on potential new evidence (15,16). These groups include Pulmonary Arterial Hypertension (PH Group I), Pulmonary Hypertension due to Left Heart Disease (PH Group II), Pulmonary Hypertension due to Lung Disease (PH Group III), Chronic Thromboembolic Pulmonary Hypertension (CTEPH) and other pulmonary artery (PA) obstructions (PH Group IV)—which includes CTEPH, pulmonary angiosarcoma, other intravascular tumours, arteritis, congenital pulmonary arteries stenoses and parasites—, and Pulmonary Hypertension due to unclear and/or multifactorial mechanisms (PH Group V). Diagnosis is not always a straightforward path due to unspecific clinical panels being common among PH patients. A diagnostic algorithm has therefore been developed to optimise the diagnostic process and minimise treatment delays (16).

WHO Group	Clinical Group
PH Group I	Pulmonary Arterial Hypertension
PH Group II	Pulmonary Hypertension due to Left Heart Disease
PH Group III	Pulmonary Hypertension due to Lung Disease
PH Group IV	Chronic Thromboembolic Pulmonary Hypertension (CTEPH) and other pulmonary artery obstructions
PH Group V	Pulmonary Hypertension associated with miscellaneous diseases

Table 1.1: Classification of the Pulmonary Hypertension spectrum of diseases by World Health Organisation.

1.3 Pulmonary Arterial Hypertension

1.3.1 PAH overview

Pulmonary arterial hypertension (PAH), also known as PH Group I, is a very rare cardiovascular disorder within the pulmonary hypertension spectrum of diseases with a prevalence of 2.1-10.6 new cases per million inhabitants per year in the normal population across different population studies (17–20). PAH diagnosis refers to a subgroup of PH patients suffering from both pre-capillary pulmonary hypertension (resting mPAP >20 mmHg) and an elevated PVR of at least 3 Wood Units, without showing any evidence of other associated disorders such as left heart disease or lung disease (16). Obliterative pulmonary vascular remodelling, including uncontrolled PAEC and PASMC proliferation, vascular smooth muscle and fibroblast hyperplasia, extracellular matrix remodelling and influx and/or activation of inflammatory cells and inflammatory mediators, are the main drivers of PAH, resulting in lumen occlusion and stiffening in small distal pulmonary arteries, as well as the formation of plexiform lesions. These processes are what cause the dramatic PVR increase observed in PAH patients and the subsequent right ventricular (RV) afterload and RV failure—the main cause of mortality in PAH (7,21–23).

1.3.2 PAH epidemiology

Average age of onset lies at ~50 years of age, while familial, heritable forms of PAH tend to induce pathogenesis at an earlier time—from early 20s to late 40s—with PAH-associated congenital heart disease patients developing the disease at the youngest ages (11,24,25). One-year PAH mortality rates average at ~15% (26), with subsequent annual mortality rates at an estimated 10% (20). Overall survival rates in PAH 5 years from diagnosis lie at 65% (27), with a mean survival of 2.8 years if there is no medical intervention (28), representing high levels of mortality. This effect is compounded by the severe effect PAH symptoms have on the quality of life of patients, profoundly affecting the daily life of both PAH patients and their families.

Female-to-male ratios of PAH incidence lie at around 3:1, hence predominantly affecting women (25,29). This effect correlates with age, with sex ratios in older patients (>75 years of age) approaching 50% (11). Nonetheless, male patients usually present worse clinical outcomes and disease prognosis for reasons yet to be understood (11,30), although recent evidence suggests sex hormones may play opposing roles in both disease pathogenesis and disease development (31).

1.3.3 PAH classification

The poorly understood, most common form of PAH in western countries (~30-50% of all PAH cases), known as idiopathic pulmonary arterial hypertension (IPAH), refers to PAH cases where disease pathogenesis is unclear and patients do not present with any known risk factor or familial history for the disease, unlike in heritable forms of the disorder (HPAH), in instances where PAH is associated with other conditions—such as congenital heart disease or connective tissue diseases like sclerosis—(APAH) or in PAH induced by drug use (DPAH) (16,32). This lies in contrast to what is observed in other regions, such as Brazil, where ~20% of PAH cases are associated with schistosomiasis infections (33), or China, where ~40% of PAH cases are associated with congenital heart disease (34).

IPAH is thought to likely originate in response to a vascular insult, such as hypoxia, infection or inflammatory processes, and likely involves a genetic predisposition (35). Further risk factors which may contribute towards PAH development also include drug use and chronic microvascular injury (16,36). Specific background conditions and triggers of the disease process in IPAH are yet to be fully characterised. Overall, this means patient heterogeneity in combination with disease rarity and poor prognosis complicate PAH research and represent some of the major challenges when trying to adequately characterise, classify, treat and prevent PAH. The specific rate of IPAH incidence in the UK lies at around 1.1 to 17.6 cases per million per year, with a prevalence of 6.6 to 26.0 per million adults (9), reaching a higher female-to-male ratio of almost 4:1 (25,37).

1.3.4 PAH pathophysiology

PAH pathology results from the combination of multiple cellular dysfunction processes, such as excessive proliferation or anti-apoptotic behaviour, which affect all main cell types within the pulmonary vasculature, including PAECs, PASMCs, fibroblasts, immune and inflammatory cells (38). These processes interact with and enhance one another, resulting in vessel wall hypertrophy, the formation of a neointimal layer in small vessels and the formation of plexiform lesions (Figure 1.1)(39).

The hyperproliferative phenotype observed in intimal PAECs in PAH is thought to be derived from a preliminary apoptotic state in PAECs triggered by the release of growth factors in response to a vascular insult—such as hypoxia, increased shear stress or genetic modifications in proliferation-related genes—and a resulting antiapoptotic subpopulation of PAECs being selected throughout this process (40,41). These effects compound with the hyperproliferative, migrating phenotype adopted by medial layer PASMCs, which results in the thickening of the vessel wall through neointimal layer formation and the neomuscularisation of small non-muscularised distal arteries (42,43).

The neointima layer consists of differentiated cells which have characteristics similar to PASMCs—or myofibroblasts—surrounded by extracellular matrix. It appears in between the intima layer and the internal elastic lamina and contributes to vessel wall thickening and arterial occlusion (44). The origin of cells comprising the neointima layer is the source of substantial debate. One theory presents evidence pointing towards fibroblasts from the tunica adventitia as the source of cells of neointima formation (45).

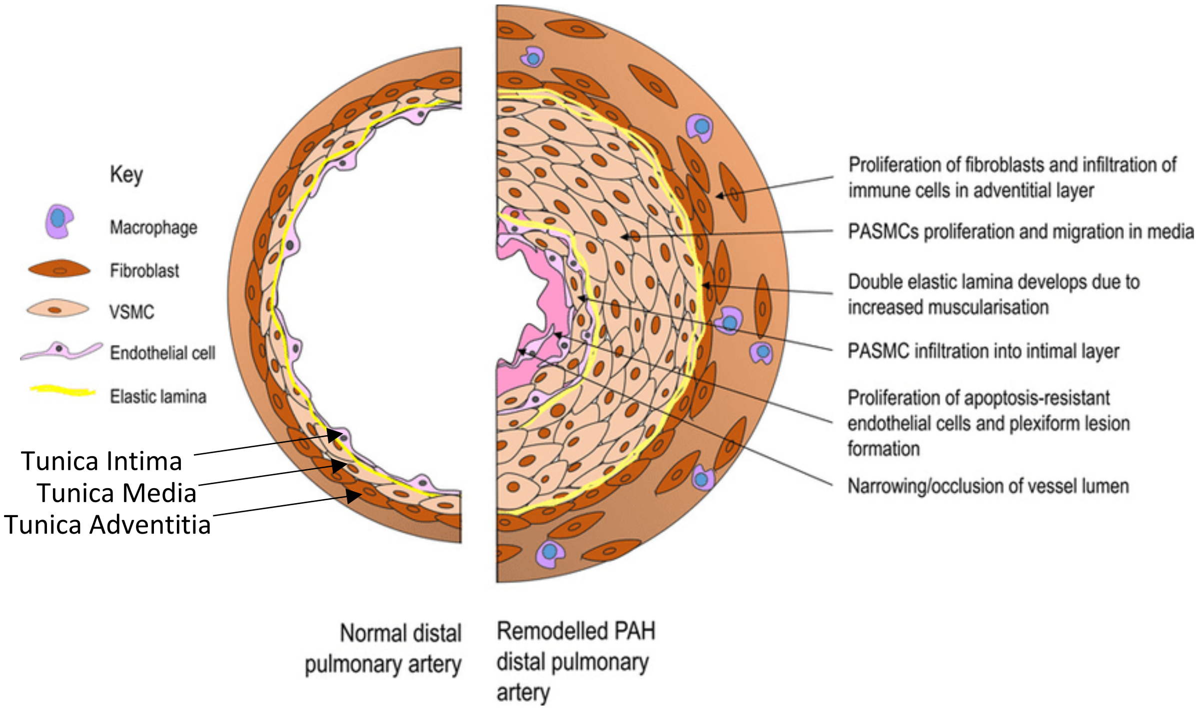

Figure 1.1: Structure of the pulmonary vasculature in health and in PAH pathology. Vessel remodelling in PAH pathology is contributed by all vascular cell types in the tunica intima, media and adventitia. The resulting occlusion of the vessel lumen contributes towards the increase in pulmonary blood pressure and right heart strain. Original diagram taken from: (46).

Hyperproliferative, migrating PASMCs from the lamina media have also been implicated in this process (42,47). Interestingly, PASMC migration into the neointima layer seems to be associated with upregulation of the Notch signalling pathway (47). Notch signalling is involved in processes such as vascular development and differentiation, response to injury and homeostasis (48,49). Notch overexpression has been previously shown to promote PAH development in mice models and in humans (50). In contrast with this, however, missense mutations in the *NOTCH3* gene found in PAH patients which lead to impaired downstream signalling were associated with increased cellular proliferation and viability (51). Furthermore, Notch signalling has been recently found to regulate EC proliferation and apoptosis in PAH (52).

PAECs which have undergone Endothelial-to-Mesenchymal Transition (EndoMT) have also been suggested as a potential origin for neointima layer formation (53). EndoMT is a key process occurring in PAH caused by a downregulation of and transcription factors such as slug, EGR1 and snail (54). The gene *BMPR2*, encoding a membrane receptor for bone morphogenic proteins (BMP) and a key component of the BMP/TGF-β pathway—central to PAH pathology (see details on Introduction 1.3.6)—is the gene most predominantly associated with familial PAH cases in HPAH. BMP/TGF-β signalling dysregulations cause PAEC reprogramming and loss of cell-cell adhesion and barrier functions, shifting PAECs towards a hyperproliferative, migrative state into small distal arteries (55–58). These transcription factors—slug, EGR1 and snail—play key roles during early arterial development, but they are aberrantly activated in PAH pathology due to yet to be understood causes (53,59,60), although recent evidence points towards shifts in haemodynamic balance and inflammatory processes as likely EndoMT inducers in early-stage PAH (61,62). Small distal artery neovascularisation also occurs because of cellular phenotype changes and is a key process in PAH pathology (7).

Another key feature in PAH pathology is the formation of plexiform lesions, complex structures arising from disorganised vascular angiogenesis (39). These plexiform lesions can be localised throughout the entire lung vasculature and their numbers are independent from the degree of remodelling and hemodynamic performance deterioration (63). They are a disease hallmark in end-stage PAH—being identified in virtually all IPAH lungs (39)—and their microenvironment triggers the release of shear stress and hypoxia-induced angiogenic factors which reach other areas in the lung vasculature and trigger the formation of more lesions (64). Excessive extracellular matrix and growth factor deposition by fibroblasts in the tunica adventitia is believed to be triggered in response to primary vascular insults and favour the formation of plexiform lesions and aberrant angiogenesis (44,65).

Immune cells, such as B-cells, T-cells and macrophages are also found within plexiform lesions (66). There is a strong immune and inflammatory component in PAH pathology (63). Inflammatory mediators, such as interleukin-1 (IL-1) and IL-6 can be detected in vascular injury sites and the blood stream. They are thought to contribute to the environment of excessive proliferation and insufficient apoptosis occurring in PAH pathogenesis (67). Levels of these inflammatory mediators are associated with poor prognosis and worse clinical phenotype (68). Systemic levels of certain immune cells, such as lymphocytes or neutrophils, have been tested for their potential as markers of disease severity (69). Nonetheless, whether immune and inflammatory processes are involved in PAH pathogenesis, or they are instead the result of the severe pathology developed in PAH remains to be understood (70).

Although most processes in PAH pathology occur within the lung microvasculature, large vessels are also affected by the disease. Fibrosis, thickening and stiffening of the vessel wall can be detected in major pulmonary arteries in PAH (71,72), with evidence of hyperproliferative behaviour, angiogenesis and arterial remodelling in some large vessels (73). The specific involvement of each of these processes and their interactions in PAH pathogenesis and disease progression is a complicated subject, and the lack of animal models which can accurately mimic the onset and disease process in PAH only further complicates research. Some of the most widely used animal models of PAH, such as the monocrotaline (MCT) and Sugen (VEGF receptor blocker SU5416)-hypoxia (SuHx) rat models, fail at either replicating the inflammatory processes or the vascular remodelling occurring in PAH (74–76). There have therefore been other animal models for PAH that have been developed in order to target the limitations of these common models and replicate specific pathological features of the disease. These models include transgenic *Bmpr2* rodents reducing BMPR2 function through different mechanisms—such as cytoplasmic *Bmpr2* tail mutations (77), heterozygous *Bmpr2* deletion (78–80), *Bmpr2* exon 1 deletion (81) or *Bmpr2* exon 1 frameshift mutations (82)—to replicate BMPR2 insufficiency (see details on Chapter 1.3.6.1), rodents transgenic for other *Bmpr2*-related genes—such as mice with heterozygous activin A receptor type II-like kinase-1 (*Alk1*) or endoglin (*Eng*) deletions (83,84)(see details on Chapter 1.3.6.1)—, mice with exacerbated inflammatory processes—such as mice overexpressing IL-6 in the airway epithelium (85)—, or mice with abnormal transcription factor activity —including mice carrying a missense gain-of-function mutation in the hypoxia inducible factor 2α (*Hif2α*) gene (86) or a combination of Egl and Hif conditional deletion (87,88)—, among others.

More sophisticated approaches are necessary to unravel the complex molecular mechanisms of PAH. These could range from the development of animal models that more accurately replicate PAH pathology, to more thorough patient analyses—such as those enabled by omic approaches—, as well as the use of artificial structures replicating biological systems—such as the Pulmonary Artery on a Chip (89), later discussed (see details on Chapter 5)—.

1.3.5 PAH vascular dysfunction and vascular therapies

A key hallmark of PAH pathology is the cell dysfunction observed across all vascular cell types in the pulmonary arteries and the subsequent dysregulation of vascular tone in processes such as vasoconstriction, vasodilation and increased vessel wall rigidity (90). These issues arise from the underlying molecular mechanisms discussed in section 1.3.4 and are the target of most current pharmacological therapies tackling PAH pathology.

These therapies tend to be administered as a combination of drugs targeting both proliferative and vasodilating pathways (91). There are three main vasoregulatory pathways impaired by PAH pathology and therapies attempting to restore balance for each of them have been developed. These pathways include the vasodilating nitric oxide (NO) (16,92) and prostacyclin (PGI2) pathways (93), both of which have been found to be downregulated in PAH patients; and the vasoconstriction mediator endothelin-1 (ET-1) pathway, which shows increased levels in PAH patients (16,94). The use of calcium channel blockers (CCBs) has also been extensively used to promote PASMC relaxation and consequent vasodilation (95,96) and there is evidence suggesting that transient receptor potential channels (TRPCs), involved in Ca^{2+} homeostasis (97), may play a role in pulmonary vascular remodelling underlying the development of hypoxia-induced PH (98).

Other molecular processes with therapeutic potential have also been targeted for PAH therapy, such as novel small-molecule therapies derived from the most recent research efforts using bone morphogenic protein (BMP) 9 analogues (99), hypoxia inducible factor (HIF) inhibitors (100) and repurposed compounds through online database—more specifically, the CMap Database (101)—screening (see details on Introduction 1.5 and in Chapter 5).

1.3.5.1 Nitric oxide

Nitric oxide is an endogenous vasodilator produced by three nitric oxide synthase enzymes (102)—neuronal NOS (nNOS), inducible NOS (iNOS) and endothelial NOS (eNOS)—from L-arginine. It triggers the synthesis of cyclic guanosine monophosphate (cGMP) and the activation of downstream anti-proliferative and vasodilating protein kinases which are dependent on cGMP through soluble guanylate cyclase (sGC) activation (103). This pathway is inhibited by the degradation of cGMP by phosphodiesterases, such as phosphodiesterase type 5 (PDE5) (104,105). Lower levels of NO and elevated levels of PDE5 have been detected in the lungs of PAH patients (92,106). Treatments targeting the NO pathway have been successful at improving clinical performance in PAH patients (106–108) and function by either stimulating sGC action, such as the compound Riociguat (107,109), or by inhibiting the action of PDE5, as in the case of sildenafil, vardenafil and tadalafil (106,108,110). Combination therapy targeting both sGC and PDE5, however, has shown no evidence of improving upon the effects of either one of these mechanisms independently and instead appear to increase the associated risk of side effects within the systemic circulatory system (111).

1.3.5.2 Prostacyclins

PAECs produce PGI2 through the action of prostacyclin synthase, metabolising it from arachidonic acid, and release it into the bloodstream so that it reaches G-protein coupled receptors (GPCRs) located on the surface of nearby PAECs, PASMCs and platelets (112). PGI2 has a pleiotropic function in these cell types through the increase of intracellular cyclic adenosine monophosphate (cAMP), which leads to increased vasodilation (113), anti-proliferative effects in PASMCs (93) and decreased platelet aggregation (112). It has been observed that PAH patients have lower blood levels of PGI2 (114) and reduced prostacyclin synthase expression in their PAECs (115). Furthermore, compounds targeting PGI2 loss have been largely utilised for PAH treatment. These include various prostanoids (such as treprostinil, iloprost or epoprostenol) , compounds mimicking PGI2 that bind to GPCRs and trigger cAMP synthesis in a similar fashion to PGI2, leading to better clinical performances and survival in PAH patients (116–119).

1.3.5.3 Endothelin

Endothelin-1 is a vasoconstriction mediator synthesised and released by ECs. ET-1 binds to and activates receptors on the surface of both PAECs and PASMCs. These receptors are endothelin receptors A (ETA; found only in PASMCs) and B (ETB; found in both PASMCs and PAECs) (120). Activation of ETA or ETB by ET-1 triggers PAEC and PASMC proliferation through an increase of mitogen activated protein kinase and phosphatidylinositol 3-kinase, as well as an increase in PASMC intracellular calcium levels, driving augmented vasoconstriction (121). Increased ET-1 blood levels have been identified in PAH patients (94), making the ET-1 pathway and, more specifically, ET-1 receptor antagonism, a common target for PAH therapeutic compounds (16). ETA and ETB antagonists, such as ambrisentan or bosentan, have been extensively shown to benefit PAH patients and improve their clinical performance and outcomes (122–124).

1.3.5.4 Ca^{2+} channel blockers

K^+ channel dysregulation is another key feature affecting vascular tone in PAH, impairing the electrochemical balance of PASMCs and leading to unwanted voltage-gated Ca^{2+} channel opening and subsequent vasoconstriction (7). Disrupting Ca^{2+} channel function in PAH has thus also become the target of PAH therapies, with numerous Ca^{2+} channel blockers (CCB) having been tested in trials and approved for their therapeutic use in PAH, such as diltiazem or nifedipine (125,126). The main caveat for therapies targeting the restoration of vascular tone is the limited number of patients (∼5-10% of all PAH patients, commonly denominated "vasoresponders) showing any meaningful response to them (127,128), although the patients that do respond positively to vasodilator treatment improve their clinical performance and extend their survival compared to non-responsive subjects, as seen by the changes identified in a study in survival rates at one, two, three and five years following vasodilator treatment, where control survival rates of 58%, 43%, 33% and 28%, respectively, climbed up to 85%, 70%, 63% and 55% (129).

1.3.5.5 Vascular therapy issues

There have been some reports of clinical performance and survival improvement in PAH patients subject to vascular therapies (130) and their use is still the first mechanism against disease progression following PAH diagnosis. Nonetheless, survival after the first year from PAH diagnosis has not climbed from 85% even after vascular therapies have become common practice (26). Furthermore, the issue of not reversing PAH pathology and vascular remodelling, and instead simply ameliorating the symptoms derived from them, has brought into light the need for a more optimised, personalised therapeutic approach. Such an approach would need to account for the molecular mechanisms underlying PAH and attempt to reverse the subsequent pathological features or, at least, halt their progression.

1.3.6 Genetic background in PAH

1.3.6.1 *BMPR2* and the BMP/TGF-β signalling pathway

Rare pathogenic genetic variants have been identified in up to 25% of PAH patients and they associate with earlier disease onset, increased disease severity, biomarkers and mortality (131). Rare mutations in the bone morphogenic protein type 2 receptor gene (*BMPR2*) were discovered early in PAH research and found to be strongly associated with PAH (132). *BMPR2* encodes a membrane receptor for bone morphogenic proteins (BMP) that is a key component of the BMP/TGF-β pathway. The BMP/TGF-β pathway regulates cell growth, proliferation, migration and apoptosis through the binding of cytokine ligands to BMP receptors and the subsequent downstream phosphorylation of intracellular SMAD ("small mothers against decapentaplegic") proteins (133,134).

Mutations in the *BMPR2* gene identified in PAH patients include both missense mutations (causing 25% of *BMPR2* variations)—which alter the aminoacid sequence of BMPR2—and premature-truncating mutations—arising from nonsense mutations (27%), frameshift mutations (23%), gene rearrangements (14%) and splice-site mutations (10%)—. The majority of nonsense mutations affect essential functional domains, such as the catalytic kinase region or the ligand-binding domain, which suggests *BMPR2* haploinsufficiency may be the primary molecular mechanism underlying hereditary PAH (131). Mutations in the active kinase domain of the BMPR2 receptor impair its function and downstream SMAD signalling (135).

Numerous studies have confirmed the association between BMP/TGF-β signalling impairment and PAH development and found that mutations in the BMP/TGF-β signalling pathway account for most familial PAH cases, with almost 70% of these accounted by mutations in the *BMPR2* gene alone (134,136). Furthermore, ~20% of apparent IPAH cases can also be attributed to unaccounted sporadic or inherited *BMPR2* mutations, although familial cases account for only ~10% of all PAH (134,137,138). As discussed above, EndoMT is promoted by BMP/TGF-β signalling dysregulation (see details on Introduction 1.3.4). Interestingly, a reduction in EndoMT has been observed following treatment with rapamycin (59), an inhibitor of protein kinase mammalian target of rapamycin (mTOR). The action of mTOR signalling promotes cell proliferation and migration, opposing that of BMP/TGF-β (139), further highlighting the pathogenic and therapeutic relevance of this signalling pathway in PAH.

Another member of the TGF- β signalling pathway, the BMPR2 upstream ligand and activator BMP9, has been shown to have a positive therapeutic effect on PAECs in vitro, restoring barrier integrity; as well as an ability to effectively reverse PAH phenotype in various murine models of PAH, including *BMPR2* knock-out mice and MCT rats (140). This lies in contrast to the also beneficial effects observed in mice when BMP9 was inhibited both through gene knock-out and through neutralising antibodies (99). Such differences may be accounted by the highly complex balance in BMP/TGF-β signalling and highlight the need for a more thorough understanding of the underlying molecular mechanisms in PAH to improve our therapeutic approach (141). Interestingly, there is a relatively low penetrance in *BMPR2* mutations, with only ~20% of carriers developing PAH (29). This would suggest that other environmental risk factors or genetic background may be required for the development of PAH pathology.

A potential mechanism for variable *BMPR2* penetrance is that of BMPR2 isoform balances impacting BMP/TGF-β signalling, as certain isoforms, such as *BMPR2* splice variant B (missing exon 12), show decreased downstream BMP/TGF-β signalling following BMP stimulation. It has been observed how serine arginine splicing factor 2 (SRSF2) favours BMPR2 isoform A (full length). The ratio of isoform A to isoform B has been found to be reduced in patients, along with a reduction in SRSF2 expression. Common genetic variants affecting levels of SRSF2 expression could therefore impact penetrance of *BMPR2* mutations in PAH (142). Another mechanism could involve common genetic variants affecting expression levels of the gene fidgetin (FIGN), a known congenital heart disease protective gene which could also help reducing penetrance for *BMPR2* carriers (143). Finally, a study has identified common genetic variants in the prostacyclin synthase (PGIS) gene located within the non-coding promoter region of the gene that could have a protective effect in *BMPR2* mutation carriers by haltering PAH pathogenesis (144).

1.3.6.2 Rare gene mutations

Although rarer than *BMPR2* mutations, mutations in other members of the BMP/TGF-β pathway have been suggested to be capable of inducing PAH pathology (137). There have been reports of mutations in PAH patients for the genes encoding *ENG*, *SMAD1*, *SMAD4*, *SMAD8*, *ALK1/ACVRL1*, *BMPR1B* and BMP9 *(GDF2)* (29,134). There is evidence suggesting there may be interplay between BMP/TGF-β and Notch signalling pathways within cells of the lung vasculature (145). Additional evidence also indicates there may be a Notch1-dependent increase in PAEC proliferation in PAH which is associated with PAEC-PASMC interaction and would require functional BMPR2 activity within both cell types (146).

Rare pathogenic mutations have also been identified in genes outside of the BMP/TGF-β signalling pathway, although these account for less than 5% of all PAH cases (147). Despite their rarity, these genes with potential PAH-causing mutations have functions associated with PAH pathology and throw insights into molecular processes that may play a role in PAH onset. Such is the case of transcription factors TBX4 (148) and KLF2 (149); the polyamine-metabolism-related ATP13A3, involved in apoptosis and proliferation (150); and the K^+ channel proteins KCNA5 (151) and KCNK3 (152).

An expert panel for gene curation in PAH was created with the purpose of assessing the strength of the evidence supporting the role of each gene which had been suggested to be potentially associated with PAH development. This panel determined that the members of the BMP/TGF-β pathway *ALK1/ACVRL1*, *ENG*, *CAV1*, *GDF2* and *SMAD9*; the protein channels *ATP13A3* and *KCNK3*; the transcription factors *EIF2AK4*, *TBX4* and *SOX17*; as well as *KDR* (VEGFR2); all had a “definitive” gene-disease relationship based off available literature. Other genes were reported to have more limited supportive evidence and were therefore not classified as “definitive”, waiting for further studies to be conducted to explore their role. These genes with limited supportive evidence are *ABCC8, GGCX, TET2, AQP1, KLF2, BMP10, KLK1, FBLN2* and *PDGFD* (153).

1.3.6.3 Common genetic polymorphisms

In contrast with rare pathogenic mutations, which have a knock-on effect in triggering pathogenesis, common genetic variation is believed to have a more subtle effect on disorders, acting more as a risk factor and creating either a protective or risk-enhancing genetic background for a given disease (154). In PAH, the overall background of all PAH-relevant common genetic polymorphisms within the genome of a given subject, along with other risk factors such as epigenetic state (155), lifestyle and environment, could determine key PAH outcomes, such as whether a rare mutation triggers PAH pathogenesis, age of onset, severity of the symptoms or survival. There is strong evidence supporting the role of some single nucleotide polymorphisms (SNPs) in PAH disease onset, disease progression and patient survival; namely the histocompatibility complex class II DP-b chain (*HLA-DPB1*) and *SOX17*, as these were found to be associated with PAH by two international genome-wide association studies (GWAS) and a meta-analysis of PAH (156). Other SNPs believed to potentially play a role in PAH include the ET-1 pathway gene *GNG2* (157), endostatin (158), several micro-RNAs (159,160), non-coding *BMPR2* gene regions (161) and *CBLN2* (162). All in all, genomic approaches have significantly contributed towards our improved understanding of the role genetics play in PAH pathology, and now the use of other omics is further improving our understanding of molecular mechanisms in PAH.

1.4 Omics applied to PAH research

1.4.1 Understanding omics

Omics are defined as “high-throughput biochemical assays that measure comprehensively and simultaneously molecules of the same type from a biological sample” (163). The term refers to our recent technical ability in biomedical research to obtain a full scan of a given layer of data, such as genomics, transcriptomics, proteomics or metabolomics, so that the information gathered is maximised and a holistic, comprehensive picture of that system is captured. This approach would therefore provide researchers with the most insights we are technologically capable of obtaining. Furthermore, these individual layers can then be combined into multi-omics sets of data with the ability to provide with even more insights and strengthen the individual results obtained from each avenue. The biggest caveat for omics and multi-omics approaches lies in the complexity of generating these comprehensive datasets, as this requires high levels of funding, labour, analytical power, and data storage. Overall, however, recent omic efforts in PAH have proven worth the trouble and shown promising results—such as the identification of distinct PAH diagnostic panels of 9 circulating proteins (164) and 16 circulating metabolites (165) capable of distinguishing between PAH patients and healthy controls—, gaining momentum within mainstream PAH research approaches as a result (163).

1.4.1.1 Omics in PAH

PAH therapeutic approaches are severely hindered by the aggressive nature of the disorder, with patients having usually developed significant pulmonary vascular remodelling by the time they undergo treatment (see details on Introduction 1.3.2). This aggressive nature in PAH pathology has the combined disadvantage of both more severe symptoms to try to reverse and less room for error when deciding the therapeutic approach. Disease rarity, along with quick disease progression, poor patient prognosis and short mean survival in PAH; also hinder research efforts through limited patient availability and a lack of patients in early-stage PAH identifiable for research collaboration (16).

There is a further limitation for PAH research in the inherent inaccessibility to the site of injury, as lung biopsies are highly hazardous and contraindicated for the severely ill PAH patients (16). Blood circulating molecules in the form of proteins, metabolites and RNA transcripts can be utilised as a "liquid biopsy" of the vascular site of injury in PAH. Through this, the comprehensive scan of the disease state at a molecular level offered by the omics approach can be used to compensate for the low numbers in PAH research cohorts—ranging between 6 and 62 patients in previous PAH lung studies (166–170) and between 15 and 72 patients in previous PAH PBMC studies (171–176)—which severely hinder the statistical power of traditional methods (177).

It is important to remark, however, the substantial effort in overcoming cohort size issues that has been made at the national and international level, bringing about the creation of networks to try and recruit as many patients as possible for biomedical research, such as the U.K. National Cohort Study of PAH, the French network, the Pulmonary Vascular Disease Omics Study (PVDOMICS) in the United States, the PH Breakthrough Initiative (PHBI), the Pulmonary Arterial Hypertension Biobank and the International PAH Genetics Consortium (178).

The comprehensive nature of omics may also help to compensate for the fact that these metrics are obtained through blood—and not directly from the primary affected cells at the site of injury—through the increased level of detail they are able to capture—especially given the important role that inflammation and immunity play in PAH (63) and that circulating factors which can be derived from the lung also affect PBMCs (171,179). Recent technological advances in high-throughput analyses have considerably reduced the costs for the performance of techniques required in omics research, alongside a reduction in costs for data storage and management (178).

Overall, when looking at all these factors in the context of PAH research, a compelling argument for the use of an omics approach for PAH research comes about naturally. The use of omics and multi-omics in PAH research could bring about better ways of diagnosing, monitoring, stratifying and treating PAH patients.

1.4.2 Understanding transcriptomics

Transcriptomics is the study and characterisation of gene expression profiles. New techniques such as microarrays, nanopore sequencing and the more comprehensive RNAseq have enabled the field of transcriptomics to develop and produce full gene expression profiles from cells, tissues and even full organs (180,181). Through these analyses, differential gene expression can be accurately identified and characterised in the context of all other transcripts being measured, allowing for key pathway identification and selection of potential therapeutic targets (182). For a more thorough description of transcriptomic methodologies see Methods 2.1 and 2.2.

1.4.2.1 Transcriptomics in PAH

As mentioned above (see details on Introduction 1.4.1.1), access to diseased tissue during PAH disease progression is a major challenge in PAH research. Most primary site of injury tissue samples are obtained from PAH patients following lung transplant, which comes with the inherent caveat of reflecting end-stage PAH and samples having been subjected to PAH therapies. The alternative comes in the form of transcriptional analyses on peripheral blood mononuclear cells (PBMCs), which can be easily obtained through patient phlebotomy, but may not accurately reflect the molecular pathology occurring within the lung vasculature.

1.4.3 Lung transcriptomics in PAH

Lung tissue RNA profiling allows for a direct measure of the differential phenotypical state of the vasculature observed in PAH. While it can only be consistently obtained from subjects undergoing lung transplant procedures, it allows for on-site analysis of the pathology and a more accurate representation of the underlying mechanisms of the disease. Although the limitations of sample collection under these conditions significantly hinders the sample size and, therefore, the analytical and statistical power of these studies, lung transcriptomics has been an insightful approach that has brought to light several pathways now believed to be central to PAH molecular pathophysiology, as well as molecular mechanisms suitable for therapy.

1.4.3.1 Lung transcriptomic studies of PAH

One of the first transcriptome studies on lung tissue compared lungs from IPAH (n= 4) and HPAH (n= 2) patients, as well as from healthy controls (n= 6) and found the gene expression pattern of HPAH patients had a closer resemblance to what was observed in healthy controls than in IPAH patients. Some of the differentially expressed genes identified in IPAH lungs belonged to pathways involved in vascular reactivity and protein synthesis and degradation, all of which linked to dysfunction in PASMCs and PAECs. These genes included eEF1A1, BMP4, EPAS1 and LamR. These findings highlighte the functional and molecular differences between heritable and idiopathic forms of PAH (166).

A similar, more recent lung microarray analysis including IPAH (n= 31), APAH (n= 18) and HPAH (n= 6) patients, along with patients suffering from similar cardiovascular disorders (n= 4) and healthy controls (failed donors; n= 25), also showed this difference between IPAH and HPAH patients. There were 1140 transcripts that were differentially expressed (FDR q< 0.001) between PAH and healthy controls, among which several targets of current therapies—EDT1, PDE5, prostacyclin receptors and calcium channels—could be found. This signature was independently validated via two different methods. First, this signature was used to try to distinguish PAH in an independent dataset of 18 PAH patients and 13 healthy controls (167) based on gene expression levels of the 1140 differentially expressed genes. Results showed PAH patients and healthy controls clustering separately except for 2 PAH patients identified as controls. Second, a literature-derived PAH gene network (183) was utilised to provide supervised analysis of results from the differential expression analysis, and only one PAH patient was misclassified by it. Downstream pathway analysis revealed several IPAH- and HPAH-specific pathways when compared to healthy controls, whereas the HPAH group (n= 6) was too small to allow for this kind of analysis. IPAH-specific pathways were associated with neutrophil and dendritic immune cell types, whereas pathways specific to APAH were associated with phospholipase C activation and extracellular matrix organization. Shared dysregulated pathways suggested a role for innate immunity, as a wide array of toll-like receptors (TLRs)— a class of proteins that play a key role in the innate immune system—were represented. Overall, these results highlight the heterogeneity inherent to PAH pathology and the role immunity and inflammation play in PAH (184).

1.4.3.2 PH-related lung transcriptomic studies

A lung tissue transcriptome study tried to identify differences between PAH and other similar PH-associated conditions, such as pulmonary fibrosis (PF). Differences between PAH patients (n= 18) and both healthy controls (n= 13) and PH secondary to IPF patients (n= 8) were observed. These changes were found predominantly in genes regulating processes such as protein ubiquitination or actin-based motility were identified, as well as downregulation of BMPR2. Altered TGF-β, nitric oxide, cAMP and MAPK signalling were also present in the lungs from PAH patients. Overall, most differentially expressed genes were involved in cell proliferation pathways, further supporting the role of vascular remodelling in PAH, in contrast with other PH associated disorders (167).

A different PAH lung transcriptome study compared transcriptional profiles from IPAH patients (n= 8), patients with PAH associated with systemic sclerosis (SSc-PAH; n= 9), pulmonary fibrosis associated with systemic sclerosis (SSc-PF; n= 9), idiopathic PF patients (IPF; n= 10) and healthy controls (n= 9). Several processes unique to PAH were identified in PAH and SSc-PAH patients, such as exacerbated inflammation and vasoconstriction, involving differential expression of genes such as IFNs, IL-4, IL-17, CCL-2, CXCL10, HLA-DR and HLA-A (168).

These potential commonalities between IPAH patients and patients with PAH secondary to other cardiovascular disorders were further explored in a study seeking to identify transcriptional differences between PF patients (n= 54), PF patients with secondary PH (PF-PAH; n= 62) and IPAH patients (n= 7). Results recapitulated previous findings, with IPAH patients showing an independent, disease-specific transcriptional signature, clustering apart from secondary PAH and other cardiovascular disorders. Furthermore, treatments targeting the therapeutic pathways identified for IPAH did not produce positive effects on secondary PAH patients (169).

Interesting insights were gathered from a different study conducted that same year, where gene expression signatures from lungs of murine models of fungus-induced PAH were compared to those of other studies performed on IPAH patients (n= 2, 7 and 18). Some molecular pathways were similarly dysregulated, while others were found to be significantly different between human patients and rodents. The most prominent shared dysregulated pathway was BMP/TGF-β signalling, including downregulation of BMPR2, ENG and ALK1. This could suggest dysregulation of the BMP/TGF-β pathway may be a key feature of PAH pathology without being essential for IPAH pathogenesis, as it was triggered as a consequence of vascular hyper-muscularisation independently of its origin. In contrast with this, evidence of upregulation in Wnt/planar cell polarity (PCP) signalling and its downstream Rho/ROCK signalling pathways was solely observed in IPAH and not in mice (170). There is abundant evidence supporting the vital role of these pathways in lung health and development (185). They have been associated with lung morphogenesis (186), BMPR2-mediated angiogenesis in hPAECs (187) and IPAH pathogenesis (188). Wnt/PCP pathway dysregulation should therefore be addressed in future IPAH transcriptomic studies for its prominent role in lung pathology and IPAH pathogenesis.

The first RNAseq analysis carried out on PAECs from PAH patients assessed transcriptional differences between cells isolated from lungs from IPAH patients (n= 6) and healthy controls (unused donors; n= 7). Dysregulation of the BMP/TGF-β signalling pathway previously described was recapitulated in this study, despite the lack of any BMPR2 mutants among IPAH patients. Functional characterisation of some of the genes found to be downregulated in IPAH PAECs, including COL4A1, COL4A2, and EFNA1; revealed lower levels of downregulated genes associated with features of endothelial dysfunction, suggesting new pathways for disease progression and potential therapeutic targets (189).

Overall, lung transcriptome studies of different forms of PH have revealed changes in pathways associated with PAH pathology, such as proliferation, inflammation, immune response and extracellular matrix turnover. The limited sample size and availability in this type of study remains as the biggest limitation for interpretation of results, along with the inherent issue of lungs analysed belonging to dead patients—hence reflecting end-stage disease—. These issues make lung transcriptomics a powerful yet insufficient stand-alone tool for PAH research, thus highlighting the need for different approaches in order to obtain more thorough reliable insights into the molecular mechanisms of disease.

1.4.4 PBMC transcriptomics in PAH

Transcriptional analysis of PBMCs offers an alternative, non-invasive insight into the molecular features of PAH. There is robust evidence supporting the ability of peripheral blood to accurately reflect changes resulting from injuries or disease processes. The constant interactions between tissue at the site of injury and PBMCs circulating in blood could very well trigger changes in their transcriptional and phenotypical state (171,179). PBMC analyses could help construct comprehensive molecular signatures without the extensive requirements of other tissue collection procedures, such as lung transplantation or localised biopsies. It would also be of relevance to find a distinct PAH transcriptional signature detectable from a blood sample, as this could allow for effective PAH diagnosis earlier or even without undergoing the invasive procedure of right heart catheterisation, the current standard PAH diagnostic test (16).

While PBMC gene expression differences have been reported between PAH patients and healthy controls, a robust PAH-specific signature separating PAH patients from other forms of PH is yet to be identified (172,173).

1.4.4.1 PH-related PBMC transcriptomic studies

One of the first PAH PBMC transcriptional studies found a 106-gene expression signature that distinguished between PAH patients (n= 15) and healthy controls (n= 6) but could not differentiate between IPAH (n= 7) and APAH (n= 8) patients. Most of the differentially expressed genes were part of pathways associated with inflammation, stress response and intracellular signalling (174). Similar results were obtained in another study comparing gene expression profiles of PBMCs from IPAH patients (n= 9), SSc-PAH patients (n= 10) and healthy controls (n= 5). Differentially expressed genes between healthy controls and both IPAH and SSc-IPAH patients were identified in pathways such as inflammation, angiogenesis and chemotaxis. However, striking similarities between the gene expression signatures of IPAH and SSc-PAH patients were also demonstrated (35).

Further evidence in this direction was gathered from several studies published in 2010. Transcriptome research conducted on limited systemic sclerosis (lSSc) patients (both with and without associated PAH), demonstrated how PBMCs from lSSc-PAH patients (n= 15) had upregulated inflammatory pathways that distinguished them from both healthy controls (n= 10) and lSSc-NoPAH patients (n= 21) (172). Analogous assays carried out on PBMCs from scleroderma patients revealed a differential gene expression signature separating scleroderma patients with associated PAH (n= 10) from scleroderma patients with no associated PAH (n= 10). Again, inflammatory and immune pathways were the most prominently dysregulated in scleroderma with associated PAH patients (173).

Similarly, a larger transcriptome study of SSc and PAH patients conducted in 2012 revealed gene expression differences ($p < 0.01$; FDR $q < 0.1$; $|\text{fold change}| > 1.5$), between SSc patients with no associated PAH (n= 19) and both IPAH (n= 30) and SSc-PAH (n= 42) patients. There were 89 up- and 136 down- regulated overlapping genes when comparing all three patient groups with healthy controls (n= 41). These numbers, however, climbed up to 207 up- and 307 down- regulated shared genes when only IPAH and SSc-PAH patients were included, while only 2 genes were shared by IPAH and SSc patients alone. Unsupervised clustering analysis of the 500 most dysregulated genes highlighted the erythrocyte maturation pathway as associated with PAH. Additionally, ALAS2 and ERAF—two of the most dysregulated genes in IPAH and SSc-PAH patients in that study—have been previously shown to be essential for terminal differentiation of erythroid cells (190), and their expression levels were validated by RT-qPCR. Data was validated using the Mouse Genomics Informatics (MGI) database (191), which identified multiple phenotypes of blood disorders in mice associated with the RNA signatures from the study; as well as by testing the identified signatures in four other independent studies (167,172–174), which also showed enrichment of genes associated with erythrocyte maturation in PH patients. Erythropoietic signatures were similarly enriched in IPAH and SSc-PAH patients within that study, although haemodynamic analyses revealed differences between them. Furthermore, disease severity was associated with the erythropoiesis signature in IPAH but not SSc-PAH patients, suggesting erythrocyte maturation could potentially be used as a IPAH-specific whole-blood disease severity transcriptional biomarker. This potential use of expression levels of erythrocyte maturation-associated genes was not validated externally, so further research is required (175).

In a later study comparing PBMC transcriptional signatures from PAH patients, it was assessed whether there was a distinct pattern of gene expression associated with patients responsive to vasodilator treatment—known as “vasoresponders”—, as these patients show a remarkable increase in survival rates compared to non-responsive PAH patients. Microarray assays followed by RT-qPCR analyses identified a signature distinguishing vasoresponders (n= 8) from non-responders (n= 32), including genes related to pathways such as rho GTPases, cytoskeleton function, cell-cell adhesion, development, and Wnt/β-catenin signalling. 13/25 genes from the list of top dysregulated genes from the microarray study were also differentially expressed (FDR $q< 0.05$) in whole blood PBMCs. Validation of results in an external cohort of vasoresponsive (n=5) and non-vasoresponsive (n= 6) PAH patients, however, showed that only 5 out of those 13 genes were significantly different in vasoresponders. Furthermore, one of those 5 transcripts (P2RY5) was dysregulated in different directions across cohorts. These results during validation suggest the identified vasoresponsive PAH RNA signature might not be as robust. No known study to date has recapitulated these findings distinguishing vasoresponsive PAH patients from non-responders (176).

1.4.5 Summary of lung and PBMC transcriptomics in PAH

Overall, there were notable differences between the gene expression signatures obtained from lung tissue and PBMCs. Lung-derived signatures identified several IPAH specific pathways that clearly differentiated them from both healthy controls and, interestingly, patients with secondary PAH. These pathways were mainly associated with cell proliferation, but also included vascular tone regulation, protein metabolism, inflammation and cell signalling, among others. In PBMC-derived signatures, however, no clear differences between IPAH and secondary PAH patients could be identified. Differentially expressed genes were mostly part of pathways associated with inflammation and immune response.

This difference between lung and PBMC PAH transcriptome signatures may reflect the limited sensitivity of PBMCs to localised changes occurring at the primary site of injury, hence pathways directly associated with PBMC functions may be more easily detectable in this context. Taken together, the current state of the field suggests there could be, in fact, IPAH-specific transcriptional changes that could provide with insights into pathogenesis, pathophysiology, molecular mechanisms and therapeutic targets for PAH. Limited sample sizes of the more informative lung studies, as well as the limited power of PBMCs studies which may have lower sensitivity to disease features remain the biggest challenges in PAH transcriptomic research. Nonetheless, the recent improved availability of new advanced techniques which provide a more thorough transcriptional characterisation, such as RNAseq, is beginning to bring about better insights and increase the analytical power of new transcriptomic studies. This, along with the global effort to recruit PAH patients into sizable cohorts, is enabling PBMC transcriptomic studies to detect more subtle changes that can better reflect disease features in PAH and thus provide with new insights into disease mechanisms.

1.4.6 Other omics in PAH

The current state of the PAH research field in terms of genomics and transcriptomics has been discussed above. Other omic approaches available, however, are also key to understand the mechanisms of PAH and for the generation of comprehensive multi-omic datasets. These include proteomics, metabolomics and epigenomics.

1.4.6.1 Proteomics in PAH

Proteins represent an intermediate step between transcriptional state and phenotype (178). Proteomic efforts in recent years have identified differential protein levels in lung tissue between PAH patients and healthy controls in proteins associated with mitochondrial function, endosomal trafficking and BMP/TGF-β signalling (192,193). A panel of 9 plasma proteins that separates PAH patients by baseline survival has also been identified from a study using an aptamer-based platform (SomaLogic's SomaScan) which measured 1100 proteins. Proteins in this panel are involved in PAH pathological processes such as PAEC stress, inflammation, immunity, myocardial stress, iron dysregulation and thrombogenesis (164). A more recent study using an updated SomaScan platform targeting over 4000 proteins has refined the proteins associated with outcomes in PAH and combined with data from the PAH GWAS, identified proteins such as netrin-4 that may be implicated in disease pathogenesis (194).

1.4.6.2 Metabolomics in PAH

Metabolites are the intermediate products of metabolic activity naturally occurring within cells. They arguably represent a closer reflection of phenotype than proteomics and transcriptomics, but it is also more complex to discern whether metabolite dysregulation is pathogenic or instead reflective of the diseased state, as they are heavily influenced by environmental factors (195). Metabolomic analyses of lung tissue have identified metabolic dysregulation in PAH patients in processes such as the tricarboxylic acid (TCA) cycle, glycolysis, arginine metabolism and fatty acid oxidation (196). Fatty acid metabolism dysregulation, a process known to be affected by BMPR2 dysfunction (197), could also be identified in RV tissue from right heart failure patients (197). Plasma levels of TCA cycle metabolites (malate, isocitrate, succinate and methylmalonate aconitate) in dyspnoeic subjects were found to be associated with PH severity and mPAP (198). Plasma levels of the lipoprotein HDL4, involved in vasodilatory, anti-inflammatory and PAEC-protective processes, were found to be associated with survival in PAH (199). Finally, a panel of 16 metabolites was identified in a prior study conducted by members of the Rhodes lab on plasma samples from PAH patients. This 16-metabolite panel was able to discern between PAH patients and both healthy controls and patients suffering from similar cardiovascular disorders ("disease controls"). The panel also correlated with survival in PAH patients (165). These results suggest PAH metabolomics may be a powerful tool for PAH research.

1.4.6.3 Epigenomics in PAH

Epigenomics studies chemical modifications of DNA and of its associated chromatin proteins that may impact phenotype and gene expression (200), such as the mostly inhibitory DNA methylation in 5′-cytosine-phosphateguanine- 3′ (CpG)-rich regions—named CpG islands—. These modifications are thought to play a role in PAH, such as the recent identified in a cohort of 5 families of an association between *BMPR2* promoter hypermethylation and reduced BMPR2 expression in PAH (201). Additionally, hypermethylation of the granulysin promoter—granulysin is a cytolytic protein that can kill microbes and tumour cells (202)—has been suggested to potentially distinguish between PAH and pulmonary veno-occlusive disease (203). There have not been many datasets of PAH epigenetic data generated to date, but the role of altered histone modifications and ncRNAs in PAH pathology should be investigated further (200).

1.4.6.4 Summary of omics in PAH – why transcriptomics?

Despite the above discussed advantages of using other omic approaches in PAH —and them being essential for PAH research—, the transcriptomics approach was selected for this study because of the benefits of utilising this methodology. More specifically, while its non-targeted nature enables the identification of novel networks of transcripts not possible with other approaches (204), techniques such as RNAseq enable the comprehensive identification of the entire transcriptional state of a biological system (205). Additionally, there have been extensive transcriptomic efforts in PAH—previously discussed (170,173–176,184)—, so there is also a considerable availability of reference datasets for comparisons. These elements combined make PAH transcriptomics a great research venue and marked it as an ideal candidate for this study.

1.5 Research compound repurposing in PAH

Research efforts over the past few years have amounted to great progress in our understanding of PAH molecular pathology. Nonetheless, this progress has not yet translated into therapeutic advances able to effectively reverse vascular remodelling and other PAH features in patients. Most currently used PAH therapies focus on halting or ameliorating the symptoms derived from PAH pathology, rather than trying to revert affected systems to their original, healthy state (see details on Introduction 1.3.5).

This results from the compound effects of an unclear molecular pathogenesis in PAH—the understanding of which would allow for more specific pathway targeting with therapeutic drugs—, low numbers of patients limiting clinical trial opportunities and the lack of animal models that accurately recapitulate PAH pathology, complicating the transfer of therapeutic candidates onto human subjects (16,75).

A research strategy that has been gaining momentum in recent years is that of therapeutic compound repurposing, where small molecule compounds already tested and, in some cases, approved for their therapeutic use in human subjects for a given disease are tested for their therapeutic potential in another disorder. This approach helps in shrinking development times, cutting research costs and reducing safety concerns (206).

This strategy has already produced fruitful results in PAH research, with examples including the compounds rapamycin and sildenafil. Rapamycin is a compound with tumour suppressor properties through mTOR pathway inhibition that has been widely used for biomedical research (207–209) and cancer therapeutics (210,211). As previously described (see details on Introduction 1.3.6.1), rapamycin has been repurposed for PAH treatment for its ability to impair the EndoMT process (59) and is undergoing clinical trials (212). Sildenafil is a compound originally marketed for its ability to prevent the effects of erectile dysfunction (213) which was later explored for its PAH therapeutic potential (106) and eventually approved for PAH therapy for its ability to improve walk distances in PAH patients through PDE5 inhibition (see details on Introduction 1.3.6.1) in the lung (214).

Drug discovery and repurposing strategies are varied, but some incur in high running costs and time investment, such as the otherwise highly effective large-scale screening through CRISPR-*Cas9* gene editing (215). A relatively new alternative to these kind of assays has been the advancement of in-silico assays such as the Connectivity Map (CMap), which allows for a low-cost approach to drug repurposing through online database querying of transcriptional signatures (216,217). These signatures are compared to those produced by “perturbagens” (any agent affecting the transcriptional state of a cell—primarily drug compounds—and gene silencing/overexpression strategies) within the database and correlation scores are produced for therapeutic potential prediction (see details on Chapter 5). The CMap has already been successfully used for drug repurposing candidate selection in anti-cellular stress therapies (218), ovarian cancer (219) and even PAH (101).

1.6 Summary

In summary, the transcriptomics field has great potential for PAH research and new studies utilising advanced, comprehensive techniques—such as RNAseq—and larger cohorts of PAH patients are necessary to deepen our knowledge of PAH mechanisms. Whole blood transcriptomic approaches could be used without the limitation of requiring lungs from patients to identify RNA profiles associated with PAH and to characterise those profiles for their associations with disease severity and progression. They could also be used to identify specific pathways and mechanisms involved in PAH pathology and to potentially implicate some of them in PAH pathogenesis. Transcriptomic approaches could also be used to assess differences between different clinical subtypes. Furthermore, there is a lack of effective therapies in PAH—with current PAH therapies having limited success in symptom reversal and improvement of survival—. Hence, the use of the CMap database in combination with transcriptomic research could lead to the identification of new candidate therapies.

1.7 Hypotheses

1. There is an RNA signature in PAH distinguishing PAH patients from healthy controls which is associated with clinical features and disease progression. A subset of these RNAs are involved in the pathogenesis of PAH.
2. There are transcriptional differences between PAH patients, patients with other forms of PH and other symptomatic patients.
3. There are existing small molecule compounds with the ability to reverse the transcriptional changes occurring in PAH patients. These compounds may also induce positive functional outcomes.

1.8 Aims

1. To identify and characterise RNA profiles associated with PAH and define genes most likely to be involved in disease development.
2. To identify differences in the RNA profiles of PAH patients, other PH patients and other symptomatic patients.
3. To identify candidate compounds that can reverse PAH-associated transcriptional changes and test their therapeutic potential.

2 - Methods

2.1 PAH Whole-Blood RNA Signature Identification and Characterisation: LASSO Model for PAH

2.1.1 Study participants and sample analysis

As part of a coordinated, multi-centred effort from across the UK—the PAH Cohort Study—, patients with different forms of pulmonary arterial hypertension (PAH), namely idiopathic, heritable or drug-induced forms of the disease, were recruited into Cohort and their diagnoses validated. This was done via right heart catheterisation following international guidelines (16) and required a mean pulmonary arterial pressure (mPAP) >25mmHG with pulmonary vascular resistance (PVR) >3 Wood Units (WU) and mean pulmonary capillary wedge pressure (mPCWP) <15mmHg following exclusion of other PH aetiologies (namely left heart disease, lung disease, chronic thromboembolic PH or other causes). Classification of PAH patients as acute vasoresponders (see details on Introduction 1.3.5) was also carried out through right-heart catherisation and required a fall in mPAP of at least 10 mmHg to ≤40 mmHg following vasodilator treatment without a significant impact on total cardiac output (16).The recruitment of healthy volunteers was also carried out at those same centres, all of which followed the same standard operating procedures. All individuals gave written, informed consent with local ethical committee approval.

For this study, 359 PAH patients from Cohort were randomised into 3 groups of RNA discovery (n=120), RNA validation (n=120) and model validation (n=119). Each group was then compared to an independent control set (n=24) of age- and sex- matched healthy volunteers with no sign of respiratory or cardiac disease (Figure 2.1 and Table 2.1).

Tempus™ Blood RNA Tubes were used to collect and store (-80ºC) 3mL of whole blood per sample. Maxwell® 16 Tissue LEV Total RNA Purification Kit (Promega, Madison, WI, USA) was used for RNA extraction from whole blood samples. Each of the samples put forward for sequencing were confirmed to have a 260/230 ratio >1.5, a 260/280 ratio between 1.9-2.1 and an RNA integrity number (RIN)>7 as determined by Bioanalyser (Agilent, Santa Clara, CA, USA).

Ribosomal RNA contamination was removed from whole blood RNA samples by using Globin-Zero Gold rRNA Removal Kits (Illumina Inc, San Diego, CA). Pooled multiplexed libraries of ~80 samples on 9 sequencing lanes were used to perform 75 base pair pared-end sequencing on a Hiseq400 system. Each pool included a randomised combination of patients and controls with similar demographic profiles (ethnicity, age, sex) so that the batch effect was minimised.

The UK NIHR BioResource Whole Genome Sequencing Rare Diseases project and a published PAH genome-wide association study were used to obtain genomics data, such as genotypes of PAH patients included in the study and summary statistics for PAH association (156).

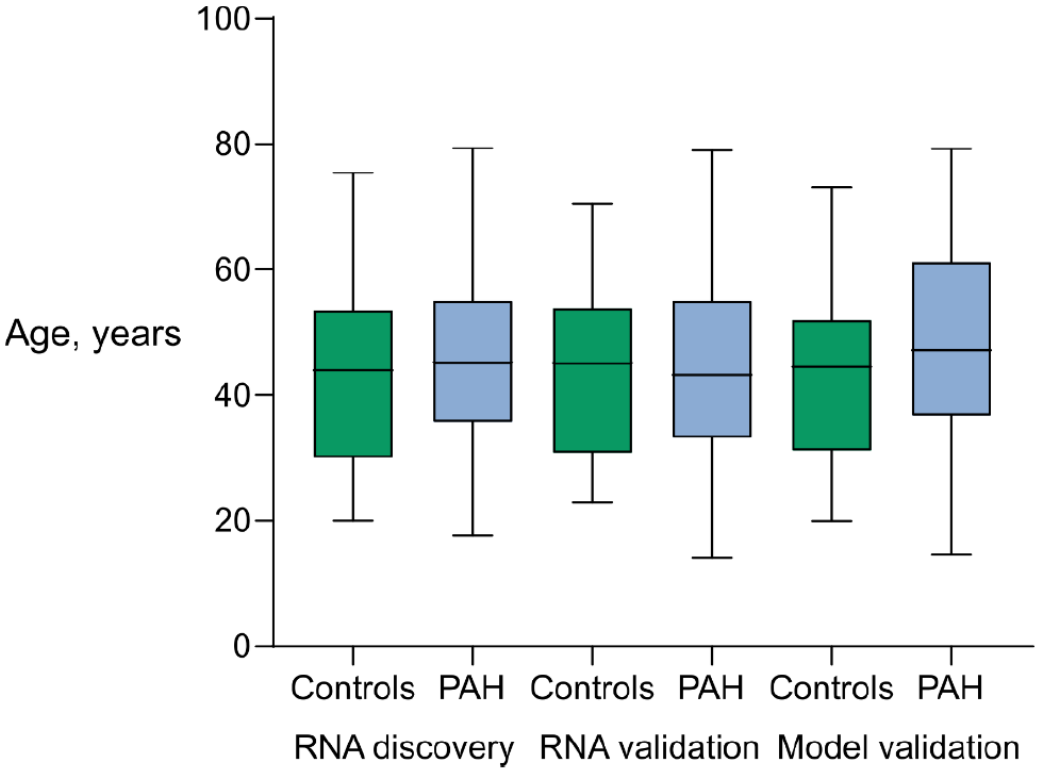

Figure 2.1: **Age in PAH RNAseq randomised groups.** Age in healthy controls (green) and PAH patients (blue) in three analysis groups (RNA Discovery, RNA Validation and Model Testing) after randomisation of PAH patients and matching of controls.

2.1.2 RNAseq data analysis

The raw reads obtained from RNA sequencing (Fastq files) were processed to produce transcript abundance estimates using Salmon v0.9.1 (220) and GENCODE release 28. These were then converted into gene expression data using tximport in R (with Rstudio) (221). The Salmon package was decided to be used based on its ability to correct for fragment GC-content bias, substantially improving the accuracy of transcript abundance estimates and the sensitivity of subsequent differential expression analyses (220). Salmon is the first transcriptome-wide quantifier that allows for that kind of correction. Genes considered for downstream analyses (n=25966) were those identified as “well detected” (2 or more reads in at least 95% of control or patient samples).

A significant outlier was identified and subsequently excluded from further analysis following principal component analysis using overall gene expression data for quality control. There were no indications of any sequencing batch effects or clustering derived from RNA extraction. Downstream correction of remaining data structure was performed using the first 3 principal components.

PAH vs HC	**A - RNA Discovery**		**B - RNA Validation**		**C - Model Validation**	
	Controls	PAH	Controls	PAH	Controls	PAH
Female	17	89	16	80	17	86
Male	7	31	8	40	7	33
Age	43.9 (30.2 - 53.4)	45.2 (35.7 - 55)	45.1 (31 - 53.5)	43.2 (33.3 - 54.8)	44.4 (31.7 - 51.6)	47.1 (36.7 - 61.2)
BMPR2 Mutants		28		19		24

PAH Patient characteristics in A, B & C	**Median (25% - 75%) or Counts**
Age at diagnosis	44.8 (34.3 - 58.1)
Female/Male	255 / 104
Ethnicity: white/other	314 / 45
WHO functional class: I/II/III/IV	36 / 138 / 155 / 18
Six-minute walk distance, m	330 (224.5 - 411)
Mean pulmonary artery pressure, mmHg	53 (46 - 61)
Mean right atrial pressure, mmHg	8 (6 - 12)
Pulmonary capillary wedge pressure, mmHg	10 (7 - 12)
Cardiac output, L/min	3.8 (3.05 - 4.9)
Cardiac index, L/min/m2	2.07 (1.68 - 2.57)
Pulmonary vascular resistance, Wood units	11.55 (7.93 - 15.78)
Years since diagnosis sampled	3.95 (1.38 - 7.7)
Years survived since sampling	3.14 (2.3 - 3.67)
Years survived since diagnosis	6.99 (4.19 - 10.88)
Vasoresponders	21

Table 2.1: **Basic demographics in PAH RNAseq randomised groups**. Demographic information of controls and PAH patients in three analysis groups (RNA Discovery, RNA Validation and Model Testing), and more detailed clinical characteristics including disease severity of PAH patients as a cohort. Controls are healthy volunteers without any cardiac or respiratory disease.

2.1.3 RNAseq white blood cell fraction deconvolution

Two different computational approaches, quanTIseq (222) and CIBERsort (223), were used for white blood cell (WBC) profile prediction based on RNA signatures obtained from the preliminary RNAseq assay (n= 25,966 genes). Correlation between available clinical data and WBC profile predictions from both computational approaches was measured through a Spearman’s rank test.

Mann-Whitney U tests were used to assess differences in WBC profiles between PAH patients and healthy controls, as WBC profiles are non-parametric in nature and samples were not paired. A linear logistic regression model for PAH based on those WBC fraction estimates which were different between PAH patients and controls was developed through a backward stepwise process based on Akaike information criterion (AIC), an estimator of relative quality of statistical models for a given set of data, where a lower AIC relative to other models for the same dataset represents a better fit (224).

WBC fractions able to independently differentiate between healthy controls and PAH patients were included as covariates in secondary differential gene expression analyses.

2.1.4 Differential gene expression analysis

The package edgeR v3.22.5 (225) was used to perform differential expression analysis with principal component correction. Analyses were carried out in distinct discovery (n_{PAH}= 120, $n_{controls}$= 24) and validation (n_{PAH}= 120, $n_{controls}$= 24) groups both with and without selected WBC fractions as covariates to identify differentially expressed genes. Genes were selected based on the following set of criteria:

- First, selected genes must be differentially expressed ($p<0.05$) in both RNA Discovery and RNA Validation groups. They must also show directional consistency between groups.
- Second, selected genes must show overlap between analyses on each group before and after accounting for WBC fractions.
- Finally, selected genes must then meet FDR in a combined analysis including both RNA Discovery and RNA Validation groups (FDR α=0.1; based on all detected genes. A higher FDR threshold than the alternative α= 0.05 was used, as this study was exploratory in nature and therefore less stringent criteria applied).

507 genes meeting these criteria were put forward for the generation of a PAH RNA model separating PAH patients from healthy controls (see details in Chapter 3).

2.1.5 RNAseq validation through RT-qPCR of dysregulated genes

Representative subjects from the model testing group were selected for validation of RNAseq results through performance of reverse transcription (RT) and quantitative-PCR (qPCR). The selection of patients was based on the RNA model score of subjects to give dynamic range. Controls (n=11) were randomly selected, from lowest score to the 55th percentile. Mid-range RNA LASSO score patients (n=18) ranged from the 40th to the 70th percentile of all scores. High RNA LASSO score patients (n=18) included those from the 90th percentile onwards.

RT-qPCR was carried out on a selection of the most significantly dysregulated and biologically relevant genes, such as those with roles in cell cycle/proliferation relevant to pulmonary vascular remodelling. Genes used and their respective primers used for qPCR can be found in Table 2.2.

There is growing evidence suggesting beta actin (ACTB) and glyceraldehyde-3-phosphate dehydrogenase (GAPDH), two common “housekeeping” genes often used as controls in qPCR analyses, are not suitable to be used in assays studying whole blood gene expression (226). It has also been recently highlighted that those same qPCR “housekeeping” control genes display variable levels in RNAseq assays that also render them unfit as controls for this kind of analysis (227). Therefore, an assessment of the most stable genes across all samples in the whole-blood RNAseq of PAH patients and healthy volunteers was conducted and a list of most stable genes was developed for control gene selection. These were defined as well expressed genes ($0 < \log10$ transcripts per million [TPM] < 2) showing the lowest possible variance (pre-selected genes—var= 0.125-0.140). The gene spastin (SPAST), involved in basic cellular functions such as membrane trafficking, intracellular motility, organelle biogenesis, protein folding, and proteolysis; was selected for this role due to its molecular function as a microtubule binding and splicing protein (228) and used as a control in RT-qPCR of PBMCs.

Gene	Direction	Oligo sequence (5' to 3')
CCDN3	F	CTGGGTGCCTGCTCCATGTC
CCND3	R	TCCCTGAGTGCAGCTTCGAT
FBLN2	F	CTACCGCTGTTCCTGCGCC
FBLN2	R	GAGCCATAGATGTTGGCACACT
GRN	F	GGGCGATCCTGCTTCCAAAG
GRN	R	ACAGCACGTGGAGAAGTCCG
NRG1	F	TGTGTGGTGGCCTACTGCAA
NRG1	R	GGGTTAGGATGGTGAGGCCC
OLFM4	F	TTAGGCAGCGGAGGTTCTGTG
OLFM4	R	CAGGTCCCACGGTCATCCAC
SESN1	F	GGATGGGCCGTTACCCCTAC
SESN1	R	GGAGCACTGATGTCTTGCCG
SMAD5	F	CCAAACAGCCCTTATCCCCCT
SMAD5	R	TAGGCAGGAGGAGGCGTATC
SPAST	F	AGCTGCAGAATCGAATGCAACC
SPAST	R	GAAGTTCTCGAGCCACAGCAAA
TRPC1	F	AGCAGAAGGACTGTGTAGGCA
TRPC1	R	TGCCACATGCGCTAAGGAGA

Table 2.2: Genes and primers for RT-qPCR validation of RNAseq results. Selection of genes for RNAseq technical validation found to be dysregulated in PAH patients in the RNAseq assay (from the 507 gene list). Genes were selected based on their PAH pathobiological relevance from literature. SPAST was used as control for its stability and cellular function.

Multiscribe Reverse Transcriptase (Applied Biosystems, ThermoFisher Scientific, UK) was used to perform Reverse Transcription on whole blood RNAseq samples. Quantitative PCR was performed on the resulting cDNA using PowerSYBRgreen mastermix (Applied Biosystems, ThermoFisher Scientific, UK). qPCR cycles started at a denaturation temperature of 95º for 15 seconds, followed by an annealing/polymerisation temperature of 60 ºC for 60 seconds, for a total of 40 cycles. The relative expression of candidate genes, compared to SPAST, was calculated as:

$$2^\wedge - (\Delta CT\ [gene] - \Delta CT\ [SPAST])$$

CT refers to the change in cycle threshold of either the target gene or the control gene. Gene expression levels of selected genes were compared by Spearman’s Rank Test with expression values from the RNAseq assay to assess the correlation between methods.

2.1.6 PAH RNA LASSO model development and testing

Least Absolute Shrinkage and Selection Operator (LASSO) regression analysis was used for the selection of a subset of RNAs best able to distinguish PAH in combination. This type of regression analysis was selected instead of more common linear regression models due to it being optimal for its use in analyses including variables displaying multicollinearity, in this case, the expression levels of 507 genes found to be dysregulated in the RNAseq differential expression analysis. LASSO regression regularises the data through shrinkage. In LASSO regression, data is shrunk towards a central point, effectively reducing many of the coefficients to zero and eliminating variables from the model. This helps creating simpler, more sparse models with fewer parameters (229).

The analysis was carried out using the glmnet v2.0-18 package from CRAN8, with k-fold cross-validation (k=10) selecting the largest value of lambda such that error is within 1 standard error of the minimum. The mRNAs selected from the original 507 genes resulting from the differential expression analysis by the LASSO analysis were used to create a linear weighted combination resulting in an individual RNA score per subject. The pROC v1.14.0 package (Bioconductor) (230) was used to perform Receiver Operating Characteristic (ROC) analysis on the Model Testing group (n_{PAH}= 119, $n_{controls}$= 24) to assess the diagnostic ability of the PAH RNA model based on its sensitivity (true positive rate) versus its specificity (false positive rate). Optimal cut-offs were determined by the maximal Youden index (sensitivity + specificity-1).

2.1.7 Functional characterisation of RNAs in PAH signature

Kaplan-Meier estimates, corrected for survival bias using left-truncation for date of sampling for this study, were used to construct survival curves from date of diagnostic (right-heart catherisation). Log-rank test was used to assess survival estimate differences. Several disease severity markers were compared to the generated RNA scores, namely 6-minute walk test (Spearman's rank), WHO functional class (Kruskal-Wallis ANOVA) and levels of cardiac biomarkers. These cardiac biomarkers were either circulating BNP or NT-proBNP as available, divided into low, intermediate or high levels as per European guidelines for PAH risk assessment (BNP <50 pg/mL, 50-300 pg/mL or >300pg/mL respectively; or NT-proBNP <300 pg/mL, 300-1400 pg/mL or >1400 pg/mL respectively)(16). Functional annotation and enrichment of the genes associated with PAH was performed using DAVID (david.ncifcrf.gov) and Ingenuity Pathway Analysis (IPA®).

2.1.8 Mendelian randomisation studies

The TwoSampleMR package (231) was used to perform mendelian randomisation (MR) analysis. Gene association with PAH was obtained from a previously published genome-wide association study (GWAS) by the Rhodes lab (156) including 9659 controls and 2085 PAH patients. All independent genome-wide significant whole blood expression quantitative trait loci (eQTLs) were obtained from two independent published studies (232,233). eQTLs in cis to the target gene (cis window of transcription start site ± 500 kb) were clumped with a linkage disequilibrium (LD) threshold of 0.01.

2.2 Whole Blood RNAseq of PH Patients and Disease Controls: Identification of a PH-Specific RNA Signature

2.2.1 Study participants and sample analysis

A new cohort was used for this study, which included 147 patients with different forms of pulmonary hypertension (PH), namely patients from PH Groups I-IV (47 Pulmonary Arterial Hypertension, 36 Pulmonary Hypertension due to Left Heart Disease, 16 Pulmonary Hypertension due to Lung Disease and 48 Chronic Thromboembolic Pulmonary Hypertension, respectively). PH patients were recruited through the National PH Service at Hammersmith Hospital and their diagnoses validated. Additionally, 45 patients originally thought to have PH but eventually diagnosed as suffering from other similar cardiovascular disorders were recruited through the same means and used as disease controls. Out of these disease controls, 27 suffered from strong co-morbidities—a full list of which can be found in Table 2.3—, while 18 of them presented with no associated co-morbidity.

Diagnosis was done following international guidelines and required following a stepwise diagnostic algorithm to identify each possible PH subtype through clinical tests such as electrocardiograms, echocardiograms, computed tomography (CT) scans or right heart catheterisation (16). All individuals gave written, informed consent with local ethical committee approval.

Three independent differential expression analyses were carried out in this cohort comparing different patient subgroupings. These subgroupings were PH Group I (n= 47) vs. disease controls (n= 45), PH Groups I-IV (n=147) vs. disease controls (n= 45) and PH Group I (n= 47) vs. PH Groups II-IV (n= 100). Each subgrouping was randomised into two groups of Discovery (A; 2/3 of samples) and Validation (B; 1/3 of samples) (Tables 2.4, 2.5 and 2.6). For each subgroup, gene expression differences between control and test subjects were assessed. Significant, directionally consistent results from both Discovery and Validation analyses were compared with a differential expression analysis of both groups combined (AB) and genes meeting FDR ($\alpha < 0.05$) were put forward for LASSO modelling. Lasso RNA modelling was carried out on subjects from each Discovery group and then tested on the corresponding Validation group.

PAXgene Blood RNA Tubes were used to collect and store (-80ºC) 3mL of whole blood per sample. Maxwell® 16 Tissue LEV Total RNA Purification Kit (Promega, Madison, WI, USA) was used for RNA extraction from whole blood samples. Each of the samples put forward for sequencing were confirmed to have a 260/230 ratio >1.5, a 260/280 ratio between 1.9-2.1 and an RNA integrity number (RIN)>7 as determined by Bioanalyser (Agilent, Santa Clara, CA, USA). Ribosomal RNA contamination was removed from whole blood RNA samples by using Globin-Zero Gold rRNA Removal Kits (Illumina Inc, San Diego, CA).

Pooled multiplexed libraries of ~80 samples on 9 sequencing lanes were used to perform 75 base pair pared-end sequencing on a Hiseq400 system. Each pool included a randomised combination of patients and controls with similar demographic profiles (ethnicity, age, sex) so that the batch effect was minimised.

Full list of co-morbidities presented by Disease Controls
Antiphospholipid syndrome and Deep vein thrombosis
Antiphospholipid syndrome
Coronary artery disease
Centrilobular emphysema
Chronic obstructive pulmonary disease
Chronic obstructive pulmonary disease and Coronary artery disease and Obstructive sleep apnoea
Chronic obstructive pulmonary disease/emphysema
Cutaneous scleroderma antinuclear antibodies positive
Deep vein thrombosis & Pulmonary embolism and Coronary artery disease
Deep vein thrombosis
Factor V Leiden deficiency and multiple Deep vein thrombosis/Pulmonary embolism plus Mitral valve replacement
Lymphangioleiomyomatosis (diagnosed at open lung biopsy)
Likely inherited narrowing of pulmonary arterial vasculature - bilateral upper lobes. Associated upper lobe bronchial collaterals.
Liver cirrhosis
Mitral valve disease
Mixed connective tissue disease
Moderate mitral regurgitation with mild prolapse of anterior leaflet
Multiple Pulmonary embolisms
Pulmonary embolism
Previous Pulmonary embolism and left leg Deep vein thrombosis
Protein S deficiency and recurrent Deep vein thrombosis
Scleroderma
Scleroderma
Scleroderma
Scleroderma affecting the bowel - chronic diarrhoea
Systemic lupus erythematosus
Venous thromboembolic disease

Table 2.3: Full list of co-morbidities presented by Disease Controls. List includes all co-morbidities presented by 27/45 Disease Controls which suffered from any.

PAH vs PH	A - Discovery		B - Validation	
	PH (controls)	PAH	PH (controls)	PAH
Female	37	19	20	13
Male	29	12	14	3
Age	70.1 (59.1 - 77.9)	64.2 (49.3 - 74.1)	59.8 (50.9 - 74.3)	47.4 (33.5 - 59.0)

Patient characteristics in A and B combined	Median (25% - 75%) or Counts	
	PH	PAH
Age at diagnosis	67.2 (54.4 - 76.9)	56.9 (38.9 - 71.7)
Female/Male	57 / 43	32 / 15
Ethnicity: white/other/non-disclosed	78 / 11 / 11	32 / 12 / 3
WHO functional class: I/II/III/IV/unavailable	2 / 8 / 18 / 1 / 71	2 / 3 / 7 / 1 / 34
Six-minute walk distance, m	288 (96 - 360)	340 (240 - 456)
Mean pulmonary artery pressure, mmHg	34 (26 - 43)	45 (32 - 53)
Mean right atrial pressure, mmHg	9 (5 - 12)	6 (3 - 10)
Pulmonary capillary wedge pressure, mmHg	12 (8 - 18)	10 (8 - 11)
Cardiac output, L/min	4.79 (3.51 - 5.95)	4.48 (3.61 - 5.27)
Cardiac index, L/min/m2	2.43 (1.79 - 3.20)	2.53 (2.08 - 2.94)
Pulmonary vascular resistance, Wood units	3.60 (2.37 - 7.17)	6.52 (3.83 - 9.58)
Years since diagnosis sampled	-0.05 (-0.12 - 0.00)	-0.01 (-0.11 - 0.03)
Years survived since sampling	4.76 (3.90 - 5.71)	4.96 (3.84 - 5.91)
Years survived since diagnosis	4.69 (3.99 - 5.93)	5.18 (4.05 - 6.19)
PAH patients (PH Group I)		47
PH-LHD patients (PH Group II)	36	
PH-LD patients (PH Group III)	16	
CTEPH patients (PH Group IV)	48	

Table 2.4: **Basic demographics in PH RNAseq randomised groups for PAH vs PH analysis**. Demographic information of controls (n= 100; PH Groups II-IV) and PAH patients (n= 47; PH Group I) in Discovery and Validation groups, and more detailed clinical characteristics including disease severity of each group as a cohort. Controls are PH patients from PH Groups II-IV, namely 36 PH-LHD (PH Group II), 16 PH-LD (PH Group III) and 48 CTEPH (PH Group IV) .

PAH vs DC	A - Discovery		B - Validation	
	Disease Controls	PAH	Disease Controls	PAH
Female	23	19	9	13
Male	7	12	6	3
Age	62.6 (47.2 - 67.2)	64.2 (49.3 - 74.1)	53.3 (40.7 - 71.1)	47.4 (33.5 - 59.0)

PAH Patient characteristics in A and B	Median (25% - 75%) or Counts
Age at diagnosis	56.9 (38.9 - 71.7)
Female/Male	32 / 15
Ethnicity: white/other/non-disclosed	32 / 12 / 3
WHO functional class: I/II/III/IV/unavailable	2 / 3 / 7 / 1 / 34
Six-minute walk distance, m	340 (240 - 456)
Mean pulmonary artery pressure, mmHg	45 (32 - 53)
Mean right atrial pressure, mmHg	6 (3 - 10)
Pulmonary capillary wedge pressure, mmHg	10 (8 - 11)
Cardiac output, L/min	4.48 (3.61 - 5.27)
Cardiac index, L/min/m2	2.53 (2.08 - 2.94)
Pulmonary vascular resistance, Wood units	6.52 (3.83 - 9.58)
Years since diagnosis sampled	-0.01 (-0.11 - 0.03)
Years survived since sampling	4.96 (3.84 - 5.91)
Years survived since diagnosis	5.18 (4.05 - 6.19)
PAH Patients (PH Group I)	47

Table 2.5: **Basic demographics in PH RNAseq randomised groups for PAH vs disease controls analysis**. Demographic information of disease controls (n= 45) and PAH patients (n= 47; PH Group I) in Discovery and Validation groups, and more detailed clinical characteristics including disease severity of PAH patients as a cohort. Disease controls are patients originally thought to have PAH but eventually diagnosed as suffering from other similar cardiovascular disorders.

PH vs DC	**A - Discovery**		**B - Validation**	
	Disease Controls	PH	Disease Controls	PH
Female	23	56	9	33
Male	7	41	6	17
Age	62.6 (47.2 - 67.2)	66.3 (55.7 - 77.2)	53.3 (40.7 - 71.1)	55.6 (46.4 - 72.6)

PH Patient characteristics in A and B	**Median (25% - 75%) or Counts**
Age at diagnosis	63.8 (52.7 - 75.7)
Female/Male	89 / 58
Ethnicity: white/other/non-disclosed	110 / 23 / 14
WHO functional class: I/II/III/IV/unavailable	4 / 11 / 25 / 2 / 105
Six-minute walk distance, m	297 (144 - 404)
Mean pulmonary artery pressure, mmHg	37 (27 - 48)
Mean right atrial pressure, mmHg	8 (4 - 12)
Pulmonary capillary wedge pressure, mmHg	11 (8 - 14)
Cardiac output, L/min	4.61 (3.56 - 5.54)
Cardiac index, L/min/m2	2.50 (1.93 - 3.11)
Pulmonary vascular resistance, Wood units	4.62 (2.86 - 8.53)
Years since diagnosis sampled	-0.03 (-0.12 - 0.00)
Years survived since sampling	4.82 (3.89 - 5.79)
Years survived since diagnosis	4.75 (4.01 - 5.95)
PAH patients (PH Group I)	47
PH-LHD patients (PH Group II)	36
PH-LD patients (PH Group III)	16
CTEPH patients (PH Group IV)	48

Table 2.6: **Basic demographics in PH RNAseq randomised groups for PH vs disease controls analysis**. Demographic information of disease controls (n= 45) and PH patients (n= 147; PH Groups I-IV) in Discovery and Validation groups, and more detailed clinical characteristics including disease severity of PH patients as a cohort. PH patients include 47 PAH (PH Group I), 36 PH-LHD (PH Group II), 16 PH-LD (PH Group III) and 48 CTEPH (PH Group IV). Disease controls are patients originally thought to have PAH but eventually diagnosed as suffering from other similar cardiovascular disorders.

2.3 PAH Whole-Blood RNA Signature Reversal: Candidate Compound Selection Using the Connectivity Map (CMap).

2.3.1 Cell culture

2.3.1.1 Human PBMC isolation and culture

10-15mL of whole peripheral blood from healthy donors were obtained via phlebotomy at the NIHR Imperial Clinical Research Facility and collected in anti-coagulation tubes containing the calcium chelator reagent ethylenediamin tetra-acetic acid (EDTA). Whole blood was diluted to a total of 35mL with R10 buffer (10% FBS, 1% Pen-Strep antibiotic in PBS) and slowly poured over 15mL Ficoll Paque medium (Sigma Aldrich) for density gradient centrifugation (2000 RPM, 20 min, minimum acceleration and brake). Following this, PBMCs were isolated from buffy coats by use of a Pasteur pipette, washed with R10 and centrifuged. 5mL of red blood cell lysis buffer was added to PBMCs for 5 mins, after which they were washed with more R10 buffer and centrifuged. PBMCs were then resuspended in cell culture medium (RPMI 1640 supplemented, 10% (v/v) heat inactivated FBS; ThermoFisher) and 1.5 million cells per well were plated in 6-well plates for 24h at 37ºC and 5% CO_2.

PBMCs were isolated in this manner from a total of 5 healthy blood donors, either 2 or 3 times per donor, and put forward for experimental drug exposure. On day two, PBMCs were exposed for 6h or 24h to one of Azithromycin, Deferiprone, Dovitinib, Homoharringtonine, Flufenamic-acid and Scopolamine at either 10µM or the concentration most used in the literature for each compound (3nM – 100µM). Following incubation with experimental compounds, mRNA extraction was performed on PBMCs using the RNeasy Plus kit (Qiagen, UK) according to the manufacturer’s instructions.

2.3.1.2 Human PAECs culture

hPAECs (PromoCell GmbH, Germany and ScienCell, USA) used in this research were at passage 4-8. hPAECs were plated (200,000 cells/well in 6-well plates for gene expression assays; 20,000 cells/well in 96-well plates for functional assays) with endothelial growth medium 2 (EGM2, 10% (v/v) heat inactivated FBS, additional growth factor and antibiotic/antimycotic supplements provided by the manufacturer; PromoCell or ScienCell) for 24h at 37°C in 5% CO2. On day two, hPAECs were exposed to Homoharringtonine for 24h for analysis of candidate gene expression (50 nM – 1 µM) or functional assays (50 nM – 100 nM).

Donor Information	PromoCell	ScienCell
Age	51	2
Sex	Female	Male
Ethnicity	Caucasian	
BMI	25.7	

2.3.2 Drug exposure

Candidate small molecule compounds for PAH whole blood RNA signature reversal (Azithromycin, Deferiprone, Dovitinib, Homoharringtonine, Flufenamic-acid and Scopolamine) were resuspended in dimethyl sulfoxide (DMSO) at 10, 50 or 100mM and kept at -20ºC.

2.3.2.1 Human PBMCs drug exposure for analysis of candidate gene expression

PBMCs were exposed to these compounds for either 6h or 24h. Vehicle (DMSO) controls were created in parallel. Information on each compound, including manufacturer, product code, and concentrations used for PBMC exposure experiments can be found in Table 2.7.

Compound	Manufacturer	Product Code	CMap Concentration	Bibliography concentration [µM]
Azithromycin	Sigma-Aldrich	PHR1088	10 µM	2 µM
Deferiprone	Sigma-Aldrich	379409	10 µM	50 µM
Dovitinib	ApexBio	A2168	10 µM	100 nM
Homoharringtonine	Sigma-Aldrich	SML1091	10 µM	50 nM
Flufenamic-acid	Supelco	F9005	10 µM	100 µM
Scopolamine	Sigma-Aldrich	S0929	10 µM	3 nM

Table 2.7 CMap candidate compounds for PAH whole-blood RNA signature. Table shows manufacturer information as well as concentrations used for biological assays.

2.3.2.2 hPAECs drug exposure for analysis of candidate gene expression and functional assays performance

hPAECs were exposed to Homoharringtonine at 50nM, 100nM, 200nM, 500nM and 1 µM for 24h for analysis of candidate gene expression and functional assays performance. Vehicle (DMSO) controls were also created at the relevant concentration and time points.

2.3.3 Analysis of candidate gene expression

2.3.3.1 Candidate gene selection for PAH whole-blood RNA signature reversal analysis

Since there are no PAH-relevant cell types within the CMap database, the ability of each compound to induce the same effect on PBMCs or hPAECs as the one identified on CMap had to be measured. For each compound, 2 of the predicted most up- and down- regulated genes from their CMap signature were selected based on significance, PAH functional relevance, expression levels in PBMCs and hPAECs, and ease of primer development. All 4 genes were used as an indicator in the analysis of candidate gene expression assays for each compound (Table 2.8).

2.3.3.2 Selection of reference genes for RT-qPCR

As with the RT-qPCR validation of whole blood PAH RNAseq results, SPAST was used as a control for the same reasons as with the RNAseq assay (see details on Methods 2.1.5). In the case of RT-qPCRs of hPAECs, ACTB was used as control since lack of stability issues have not been flagged in this cellular type.

2.3.3.3 RT-qPCR of candidate genes

Total mRNA was extracted from hPAECs, processed and analysed utilising the same methodology as with the RT-qPCR validation of whole blood PAH RNAseq results (see details on Methods 2.1.5). Genes used for validation and primers used for qPCR can be found in Table 2.9. Relative expression of candidate genes was compared to either SPAST or ACTB.

Gene	Compound	Predicted Direction	Role(s)
PANK4	Azithromycin	Up	Metabolism / Energy production
GOLGA4	Azithromycin	Up	Vesicular transport
CHP1	Azithromycin	Down	Pleiotropic
CPT1A	Azithromycin	Down	Metabolism / Energy production
TRIP10	Deferiprone	Up	Endocytosis and signal transduction
ATG12	Deferiprone	Up	Autophagy and apoptosis
DGCR11	Deferiprone	Down	Non-coding
BACE1	Deferiprone	Down	Amyloid beta cleavage
DHX15	Dovitinib	Up	RNA splicing
XPC	Dovitinib	Up	DNA damage repair
ATG12	Dovitinib	Down	Autophagy and apoptosis
PTTG2	Dovitinib	Down	Cell cycle regulation
RANBP2	Imatinib	Up	Nuclear transport
ITGA6	Imatinib	Up	Cell-cell and cell-matrix adhesion
CPT1A	Imatinib	Down	Fatty acid oxidation Apoptosis prevention
RALA	Imatinib	Down	GTPase — Variety of cellular processes
PCF11	Homoharringtonine	Up	Cell Proliferation and Differentiation
BCLAF1	Homoharringtonine	Up	Cell Senescence and Apoptosis
PCBP1	Homoharringtonine	Down	Tumour suppressor Cell growth inhibition
CPT1A	Homoharringtonine	Down	Fatty acid oxidation Aapoptosis prevention
PCF11	Flufenamic-acid	Up	Cell Proliferation and Differentiation
PANK4	Flufenamic-acid	Up	Metabolism / Energy production
VPS37B	Flufenamic-acid	Down	Regulator of vesicular trafficking
DCAF7	Flufenamic-acid	Down	Protein ubiquitination
KDM1A	Scopolamine	Up	Epigenetic modifier Regulation of cell growth and differentiation
C12orf29	Scopolamine	Up	Structural protein Extracellular matrix cohesion
ZFP36L2	Scopolamine	Down	Anti-inflammatory modulator
ACAA2	Scopolamine	Down	Catalysation of last step of mitochondrial fatty acid beta-oxidation

Table 2.8: Candidate genes for RT-qPCR validation of CMap predictions. Selection of genes for RT-qPCR validation of PAH whole-blood RNA signature reversal analysis. Genes were selected based on significance in RNA signature, PAH functional relevance, expression levels in PBMCs and hPAECs, and ease of primer development.

Gene	Direction	Oligo sequence (5' to 3')
ACAA2	F	ACTGCACACCTGGTTCACGA
ACAA2	R	GCCACCTCCAATGCAAGCTG
ATG12	F	AGAGCGAACACGAACCATCCA
ATG12	R	CATCCCCACGCCTGAGACTT
BACE1	F	CCCGGGAGACCGACGAAGA
BACE1	R	GCAGCACCCACTGCAAAGTT
BCLAF1	F	CTAGGGGCCGTTCCTCGTTT
BCLAF1	R	ATTCTCCCTCTGCCCTCCCT
C12orf29	F	TGCCGTGTGTGTTTGTGACG
C12orf29	R	CGAGCCCAAAGGTATGGCTG
CHP1	F	GGCTCATTTCCGCCCCATTG
CHP1	R	CGACCATCATGCGTAGCACC
CPT1A	F	CCGGATCCCAGGAGAGGAGA
CPT1A	R	AGCGTCCTCGATGGTACACG
DCAF7	F	GCAGGTGTTAGGGCGAGTGA
DCAF7	R	AGGTCAAACATCCGCACCGA
DGCR11	F	CTGCCTTGCCACTCTGTCCA
DGCR11	R	GGGCCCTGCTCTGCTAAGAA
DHX15	F	GTTTTGTTCGCCCCACGGAG
DHX15	R	TGTCTGCGGACATCAGGGAC
GOLGA4	F	GCAGGAGGAGAACCCTGGC
GOLGA4	R	GGTGTCCCCACAGTTGTTGC
KDM1A	F	TCGTGTGGGTGGACGAGTTG
KDM1A	R	GACAGTGTCAGCTTGTCCGTTG
PANK4	F	TGACGCTCTGGCCCGAAAAT
PANK4	R	CAGGGTCCCATAGGCGAAGG
PCBP1	F	GACCATTCCGTACCAGCCCA
PCBP1	R	GGCCAGATCGAGCGGAGAAA
PCF11	F	GTGGAGCACAGTTTGACAGAAAAGA
PCF11	R	TGGAGATCTCTGCTCTTCTCGC
PTTG2	F	TGGCTGTTGAGAGCGGCAAT
PTTG2	R	AGGCTGATGGAGCATCGTATGT
TRIP10	F	GCGCATCACAGGACACCAAG
TRIP10	R	CCCTCGCTGGACCCTTCAAA
VPS37B	F	CTGTCGCTGGTGCAGCTCAA
VPS37B	R	GCGTGCTTTCAACGTGTCCA
XPC	F	TCCAAGGCCAAGAGCAAGGC
XPC	R	ACCATCTGCTGAACCCCCAG

Table 2.9: Primers of genes used for RT-qPCR validation of CMap predictions.

2.3.5 Functional assays

The effect of Homoharringtonine on hPAECs function was assessed through apoptosis, cell viability and proliferation assays. These assays were chosen as they investigate functions which are known to be impacted in PAH. The cell viability assay (Cell Titre) is used as a control against apoptotic activity (Caspase 3/7) so that higher/lower results due to higher/lower cell numbers can be identified. Each experiment included 3 technical replicates for each condition tested. Averages from 3 experiments were used to perform unpaired, one-way student's t-test using GraphPad Prism (version 8.0.2, GraphPad Software, San Diego, California, USA) comparing vehicle controls (DMSO) and compound exposure groups.

2.3.5.1 Caspase 3/7 assay

To assess cell apoptosis, the Caspase-Glo 3/7 assay (Promega) was performed according to the manufacturer's instructions. This assay measures cellular levels of both caspase-3 and caspase-7, key components of the cellular apoptotic machinery through their roles in DNA fragmentation and loss of cellular viability. Therefore, levels of Caspase-3/7 serve as a readout of apoptotic activity. hPAECs (PromoCell or Sciencell) were plated in EGM2 (10% FBS) in 96-well plates at 20,000/well and allowed to grow for 24h. Following this, cells were washed with PBS and medium was changed to EGM2 (2% FBS). hPAECS were then exposed to Homoharringtonine (see details on Methods 2.3.3) or vehicle (DMSO) and TNF-α [10ng/ml] or vehicle (PBS) for 24 hours. After that period, blank wells were created and the caspase assay was performed.

2.3.5.2 CellTitre-Glo assay

To assess viability of cells, the CellTitre-Glo cell viability kit (Promega) was used according to the manufacturer's instructions. This assay measures ATP as an indicator of cell viability and produces a luminescent readout. hPAECs (PromoCell or Sciencell) were plated in EGM2 (10% FBS) in 96-well plates at 20,000/well and allowed to grow for 24h. Following this, cells were washed with PBS and medium was changed to EGM2 (2% FBS). hPAECS were then exposed to Homoharringtonine (see details on Methods 2.3.3) or vehicle (DMSO) and TNF-α [10ng/mL] or vehicle (PBS) for 24 hours. After that period, blank wells were created and the CellTitre-Glo assay was performed.

2.3.5.3 MTT assay

To further assess cell viability, an MTT assay was used. This colorimetric assay measures cellular metabolism to give a readout on cell viability and proliferation. In the reaction, yellow tetrazolium salt (MTT) is converted to purple formazan crystals by metabolically active cells. These crystals are then dissolved and the change in colour measured on a plate reader. Here, hPAECs (PromoCell or Sciencell) were plated in EGM2 (10% FBS) in 96-well plates at 20,000/well and allowed to grow overnight. Cells were then washed with PBS and medium was changed to EGM2 (0.2% FBS). Following this, hPAECS were exposed to Homoharringtonine (see details on Methods 2.3.3) or vehicle (DMSO) and VEGF [100ng/ml] or vehicle (PBS) for 24 hours. On the day of the MTT, medium was changed to EGM2 (10% FBS) and 10µL of MTT [5mg/mL] reagent was added to each well and cells were incubated for 4 hours. Blank wells were also created. Following this, 100µL of MTT detergent (94.65% isopropanol, 5% NP40, 0.35% HCL [1M]) was added to each well and the plate shaken for 10 minutes. A plate reader was used to test absorbance at 570nM.

3 - Whole Blood RNAseq of PAH Patients and Healthy Controls: Development of a PAH RNA Model Associated with Clinical Outcome

3.1 Introduction

Pulmonary arterial hypertension (PAH) is a very complex disorder with unclear pathogenesis, where genetic predisposition is not sufficient for disease development. Patient responses to treatment and general disease progression vastly differ between PAH patients (see details on Introduction 1.3), so it is essential to factor in disease heterogeneity to find better predictors of clinical outcome and tools to inform drug selection. Following this research process has the further benefit of an added potential to find other pathogenic elements triggering PAH development.

A prominent technology with great potential for better risk stratification and more personalised treatment selection is that of molecular profiling through combined omics (see details on Introduction 1.4). Molecular profiling results in greater granularity (i.e., greater level of detail in profiling) when characterising PAH patients than that of current clinical guidelines. Moreover, molecular profiling could provide valuable insights into pathologic molecular pathways that have not yet been addressed in research or for therapeutic purposes (164,165).

Transcriptomics is the study and characterisation of gene expression profiles. Analysis of differential gene expression between patients and relevant controls is a very powerful tool when trying to understand the underlying mechanisms of a disease, stratify clinical phenotypes or assess risk (182). RNA sequencing assays (RNAseq) are a potent device for transcriptome profiling. They allow for a thorough characterisation of gene expression profiles in tissue samples. For this study, we used a whole blood RNAseq analysis, since this type of “liquid biopsy” can easily be performed sequentially and it carries less risk than the alternative lung biopsy. Whole blood RNAseq also has the benefit of allowing for research onto PAH changes in immune processes recently highlighted by the literature, since the cells being sequenced are PBMCs (234).

The purpose of this PAH RNAseq study was to identify molecular pathways linked to PAH and test their association with disease heterogeneity, clinical features and pathogenesis. These include metrics of disease severity and progression, survival, responsiveness to vasodilator therapy and genetic background. Gene expression profiles were generated for a study cohort of 359 PAH patients with idiopathic, heritable or drug induced forms of PAH from the UK PAH Cohort study, as well as 72 age- and sex-matched healthy volunteers without any cardiac or respiratory disease as controls (see details on Methods 2.1.1).

Whole blood RNAseq is a technique which studies gene expression levels in white blood cells (WBC) from study subjects. WBC numbers vary greatly from subject to subject, especially under diseased conditions where the immune system may be affected or there may be an inflammatory response (235). This, compounded with the different gene expression profiles across different WBC types (236), results in a potential confounding factor which must be accounted for in this kind of analysis (222,225).

Predictions of WBC fraction profile estimates were therefore used in this RNAseq analysis to account for variable WBC numbers potentially impacting gene expression levels across different samples. These predictions were calculated by using two different computational approaches, then validated and used as covariates in subsequent analyses (see details on Methods 2.1.3).

Gene expression differences were identified and validated in two independent groups of 120 PAH patients and 24 healthy controls. Differentially expressed genes were then put forward for the generation of a PAH predictive model which was tested on a third group of 119 PAH patients and 24 healthy controls. Model scores were found to be associated with patient survival and other metrics of disease severity.

The work carried out in this thesis was, at the time it was performed, the first ever RNAseq analysis on PBMCs from PAH patients. As discussed in earlier sections, there have been multiple prior PH transcriptomic studies of a relatively smaller size conducted on either white blood cells from peripheral blood or lung tissue biopsies (see details on Introduction 1.4.3 and 1.4.4). In order to further validate results from the RNAseq described here, the identified PAH RNA signature was externally validated using two of these prior studies, one performed using white blood cells (237) and the other using lung tissue (184).

Genetic variants associated with different levels of gene expression (eQTLs) in genes found in this study to be associated with PAH were found to be elevated in PAH patients. This would suggest they could in fact be implicated in PAH pathogenesis.

Metabolomics is another area of research within the larger omics family where the study of substrates and products of metabolism is used to characterise subjects. For this study, previous work carried out by other members of the Rhodes lab was used to perform clustering analysis combining available transcriptomics and metabolomics data, testing the power of multi-omics as a more advanced diagnostic tool.

3.2 Hypotheses

- There is an RNA signature in PAH distinguishing patients from healthy controls.
- This RNA signature is associated with clinical features and disease progression.
- A subset of these RNAs are involved in the pathogenesis of PAH.

3.3 Aims

- To identify and optimise blood RNA profiles associated with PAH.
- To develop a model for PAH based on the identified RNA profiles.
- To use the model to further characterise the association of the RNA signature with clinical features such as mortality, functional class and levels of cardiac biomarkers.
- To find evidence of potential pathogenic gene/pathway dysregulations.
- To test combined transcriptomic and metabolomic data and create an omics diagnostic panel.

3.4 Methods

3.4.1 Study design

Three equally sized independent groups of PAH patients and healthy controls were randomly generated for this RNAseq study. Study subjects included 359 consecutively recruited PAH patients from the UK National Cohort study of PAH and 72 age- and sex-matched healthy volunteers from the same study as controls. The three independent groups were RNA Discovery (n_{PAH}= 120, $n_{controls}$= 24), RNA Validation (n_{PAH}= 120, $n_{controls}$= 24) and Model Testing (n_{PAH}= 119, $n_{controls}$= 24). The first two groups were analysed separately for RNA discovery and RNA validation and then combined for LASSO modelling of the best combination of RNAs to distinguish between controls and PAH. The LASSO model was tested in the Model Testing group. Analyses of clinical features were performed with all subjects combined into PAH and control groups (Figure 3.1).

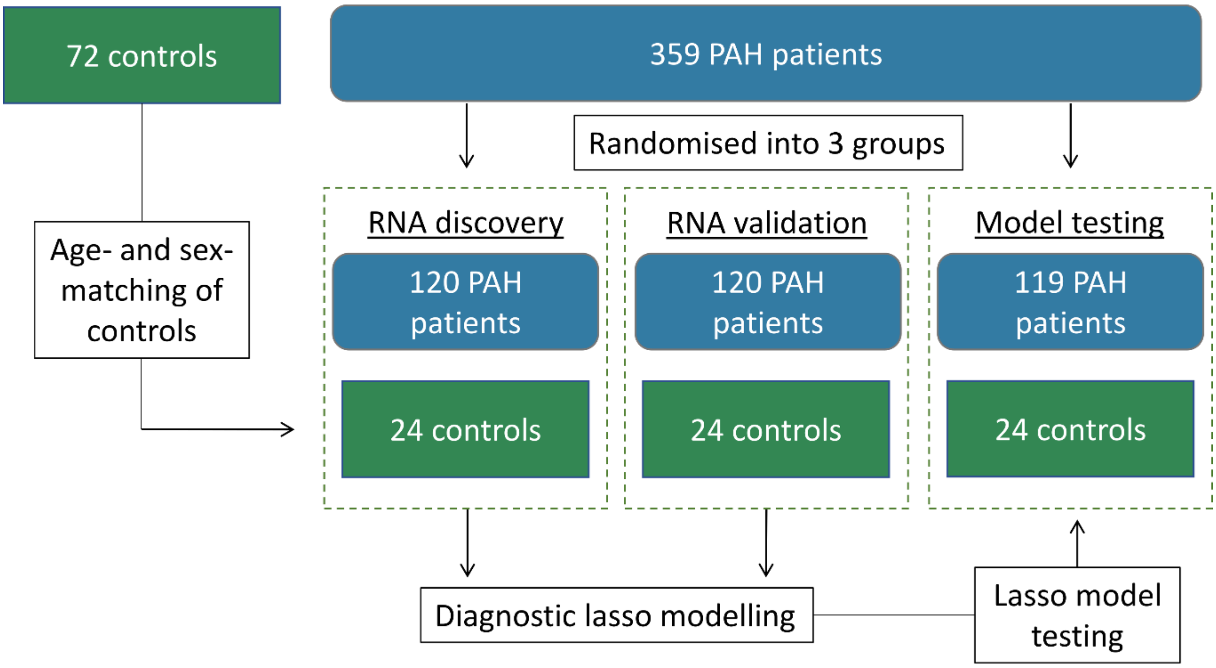

Figure 3.1: Study design for whole blood PAH RNAseq analysis.

3.5 Results

3.5.1 RNAseq white blood cell fraction deconvolution

White blood cell (WBC) fraction variability in whole blood samples represents a key accuracy issue that must be addressed in RNAseq assays such as the present one. For this analysis, there was clinical data on blood cell fractions available only in a subset of PAH patients, so two different computational approaches were used for WBC profile prediction based on RNA signatures obtained from a preliminary RNAseq analysis (see details on Methods 2.1.3). WBC profile predictions from both approaches correlated (rho= 0.44-0.73) with the limited patient clinical data available (Table 3.1, Table 3.2 and Figure 3.2). Mann-Whitney U tests identified differences between healthy controls and PAH patients for 6 WBC fractions for each computational approach (Table 3.3). All 12 WBC fractions were subsequently included as covariates in a PAH logistic regression model.

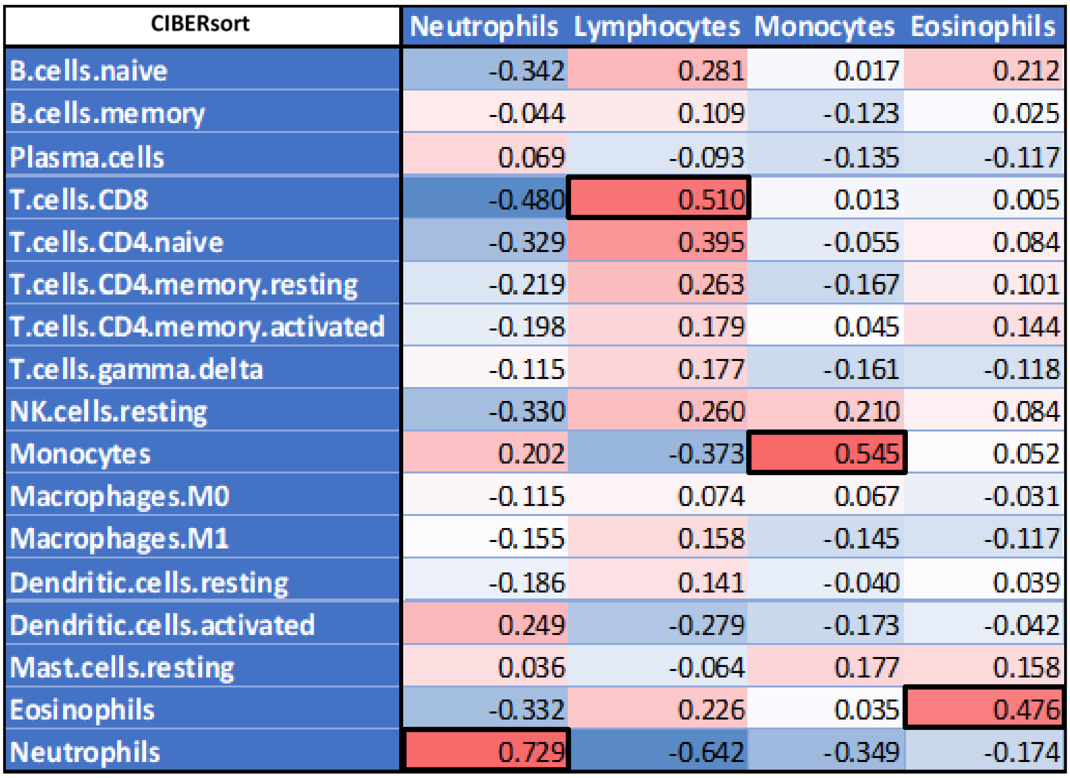

CIBERsort	Neutrophils	Lymphocytes	Monocytes	Eosinophils
B.cells.naive	-0.342	0.281	0.017	0.212
B.cells.memory	-0.044	0.109	-0.123	0.025
Plasma.cells	0.069	-0.093	-0.135	-0.117
T.cells.CD8	-0.480	0.510	0.013	0.005
T.cells.CD4.naive	-0.329	0.395	-0.055	0.084
T.cells.CD4.memory.resting	-0.219	0.263	-0.167	0.101
T.cells.CD4.memory.activated	-0.198	0.179	0.045	0.144
T.cells.gamma.delta	-0.115	0.177	-0.161	-0.118
NK.cells.resting	-0.330	0.260	0.210	0.084
Monocytes	0.202	-0.373	0.545	0.052
Macrophages.M0	-0.115	0.074	0.067	-0.031
Macrophages.M1	-0.155	0.158	-0.145	-0.117
Dendritic.cells.resting	-0.186	0.141	-0.040	0.039
Dendritic.cells.activated	0.249	-0.279	-0.173	-0.042
Mast.cells.resting	0.036	-0.064	0.177	0.158
Eosinophils	-0.332	0.226	0.035	0.476
Neutrophils	0.729	-0.642	-0.349	-0.174

Table 3.1: Correlation analysis of WBC fractions between CIBERsort and clinical data. Table shows rho values from correlation analysis. Highlighted boxes indicate matching WBC types. Colour coding represents correlation strength (red: strong positive correlation).

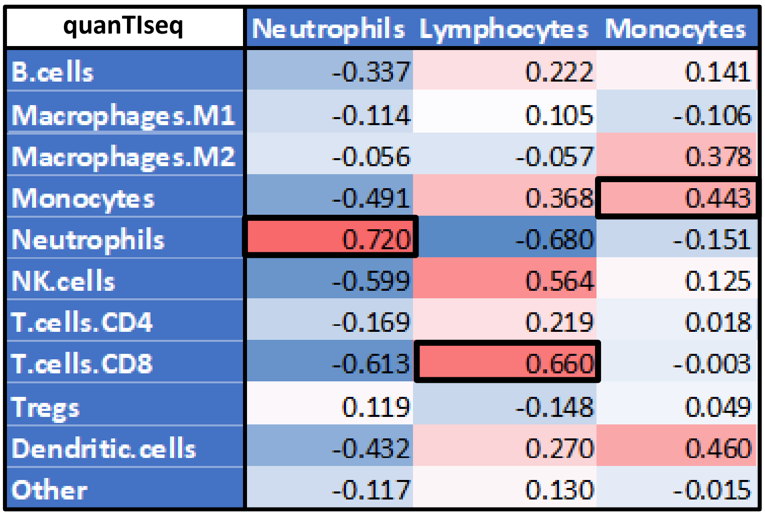

quanTIseq	Neutrophils	Lymphocytes	Monocytes
B.cells	-0.337	0.222	0.141
Macrophages.M1	-0.114	0.105	-0.106
Macrophages.M2	-0.056	-0.057	0.378
Monocytes	-0.491	0.368	0.443
Neutrophils	0.720	-0.680	-0.151
NK.cells	-0.599	0.564	0.125
T.cells.CD4	-0.169	0.219	0.018
T.cells.CD8	-0.613	0.660	-0.003
Tregs	0.119	-0.148	0.049
Dendritic.cells	-0.432	0.270	0.460
Other	-0.117	0.130	-0.015

Table 3.2: Correlation analysis of WBC fractions between quanTIseq and clinical data. Table shows rho values from correlation analysis. Highlighted boxes indicate matching WBC types. Colour coding represents correlation strength (red: strong positive correlation).

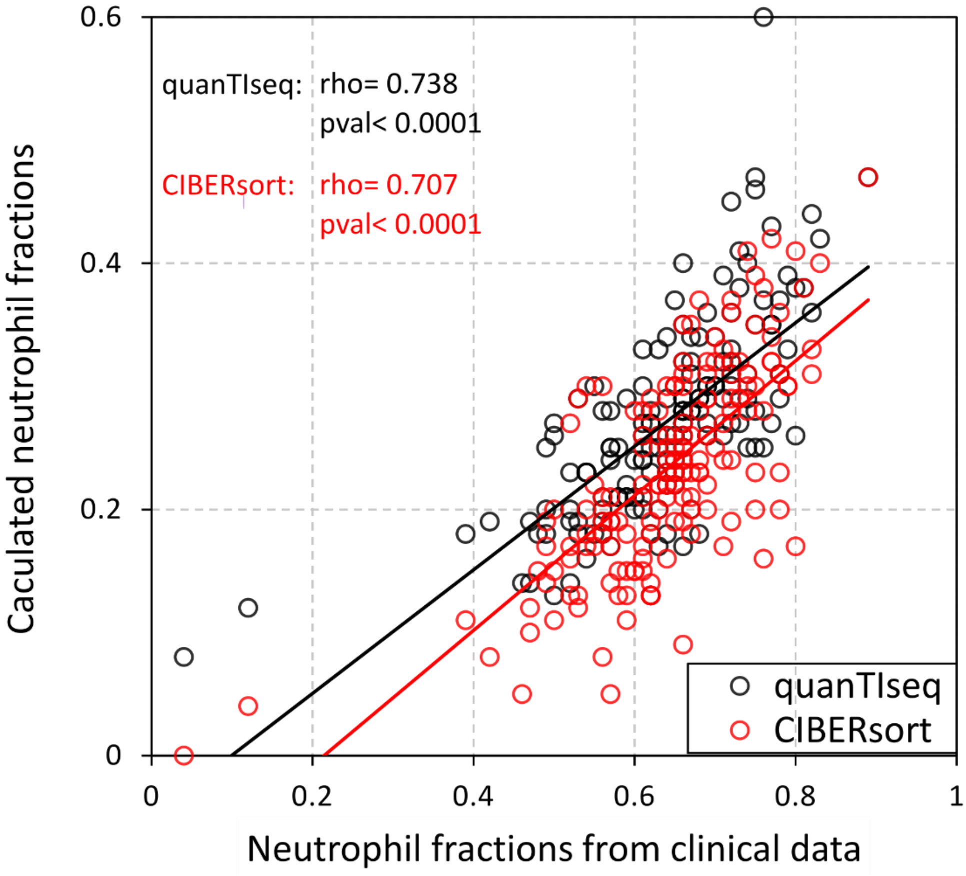

Figure 3.2: Correlation between predicted neutrophil fractions and clinical data. Scatter plot of calculated neutrophil WBC fractions by RNAseq deconvolution methods quanTIseq (black) and CIBERsort (red) in PAH patients where clinical measurements were also available.

White cell fractions predicted by QuanTIseq

	White cell fractions Means, Controls	Standard dev . Controls	Variance Controls	White cell fractions Means, PAH	Standard dev. PAH	Variance PAH	Sig. MW-U test	FDR-adjusted q value
Tregs	0.110	0.080	0.725	0.172	0.099	0.575	1.26x10^{-08}	**1.26x10^{-07}**
T cells CD4	0.039	0.046	1.173	0.018	0.035	1.932	4.58x10^{-05}	**2.00x10^{-04}**
Monocytes	0.007	0.010	1.460	0.004	0.009	2.167	2.21x10^{-04}	**7.00x10^{-04}**
Neutrophils	0.249	0.097	0.391	0.280	0.079	0.281	5.02x10^{-04}	**1.30x10^{-03}**
T cells CD8	0.070	0.039	0.554	0.057	0.032	0.569	4.28x10^{-03}	**8.60x10^{-03}**
NK cells	0.026	0.012	0.452	0.024	0.015	0.632	0.0252	**0.0420**
Macrophages M1	0.000	0.000	3.118	0.000	0.001	5.492	0.1694	0.2420
Macrophages M2	0.022	0.007	0.322	0.021	0.008	0.356	0.3685	0.4606
Dendritic cells	0.009	0.007	0.790	0.010	0.010	0.942	0.4444	0.4938
B cells	0.031	0.012	0.394	0.031	0.016	0.504	0.7967	0.7967

White cell fractions predicted by CIBERsort

	White cell fractions Means, Controls	Standard dev. Controls	Variance Controls	White cell fractions Means, PAH	Standard dev. PAH	Variance PAH	Sig. MW-U test	FDR-adjusted q value
T cells CD4 naive	0.178	0.054	0.302	0.145	0.047	0.326	1.28x10-6	**2.30x10^{-05}**
Neutrophils	0.202	0.108	0.534	0.252	0.091	0.362	2.30x10-5	**2.00x10^{-04}**
B cells memory	0.022	0.017	0.757	0.015	0.016	1.050	2.23x10-4	**1.30x10^{-03}**
Mast cells resting	0.017	0.009	0.498	0.020	0.009	0.422	3.07x10-3	**0.0138**
Dendritic cells resting	<0.001	0.001	3.814	<0.001	<0.001	7.905	4.00x10-3	**0.0144**
T cells CD4 memory resting	0.124	0.048	0.387	0.107	0.038	0.357	0.0138	**0.0413**
Macrophages M1	<0.001	<0.001	6.368	<0.001	<0.001	18.947	0.0206	0.0531
Macrophages M0	0.003	0.008	2.236	0.002	0.004	2.471	0.0432	0.0973
Monocytes	0.310	0.060	0.194	0.325	0.064	0.197	0.0986	0.1971
Eosinophils	0.004	0.007	1.734	0.003	0.006	2.465	0.1181	0.2126
T cells gamma delta	0.004	0.011	2.454	0.003	0.009	3.655	0.1840	0.3010
NK cells activated	<0.001	<0.001	8.485	<0.001	<0.001	18.947	0.2095	0.3143
NK cells resting	0.054	0.023	0.424	0.052	0.025	0.480	0.2640	0.3655
T cells CD4 memory active	0.026	0.010	0.386	0.025	0.013	0.521	0.3224	0.4027
T cells CD8	0.032	0.041	1.314	0.029	0.040	1.407	0.3356	0.4027
Dendritic cells activated	0.004	0.002	0.568	0.004	0.002	0.585	0.4507	0.5071
Plasma cells	0.006	0.005	0.803	0.007	0.008	1.147	0.5664	0.5997
B cells naive	0.013	0.020	1.482	0.013	0.017	1.364	0.8277	0.8277

Table 3.3: Deconvoluted white blood cell fractions show differences between healthy controls and PAH patients. Mann Whitney U tests were conducted comparing WBC fractions in healthy controls against PAH patients. Q-values produced from FDR-correction of p-values. Highlighted are WBC fractions found to be significantly different. Genes sorted by FDR-corrected significance (weakest q-value). Sig: significance.

5 out of the 12 WBC fractions found to be different between healthy controls and PAH patients were identified by the PAH logistic regression model as able to independently differentiate between healthy controls and PAH patients. These were CD4+ T cells and regulatory T cells (Tregs) estimated by quanTIseq and resting mast cells, memory B cells and naïve CD4+ T cells estimated by CIBERsort. While resting dendritic cells were not able to independently differentiate between healthy controls and PAH patients (p= 0.113), their inclusion in the model increased its performance and it was ultimately decided to include them in downstream analyses. (Table 3.4). These WBC profiles were subsequently included as covariates in secondary differential gene expression analyses.

Coefficients:	Estimate	Std. Error	Significance (p)
(Intercept)	1.263	0.572	2.72×10^{-02}
CIBERsort T cells, CD4, naive	-11.033	2.850	1.00×10^{-04}
CIBERsort B cells, memory	-14.201	6.167	2.13×10^{-02}
CIBERsort Mast cells, resting	27.531	13.545	4.21×10^{-02}
CIBERsort Dendritic cells, resting	-391.501	246.855	1.13×10^{-01}
quanTIseq Tregs	7.136	1.734	3.90×10^{-05}
quanTIseq T cells, CD4	8.229	3.993	3.93×10^{-02}

Table 3.4: Logistic regression model of white blood cell fractions which differentiate PAH versus healthy controls. These WBC fractions were included as covariates in secondary differential gene expression analyses. Std: standard.

3.5.2 Identification of differentially expressed RNAs in PAH patients

Independent differential gene expression analyses were carried out in both RNA Discovery and RNA Validation groups. From these analyses, 507 genes were selected (Figure 3.3, Table 3.5 and Supplementary Table 1) based on significance (p< 0.05) and directional consistency in both RNA Discovery and RNA Validation groups (Figure 3.4), overlap before and after accounting for WBC fractions, and significance in the combined analysis (FDR α< 0.1; based on all detected genes; Table 3.5 and Supplementary Table 1; see details on Methods 2.1.4).

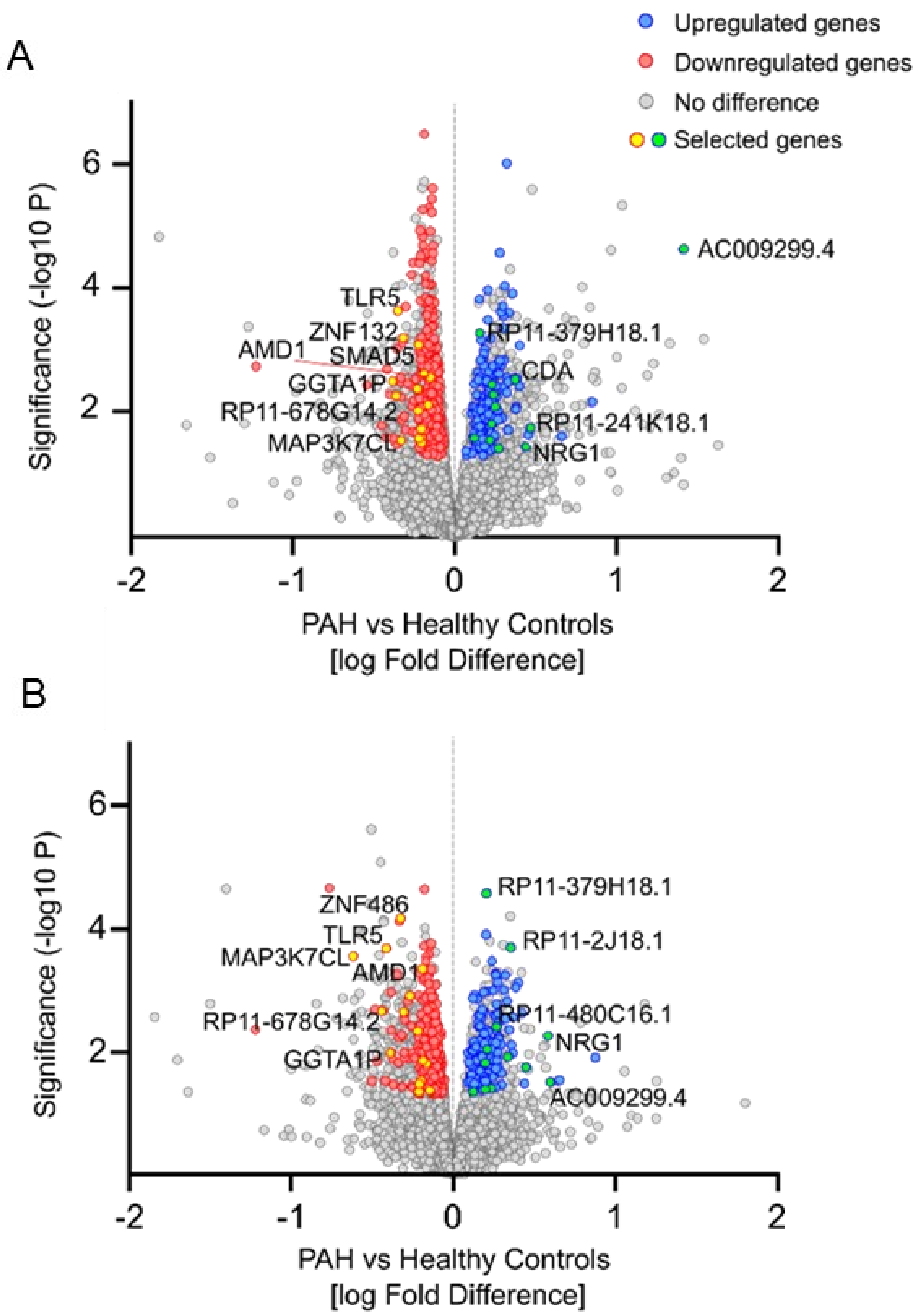

Figure 3.3: Differential expression analyses in whole blood PAH RNAseq independent groups. Volcano plots showing log fold changes of differentially expressed ($p < 0.05$) and directionally consistent (between Discovery and Validation groups) genes between PAH patients (n= 120) and healthy controls (n= 24) in the A) RNA Discovery and B) RNA Validation groups when including WBC fractions as covariates. Highlighted genes include those identified by downstream analyses presented in this manuscript, such as PAH RNA LASSO modelling, Mendelian randomisation and external dataset validation.

	RNA Discovery		RNA Validation		Combined Discovery and Validation		
GeneName	**logFC A**	**Sig. A**	**logFC B**	**Sig. B**	**logFC AB**	**Sig. AB**	**FDR q AB**
RSRC2	-0.188	3.00x10^{-07}	-0.110	8.64x10^{-04}	-0.142	4.85x10^{-09}	4.37x10^{-05}
PTAR1	-0.197	5.01x10^{-06}	-0.140	1.10x10^{-03}	-0.164	3.16x10^{-08}	1.90x10^{-04}
RP11-379H18.1	0.155	5.00x10^{-04}	0.209	2.88x10^{-05}	0.177	5.20x10^{-08}	2.34x10^{-04}
C1orf27	-0.196	1.39x10^{-05}	-0.158	1.23x10^{-03}	-0.175	8.08x10^{-08}	2.91x10^{-04}
AP004289.1	0.321	9.03x10^{-07}	0.202	4.61x10^{-03}	0.255	1.26x10^{-07}	3.16x10^{-04}
BTAF1	-0.192	2.75x10^{-05}	-0.130	1.26x10^{-03}	-0.157	1.76x10^{-07}	3.16x10^{-04}
TEX10	-0.141	5.52x10^{-06}	-0.087	5.53x10^{-03}	-0.113	1.39x10^{-07}	3.16x10^{-04}
TLR5	-0.349	2.18x10^{-04}	-0.410	2.23x10^{-04}	-0.368	1.49x10^{-07}	3.16x10^{-04}
ARFGAP3	-0.160	1.93x10^{-04}	-0.150	6.01x10^{-04}	-0.155	2.69x10^{-07}	3.24x10^{-04}
HLTF	-0.212	1.08x10^{-05}	-0.150	5.06x10^{-03}	-0.179	2.70x10^{-07}	3.24x10^{-04}
RBM27	-0.136	6.00x10^{-04}	-0.135	4.90x10^{-04}	-0.140	2.08x10^{-07}	3.24x10^{-04}
SAMD8	-0.125	2.76x10^{-03}	-0.177	2.46x10^{-05}	-0.149	2.23x10^{-07}	3.24x10^{-04}
SCYL3	-0.142	3.37x10^{-06}	-0.085	1.11x10^{-02}	-0.113	2.36x10^{-07}	3.24x10^{-04}
SCFD2	-0.257	3.63x10^{-05}	-0.211	5.53x10^{-04}	-0.227	2.99x10^{-07}	3.37x10^{-04}
ZNF211	-0.182	7.91x10^{-05}	-0.154	6.68x10^{-04}	-0.163	3.26x10^{-07}	3.45x10^{-04}
DDX17	-0.159	4.61x10^{-06}	-0.083	1.34x10^{-02}	-0.118	3.68x10^{-07}	3.68x10^{-04}
AL844908.5	-0.300	1.86x10^{-04}	-0.280	1.62x10^{-03}	-0.297	4.76x10^{-07}	4.29x10^{-04}
RALA	0.160	1.36x10^{-03}	0.204	1.33x10^{-04}	0.181	5.22x10^{-07}	4.48x10^{-04}
PTEN	-0.181	1.32x10^{-04}	-0.176	6.67x10^{-04}	-0.171	5.73x10^{-07}	4.69x10^{-04}
CCNB1IP1	-0.148	9.46x10^{-04}	-0.150	2.80x10^{-04}	-0.149	6.17x10^{-07}	4.84x10^{-04}
AP000240.5	0.324	2.64x10^{-03}	0.400	8.03x10^{-04}	0.389	6.86x10^{-07}	5.15x10^{-04}
RBM5	-0.137	2.28x10^{-06}	-0.062	4.48x10^{-02}	-0.101	7.51x10^{-07}	5.41x10^{-04}
KCNQ1OT1	0.152	1.41x10^{-04}	0.132	1.26x10^{-03}	0.140	9.24x10^{-07}	6.17x10^{-04}
ZNF224	-0.135	2.53x10^{-05}	-0.090	9.32x10^{-03}	-0.112	9.08x10^{-07}	6.17x10^{-04}
RP11-138A9.2	0.223	6.17x10^{-04}	0.238	3.59x10^{-04}	0.225	1.08x10^{-06}	6.72x10^{-04}
ZFAND1	-0.151	8.35x10^{-04}	-0.167	3.08x10^{-04}	-0.157	1.06x10^{-06}	6.72x10^{-04}
AC010746.2	0.206	3.04x10^{-04}	0.213	1.10x10^{-03}	0.207	1.33x10^{-06}	8.01x10^{-04}
CCDC186	-0.153	1.45x10^{-04}	-0.109	6.54x10^{-03}	-0.132	1.52x10^{-06}	8.24x10^{-04}
CHD9	-0.157	3.20x10^{-04}	-0.178	2.04x10^{-04}	-0.155	1.49x10^{-06}	8.24x10^{-04}
RASA2	-0.145	2.57x10^{-04}	-0.113	7.17x10^{-03}	-0.135	1.56x10^{-06}	8.24x10^{-04}
UBR1	-0.150	1.13x10^{-05}	-0.089	1.01x10^{-02}	-0.114	1.52x10^{-06}	8.24x10^{-04}
ZNF141	-0.159	1.49x10^{-04}	-0.110	2.62x10^{-03}	-0.130	1.64x10^{-06}	8.46x10^{-04}
AC009299.4	1.414	2.20x10^{-05}	0.600	3.22x10^{-02}	1.048	1.74x10^{-06}	8.69x10^{-04}
ARHGAP12	-0.195	1.89x10^{-05}	-0.099	3.39x10^{-02}	-0.151	1.84x10^{-06}	8.78x10^{-04}
ZNF486	-0.229	3.96x10^{-03}	-0.321	7.27x10^{-05}	-0.266	1.85x10^{-06}	8.78x10^{-04}
BCLAF1	-0.166	3.01x10^{-05}	-0.092	1.53x10^{-02}	-0.127	2.00x10^{-06}	9.25x10^{-04}
SMARCD2	-0.158	8.08x10^{-05}	-0.114	5.20x10^{-03}	-0.132	2.23x10^{-06}	1.00x10^{-03}
RP11-158K1.3	-0.160	5.37x10^{-04}	-0.138	3.47x10^{-03}	-0.151	2.30x10^{-06}	1.01x10^{-03}
DENND4C	-0.176	2.52x10^{-05}	-0.094	1.63x10^{-02}	-0.132	2.48x10^{-06}	1.04x10^{-03}
RP11-154H23.1	0.279	2.47x10^{-05}	0.172	1.24x10^{-02}	0.221	2.48x10^{-06}	1.04x10^{-03}

Table 3.5: Top dysregulated RNAs in whole blood PAH RNAseq. List of 40 genes most significantly associated with PAH from 507 gene list of differentially expressed, overlapping and directionally consistent genes in differential expression analysis in the RNA Discovery and RNA Validation groups. $N_{controls}$= 24 per group; N_{PAH}= 120 per group. Genes listed by significance (lowest FDR q first). LogFC: log2 fold-change.

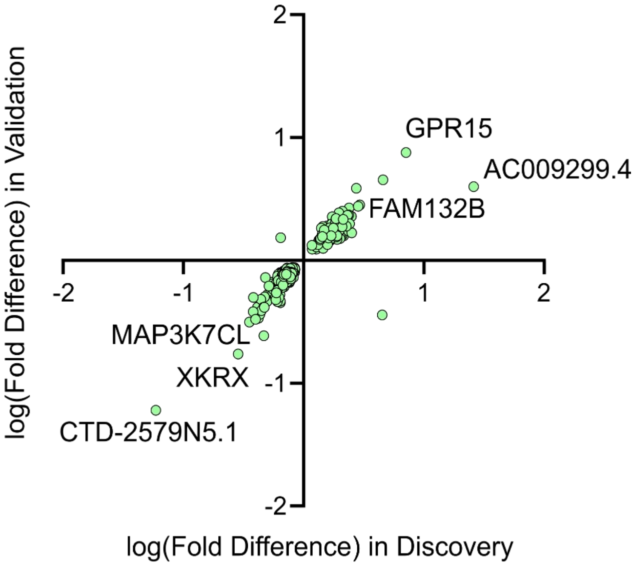

Figure 3.4: Directional consistence in differentially expressed genes from RNAseq across study groups. Scatter plot showing fold-differences in 509 RNAs reaching significance ($p<0.05$) in both RNA Discovery and RNA Validation group analyses. 507 directionally consistent genes were taken forward in the main analysis.

Included in the 507 gene list were RNAs from pathways known to be associated with PAH pathology. For instance, a downstream BMPR2 signalling mediator, the gene Mothers Against Decapentaplegic Homolog-5 (SMAD5; combined analysis FDR = $6.59\text{x}10^{-03}$; Supplementary Table 1), was reduced in PAH patients across all three study groups (Figure 3.5A). This reduction is consistent with evidence of BMP/TGF-β signalling impairment in PAH (see details on Introduction 1.3.6.1). SMAD5 is also one of two genes in the 507-gene PAH signature reaching significance in an MR analysis for PAH (see details on Chapter 3.5.8). The Transient Receptor Potential Cation channel (TRPC1; combined analysis FDR = $5.36\text{x}10^{-02}$; Supplementary Table 1), another gene where evidence of an association with PH development has been documented (98), was also downregulated in PAH patients across groups (Figure 3.5B). This gene plays an important metabolic role and was identified in previous metabolomic assays conducted in the Rhodes lab (see details on Chapter 3.5.9). It is also believed to play a role in hypoxia-induced PAH (see details on Chapter 3.6).

In order to assess the association between gene expression changes and PAH therapy exposure, a differential expression analysis was carried out evaluating exposure to the main current PAH therapies, namely ET-1 receptor antagonists, PDE5 inhibitors and prostanoids (see details on Introduction 1.3.5). Study subjects were divided into Discovery and Validation groups as in the original analysis and results were corrected using white blood cell profiles (see details on Methods 2.1.3 and Chapter 3.5.1) and 3 principal components. Differential expression in 7 genes was identified in PAH patients exposed to ET-1 receptor antagonists. In the case of patients treated with PDE5 inhibitors, the number of differentially expressed genes was 4. Finally, there were 50 genes differentially expressed in PAH patients exposed to prostanoids prior to sampling for the study (Table 3.6).

None of the genes associated with PAH therapies were part of the 507 gene list of transcripts associated with PAH diagnosis, indicating these therapies were not associated with changes in the genes most dysregulated by PAH pathology and potentially reflecting an independent mechanism of action with low impact on gene expression in white blood cells. Significantly dysregulated genes associated with vasodilator therapy were involved in pathways such as prostanoids biosynthesis, cell proliferation or platelet aggregation, which are in accordance with the expected effects of these therapies. It would be of interest to test whether these sets of genes may represent a signal of response to therapy or even for dosing.

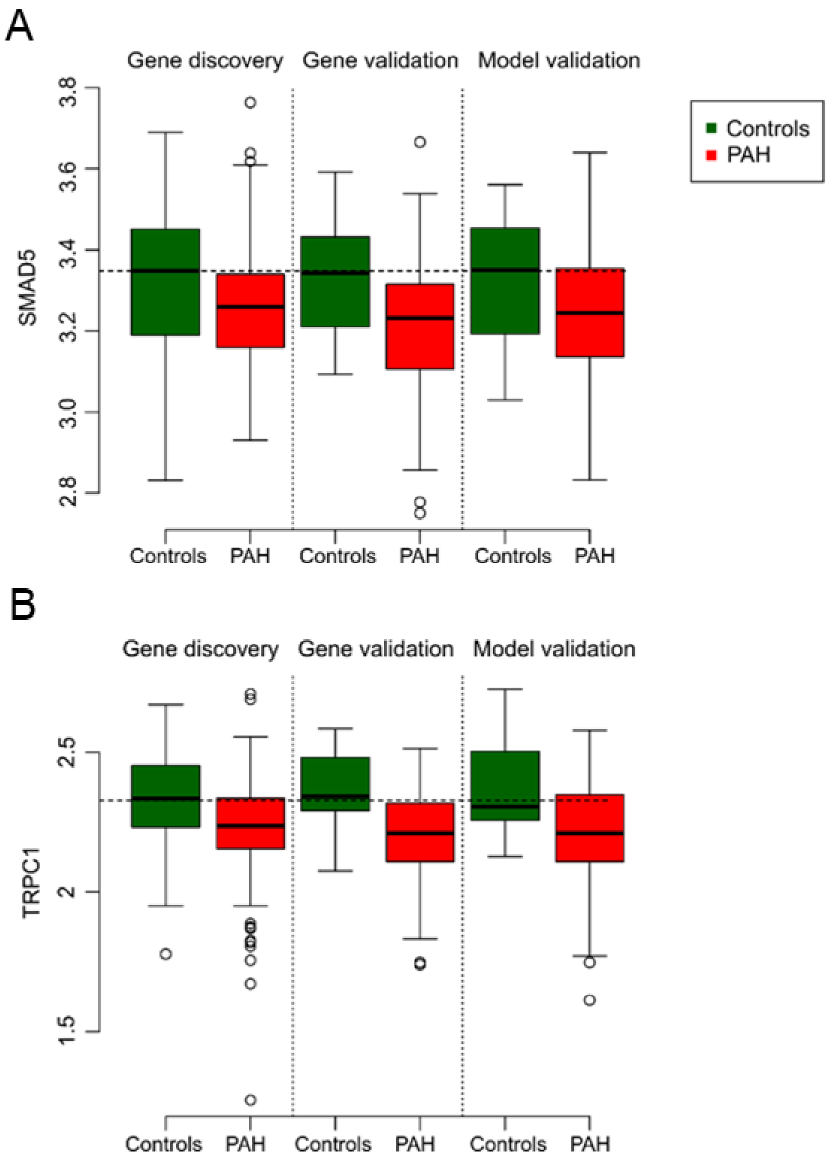

Figure 3.5: Levels of PAH-relevant genes in all whole blood PAH RNAseq independent groups. Boxplots showing log10 reads of A) SMAD5 B) TRPC1 in PAH patients (red) and healthy controls (green) across the RNA Discovery, RNA Validation and Model Testing groups. . $N_{controls}$= 24 per group; N_{PAH}= 119/120 per group

		Discovery		Validation		Combined		
Gene	**Drug class**	**logFC**	**Sig.**	**logFC**	**Sig.**	**logFC**	**Sig.**	**FDR**
RP5-857K21.6	PDE5 inhibitors	-2.529	1.77x10^{-05}	-0.845	3.61x10^{-02}	-1.887	2.47x10^{-07}	4.36x10^{-03}
PTGS2	PDE5 inhibitors	-0.442	2.42x10^{-03}	-0.254	4.66x10^{-03}	-0.378	9.34x10^{-06}	3.96x10^{-02}
FOS	PDE5 inhibitors	-0.595	1.01x10^{-03}	-0.355	1.12x10^{-03}	-0.465	1.12x10^{-05}	3.96x10^{-02}
MIDN	PDE5 inhibitors	-0.124	4.21x10^{-02}	-0.218	4.96x10^{-04}	-0.180	1.89x10^{-05}	5.57x10^{-02}
LRP12	ERAs	-1.332	4.01x10^{-04}	-0.692	6.91x10^{-03}	-1.651	2.42x10^{-10}	4.27x10^{-06}
EGR3	ERAs	1.144	2.68x10^{-04}	0.697	5.32x10^{-03}	1.046	2.36x10^{-06}	8.32x10^{-03}
PHGDH	ERAs	-0.389	2.74x10^{-04}	-0.284	5.42x10^{-03}	-0.332	4.41x10^{-06}	1.10x10^{-02}
RN7SKP71	ERAs	1.747	1.17x10^{-03}	1.465	2.52x10^{-03}	1.667	4.98x10^{-06}	1.10x10^{-02}
PCYOX1L	ERAs	-0.168	1.94x10^{-03}	-0.170	1.05x10^{-02}	-0.180	1.63x10^{-05}	2.88x10^{-02}
IGLV7-46	ERAs	-0.768	7.40x10^{-03}	-0.867	1.19x10^{-03}	-0.757	6.31x10^{-05}	9.24x10^{-02}
ANKUB1	ERAs	0.132	4.24x10^{-02}	0.223	9.17x10^{-05}	0.168	7.33x10^{-05}	9.24x10^{-02}
ACCSL	Prostanoids	1.024	1.81x10^{-05}	1.018	2.22x10^{-06}	0.967	2.35x10^{-10}	2.07x10^{-06}
VWF	Prostanoids	0.712	5.16x10^{-03}	1.143	5.07x10^{-06}	0.987	2.41x10^{-08}	1.42x10^{-04}
TPM4	Prostanoids	0.185	2.26x10^{-02}	0.457	1.36x10^{-07}	0.316	3.76x10^{-08}	1.66x10^{-04}
GCSAML	Prostanoids	0.404	2.13x10^{-04}	0.449	3.11x10^{-05}	0.400	7.49x10^{-08}	2.63x10^{-04}
NFIB	Prostanoids	0.537	3.89x10^{-03}	0.767	3.56x10^{-06}	0.649	8.93x10^{-08}	2.63x10^{-04}
TPM1	Prostanoids	0.296	3.54x10^{-03}	0.445	9.06x10^{-06}	0.361	1.15x10^{-07}	2.90x10^{-04}
ITGB3	Prostanoids	0.572	3.71x10^{-03}	0.753	9.06x10^{-05}	0.619	3.43x10^{-06}	4.65x10^{-03}
MSANTD3	Prostanoids	0.186	6.67x10^{-03}	0.305	6.84x10^{-05}	0.227	4.37x10^{-06}	5.51x10^{-03}
TDRP	Prostanoids	0.399	9.99x10^{-03}	0.542	1.93x10^{-04}	0.470	5.27x10^{-06}	6.02x10^{-03}
WRB	Prostanoids	0.290	7.14x10^{-03}	0.400	2.35x10^{-05}	0.315	5.45x10^{-06}	6.02x10^{-03}
SLC18A2	Prostanoids	0.256	1.61x10^{-02}	0.418	3.77x10^{-05}	0.319	6.37x10^{-06}	6.62x10^{-03}
RP11-354E11.2	Prostanoids	0.386	1.24x10^{-02}	0.544	2.26x10^{-05}	0.436	7.10x10^{-06}	6.97x10^{-03}
SERPINE2	Prostanoids	0.357	8.85x10^{-03}	0.546	7.06x10^{-05}	0.409	1.42x10^{-05}	1.32x10^{-02}
MGLL	Prostanoids	0.346	2.78x10^{-02}	0.581	6.30x10^{-05}	0.439	1.82x10^{-05}	1.53x10^{-02}
UBE2C	Prostanoids	0.502	3.77x10^{-04}	0.217	2.89x10^{-02}	0.369	1.99x10^{-05}	1.60x10^{-02}
CSRP1	Prostanoids	0.123	3.23x10^{-02}	0.256	2.13x10^{-04}	0.185	2.19x10^{-05}	1.65x10^{-02}
PRTFDC1	Prostanoids	0.312	2.47x10^{-02}	0.537	9.52x10^{-05}	0.397	2.47x10^{-05}	1.74x10^{-02}
PDLIM1	Prostanoids	0.234	4.71x10^{-02}	0.542	3.48x10^{-05}	0.359	2.85x10^{-05}	1.86x10^{-02}
IGF2BP3	Prostanoids	0.254	8.52x10^{-03}	0.312	2.17x10^{-03}	0.282	3.38x10^{-05}	2.06x10^{-02}
PF4	Prostanoids	0.443	2.19x10^{-03}	0.498	1.87x10^{-03}	0.436	3.69x10^{-05}	2.08x10^{-02}
C9orf16	Prostanoids	0.183	5.29x10^{-03}	0.189	2.87x10^{-03}	0.179	3.70x10^{-05}	2.08x10^{-02}
GP9	Prostanoids	0.521	4.25x10^{-04}	0.454	5.62x10^{-03}	0.444	3.78x10^{-05}	2.08x10^{-02}
ADRA2A	Prostanoids	0.666	4.86x10^{-04}	0.552	9.11x10^{-03}	0.572	3.92x10^{-05}	2.10x10^{-02}
PDE5A	Prostanoids	0.209	1.91x10^{-02}	0.313	1.62x10^{-04}	0.239	4.76x10^{-05}	2.41x10^{-02}
ZC3HAV1L	Prostanoids	0.220	1.20x10^{-02}	0.215	5.08x10^{-03}	0.225	4.77x10^{-05}	2.41x10^{-02}
ICA1	Prostanoids	0.211	1.13x10^{-02}	0.225	1.02x10^{-02}	0.235	5.91x10^{-05}	2.73x10^{-02}
DNM3	Prostanoids	0.326	7.84x10^{-03}	0.350	1.97x10^{-03}	0.329	6.04x10^{-05}	2.73x10^{-02}

P2RY1	Prostanoids	0.280	1.18x10^{-02}	0.352	3.53x10^{-03}	0.317	6.97x10^{-05}	3.07x10^{-02}
DGKI	Prostanoids	0.633	3.60x10^{-02}	1.028	2.07x10^{-05}	0.746	8.75x10^{-05}	3.59x10^{-02}
CAV2	Prostanoids	0.556	1.60x10^{-03}	0.428	6.85x10^{-03}	0.438	9.16x10^{-05}	3.59x10^{-02}
FAM69B	Prostanoids	0.278	3.99x10^{-02}	0.314	7.92x10^{-03}	0.335	1.11x10^{-04}	4.18x10^{-02}
LY6G6E	Prostanoids	0.393	2.52x10^{-02}	0.544	1.14x10^{-03}	0.448	1.22x10^{-04}	4.40x10^{-02}
MEST	Prostanoids	0.295	2.65x10^{-02}	0.492	2.41x10^{-04}	0.352	1.51x10^{-04}	4.77x10^{-02}
LYPD2	Prostanoids	-0.953	3.32x10^{-03}	-0.819	1.35x10^{-02}	-0.861	1.61x10^{-04}	4.97x10^{-02}
NDUFAF3	Prostanoids	0.141	1.16x10^{-02}	0.179	3.41x10^{-03}	0.148	1.66x10^{-04}	4.97x10^{-02}
C2orf88	Prostanoids	0.318	1.19x10^{-03}	0.219	2.52x10^{-02}	0.255	1.72x10^{-04}	5.06x10^{-02}
IGFBP2	Prostanoids	-0.696	2.69x10^{-02}	-0.667	1.30x10^{-02}	-0.750	2.17x10^{-04}	5.99x10^{-02}
LLNLF-96A1.1	Prostanoids	-2.363	1.28x10^{-02}	-2.141	5.41x10^{-03}	-2.206	2.21x10^{-04}	5.99x10^{-02}
RTKN2	Prostanoids	0.290	7.91x10^{-03}	0.285	4.35x10^{-03}	0.264	2.34x10^{-04}	6.20x10^{-02}
CENPM	Prostanoids	0.231	1.49x10^{-02}	0.207	1.65x10^{-02}	0.225	2.52x10^{-04}	6.55x10^{-02}
L1TD1	Prostanoids	-0.500	2.63x10^{-02}	-0.674	2.77x10^{-03}	-0.562	2.63x10^{-04}	6.63x10^{-02}
AC010970.2	Prostanoids	-1.755	4.99x10^{-02}	-2.698	3.72x10^{-04}	-2.064	3.14x10^{-04}	7.52x10^{-02}
CTTN	Prostanoids	0.344	1.25x10^{-02}	0.348	5.85x10^{-03}	0.325	3.15x10^{-04}	7.52x10^{-02}
ARHGEF18	Prostanoids	0.184	2.20x10^{-03}	0.101	4.59x10^{-02}	0.133	3.30x10^{-04}	7.66x10^{-02}
ZNF367	Prostanoids	0.190	1.66x10^{-02}	0.190	7.05x10^{-03}	0.182	4.21x10^{-04}	9.28x10^{-02}
RAB11A	Prostanoids	0.175	8.66x10^{-03}	0.183	1.34x10^{-02}	0.168	4.33x10^{-04}	9.42x10^{-02}
WASF3	Prostanoids	0.380	1.43x10^{-02}	0.375	1.69x10^{-02}	0.370	4.47x10^{-04}	9.42x10^{-02}
LGALSL	Prostanoids	0.289	3.39x10^{-02}	0.353	8.99x10^{-03}	0.329	4.54x10^{-04}	9.42x10^{-02}
LIMS1	Prostanoids	0.193	4.80x10^{-02}	0.339	9.70x10^{-04}	0.242	4.93x10^{-04}	9.85x10^{-02}
IGHV3-15	Prostanoids	0.555	8.48x10^{-03}	0.439	1.89x10^{-02}	0.484	4.99x10^{-04}	9.85x10^{-02}

Table 3.6: Association of main PAH therapies with gene expression levels. A differential expression analysis between PAH patients exposed or not exposed to PAH therapies was conducted in Discovery (N_{total}= 120) and Validation (N_{total}= 120) groups and then in the combined Discovery and Validation (N_{total}= 240). Genes meeting FDR (α< 0.01) in the combined analysis were included. Genes listed by associated PAH therapy and then by significance (weakest FDR first). ERAs: ET-1 receptor antagonists.

3.5.3 RNAseq validation through RT-qPCR of dysregulated genes

In order to technically validate RNAseq results it was decided to perform RT-qPCR in a subset of subjects from the model testing group including 11 controls and 36 PAH patients with either average or high RNAseq model scores (see details on Methods 2.1.5). The genes tested, namely TRPC1, SESN1, GRN, CCND3, NRG1, OLFM4, FBLN2 and SMAD5; were selected because of their pathobiological relevance to PAH and the strength of dysregulation observed in PAH patients (see details on Methods 2.1.5). The gene SPAST was selected to be used as control for this assay because of its biological role and its stability across RNAseq samples (see details on Methods 2.1.5).

Following analysis of RT-qPCR results, all measurements showed a significant correlation with RNAseq results ($p<0.05$, Spearman's rho = 0.3 - 0.89, Table 3.7).

Gene	P-value	Rho
NRG1	2.20×10^{-16}	**0.89**
OLFM4	2.20×10^{-16}	**0.88**
TRPC1	2.20×10^{-16}	**0.77**
FBLN2	1.63×10^{-07}	**0.71**
SESN1	2.69×10^{-06}	**0.64**
SMAD5	3.00×10^{-04}	**0.51**
GRN	0.004	**0.42**
SPAST	0.030	**0.32**
CCND3	0.041	**0.30**

Table 3.7: RT-qPCR validation of RNAseq results. Table shows correlation (rho) between RNAseq and RT-qPCR measurements of gene expression for a selection of genes found to be dysregulated in PAH patients in the RNAseq assay (from the 507 gene list). Genes were selected based on their PAH pathobiological relevance from literature. SPAST was used as control for its stability and cellular function.

3.5.4 PAH RNA LASSO model development and testing

LASSO analysis and modelling were used downstream of the differential expression analysis to generate a PAH RNA model able to effectively separate healthy controls from PAH patients (see details on Methods 2.1.6). RNA Discovery and RNA Validation groups were then combined and results for 48 healthy controls and 240 PAH patients were put forward for LASSO analysis. A LASSO regression model, utilising the combination of 25 RNAs best able to best discriminate between healthy controls and PAH patients, was then developed (Table 3.8). Following this, the Model Testing group (n_{PAH}= 119, $n_{controls}$= 24) was used as an independent validation set to test the LASSO model. It was found the model was able to significantly separate healthy controls from PAH patients ($p= 1.39 \times 10^{-8}$; Figure 3.6A). Receiver operating curve (ROC) analysis demonstrated an area under the curve (AUC) of 0.868 (95% CI: 0.791- 0.945; Figure 3.6B). The optimum cut-off for identifying PAH patients in the RNA Discovery and RNA Validation groups with the LASSO model (1.768) was able to identify 88.9% of patients with 72.2% specificity in the Model Testing group. Other modelling methods—alternative to LASSO—which could also be used to analyse this data will be later discussed in Chapter 3.6.

It is worth noting that, despite their aforementioned relevance for PAH pathology, SMAD5 and TRPC1 were not a part of the LASSO model, since the purpose of the model was not to prove causality, but rather to numerically show the value of the RNA signature for purposes such as a diagnostic tool.

VARIABLE	COEFFICIENT
(Intercept)	1.861
RP11-574K11.28	$7.81\text{x}10^{-04}$
RP11-2J18.1	$6.04\text{x}10^{-04}$
NRG1	$1.63\text{x}10^{-04}$
AC009299.4	$1.51\text{x}10^{-04}$
RP11-241K18.1	$1.51\text{x}10^{-04}$
RP11-480C16.1	$1.35\text{x}10^{-04}$
RP11-379H18.1	$1.05\text{x}10^{-04}$
RP4-534N18.4	$9.08\text{x}10^{-05}$
CTD-2192J16.20	$4.68\text{x}10^{-05}$
CPT1A	$3.20\text{x}10^{-05}$
ZFP36L2	$1.74\text{x}10^{-05}$
CDA	$3.87\text{x}10^{-06}$
CCND3	$-3.70\text{x}10^{-06}$
MAP3K7CL	$-1.10\text{x}10^{-05}$
ZNF486	$-1.50\text{x}10^{-05}$
RP11-678G14.2	$-2.80\text{x}10^{-05}$
ZNF763	$-5.40\text{x}10^{-05}$
GGTA1P	$-5.40\text{x}10^{-05}$
TLR5	$-5.90\text{x}10^{-05}$
FAM213A	$-8.20\text{x}10^{-05}$
ZNF132	$-9.20\text{x}10^{-05}$
TRIP10	$-3.20\text{x}10^{-04}$
RP4-751H13.6	$-3.40\text{x}10^{-04}$
B4GAT1	$-5.50\text{x}10^{-04}$
RP11-701H24.5	$-5.70\text{x}10^{-04}$

Table 3.8: 25 RNAs included in the PAH RNA LASSO model. Combination of 25 genes best able to distinguish between healthy controls and PAH patients. Selected by LASSO analysis of the combined RNA Discovery and RNA validation groups including 48 healthy controls and 240 PAH patients

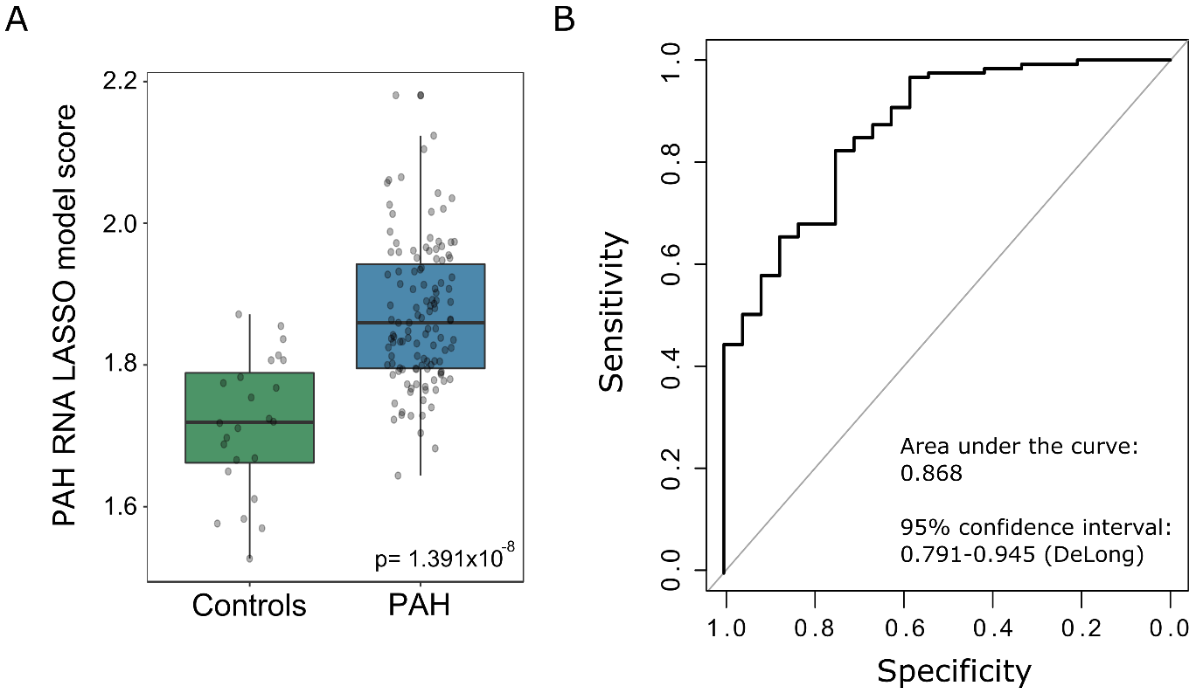

Figure 3.6: PAH RNA LASSO model performance in Model Testing group. A) Boxplot showing PAH RNA LASSO model scores for healthy controls (n=24) and PAH patients (n=119). **B**) Receiver operating curve (ROC) showing the performance of PAH RNA LASSO model scores for determining PAH status in the Model Testing group. p: p-value for Mann Whitney U test.

As a further validation for the PAH RNAseq LASSO model, 20 regression models for PAH diagnosis prediction were constructed on the Discovery and Validation groups based on random, non-repeating 25-gene sets from the list of 507 top differentially expressed genes in PAH. Performance of these 20 regression models was the tested on the Model Testing groups, following the study design used for the development and testing of the PAH RNAseq LASSO model in the main analysis. In contrast with the AUC of 0.868 for the PAH RNAseq LASSO model, the mean AUC for the 20 regression models was 0.679 (0.595 – 0.779), showing the PAH RNAseq LASSO model performed better at distinguishing PAH patients from healthy controls than all 20 regression models based on random 25-gene sets of PAH-associated genes (Figure 3.7).

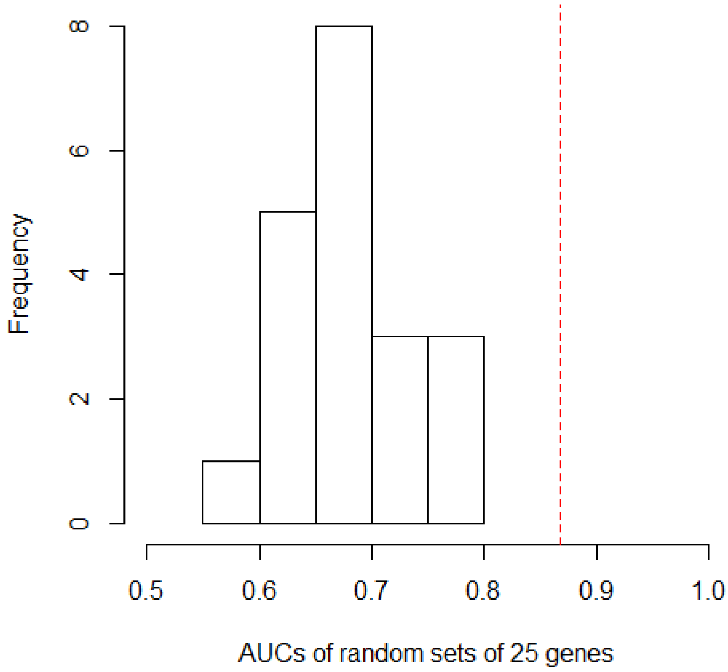

Figure 3.7: PAH RNAseq LASSO model performance comparison. The performance (AUC) when separating PAH patients from healthy controls of 20 regression models developed from random sets of 25 genes from the list of 507 PAH-associated genes (without repeating genes) is shown in the histogram. Red line indicates PAH RNAseq LASSO model performance (AUC= 0.868).

3.5.5 PAH RNA model association with PAH clinical features

3.5.5.1 PAH RNA model and survival

All 359 PAH patients were combined for the testing of the association between PAH RNA model scores and survival. This analysis yielded an optimum PAH RNA model score cut-off (1.910) separating surviving from non-surviving PAH patients (AUC= 0.704; Figure 3.8). This cut-off also separated PAH survivors from non-survivors in each of the three experimental groups (RNA Discovery, RNA Validation and Model Testing (Figure 3.9).

Downstream survival analysis was then performed and the optimum PAH RNA model score cut-off was used to separate PAH patients into low- and high-risk groups. These groups showed different survival patterns (p= $4.66x10^{-6}$), with PAH patients in the high-risk group performing poorly (Figure 3.10). A similar pattern was observed when independent survival analyses were performed in each of the three experimental groups (Figure 3.11).

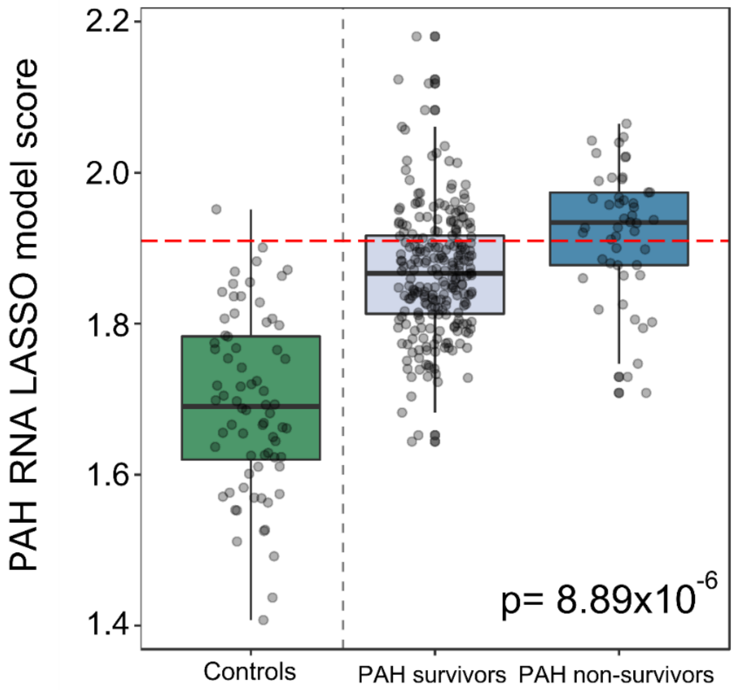

Figure 3.8: PAH RNA model scores and survival in all study subjects. Boxplot showing LASSO model score in healthy controls (n=72) and PAH patients (n=359) divided into survivors and non-survivors in follow-up assessments. Dashed line represents the cut-off to best distinguish surviving from non-surviving PAH patients.

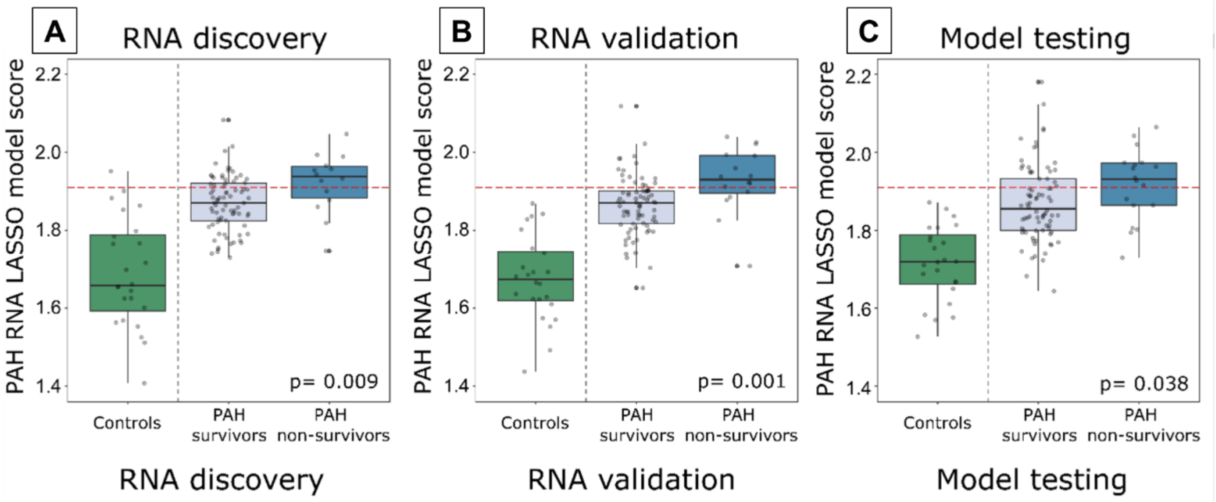

Figure 3.9: PAH RNA model scores and survival in differential expression analysis groups. Boxplot showing LASSO model scores in **A**) RNA Discovery, **B**) RNA Validation, **C**) Model Testing groups for healthy controls (n=24 per group) and PAH patients (n=120/120/119, respectively) divided into survivors and non-survivors in follow-up assessments. Dashed line represents the cut-off to best distinguish surviving from non-surviving PAH patients.

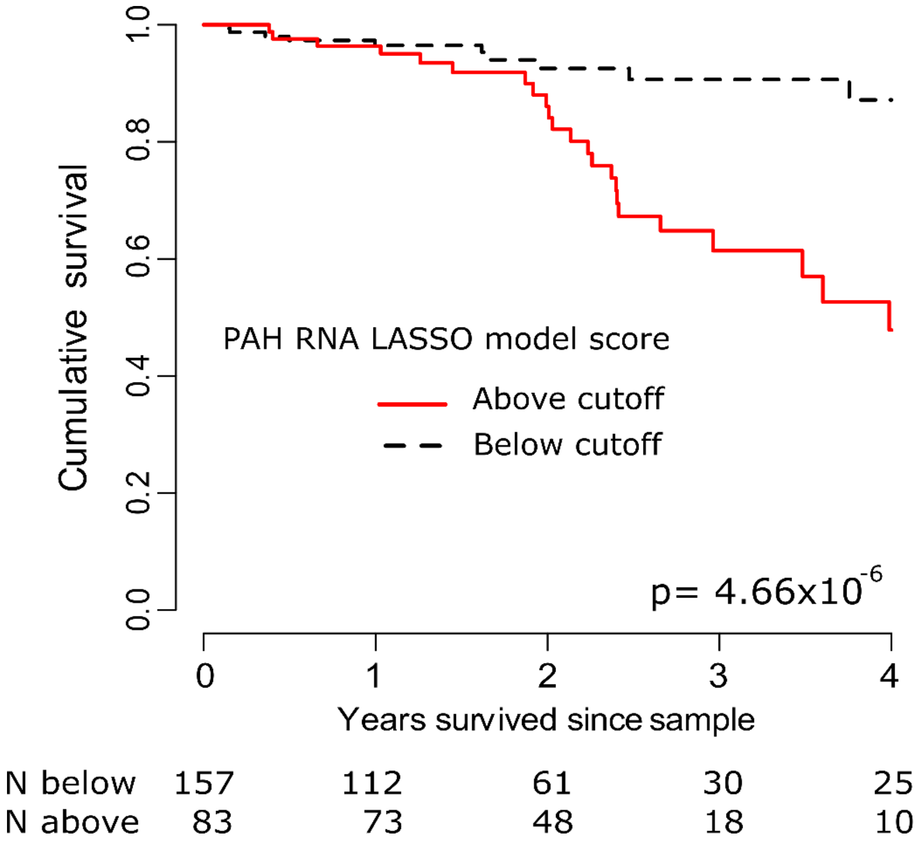

Figure 3.10: Combined PAH patients divided by survival in follow-up. Kaplan-Meier survival plot separating patients on basis of the best cut-off distinguish surviving from non-surviving PAH patients. Red line indicates higher score than cut-off and dashed black line not higher than cut-off.

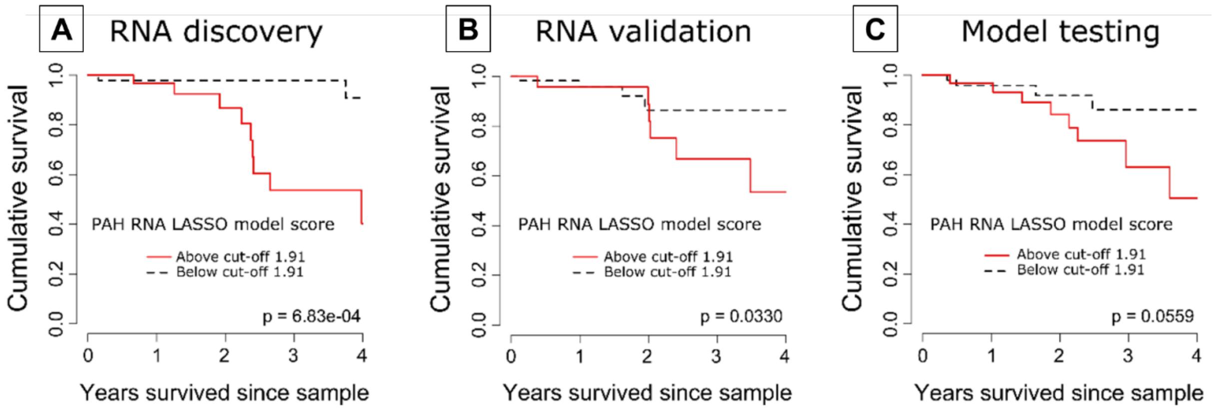

Figure 3.11: PAH patients divided by survival in follow-up by differential expression analysis groups. Kaplan-Meier survival plot separating patients on basis of the best cut-off distinguish surviving from non-surviving PAH patients in **A**) RNA Discovery, **B**) RNA Validation, **C**) Model Testing groups. Red lines indicate higher score than cut-off and dashed black lines not higher than cut-off.

All 25 RNAs in the diagnostic PAH RNA LASSO model were tested for association with mortality during follow-up to assess which were responsible for the association with survival in PAH patients. Following correction for multiple testing false discovery rate (FDR; α< 0.05), 4/25 RNAs from the model were found to be independently associated with survival in PAH patients, but optimal survival cut-offs only effectively distinguished between low- and high-risk patient groups for 3 of those transcripts. All 3 RNAs were intronic long non-coding transcripts, namely RP4-751H13.6/ATP6V0E2-AS1, RP4-534N18.4/AL136115.3/Lnc-PTP4A2-13 and RP11-701H24.5/lnc-SNRPN-1:6 ($p<0.05$; Figure 3.12 and Table 3.9). Neuregulin-1 (NRG1), the other transcript significantly associated with survival in PAH, is a cardioactive growth factor released from ECs that plays a cardioprotective role through EC-cardiomyocyte interactions. It induces cell proliferation, differentiation and survival in several cell types, including cardiomyocytes (238,239).

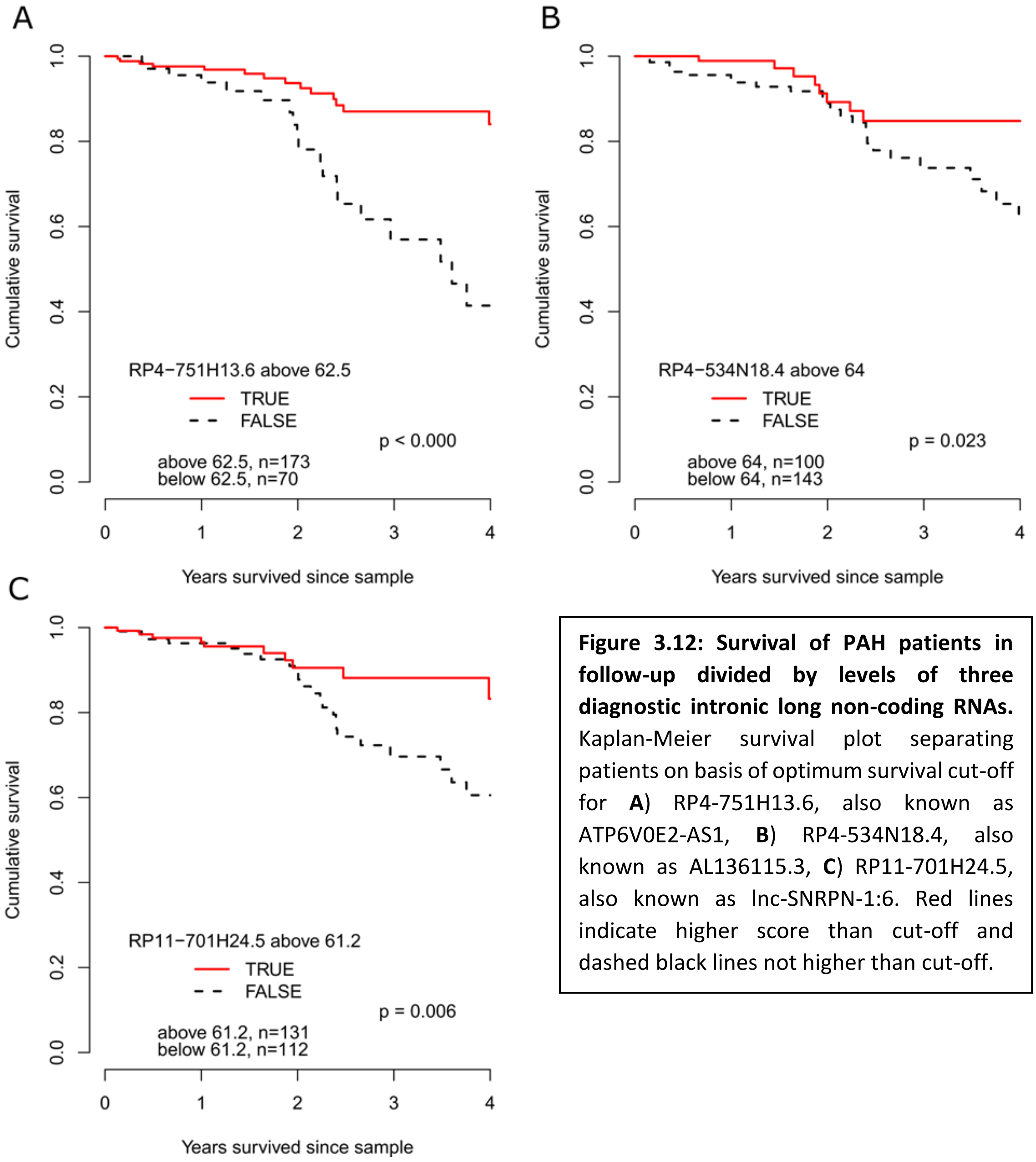

Figure 3.12: Survival of PAH patients in follow-up divided by levels of three diagnostic intronic long non-coding RNAs. Kaplan-Meier survival plot separating patients on basis of optimum survival cut-off for **A**) RP4-751H13.6, also known as ATP6V0E2-AS1, **B**) RP4-534N18.4, also known as AL136115.3, **C**) RP11-701H24.5, also known as lnc-SNRPN-1:6. Red lines indicate higher score than cut-off and dashed black lines not higher than cut-off.

Gene	AUC	Best cut-off	Sensitivity	Specificity	Sig.	FDR q
RP4-751H13.6	0.683	62.5	0.563	0.761	6.50x10^{-05}	**0.002**
RP11-701H24.5	0.644	61.2	0.729	0.586	0.002	**0.022**
RP4-534N18.4	0.633	64.0	0.813	0.444	0.004	**0.031**
NRG1	0.625	295.6	0.771	0.483	0.006	**0.040**
MAP3K7CL	0.617	2161.0	0.458	0.731	0.011	0.055
B4GAT1	0.610	177.5	0.771	0.462	0.017	0.069
CDA	0.595	238.0	0.604	0.628	0.039	0.123
CPT1A	0.595	1584.0	0.458	0.727	0.039	0.123
ZNF132	0.584	195.5	0.646	0.534	0.067	0.187
TLR5	0.578	1167.7	0.563	0.671	0.088	0.204
ZFP36L2	0.578	3777.5	0.521	0.697	0.090	0.204
ZNF763	0.573	212.6	0.396	0.761	0.111	0.221
FAM213A	0.572	187.0	0.625	0.539	0.115	0.221
CCND3	0.562	3116.2	0.458	0.671	0.178	0.297
RP11-241K18.1	0.561	59.0	0.667	0.483	0.185	0.297
AC009299.4	0.560	20.5	0.563	0.581	0.190	0.297
RP11-480C16.1	0.556	278.2	0.625	0.530	0.222	0.327
RP11-2J18.1	0.549	56.4	0.167	0.692	0.290	0.403
ZNF486	0.545	663.7	0.417	0.748	0.332	0.437
GGTA1P	0.542	884.5	0.188	0.940	0.363	0.453
RP11-379H18.1	0.534	157.1	0.417	0.688	0.454	0.54
TRIP10	0.530	94.5	0.833	0.291	0.516	0.587
RP11-574K11.28	0.515	156.2	0.583	0.517	0.751	0.816
CTD-2192J16.20	0.505	93.3	0.750	0.141	0.919	0.937
RP11-678G14.2	0.504	38.0	0.729	0.415	0.937	0.937

Table 3.9: Survival analysis of 25 RNAs in the diagnostic PAH RNA LASSO model. Sig: significance. AUC: area under ROC curve. Best cut-off expressed in transcripts per million. Genes listed by significance (lowest FDR q first).

3.5.5.2 PAH RNA model and other functional metrics

The diagnostic PAH RNA model was then used to further characterise the RNA signature identified in PAH patients. The association of PAH RNA model scores with different measurements of clinical performance, such as WHO functional class, exercise capacity (6-minute walk) and levels of cardiac biomarkers (BNP or NT-proBNP) was then tested.

Significant differences were observed in the PAH RNA model scores from patients in different WHO functional classes (p= 0.008; Figure 3.13), where an increase in PAH RNA model score was associated with a worse symptomatic profile. Similarly, PAH patients with higher PAH RNA model scores also showed significantly higher blood levels of markers of cardiac dysfunction (p= 5.10x10^{-4}; Figure 3.14). Finally, there was a significant negative correlation between PAH RNA model scores in PAH patients and exercise capacity (Spearman's rho= -0.256; p= 8.7x10^{-5}).

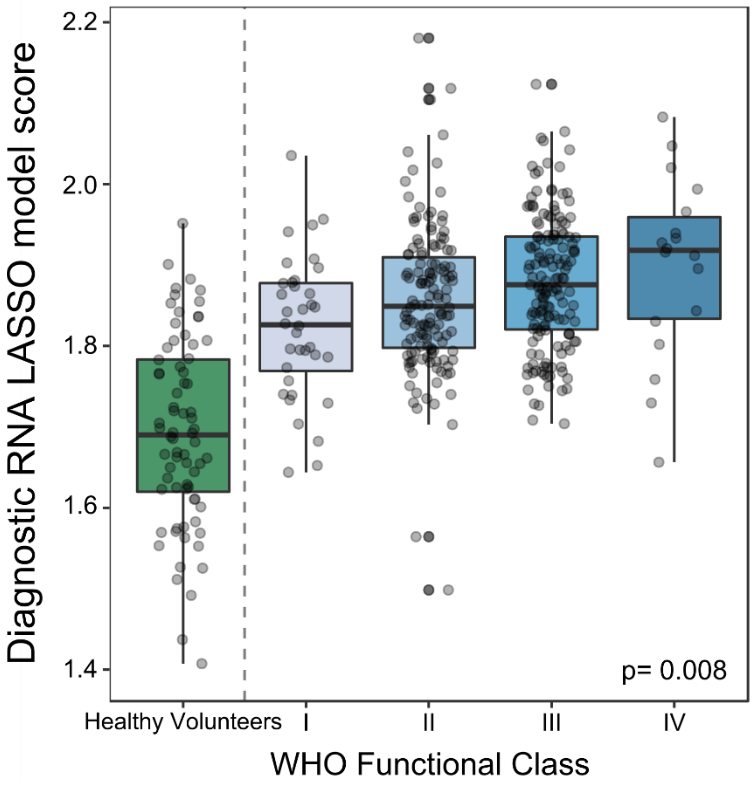

Figure 3.13: Boxplot showing PAH RNA model scores in heathy controls (n=72) and PAH patients (n=359) separated by WHO functional class (I-IV). Functional Class (FC) I patients= 36; FC II patients= 138; FC III patients= 155; FC IV patients = 18.

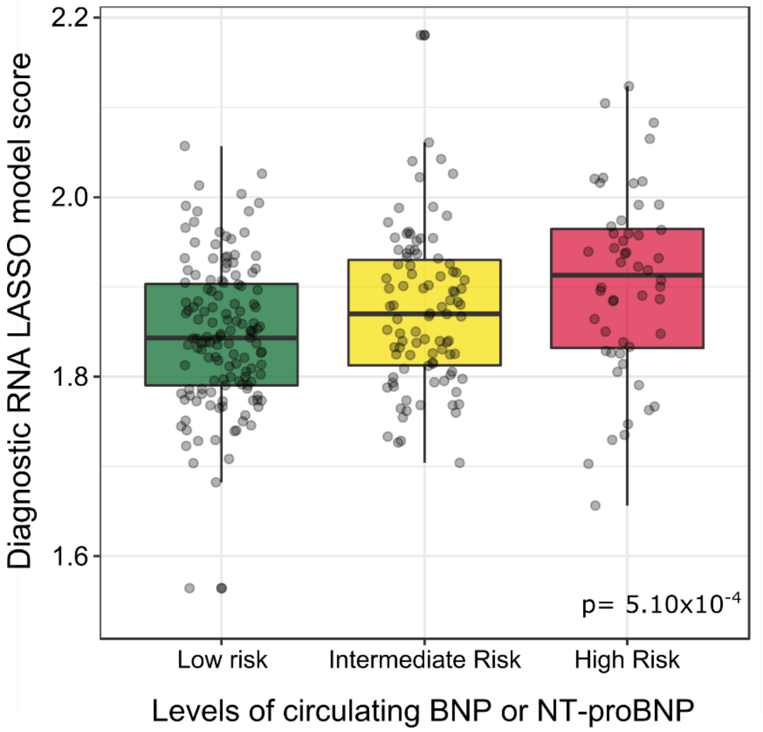

Figure 3.14: Boxplot showing PAH RNA model scores in PAH patients (n=359) separated by blood levels of cardiac biomarkers. BNP (<50 pg/ml, 50-300 pg/ml or >300pg/ml) or NT-proBNP (<300 pg/ml, 300-1400 pg/ml or >1400 pg/ml), as per European guidelines for PAH assessment.

3.5.5.3 PAH RNA model and responsiveness to vasodilator therapy

PAH patients responsive to calcium antagonist treatment ("vasoresponders") have been previously suggested to be identifiable through expression levels of certain RNAs based on in-vitro assays conducted on lymphocytes (176). Gene expression profiles of 240 PAH patients in the Discovery and Validation groups ($N_{vasoresponders}$= 17; $N_{non\text{-}vasoresponders}$= 223) were assessed, but no transcripts consistently distinguished responders and non-responders and no significant difference in any of the transcripts previously identified in lymphocyte assays was observed (Table 3.10).

	Discovery		**Validation**		**Combined**	
Gene	**log FC**	**Sig.**	**log FC**	**Sig.**	**log FC**	**Sig.**
EPDR1	0.25	0.21	-0.12	0.59	0.09	0.53
LPAR6	-0.09	0.33	<0.01	0.99	-0.01	0.82
MGAT5	-0.12	0.21	0.01	0.92	-0.10	0.15
MKLN1	-0.05	0.59	-0.01	0.92	-0.09	0.24
PIAS1	0.02	0.82	-0.03	0.80	-0.01	0.89
RALGPS2	-0.10	0.57	-0.03	0.87	-0.06	0.61
RAPGEF2	0.05	0.58	<0.01	0.98	<0.01	0.98
RHOQ	-0.04	0.68	<0.01	0.99	-0.02	0.74
SCD5	-0.05	0.70	-0.05	0.72	<0.01	0.99
TPD52	-0.10	0.39	-0.07	0.54	-0.11	0.20
ZNF652	-0.05	0.57	-0.04	0.71	-0.06	0.34

Table 3.10: Analysis of transcripts suggested to be associated with vasoresponsivity. Differential expression analysis comparing expression levels in vasoreponder/non-vasoresponder PAH patients of transcripts suggested to be associated with vasoresponsivity to calcium antagonist treatment in Discovery (n= 120), Validation (n= 120) and combined Discovery and Validation groups (n=240).

3.5.6 External validation of RNAseq analysis results

The PAH RNA signature identified in this study was further validated by comparing results with two other prior transcriptomic studies. First, a meta-analysis of PAH transcriptomic studies using blood samples from patients (237). Second, a microarray analysis of lung tissue isolated from PAH patients (184). The list of 507 top dysregulated genes in PAH from the differential expression analysis was used for this analysis.

3.5.6.1 Whole blood PAH RNA signature validation

The list of 507 top dysregulated genes in PAH from the differential expression analysis was used for this analysis and compared with the lists of significantly dysregulated genes from each study. In the case of the meta-analysis of whole blood studies in PAH (237), the list comprised 1269 significantly PAH-associated genes (FDR q< 0.01) out of the 22753 transcripts detected in the study (5.58%); and for the lung tissue microarray study (184), it comprised 1140 genes (FDR q< 0.001) out of the 33297 detected transcripts (3.42%).

A total of 416 genes from the PAH RNAseq list were present in the meta-analysis of whole blood studies in PAH (237). Directional consistence between dysregulated genes from both studies could be detected in 278/416 genes (66.8%). Out of those, 118/278 (42.4%) reached nominal significance. FDR corrected significance was met by a total of 67 genes, 34 of which also met FDR corrected significance in the IPAH subgroup analysis from that study (Table 3.11 and Supplementary table 2).

When comparing the PAH RNA signature 507 gene list with the lung tissue microarray study, a total of 372 genes from that PAH RNAseq list were also found in such analysis (184). Directional consistence between dysregulated genes from both studies could be detected in 161/372 genes (43.2%). Out of those, 41/161 (25.5%) reached nominal significance. FDR corrected significance was met by a total of 26 genes (Table 3.12 and Supplementary table 3)

Overall, the external validation process showed that 118/416 (28.4%) genes from the PAH RNA signature present in the meta-analysis of whole blood studies in PAH (237) and 41/372 (11.0%) genes from the PAH RNA signature present in the PH lung tissue microarray study (184) were found to be significantly dysregulated and directionally consistent across studies. These results show high levels of agreement between analyses—as the ratio of significant genes from each of those studies was 1269/22753 (5.58%) and 1140/33297 (3.42%) respectively. To further confirm this, a Fisher's exact test was conducted comparing significant results from each study—this is, 118/416 vs. 1269/22753 for the meta-analysis of whole blood studies in PAH, and 41/372 vs. 1140/33297 for the PH lung tissue microarray study—. For both comparisons, it was found that the proportion of associated genes was significantly different between studies ($p_{\text{meta-analysis}} < 2.2\text{x}10^{-16}$; $p_{\text{lung}} = 1.2\text{x}10^{-10}$), meaning that the overlap was higher than what would be expected by chance. Still, these results should be validated utilising another study cohort and a new analysis.

The gene adenosylmethionine decarboxylase 1 (AMD1) was the only significantly dysregulated gene meeting FDR corrected significance in all three analyses. This gene encodes a polyamine biosynthesis intermediate enzyme.

	PAH Cohort		PAH Meta-analysis			IPAH Meta-analysis	
Genes	**logFC AB**	**Sig. AB**	**log2(FC)**	**Sig.**	**FDR q**	**log2(FC)**	**Sig.**
Same direction, significant, meeting FDR in both meta-analyses							
DDX17	-0.117	4.30x10^{-07}	-0.590	2.00x10^{-03}	2.30x10^{-02}	-0.817	2.00x10^{-03}
RASA2	-0.135	4.60x10^{-07}	-0.861	5.00x10^{-04}	8.00x10^{-03}	-0.597	5.00x10^{-04}
ATM	-0.131	3.40x10^{-06}	-0.767	7.00x10^{-08}	9.00x10^{-06}	-0.831	5.00x10^{-06}
UHRF2	-0.141	3.70x10^{-06}	-0.493	6.00x10^{-04}	1.00x10^{-02}	-0.586	2.00x10^{-03}
ITGA6	-0.204	9.50x10^{-06}	-1.137	1.00x10^{-04}	3.00x10^{-03}	-0.874	2.00x10^{-03}
OXNAD1	-0.183	1.00x10^{-05}	-1.118	9.00x10^{-07}	7.00x10^{-05}	-1.099	2.00x10^{-08}
ATG12	-0.118	1.00x10^{-05}	-0.634	7.00x10^{-04}	1.10x10^{-02}	-0.690	1.00x10^{-04}
SESN1	-0.205	2.00x10^{-05}	-1.194	7.00x10^{-05}	2.00x10^{-03}	-1.212	7.00x10^{-04}
ZNF160	-0.113	3.30x10^{-05}	-0.806	6.00x10^{-08}	8.00x10^{-06}	-0.717	1.00x10^{-04}
KLHL28	-0.105	3.50x10^{-05}	-0.501	3.00x10^{-03}	3.20x10^{-02}	-0.592	1.00x10^{-03}
GPRASP1	-0.230	3.70x10^{-05}	-0.952	4.00x10^{-04}	7.00x10^{-03}	-0.688	1.00x10^{-04}
ZNF506	-0.155	4.50x10^{-05}	-0.953	1.00x10^{-04}	2.00x10^{-03}	-1.200	9.00x10^{-06}
PEX1	-0.108	5.40x10^{-05}	-0.940	1.00x10^{-06}	9.00x10^{-05}	-0.915	2.00x10^{-07}
BBX	-0.102	5.90x10^{-05}	-1.115	2.00x10^{-05}	6.00x10^{-04}	-1.205	2.00x10^{-05}
PPP1R2	-0.104	5.90x10^{-05}	-0.822	3.00x10^{-05}	1.00x10^{-03}	-1.013	1.00x10^{-08}
TRMT11	-0.137	7.30x10^{-05}	-0.906	2.00x10^{-010}	8.00x10^{-08}	-0.934	3.00x10^{-07}
ZNF329	-0.152	1.40x10^{-04}	-1.047	6.00x10^{-012}	6.00x10^{-09}	-0.990	3.00x10^{-07}
HSF2	-0.137	1.90x10^{-04}	-1.207	2.00x10^{-06}	1.00x10^{-04}	-0.950	3.00x10^{-04}
CEP85L	-0.100	2.00x10^{-04}	-1.107	5.00x10^{-012}	5.00x10^{-09}	-1.100	1.00x10^{-07}
MIGA1	-0.081	2.20x10^{-04}	-0.430	3.00x10^{-03}	2.90x10^{-02}	-0.592	2.00x10^{-03}
ZNF549	-0.104	3.00x10^{-04}	-0.500	3.00x10^{-03}	3.30x10^{-02}	-0.578	2.00x10^{-03}
SYNJ2BP	-0.110	3.10x10^{-04}	-0.736	1.00x10^{-03}	1.40x10^{-02}	-0.820	6.00x10^{-04}
FAM213A	-0.206	3.30x10^{-04}	-0.769	2.00x10^{-07}	2.00x10^{-05}	-0.705	2.00x10^{-04}
UFM1	-0.099	3.30x10^{-04}	-0.502	2.00x10^{-04}	4.00x10^{-03}	-0.508	3.00x10^{-03}
L3MBTL3	-0.118	4.00x10^{-04}	-0.731	6.00x10^{-07}	5.00x10^{-05}	-0.816	3.00x10^{-04}
ATF2	-0.085	5.10x10^{-04}	-0.816	9.00x10^{-04}	1.30x10^{-02}	-1.297	2.00x10^{-04}
ZCCHC7	-0.164	5.20x10^{-04}	-0.888	2.00x10^{-03}	2.20x10^{-02}	-0.730	1.00x10^{-04}
SLC38A1	-0.125	9.40x10^{-04}	-1.299	2.00x10^{-05}	6.00x10^{-04}	-1.116	4.00x10^{-06}
PLCG1	-0.145	1.17x10^{-03}	-0.804	1.00x10^{-08}	2.00x10^{-06}	-0.826	2.00x10^{-06}
EPHX2	-0.127	1.65x10^{-03}	-0.874	8.00x10^{-010}	2.00x10^{-07}	-0.883	1.00x10^{-06}
IL6ST	-0.148	1.76x10^{-03}	-0.951	5.00x10^{-06}	3.00x10^{-04}	-1.013	3.00x10^{-07}
TSR1	-0.100	1.92x10^{-03}	-0.499	3.00x10^{-04}	6.00x10^{-03}	-0.579	1.00x10^{-03}
TXK	-0.159	3.51x10^{-03}	-0.636	3.00x10^{-05}	9.00x10^{-04}	-0.619	3.00x10^{-04}
MALT1	-0.074	4.18x10^{-03}	-0.662	2.00x10^{-05}	6.00x10^{-04}	-0.852	4.00x10^{-04}
Same direction, significant, meeting FDR in PAH meta-analysis							
PTAR1	-0.168	1.30x10^{-08}	-0.743	5.00x10^{-04}	8.00x10^{-03}	-0.713	1.03x10^{-01}
RBM27	-0.137	1.30x10^{-07}	-0.736	5.00x10^{-04}	9.00x10^{-03}	-0.589	4.80x10^{-02}
ZNF211	-0.166	1.70x10^{-07}	-0.438	1.00x10^{-03}	1.50x10^{-02}	-0.506	3.00x10^{-03}

UBR1	-0.119	4.50x10^{-07}	-0.399	5.00x10^{-03}	4.70x10^{-02}	-0.364	7.60x10^{-02}
CCNB1IP1	-0.150	5.60x10^{-07}	-0.715	4.00x10^{-05}	1.00x10^{-03}	-0.334	2.95x10^{-01}
AMD1	-0.160	2.00x10^{-06}	-0.614	1.00x10^{-05}	5.00x10^{-04}	-0.266	4.66x10^{-01}
ARHGAP12	-0.149	2.10x10^{-06}	-0.708	2.00x10^{-03}	2.30x10^{-02}	-0.657	3.30x10^{-02}
BCLAF1	-0.127	2.20x10^{-06}	-0.927	5.00x10^{-06}	2.00x10^{-04}	-0.706	3.20x10^{-02}
ZNF33A	-0.122	6.50x10^{-06}	-0.459	5.00x10^{-03}	4.60x10^{-02}	-0.594	4.80x10^{-02}
CEP120	-0.126	7.10x10^{-06}	-0.695	6.00x10^{-04}	1.00x10^{-02}	-0.627	1.90x10^{-02}
EIF4A2	-0.141	7.60x10^{-06}	-0.825	5.00x10^{-04}	8.00x10^{-03}	-0.698	1.10x10^{-02}
NR1D2	-0.150	9.80x10^{-06}	-0.870	9.00x10^{-05}	2.00x10^{-03}	-0.844	4.00x10^{-03}
C12orf45	-0.177	1.00x10^{-05}	-0.497	5.00x10^{-03}	4.40x10^{-02}	-0.224	3.89x10^{-01}
TUBE1	-0.136	1.70x10^{-05}	-0.409	4.00x10^{-03}	4.00x10^{-02}	-0.496	8.00x10^{-03}
CREBRF	-0.116	3.20x10^{-05}	-0.551	3.00x10^{-04}	6.00x10^{-03}	-0.338	8.30x10^{-02}
ZBTB14	-0.119	7.10x10^{-05}	-0.662	1.00x10^{-03}	1.40x10^{-02}	-0.604	8.00x10^{-03}
DENND6A	-0.114	1.90x10^{-04}	-0.613	1.00x10^{-03}	1.50x10^{-02}	-0.596	2.70x10^{-02}
CSE1L	-0.115	3.10x10^{-04}	-0.505	2.00x10^{-04}	3.00x10^{-03}	-0.490	4.00x10^{-03}
CDA	0.291	3.40x10^{-04}	0.721	1.00x10^{-03}	1.80x10^{-02}	0.320	5.70x10^{-02}
SNRK	-0.099	4.00x10^{-04}	-0.884	5.00x10^{-05}	1.00x10^{-03}	-0.724	3.20x10^{-02}
ZNF525	-0.181	4.40x10^{-04}	-0.499	1.00x10^{-03}	1.60x10^{-02}	-0.705	1.70x10^{-02}
CASD1	-0.097	5.60x10^{-04}	-0.427	2.00x10^{-03}	2.30x10^{-02}	-0.372	3.40x10^{-02}
ZNF121	-0.113	6.90x10^{-04}	-0.398	6.00x10^{-03}	4.80x10^{-02}	-0.281	1.26x10^{-01}
HIP1R	-0.170	9.10x10^{-04}	-0.745	1.00x10^{-04}	3.00x10^{-03}	-0.391	1.06x10^{-01}
ZNF589	-0.112	1.25x10^{-03}	-0.476	1.00x10^{-03}	1.50x10^{-02}	-0.490	1.00x10^{-02}
FAM20C	0.309	1.79x10^{-03}	0.700	1.00x10^{-03}	1.80x10^{-02}	0.679	6.20x10^{-02}
SASH1	0.437	1.98x10^{-03}	0.564	3.00x10^{-03}	3.30x10^{-02}	0.446	1.20x10^{-02}
CNOT7	-0.089	2.16x10^{-03}	-0.734	2.00x10^{-03}	2.20x10^{-02}	-0.302	2.72x10^{-01}
CYTIP	-0.080	2.85x10^{-03}	-0.474	5.00x10^{-03}	4.70x10^{-02}	-0.591	3.60x10^{-02}
FBLN2	-0.355	2.99x10^{-03}	-0.707	3.00x10^{-04}	6.00x10^{-03}	-0.493	5.00x10^{-03}
DLG1	-0.099	3.26x10^{-03}	-0.815	3.00x10^{-03}	2.80x10^{-02}	-0.600	1.00x10^{-02}
FAN1	-0.096	5.45x10^{-03}	-0.454	2.00x10^{-03}	2.10x10^{-02}	-0.504	5.70x10^{-02}
TRPC1	-0.197	5.71x10^{-03}	-0.691	8.00x10^{-04}	1.10x10^{-02}	-0.783	4.00x10^{-03}

Table 3.11: Top results of meta-analysis of PAH transcriptomic studies in blood samples for RNAs associated with PAH in RNAseq. Table shows genes meeting FDR significance in the meta-analysis of PAH (n=67). Data ordered based on dysregulation significance (p-value) in current PAH RNAseq analysis. For full table of 416 genes see Supplementary Table 2.

	PAH Cohort		PAH Meta-analysis		
Genes	**logFC AB**	**Sig. AB**	**Average FC**	**Sig.**	**FDR q**
Same direction, significant, meeting FDR					
TLR5	-0.350	1.90x10^{-08}	0.810	<1.00x10^{-04}	2.00x10^{-03}
PTEN	-0.170	7.70x10^{-08}	0.889	7.00x10^{-03}	3.20x10^{-02}
BROX	-0.119	8.00x10^{-07}	0.886	1.00x10^{-03}	7.00x10^{-03}
AMD1	-0.160	2.00x10^{-06}	0.813	<1.00x10^{-04}	<1.00x10^{-04}
XKRX	-0.587	2.70x10^{-06}	0.709	<1.00x10^{-04}	<1.00x10^{-04}
MEFV	-0.193	5.40x10^{-06}	0.783	<1.00x10^{-04}	<1.00x10^{-04}
ZNF252P	-0.146	6.70x10^{-06}	0.849	<1.00x10^{-04}	3.00x10^{-03}
RP11-43D4.3	0.217	3.20x10^{-05}	1.255	6.00x10^{-03}	3.00x10^{-02}
TWF1	-0.117	4.00x10^{-05}	0.861	1.00x10^{-03}	8.00x10^{-03}
SLC25A16	-0.126	1.00x10^{-04}	0.875	1.00x10^{-03}	9.00x10^{-03}
STAT5A	-0.118	1.20x10^{-04}	0.860	2.00x10^{-03}	1.60x10^{-02}
LRCH1	0.131	1.20x10^{-04}	1.285	<1.00x10^{-04}	4.00x10^{-03}
SDCCAG3	-0.133	2.10x10^{-04}	0.872	<1.00x10^{-04}	3.00x10^{-03}
CYP2R1	-0.109	2.30x10^{-04}	0.828	<1.00x10^{-04}	2.00x10^{-03}
ZFP36L2	0.200	3.10x10^{-04}	1.263	<1.00x10^{-04}	2.00x10^{-03}
ATXN1	0.112	3.70x10^{-04}	1.164	<1.00x10^{-04}	<1.00x10^{-04}
TECPR1	-0.136	3.90x10^{-04}	0.929	8.00x10^{-03}	3.80x10^{-02}
UBE4A	-0.123	4.90x10^{-04}	0.893	<1.00x10^{-04}	<1.00x10^{-04}
ZNF233	0.161	5.10x10^{-04}	1.040	6.00x10^{-03}	3.00x10^{-02}
CEPT1	-0.080	7.70x10^{-04}	0.875	1.00x10^{-03}	6.00x10^{-03}
LIN52	-0.142	8.10x10^{-04}	0.855	2.00x10^{-03}	1.10x10^{-02}
GTF2H1	-0.076	9.40x10^{-04}	0.890	8.00x10^{-03}	3.70x10^{-02}
TYW3	-0.096	1.10x10^{-03}	0.918	1.00x10^{-02}	4.20x10^{-02}
CCDC18	-0.187	1.20x10^{-03}	0.927	<1.00x10^{-04}	2.00x10^{-03}
NDC1	-0.131	1.70x10^{-03}	0.872	7.00x10^{-03}	3.20x10^{-02}
TAF6L	-0.131	1.80x10^{-03}	0.891	1.00x10^{-03}	7.00x10^{-03}

Table 3.12: Top results of meta-analysis of PAH transcriptomic studies in lung tissue for RNAs associated with PAH in RNAseq. Table shows genes meeting FDR significance (n=26). Data ordered based on dysregulation significance (p-value) in current PAH RNAseq analysis. For full table of 372 genes see Supplementary Table 3.

3.5.6.2 Validation of external analyses using whole blood RNA PAH signature

The lists of detected genes significantly associated with PAH from each external analysis were used for this analysis and compared with the total number of detected genes in the PAH RNAseq study (17038 genes).

1087 out of 1269 genes in the meta-analysis of whole blood studies could be found in the PAH RNAseq analysis. Directional consistence between dysregulated genes from both studies could be detected in 639/1087 genes (58.8%). Out of those, 206/639 (32.2%) reached nominal significance. FDR corrected significance was met by a total of 96 genes (Table 3.13 and Supplementary table 4).

777 out of 1140 genes in the lung tissue microarray study could be found in the PAH RNAseq analysis. Directional consistence between dysregulated genes from both studies could be detected in 411/777 genes (52.9%). Out of those, 118/411 (28.7%) reached nominal significance and 46 met FDR corrected significance (Table 3.14 and Supplementary table 5).

	PAH Meta-analysis			**PAH Cohort**		
Gene	**log2FC**	**Sig.**	**FDR**	**logFC**	**Sig.**	**FDR q**
Same direction, significant, meeting FDR						
YTHDC1	-1.039	7.34x10^{-13}	1.64x10^{-09}	-0.118	7.82x10^{-05}	4.39x10^{-03}
NCR3	-1.084	1.32x10^{-12}	2.15x10^{-09}	-0.201	1.49x10^{-03}	2.35x10^{-02}
CEP85L	-1.107	4.52x10^{-12}	5.14x10^{-09}	-0.100	2.00x10^{-04}	7.55x10^{-03}
ZNF329	-1.047	6.31x10^{-12}	6.24x10^{-09}	-0.152	1.41x10^{-04}	6.16x10^{-03}
EPC1	-0.952	1.92x10^{-10}	7.80x10^{-08}	-0.062	1.04x10^{-03}	1.93x10^{-02}
TRMT11	-0.906	2.12x10^{-10}	8.32x10^{-08}	-0.137	7.33x10^{-05}	4.23x10^{-03}
GON4L	-0.885	5.56x10^{-10}	1.83x10^{-07}	-0.119	2.76x10^{-03}	3.36x10^{-02}
EPHX2	-0.874	7.98x10^{-10}	2.42x10^{-07}	-0.127	1.65x10^{-03}	2.48x10^{-02}
TMIGD2	-1.071	1.27x10^{-09}	3.66x10^{-07}	-0.249	1.28x10^{-03}	2.17x10^{-02}
BRWD1	-0.872	5.15x10^{-09}	1.23x10^{-06}	-0.108	3.80x10^{-04}	1.05x10^{-02}
PLCG1	-0.804	1.16x10^{-08}	2.26x10^{-06}	-0.145	1.17x10^{-03}	2.07x10^{-02}
IFI27	0.829	2.23x10^{-08}	3.65x10^{-06}	1.240	1.89x10^{-03}	2.70x10^{-02}
HIST2H3C	1.065	2.41x10^{-08}	3.81x10^{-06}	0.501	1.60x10^{-04}	6.50x10^{-03}
ZNF14	-0.949	3.72x10^{-08}	5.43x10^{-06}	-0.118	4.07x10^{-03}	4.22x10^{-02}
ZNF160	-0.806	6.32x10^{-08}	7.86x10^{-06}	-0.113	3.30x10^{-05}	2.86x10^{-03}
ATM	-0.767	7.01x10^{-08}	8.53x10^{-06}	-0.131	3.41x10^{-06}	8.29x10^{-04}
MTX3	-0.791	7.96x10^{-08}	9.38x10^{-06}	-0.101	1.45x10^{-03}	2.32x10^{-02}
URI1	-0.774	1.74x10^{-07}	1.78x10^{-05}	-0.090	9.44x10^{-04}	1.81x10^{-02}
DHX9	-0.695	2.71x10^{-07}	2.52x10^{-05}	-0.083	3.74x10^{-04}	1.04x10^{-02}
NR2C1	-0.708	5.70x10^{-07}	4.57x10^{-05}	-0.099	1.36x10^{-03}	2.25x10^{-02}
L3MBTL3	-0.731	5.91x10^{-07}	4.65x10^{-05}	-0.118	3.96x10^{-04}	1.08x10^{-02}
ATF7IP2	-0.862	6.10x10^{-07}	4.72x10^{-05}	-0.185	2.19x10^{-04}	7.96x10^{-03}
SOCS7	-0.712	1.13x10^{-06}	7.72x10^{-05}	-0.151	3.78x10^{-04}	1.05x10^{-02}

RPS25	-0.682	1.24x10^{-06}	8.42x10^{-05}	-0.112	3.27x10^{-03}	3.72x10^{-02}
ARGLU1	-0.707	1.30x10^{-06}	8.75x10^{-05}	-0.121	3.81x10^{-03}	4.08x10^{-02}
PEX1	-0.940	1.33x10^{-06}	8.87x10^{-05}	-0.108	5.43x10^{-05}	3.72x10^{-03}
ZMYM5	-0.860	1.43x10^{-06}	9.38x10^{-05}	-0.087	2.48x10^{-03}	3.15x10^{-02}
UTP23	-0.796	1.46x10^{-06}	9.52x10^{-05}	-0.078	2.89x10^{-03}	3.45x10^{-02}
NOG	-0.702	1.47x10^{-06}	9.56x10^{-05}	-0.357	1.79x10^{-03}	2.60x10^{-02}
JADE1	-0.848	2.26x10^{-06}	1.35x10^{-04}	-0.086	5.32x10^{-03}	4.92x10^{-02}
PDE6B	-0.762	2.42x10^{-06}	1.42x10^{-04}	-0.118	3.05x10^{-03}	3.57x10^{-02}
HNRNPK	-0.657	2.69x10^{-06}	1.55x10^{-04}	-0.102	2.40x10^{-05}	2.43x10^{-03}
MS4A4A	0.825	3.23x10^{-06}	1.79x10^{-04}	0.264	5.28x10^{-03}	4.89x10^{-02}
ANAPC16	-0.678	3.25x10^{-06}	1.79x10^{-04}	-0.088	1.57x10^{-03}	2.42x10^{-02}
NT5E	-0.657	3.24x10^{-06}	1.79x10^{-04}	-0.286	2.44x10^{-03}	3.13x10^{-02}
DBP	-0.618	4.43x10^{-06}	2.28x10^{-04}	-0.133	5.40x10^{-03}	4.97x10^{-02}
RABGGTB	-0.782	4.39x10^{-06}	2.28x10^{-04}	-0.094	1.59x10^{-03}	2.44x10^{-02}
FAM185A	-0.652	7.15x10^{-06}	3.31x10^{-04}	-0.168	2.49x10^{-03}	3.15x10^{-02}
SNHG1	-1.154	8.20x10^{-06}	3.64x10^{-04}	-0.124	7.89x10^{-04}	1.64x10^{-02}
ACAP1	-0.621	9.97x10^{-06}	4.19x10^{-04}	-0.117	2.28x10^{-03}	3.02x10^{-02}
ARHGEF18	-0.646	1.07x10^{-05}	4.37x10^{-04}	-0.111	3.39x10^{-03}	3.79x10^{-02}
INTS6	-0.832	1.17x10^{-05}	4.65x10^{-04}	-0.087	9.21x10^{-05}	4.82x10^{-03}
TMEM45A	0.638	1.31x10^{-05}	5.12x10^{-04}	0.124	4.64x10^{-04}	1.18x10^{-02}
AMD1	-0.614	1.33x10^{-05}	5.17x10^{-04}	-0.160	1.96x10^{-06}	6.42x10^{-04}
EIF4A2	-0.667	1.47x10^{-05}	5.58x10^{-04}	-0.141	7.62x10^{-06}	1.32x10^{-03}
TSGA10	-0.663	1.53x10^{-05}	5.71x10^{-04}	-0.140	3.47x10^{-03}	3.84x10^{-02}
COQ10A	-0.663	1.55x10^{-05}	5.75x10^{-04}	-0.096	3.79x10^{-03}	4.07x10^{-02}
MALT1	-0.662	1.75x10^{-05}	6.31x10^{-04}	-0.073	4.18x10^{-03}	4.28x10^{-02}
SLC30A4	-0.613	2.41x10^{-05}	8.15x10^{-04}	-0.097	4.34x10^{-03}	4.37x10^{-02}
TXK	-0.636	2.66x10^{-05}	8.78x10^{-04}	-0.159	3.51x10^{-03}	3.88x10^{-02}
ZNF432	-0.617	2.66x10^{-05}	8.78x10^{-04}	-0.145	6.03x10^{-06}	1.17x10^{-03}
ELANE	0.560	3.00x10^{-05}	9.75x10^{-04}	0.835	4.41x10^{-04}	1.16x10^{-02}
GALNT11	-0.768	3.18x10^{-05}	1.01x10^{-03}	-0.066	4.37x10^{-03}	4.38x10^{-02}
RAPH1	0.635	3.41x10^{-05}	1.07x10^{-03}	0.290	1.63x10^{-03}	2.47x10^{-02}
CAPN10	-0.635	3.40x10^{-05}	1.07x10^{-03}	-0.110	4.97x10^{-04}	1.24x10^{-02}
CCNB1IP1	-0.715	3.63x10^{-05}	1.13x10^{-03}	-0.150	5.61x10^{-07}	3.06x10^{-04}
ING3	-0.783	4.83x10^{-05}	1.41x10^{-03}	-0.087	8.18x10^{-04}	1.67x10^{-02}
MITF	0.558	6.26x10^{-05}	1.73x10^{-03}	0.155	1.82x10^{-03}	2.63x10^{-02}
UBASH3B	0.767	6.43x10^{-05}	1.77x10^{-03}	0.145	5.60x10^{-04}	1.33x10^{-02}
ANKRD44	-0.605	7.27x10^{-05}	1.94x10^{-03}	-0.067	4.46x10^{-03}	4.42x10^{-02}
ZNF506	-0.953	9.53x10^{-05}	2.38x10^{-03}	-0.155	4.51x10^{-05}	3.35x10^{-03}
CREBZF	-0.736	1.11x10^{-04}	2.66x10^{-03}	-0.138	1.85x10^{-04}	7.18x10^{-03}
HIP1R	-0.745	1.20x10^{-04}	2.80x10^{-03}	-0.169	9.14x10^{-04}	1.79x10^{-02}
TRABD2A	-0.976	1.20x10^{-04}	2.80x10^{-03}	-0.190	1.55x10^{-03}	2.40x10^{-02}

SUPT20H	-0.526	1.52x10^{-04}	3.37x10^{-03}	-0.076	1.96x10^{-03}	2.75x10^{-02}
CSE1L	-0.505	1.56x10^{-04}	3.42x10^{-03}	-0.115	3.10x10^{-04}	9.55x10^{-03}
ZNF626	-0.546	1.59x10^{-04}	3.49x10^{-03}	-0.181	1.94x10^{-03}	2.73x10^{-02}
UFM1	-0.502	1.70x10^{-04}	3.65x10^{-03}	-0.099	3.26x10^{-04}	9.81x10^{-03}
ZNF75A	-0.585	1.70x10^{-04}	3.65x10^{-03}	-0.101	5.72x10^{-04}	1.35x10^{-02}
ESYT2	-0.781	1.81x10^{-04}	3.83x10^{-03}	-0.131	9.19x10^{-05}	4.82x10^{-03}
CTNNB1	-0.668	2.00x10^{-04}	4.13x10^{-03}	-0.096	3.09x10^{-05}	2.80x10^{-03}
HAUS6	-0.515	2.11x10^{-04}	4.31x10^{-03}	-0.115	2.62x10^{-04}	8.77x10^{-03}
TMEM200A	0.564	2.23x10^{-04}	4.50x10^{-03}	0.328	9.51x10^{-04}	1.82x10^{-02}
LONP1	-0.510	2.37x10^{-04}	4.72x10^{-03}	-0.079	3.90x10^{-03}	4.13x10^{-02}
POLE3	-0.583	2.45x10^{-04}	4.84x10^{-03}	-0.085	1.28x10^{-03}	2.17x10^{-02}
MRI1	-0.557	2.58x10^{-04}	5.04x10^{-03}	-0.163	1.17x10^{-04}	5.58x10^{-03}
MAOB	0.504	2.73x10^{-04}	5.28x10^{-03}	0.282	4.38x10^{-03}	4.39x10^{-02}
RSAD1	-0.502	2.98x10^{-04}	5.65x10^{-03}	-0.100	3.84x10^{-03}	4.10x10^{-02}
CREBRF	-0.551	3.05x10^{-04}	5.75x10^{-03}	-0.116	3.23x10^{-05}	2.85x10^{-03}
TSR1	-0.499	3.16x10^{-04}	5.91x10^{-03}	-0.100	1.92x10^{-03}	2.72x10^{-02}
CYP20A1	-0.499	3.20x10^{-04}	5.95x10^{-03}	-0.077	3.91x10^{-03}	4.14x10^{-02}
FBLN2	-0.707	3.37x10^{-04}	6.21x10^{-03}	-0.355	2.99x10^{-03}	3.52x10^{-02}
DFFA	-0.477	3.62x10^{-04}	6.55x10^{-03}	-0.069	5.40x10^{-03}	4.97x10^{-02}
ZNF766	-0.539	4.02x10^{-04}	7.05x10^{-03}	-0.082	3.79x10^{-03}	4.07x10^{-02}
WTAP	-0.603	4.19x10^{-04}	7.24x10^{-03}	-0.060	4.12x10^{-03}	4.24x10^{-02}
HORMAD1	0.508	4.28x10^{-04}	7.32x10^{-03}	0.271	1.63x10^{-03}	2.47x10^{-02}
PRKRIP1	-0.487	4.54x10^{-04}	7.64x10^{-03}	-0.073	3.85x10^{-03}	4.10x10^{-02}
ZNF518B	-0.505	4.67x10^{-04}	7.79x10^{-03}	-0.149	2.67x10^{-05}	2.57x10^{-03}
PTAR1	-0.743	5.09x10^{-04}	8.33x10^{-03}	-0.168	1.35x10^{-08}	4.48x10^{-05}
RBM27	-0.736	5.29x10^{-04}	8.59x10^{-03}	-0.137	1.33x10^{-07}	1.49x10^{-04}
CCNB2	0.480	5.37x10^{-04}	8.70x10^{-03}	0.370	2.05x10^{-03}	2.83x10^{-02}
LCN2	0.548	5.57x10^{-04}	8.96x10^{-03}	0.435	3.29x10^{-03}	3.74x10^{-02}
URGCP	-0.482	5.67x10^{-04}	9.08x10^{-03}	-0.097	1.08x10^{-03}	1.97x10^{-02}
UHRF2	-0.493	6.05x10^{-04}	9.51x10^{-03}	-0.141	3.70x10^{-06}	8.70x10^{-04}
CEP120	-0.695	6.12x10^{-04}	9.58x10^{-03}	-0.126	7.14x10^{-06}	1.28x10^{-03}
MFNG	-0.473	6.16x10^{-04}	9.61x10^{-03}	-0.096	5.42x10^{-03}	4.97x10^{-02}

Table 3.13: Top results of whole blood PAH RNA signature in the meta-analysis of PAH transcriptomic studies in blood samples. Table shows genes meeting FDR significance (n=96). Data ordered based on dysregulation significance (p-value) in meta-analysis of PAH transcriptomic studies in blood samples. For full table of 1087 genes see Supplementary Table 4.

	PAH Meta-analysis			PAH Cohort		
Gene	**Average FC**	**Sig.**	**FDR q**	**logFC AB**	**Sig. AB**	**FDR q AB**
Same direction, significant, meeting FDR						
TLR8	-0.451	8.37x10^{-14}	2.50x10^{-10}	-0.166	2.60x10^{-04}	8.76x10^{-03}
TALDO1	-0.349	1.25x10^{-13}	2.90x10^{-10}	-0.099	4.04x10^{-03}	4.21x10^{-02}
TXNRD1	-0.416	7.09x10^{-13}	8.24x10^{-10}	-0.099	2.04x10^{-03}	2.82x10^{-02}
TLR1	-0.421	7.36x10^{-11}	3.14x10^{-08}	-0.117	6.36x10^{-04}	1.44x10^{-02}
FAM45A	-0.209	8.86x10^{-11}	3.56x10^{-08}	-0.097	1.36x10^{-04}	6.03x10^{-03}
ACOT13	-0.266	1.16x10^{-10}	4.25x10^{-08}	-0.077	3.29x10^{-03}	3.73x10^{-02}
MAOB	0.533	8.01x10^{-10}	2.09x10^{-07}	0.282	4.38x10^{-03}	4.39x10^{-02}
DSEL	-0.383	8.82x10^{-10}	2.25x10^{-07}	-0.252	3.22x10^{-03}	3.69x10^{-02}
LILRB3	-0.476	1.07x10^{-09}	2.57x10^{-07}	-0.186	3.93x10^{-03}	4.14x10^{-02}
MMP25	-0.248	1.51x10^{-09}	3.35x10^{-07}	-0.261	8.42x10^{-04}	1.70x10^{-02}
TMEM184C	-0.176	5.20x10^{-09}	8.43x10^{-07}	-0.085	1.90x10^{-03}	2.70x10^{-02}
TLR4	-0.334	5.86x10^{-09}	9.01x10^{-07}	-0.143	1.61x10^{-03}	2.46x10^{-02}
MEG3	0.507	1.97x10^{-08}	2.34x10^{-06}	0.492	3.25x10^{-03}	3.71x10^{-02}
PFKFB4	-0.158	4.95x10^{-08}	4.81x10^{-06}	-0.123	2.58x10^{-04}	8.75x10^{-03}
TNKS	0.180	6.30x10^{-08}	5.77x10^{-06}	0.092	4.26x10^{-03}	4.32x10^{-02}
GSR	-0.248	8.27x10^{-08}	7.21x10^{-06}	-0.100	1.30x10^{-03}	2.19x10^{-02}
C6orf89	-0.118	1.08x10^{-07}	8.72x10^{-06}	-0.081	4.04x10^{-03}	4.21x10^{-02}
SMAD3	0.334	2.31x10^{-07}	1.55x10^{-05}	0.165	1.41x10^{-03}	2.29x10^{-02}
PLXNC1	-0.384	3.20x10^{-07}	1.98x10^{-05}	-0.149	1.06x10^{-05}	1.54x10^{-03}
INHBA	0.780	4.25x10^{-07}	2.44x10^{-05}	0.579	2.24x10^{-03}	2.98x10^{-02}
CXCR1	-0.528	4.77x10^{-07}	2.67x10^{-05}	-0.196	2.69x10^{-03}	3.31x10^{-02}
MEFV	-0.217	5.59x10^{-07}	3.05x10^{-05}	-0.193	5.37x10^{-06}	1.06x10^{-03}
FLT3	-0.251	7.54x10^{-07}	3.90x10^{-05}	-0.323	3.13x10^{-03}	3.62x10^{-02}
ATP6V1B2	-0.194	1.17x10^{-06}	5.47x10^{-05}	-0.104	9.20x10^{-04}	1.80x10^{-02}
RNF141	-0.214	2.99x10^{-06}	1.12x10^{-04}	-0.132	1.49x10^{-04}	6.30x10^{-03}
TLR2	-0.331	3.02x10^{-06}	1.12x10^{-04}	-0.168	1.59x10^{-03}	2.44x10^{-02}
XKRX	-0.291	3.39x10^{-06}	1.24x10^{-04}	-0.587	2.66x10^{-06}	7.45x10^{-04}
MAPKAP1	-0.131	4.39x10^{-06}	1.50x10^{-04}	-0.065	1.19x10^{-03}	2.10x10^{-02}
MBD2	-0.098	4.49x10^{-06}	1.53x10^{-04}	-0.084	3.19x10^{-03}	3.68x10^{-02}
DUSP4	0.154	5.13x10^{-06}	1.69x10^{-04}	0.353	5.02x10^{-04}	1.24x10^{-02}
MED11	-0.159	5.12x10^{-06}	1.69x10^{-04}	-0.080	1.53x10^{-03}	2.38x10^{-02}
HCK	-0.423	5.69x10^{-06}	1.82x10^{-04}	-0.137	2.08x10^{-04}	7.68x10^{-03}
TBC1D14	-0.162	6.42x10^{-06}	1.99x10^{-04}	-0.091	2.14x10^{-03}	2.91x10^{-02}
MCOLN3	0.560	6.93x10^{-06}	2.11x10^{-04}	0.162	5.00x10^{-04}	1.24x10^{-02}
IRAK4	-0.181	9.40x10^{-06}	2.64x10^{-04}	-0.075	1.08x10^{-03}	1.97x10^{-02}
NCF2	-0.306	1.04x10^{-05}	2.84x10^{-04}	-0.111	3.97x10^{-04}	1.08x10^{-02}
UBE4A	-0.107	1.36x10^{-05}	3.45x10^{-04}	-0.123	4.92x10^{-04}	1.23x10^{-02}

CYTH4	-0.341	$1.47x10^{-05}$	$3.66x10^{-04}$	-0.119	$7.67x10^{-04}$	$1.61x10^{-02}$
GMPR2	-0.140	$1.54x10^{-05}$	$3.78x10^{-04}$	-0.099	$3.27x10^{-04}$	$9.84x10^{-03}$
AMD1	-0.187	$1.90x10^{-05}$	$4.48x10^{-04}$	-0.160	$1.96x10^{-06}$	$6.42x10^{-04}$
ATXN1	0.164	$2.05x10^{-05}$	$4.76x10^{-04}$	0.112	$3.67x10^{-04}$	$1.03x10^{-02}$
YIPF1	-0.154	$2.08x10^{-05}$	$4.82x10^{-04}$	-0.123	$1.81x10^{-04}$	$7.14x10^{-03}$
NUCB2	-0.248	$2.54x10^{-05}$	$5.65x10^{-04}$	-0.109	$2.24x10^{-03}$	$2.98x10^{-02}$
GOLGA5	-0.125	$3.82x10^{-05}$	$7.63x10^{-04}$	-0.081	$8.96x10^{-05}$	$4.80x10^{-03}$
SLC25A45	0.126	$5.32x10^{-05}$	$9.79x10^{-04}$	0.106	$5.07x10^{-03}$	$4.78x10^{-02}$
ALG13	0.185	$5.40x10^{-05}$	$9.92x10^{-04}$	0.136	$3.97x10^{-03}$	$4.17x10^{-02}$

Table 3.14: Top results of whole blood PAH RNA signature in the lung tissue microarray study. Table shows genes meeting FDR significance (n=46). Data ordered based on dysregulation significance (p-value) in lung tissue microarray study. For full table of 777 genes see Supplementary Table 5.

3.5.7 Functional characterisation of RNAs in PAH signature

Functional characterisation of differentially expressed genes in PAH patients was performed using DAVID, an online tool for bioinformatic functional interpretation of large lists of genes resulting from biological assays (240). In the functional annotation database in DAVID—which included data on functional annotations, gene ontology, pathways, disease association, interactions and protein domains—, 435/507 differentially expressed genes in PAH patients could be found. The main class of genes enriched in PAH patients was that of DNA-binding transcription factors (TFs). These included genes such as Krüppel-like factor 10 (KLF10), hypoxia-inducible factor 1α (HIF1α) and many zinc-finger containing TFs (Table 3.15).

Another resource used for functional characterisation of differentially expressed genes in PAH patients was the Ingenuity Pathway Analysis (IPA®) from the Ingenuity Knowledge Base (241). It is an online tool for analysis, integration, and understanding of data from assays such as RNAseq, among others. In the Ingenuity Knowledge Base, 505/507 differentially expressed genes in PAH patients were mapped. Some of the top canonical pathways highlighted by the IPA® included PI3K signalling in B lymphocytes, hypoxia signalling, the role of JAK family kinases in IL6-type cytokine signalling, double-stranded DNA repair, T-cell receptor signalling (Figure 3.15).

The only gene differentially expressed gene in this RNAseq analysis which was also found to be significantly dysregulated in the PAH differential expression assay of lung tissue and the PAH differential expression meta-analysis of PBMC assays, *AMD1* (see details on Chapter 3.5.6.1), was found to be part of the top IPA® gene network (Figure 3.16).

Term	Count	%	Sig.	Fold Enrichment	Bonferroni	Benjamini	FDR q
Krueppel-associated box	51	11.72	$3.00x10^{-25}$	6.245	$2.00x10^{-22}$	$2.00x10^{-22}$	$5.00x10^{-22}$
KRAB domain	46	10.57	$2.20x10^{-24}$	6.864	$2.00x10^{-21}$	$2.00x10^{-21}$	$4.00x10^{-21}$
Zinc finger C2H2-type / Integrase DNA-binding domain	65	14.94	$3.30x10^{-24}$	4.494	$2.00x10^{-21}$	$1.00x10^{-21}$	$5.00x10^{-21}$
Zinc finger, C2H2	68	15.63	$1.20x10^{-23}$	4.190	$9.00x10^{-21}$	$3.00x10^{-21}$	$2.00x10^{-20}$
Zinc finger C2H2-type 10	45	10.34	$1.50x10^{-23}$	6.754	$2.00x10^{-20}$	$8.00x10^{-21}$	$2.00x10^{-20}$
KRAB	51	11.72	$1.80x10^{-23}$	5.475	$3.00x10^{-21}$	$3.00x10^{-21}$	$2.00x10^{-20}$
Zinc-finger	101	23.22	$2.20x10^{-23}$	2.940	$7.00x10^{-21}$	$7.00x10^{-21}$	$3.00x10^{-20}$
Zinc finger C2H2-like	66	15.17	$2.40x10^{-23}$	4.264	$2.00x10^{-20}$	$4.00x10^{-21}$	$4.00x10^{-20}$
Zinc finger C2H2-type 6	53	12.18	$3.00x10^{-23}$	5.414	$3.00x10^{-20}$	$1.00x10^{-20}$	$5.00x10^{-20}$
Zinc finger C2H2-type 9	47	10.8	$3.50x10^{-23}$	6.248	$4.00x10^{-20}$	$1.00x10^{-20}$	$6.00x10^{-20}$
Zinc finger C2H2-type 7	51	11.72	$3.80x10^{-23}$	5.638	$4.00x10^{-20}$	$8.00x10^{-21}$	$6.00x10^{-20}$
Nucleus	190	43.68	$3.40x10^{-22}$	1.878	$1.00x10^{-19}$	$5.00x10^{-20}$	$5.00x10^{-19}$
Zinc finger:C2H2-type 8	48	11.03	$3.80x10^{-22}$	5.753	$4.00x10^{-19}$	$7.00x10^{-20}$	$6.00x10^{-19}$
Zinc finger:C2H2-type 11	41	9.425	$5.60x10^{-22}$	6.972	$6.00x10^{-19}$	$9.00x10^{-20}$	$9.00x10^{-19}$
Nucleic acid binding	74	17.01	$1.50x10^{-21}$	3.533	$8.00x10^{-19}$	$8.00x10^{-19}$	$2.00x10^{-18}$
Zinc finger C2H2-type 5	53	12.18	$2.10x10^{-21}$	4.932	$2.00x10^{-18}$	$3.00x10^{-19}$	$3.00x10^{-18}$
Zinc finger C2H2-type 4	54	12.41	$7.40x10^{-21}$	4.700	$8.00x10^{-18}$	$9.00x10^{-19}$	$1.00x10^{-17}$
Zinc finger C2H2	66	15.17	$8.30x10^{-21}$	3.645	$2.00x10^{-18}$	$8.00x10^{-19}$	$1.00x10^{-17}$
Zinc finger C2H2-type 3	56	12.87	$8.80x10^{-21}$	4.507	$1.00x10^{-17}$	$1.00x10^{-18}$	$1.00x10^{-17}$
Transcription regulation	110	25.29	$2.20x10^{-19}$	2.445	$7.00x10^{-17}$	$2.00x10^{-17}$	$3.00x10^{-16}$
Zinc finger C2H2-type 2	53	12.18	$2.90x10^{-19}$	4.411	$3.00x10^{-16}$	$3.00x10^{-17}$	$5.00x10^{-16}$
Transcription	111	25.52	$5.70x10^{-19}$	2.400	$2.00x10^{-16}$	$4.00x10^{-17}$	$8.00x10^{-16}$
DNA-templated transcription regulation	88	20.23	$2.40x10^{-18}$	2.722	$4.00x10^{-15}$	$4.00x10^{-15}$	$4.00x10^{-15}$
Zinc	108	24.83	$3.30x10^{-18}$	2.385	$1.00x10^{-15}$	$2.00x10^{-16}$	$4.00x10^{-15}$
Zinc finger C2H2-type 12	34	7.816	$6.50x10^{-18}$	6.797	$7.00x10^{-15}$	$6.00x10^{-16}$	$1.00x10^{-14}$
DNA-binding	98	22.53	$1.70x10^{-17}$	2.478	$5.00x10^{-15}$	$9.00x10^{-16}$	$2.00x10^{-14}$
DNA-templated transcription	100	22.99	$5.30x10^{-17}$	2.379	$9.00x10^{-14}$	$5.00x10^{-14}$	$9.00x10^{-14}$
Zinc finger C2H2-type 13	27	6.207	$3.30x10^{-14}$	6.774	$4.00x10^{-11}$	$3.00x10^{-12}$	$5.00x10^{-11}$
Zinc finger C2H2-type 1; degenerate	21	4.828	$3.10x10^{-13}$	8.738	$3.00x10^{-10}$	$2.00x10^{-11}$	$5.00x10^{-10}$
Metal-binding	129	29.66	$8.00x10^{-13}$	1.837	$2.00x10^{-10}$	$3.00x10^{-11}$	$1.00x10^{-09}$
Zinc finger C2H2-type 15	21	4.828	$1.40x10^{-12}$	8.081	$2.00x10^{-09}$	$1.00x10^{-10}$	$2.00x10^{-09}$
Metal ion binding	93	21.38	$1.80x10^{-12}$	2.114	$9.00x10^{-10}$	$4.00x10^{-10}$	$3.00x10^{-09}$
Phosphoprotein	227	52.18	$4.10x10^{-12}$	1.427	$1.00x10^{-09}$	$2.00x10^{-10}$	$6.00x10^{-09}$
Nucleus	174	40	$7.10x10^{-12}$	1.562	$3.00x10^{-09}$	$3.00x10^{-09}$	$1.00x10^{-08}$
Zinc finger C2H2-type 1	39	8.966	$1.90x10^{-11}$	3.603	$2.00x10^{-08}$	$1.00x10^{-09}$	$3.00x10^{-08}$
Zinc finger C2H2-type 14	21	4.828	$2.90x10^{-11}$	6.890	$3.00x10^{-08}$	$2.00x10^{-09}$	$5.00x10^{-08}$
Intracellular	66	15.17	$4.60x10^{-11}$	2.408	$2.00x10^{-08}$	$8.00x10^{-09}$	$6.00x10^{-08}$

Transcription factor activity, sequence-specific DNA binding	53	12.18	4.30x10^{-10}	2.593	2.00x10^{-07}	7.00x10^{-08}	6.00x10^{-07}
DNA binding	74	17.01	1.60x10^{-09}	2.079	8.00x10^{-07}	2.00x10^{-07}	2.00x10^{-06}
Zinc finger C2H2-type 16	15	3.448	1.30x10^{-08}	7.454	1.00x10^{-05}	8.00x10^{-07}	2.00x10^{-05}
Alternative splicing	255	58.62	1.80x10^{-07}	1.249	5.00x10^{-05}	6.00x10^{-06}	2.00x10^{-04}
Nucleoplasm	95	21.84	3.80x10^{-07}	1.658	1.00x10^{-04}	5.00x10^{-05}	5.00x10^{-04}
Repressor	32	7.356	5.20x10^{-07}	2.802	2.00x10^{-04}	2.00x10^{-05}	7.00x10^{-04}
Zinc finger C2H2-type 18	10	2.299	4.50x10^{-06}	7.874	0.005	3.00x10^{-04}	7.00x10^{-03}
DNA-templated negative transcription regulation	28	6.437	1.10x10^{-05}	2.610	0.019	6.00x10^{-03}	1.80x10^{-02}
Zinc finger C2H2-type 2; degenerate	10	2.299	1.70x10^{-05}	6.734	0.018	9.00x10^{-04}	2.70x10^{-02}
Cytoplasm	145	33.33	2.20x10^{-05}	1.349	0.008	2.00x10^{-03}	3.00x10^{-02}
Zinc finger C2H2-type 17	10	2.299	3.10x10^{-05}	6.242	0.034	2.00x10^{-03}	4.90x10^{-02}
Isopeptide bond	42	9.655	7.80x10^{-05}	1.923	0.023	2.00x10^{-03}	0.11
Cytoplasm	126	28.97	1.10x10^{-04}	1.356	0.032	3.00x10^{-03}	0.15
Armadillo-type fold	19	4.368	3.10x10^{-04}	2.665	0.202	0.04	0.47
Helicase	11	2.529	4.60x10^{-04}	3.988	0.13	0.01	0.61
Ubl conjugation	53	12.18	6.20x10^{-04}	1.611	0.172	0.01	0.83
Zinc finger C2H2-type 20	6	1.379	6.30x10^{-04}	8.530	0.503	0.03	1.00
DNA damage	17	3.908	1.38x10^{-03}	2.504	0.342	0.03	1.83
Protein transport	24	5.517	1.78x10^{-03}	2.040	0.419	0.03	2.36

Table 3.15: Functional annotation enrichment analysis results for genes associated with PAH. 435/507 PAH-associated genes from RNAseq differential expression analysis were found in DAVID and used for functional characterisation of PAH RNA signature. Gene classes listed by significance (lowest FDR q first).

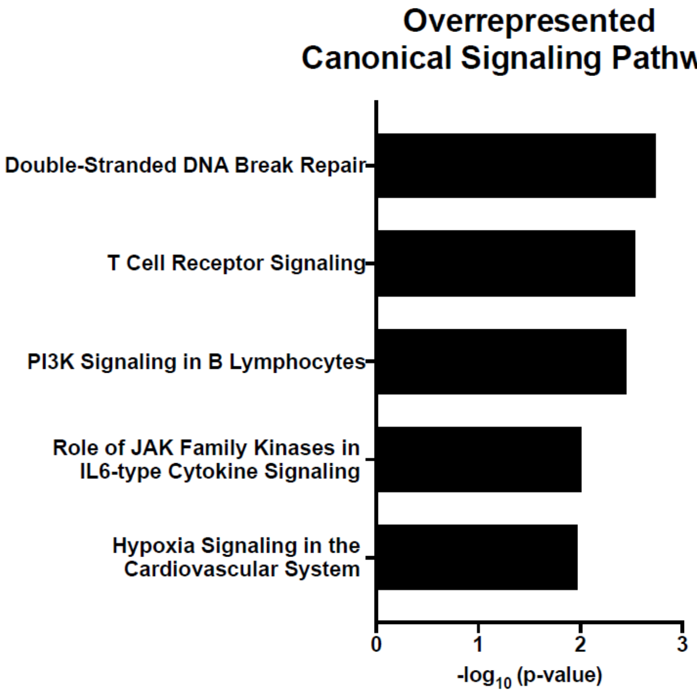

Figure 3.15: Overrepresented canonical signalling pathways in PAH patients. Selected top canonical pathways identified by IPA® through Fisher's exact test (uncorrected p-value < 0.01).

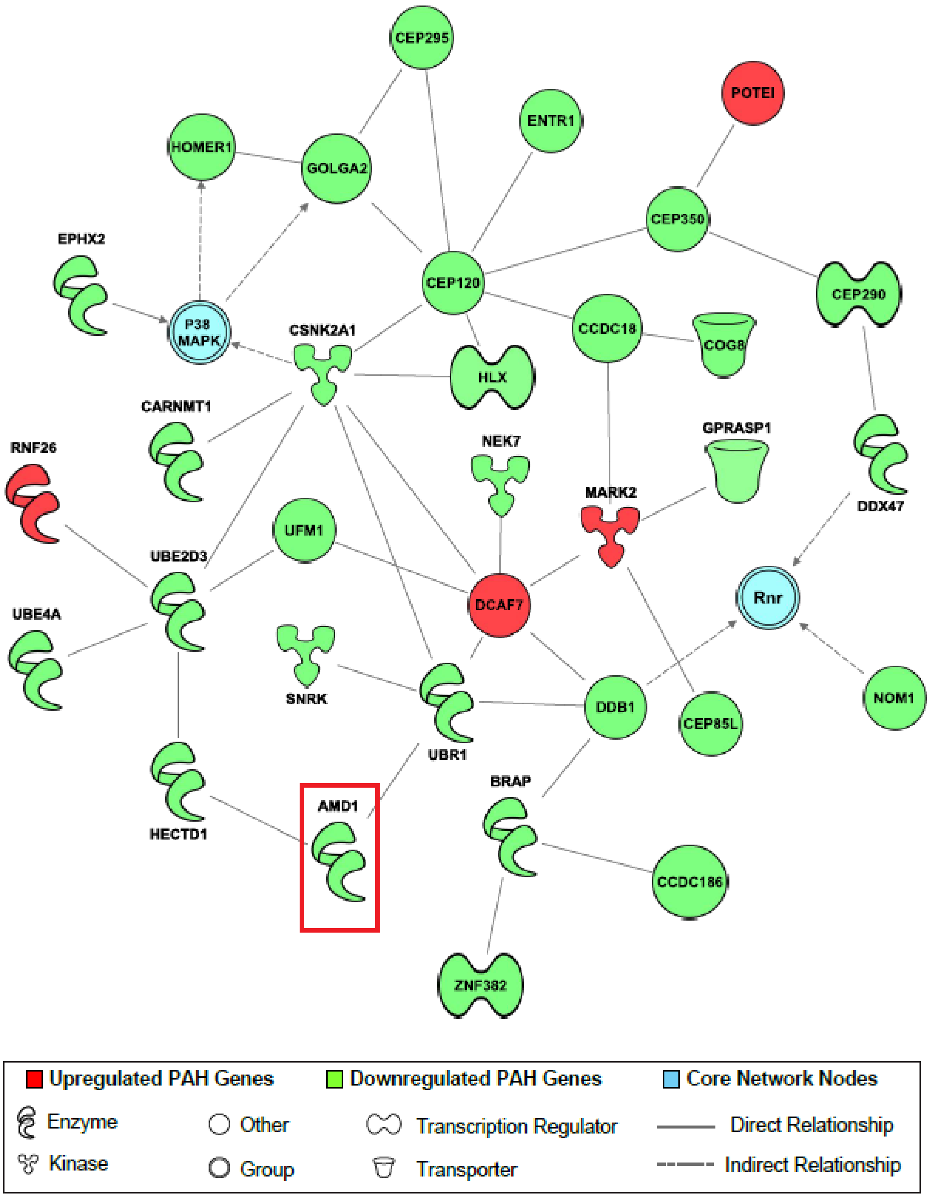

Figure 3.16: Double-stranded DNA break repair gene network. Diagram showing the top dysregulated gene network identified by IPA® from the 507-gene PAH signature. AMD1, a gene previously highlighted in this analysis (see details on Chapter 3.5.6.1), is marked by a red box.

3.5.8 Mendelian randomisation analysis for RNAs associated with PAH pathogenesis

Expression quantitative trait loci (eQTLs) are genetic locations that explain a fraction of the genetic variance of a gene expression phenotype, resulting in different gene expression profiles for that gene depending on genotype. Mendelian randomisation (MR) analyses are used to identify whether a given eQTL is also associated with a different phenotype (other than gene expression levels). In this case, the goal of the study was to test the association between known eQTLs and development of PAH.

We carried out a two-sample mendelian randomisation (MR) analysis testing the association of 293 whole-blood eQTLs (from the total 507 genes in the PAH RNA signature) from two population-based studies and genetic data from a previously published PAH GWAS (see details on Methods 2.1.8). Nominal significance was reached with eQTLs from both datasets for the genes *SMAD5* and *SESN1* (Sestrin-1). There were 11 more genes which reached nominal significance in just one of the two studies while no eQTL for that given gene was included in the other study. There were 15 genes that reached nominal significance in one study but not in the other (Table 3.16, Supplementary tables 6 and 7).

RNAseq gene	Study 1 Gene(s) tested	N SNPs	OR	Sig.	Study 2 Gene(s) tested	N SNPs	OR	Sig.	Max p-value
STAT5A	STAT5A STAT5B	1	16.04	0.016					**0.02**
TYW3	TYW3 CRYZ	1	3.856	0.023					**0.02**
C1orf27	C1orf27	1	0.123	0.023					**0.02**
SESN1	SESN1	2	0.222	0.020	SESN1	1	0.819	0.025	**0.02**
SMAD5	SMAD5	1	0.317	0.012	SMAD5	1	0.883	0.028	**0.03**
ZNF430	ZNF100 ZNF430 LOC400682	5	0.679	0.031					**0.03**
ZNF638	ZNF638	1	8.019	0.032					**0.03**
ZNF577	ZNF577	1	0.123	0.032					**0.03**
LRCH1	LRCH1	1	0.066	0.036					**0.04**
CHP1	CHP1	1	0.111	0.037					**0.04**
SCFD2	SCFD2	1	16.80	0.038					**0.04**
FBLN2					FBLN2	1	1.727	0.039	**0.04**
ZNF28	ZNF468 ZNF28	1	0.565	0.042					**0.04**

Table 3.16: Mendelian randomisation analysis for eQTLs associated with PAH development. Nominally significant results from 2 separate analyses using eQTLs from different studies. N SNPs: number of relevant single nucleotide polymorphisms within that locus. OR: odds ratio for that SNP. Sig.: significance. Max p-value: highest p-value reached for that eQTL in either of the studies. For full list of results see Supplementary Table 6. For full list of eQTLs included in each study see Supplementary Table 7.

When looking at the genes highlighted by the MR study, it was found that, in PAH patients from the PAH RNAseq study, there was in fact a strong association between the *SMAD5* eQTL SNP rs4146187 (gnomAD database allele frequency in non-Finnish European Population = 0.275) and expression levels of *SMAD5* ($p = 3.56 \times 10^{-6}$; Figure 3.17). PAH patients homozygous for the C allele (C/C genotype) had a median *SMAD5* expression 18% lower than that of healthy controls. On the other hand, PAH patients homozygous for the A allele (A/A genotype), showed very similar *SMAD5* expression levels to healthy controls. In the PAH GWAS used for the MR analysis (156), PAH risk was reduced by 8.5% for each A allele copy (odds ratio:0.915, 95% confidence intervals:0.846-0.990, p=0.0266). The A allele was therefore associated with both reduced risk for PAH development and increased SMAD5 expression.

Since the purpose of the MR analysis was to identify potential associations with PAH development, and given the key role of *SMAD5* in BMP/TGF-β signalling (a prominent pathway in PAH pathology; see details on Introduction 1.3.6.1), it was then decided to look at *SMAD5* levels in PAH patients with and without pathogenic *BMPR2* variants. The reduction in *SMAD5* in PAH patients compared with healthy controls occurred similarly for patients both with and without pathogenic *BMPR2* variants (Figure 3.18). BMP/TGF-β pathway signalling is affected regardless of *BMPR2* mutation status (131), which may be why SMAD5 levels were not related to it. This would suggest that impaired BMP/TGF-β pathway signalling is more prevalent in PAH pathology than what rare *BMPR2* mutations could indicate. Additionally, PAH RNA model scores in PAH patients were also higher than those of controls in a similar manner for patients both with and without pathogenic *BMPR2* variants (Figure 3.19).

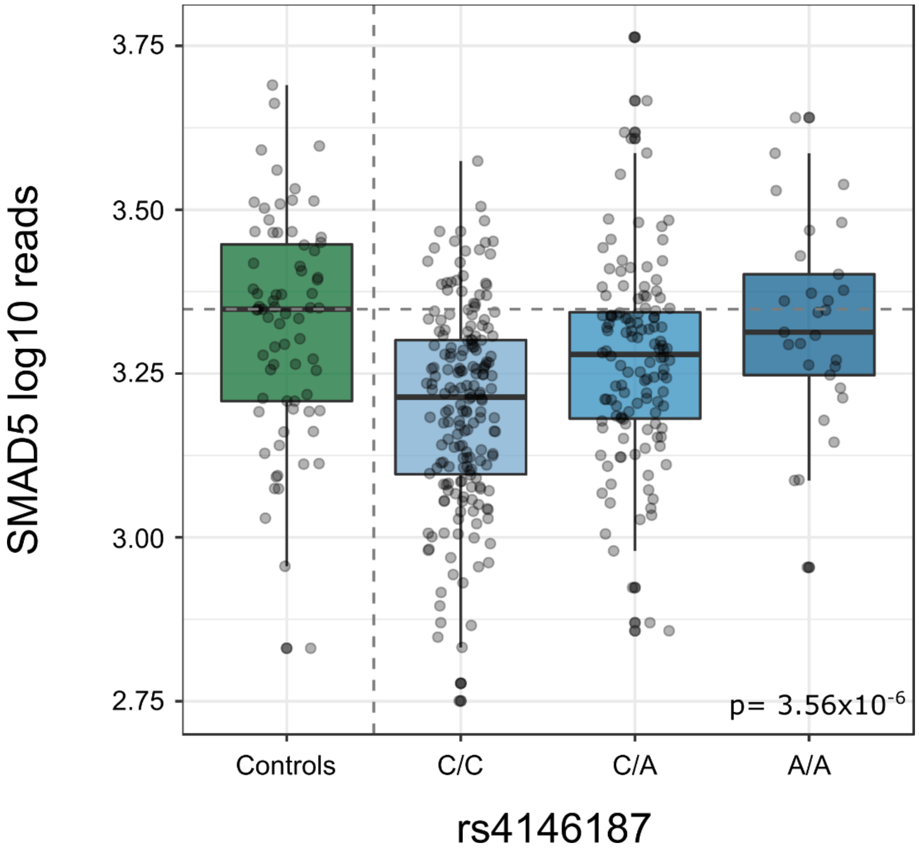

Figure 3.17: SMAD5 expression levels in whole blood RNAseq by eQTL phenotype. Boxplot shows log10 reads in RNAseq analysis for SMAD5 in healthy controls (n= 72) and in PAH patients (n= 359) separated by the SMAD5 eQTL rs4146187 genotype. Genotypes for healthy controls were not available.

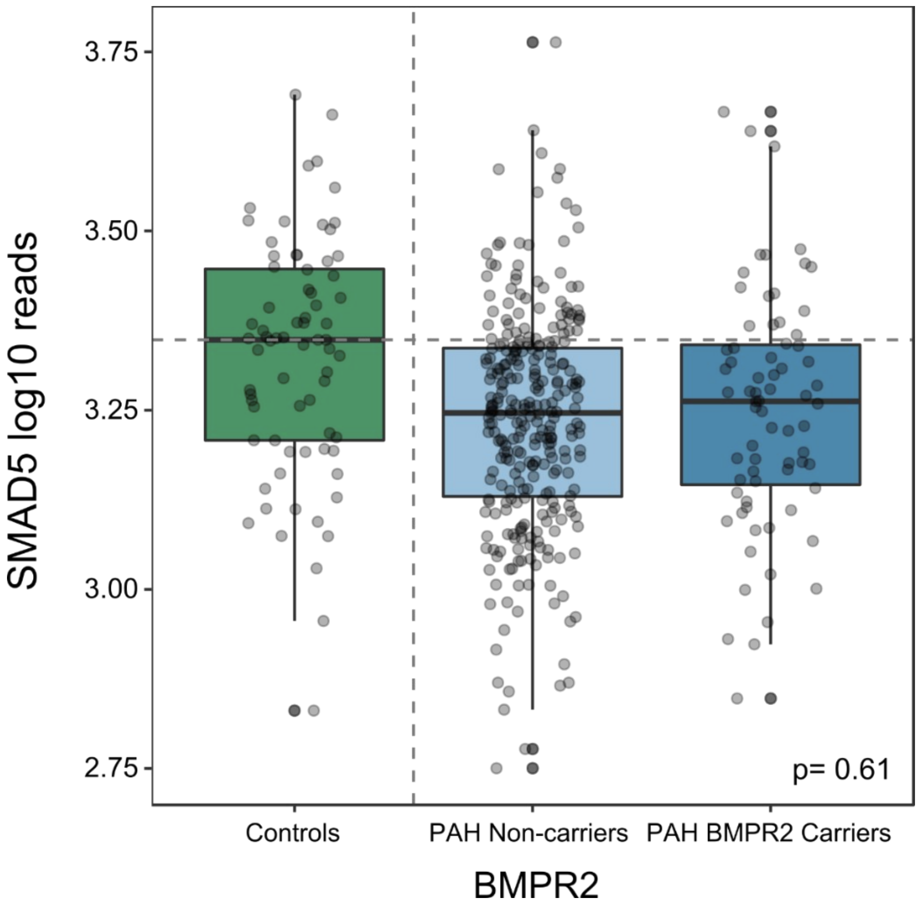

Figure 3.18: SMAD5 expression levels in whole blood RNAseq by BMPR2 mutation status. Boxplot shows log10 reads in RNAseq analysis for SMAD5 in healthy controls (n= 72) and in PAH patients (n= 359) separated by carrier or non-carrier status for known *BMPR2* pathogenic mutations. P value reflects comparison between PAH groups.

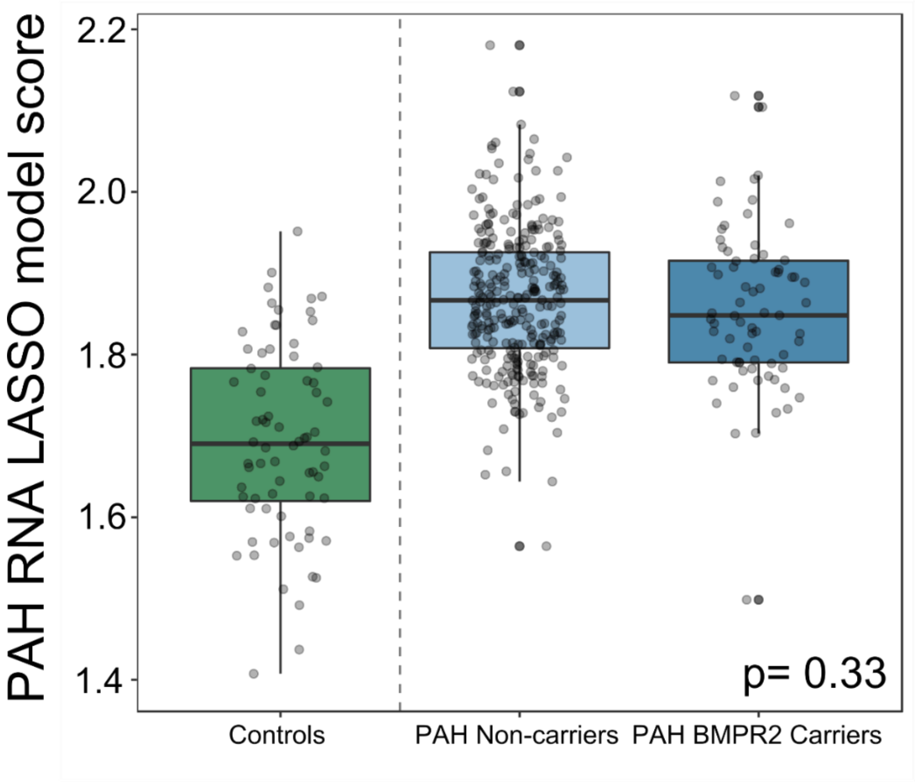

Figure 3.19: PAH RNA model scores by BMPR2 mutation status. Boxplot shows PAH RNA LASSO model scores in healthy controls (n= 72) and in PAH patients (n= 359) separated by carrier or non-carrier status for known *BMPR2* pathogenic mutations. P value reflects comparison between PAH groups

3.5.9 PAH RNA model association with metabolomic profiles

Previous work carried out on samples collected at the same time by other members of the Rhodes lab had produced metabolomic data for 240 individuals from the study cohort. These included 22 healthy controls and 218 PAH patients (165). I used this data to perform clustering analysis combining available data from both the transcriptomics and metabolomics sets. Through this analysis, several groups of metabolites were found to be dysregulated in PAH patients with higher PAH RNA model scores (Figure 3.20).

When trying to correlate levels of gene expression and metabolite levels, indirect correlation of molecules associated with disease will account for some of the hits, but some may be mechanistically linked. It was identified that *MAP3K7CL* (also known as TGF-beta activated kinase) clustered and correlated with dehydroisoandrosterone-sulfate (DHEA-S; Spearman's rho=0.26, p=2.8×10^{-5}) and asparagine (Spearman's rho=0.15; p=0.0179). Additionally, TRPC1 levels significantly correlated with levels of sphingomyelin-d18:1/20:0, d16:1/22:0 (Spearman's rho=0.237, p<0.001). Interestingly, TRPC1 regulates sphingolipids (242) and is itself regulated by sphingosine-1 phosphate (243); while it was previously shown by the metabolomic assays from other members of the Rhodes lab that sphingolipids are dysregulated in PAH (165).

Another finding of the previous metabolomic studies was the identification of a combined metabolite panel of 7 molecules able to effectively distinguish between PAH patients and healthy controls. These metabolites were dehydroisoandrosterone sulfate/DHEA-S, methionine sulfone, N1-methylinosine, oleoylcarnitine, palmitoylcholine, sphingomyelin-d18:1/20:0, d16:1/22:0, unknown metabolite X-24513. When comparing PAH metabolite model scores and PAH RNA model scores, it was observed that 65% of PAH patients demonstrated scores above the identified diagnostic threshold for both omic models, while 30% were negative for either one of them. This combination therefore allowed to identify PAH patients that would be missed if only of the diagnostic models was used in isolation. Furthermore, only 2 healthy controls had a score higher than the diagnostic threshold for at least one of the models (Figure 3.21A). ROC analysis showed the combination of metabolite and RNA scores significantly improved the distinction of PAH from healthy controls by metabolite profiles alone (p= 1.75×10^{-03}, Figure 3.21B).

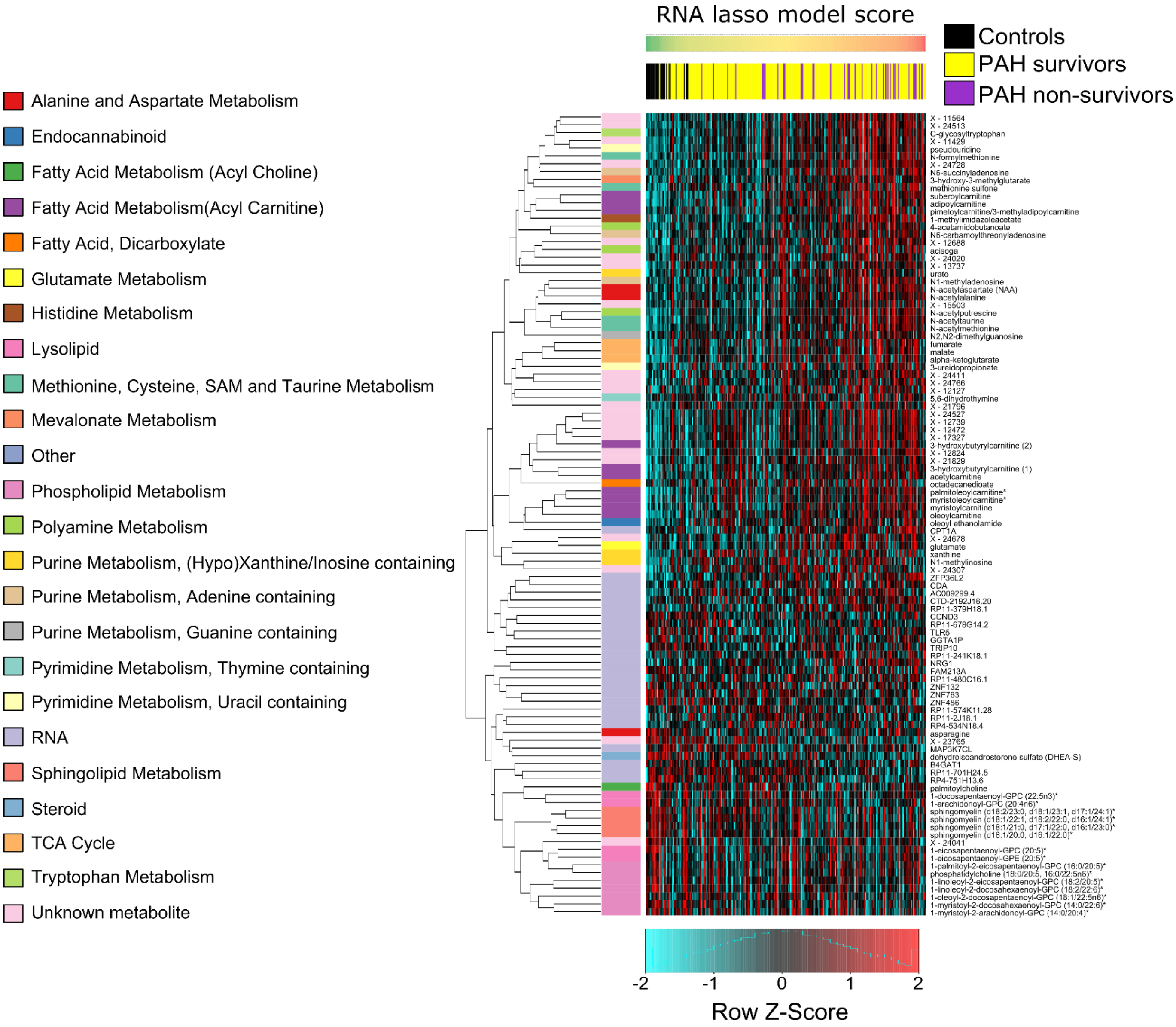

Figure 3.20: Heatmap of metabolite profiles in healthy controls and PAH patients ordered by PAH RNA model scores. The black, yellow and purple-coloured bar at the top indicates which columns relate to controls and PAH patients who survived or did not survive during the follow-up. The RNAs and metabolites were cluster by Euclidean-distance based hierarchical clustering, as shown by the dendrogram, with the coloured bar on the left indicating groups of related metabolites and RNA species.

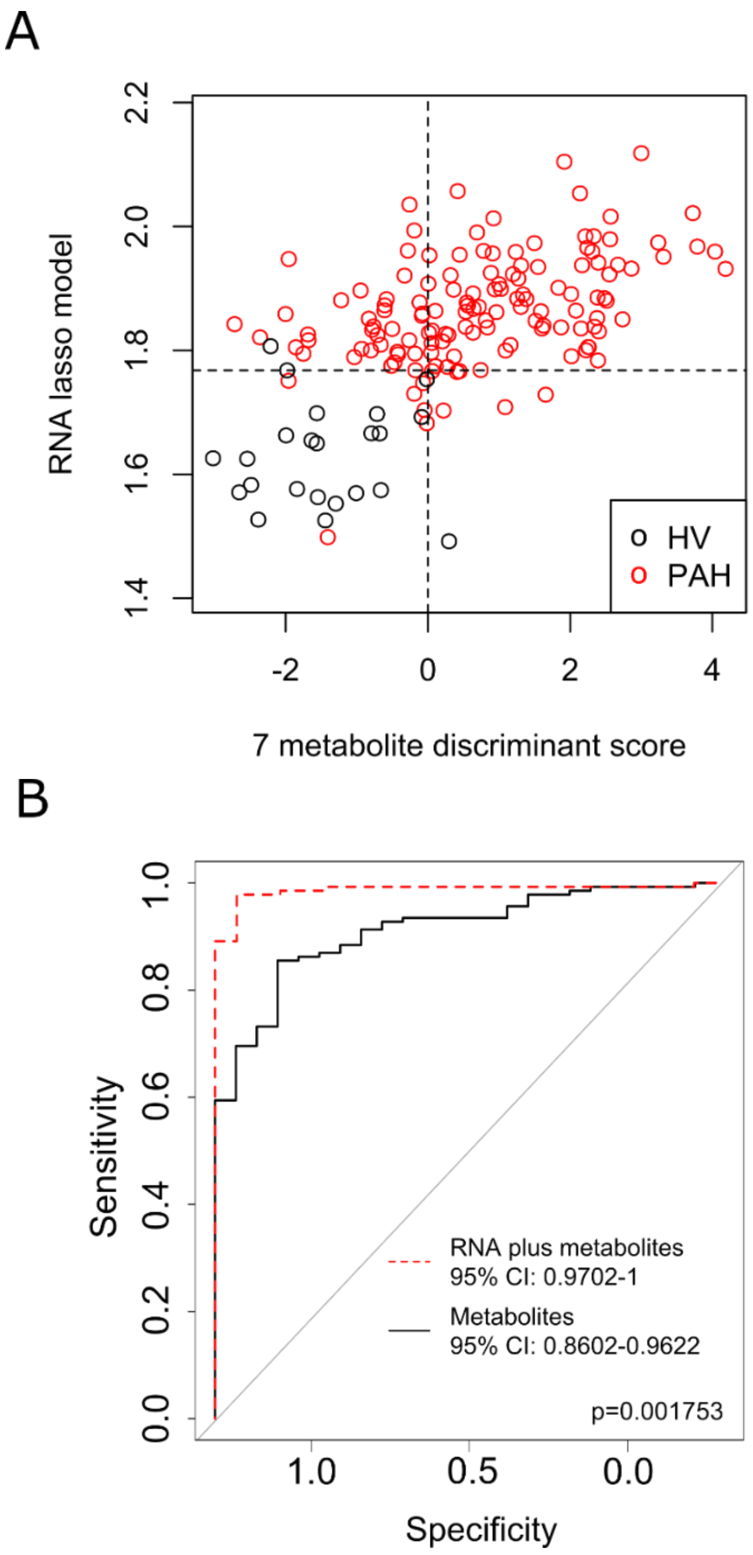

Figure 3.21: Combination of PAH metabolite and RNA diagnostic models. **A**) Scatter plot of metabolite and RNA diagnostic scores in healthy controls (HV) and PAH patients. Upper-left and lower-right quadrants contain individuals positive for only one of the two scores, which may be better identified by the combination of both profiles. **B**) Receiver operating characteristic (ROC) curve illustrating the ability of the combined metabolite and RNA score versus metabolite score alone in distinguishing PAH from controls. Significance shown from De Long test for comparing ROC curves.

3.6 Discussion

The first aim of the work presented in this chapter was to assess differences in gene expression profiles between PAH patients and healthy controls by performing whole blood RNAseq followed by differential expression analysis. A signature of 507 RNAs associated with PAH has been identified, optimised and validated in this study. Identification of RNAs was performed through two independent differential expression analyses and only transcripts significant ($p < 0.05$) in both and directionally consistent were considered. Furthermore, only those transcripts also meeting FDR corrected significance ($\alpha < 0.1$) in a further differential expression analysis combining both groups were considered for downstream analyses.

An important limitation of whole blood transcriptomics is the mix of white blood cell populations in blood samples, introducing high levels of variability in transcripts that differ across PBMCs. Furthermore, there is existing evidence suggesting certain PBMC populations have altered numbers in PAH patients (244–247). RNA signature optimisation using established white blood cell deconvolution methodologies (222,223) was therefore performed and identified specific white blood cell type fractions associated with PAH and included those PBMC profiles as covariates in the differential expression analysis to correct for potential confounding effects. Only transcripts meeting inclusion criteria in analyses both including and not including WBC fractions were further considered, resulting in the final 507 gene list of dysregulated expression in PAH. Interestingly, numbers of CD8-positive T-cells and regulatory T-cells were found to be dysregulated in PAH patients, which is consistent with previous reports (245,246). There is, however, an ongoing debate over the specific changes in PBMC fractions occurring in PAH, potentially due to differing experimental approaches and PBMC classification (247).

RNA signature validation procedures included technical validation of RNAseq methodology through correlation analysis of RT-qPCR results using the same whole blood samples, which showed high levels of correlation between assays; and external validation through comparison with two independent studies, a meta-analysis of PAH transcriptomic studies using whole blood samples from patients (237) and a microarray analysis of lung tissue isolated from PAH patients (184). The external validation process showed that 118/416 (28.4%) genes from the PAH RNA signature present in the meta-analysis of whole blood studies in PAH (237) and 41/372 (11.0%) genes from the PAH RNA signature present in the PH lung tissue microarray study (184) were found to be significantly dysregulated and directionally consistent. A Fisher's exact test showed that this overlap was significantly higher than what would be expected by chance, supporting the robustness of these findings. When results from those analyses were validated using results from the current PAH RNA differential expression analysis, 206/1087 (19.0%) genes from the meta-analysis of whole blood studies in PAH (237) present in the PAH RNA signature and 118/777 (15.2%) genes from the PH lung tissue microarray study (184) present in the PAH RNA signature were found to be significantly dysregulated and directionally consistent. Again, high levels of agreement were identified, particularly between analyses of PBMCs. Lower agreement with assays performed on lung can be accounted by the inherent differences in tissues analysed and proximity to the site of injury.

The polyamine biosynthesis intermediate enzyme AMD1 was the only gene consistently dysregulated (downregulated in PAH patients) in both independent studies and the current PAH dataset. AMD1 controls polyamine biosynthesis through regulation of decarboxylated S-adenosylmethionine supply.

Its action is itself regulated by mRNA translation inhibition by spermine and spermidine and by polyamine-mediated protein degradation (248). A previous metabolomic study by members of the Rhodes lab highlighted the association between high levels of certain circulating polyamines, such as N-acetylputrescine, 4-acetamidobutanoate and acisoga, and poor prognosis in PAH patients (165). These findings starkly contrast with evidence of mice exposed to hypoxia. Increased *Amd1* expression was observed in hypoxic mice, while both an AMD1-inhibitor (SAM486a) and a haploid knock-out of AMD1(+/-) showed partial protection against hypoxic PH development (249). Incidentally, expression levels of the transient receptor potential channel TRPC1, also found in this study to be downregulated in PAH patients and suspected of playing a role in hypoxia-induced PAH (see details on Introduction 1.3.5), were also elevated in mice exposed to hypoxia (98). These differences may arise from the inherent limitations of current hypoxic mice models of PAH previously discussed in this thesis (see details on Introduction 1.3.4). Additionally, previously discussed rare mutations in the polyamine-metabolism-related ATP13A3 (see details on Introduction 1.3.6.2), involved in apoptosis and proliferation (150), further support the need for further research conducted into polyamine metabolism in PAH.

Other datasets could be used for further validation of the data and analysis presented here, such as a recent study that investigated transcriptional changes in hMVECs and PASMCs between PAH patients and healthy controls through RNAseq (250). Signatures of 1008 DEGs in hMVECs and of 229 DEGs in PASMCs between PAH patients and healthy controls were identified ($p \leq 0.0001$); and associated with barrier function and vascular permeability in hMVECs and energy-driven proliferation in PASMCs. Studying the overlap of these signatures with the data here presented could through further insights into the specific molecular mechanisms affecting each relevant cell type in PAH pathology.

Overall, a 507 RNA signature for PAH was identified through RNAseq and differential gene expression analysis; optimised through PBMC deconvolution; validated technically through RT-PCR and by using other, independent studies; highlighted mechanisms potentially implicated in PAH pathology; and was put forward for downstream analysis. A potential limitation of this analysis is the predominantly white population cohort (314/359 patients; 87.5%) from which samples were gathered. Evidence has shown variability in PAH prevalence and presentation across different populations (9), so a similar study utilising different ethnicities may reflect different changes occurring in different kinds of PAH patients.

The second aim was to develop an RNA model for PAH using the results derived from the differential expression analysis. LASSO regression modelling was used to generate a 25 RNA model using the combined sample group from the differential expression analysis which was tested on an independent group. The PAH RNA model showed it was able to effectively separate between PAH patients and healthy controls. When the model was validated using 20 randomly generated models using RNAs from the PAH signature, the mean AUC from these models (0.679) was over 20% lower than the AUC for the PAH RNA model (0.868). These results suggest LASSO regression modelling was an effective method of developing a PAH diagnostic model based on results from the differential expression analysis.

Alternative modelling approaches, such as standard multiple linear regression, Ridge regression or random forest, could be used for further validation of model results. There are, however, several benefits to performing LASSO regression as the primary modelling approach in the current study over the alternatives. These benefits include the regularisation of LASSO accounting for the inherent multicollinearity found in gene expression profiles due to linkage disequilibrium and signalling pathway interaction and thus preventing data overfitting observed when using regular multiple linear regression (229). L1 regularisation in LASSO regression (shrinking parameters to 0) is also more optimal in this setting than the L2 regularisation occurring in Ridge regression (reducing parameters without eliminating them), as it performs better at variable selection and is more robust to outliers (229). Finally, LASSO regression generally performs better at variable selection than random forest (251,252), although a combined LASSO-random forest model has been suggested as a potential improvement (252). Another important method of approaching this type of transcriptomic data is unsupervised clustering, which attempts to discover the "natural" groupings arising from transcriptional changes across patients (253). This work, however, was carried out in tandem to the work presented here by another research team at the University of Sheffield. They identified and validated the existence of three major transcriptional subgroups of PAH patients that accounted for over 90% of individuals. These subgroups were associated with prognosis, ranging from good, to moderate and bad. The worst prognosis correlated with an upregulation of ALAS2 and downregulation of several immunoglobulin genes. The subgroup presenting with best prognosis was associated with upregulation of the bone morphogenetic protein signalling regulator NOG, and the C/C variant of HLA-DPA1/DPB1 (independently associated with survival)(254).

The third aim was to use the model to evaluate the association between PAH gene expression profiles and different clinical features. The model was tested on all PAH patients from the study combined and showed a strong association with survival, WHO functional class and levels of cardiac biomarkers. The ability of the RNA model to effectively identify PAH patients and stratify them according to clinical features adds plausibility to the association of the identified gene expression profiles with PAH pathology. Additionally, these associations suggest RNA profiling could be used to identify PAH patients which may require a more aggressive treatment strategy or give priority in clinical trials to those PAH patients with higher likelihood to have events increasing statistical power. Furthermore, levels of 3 lncRNAs found to be downregulated in PAH patients associated with poor prognosis and could be used to separate patients by survival. These RNAs have not been extensively studied and had not been previously implicated in PAH pathology. They are believed to play a role in regulating small nuclear ribonucleoprotein-associated protein N—which plays a role in pre-mRNA processing, may contribute to tissue-specific alternative splicing and has been associated with the rare Prader Willi Syndrome (255)—, protein tyrosine phosphatase PTP4A2—which regulates the activity of several protein tyrosine phosphatases (256)—and lysosomal proton pump protein ATP6V0E2—critical for maintaining lysosomal function, autophagy, and degradation of oxidized low-density lipid protein (257)—, but their specific features have not yet been identified. Their strong association with survival in PAH suggests further research could provide useful insights into PAH pathology and treatment.

Contrasting with previous reports, however, no consistent differences in gene expression were observed between vasoresponsive and non-vasoresponsive PAH patients, and none of the genes previously suggested to be associated with vasoresponsivity were found to be different either (176). The number of PAH patients included in this study, 359, is close to an order of magnitude larger than most other PAH transcriptomic studies (171–173,175,176). This helps increasing statistical power and hence the confidence of results obtained. Previous reports relied on much smaller numbers of PAH patients. External validation of the results reported here with other PAH transcriptome studies further supports the robustness of the methodology utilised for this study.

The fourth aim was to find evidence of PAH pathogenic dysregulations of specific genes or signalling pathways, which was done through functional characterisation and mendelian randomisation analysis. Functional characterisation of 507 PAH RNA signature using DAVID (240) and IPA® (241) highlighted transcription factors, such as KLF10 and HIF1α, as the main class of genes associated with PAH; featured signalling pathways such as hypoxia signalling, PI3K signalling in B lymphocytes, the role of JAK family kinases in IL6-type cytokine signalling, double-stranded DNA repair and T-cell receptor signalling; and highlighted the polyamine biosynthesis intermediate enzyme AMD1, which was also the only significantly dysregulated gene meeting FDR corrected across all analyses in the PAH signature external validation and has been discussed above.

Mendelian randomisation is a powerful tool to identify potential pathogenic gene dysregulation, as it connects variants associated with expression levels of a gene with independent genome-wide association studies (GWAS) identifying that gene as associated with the disorder. The two-sample mendelian randomisation analysis performed here, using publicly available data from a published international GWAS (156) and eQTLs from two large studies on whole blood RNA (232,233), highlighted an eQTL for the gene SMAD5 as associated with PAH. These findings potentially implicate SMAD5 in the pathogenesis of PAH and are in line with the known role of SMAD5 as a downstream signal mediator of BMPR2 ligand binding activation. The relevance of BMPR2 and the associated BMP/TGF-β signalling pathway in PAH is extensively covered in Introduction 1.3.6.1. Furthermore, levels of SMAD5 were also associated with SMAD5 eQTL SNP genotype in PAH patients and were independent of *BMPR2* mutation status. This is of particular interest, as SMAD5 plays other non-BMPR2-related roles, such as mediating the response to intracellular pH level changes (258), its direct interaction with hexokinase to increase glycolysis (258) and the regulation of the master iron regulator hepcidin (259) which is believed to be elevated and promote iron deficiency (associated with poor clinical prognosis) in PAH (260). It could be of great benefit to utilise genes with known eQTLs to stratify PAH patients and identify those more likely to show a positive response to therapeutic approaches targeting specific mechanisms. More specifically, SMAD5 levels or SMAD5 eQTL phenotype could be used to determine which patients may respond to novel therapies targeting the BMP/TGF-β signalling pathway, such as the TGF-beta ligand trap, Sotatercept (261). Overall, findings in this study suggest SMAD5 dysregulation may be implicated in PAH pathogenesis and highlight SMAD5 as a potential biomarker for BMP/TGF-β signalling pathway dysfunction in PAH.

The fifth and final aim was to create a combined omics diagnostic panel to improve upon the results obtained from transcriptomic analyses alone. A combination of current differential expression results and a prior analysis of PAH metabolomics carried out by the Rhodes lab showed there was an association between PAH RNA model scores and metabolite levels. Furthermore, the combination of a 7-metabolite panel able to effectively distinguish between PAH patients and healthy controls and the 25-transcript PAH RNA model significantly improved the diagnostic power of each individual panel alone. These results suggest the creation of a full-omics panel (integrating transcriptomics, metabolomics, proteomics, genomics and epigenomics) could provide with even greater granularity in PAH stratification and provide further insights into the pathologic molecular interplay underlying PAH pathology.

Furthermore, the recent successful use of platelet transcriptomics in pulmonary hypertension, with the identification of a platelet-derived predictive 408-gene PH RNA signature able to differentiate PH patients from healthy controls (262), adds another potential layer to the combined omics approach and suggests there is potential for a multi-layered transcriptomics approach in PAH, combining gene expression profiles from PBMCs, platelets and vascular cells. These multi-layered and multi-omics approaches, however, would incur high costs and take a great amount of time.

Overall, a 507-gene RNA signature separating PAH patients from healthy controls was identified, optimised and validated in this study. This signature was also found to be associated with survival and several metrics of disease progression, but not with vasoresponsivity. SMAD5 was found to be potentially implicated in PAH pathogenesis through integration of transcriptomics and genomics data, and integration with metabolomics data showed increased diagnostic power and highlighted the potential of combined omics for PAH research. The role of post-translational modifications in PAH pathogenesis, however, was not evaluated in this study and could provide with further insights into PAH molecular mechanisms. Furthermore, all patients from the study presented with idiopathic, heritable or drug-induced forms of PAH, so assessing gene expression changes in other PAH presentations or similar cardiovascular disorders (PH Groups II-IV or other diseases altogether) may be of interest to further characterise the identified PAH RNA signature. The number of healthy controls (n=24 per group) used in this study was also relatively low when compared to the number of PAH patients (n= 119/120 per group), which could impact and skew the healthy signature for the study. Nonetheless, this was done under the assumption that there may be less variability within healthy individuals in the genes affected by PAH pathology, so a lower number of controls may not affect the study outcome negatively. High levels of heterogeneity in results from PAH patients could also be observed throughout this study and reflect the highly heterogenous profile in PAH that greatly complicates accurate diagnosis and clinical treatment. This highlights the paramount relevance of finding better ways to characterise the underlying molecular pathology in PAH and improve our ability to stratify patients and optimise their treatment. It would therefore be of great importance for further mechanistic research to investigate the transcripts and pathways highlighted in this analysis.

4 - Whole Blood RNAseq of PH Patients and Disease Controls: Identification of a PH-Specific RNA Signature

4.1 Introduction

In our prior PAH RNAseq study, gene expression levels in whole blood samples from 359 PAH patients were compared with those from 72 age- and sex-matched healthy controls (see details on Chapter 3). In this analysis, a whole blood PAH RNA signature was identified, optimised, validated, and thoroughly characterised. This signature included RNAs relevant to disease pathogenesis, was associated with disease severity and identified patients with poor clinical outcomes.

An inherent limitation in the design of this PAH RNAseq study is the vastly different phenotypic profile between the severely ill PAH patients and the healthy volunteers used as controls. Such dramatic differences may result in an unspecific, generic "diseased" RNA signature being detected in the differential expression analysis. This unspecific RNA signature could potentially lack the nuance and power to separate pathogenic or disease-specific elements from the downstream, more generic effects of being as severely ill as PAH patients are.

For that reason, it was decided to perform an analysis more sensitive to the specific characteristics of PAH and assess the differences in gene expression that may exist between different forms of PH (with PAH being PH Group I). This analysis would also attempt to identify gene expression differences between PH patients and other patients suffering from other similar cardiovascular disorders (see details on Methods 2.2.1 and Table 2.3). These other patients (referred to as "disease controls" from this point onwards; DCs) were patients originally thought to potentially suffer from PH due to their symptomatic panel, which were then determined not to have PH at the expert PH clinic at Hammersmith Hospital, London. A new cohort was used for this analysis, which included a total of 147 PH patients from the PH spectrum—47 PAH (PH Group I), 36 PH-LHD (PH Group II), 16 PH-LD (PH Group III) and 48 CTEPH (PH Group IV)—and 45 disease controls.

Firstly, the performance of the whole blood PAH RNA LASSO model—developed on the cohort of 359 PAH patients and 72 healthy controls—was tested in this cohort to evaluate whether it was able to also distinguish between PAH patients and disease controls. This also allowed assessment of whether the model was able to distinguish between different PH diagnostic subgroups (PH Groups I-IV).

Next, three independent differential expression analyses were carried out in this cohort comparing different patient subgroups in order to newly identify genes best able to distinguish between PH groups (PH Group I vs. PH Groups II-IV) as well as between PH patients (either PH Group I or PH Groups I-IV) and disease controls (see details on Chapter 4.4.1).

4.2 Hypotheses

- The PAH RNA model identified in a cohort of PAH patients and healthy controls is able to distinguish between PAH, other forms of PH and other symptomatic individuals.
- There is an RNA signature distinguishing PAH patients (PH Group I) from other forms of PH (PH Groups II-IV).
- There is an RNA signature distinguishing PAH patients (PH Group I) from disease controls.
- There is an RNA signature distinguishing PH patients (PH groups I-IV) from disease controls.

4.3 Aims

- To evaluate the ability of the previous PAH RNA model to separate between PAH patients, PH patients and patients with other cardiovascular disorders.
- To identify blood RNA profiles separating PAH/PH patients and other symptomatic patients.
- To develop diagnostic models based on those RNA profiles.
- To find evidence of potential pathogenic pathway dysregulations in PH RNA profiles.

4.4 Methods

4.4.1 Study design

The study cohort included patients from PH groups I-IV, namely 47 PAH (PH Group I), 36 PH-LHD (PH Group II), 16 PH-LD (PH Group III) and 48 CTEPH (PH Group IV); and 45 disease controls. Three differential expression analyses were carried out assessing gene expression differences between the following groupings (Table 4.1):

A) PAH patients (PH Group I; n= 47) and other PH patients (PH Groups II-IV; n= 100).
B) PAH patients (PH Group I; n= 47) and disease controls (n=45).
C) All PH patients (PH Groups I-IV; n= 147) and disease controls (n= 45).

	Disease controls	**PH patients**				**Total control group**	**Total test group**
		Group I PAH	Group II PH-LHD	Group III PH-LD	Group IV CTEPH		
A: PAH vs PH	-	47	36	16	48	100	47
B: PAH vs DCs	45	47	-	-	-	45	47
C: PH vs DCs	45	47	36	16	48	45	147

Table 4.1: Number of subjects per study group in cohort of PH patients and disease controls. Different groupings and subject counts relevant to downstream analyses have been highlighted. Samples used as controls in each analysis are highlighted in yellow. DCs: disease controls.

Subjects from each analysis were divided into study groups, but the more limited number of samples was unlikely to be sufficiently powered for a division into three groups as in the PAH RNAseq analysis (see details on Chapter 3.4.1). Therefore, in each of the three differential expression analyses, subjects were divided into just Discovery (2/3 of samples) and Validation (1/3 of samples) groups to maximise the number of subjects per group, with an emphasis on Discovery where all genes would have to be analysed, versus Validation where only smaller numbers of genes and the models would need to be sufficiently powered. Directionally consistent, differentially expressed ($p < 0.05$) genes from each analysis in both Discovery and Validation groups were identified and highlighted. Highlighted genes which met false discovery rate (FDR) corrected significance ($\alpha < 0.05$) in the combined analysis (combined Discovery and Validation, including all samples) were put forward for the generation of a predictive LASSO RNA model on the Discovery group which was then tested on the Validation group (Figure 4.1).

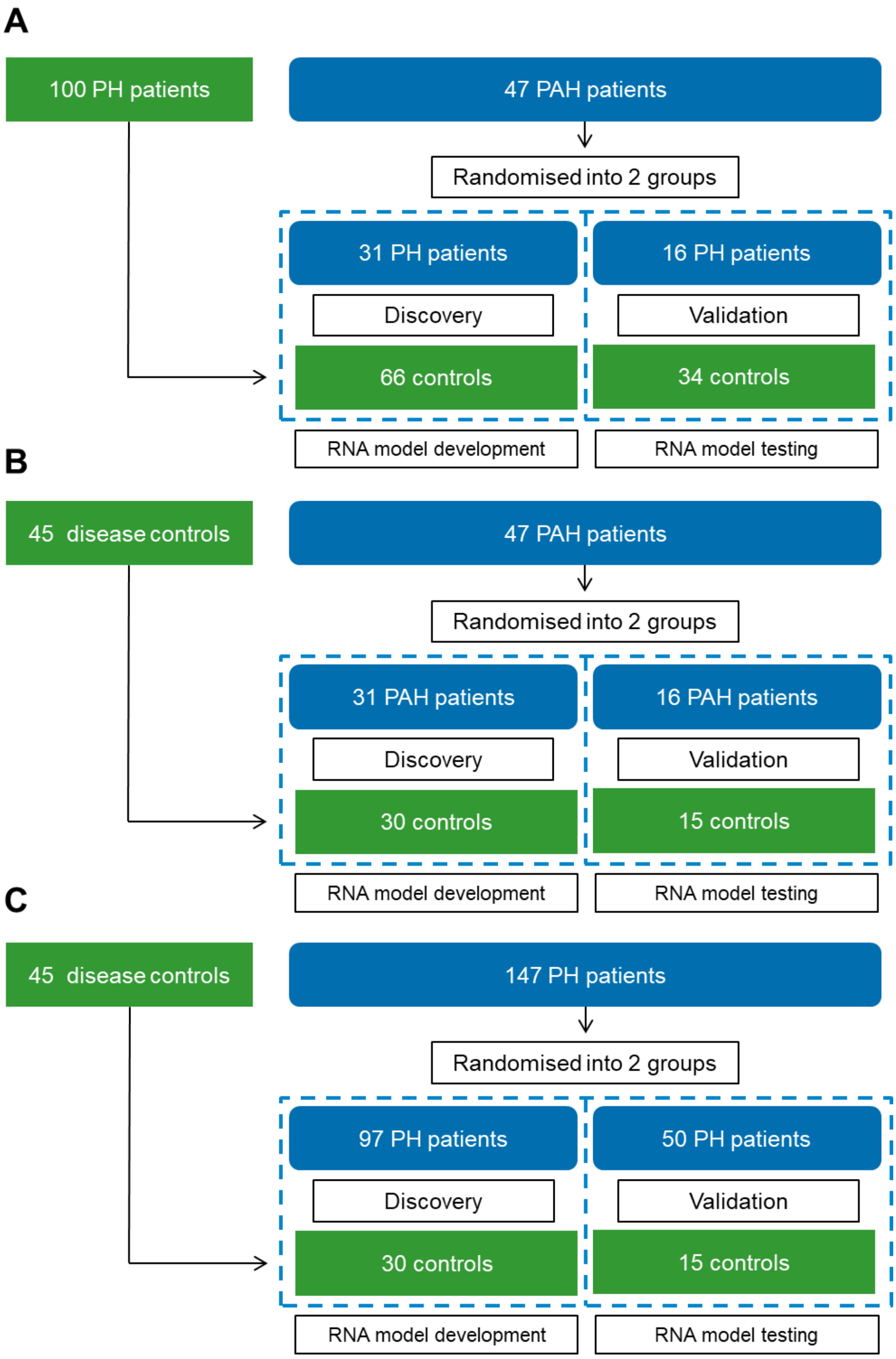

Figure 4.1: Study design for three distinct analyses of an RNAseq in a cohort of PH patients and disease controls. Study design in a cohort including patients from PH Groups I-IV (47 PAH, 36 PH with Left Heart Disease, 16 PH-Lung Disease and 48 Chronic Thromboembolic PH respectively). Three differential expression analyses were carried out on different sample subgroupings divided into Discovery (2/3 of samples) and Validation (1/3 of samples). Discovery group results were used for RNA model development, which was tested in the corresponding Validation groups. These subgroupings included **A**) PAH vs PH patients, **B**) PAH patients vs disease controls and **C**) PH patients vs disease controls. Disease controls are patients originally thought to suffer from PH but eventually diagnosed with a different cardiovascular pathology.

4.5 Results

4.5.1 Testing previous PAH RNA LASSO model in this new cohort

No significant differences between disease controls and any of the PH subgroups were identified in this analysis. PAH RNA model scores were also similar in patients from different PH diagnostic groups (Figure 4.2). These results contrasted with those obtained when the PAH RNA model was applied to an independent group of PAH patients (n= 119) and healthy controls (n=24), where the model was able to accurately distinguish between PAH patients and healthy controls (p= 1.39×10^{-8}; AUC= 0.868; see details on Chapter 3.5.4).

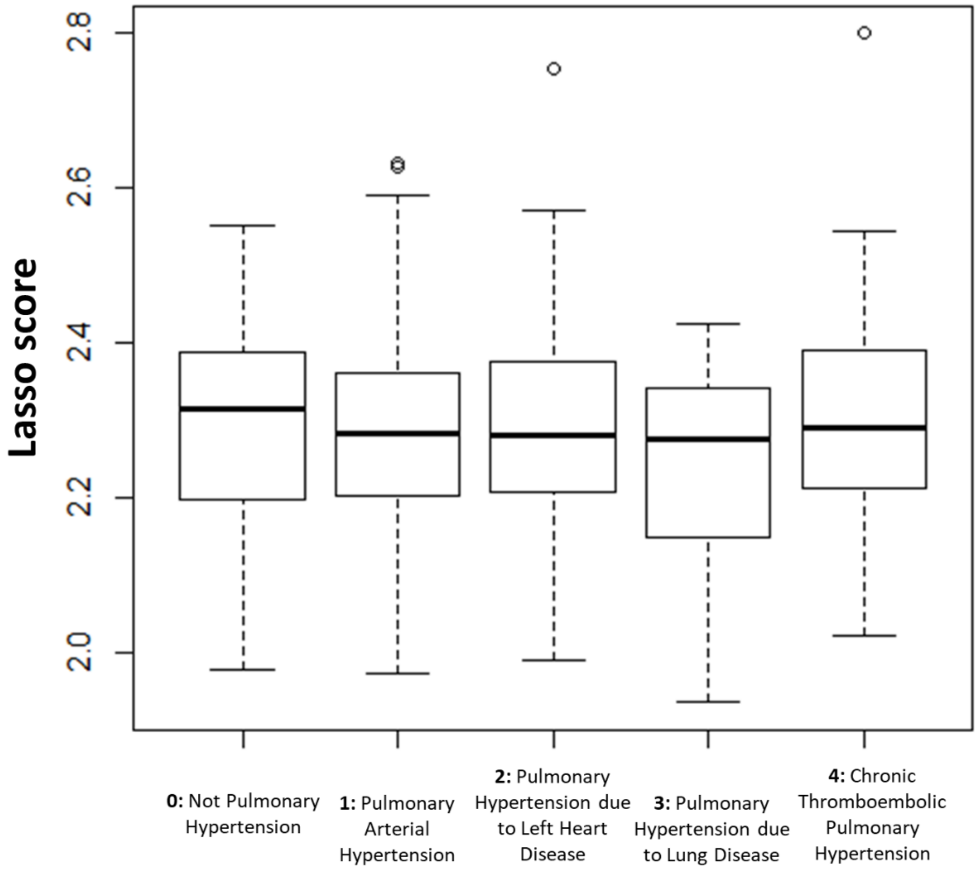

Figure 4.2: PAH RNA LASSO model performance in a cohort including PH patients from groups I-IV. Groups are **0**) Disease controls (n= 45), **1**) PAH (n= 47), **2**) PH-LHD (n= 36), **3**) PH-LD (n= 16) and **4**) CTEPH (n= 48). Disease controls are patients originally thought to potentially suffer from PH due to their symptomatic panel, which were then determined not to have PH.

4.5.2 Differentially expressed RNAs across different groups of patients

Independent differential gene expression analyses were carried out in both Discovery and Validation groups for each of the three RNAseq analyses of PAH (PH Group I; n= 47) vs. other PH (PH Groups II-IV; n= 100), PAH (PH Group I; n= 47) vs. DCs (n= 45) and all PH (PH Groups I-IV; n= 147) vs. DCs (n= 45) (see details on Chapter 4.4.1). There were 276 RNAs found to be significantly different ($p < 0.05$) and directionally consistent across Discovery and Validation groups between PAH and PH patients. Out of these 276 RNAs, 253 met multiple testing false discovery rate (FDR) corrected significance ($q < 0.05$) in the combined (Discovery plus Validation) analysis (Figure 4.3, Table 4.2 and Supplementary Table 8). When comparing PAH patients against DCs, there were 770 differentially expressed ($p < 0.05$), directionally consistent RNAs, with 727 of them meeting FDR ($q < 0.05$) in the combined analysis (Figure 4.4, Table 4.3 and Supplementary Table 9). When all PH patients were compared with DCs, 159 differentially expressed ($p < 0.05$), directionally consistent RNAs were found, with 87 of these meeting FDR ($q < 0.05$) in the combined analysis (Figure 4.5, Table 4.4 and Supplementary Table 10).

When comparing lists of most significantly dysregulated genes across analyses, only three genes— namely ZNF254, PPA2 and SEC22B— were found to be different in PAH both when compared to other PH forms (Supplementary Table 8) and with DCs (Supplementary Table 9), all of them downregulated in PAH. Both ZNF254 and PPA2 were also found to be downregulated in PAH patients in the whole blood PAH RNA signature (see details on Chapter 3). ZNF254 is a zinc-finger which has been previously implicated in ovarian cancer (263). PPA2 encodes an enzyme that catalyses inorganic pyrophosphate hydrolysis and plays a key role in the regulation of mitochondrial membrane potential and mitochondrial organization and function (264). It has been implicated in sudden infant cardiac arrest (265) and kidney renal clear cell carcinoma (264). Most interestingly, SEC22B encodes a member of the SEC22 family of proteins thought to play a role in membrane fusion of vesicle trafficking between the endoplasmic reticulum and the Golgi apparatus, antigen cross-presentation, secretory autophagy, and other biological processes (266), and will be later discussed.

There were also three genes which levels stratified between different groups—namely CAMKMT, EDEM1 and FER (Supplementary Tables 9 and 10)—. This may reflect pathways specific to PAH pathology, especially since DCs show a more similar gene expression to PAH than other PH forms. CAMKMT was also downregulated in PAH patients in the whole blood PAH RNA signature. Calmodulin lysine methyl transferase (CAMKMT) is an enzyme that trimethylates Lys-115 in calmodulin—a key mediator of calcium-dependent signalling—that has been shown to be required for growth, muscle strength, somatosensory development and brain function (267). CAMKMT was downregulated in PAH patients when compared with DCs (average logFC= -0.158) and upregulated in all PH when compared with DCs (average logFC= 0.124). The endoplasmic reticulum degradation-enhancing α-mannosidase-like protein 1 (EDEM1) plays a role in misfolded protein degradation by extracting terminally misfolded proteins from productive folding cycles (268), has been associated with Alzheimer's disease (268) and implicated in several types of cancer (269,270). EDEM1 was upregulated in PAH patients when compared with DCs (average logFC= 0.138) and downregulated in all PH when compared with disease controls (average logFC= -0.083). The feline sarcoma-related (FER) gene is a member of the FPS/FES family of non-transmembrane receptor tyrosine kinases. It regulates cell-cell adhesion and mediates cell signalling via growth factor receptors (271). It was downregulated in PAH patients when compared with DCs (average logFC= -0.133) and upregulated in all PH when compared with DCs (average logFC= 0.084). It will also be later discussed.

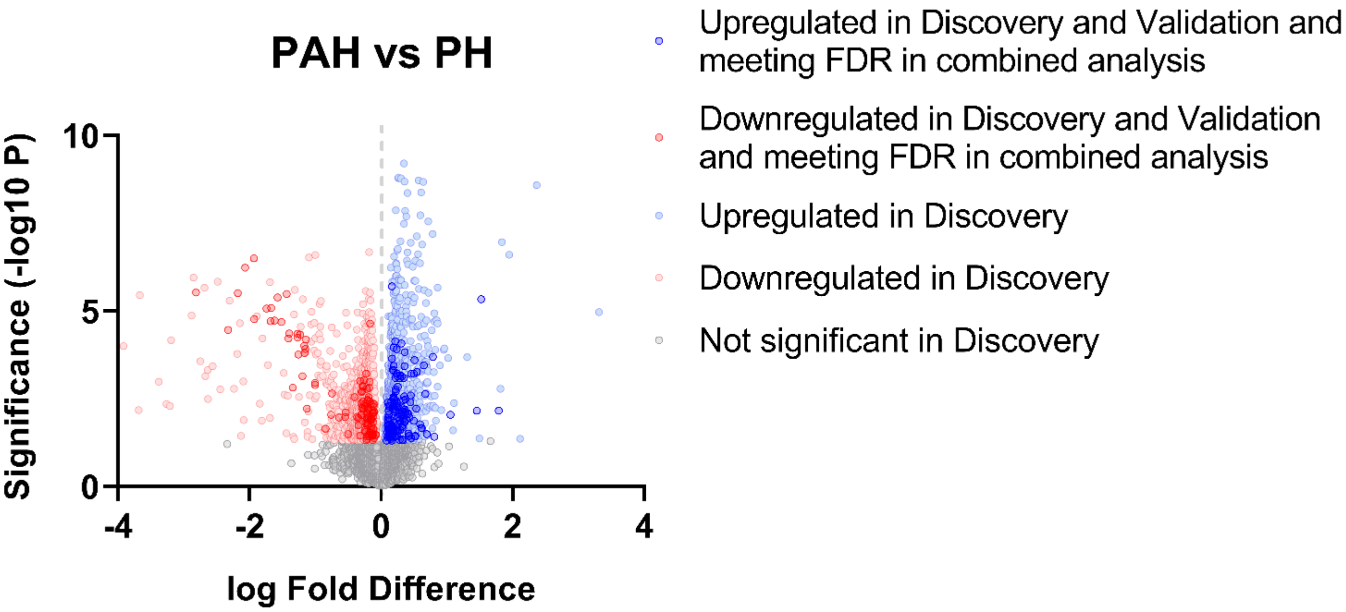

Figure 4.3: Differential expression analysis in whole blood RNAseq comparing PAH and other PH patients. Volcano plot showing log fold-differences of differentially expressed ($p < 0.05$) genes in the Discovery analysis (2/3 of samples) comparing PAH patients (PH Group I) with patients suffering from other cardiovascular disorders. Highlighted genes include 253 genes which were also significantly dysregulated ($p < 0.05$) and directionally consistent in the Validation analysis (1/3 samples) and met FDR corrected significance ($q < 0.05$) in the combined Discovery and Validation analysis (all samples).

	RNA Discovery		**RNA Validation**		**Combined Discovery and Validation**		
Gene	**logFC**	**Sig**	**logFC**	**Sig**	**logFC**	**Sig**	**FDR**
EGR1	2.808	6.23x10^{-11}	0.444	4.94x10^{-02}	2.441	2.64x10^{-15}	6.06x10^{-11}
SNORD3A	-2.063	5.90x10^{-07}	-1.737	1.92x10^{-03}	-2.039	1.21x10^{-09}	6.94x10^{-06}
SNORD17	-1.931	3.21x10^{-07}	-1.609	7.65x10^{-03}	-1.905	5.38x10^{-09}	2.06x10^{-05}
SNORA53	-2.811	3.01x10^{-06}	-3.044	7.31x10^{-04}	-2.995	6.34x10^{-09}	2.08x10^{-05}
SCARNA10	-2.174	3.14x10^{-06}	-1.972	3.71x10^{-03}	-2.169	2.42x10^{-08}	4.64x10^{-05}
SNORA23	-1.740	8.70x10^{-06}	-1.627	3.38x10^{-03}	-1.756	3.42x10^{-08}	6.05x10^{-05}
POLDIP3	0.166	2.02x10^{-06}	0.118	3.78x10^{-02}	0.155	4.51x10^{-08}	7.40x10^{-05}
SNORA12	-1.433	3.33x10^{-06}	-0.930	2.64x10^{-02}	-1.333	7.06x10^{-08}	1.08x10^{-04}
RPPH1	-1.928	1.73x10^{-05}	-1.791	4.32x10^{-03}	-1.971	8.74x10^{-08}	1.25x10^{-04}
SCARNA6	-1.667	8.29x10^{-06}	-1.413	1.09x10^{-02}	-1.662	1.08x10^{-07}	1.31x10^{-04}
RNU12	-2.324	3.51x10^{-05}	-2.841	1.59x10^{-03}	-2.671	1.05x10^{-07}	1.31x10^{-04}
SCARNA5	-1.680	1.97x10^{-05}	-1.553	6.13x10^{-03}	-1.734	1.25x10^{-07}	1.43x10^{-04}
IFI27	1.788	6.95x10^{-03}	2.557	5.91x10^{-03}	2.671	1.67x10^{-07}	1.75x10^{-04}
RNU2-2P	-1.511	2.10x10^{-05}	-1.509	6.47x10^{-03}	-1.578	1.83x10^{-07}	1.83x10^{-04}
SNORA74B	-1.165	9.89x10^{-05}	-1.568	2.29x10^{-03}	-1.367	2.85x10^{-07}	2.45x10^{-04}
SNORD97	-1.271	5.78x10^{-05}	-1.271	4.83x10^{-03}	-1.298	4.28x10^{-07}	3.51x10^{-04}
RP11-734I18.1	1.522	4.71x10^{-06}	0.919	2.38x10^{-02}	1.326	6.09x10^{-07}	4.00x10^{-04}
SNORA57	-1.573	4.19x10^{-06}	-1.094	3.01x10^{-02}	-1.401	7.07x10^{-07}	4.28x10^{-04}
RNU4-2	-1.614	1.88x10^{-05}	-1.421	1.80x10^{-02}	-1.629	7.26x10^{-07}	4.28x10^{-04}
RP11-206L10.9	-0.165	2.32x10^{-05}	-0.139	4.37x10^{-02}	-0.160	1.23x10^{-06}	5.24x10^{-04}
GPKOW	0.238	1.24x10^{-04}	0.183	1.41x10^{-02}	0.230	1.18x10^{-06}	5.24x10^{-04}
NATD1	0.511	2.54x10^{-04}	0.650	8.24x10^{-03}	0.616	1.23x10^{-06}	5.24x10^{-04}
NAPA	0.501	6.27x10^{-04}	0.634	5.93x10^{-04}	0.559	1.13x10^{-06}	5.24x10^{-04}
RP11-85G21.3	0.788	2.07x10^{-04}	0.978	6.69x10^{-03}	0.898	1.41x10^{-06}	5.63x10^{-04}
UNC45A	0.192	3.70x10^{-04}	0.281	4.98x10^{-03}	0.229	1.47x10^{-06}	5.64x10^{-04}
SNORA38B	-1.161	1.60x10^{-04}	-1.217	1.30x10^{-02}	-1.251	1.88x10^{-06}	6.98x10^{-04}
RNU4-1	-1.392	4.43x10^{-05}	-1.190	2.10x10^{-02}	-1.371	2.16x10^{-06}	7.66x10^{-04}
FOXO4	0.651	3.61x10^{-04}	0.593	3.39x10^{-02}	0.732	2.23x10^{-06}	7.68x10^{-04}
OTOF	1.457	7.04x10^{-03}	2.680	9.38x10^{-04}	2.093	2.24x10^{-06}	7.68x10^{-04}
RNU1-1	-1.227	4.80x10^{-05}	-1.192	3.44x10^{-02}	-1.290	2.77x10^{-06}	9.09x10^{-04}
SCARNA1	-1.409	6.12x10^{-05}	-1.139	4.61x10^{-02}	-1.455	2.87x10^{-06}	9.30x10^{-04}
SNORA73B	-1.139	6.66x10^{-05}	-0.842	4.26x10^{-02}	-1.093	3.88x10^{-06}	1.17x10^{-03}
KHNYN	0.165	2.30x10^{-04}	0.210	2.58x10^{-02}	0.197	4.75x10^{-06}	1.36x10^{-03}
CHMP4B	0.361	1.51x10^{-04}	0.390	2.62x10^{-02}	0.400	4.94x10^{-06}	1.37x10^{-03}
E2F2	0.676	2.35x10^{-03}	1.114	8.45x10^{-03}	0.967	5.00x10^{-06}	1.37x10^{-03}
SNORD94	-1.270	4.48x10^{-05}	-1.064	4.58x10^{-02}	-1.238	5.07x10^{-06}	1.37x10^{-03}
SCARNA2	-1.255	1.75x10^{-04}	-1.215	1.72x10^{-02}	-1.257	5.65x10^{-06}	1.46x10^{-03}
DCAF11	0.287	8.36x10^{-04}	0.421	7.45x10^{-03}	0.352	5.64x10^{-06}	1.46x10^{-03}
KDELR1	0.194	1.12x10^{-04}	0.187	4.41x10^{-02}	0.195	8.69x10^{-06}	1.83x10^{-03}

Table 4.2: Top dysregulated RNAs in whole blood RNAseq comparing PAH and other PH patients. List of 40 genes most significantly dysregulated between PAH (PH Group I) and other PH (PH Groups II-IV) patients from 253 gene list of differentially expressed ($p < 0.05$), directionally consistent genes in Discovery (2/3 samples) and Validation (1/3 samples) groups which also met FDR corrected significance ($q < 0.05$) in combined Discovery and Validation analysis (all samples). Genes listed by significance (lowest FDR q first).

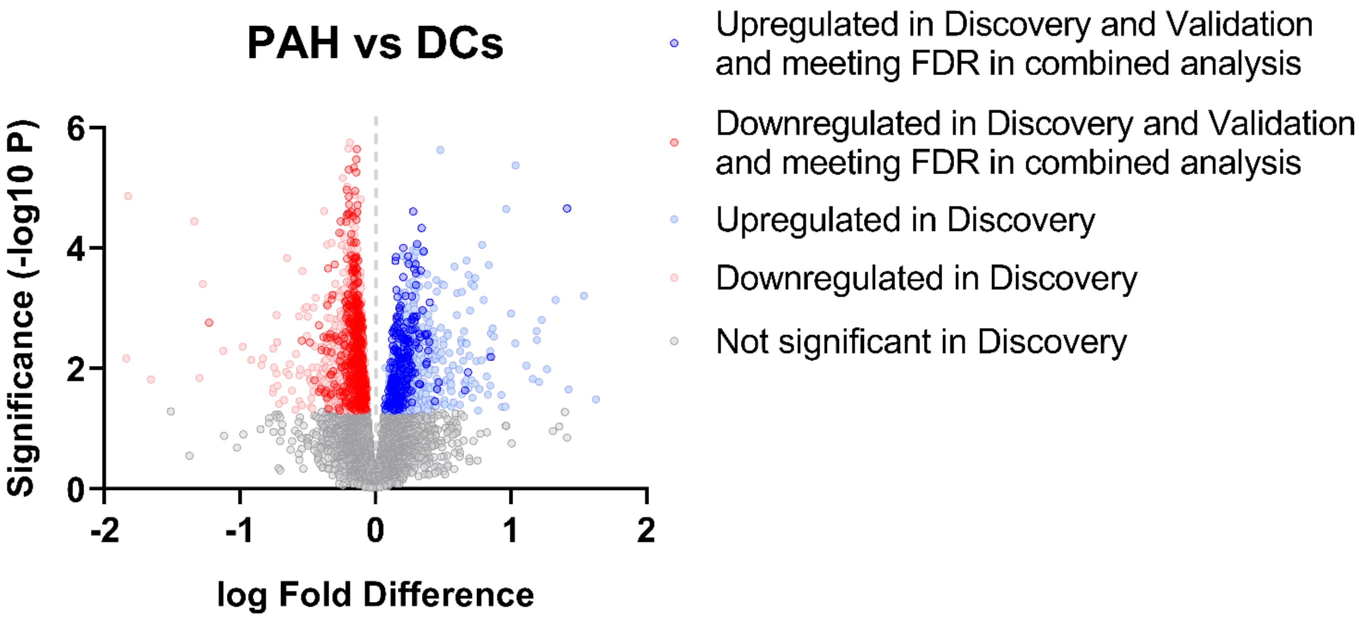

Figure 4.4: Differential expression analysis in whole blood RNAseq comparing PAH patients and disease controls. Volcano plot showing log fold-differences of differentially expressed ($p < 0.05$) genes in the Discovery analysis (2/3 of samples) comparing PAH patients (PH Group I) with patients suffering from other cardiovascular disorders. Highlighted genes include 727 genes which were also significantly dysregulated ($p < 0.05$) and directionally consistent in the Validation analysis (1/3 samples) and met FDR corrected significance ($q < 0.05$) in the combined Discovery and Validation analysis (all samples).

	RNA Discovery		RNA Validation		Combined Discovery and Validation		
Gene	**logFC**	**Sig**	**logFC**	**Sig**	**logFC**	**Sig**	**FDR**
RSRC2	-0.188	3.00x10^{-07}	-0.110	8.64x10^{-04}	-0.142	4.85x10^{-09}	4.37x10^{-05}
PTAR1	-0.197	5.01x10^{-06}	-0.140	1.10x10^{-03}	-0.164	3.16x10^{-08}	1.90x10^{-04}
RP11-379H18.1	0.155	5.00x10^{-04}	0.209	2.88x10^{-05}	0.177	5.20x10^{-08}	2.34x10^{-04}
C1orf27	-0.196	1.39x10^{-05}	-0.158	1.23x10^{-03}	-0.175	8.08x10^{-08}	2.91x10^{-04}
AP004289.1	0.321	9.03x10^{-07}	0.202	4.61x10^{-03}	0.255	1.26x10^{-07}	3.16x10^{-04}
BTAF1	-0.192	2.75x10^{-05}	-0.130	1.26x10^{-03}	-0.157	1.76x10^{-07}	3.16x10^{-04}
TEX10	-0.141	5.52x10^{-06}	-0.087	5.53x10^{-03}	-0.113	1.39x10^{-07}	3.16x10^{-04}
TLR5	-0.349	2.18x10^{-04}	-0.410	2.23x10^{-04}	-0.368	1.49x10^{-07}	3.16x10^{-04}
ARFGAP3	-0.160	1.93x10^{-04}	-0.150	6.01x10^{-04}	-0.155	2.69x10^{-07}	3.24x10^{-04}
HLTF	-0.212	1.08x10^{-05}	-0.150	5.06x10^{-03}	-0.179	2.70x10^{-07}	3.24x10^{-04}
RBM27	-0.136	6.00x10^{-04}	-0.135	4.90x10^{-04}	-0.140	2.08x10^{-07}	3.24x10^{-04}
SAMD8	-0.125	2.76x10^{-03}	-0.177	2.46x10^{-05}	-0.149	2.23x10^{-07}	3.24x10^{-04}
SCYL3	-0.142	3.37x10^{-06}	-0.085	1.11x10^{-02}	-0.113	2.36x10^{-07}	3.24x10^{-04}
SCFD2	-0.257	3.63x10^{-05}	-0.211	5.53x10^{-04}	-0.227	2.99x10^{-07}	3.37x10^{-04}
ZNF211	-0.182	7.91x10^{-05}	-0.154	6.68x10^{-04}	-0.163	3.26x10^{-07}	3.45x10^{-04}
DDX17	-0.159	4.61x10^{-06}	-0.083	1.34x10^{-02}	-0.118	3.68x10^{-07}	3.68x10^{-04}
AL844908.5	-0.300	1.86x10^{-04}	-0.280	1.62x10^{-03}	-0.297	4.76x10^{-07}	4.29x10^{-04}
ZNF702P	-0.261	2.45x10^{-02}	-0.505	2.63x10^{-06}	-0.406	4.56x10^{-07}	4.29x10^{-04}
RALA	0.160	1.36x10^{-03}	0.204	1.33x10^{-04}	0.181	5.22x10^{-07}	4.48x10^{-04}
PTEN	-0.181	1.32x10^{-04}	-0.176	6.67x10^{-04}	-0.171	5.73x10^{-07}	4.69x10^{-04}
CCNB1IP1	-0.148	9.46x10^{-04}	-0.150	2.80x10^{-04}	-0.149	6.17x10^{-07}	4.84x10^{-04}
AP000240.5	0.324	2.64x10^{-03}	0.400	8.03x10^{-04}	0.389	6.86x10^{-07}	5.15x10^{-04}
RBM5	-0.137	2.28x10^{-06}	-0.062	4.48x10^{-02}	-0.101	7.51x10^{-07}	5.41x10^{-04}
KCNQ1OT1	0.152	1.41x10^{-04}	0.132	1.26x10^{-03}	0.140	9.24x10^{-07}	6.17x10^{-04}
ZNF224	-0.135	2.53x10^{-05}	-0.090	9.32x10^{-03}	-0.112	9.08x10^{-07}	6.17x10^{-04}
RP11-138A9.2	0.223	6.17x10^{-04}	0.238	3.59x10^{-04}	0.225	1.08x10^{-06}	6.72x10^{-04}
ZFAND1	-0.151	8.35x10^{-04}	-0.167	3.08x10^{-04}	-0.157	1.06x10^{-06}	6.72x10^{-04}
AC010746.2	0.206	3.04x10^{-04}	0.213	1.10x10^{-03}	0.207	1.33x10^{-06}	8.01x10^{-04}
CCDC186	-0.153	1.45x10^{-04}	-0.109	6.54x10^{-03}	-0.132	1.52x10^{-06}	8.24x10^{-04}
CHD9	-0.157	3.20x10^{-04}	-0.178	2.04x10^{-04}	-0.155	1.49x10^{-06}	8.24x10^{-04}
RASA2	-0.145	2.57x10^{-04}	-0.113	7.17x10^{-03}	-0.135	1.56x10^{-06}	8.24x10^{-04}
UBR1	-0.150	1.13x10^{-05}	-0.089	1.01x10^{-02}	-0.114	1.52x10^{-06}	8.24x10^{-04}
ZNF141	-0.159	1.49x10^{-04}	-0.110	2.62x10^{-03}	-0.130	1.64x10^{-06}	8.46x10^{-04}
AC009299.4	1.414	2.20x10^{-05}	0.600	3.22x10^{-02}	1.048	1.74x10^{-06}	8.69x10^{-04}
ARHGAP12	-0.195	1.89x10^{-05}	-0.099	3.39x10^{-02}	-0.151	1.84x10^{-06}	8.78x10^{-04}
ZNF486	-0.229	3.96x10^{-03}	-0.321	7.27x10^{-05}	-0.266	1.85x10^{-06}	8.78x10^{-04}
BCLAF1	-0.166	3.01x10^{-05}	-0.092	1.53x10^{-02}	-0.127	2.00x10^{-06}	9.25x10^{-04}
SMARCD2	-0.158	8.08x10^{-05}	-0.114	5.20x10^{-03}	-0.132	2.23x10^{-06}	1.00x10^{-03}
RP11-158K1.3	-0.160	5.37x10^{-04}	-0.138	3.47x10^{-03}	-0.151	2.30x10^{-06}	1.01x10^{-03}

Table 4.3: Top dysregulated RNAs in whole blood RNAseq comparing PAH patients and disease controls. List of 40 genes most significantly dysregulated between PAH patients and patients with other cardiovascular disorders from 727 gene list of differentially expressed ($p < 0.05$), directionally consistent genes in Discovery (2/3 samples) and Validation (1/3 samples) groups which also met FDR corrected significance ($q < 0.05$) in combined Discovery and Validation analysis (all samples). Genes listed by significance (lowest FDR q first).

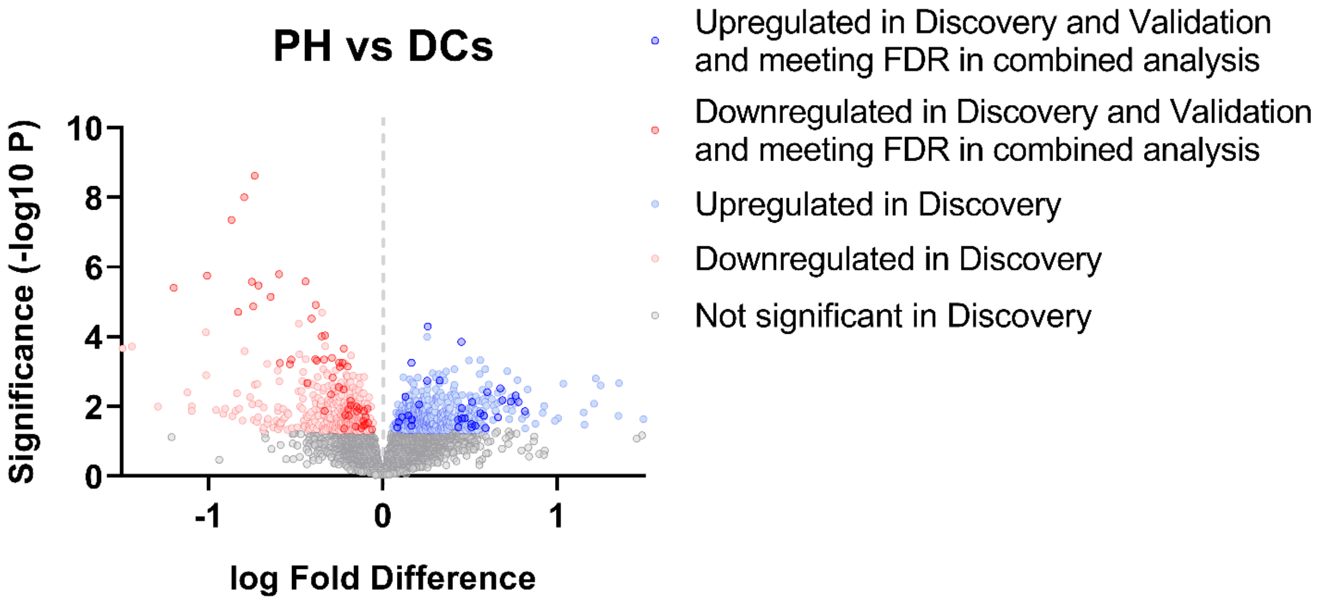

Figure 4.5: Differential expression analysis in whole blood RNAseq comparing all PH patients and disease controls. Volcano plot showing log fold-differences of differentially expressed ($p < 0.05$) genes in the Discovery analysis (2/3 of samples) comparing PH patients (PH Groups I-IV) with patients suffering from other cardiovascular disorders. Highlighted genes include 87 genes which were also significantly dysregulated ($p < 0.05$) and directionally consistent in the Validation analysis (1/3 samples) and met FDR corrected significance ($q < 0.05$) in the combined Discovery and Validation analysis (all samples).

	RNA Discovery		RNA Validation		Combined Discovery and Validation		
Gene	**logFC**	**Sig**	**logFC**	**Sig**	**logFC**	**Sig**	**FDR**
NEUROD2	-0.734	2.39x10^{-09}	-1.023	1.80x10^{-11}	-0.830	2.92x10^{-17}	3.40x10^{-13}
FGF23	-0.793	9.82x10^{-09}	-0.813	1.53x10^{-11}	-0.832	1.81x10^{-15}	1.41x10^{-11}
PRRG3	-0.867	4.42x10^{-08}	-0.708	3.00x10^{-08}	-0.868	1.34x10^{-13}	7.82x10^{-10}
HEPACAM	-0.594	1.61x10^{-06}	-0.799	2.08x10^{-09}	-0.679	7.68x10^{-13}	3.58x10^{-09}
SLC25A48	-0.751	2.62x10^{-06}	-0.651	3.94x10^{-06}	-0.749	1.23x10^{-10}	4.77x10^{-07}
GPM6A	-1.008	1.77x10^{-06}	-0.637	2.36x10^{-05}	-0.972	2.37x10^{-10}	7.88x10^{-07}
GPT2	-0.183	9.22x10^{-03}	-1.182	1.84x10^{-05}	-0.684	4.39x10^{-10}	1.28x10^{-06}
SOX11	-0.442	2.58x10^{-06}	-0.381	5.30x10^{-04}	-0.435	8.46x10^{-10}	1.79x10^{-06}
RP11-69P2.1	-0.743	1.34x10^{-05}	-0.699	4.67x10^{-08}	-0.754	8.30x10^{-10}	1.79x10^{-06}
RP1-17K7.2	-0.712	3.38x10^{-06}	-0.714	3.13x10^{-05}	-0.715	9.42x10^{-10}	1.83x10^{-06}
RP11-217O12.1	-1.200	3.94x10^{-06}	-0.676	4.44x10^{-06}	-1.114	1.75x10^{-09}	2.92x10^{-06}
AC079779.4	-0.829	1.94x10^{-05}	-0.766	1.82x10^{-06}	-0.868	1.71x10^{-09}	2.92x10^{-06}
KCNJ3	-0.407	3.02x10^{-05}	-0.446	6.98x10^{-05}	-0.428	8.62x10^{-09}	9.56x10^{-06}
FAM184B	-0.330	9.23x10^{-05}	-0.409	1.37x10^{-05}	-0.363	9.78x10^{-09}	1.04x10^{-05}
CTB-129P6.7	-0.385	1.22x10^{-05}	-0.236	1.18x10^{-03}	-0.351	2.91x10^{-08}	2.82x10^{-05}
ZPR1	-0.223	2.19x10^{-04}	-0.311	9.93x10^{-06}	-0.254	3.26x10^{-08}	2.92x10^{-05}
DPPA4	-0.642	7.16x10^{-06}	-0.261	5.40x10^{-03}	-0.562	3.87x10^{-08}	3.33x10^{-05}
RP11-87N24.3	-0.250	2.77x10^{-03}	-0.626	2.33x10^{-06}	-0.379	7.04x10^{-08}	5.29x10^{-05}
RP11-113I24.1	-0.246	7.35x10^{-04}	-0.365	2.01x10^{-05}	-0.296	9.76x10^{-08}	7.10x10^{-05}
AP000339.4	0.260	5.10x10^{-05}	0.295	6.01x10^{-04}	0.273	1.12x10^{-07}	7.93x10^{-05}
RP11-38O23.4	-0.524	4.51x10^{-04}	-0.636	2.15x10^{-06}	-0.569	1.77x10^{-07}	1.15x10^{-04}
RP5-857K21.6	2.045	2.35x10^{-05}	1.618	1.87x10^{-02}	2.033	2.49x10^{-07}	1.52x10^{-04}
RNF168	-0.349	9.66x10^{-05}	-0.203	1.46x10^{-03}	-0.323	2.77x10^{-07}	1.65x10^{-04}
AC009404.2	-0.533	6.10x10^{-04}	-0.519	8.05x10^{-06}	-0.570	3.17x10^{-07}	1.85x10^{-04}
SNORA48	0.600	3.86x10^{-03}	1.156	1.81x10^{-05}	0.812	6.26x10^{-07}	3.42x10^{-04}
CTA-414D7.1	-0.291	3.99x10^{-04}	-0.282	1.36x10^{-04}	-0.295	6.53x10^{-07}	3.46x10^{-04}
RASSF6	-0.194	1.88x10^{-02}	-0.667	1.95x10^{-04}	-0.384	2.09x10^{-06}	1.02x10^{-03}
S1PR2	-0.231	5.61x10^{-04}	-0.214	1.11x10^{-03}	-0.231	2.45x10^{-06}	1.14x10^{-03}
SNORA70	0.764	4.86x10^{-03}	1.315	8.53x10^{-05}	0.972	3.12x10^{-06}	1.37x10^{-03}
TPH1	-0.386	4.38x10^{-04}	-0.309	3.71x10^{-03}	-0.369	3.96x10^{-06}	1.68x10^{-03}
PARD6B	-0.250	5.43x10^{-04}	-0.156	1.30x10^{-03}	-0.227	5.94x10^{-06}	2.43x10^{-03}
CENPP	0.452	1.39x10^{-04}	0.373	2.86x10^{-02}	0.427	6.46x10^{-06}	2.55x10^{-03}
MCM2	-0.377	4.89x10^{-04}	-0.470	6.00x10^{-03}	-0.400	7.55x10^{-06}	2.70x10^{-03}
RPS6KA6	-0.590	5.70x10^{-04}	-0.290	2.25x10^{-03}	-0.541	7.22x10^{-06}	2.70x10^{-03}
AC096655.2	-0.123	4.17x10^{-02}	-0.372	5.35x10^{-06}	-0.215	7.48x10^{-06}	2.70x10^{-03}
NTNG1	-0.432	2.13x10^{-03}	-0.559	3.23x10^{-03}	-0.495	8.72x10^{-06}	3.03x10^{-03}
SNORA67	0.736	7.28x10^{-03}	1.454	9.66x10^{-04}	1.012	1.00x10^{-05}	3.43x10^{-03}
ZNF395	-0.135	1.16x10^{-02}	-0.237	2.30x10^{-03}	-0.182	1.92x10^{-05}	5.98x10^{-03}
BICC1	-0.295	4.55x10^{-03}	-0.394	1.61x10^{-03}	-0.342	1.96x10^{-05}	6.00x10^{-03}

Table 4.4: Top dysregulated RNAs in whole blood RNAseq comparing PH patients and disease controls. List of 40 genes most significantly dysregulated between all PH patients (PH Groups I-IV) and patients with other cardiovascular disorders from 87 gene list of differentially expressed ($p< 0.05$), directionally consistent genes in Discovery (2/3 samples) and Validation (1/3 samples) groups which also met FDR corrected significance ($q< 0.05$) in combined Discovery and Validation analysis (all samples). Genes listed by significance (lowest FDR q first).

4.5.3 Diagnostic RNA LASSO models development and testing

Predictive diagnostic models were developed using LASSO regression modelling (see details on Methods 2.1.6). For each of the three differential expression analyses (PAH vs PH, PAH vs DCs and PH vs DCs), significantly dysregulated, directionally consistent genes in Discovery and Validation groups which also met FDR corrected significance ($q < 0.05$) in the combined analysis (all samples) were put forward for LASSO modelling. Gene expression results from each Discovery analysis were used for model development. Models were tested using results from each respective Validation analysis.

For the analysis comparing PAH (PH Group I) and other PH (PH Groups II-IV) patients, the predictive model utilised a combination of 8 RNAs and age (Table 4.5) that could best discriminate between PAH and other PH in the Discovery group ($n_{PAH}= 31$, $n_{PH}= 66$). When this RNA model was tested in the Validation group ($n_{PAH}= 16$, $n_{PH}= 34$), it was found the model was not able to significantly separate PAH from other PH patients ($p= 0.719$; Figure 4.6A). Receiver operating curve (ROC) analysis demonstrated an area under the curve (AUC) of 0.533 (95% CI: 0.349- 0.717; Figure 4.6B).

When comparing PAH (PH Group I) patients with disease controls, the predictive model utilised a combination of 16 RNAs (Table 4.6) that could best discriminate between groups in Discovery ($n_{PAH}=$ 31, $n_{DCs}= 30$). When this RNA model was tested in the Validation group ($n_{PAH}= 16$, $n_{PH}= 15$), it was found the model was able to significantly separate PAH patients from patients suffering from other cardiovascular disorders ($p= 0.049$; Figure 4.7A). ROC analysis demonstrated an AUC of 0.708 (95% CI: 0.522- 0.895; Figure 4.7B).

When comparing all PH (PH Groups I-IV) patients with disease controls, the predictive model utilised a combination of 6 RNAs (Table 4.7) that could best discriminate between groups in Discovery ($n_{PH}=$ 97, $n_{DCs}= 30$). When this RNA model was tested in the Validation group ($n_{PH}= 50$, $n_{PH}= 15$), it was found the model was able to significantly separate PH patients from patients suffering from other cardiovascular disorders ($p= 1.92\text{x}10^{-5}$; Figure 4.8A). ROC analysis demonstrated an AUC of 0.867 (95% CI: 0.744- 0.989; Figure 4.8B).

VARIABLE	COEFFICIENT
(Intercept)	0.175
Age at sample	-4.70×10^{-04}
AC010731.3	-6.86×10^{-03}
AC096664.2	-3.97×10^{-02}
AC105402.3	7.55×10^{-03}
C1QL4	2.74×10^{-02}
CAPN1	6.53×10^{-05}
CTD-2014N11.1	-1.67×10^{-02}
IL6R	1.73×10^{-05}
MT-TK	3.63×10^{-03}

Table 4.5: 8 RNAs and age included in the PAH vs PH RNA LASSO model. Combination of 8 genes and age best able to distinguish between PAH (PH Group I) and other PH (PH Groups II-IV) patients in Discovery analysis (nPAH= 31, nPH= 66). Genes were selected by LASSO regression modelling.

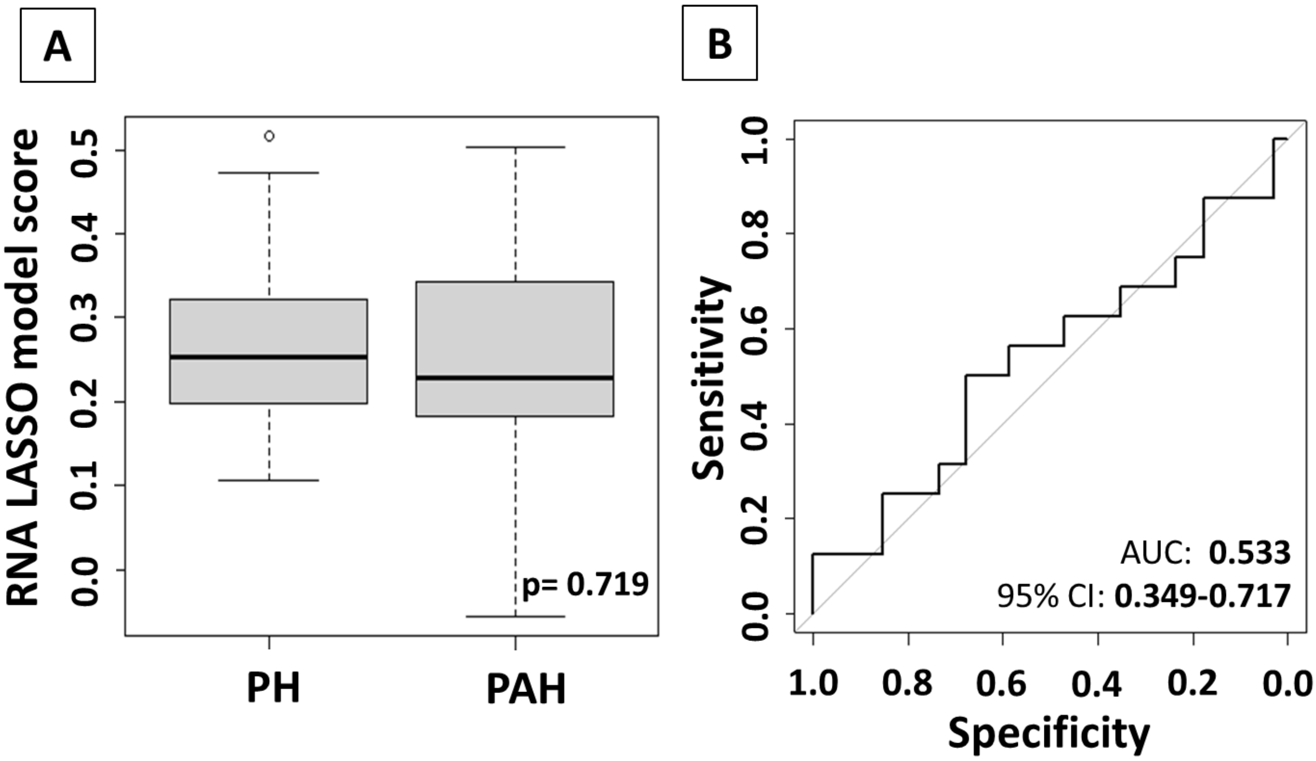

Figure 4.6: PAH vs PH RNA LASSO model performance in Validation group. A) Boxplot showing RNA LASSO model scores for PAH (PH Group I; n= 16) and other PH (PH Groups II-IV; n= 34) patients. **B**) Receiver operating curve (ROC) showing the performance of RNA LASSO model scores for determining PAH or PH status in the Validation group. p: p-value. AUC: Area under curve.

VARIABLE	COEFFICIENT
(Intercept)	0.178
AC007405.8	0.233
AC092664.1	$-3.37\text{x}10^{-02}$
AC138035.3	$8.04\text{x}10^{-04}$
ASS1P5	$-6.90\text{x}10^{-04}$
BTBD19	$1.77\text{x}10^{-04}$
CAMKV	$6.04\text{x}10^{-03}$
COL4A6	$1.56\text{x}10^{-02}$
CPHXL	$7.50\text{x}10^{-03}$
CRYBB2	$-5.63\text{x}10^{-02}$
CTA-363E6.6	$1.58\text{x}10^{-05}$
CTD-3092A11.1	$4.18\text{x}10^{-04}$
CTD-3214H19.6	$2.11\text{x}10^{-03}$
DCSTAMP	$6.71\text{x}10^{-04}$
GPS2	$2.80\text{x}10^{-06}$
MIR3651	$-5.02\text{x}10^{-02}$
MIR548AQ	$-9.72\text{x}10^{-03}$

Table 4.6: 16 RNAs included in the PAH vs DCs RNA LASSO model. Combination of 16 genes best able to distinguish between PAH (PH Group I) patients and disease controls in Discovery analysis (n_{PAH}= 31, n_{DCs}= 30). Genes were selected by LASSO regression modelling.

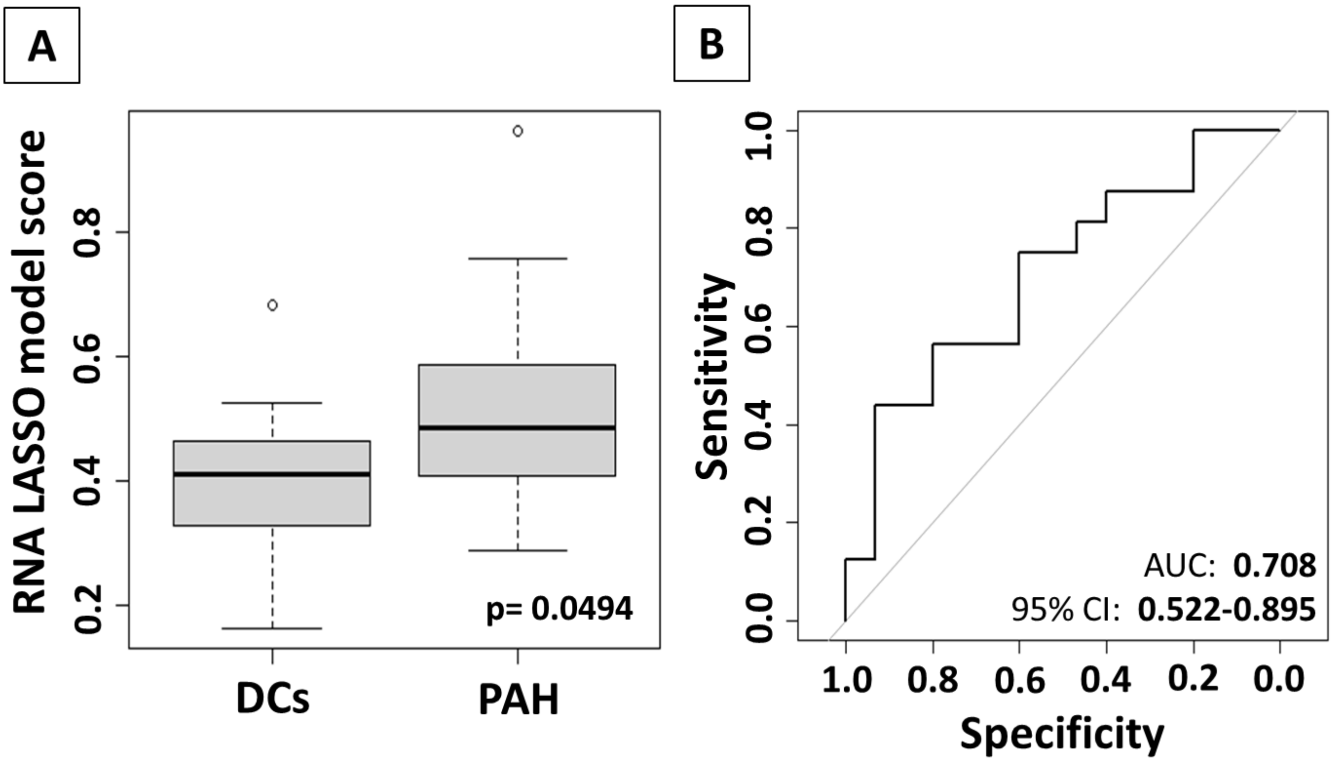

Figure 4.7: PAH vs DCs RNA LASSO model performance in Validation group. A) Boxplot showing RNA LASSO model scores for PAH patients (PH Group I; n= 16) and disease controls (n= 15). **B**) Receiver operating curve (ROC) showing the performance of RNA LASSO model scores for determining PAH status in the Validation group. p: p-value. AUC: Area under curve.

VARIABLE	COEFFICIENT
(Intercept)	0.799
C2orf78	4.04×10^{-03}
CCDC74B	1.20×10^{-03}
HEPACAM	-7.66×10^{-04}
HSD17B7P1	-2.06×10^{-02}
LRP10	2.06×10^{-06}
NADSYN1	1.06×10^{-05}

Table 4.7: 6 RNAs included in the PH vs DC RNA LASSO model. Combination of 6 genes best able to distinguish between PH (PH Groups I-IV) patients and disease controls in Discovery analysis (n_{PH}= 97, n_{DCs}= 30). Genes were selected by LASSO regression modelling.

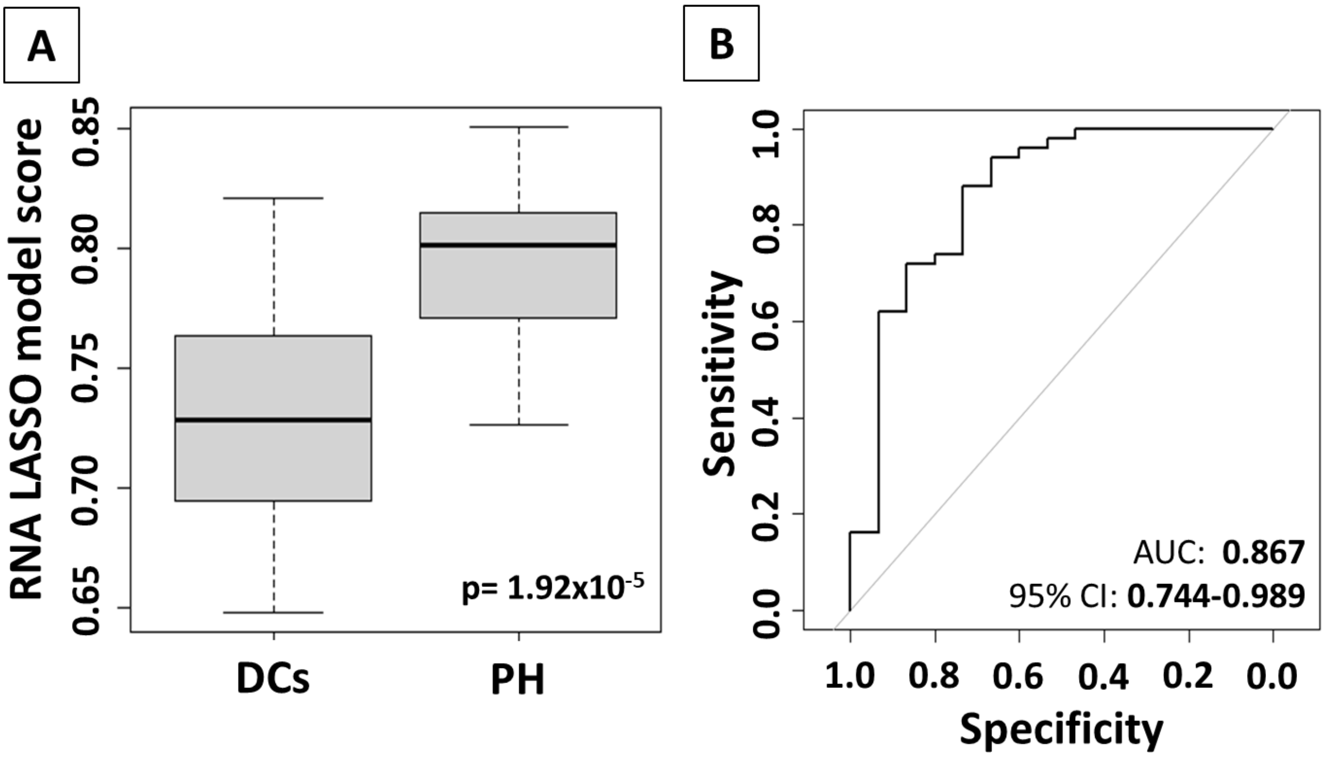

Figure 4.8: PH vs DCs RNA LASSO model performance in Validation group. A) Boxplot showing RNA LASSO model scores for PH patients (PH Groups I-IV; n= 50) and disease controls (n= 15). **B**) Receiver operating curve (ROC) showing the performance of RNA LASSO model scores for determining PH status in the Validation group. p: p-value. AUC: Area under curve.

4.5.4 Functional characterisation of RNAs in PAH/PH signatures

Functional characterisation of differentially expressed genes for each of the three differential expression analyses was performed using DAVID, an online tool for bioinformatic functional interpretation of large lists of genes resulting from biological assays (240).

Across all three analyses, the main classes of genes enriched (FDR; $q < 0.05$) were those of DNA-binding zinc-finger transcription factors (ZNF-TFs) in PAH patients, and of small nucleolar RNAs (SNORD)—a type of RNA processing genes—in both PAH and PH patients (Table 4.8). RNA processing was highlighted the two analyses of PH (PAH vs. PH and PH vs. DCs), which could reflect it may be a pathway specific to PH groups 2-4. This could also mean the pathways highlighted by the PAH vs. DCs analysis may be more specific to PAH aetiology.

Term	Count	%	Sig.	Fold Enrichment	Bonferroni	Benjamini	FDR
PAH vs PH patients							
Phosphoprotein	98	47.80	2.25×10^{-04}	1.258	3.82×10^{-03}	4.05×10^{-03}	4.05×10^{-03}
Cytoplasm	66	32.20	1.77×10^{-04}	1.480	5.81×10^{-03}	5.83×10^{-03}	5.47×10^{-03}
RNA processing	19	9.27	6.30×10^{-06}	3.572	6.71×10^{-03}	6.73×10^{-03}	6.72×10^{-03}
Cytosol	74	36.10	1.07×10^{-04}	1.487	2.85×10^{-02}	2.90×10^{-02}	2.87×10^{-02}
PAH patients vs Disease controls							
Zinc finger: C2H2-type 7	60	14.05	7.88×10^{-30}	6.294	1.45×10^{-26}	1.06×10^{-26}	1.04×10^{-26}
Zinc finger: C2H2-type 8	58	13.58	1.19×10^{-29}	6.528	2.20×10^{-26}	1.06×10^{-26}	1.04×10^{-26}
Zinc finger: C2H2-type 10	53	12.41	1.72×10^{-29}	7.323	3.17×10^{-26}	1.06×10^{-26}	1.04×10^{-26}
Zinc finger: C2H2-type 6	61	14.29	3.66×10^{-29}	5.992	6.75×10^{-26}	1.69×10^{-26}	1.67×10^{-26}
Zinc finger: C2H2-type 9	55	12.88	4.69×10^{-29}	6.822	8.65×10^{-26}	1.73×10^{-26}	1.71×10^{-26}
PH patients vs Disease controls							
RNA processing	18	40.00	9.71×10^{-16}	14.166	2.67×10^{-13}	2.59×10^{-13}	2.59×10^{-13}
Nucleolus	19	42.22	1.97×10^{-11}	6.885	1.95×10^{-09}	1.95×10^{-09}	1.95×10^{-09}

Table 4.8: Functional annotation enrichment analysis results for genes associated with PAH or PH. Genes from each differential expression analysis were used for functional characterisation of the respective RNA signature. Shown are top 5 gene classes meeting FDR corrected significance ($\alpha < 0.05$). Gene classes listed by significance (weakest FDR first).

4.6 Discussion

The first aim of the work presented in this chapter was to evaluate the ability of the previous PAH RNA model to separate between PAH patients, PH patients and symptomatic patients with PH ruled out. When the PAH RNA model was applied to subjects in the current cohort, no significant differences in LASSO scores were identified between any of the disease subgroups. These results highlight the similarities between PH subgroups (PH Groups I-IV) and between PH and patients who have other cardiovascular or respiratory disorders. It is worth noting that the PAH RNA model was developed on a cohort comparing PAH patients from healthy controls. It is likely that the most dysregulated genes included in the 25-transcript model reflected the severely ill status of PAH patients instead of more subtle differences that may reflect PAH-specific mechanisms.

The second aim was to assess differences in gene expression profiles between PAH patients, PH patients and disease controls through whole blood RNAseq followed by differential expression analysis. Three RNA signatures were identified, and the most significantly dysregulated transcripts were put forward for downstream analyses. The gene SEC22B, part of the soluble N-ethylmaleimide-sensitive factor attachment protein family of receptors (SNAREs) involved in intracellular protein trafficking, was found to be specifically dysregulated (reduced expression) in PAH. SNAREs have been previously found to play a role in PAH pathogenesis (272). SEC22B has also been found to fuse with NOTCH2 in aggressive breast cancers and increase Notch signalling, enhancing proliferation and survival in cancer cells (273). Additionally, SEC22B has also been implicated in other tumorigenic processes and may play a role in autophagy (274–276). It has been previously highlighted in this thesis how Notch signalling plays a key role in hPAEC differentiation, vascular development, response to injury and homeostasis (48,49). Notch signalling dysregulation has been implicated in vascular disease and, more specifically, PAH pathology through the role of NOTCH1 in increasing proliferation and reducing apoptosis in hPAECs in PAH (52) and migration into the neointima layer in PASMCs (47). These links with Notch signalling, SNAREs and PAH pathology, along with the PAH specific dysregulation identified in this analysis, suggest SEC22B be involved in mechanisms specific to PAH pathology. Further research into SEC22B is therefore needed and could provide with tools to help identify and molecularly characterise PAH patients.

The feline sarcoma-related gene FER was also identified as differentially expressed across groups, showing the lowest expression levels in PAH patients and the highest in other PH groups, with other non-PH patients showing intermediate expression levels. Recent evidence in *Drosophila* showed that FER overexpression promoted cell migration and enhanced JNK signalling, hinting at a potential role in cancer metastasis (277). JNK signalling is ubiquitous and involved in the regulation of proliferation, migration, survival, and cytokine production (278). It has been implicated in PH pathology via its activation in pulmonary arteries under hypoxic conditions (279) and in murine PH models (280), as well as in the PASMCs of PAH patients (281). It has also been shown that hypoxia-induced pathological angiogenesis is JNK1-dependent (282) and that JNK2 null mice are protected from the development of hypoxia-induced PH (283). Recent evidence in hypoxic rats suggests this protective role of JNK2 occurs through the prevention of hypoxia-induced vascular remodelling (284). The JNK signalling enhancing role of FER could therefore be an interesting research venue and further investigations into the role of FER in PAH and other PH forms should be conducted. These results suggest FER expression levels could also be potentially used to identify and stratify patients referred to PH clinics, or explored for more utility in more general settings, for example in breathlessness clinics.

The third aim of this chapter was to develop RNA models derived from each of the three gene expression signatures identified in the differential expression analyses. LASSO regression modelling was used to generate diagnostic models in each Discovery group and test them in the respective Validation group. While the RNA model to separate PAH patients from other PH groups (PH Groups II-IV) could not effectively distinguish between them, the other two models separating PAH and PH patients from other cardiovascular patients did effectively distinguish between groups. These results highlight once again the similarities between different forms of PH but suggest there may be an opportunity for preliminary transcriptome-based PH diagnosis to rule out the possibility of other symptom-driving pathology. It is also worth noting the limited number of available PH patients of each group, which may limit the power of this analysis to identify potential transcriptional differences between them. Also worth noting is the inherent limitation in this study design, where transcripts already shown to be significant in the Validation group are tested as part of the RNA model. This also meant it was not possible to validate the genes in a separate group following FDR. Ultimately, the best test would be to test the RNA models in a new cohort from an independent centre. Further recruiting efforts and research are needed to get a better understanding of the transcriptional differences which may exist between PH patients.

The limited amount of time and study subjects available also hindered my ability to try and evaluate the association of the identified RNA signatures with clinical features such as survival or levels of circulating cardiac biomarkers. As evidenced by results in the previous chapter (see details on Chapter 3), there is potential in testing these associations and a great deal of insights can be inferred from this kind of analysis. Further research should therefore try to also establish whether the transcriptional states of PAH, PH and non-PH symptomatic patients correlate with their clinical performance.

The fourth aim was to evaluate evidence of potential pathogenic pathway dysregulations through functional characterisation of the identified RNA profiles using enrichment analyses (240). This analysis highlighted DNA-binding zinc-finger transcription factors (ZNF-TFs) and small nucleolar RNAs (SNORD)—a type of RNA processing genes—as the main gene enriched in PAH and in both PAH and PH patients respectively. DNA-binding ZNFs were part of the main class of genes—TFs—found to be enriched in PAH patients in results from the PAH RNA signature, further supporting results from both assays. RNA processing genes, however, were not previously highlighted and separate patients of the PH spectrum from other non-PH symptomatic patients. This could reflect PH-specific transcriptional changes.

In summary, three RNA signatures separating PAH patients from other PH patients, and both PAH and PH patients from other non-PH patients, have been identified in this chapter. Diagnostic models were developed from those RNA signatures and were effective in distinguishing both PAH and all PH patients from other non-PH patients. These results suggest transcriptional differences may be useful in stratifying patients in PH clinics, which needs confirmation in larger, prospective studies. Further research should be conducted to try and identify potential mechanistic differences between PH groups and any association with disease progression and pathogenesis.

5 - The Connectivity Map: *in vitro* Testing of Predicted Rescue Compounds

5.1 Introduction

Research into druggable targets for disease treatment is a long, costly process. The average cost for a company to develop a new drug, from early laboratory research until it reaches the patient commercially, has been recently estimated at an average of $985 billion, taking over 12 years to fully complete (285,286). From basic research to clinical trials, each step towards the approval of a new drug treatment involves new hurdles and incurs costs in the form of work hours, funding, safety concerns, healthcare personnel and patient contributions. Finding ways of minimising the impact of these issues is key when trying to make this process more time- and cost- effective and achieve higher success rates.

The Connectivity Map project (CMap) can be used to tackle some of these issues (217). It contains a large database of different transcriptional signatures from various cell types exposed to a wide range of "perturbagens". A CMap perturbagen is any agent affecting the transcriptional state of a cell, such as small molecule compounds, gene overexpression or RNA interference. The CMap allows for a list of genes of interest to be queried against it to assess which perturbagen is most or least correlated to that specific signature (see details on Introduction 1.5). Only about 10% of compounds reaching pre-clinical testing ever make it into trials on human subjects. When focusing on human clinical trials specifically, safety concerns about the use of small molecule compounds on human subjects represents a large proportion of the high rate of failure for potential new treatments, with just about 20% of compounds reaching this stage getting approved for safe clinical use on humans (286). Many compounds within the CMap database have previously undergone clinical trials and their safety has therefore been assessed. Hence, repurposing of compounds approved or investigated for a different disease is a great mechanism for optimisation of the long treatment development process, although a successful repurposing process still requires new human clinical trials to be conducted.

As outlined in previous chapters from this thesis, I have identified and characterised a whole-blood RNA signature for PAH which strongly associated with clinical features and survival (see details on Chapter 3). Consequently, I then queried a list of differentially expressed genes from my DE analysis in CMap to identify small molecule compounds predicted to be capable of inducing the opposite transcriptional effects as those observed in PAH. These compounds were tested on PBMCs in vitro for their potential for PAH treatment.

PAH pathology has a strong immune and inflammatory component, but its primary site of injury occurs within the lung vasculature (see details on Introduction 1.3.4). It is also proposed there exists a relationship between systemic changes in the transcriptional state of PBMCs from PAH patients and changes occurring in vascular cells at the primary site of injury (see details on Introduction 1.4.4). It would therefore be of relevance to study the effects of candidate compounds on vascular cells. Reversing the transcriptional changes observed in PAH on those vascular cells may also have therapeutic potential. For those reasons, I decided to test the effects on transcriptional state and cellular function of the stronger CMap compound candidates on hPAECs in vitro.

5.2 Hypotheses

- There are existing small molecule compounds with the ability to reverse the transcriptional effects observed in PBMCs in PAH patients.
- These compounds may also induce positive outcomes in vascular cells at the site of injury.

5.3 Aims

- To query the CMap database for identification of small molecule compounds which induce transcriptional signatures opposite to that identified in the whole blood of PAH patients.
- To assess the ability of these compounds to effect those transcriptional changes in PBMCs from healthy donors.
- To assess the transcriptional and functional changes of the strongest compound candidates in vascular cells (hPAECs).

5.4 Methods

5.4.1 DEG lists for CMap querying

The CMap platform uses the Entrez Gene database. It allows for a list of up to 150 Entrez IDs of DEGs in each direction (up- or down- regulated) to be used in a query. 439/507 genes (86.6%) from the PAH whole-blood RNA signature could be found in the Entrez Gene database, 90 upregulated and 349 downregulated. Queries in CMap only use genes within their own defined space of Best INferred Genes (BING). Using this system, they can infer the expression of up to 10,174 genes from measuring only 978 landmark genes. This further reduced the number of genes used in the query. After filtering out genes not included in the CMap BING space, DEG lists included 44 upregulated and 236 downregulated genes. Finally, downregulated genes were selected based on significance (p-value) to form the final lists of 44 upregulated and 150 downregulated DEGs used to query the CMap.

5.4.2 CMap query

CMap queries yield a list of perturbagens and their tau score in relationship with the input signature, from -100 to +100. The tau score represents the percentage of perturbagens within the database that are more weakly correlated in that direction to the input signature, with higher values reflecting a stronger positive correlation and lower values a stronger negative correlation. For example, a tau score of +98 means that perturbagen's signature is more strongly positively correlated with the input signature than 98% of the entire CMap database. The top 6 candidate compounds for PAH whole-blood RNA signature reversal were selected on the basis of lower tau scores (as close to -100 as possible) and lack of overlapping molecular function with other compounds. These compounds were put forward for in vitro assays.

5.5 Results

5.5.1 Identification of candidate drug compounds for PAH RNA signature reversal

The CMap database was queried using DEG lists including 44 up- and 150 down- regulated genes derived from the 507 genes within the PAH whole-blood RNA signature (see details on Methods 2.3.1.1). Only small molecule compound perturbagens were selected. The top 6 commercially available compounds with the strongest negative correlations (tau scores closer to -100) to the PAH whole-blood RNA signature and no overlapping function were selected and put forward for in vitro assays. These compounds were Azithromycin, Dovitinib, Deferiprone, Homoharringtonine, Flufenamic-acid and Scopolamine (Figure 5.1).

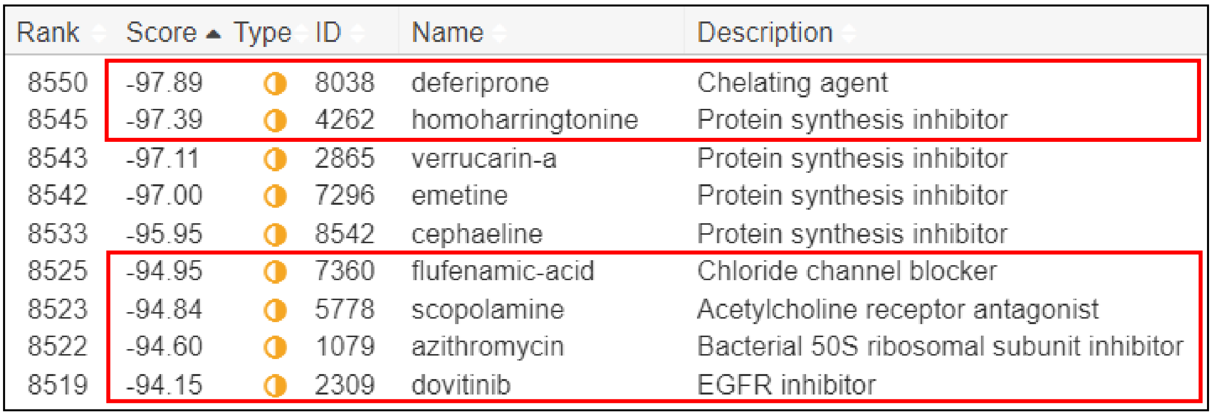

Rank	Score ▲	Type	ID	Name	Description
8550	-97.89	◑	8038	deferiprone	Chelating agent
8545	-97.39	◑	4262	homoharringtonine	Protein synthesis inhibitor
8543	-97.11	◑	2865	verrucarin-a	Protein synthesis inhibitor
8542	-97.00	◑	7296	emetine	Protein synthesis inhibitor
8533	-95.95	◑	8542	cephaeline	Protein synthesis inhibitor
8525	-94.95	◑	7360	flufenamic-acid	Chloride channel blocker
8523	-94.84	◑	5778	scopolamine	Acetylcholine receptor antagonist
8522	-94.60	◑	1079	azithromycin	Bacterial 50S ribosomal subunit inhibitor
8519	-94.15	◑	2309	dovitinib	EGFR inhibitor

Figure 5.1: Top compounds most negatively correlated with PAH whole-blood RNA signature in CMap query. Highlighted in red are 6 selected compounds with scores closest to -100 and no overlapping molecular function. These 6 compounds were put forward for in vitro analysis.

5.5.2 PBMC gene expression changes following exposure to CMap candidate compounds

The top 6 candidate compounds resulting from the CMap query were used for PBMC exposure. To assess the ability of each compound to reverse the PAH whole-blood RNA signature, expression levels of the 4 selected genes per compound were assessed through RT-qPCR after 6h or 24h of exposure to two different concentrations for each compound (see details on Methods 2.3.4.1).

5.5.2.1 Optimisation of experimental conditions

Preliminary experiments with PBMCs isolated from a single donor were used to optimise experimental conditions and drug candidates so that all experiments could be carried out in the available timeline. These preliminary experiments showed similar gene expression changes in both the 6h and the 24h exposure periods, so it was decided to continue with only the 24h exposure period.

Gene expression across the whole blood RNAseq, CMap database and PBMC exposure assays of the 4 selected genes per compound for Deferiprone, Dovitinib, Flufenamic Acid and Scopolamine were inconsistent (figures 5.2, 5.3, 5.4 and 5.5). CMap database results are filtered for the conditions which were later decided to be used (10µM and 24h), which may result in CMap results shown in the figures being different to the overall CMap score originally used to choose each compound. On the other hand, Azithromycin and Homoharringtonine showed the most consistent gene expression changes in the CMap-predicted direction (showing some degree of change in at least 3/4 genes across experimental repeats) out of the 6 candidate compounds in preliminary results and were therefore tested across all 5 PBMC donors.

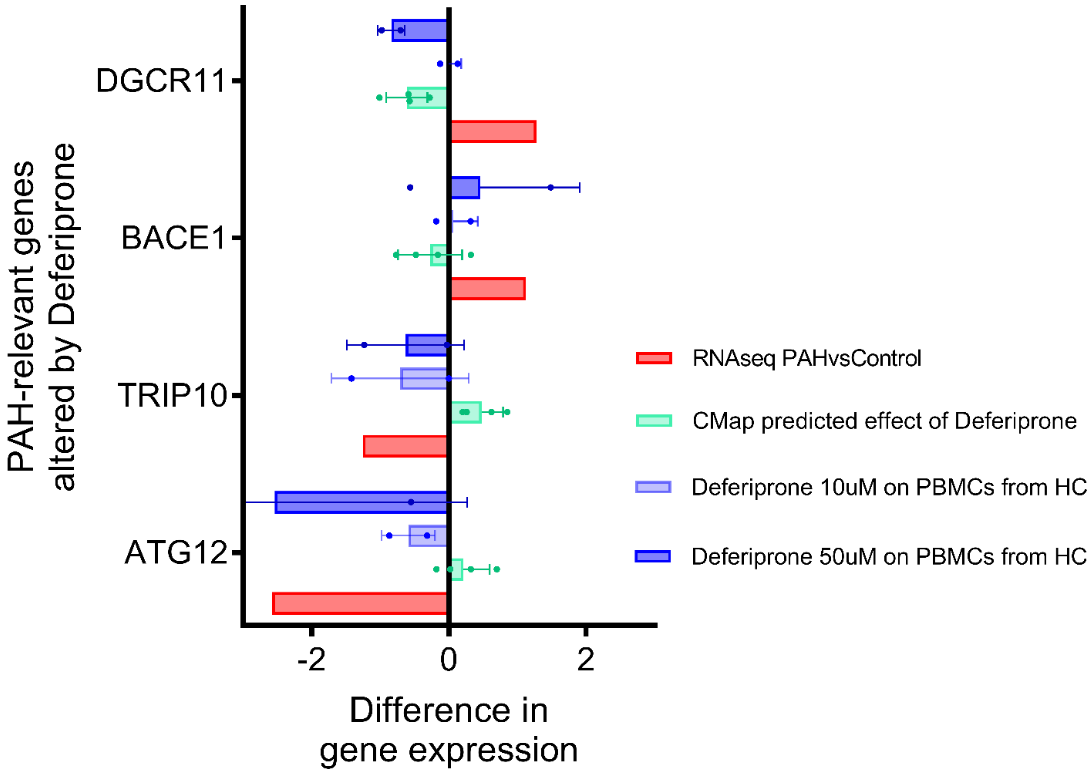

Figure 5.2: Expression levels of selected differentially expressed PAH RNAseq genes for Deferiprone exposure across assays. Gene expression of ATG12, TRIP10, BACE1 and DGCR11 in PBMCs from PAH patients (Fold Change vs. Healthy Controls; Red), the CMap database (z-score; Green) and in PBMCs from a healthy donor following Deferiprone exposure (relative expression to PBMCs exposed to vehicle; Blue; 10µM or 50µM Deferiprone in DMSO). Points represent different cell lines (CMap database; Green) or individual experiments (Deferiprone exposure of PBMCs; Blue).

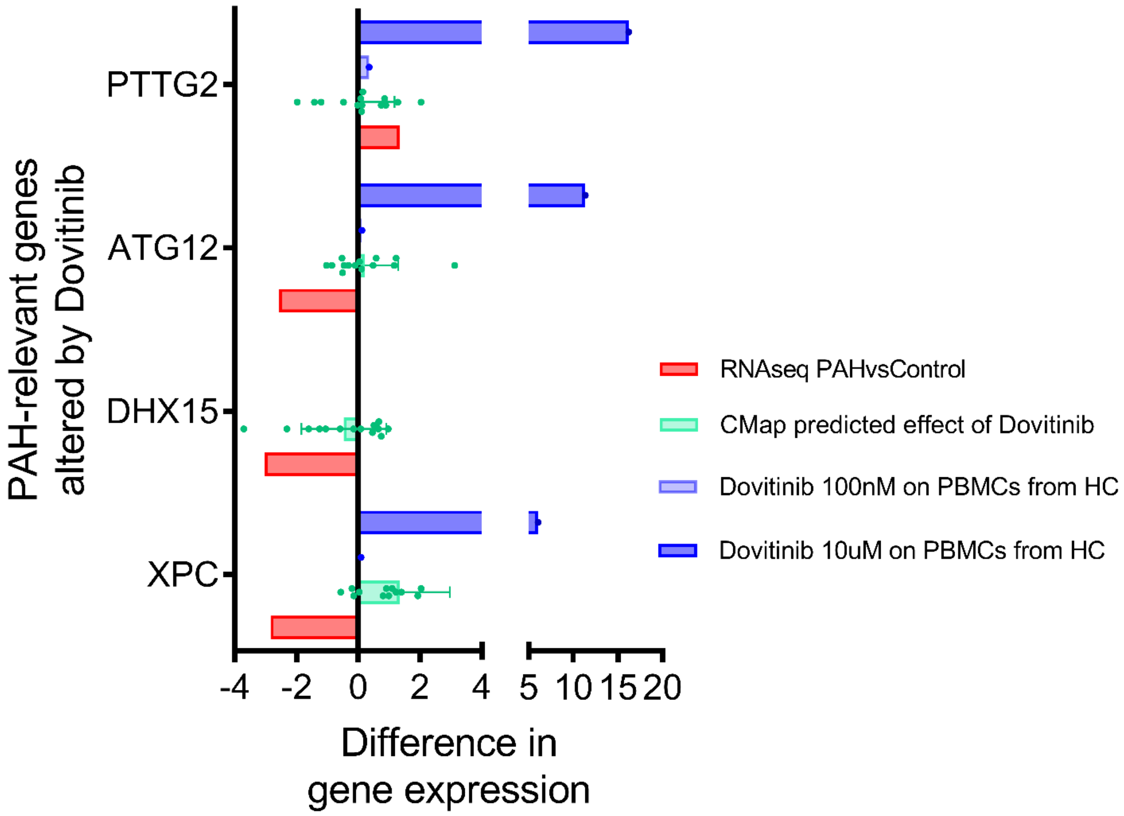

Figure 5.3 (below): Expression levels of selected differentially expressed PAH RNAseq genes for Dovitinib exposure across assays. Gene expression of XPC, DHX15, ATG12 and PTTG2 in PBMCs from PAH patients (Fold Change vs. Healthy Controls; Red), the CMap database (z-score; Green) and in PBMCs from a healthy donor following Dovitinib exposure (relative expression to PBMCs exposed to vehicle; Blue; 100nM or 10µM Dovitinib in DMSO). Points represent different cell lines (CMap database; Green) or individual experiments (Dovitinib exposure of PBMCs; Blue).

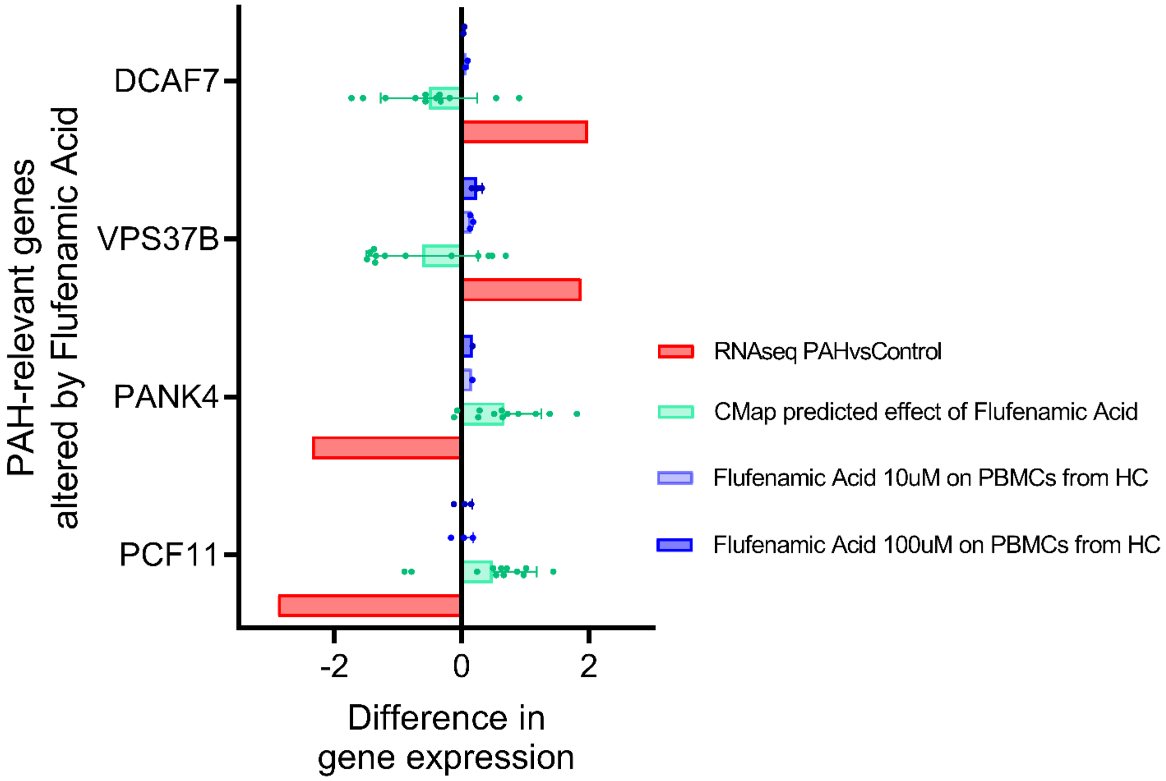

Figure 5.4: Expression levels of selected differentially expressed PAH RNAseq genes for Flufenamic Acid exposure across assays. Gene expression of PCF11, PANK4, VPS37B and DCAF7 in PBMCs from PAH patients (Fold Change vs. Healthy Controls; Red), the CMap database (z-score; Green) and in PBMCs from a healthy donor following Flufenamic Acid exposure (relative expression to PBMCs exposed to vehicle; Blue; 10µM or 100µM Flufenamic Acid in DMSO). Points represent different cell lines (CMap database; Green) or individual experiments (Flufenamic Acid exposure of PBMCs; Blue).

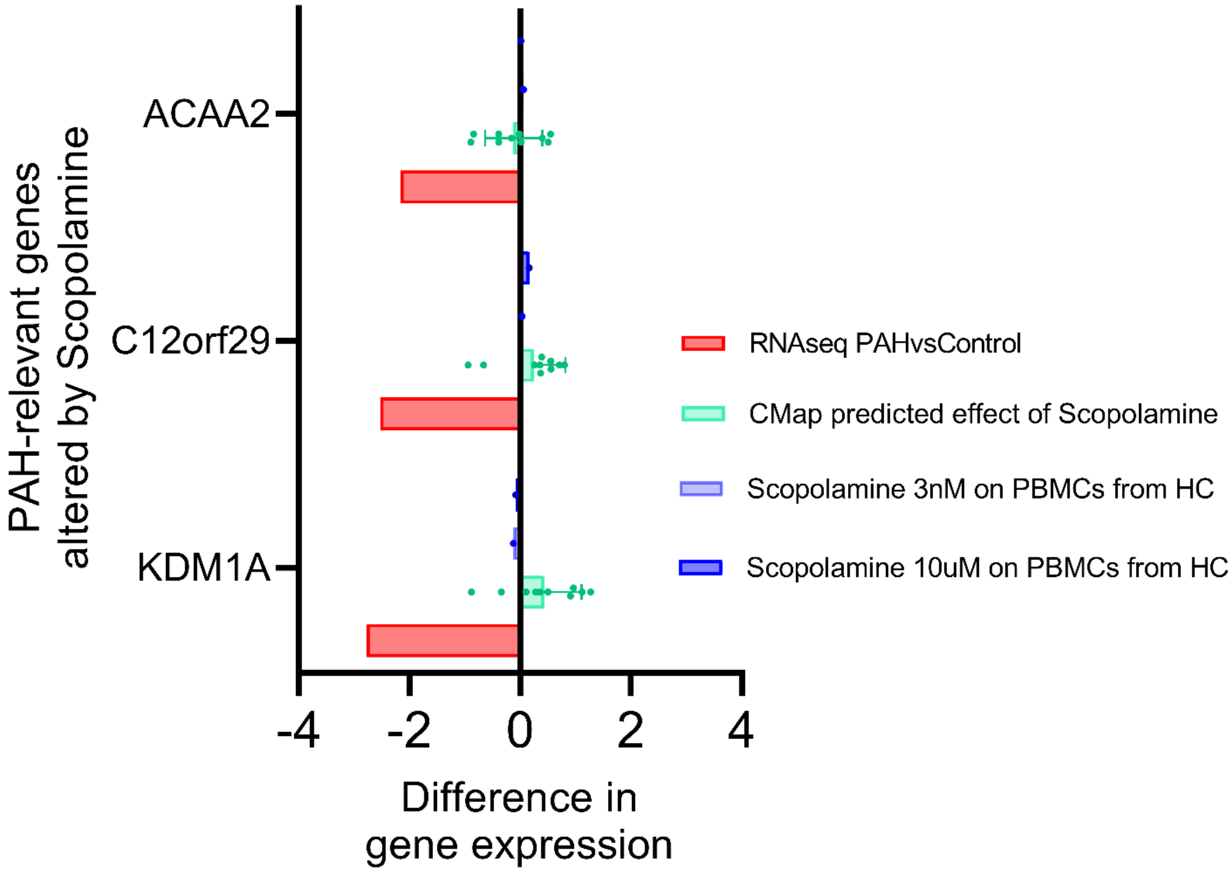

Figure 5.5 (below): Expression levels of selected differentially expressed PAH RNAseq genes for Scopolamine exposure across assays. Gene expression of KDM1A, C12orf29 and ACAA2 in PBMCs from PAH patients (Fold Change vs. Healthy Controls; Red), the CMap database (z-score; Green) and in PBMCs from a healthy donor following Scopolamine exposure (relative expression to PBMCs exposed to vehicle; Blue; 3nM or 10µM Scopolamine in DMSO). Points represent different cell lines (CMap database; Green) or individual experiments (Scopolamine exposure of PBMCs; Blue).

5.5.2.2 Gene expression changes following PBMC exposure to Azithromycin and Homoharringtonine

RNA yields in extracts from PBMCs incubated with 10 µM Homoharringtonine were greatly reduced, suggesting a potential negative impact of high concentrations of Homoharringtonine on cell survivability. Concentrations found to be used in the existing literature ranged from 50 nM to 1 µM, so the latter was decided to be used as the upper range to prevent the reduction in the yield of genetic material observed at 10 µM.

PBMC exposure to Homoharringtonine showed significant changes ($p< 0.01$; $n= 5$) in the expression of 3/4 genes (*PCF11*, *BCLAF1* and *CPT1A*) at the higher experimental concentration (1 µM), as well as significant changes ($p< 0.01$; n= 2-3 per donor) in the expression of 2/4 genes (*PCF11* and *CPT1A*) at the lower experimental concentration (50 nM), in the direction predicted by CMap (Figure 5.6). PBMC exposure to Azithromycin showed significant changes ($p< 0.01$; $n= 5$) in the expression of 1/4 genes (GOLGA4) at the higher experimental concentration (10 µM) in the direction predicted by CMap. No other significant change could be observed in any gene or concentration following exposure of PBMCs to Azithromycin (Figure 5.7).

Overall, Homoharringtonine showed changes in gene expression directionally consistent with CMap predictions and opposing what was observed in the whole blood of PAH patients in 3/4 genes (Figure 5.8), while Azithromycin replicated the predicted changes in 1/4 genes (Figure 5.9).

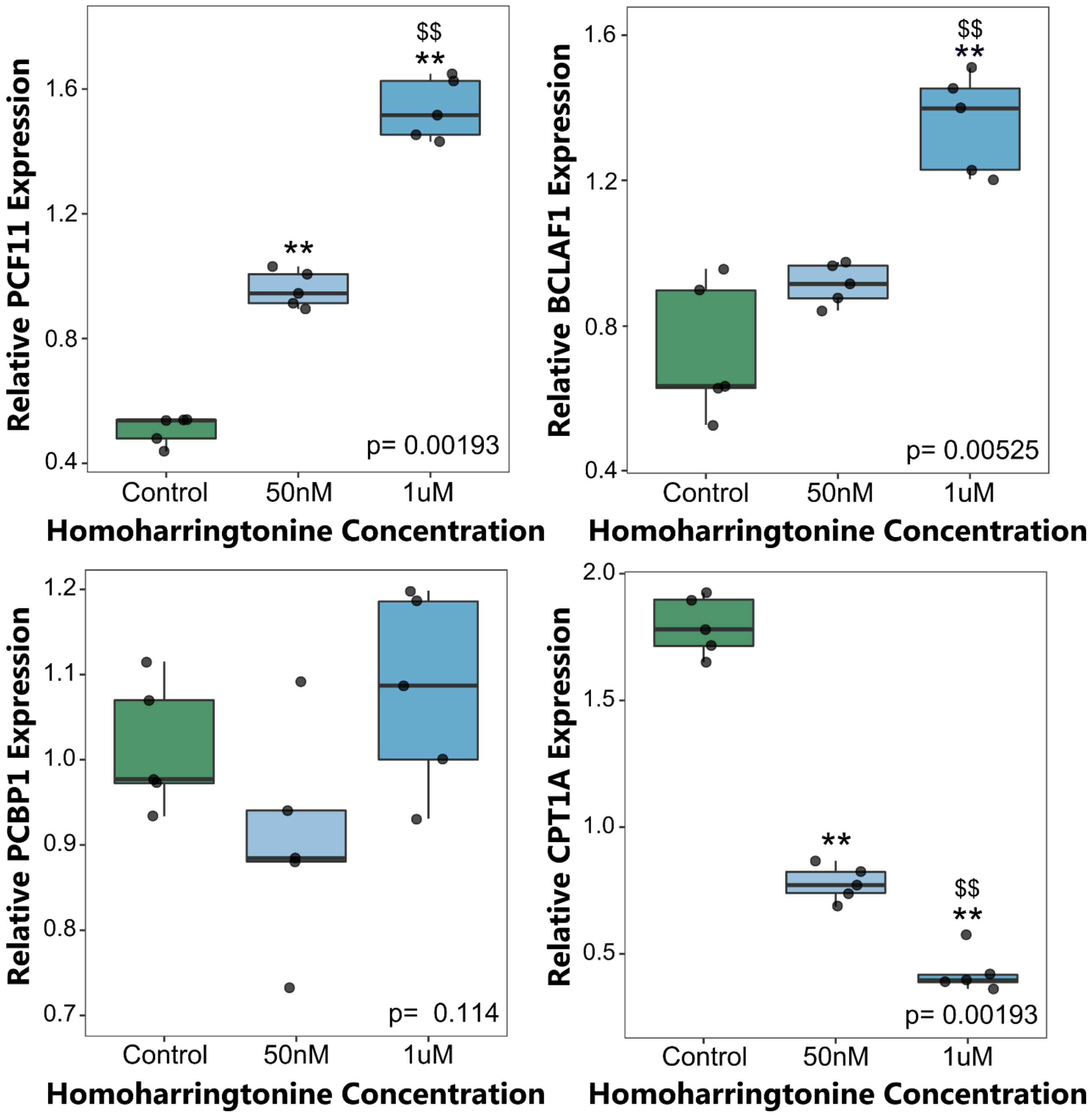

Figure 5.7: Relative expression of selected genes on PBMCs following exposure to Homoharringtonine. PBMCs were exposed to either 50 nM or 1 µM Homoharringtonine or vehicle (DMSO) for 24h. Gene expression was measured by RT-qPCR and relative expression to the experimental average calculated. Kruskal–Wallis one-way analysis of variance was used. Overall differences shown by p-value on each panel. For individual differences across conditions: ***-** $p < 0.05$; ****-** $p < 0.01$ (vs. Control). **$-** $p < 0.05$; **$$-** $p < 0.01$ (vs. 50 nM). Individual dots are averages of 2-3 experiments (n= 5).

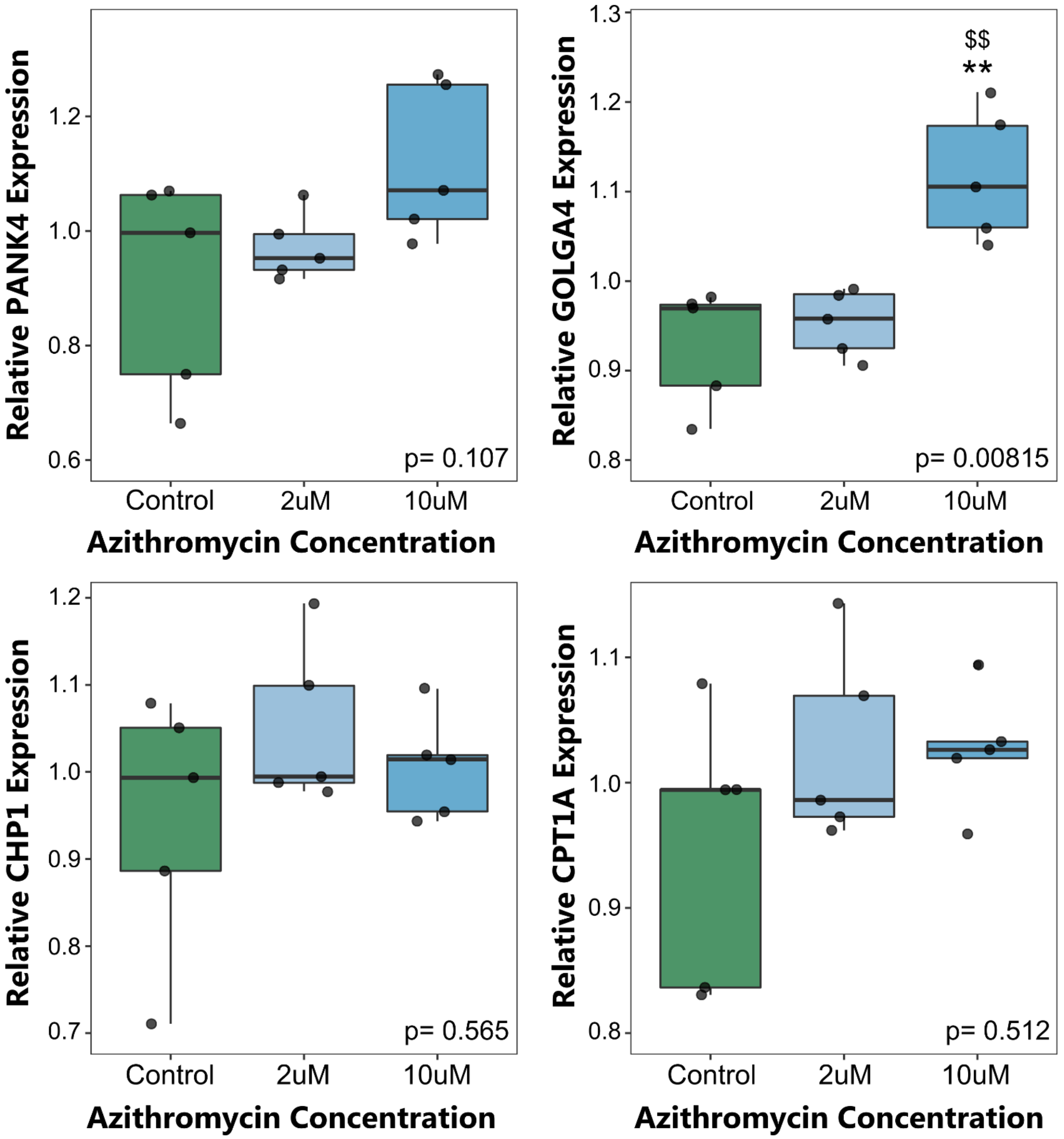

Figure 5.7: Relative expression of selected genes on PBMCs following exposure to Azithromycin. PBMCs were exposed to either 2 µM or 10 µM Azithromycin or vehicle (DMSO) for 24h. Gene expression was measured by RT-qPCR and relative expression to the experimental average calculated. Kruskal–Wallis one-way analysis of variance was used. Overall differences shown by p-value on each panel. For individual differences across conditions: ***-** $p< 0.05$; ****-** $p< 0.01$ (vs. Control). **$-** $p< 0.05$; **$$-** $p< 0.01$ (vs. 2 µM). Individual dots are averages of 2-3 experiments (n= 5).

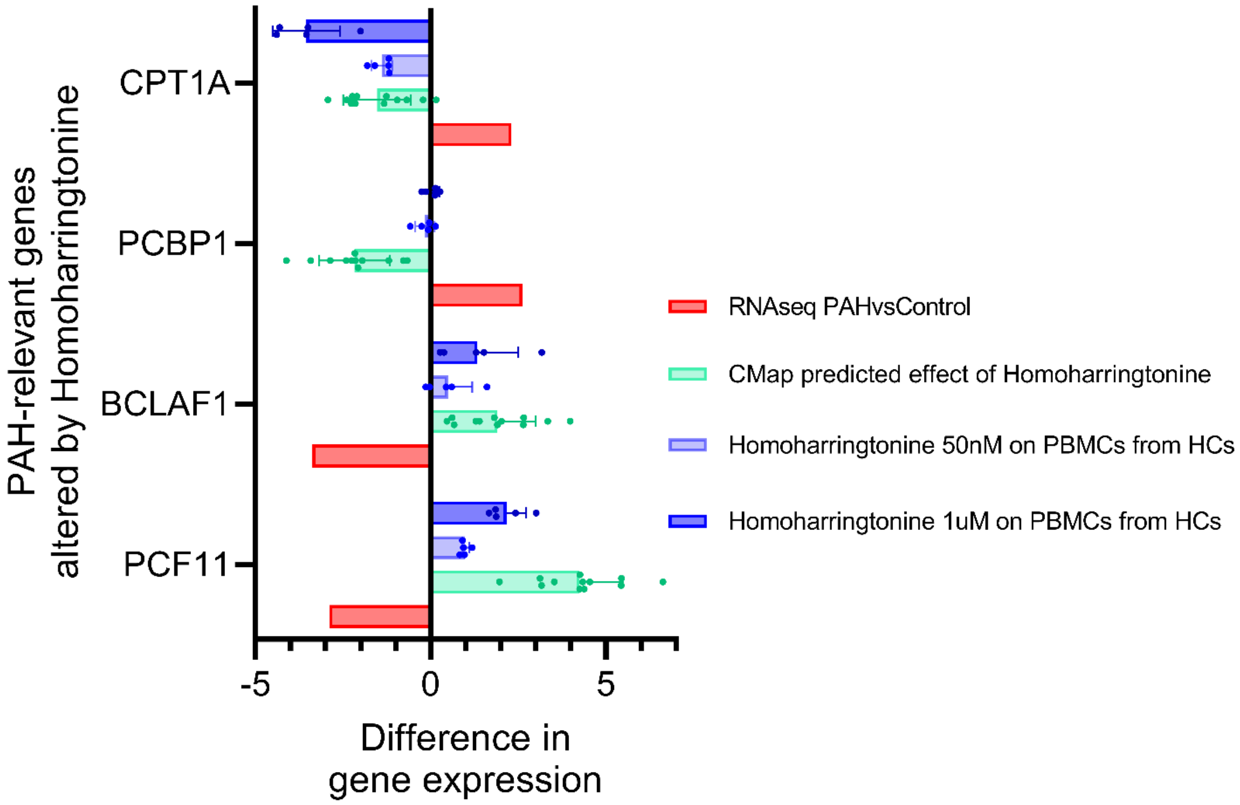

Figure 5.8: Expression levels of selected differentially expressed PAH RNAseq genes for Homoharringtonine exposure across assays. Gene expression of PCF11, BCLAF1, PCBP1 and CPT1A in PBMCs from PAH patients (Fold Change vs. Healthy Controls; Red), the CMap database (z-score; Green) and in PBMCs from 5 healthy donors following Homoharringtonine exposure (relative expression to PBMCs exposed to vehicle; Blue; 50 nM or 1 µM Homoharringtonine in DMSO). Points represent different cell lines (CMap database; Green) or averages of individual donors (Homoharringtonine exposure of PBMCs; Blue).

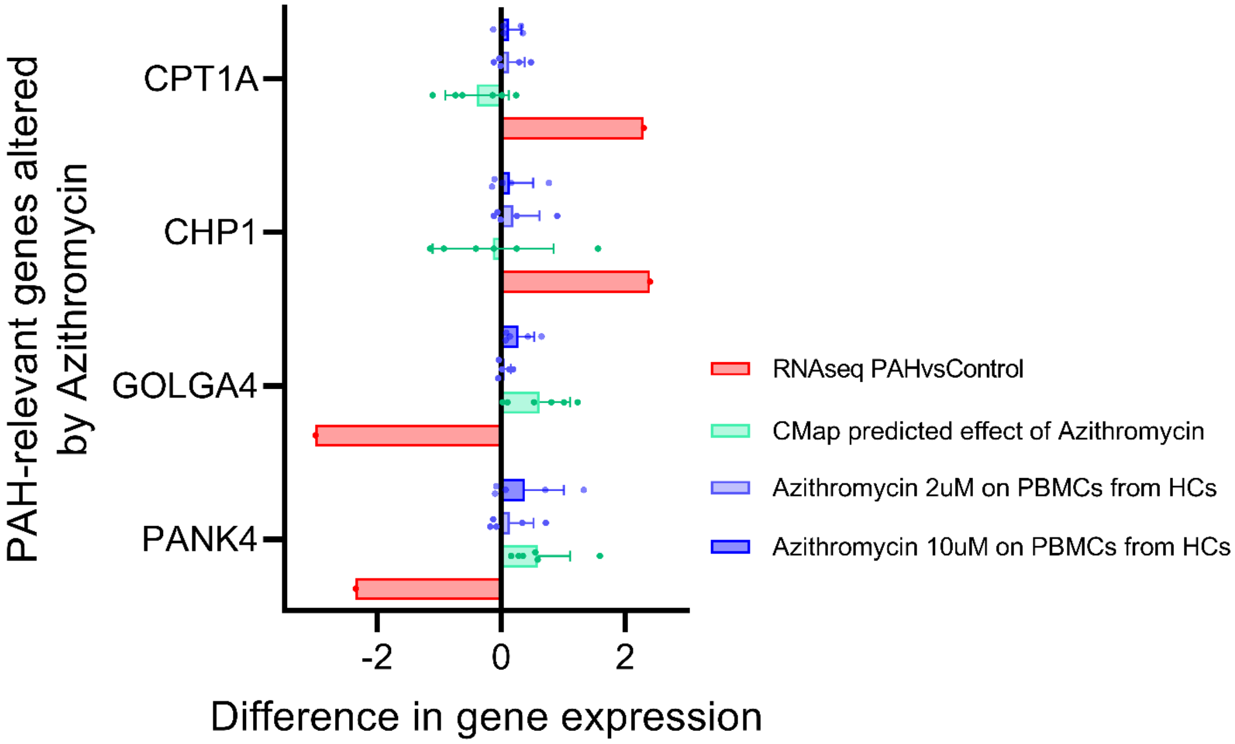

Figure 5.9: Expression levels of selected differentially expressed PAH RNAseq genes for Azithromycin exposure across assays. Gene expression of PANK4, GOLGA4, CHP1 and CPT1A in PBMCs from PAH patients (Fold Change vs. Healthy Controls; Red), the CMap database (z-score; Green) and in PBMCs from 5 healthy donors following Azithromycin exposure (relative expression to PBMCs exposed to vehicle; Blue; 2 µM or 10 µM Azithromycin in DMSO). Points represent different cell lines (CMap database; Green) or averages of individual donors (Azithromycin exposure of PBMCs; Blue).

5.5.3 hPAEC gene expression changes following Homoharringtonine exposure

The top CMap compound, Homoharringtonine, highlighted by differential gene expression analysis following PBMC exposure to all 6 CMap candidate compounds (Azithromycin, Deferiprone, Dovitinib, Flufenamic Acid, Homoharringtonine and Scopolamine), was put forward for hPAEC exposure and subsequential differential expression analysis, as hPAECs are a key cell type in PAH pathology.

In experiments performed by my laboratory colleague, Dr. Yukyee Wu, hMVECs (human MicroVasculature Endothelial Cells were exposed for 24h to LPS (Lipopolysaccharide) [2µg/mL], a proinflammatory stimulus producing a response akin to the inflammation occurring in PAH, followed by RNA extraction. Gene expression analysis of RNA extracted from these hMVECs revealed a reduction in the expression levels of all 4 selected CMap genes (PCF11, BCLAF1, PCBP1 and CPT1A) following LPS exposure (Figure 5.10), which is in contrast to what was observed in the PAH RNAseq (where there were 2 genes up- and 2 down- regulated in PAH patients). This may be due to a tissue-specific response to LPS.

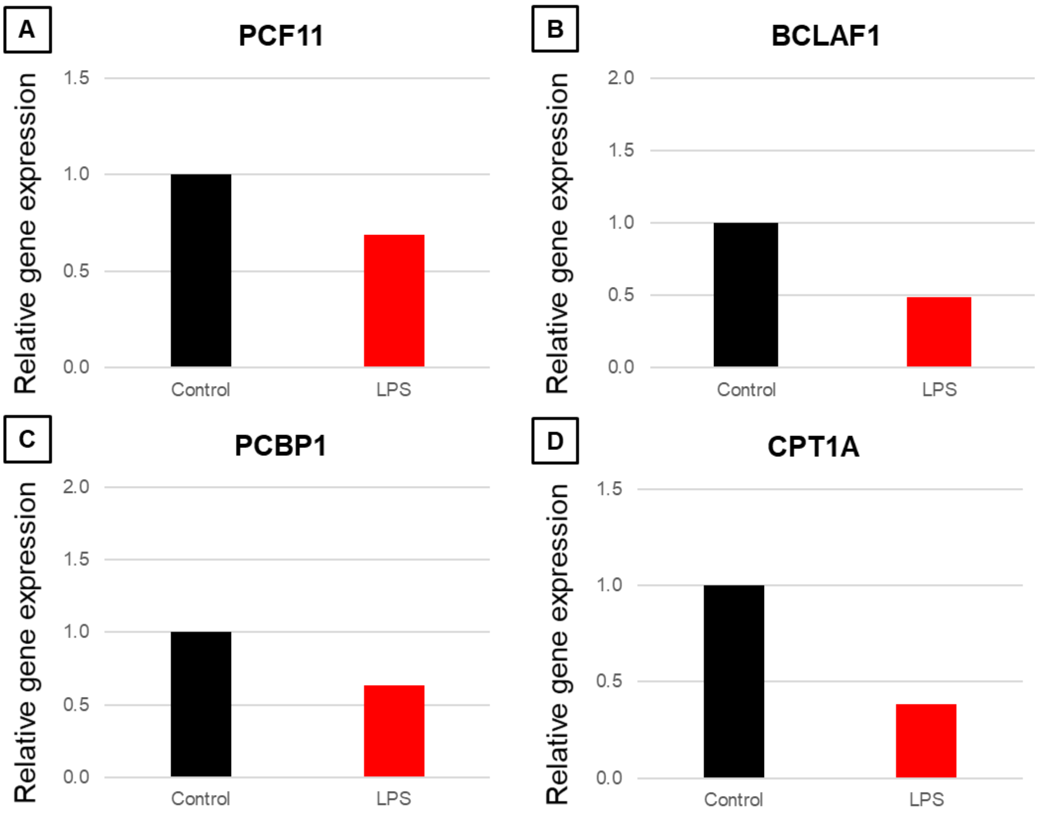

Figure 5.10: Relative expression of selected differentially expressed PAH RNAseq genes in hMVECs following PAH-relevant stimuli. Relative gene expression of **A)** PCF11, **B)** BCLAF1, **C)** PCBP1 and **D)** CPT1A vs. controls in hMVECs following exposure to LPS (Red; Lipopolysaccharide) [2 µg/mL].

To assess the effect of Homoharringtonine on the expression of PCF11, BCLAF1, PCBP1 and CPT1A in hPAECs, cells were exposed to increasing concentrations [50 nM – 1 µM] of Homoharringtonine for 24h and RNA levels of these 4 genes were measured by RT-qPCR. The expression of all 4 genes was upregulated by Homoharringtonine in a concentration-dependent manner (Figure 5.11), which again differs from what was observed in PBMCs *in-vitro* (see details in Chapter 5.5.2.2). These differences in responses to PAH-relevant stimuli between tissues suggest there may be a tissue-specific transcriptional response.

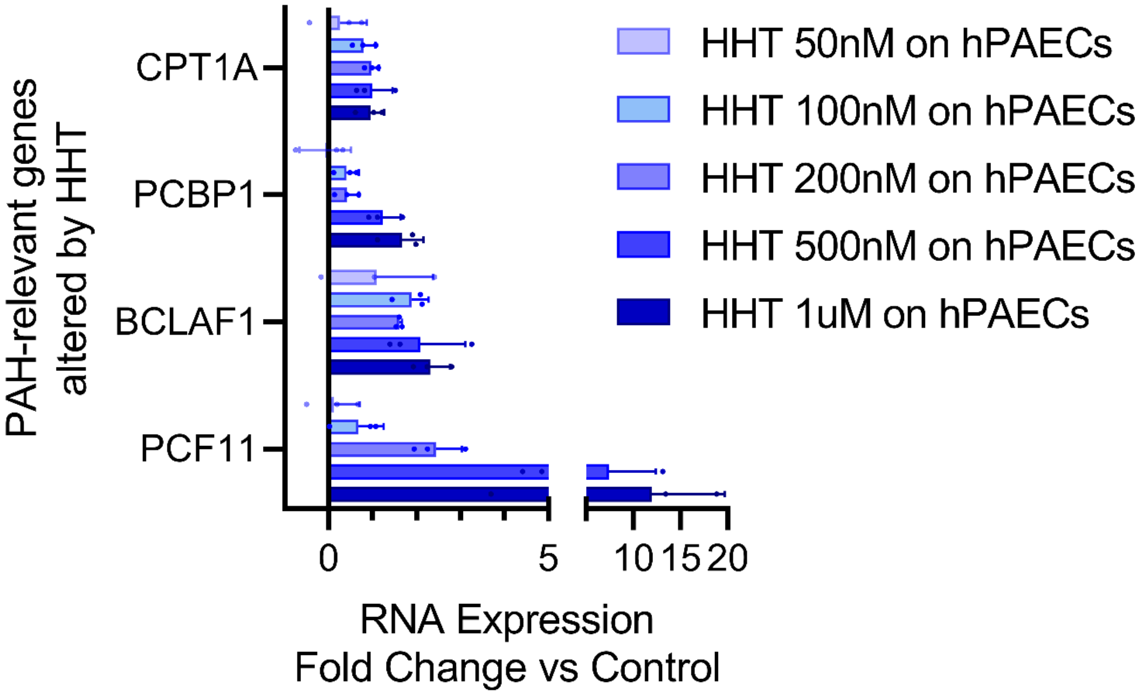

Figure 5.11: Gene expression levels of selected differentially expressed PAH RNAseq genes in hPAECs following exposure to increasing concentrations of Homoharringtonine. Fold change of PCF11, BCLAF1, PCBP1 and CPT1A vs. controls in hPAECs following 24h exposure to 50nM, 100nM, 200nM, 500nM and 1µM Homoharringtonine. DMSO used as vehicle.

5.5.4 hPAEC function changes following Homoharringtonine exposure

To determine the functional impact of Homoharringtonine exposure in hPAECs, the functional responses to relevant PAH stimuli on hPAECs in culture were investigated. Specifically, cell viability inferred via metabolic activity was measured through MTT assay, cell viability inferred via ATP levels was measured through Cell Titre assay and cell apoptosis inferred through caspase activity was measured through Caspase assay.

Preliminary MTT and Caspase assays for hPAEC 24h exposure using a range of Homoharringtonine concentrations [50 nM – 1 µM] revealed decreased metabolic activity and increased apoptosis at higher Homoharringtonine concentrations [200 nM – 1 µM]. Conversely, lower concentrations [50 nM – 100 nM] suggested a potential protective anti-apoptotic and proliferation-neutral effect of low doses of Homoharringtonine in hPAECs (Figure 5.12)

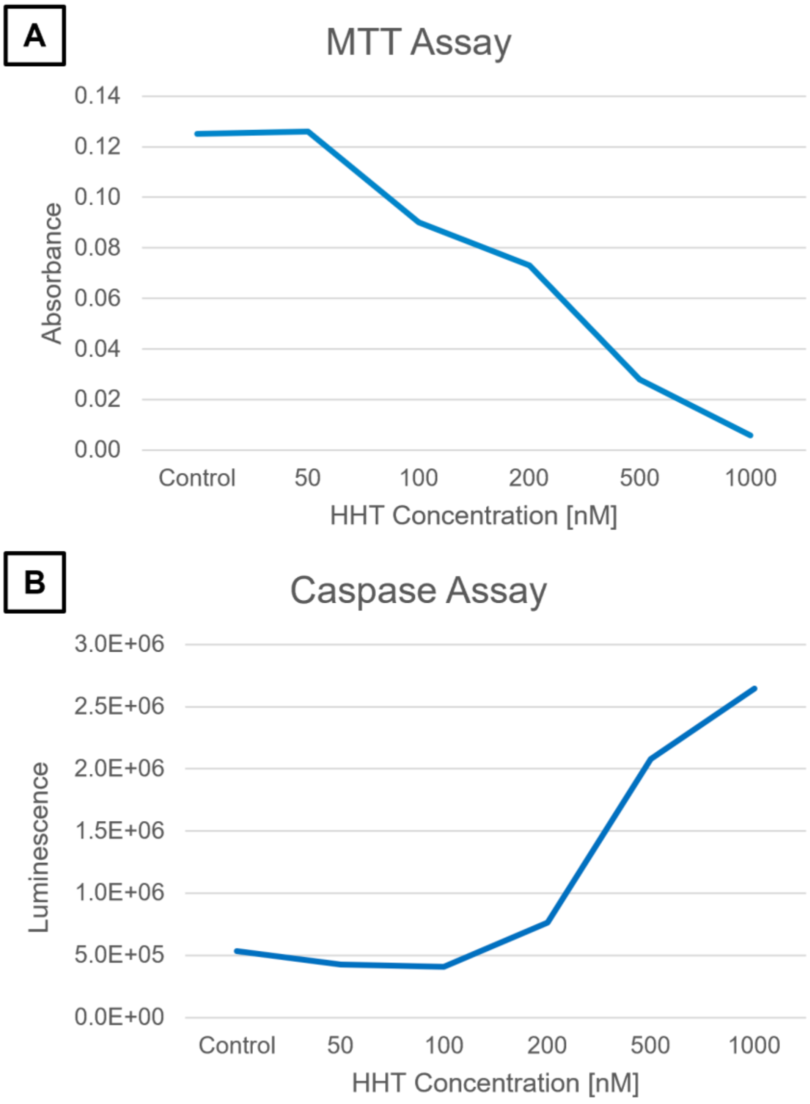

Figure 5.12: Preliminary functional assays on hPAECs exposed to Homoharringtonine. A) MTT (cell viability) and **B**) Caspase (apoptosis) assays performed on hPAECs following 24h exposure to 50 nM, 100 nM, 200 nM, 500 nM and 1 µM Homoharringtonine. DMSO used as vehicle. Y-axis shows average (n= 3 wells per condition) absorbance (MTT) or luminescence (Caspase) per condition.

Following these preliminary results, it was decided to continue the functional assays using the lower concentrations of Homoharringtonine [50nM and 100nM]. The Cell Titre assay was used as a control for the results obtained from the Caspase assay (see details on Methods 2.3.5). The PAH-relevant stimuli TNFα and VEGF were used to further characterise the effects of Homoharringtonine. TNFα induces pro-inflammatory and pro-apoptotic conditions by suppressing BMPR2 and altering Notch signalling (145). It was used for the Caspase 3/7 and Cell Titre assays [10 ng/mL]. VEGF induces pro-angiogenic and pro-proliferative conditions (287). It was used for the MTT assay [100 ng/mL].

A significant difference (p= 0.041) in the ratio of caspase activity to cell viability was observed between conditions, but no individual differences between any of the groups were identified. Nonetheless, a trend for a reduction in the apoptotic activity of hPAECs after exposure to low concentrations of Homoharringtonine [50 nM and 100 nM] was observed both with and without co-exposure to TNFα (Figure 5.13). A non-parametric test on the same data (Kruskal-Wallis test) resulted in no significant differences identified between conditions (p= 0.092). These results should therefore be validated utilizing larger sample sizes and experimental repeats.

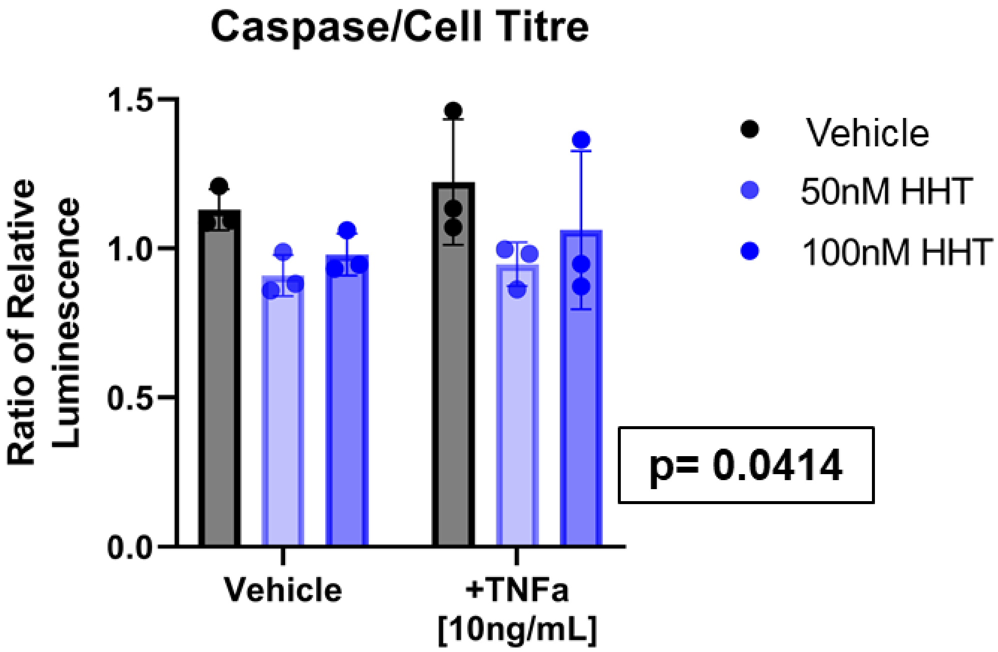

Figure 5.13: Ratio of caspase activity to cell viability in hPAECs exposed to low doses of Homoharringtonine. Caspase (apoptosis) and Cell Titre (cell viability) assays performed on hPAECs following 24h exposure to 50 nM, or 100 nM Homoharringtonine; with and without 10 ng/mL TNFα. DMSO used as vehicle. Individual dots show average ratio of relative luminescence per assays (n= 3). Statistical tests used are ordinary two-way ANOVA with Dunnett's multiple comparisons test.

A significant difference (p< 0.0001) in the MTT proliferation assay results was observed, with hPAECs in the 100 nM Homoharringtonine groups (both with and without VEGF) showing a significant reduction in the number of metabolically active cells when compared to both hPAECs exposed to 50 nM Homoharringtonine and hPAECs in the vehicle group. hPAECs exposed to 50 nM Homoharringtonine also showed a reduction in the number of metabolically active cells when compared to the vehicle group when also co-exposed to VEGF, while this was not the case for the group without VEGF co-exposure. Overall, low concentrations of Homoharringtonine [50 nM and 100 nM] significantly reduced the number of metabolically active hPAECs (Figure 5.14).

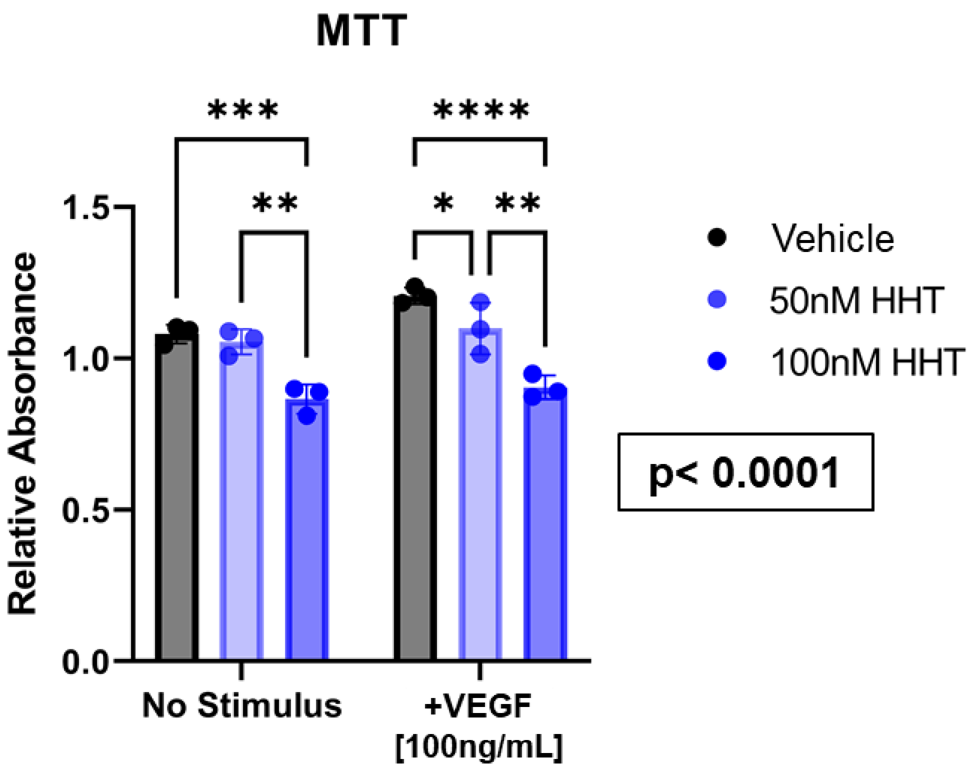

Figure 5.14: MTT assay in hPAECs exposed to low doses of Homoharringtonine. MTT (cell viability through metabolic activity) assay performed on hPAECs following 24h exposure to 50 nM, or 100 nM Homoharringtonine; with and without 100 ng/mL VEGF. DMSO used as vehicle. Individual dots show average relative absorbance per assay (n= 3). Statistical tests used are ordinary two-way ANOVA with Tukey's multiple comparisons test. *: p< 0.05; **= p< 0.01; ***= p< 0.001; ****= p< 0.0001.

5.5.5 Changes in hPAEC gene expression following exposure to Homoharringtonine and LPS

Following preliminary results in functional assays in hPAECs revealing a potential therapeutic effect of Homoharringtonine at low concentrations [50 nM and 100 nM] (Figure 5.12), it was decided to explore the ability of these concentrations of Homoharringtonine to rescue the changes caused by LPS in gene expression on endothelial cells—namely, a reduction in gene expression of the 4 genes highlighted from the PAH RNAseq signature: PCF11, BCLAF1, PCBP1 and CPT1A (Figure 5.10). Previous results on hPAECs showed that exposure to Homoharringtonine alone increased the expression of all 4 genes, even at these low concentrations (Figure 5.11).

In this assay, as seen in previous results from the Rhodes lab (Figure 5.10), LPS [2 µg/mL] alone induced a general reduction in gene expression in hPAECs across all 4 genes. Similarly, as previously showed (Figure 5.11), expression of 3 genes (PCF11, BCLAF1 and CPT1A) was significantly increased ($p < 0.05$) by 100 nM Homoharringtonine (dark blue), while PCBP1 expression was also increased but did not meet significance. Expression for all 4 genes was increased by 50 nM Homoharringtonine (light blue), but only significantly in the case of BCLAF1 ($p = 0.011$). Co-exposure to LPS and 100 nM Homoharringtonine (dark green) also resulted in significantly increased ($p < 0.05$) gene expression in PCF11, BCLAF1 and CPT1A, similar to 100 nM Homoharringtonine. Co-exposure to both LPS and 50 nM Homoharringtonine (light green) resulted in increased gene expression of PCF11, BCLAF1 and PCBP1, although changes were not significant. Overall, low concentrations of Homoharringtonine, particularly at 100 nM, were able to prevent the reduction in gene expression of the selected PAH RNAseq signature genes induced by LPS in hPAECs (Figure 5.15).

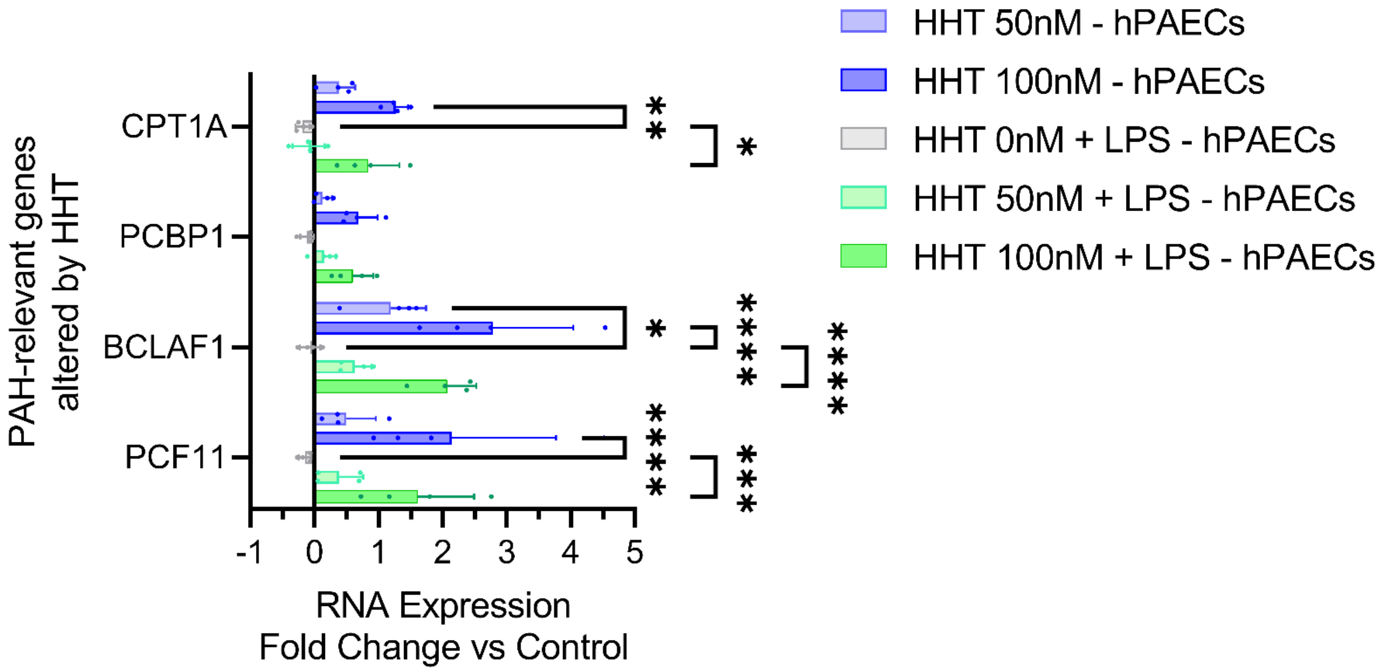

Figure 5.15: Gene expression levels of selected differentially expressed PAH RNAseq genes in hPAECs following co-exposure to Homoharringtonine and LPS. Fold change of PCF11, BCLAF1, PCBP1 and CPT1A vs. controls (no Homoharringtonine and no LPS) in hPAECs following 24h exposure to 50 nM or 100 nM Homoharringtonine or vehicle and either LPS or vehicle. DMSO used as vehicle. Statistical tests used are ordinary two-way ANOVA with Dunnett's multiple comparisons test vs. control (0 nM). *: $p < 0.05$; **= $p < 0.01$; ***= $p < 0.001$; ****= $p < 0.0001$.

5.6 Discussion

The first aim of the work presented in this chapter was to utilise the CMap database to identify small molecule compounds that could induce gene expression profiles opposite to the whole blood PAH RNA signature described throughout this thesis (see details in Chapter 3). When the CMap database was queried using the top dysregulated genes from the 507-gene PAH signature, 6 commercially available compounds, namely Azithromycin, Dovitinib, Deferiprone, Homoharringtonine, Flufenamic-acid and Scopolamine were highlighted as potential candidates for PAH signature reversal and put forward for downstream analyses.

The second aim was to evaluate the ability of candidate compounds to effect opposite transcriptional changes to those observed in PAH patients in *in-vitro* assays in PBMCs from healthy donors. A selection of 4 genes from the PAH RNA signature predicted by the CMap database to change in the opposite direction following exposure to a given compound, 2 with increased and 2 with decreased expression, was performed. Selection was based on dysregulation significance, PAH functional relevance, expression levels in PBMCs and hPAECs, and ease of primer development. Two different compound concentrations were utilised for each candidate, one being the most widely used across literature in relevant cell types, the other 10 µM as per CMap methodology. Homoharringtonine, the candidate compound that most closely replicated the gene expression changes predicted by CMap in PBMCs from healthy donors, showed significant changes in the predicted direction in 3/4 genes selected and 2/3 genes (PCF11 and CPT1A) were still significantly dysregulated by Homoharringtonine even when a much lower compound concentration (50 nM) was utilised. These results suggest Homoharringtonine may be able to produce opposite effects on gene expression in PBMCs as those identified in PAH. PAH pathology, despite mainly occurring in the lung vasculature, includes a strong immune and inflammatory process thought to contribute to disease severity and progression (see details on Introduction 1.3.4) (62, 65-69). Additionally, gene expression changes identified in PBMCs from PAH patients have been shown to strongly correlate with clinical performance (see details on Chapter 3). PAH signature reversal on whole-blood PBMCs in systemic circulation could therefore have positive, therapeutic effects independently from what may be occurring within the lung vasculature itself.

The main caveat of these findings lies in the limited nature of the CMap signature validation performed through this mechanism, as only 4 genes were tested per compound. Despite these 4 genes being selected accounting for biological relevance and dysregulation significance, their changes may not be representative of other gene expression changes occurring following compound exposure. Further validation using a wider selection of dysregulated genes (perhaps even full RNAseq analysis or another high-throughput methodology) could overcome this issue and provide a clearer picture of the gene expression perturbation elicited by each compound. Another potential limitation lies in the number of different compound concentrations used for candidate compound exposure. Assays were carried out using healthy donor PBMCs. PBMC isolation is a complicated process requiring fresh blood from on-site phlebotomies. This technical difficulty significantly limits the number of experimental conditions that can be tested per compound. Where possible, an increased number of donors, experimental conditions (including compound concentration) and technical repeats would be useful and yield more comprehensive results. This would help to more robustly identify the strongest candidate compounds.

The third and final aim for this chapter was to assess changes in gene expression and cellular function in *in-vitro* assays in relevant vascular cells (hPAECs) induced by Homoharringtonine, the strongest candidate compound from previous assays. Transcriptional changes induced by LPS (a proinflammatory stimulus producing a response akin to the inflammation occurring in PAH) on hMVECs, namely a reduction in all four selected genes, were used for reference. In contrast to this, when hPAECs were exposed to Homoharringtonine, an upregulation in all 4 genes was identified. Furthermore, hPAECs exposed to LPS replicated results observed in hMVECs, but co-culture with LPS and Homoharringtonine (50 nM and 100 nM), prevented this reduction of gene expression levels and resulted in upregulation in all four genes. These observations suggest Homoharringtonine may be able to effectively reverse transcriptional changes elicited by PAH pathology on hPAECs, even under disease conditions. Given this, I hypothesised Homoharringtonine may have a therapeutic effect not only in PBMCs but also in hPAECs, a vascular cell intrinsic to PAH pathology. This would increase the therapeutic potential of Homoharringtonine action. Again, the main caveat for these results lies in the limited number of genes selected for PAH RNA signature reversal validation and utilising more genes would yield more insights into transcriptional changes induced by Homoharringtonine expression. Furthermore, transcriptional effects of PAH pathology on hPAECs were inferred from LPS exposure on hMVECs. While LPS is a pro-inflammatory stimulus capable of inducing PAH-like effects and hMVECs are very similar in nature to hPAECs, hPAECs isolated from PAH patients would be the ideal model from which to compare results in our assays. A more meaningful approach, if it had been available, would have entailed the study of behavioural changes in hPAECs isolated from PAH patients followed by a study of whether these changes were corrected by Homoharringtonine.

Functional assays were also conducted on hPAECs exposed to Homoharringtonine. This included MTT, Caspase 3/7 and Cell Titre assays. Preliminary MTT and Caspase assays showed that, while high concentrations of Homoharringtonine reduced cell viability and increased apoptosis, low Homoharringtonine concentrations (50 nM – 100 nM) seemed to have a protective effect on hPAECs. Further assays conducted using these lower Homoharringtonine concentrations along with PAH relevant stimuli (TNFα or VEGF) showed a significant difference in Caspase/Cell Titre ratios (potentially reflecting a reduction in apoptotic activity, although further repeats will be needed to achieve statistically robust results) as well as a significant reduction in MTT assay results (reflecting a reduction in the number of metabolically active cells) following Homoharringtonine exposure independently of PAH stimuli. PAH pathogenesis involves dysregulation of normal vascular physiology, where vascular cells develop hyperproliferative, migratory phenotypes while becoming resistant to apoptosis (see details on Introduction 1.3.4). There is evidence suggesting PAEC apoptosis may be increased early during PAH pathogenesis, which may lead to the selection of apoptosis-resistant cells and result in the angioproliferative phenotype that is a hallmark of severe PAH (288,289). Apoptosis prevention could therefore eliminate this selection process and facilitate the stabilisation of a more normal endothelium. Furthermore, reducing the number of metabolically active hPAECs could interfere with the pathologic hyperproliferative phenotype these cells acquire in PAH. Our results therefore suggest Homoharringtonine could have beneficial effects for PAH pathology on hPAECs through decreased apoptosis and limited proliferation.

Further functional work on other physiological functions of hPAECs, such as barrier function or adhesion, would need to be explored to get a clearer view of the functional effects of Homoharringtonine on hPAECs and get a better understanding of the overall effect of this candidate compound on hPAECs. Future Homoharringtonine research should also investigate transcriptional and functional effects of Homoharringtonine on PASMCs. PASMCs are, along with hPAECs, the most prominent cell types affected by PAH pathology (see details on Introduction 1.3.4). If PASMC research yielded positive results, the effects of this compound on more complex biological systems should be studied next. These biological systems could range from rodent models of PAH to biomimetic structures replicating the arterial vasculature, such as the Pulmonary Artery on a Chip (89). This kind of model would also enable investigating a crucial element of normal and PAH physiology not explored in this work—the interplay and communication between different cell types. Cell-cell communication is a key physiological component and several changes in PAH occur through perturbations of these signalling mechanisms (see details on Introduction 1.3.4). Another element these models enable exploring is the effect of blood flow, previously shown to affect vascular homeostasis (290), on cell physiology and communication in the context of PAH. Increased blood flow has also been shown to elicit pathological changes in PAH (291–294).

Candidate compounds were chosen on the basis of their respective gene expression signatures showing the strongest negative correlation with the input PAH RNA signature. It is important to note, however, that there were 3 compounds that showed the third, fourth and fifth strongest negative correlation with the input signature but were not chosen to be used for this study. These compounds were Verrucarin-a, Emetine and Cephaeline. The rationale for these exclusions was on the basis of underlying molecular mechanisms, as these compounds had the same general function—protein synthesis inhibitors—as Homoharringtonine, which had a stronger negative correlation as the second most associated compound and was selected to be put forward for the study. Since this work does not actually explore the mechanism by which Homoharringtonine is inducing the reported positive effects on PBMC and hPAEC physiology and transcriptional state, it is yet unknown whether these are Homoharringtonine-specific effects or if they arise from exposing these cells to a protein synthesis inhibitor. Thus, exploring the therapeutic potential of these discarded compounds would also be of relevance in the context of PAH therapeutics and even for investigating the underlying pathological processes that are being reverted by exposure to a protein synthesis inhibitor.

The CMap database originated as a pilot study, including only 3 cancer cell lines and studying gene perturbations derived from exposure to just 164 small molecule compounds (216). In order to scale up the project and produce a large database following the CMap proof of concept, the number of core cell lines used was increased to 9, the number of small molecule compounds was increased to 19,811 and a new sequencing method was developed (L1000) where measuring expression levels of just 1000 landmark genes was sufficient to recover 82% of the information in the full transcriptome (217). While this method enabled a dramatic reduction in sequencing costs versus full-scale sequencing approaches such as RNAseq, this also means a considerable portion of the transcriptomic information is lost as a result. Furthermore, despite the increase in core cell lines and small molecule compounds used, the database is not entirely comprehensive. This is evidenced by the lack of a PAH-relevant cell line within the CMap database, as the types of cells used do not include hPAECs, PASMCs, PBMCs or any other related cell lines (such as other types of ECs). Therefore, predictions of gene perturbation following compound exposure require validation in the cell type of interest. It is also worth noting how current commercially available small molecule compound repositories offer research libraries more than an order of magnitude larger than the total number of compounds used for the CMap database generation (295), so there may be more optimal compounds not included in the assays. Additionally, compound concentrations during exposure are limited and only 10 µM is used across all compounds, with some instances including ranges of lower concentrations (up to 3 nM on occasion). This means the observed gene perturbation may be occurring at biologically irrelevant doses. Hence, biologically relevant concentrations must be identified in the literature and tested as well. It would thus be of great interest to revisit the CMap database in the future if the number of cell lines, compounds tested or compound concentrations gets expanded, or to query the PAH RNA signature in a new, different database, as this may yield more directly relevant, insightful results.

Overall, I used the CMap database to identify six PAH RNA signature reversal candidate compounds and selected Homoharringtonine as the strongest candidate based on its ability to induce the desired transcriptional changes in healthy donor PBMCs and in hPAECs *in vitro*, as well as functional changes in hPAECs. Further research into the molecular mechanisms of Homoharringtonine action, or of other protein synthesis inhibitors, is required to investigate its therapeutic potential in PAH. This should include assays on PASMCs and in more complex physiological models, such as the Pulmonary Artery on a Chip or rodent PAH models. These results also highlight the potential of whole blood RNA profiling to generate candidate therapeutic approaches which may also act on pathologic tissues (such as vascular cells), strengthening the possibility of harnessing this approach in other presentations of PH. Furthermore, an RNA signature based on circulating blood cells (PBMCs) could be easily used as a strategy for selecting patients potentially more likely to respond to therapies derived from that signature.

6 – Discussion

The biomedicine field now finds itself at a remarkable crossroad. Exponential, ever-growing improvements in our technological capabilities and infrastructure over the past few decades have finally enabled research to not be mainly limited by technical issues, but rather by research ingenuity and innovation. Comprehensive, real-time snapshots of biological systems are now attainable, and we are able to analyse, compare, store and share vast amounts of information instantly with astounding computing power. Optimally harnessing that technological power to broaden our understanding of disease beyond what was previously possible is now the primary challenge of biomedical research efforts, as we are now essentially able to test most hypotheses if we are able to find the right question and capable of interpreting the results. The personalised medicine approach, where each patient is treated as an individual biological system we can fully understand and design an optimal treatment for, is rapidly shifting from a utopic, distant goal into a fast-approaching reality; and the current paradigm is no longer whether personalised medicine is possible, but rather how quickly we can materialise it.

At the forefront of this vision lies the omics field and its—to a great extent—untapped potential, and no other recipient for this strategic approach has greater potential than that of the very rare and very deadly diseases. Unless pathogenesis arises from clear, relatively direct causes, such as monogenic mutations, low incidence and high mortality vastly limit sample availability. This creates crucial issues when trying to attain statistical power, identify underlying mechanisms and develop effective therapies. PAH research suffers from all these issues and recent omic approaches have shown great levels of success in lifting the veil that for decades has haltered meaningful advances in our understanding of this disorder (164,165).

The work presented throughout this manuscript attempts to begin to fully harness these new research possibilities and methodologies through a transcriptomics approach to generate a thorough evaluation of changes occurring in PAH patients at the RNA level, establish connections between RNA profiles and other features of PAH pathology—both clinical and mechanistic—, and use them directly to identify candidate therapies to bring back into a patient setting. It also attempts to show instances of omic layer combinations and their potential to generate further, more nuanced results.

In this thesis, transcriptional changes occurring in the whole blood of PAH patients were assessed by comparing PAH RNA profiles with RNA profiles from healthy controls. An RNA signature for PAH was identified, validated and used to generate an RNA model associated with clinical outcomes. This signature was also utilised to identify potentially pathogenic gene dysregulations—implicating SMAD5, TRPC1 and AMD1—and combined with metabolomic data to further improve its diagnostic power. These findings highlight the potential of whole blood RNA—but also of multi-omics—profiling as a useful diagnostic and stratifying tool for PAH. This simple, readily available method could not only provide with accurate results and greater granularity, but also circumvent the invasive clinical diagnostic procedures currently used for this purpose. Results also emphasize the potential role in PAH pathogenesis of known pathways and processes previously implicated in PAH pathology, such as BMP/TGF-β signalling (SMAD5), calcium channel dysfunction (TRPC1) and polyamine metabolism (AMD1). Interestingly, polyamine metabolism had also been flagged for its association with PAH in previous metabolomic efforts (165).

While other PAH transcriptomic studies had been conducted previously (see details on Introduction 1.4), this PAH RNAseq study was, to my knowledge—and based on subsequent publications—, the first whole blood RNAseq performed on a cohort including PAH patients. Since, another whole blood RNAseq study of PAH patients has been published (296) and, notably, one of the top dysregulated genes highlighted in that study—ZNF841—was also one of the top 507 dysregulated genes identified in the present RNAseq. ZNF841 was downregulated in the PBMCs of PAH patients from both that PAH RNAseq study and the current one, as well as in hPAECs from PAH patients also described in that publication. This emphasises the robustness of the analyses conducted throughout the work presented in this manuscript and suggests there may be potential in investigating the role of ZNF841 in the context of PAH pathology. Multi-omic approaches to PAH research have also been recently attempted, such as a study combining transcriptomic, proteomic and epigenomic data derived from pulmonary arteries of hypoxia-induced PAH rat models (297), but none of the top 9 genes highlighted in that analysis were found in the current PAH RNA signature. Differences between rat PAH models and human PAH patients, as well as between vascular cells in pulmonary arteries and PBMCs in whole blood may account for these different results. Such differences may reflect a key issue in PAH research—tissue and model selection—. Interpretation and external validation of study results must account for this heterogeneity across PAH research strategies. This can be further observed in other recently published transcriptomic studies of PAH, including a hPAEC single-cell RNAseq (298) for which only 1 of the top 80 dysregulated genes (HLX; downregulated in PAH) was found to overlap with results from the present study. Similarly, in a monocrotaline rat RNAseq of lung tissue (299), none of the top 10 dysregulated genes overlapped with the current PAH RNA signature. New research following a similar methodological approach as the one followed in the work presented in this thesis is required to assess whether the results presented here are reproducible and whether further support for the pathological PAH mechanisms identified can be obtained.

SMAD5 has been implicated in PAH pathology and potentially in PAH pathogenesis throughout the work here presented, both by its dysregulation in the PBMCs of PAH patients and the results of a Mendelian Randomisation study showing lower levels of SMAD5 associated with genotype of a known *SMAD5* eQTL also associated with PAH phenotype (see details on Chapter 3). Its role within the BMP/TGF-β signalling pathway and its other independent cellular functions have also been outlined (see details on Intro 1.3.6 and Chapter 3). SMAD5 has been found to be downregulated in the PASMCs of hypoxic rat models of PAH (300). Evidence of microRNA-mediated SMAD5 downregulation, such as that induced by miR-21 in periodontal ligament formation (301), highlights a *BMPR2* mutation-independent regulation of BMP/TGF-β signalling through SMAD5 dysregulation. Furthermore, a recent study on hypoxic rats and hPAECs showed how miR-27a, a microRNA upregulated in ECs under hypoxic conditions, promoted EndoMT through inhibition of Smad5 translation (302), suggesting another molecular mechanism by which SMAD5 downregulation may promote PAH pathogenesis independently of upstream BMP/TGF-β signalling. Overall, this suggests SMAD5 may play a key role in PAH pathology and pathogenesis independent of BMP/TGF-β signalling, and further research should be conducted to elucidate the specific role of SMAD5 in PAH. It has been shown how germline knock-out of *SMAD5* results in embryonic lethality in mice (303), but conditional tissue-specific *SMAD5* knock-outs both in ECs and in SMCs result in viable animals with only slight cardiac defects in the case of the SMC *SMAD5* KO (304). These conditional *SMAD5* KO lines could be studied in the context of hypoxia-induced PH and assess whether *SMAD5* deficiency induces changes in disease progression. Other approaches for conditional SMAD5 depletion may include the use of siRNA to test whether there is a temporal component to the role of SMAD5 levels in PAH and its potential action during PAH pathogenesis. Rescue experiments could then be performed to assess whether restoration of normal SMAD5 levels shows any beneficial effect. SMAD5 overexpression assays both in rodent models of PAH and in the context of *BMPR2* mutations would also be useful to understand the role SMAD5 levels play in PAH pathology.

A downregulation of TRPC1 has been identified in the current PAH RNAseq in PBMCs from PAH patients. It has been previously discussed in this thesis the contrasting results obtained by previous research implicating hypoxia-induced TRPC1 upregulation in mice PASMCs in pulmonary vascular remodelling through an increase in PASMC proliferation (98). Further evidence in mice showed that siRNA-mediated TRPC1 downregulation ameliorated RVSP in hypoxic PH models (305) and that TRPC1 KO mice did not develop hypoxia-induced PH (306). These notable differences between rodent models of PH and PAH patients, and between PASMCs and PBMCs, which could account for these opposing roles of TRPC1 across this and other studies, have also been noted in this manuscript (see details on Chapter 3). All in all, the relevance of Ca^{2+} homeostasis and, therefore, of TRPC channels in PAH pathology cannot be understated. Additionally, the role of TRPC1 in regulating sphingolipids in myoblasts (243), which were previously found to be dysregulated in PAH (165) suggest there may be a different mechanism by which TRPC1 dysregulation may play a role in PAH pathology. TRPC1 downregulation has also been identified in the PBMCs of patients suffering from inflammatory bowel disease (307), a disorder which, similarly to PAH, has a strong inflammatory component. It has also been shown that TRPC1 may prevent cell death through a reduction in autophagy (308), so it is possible that a reduction in TRPC1 levels could result in higher levels of cell death. Early apoptosis of vulnerable hPAECs plays a key role in PAH pathogenesis (288,289) and has been previously described in this thesis (see details on Chapter 5). This potential association between lower TRPC1 levels and cell death, along with lower levels of TRPC1 being identified in PAH patients and the early hPAEC apoptosis occurring in PAH, suggest a mechanism by which TRPC1 dysregulation could play a role in PAH pathogenesis. Further research should be conducted to elucidate the specific role of TRPC1 in PAH pathology, both via its downregulation in PAH patients and its regulation of sphingolipids found to be dysregulated in PAH.

The work presented in this thesis also entailed a second whole blood RNAseq in a cohort including PAH patients, patients from different PH groups and symptomatic patients found not to have PH but likely suffering from other cardiovascular or respiratory disorders. Results demonstrated the remarkable similarities between these patients, especially between different PH groups, but also identified differences in their transcriptomic profiles that emphasised the potential of transcriptomics—and of omics as a whole—to unveil previously unidentified disease mechanisms. These results suggest the utility of transcriptomics in distinguishing between PH groups should be investigated in a larger cohort with comprehensive patient clinical information. This would also allow testing of whether the identified differences in RNA profiles also correlate with metrics of disease progression and implicate transcripts in the pathogenesis of specific disease types—as was the case with the PAH RNA signature. Research efforts attempting to use combined omics to create more sophisticated diagnostic panels and identify stronger candidates of pathological mechanisms should also take place.

Also outlined in this thesis was the use of the Connectivity Map (CMap) database to identify small molecule candidates that could reverse the identified PAH RNA signature in PBMCs and investigate their potential therapeutic effect on PBMCs and vascular cells. These investigations yielded Homoharringtonine, a protein synthesis inhibitor, as the strongest therapeutic candidate. It effectively reversed the whole blood PAH RNA signature in PBMCs, reversed transcriptional changes in hPAECs induced by a PAH-like inflammatory stimulus, and induced positive functional changes in hPAECs through reduced apoptotic activity and limited proliferation. These results strongly suggest further research into Homoharringtonine must be conducted, both to more thoroughly explore its therapeutic potential in PAH—not only in PBMCs and hPAECs, but also in PASMCs and in more complex biological systems—and to investigate the mechanism by which these effects occur. These mechanistic investigations are of great relevance, as elucidating whether changes induced in PBMCs and hPAECs are Homoharringtonine-specific or, instead, reflect a more general therapeutic effect common to all protein synthesis inhibitors, could help identify other compounds which may display greater therapeutic potential than that of Homoharringtonine. Further research should therefore also include other protein synthesis inhibitors as well, particularly those highlighted by the CMap query which identified Homoharringtonine.

The used of the CMap database is gaining momentum within the PAH transcriptomics field. A recent single-cell study of 28 different cell types in the lungs of MCT and SuHx rat PAH models (309) queried those RNA signatures against the CMap database, which yielded treprostinil—the most effective PAH therapy available for patients currently—as the top candidate drug for PAH RNA signature reversal in non-classical monocytes. Other candidate compounds yielded by that analysis are reported to be undergoing further testing. Another study integrating three datasets of gene expression signatures from the lungs of PAH patients queried the RNA signatures identified in their analysis against the CMap database, which yielded 9 candidate compounds, one of which (ruxolitinib) induced a reduction in proliferation and migration in rat PASMCs *in vitro* (310). A study previously mentioned in this manuscript, which attempted to identify transcriptional differences between vasoresponsive and non-vasoresponsive PAH patients (176), then utilised the CMap in a different manner, using it to define genetic profiles that may reflect vasoresponsivity (311). All in all, the use of CMap for compound repurposing in PAH is now an increasingly popular tool in PAH research and its use should be considered in most transcriptomic investigative approaches for its great potential. Differences in transcriptomic signatures identified in different tissues and biological systems are reflected by differences in candidate compounds yielded by CMap queries utilising those signatures. Still, the limitations of the CMap database must be kept in mind when utilising this tool. Future improvements in the cell types used in assays that expand the CMap database or the utilisation of other, new compound repurposing databases should be considered.

Homoharringtonine, the top candidate compound resulting from the work outlined throughout this thesis, is a plant alkaloid that exhibits antitumor properties. It acts as a protein synthesis inhibitor through a unique mechanism of action by preventing the initial elongation step of protein synthesis. This occurs as a result of Homoharringtonine binding to the 80S ribosome in eukaryotic cells and interfering with aminoacid chain elongation (312,313). Its main serious adverse side effects include myelosuppression and reversible cardiotoxicity (314), as well as the more common, diarrhoea, fever, chills, nausea and vomiting (315). The potential severity of these side effects suggests identifying a compound with similar molecular mechanism but less side effects would be of great therapeutic interest. It has been extensively used for the treatment of chronic and acute myeloid leukaemia (CML and AML) with resistance and/or intolerance to two or more tyrosine kinase inhibitors since its approval in 2012 (316), due to its ability to block leukemic cells from progressing from G1 phase into S phase and from G2 phase into M phase. Since results presented throughout this thesis suggest Homoharringtonine is probably cytotoxic at high doses, identifying the therapeutic range would be of great interest, as its molecular mechanism suggests it could induce cell cycle arrest even under healthy conditions.

Homoharringtonine has also been used in a phase II open-label study for the treatment of myelodysplastic syndrome (317) and in bone marrow mononuclear cells of multiple myeloma patients *in vitro* (318). Homoharringtonine has also been suggested for its potential use in the treatment of several cancers because of results obtained in non-small cell lung cancer in mice (319), colon rectal cancer *in vitro* (320) and renal cell carcinoma *in vitro* (321). The only prior study exposing ECs to Homoharringtonine showed it induced apoptosis in a human umbilical vein endothelial cell line (ECV304) at doses similar to those which also promoted apoptosis in the present study (322). Another study focused on ischemic vulnerability of diabetic hearts also showed how a high dose of 500 nM Homoharringtonine administration induced cardiomyocyte apoptosis in mice (323), again similar to results obtained in the present study at those Homoharringtonine concentration ranges. It would therefore be of interest to test lower doses (50 – 100 nM) of Homoharringtonine for cardiomyocyte toxicity—which would be unwanted and would mean mean another compound with similar transcriptional effects but less toxic would be better suited for PAH treatment—. These results, nonetheless, highlight the ability of Homoharringtonine to exert its molecular action independently of the cell type exposed, which may help account for the effects of Homoharringtonine in both PBMCs and hPAECs described in this manuscript. It also suggests the effects observed throughout this work at lower doses (50 – 100 nM) could potentially induce similar effects at those doses in other cell types. Interestingly, a recent study identified a mechanism by which Homoharringtonine induced EndoMT reversal in TGF-β-induced hepatocellular carcinoma (324). This mechanism entailed Homoharringtonine-induced suppression of erythropoietin-producing hepatocyte receptor B4 (EphB4), a member of the tyrosine kinase family that plays a crucial role in tumour progression via inhibition of HIF1-α (325). This EphB4 suppression promoted the phosphorylation and loss of β-catenin and triggered downstream E-cadherin overexpression and Snail, MMP2 and MMP9 inhibition that inhibited migration. These results outline a mechanism by which Homoharringtonine may be able to inhibit or reverse EndoMT, a hallmark of PAH pathology. Future PAH research should investigate this mechanism in vascular cells which have shown some degree of EndoMT in PAH, namely hPAECs (see details on Introduction 1.3.4). To date, there has been no other attempt at utilising Homoharringtonine for PAH research.

In summary, the work presented throughout this manuscript has harnessed transcriptomic approaches to identify a whole blood RNA signature for PAH which correlates with disease progression and survival. This RNA signature has been utilised to identify genes and pathways that may play a role in PAH pathogenesis, such as SMAD5, TRPC1, AMD1, SEC22B and FER. It has also been used to infer a new candidate small molecule therapeutic compound—the protein synthesis inhibitor Homoharringtonine—which has shown great therapeutic potential in both PBMCs and hPAECs and should be investigated further for its potential in clinical therapeutic use. Distinct RNA signatures separating PAH from other PH and non-PH patients have been identified and shown the potential of transcriptomics—and multi-omics—to produce further advances in our understanding of PAH.

7 – References

1. Huang W, Yen RT, McLaurine M, Bledsoe G. Morphometry of the human pulmonary vasculature. J Appl Physiol. 1996 Nov;81(5):2123–33.

2. Townsley MI. Structure and composition of pulmonary arteries, capillaries and veins. Compr Physiol. 2012 Jan 1;2:675–709.

3. Leslie KO, Wick MR. Practical Pulmonary Pathology: A Diagnostic Approach (Third Edition). Elsevier; 2018.

4. Villa N, Walker L, Lindsell CE, Gasson J, Iruela-Arispe ML, Weinmaster G. Vascular expression of Notch pathway receptors and ligands is restricted to arterial vessels. Mech Dev. 2001 Oct 1;108(1):161–4.

5. Hislop AA, Pierce CM. Growth of the vascular tree. Paediatr Respir Rev. 2000 Dec;1(4):321–7.

6. Burri PH. Structural aspects of postnatal lung development - alveolar formation and growth. Biol Neonate. 2006;89(4):313–22.

7. Humbert M, Morrell NW, Archer SL, Stenmark KR, MacLean MR, Lang IM, et al. Cellular and molecular pathobiology of pulmonary arterial hypertension. J Am Coll Cardiol. 2004 Jun 16;43(12 Suppl S):13S-24S.

8. Rabinovitch M. Molecular pathogenesis of pulmonary arterial hypertension. J Clin Invest. 2012 Dec;122(12):4306–13.

9. Hoeper MM, Humbert M, Souza R, Idrees M, Kawut SM, Sliwa-Hahnle K, et al. A global view of pulmonary hypertension. Lancet Respir Med. 2016 Apr;4(4):306–22.

10. Kovacs G, Berghold A, Scheidl S, Olschewski H. Pulmonary arterial pressure during rest and exercise in healthy subjects: a systematic review. Eur Respir J. 2009 Oct;34(4):888–94.

11. Hoeper MM, Bogaard HJ, Condliffe R, Frantz R, Khanna D, Kurzyna M, et al. Definitions and diagnosis of pulmonary hypertension. J Am Coll Cardiol. 2013 Dec 24;62(25 Suppl):D42-50.

12. Lau EMT, Humbert M, Celermajer DS. Early detection of pulmonary arterial hypertension. Nat Rev Cardiol. 2015 Mar;12(3):143–55.

13. Maron BA, Hess E, Maddox TM, Opotowsky AR, Tedford RJ, Lahm T, et al. Association of Borderline Pulmonary Hypertension With Mortality and Hospitalization in a Large Patient Cohort: Insights From the Veterans Affairs Clinical Assessment, Reporting, and Tracking Program. Circulation. 2016 Mar 29;133(13):1240–8.

14. Simonneau G, Hoeper MM. The revised definition of pulmonary hypertension: exploring the impact on patient management. Eur Heart J Suppl J Eur Soc Cardiol. 2019 Dec;21(Suppl K):K4–8.

15. Galiè N, McLaughlin VV, Rubin LJ, Simonneau G. An overview of the 6th World Symposium on Pulmonary Hypertension. Eur Respir J. 2019 Jan 24;53(1):1802148.

16. Galiè N, Humbert M, Vachiery JL, Gibbs S, Lang I, Torbicki A, et al. 2015 ESC/ERS Guidelines for the diagnosis and treatment of pulmonary hypertension: The Joint Task Force for the Diagnosis and Treatment of Pulmonary Hypertension of the European Society of Cardiology (ESC) and the

European Respiratory Society (ERS): Endorsed by: Association for European Paediatric and Congenital Cardiology (AEPC), International Society for Heart and Lung Transplantation (ISHLT). Eur Respir J. 2015 Oct;46(4):903–75.

17. Hoeper MM, Huscher D, Pittrow D. Incidence and prevalence of pulmonary arterial hypertension in Germany. Int J Cardiol. 2016 Jan 15;203:612–3.

18. Humbert M, Sitbon O, Chaouat A, Bertocchi M, Habib G, Gressin V, et al. Pulmonary arterial hypertension in France: results from a national registry. Am J Respir Crit Care Med. 2006 May 1;173(9):1023–30.

19. Peacock AJ, Murphy NF, McMurray JJV, Caballero L, Stewart S. An epidemiological study of pulmonary arterial hypertension. Eur Respir J. 2007 Jul;30(1):104–9.

20. McGoon MD, Benza RL, Escribano-Subias P, Jiang X, Miller DP, Peacock AJ, et al. Pulmonary arterial hypertension: epidemiology and registries. J Am Coll Cardiol. 2013 Dec 24;62(25 Suppl):D51-59.

21. Schermuly RT, Ghofrani HA, Wilkins MR, Grimminger F. Mechanisms of disease: pulmonary arterial hypertension. Nat Rev Cardiol. 2011 Jun 21;8(8):443–55.

22. Lan NSH, Massam BD, Kulkarni SS, Lang CC. Pulmonary Arterial Hypertension: Pathophysiology and Treatment. Dis Basel Switz. 2018 May 16;6(2):E38.

23. Wagenvoort CA. The pathology of primary pulmonary hypertension. J Pathol. 1970 Aug;101(4):Pi.

24. Badesch DB, Raskob GE, Elliott CG, Krichman AM, Farber HW, Frost AE, et al. Pulmonary arterial hypertension: baseline characteristics from the REVEAL Registry. Chest. 2010 Feb;137(2):376–87.

25. Ling Y, Johnson MK, Kiely DG, Condliffe R, Elliot CA, Gibbs JSR, et al. Changing demographics, epidemiology, and survival of incident pulmonary arterial hypertension: results from the pulmonary hypertension registry of the United Kingdom and Ireland. Am J Respir Crit Care Med. 2012 Oct 15;186(8):790–6.

26. Thenappan T, Shah SJ, Rich S, Gomberg-Maitland M. A USA-based registry for pulmonary arterial hypertension: 1982–2006. Eur Respir J. 2007 Dec 1;30(6):1103–10.

27. Farber HW, Miller DP, Poms AD, Badesch DB, Frost AE, Muros-Le Rouzic E, et al. Five-Year outcomes of patients enrolled in the REVEAL Registry. Chest. 2015 Oct;148(4):1043–54.

28. Humbert M, Sitbon O, Yaïci A, Montani D, O'Callaghan DS, Jaïs X, et al. Survival in incident and prevalent cohorts of patients with pulmonary arterial hypertension. Eur Respir J. 2010 Sep;36(3):549–55.

29. Evans JDW, Girerd B, Montani D, Wang XJ, Galiè N, Austin ED, et al. BMPR2 mutations and survival in pulmonary arterial hypertension: an individual participant data meta-analysis. Lancet Respir Med. 2016 Feb;4(2):129–37.

30. Ventetuolo CE, Gabler NB, Fritz JS, Smith KA, Palevsky HI, Klinger JR, et al. Are hemodynamics surrogate end points in pulmonary arterial hypertension? Circulation. 2014 Aug 26;130(9):768–75.

31. White RJ. Estrogen: Friend or Foe in Pulmonary Hypertension? Am J Respir Crit Care Med. 2016 May 15;193(10):1084–6.

32. Simonneau G, Galiè N, Rubin LJ, Langleben D, Seeger W, Domenighetti G, et al. Clinical classification of pulmonary hypertension. J Am Coll Cardiol. 2004 Jun 16;43(12 Suppl S):5S-12S.

33. Alves JL, Gavilanes F, Jardim C, Fernandes CJCDS, Morinaga LTK, Dias B, et al. Pulmonary arterial hypertension in the southern hemisphere: results from a registry of incident Brazilian cases. Chest. 2015 Feb;147(2):495–501.

34. Lau EMT, Giannoulatou E, Celermajer DS, Humbert M. Epidemiology and treatment of pulmonary arterial hypertension. Nat Rev Cardiol. 2017 Oct;14(10):603–14.

35. Grigoryev DN, Mathai SC, Fisher MR, Girgis RE, Zaiman AL, Housten-Harris T, et al. Identification of candidate genes in scleroderma-related pulmonary arterial hypertension. Transl Res J Lab Clin Med. 2008 Apr;151(4):197–207.

36. Farber HW, Loscalzo J. Pulmonary arterial hypertension. N Engl J Med. 2004 Oct 14;351(16):1655–65.

37. Newman JH, Phillips JA, Loyd JE. Narrative review: the enigma of pulmonary arterial hypertension: new insights from genetic studies. Ann Intern Med. 2008 Feb 19;148(4):278–83.

38. Savai R, Pullamsetti SS, Kolbe J, Bieniek E, Voswinckel R, Fink L, et al. Immune and inflammatory cell involvement in the pathology of idiopathic pulmonary arterial hypertension. Am J Respir Crit Care Med. 2012 Nov 1;186(9):897–908.

39. Stacher E, Graham BB, Hunt JM, Gandjeva A, Groshong SD, McLaughlin VV, et al. Modern age pathology of pulmonary arterial hypertension. Am J Respir Crit Care Med. 2012 Aug 1;186(3):261–72.

40. Campbell AI, Zhao Y, Sandhu R, Stewart DJ. Cell-based gene transfer of vascular endothelial growth factor attenuates monocrotaline-induced pulmonary hypertension. Circulation. 2001 Oct 30;104(18):2242–8.

41. Zhao YD, Campbell AIM, Robb M, Ng D, Stewart DJ. Protective role of angiopoietin-1 in experimental pulmonary hypertension. Circ Res. 2003 May 16;92(9):984–91.

42. Runo JR, Loyd JE. Primary pulmonary hypertension. Lancet Lond Engl. 2003 May 3;361(9368):1533–44.

43. Sheikh AQ, Misra A, Rosas IO, Adams RH, Greif DM. Smooth muscle cell progenitors are primed to muscularize in pulmonary hypertension. Sci Transl Med. 2015 Oct 7;7(308):308ra159.

44. Yi ES, Kim H, Ahn H, Strother J, Morris T, Masliah E, et al. Distribution of obstructive intimal lesions and their cellular phenotypes in chronic pulmonary hypertension. A morphometric and immunohistochemical study. Am J Respir Crit Care Med. 2000 Oct;162(4 Pt 1):1577–86.

45. Stenmark KR, Gerasimovskaya E, Nemenoff RA, Das M. Hypoxic activation of adventitial fibroblasts: role in vascular remodeling. Chest. 2002 Dec;122(6 Suppl):326S-334S.

46. Morris HE, Neves K, Montezano A, MacLean MR, Touyz R. Notch3 signalling and vascular remodelling in pulmonary arterial hypertension. Clin Sci. 2019 Dec 20;133:2481–98.

47. Steffes LC, Froistad AA, Andruska A, Boehm M, McGlynn M, Zhang F, et al. A Notch3-Marked Subpopulation of Vascular Smooth Muscle Cells Is the Cell of Origin for Occlusive Pulmonary Vascular Lesions. Circulation. 2020 Oct 20;142(16):1545–61.

48. Hofmann JJ, Iruela-Arispe ML. Notch signaling in blood vessels: who is talking to whom about what? Circ Res. 2007 Jun 8;100(11):1556–68.

49. Lindner V, Booth C, Prudovsky I, Small D, Maciag T, Liaw L. Members of the Jagged/Notch Gene Families Are Expressed in Injured Arteries and Regulate Cell Phenotype via Alterations in Cell Matrix and Cell-Cell Interaction. Am J Pathol. 2001 Sep;159(3):875–83.

50. Li X, Zhang X, Leathers R, Makino A, Huang C, Parsa P, et al. Notch3 signaling promotes the development of pulmonary arterial hypertension. Nat Med. 2009 Nov;15(11):1289–97.

51. Chida A, Shintani M, Matsushita Y, Sato H, Eitoku T, Nakayama T, et al. Mutations of NOTCH3 in childhood pulmonary arterial hypertension. Mol Genet Genomic Med. 2014 May;2(3):229–39.

52. Dabral S, Tian X, Kojonazarov B, Savai R, Ghofrani HA, Weissmann N, et al. Notch1 signalling regulates endothelial proliferation and apoptosis in pulmonary arterial hypertension. Eur Respir J. 2016 Oct;48(4):1137–49.

53. Qiao L, Nishimura T, Shi L, Sessions D, Thrasher A, Trudell JR, et al. Endothelial fate mapping in mice with pulmonary hypertension. Circulation. 2014 Feb 11;129(6):692–703.

54. Reynolds AM, Holmes MD, Danilov SM, Reynolds PN. Targeted gene delivery of BMPR2 attenuates pulmonary hypertension. Eur Respir J. 2012 Feb;39(2):329–43.

55. Jones R, Jacobson M, Steudel W. alpha-smooth-muscle actin and microvascular precursor smooth-muscle cells in pulmonary hypertension. Am J Respir Cell Mol Biol. 1999 Apr;20(4):582–94.

56. Hopper RK, Moonen JRAJ, Diebold I, Cao A, Rhodes CJ, Tojais NF, et al. In Pulmonary Arterial Hypertension, Reduced BMPR2 Promotes Endothelial-to-Mesenchymal Transition via HMGA1 and Its Target Slug. Circulation. 2016 May 3;133(18):1783–94.

57. Good RB, Gilbane AJ, Trinder SL, Denton CP, Coghlan G, Abraham DJ, et al. Endothelial to Mesenchymal Transition Contributes to Endothelial Dysfunction in Pulmonary Arterial Hypertension. Am J Pathol. 2015 Jul;185(7):1850–8.

58. Stenmark KR, Frid M, Perros F. Endothelial-to-Mesenchymal Transition: An Evolving Paradigm and a Promising Therapeutic Target in PAH. Circulation. 2016 May 3;133(18):1734–7.

59. Ranchoux B, Antigny F, Rucker-Martin C, Hautefort A, Péchoux C, Bogaard HJ, et al. Endothelial-to-mesenchymal transition in pulmonary hypertension. Circulation. 2015 Mar 17;131(11):1006–18.

60. Cheng JC, Chang HM, Leung PCK. Egr-1 mediates epidermal growth factor-induced downregulation of E-cadherin expression via Slug in human ovarian cancer cells. Oncogene. 2013 Feb 21;32(8):1041–9.

61. Suzuki T, Carrier EJ, Talati MH, Rathinasabapathy A, Chen X, Nishimura R, et al. Isolation and characterization of endothelial-to-mesenchymal transition cells in pulmonary arterial hypertension. Am J Physiol - Lung Cell Mol Physiol. 2018 Jan 1;314(1):L118–26.

62. Krenning G, Barauna VG, Krieger JE, Harmsen MC, Moonen JRAJ. Endothelial Plasticity: Shifting Phenotypes through Force Feedback. Stem Cells Int. 2016;2016:9762959.

63. Tuder RM, Stacher E, Robinson J, Kumar R, Graham BB. Pathology of pulmonary hypertension. Clin Chest Med. 2013 Dec;34(4):639–50.

64. Jonigk D, Golpon H, Bockmeyer CL, Maegel L, Hoeper MM, Gottlieb J, et al. Plexiform lesions in pulmonary arterial hypertension composition, architecture, and microenvironment. Am J Pathol. 2011 Jul;179(1):167–79.

65. Stenmark KR, Fagan KA, Frid MG. Hypoxia-induced pulmonary vascular remodeling: cellular and molecular mechanisms. Circ Res. 2006 Sep 29;99(7):675–91.

66. Dorfmüller P, Chaumais MC, Giannakouli M, Durand-Gasselin I, Raymond N, Fadel E, et al. Increased oxidative stress and severe arterial remodeling induced by permanent high-flow challenge in experimental pulmonary hypertension. Respir Res. 2011 Dec 1;12(1):119.

67. Cool CD, Kennedy D, Voelkel NF, Tuder RM. Pathogenesis and evolution of plexiform lesions in pulmonary hypertension associated with scleroderma and human immunodeficiency virus infection. Hum Pathol. 1997 Apr;28(4):434–42.

68. Soon E, Holmes AM, Treacy CM, Doughty NJ, Southgate L, Machado RD, et al. Elevated levels of inflammatory cytokines predict survival in idiopathic and familial pulmonary arterial hypertension. Circulation. 2010 Aug 31;122(9):920–7.

69. Harbaum L, Baaske KM, Simon M, Oqueka T, Sinning C, Glatzel A, et al. Exploratory analysis of the neutrophil to lymphocyte ratio in patients with pulmonary arterial hypertension. BMC Pulm Med. 2017 Apr 26;17(1):72.

70. Tuder RM, Groves B, Badesch DB, Voelkel NF. Exuberant endothelial cell growth and elements of inflammation are present in plexiform lesions of pulmonary hypertension. Am J Pathol. 1994 Feb;144(2):275–85.

71. Tabima DM, Chesler NC. The effects of vasoactivity and hypoxic pulmonary hypertension on extralobar pulmonary artery biomechanics. J Biomech. 2010 Jul 20;43(10):1864–9.

72. Ooi CY, Wang Z, Tabima DM, Eickhoff JC, Chesler NC. The role of collagen in extralobar pulmonary artery stiffening in response to hypoxia-induced pulmonary hypertension. Am J Physiol - Heart Circ Physiol. 2010 Dec;299(6):H1823–31.

73. Ghigna MR, Guignabert C, Montani D, Girerd B, Jaïs X, Savale L, et al. BMPR2 mutation status influences bronchial vascular changes in pulmonary arterial hypertension. Eur Respir J. 2016 Dec;48(6):1668–81.

74. Gomez-Arroyo JG, Farkas L, Alhussaini AA, Farkas D, Kraskauskas D, Voelkel NF, et al. The monocrotaline model of pulmonary hypertension in perspective. Am J Physiol Lung Cell Mol Physiol. 2012 Feb 15;302(4):L363-369.

75. Bonnet S, Provencher S, Guignabert C, Perros F, Boucherat O, Schermuly RT, et al. Translating Research into Improved Patient Care in Pulmonary Arterial Hypertension. Am J Respir Crit Care Med. 2017 Mar 1;195(5):583–95.

76. Stenmark KR, Meyrick B, Galie N, Mooi WJ, McMurtry IF. Animal models of pulmonary arterial hypertension: the hope for etiological discovery and pharmacological cure. Am J Physiol Lung Cell Mol Physiol. 2009 Dec;297(6):L1013-1032.

77. West J, Harral J, Lane K, Deng Y, Ickes B, Crona D, et al. Mice expressing BMPR2R899X transgene in smooth muscle develop pulmonary vascular lesions. Am J Physiol - Lung Cell Mol Physiol. 2008 Nov;295(5):L744–55.

78. Beppu H, Ichinose F, Kawai N, Jones RC, Yu PB, Zapol WM, et al. BMPR-II heterozygous mice have mild pulmonary hypertension and an impaired pulmonary vascular remodeling response to prolonged hypoxia. Am J Physiol-Lung Cell Mol Physiol. 2004 Dec;287(6):L1241–7.

79. Song Y, Jones JE, Beppu H, Keaney JF, Loscalzo J, Zhang YY. Increased Susceptibility to Pulmonary Hypertension in Heterozygous BMPR2-Mutant Mice. Circulation. 2005 Jul 26;112(4):553–62.

80. Long L, MacLean MR, Jeffery TK, Morecroft I, Yang X, Rudarakanchana N, et al. Serotonin Increases Susceptibility to Pulmonary Hypertension in BMPR2-Deficient Mice. Circ Res. 2006 Mar 31;98(6):818–27.

81. A H, P MF, J S, G M, T B, C RM, et al. Bmpr2 Mutant Rats Develop Pulmonary and Cardiac Characteristics of Pulmonary Arterial Hypertension. Circulation [Internet]. 2019 Dec 2 [cited 2022 Nov 2];139(7). Available from: https://pubmed.ncbi.nlm.nih.gov/30586714/

82. Tian W, Jiang X, Sung YK, Shuffle E, Wu TH, Kao PN, et al. Phenotypically-Silent Bone Morphogenetic Protein Receptor 2 (Bmpr2) Mutations Predispose Rats to Inflammation-Induced Pulmonary Arterial Hypertension by Enhancing The Risk for Neointimal Transformation. Circulation. 2019 Oct 22;140(17):1409–25.

83. Jerkic M, Kabir MG, Davies A, Yu LX, McIntyre BAS, Husain NW, et al. Pulmonary hypertension in adult Alk1 heterozygous mice due to oxidative stress. Cardiovasc Res. 2011 Dec 1;92(3):375–84.

84. Toporsian M, Jerkic M, Zhou YQ, Kabir MG, Yu LX, McIntyre BAS, et al. Spontaneous Adult-Onset Pulmonary Arterial Hypertension Attributable to Increased Endothelial Oxidative Stress in a Murine Model of Hereditary Hemorrhagic Telangiectasia. Arterioscler Thromb Vasc Biol. 2010 Mar;30(3):509–17.

85. Steiner MK, Syrkina OL, Kolliputi N, Mark EJ, Hales CA, Waxman AB. IL-6 Overexpression Induces Pulmonary Hypertension. Circ Res. 2009 Jan 30;104(2):236–44.

86. Tan Q, Kerestes H, Percy MJ, Pietrofesa R, Chen L, Khurana TS, et al. Erythrocytosis and pulmonary hypertension in a mouse model of human HIF2A gain of function mutation. J Biol Chem. 2013 Jun 14;288(24):17134–44.

87. Kapitsinou PP, Rajendran G, Astleford L, Michael M, Schonfeld MP, Fields T, et al. The Endothelial Prolyl-4-Hydroxylase Domain 2/Hypoxia-Inducible Factor 2 Axis Regulates Pulmonary Artery Pressure in Mice. Mol Cell Biol. 2016 May 2;36(10):1584–94.

88. Dai Z, Li M, Wharton J, Zhu MM, Zhao YY. PHD2 Deficiency in Endothelial Cells and Hematopoietic Cells Induces Obliterative Vascular Remodeling and Severe Pulmonary Arterial Hypertension in Mice and Humans through HIF-2α. Circulation. 2016 Jun 6;133(24):2447.

89. Al-Hilal TA, Keshavarz A, Kadry H, Lahooti B, Al-Obaida A, Ding Z, et al. Pulmonary-arterial-hypertension (PAH)-on-a-chip: fabrication, validation and application. Lab Chip. 2020 Sep 15;20(18):3334–45.

90. Hoeper MM, McLaughlin VV, Dalaan AMA, Satoh T, Galiè N. Treatment of pulmonary hypertension. Lancet Respir Med. 2016 Apr;4(4):323–36.

91. Sommer N, Ghofrani HA, Pak O, Bonnet S, Provencher S, Sitbon O, et al. Current and future treatments of pulmonary arterial hypertension. Br J Pharmacol. 2021;178(1):6–30.

92. Giaid A, Saleh D. Reduced expression of endothelial nitric oxide synthase in the lungs of patients with pulmonary hypertension. N Engl J Med. 1995 Jul 27;333(4):214–21.

93. Wharton J, Davie N, Upton PD, Yacoub MH, Polak JM, Morrell NW. Prostacyclin analogues differentially inhibit growth of distal and proximal human pulmonary artery smooth muscle cells. Circulation. 2000 Dec 19;102(25):3130–6.

94. Giaid A, Yanagisawa M, Langleben D, Michel RP, Levy R, Shennib H, et al. Expression of endothelin-1 in the lungs of patients with pulmonary hypertension. N Engl J Med. 1993 Jun 17;328(24):1732–9.

95. Yuan XJ, Wang J, Juhaszova M, Gaine SP, Rubin LJ. Attenuated K+ channel gene transcription in primary pulmonary hypertension. Lancet Lond Engl. 1998 Mar 7;351(9104):726–7.

96. Sitbon O, Humbert M, Jaïs X, Ioos V, Hamid AM, Provencher S, et al. Long-term response to calcium channel blockers in idiopathic pulmonary arterial hypertension. Circulation. 2005 Jun 14;111(23):3105–11.

97. Dietrich A, Kalwa H, Fuchs B, Grimminger F, Weissmann N, Gudermann T. In vivo TRPC functions in the cardiopulmonary vasculature. Cell Calcium. 2007 Aug;42(2):233–44.

98. Malczyk M, Veith C, Fuchs B, Hofmann K, Storch U, Schermuly RT, et al. Classical transient receptor potential channel 1 in hypoxia-induced pulmonary hypertension. Am J Respir Crit Care Med. 2013 Dec 15;188(12):1451–9.

99. Tu L, Desroches-Castan A, Mallet C, Guyon L, Cumont A, Phan C, et al. Selective BMP-9 Inhibition Partially Protects Against Experimental Pulmonary Hypertension. Circ Res. 2019 Mar 15;124(6):846–55.

100. Dai Z, Zhu MM, Peng Y, Machireddy N, Evans CE, Machado R, et al. Therapeutic Targeting of Vascular Remodeling and Right Heart Failure in Pulmonary Arterial Hypertension with a HIF-2α Inhibitor. Am J Respir Crit Care Med. 2018 Dec 1;198(11):1423–34.

101. Gu M, Donato M, Guo M, Wary N, Miao Y, Mao S, et al. iPSC-endothelial cell phenotypic drug screening and in silico analyses identify tyrphostin-AG1296 for pulmonary arterial hypertension. Sci Transl Med. 2021 May 5;13(592):eaba6480.

102. Förstermann U, Sessa WC. Nitric oxide synthases: regulation and function. Eur Heart J. 2012 Apr;33(7):829–37.

103. Chen C nien, Watson G, Zhao L. Cyclic guanosine monophosphate signalling pathway in pulmonary arterial hypertension. Vascul Pharmacol. 2013 Mar;58(3):211–8.

104. Wharton J, Strange JW, Møller GMO, Growcott EJ, Ren X, Franklyn AP, et al. Antiproliferative effects of phosphodiesterase type 5 inhibition in human pulmonary artery cells. Am J Respir Crit Care Med. 2005 Jul 1;172(1):105–13.

105. Omori K, Kotera J. Overview of PDEs and their regulation. Circ Res. 2007 Feb 16;100(3):309–27.

106. Galiè N, Ghofrani HA, Torbicki A, Barst RJ, Rubin LJ, Badesch D, et al. Sildenafil citrate therapy for pulmonary arterial hypertension. N Engl J Med. 2005 Nov 17;353(20):2148–57.

107. Ghofrani HA, Galiè N, Grimminger F, Grünig E, Humbert M, Jing ZC, et al. Riociguat for the treatment of pulmonary arterial hypertension. N Engl J Med. 2013 Jul 25;369(4):330–40.

108. Galiè N, Brundage BH, Ghofrani HA, Oudiz RJ, Simonneau G, Safdar Z, et al. Tadalafil therapy for pulmonary arterial hypertension. Circulation. 2009 Jun 9;119(22):2894–903.

109. Stasch JP, Pacher P, Evgenov OV. Soluble guanylate cyclase as an emerging therapeutic target in cardiopulmonary disease. Circulation. 2011 May 24;123(20):2263–73.

110. Jing ZC, Yu ZX, Shen JY, Wu BX, Xu KF, Zhu XY, et al. Vardenafil in pulmonary arterial hypertension: a randomized, double-blind, placebo-controlled study. Am J Respir Crit Care Med. 2011 Jun 15;183(12):1723–9.

111. Galiè N, Müller K, Scalise AV, Grünig E. PATENT PLUS: a blinded, randomised and extension study of riociguat plus sildenafil in pulmonary arterial hypertension. Eur Respir J. 2015 May;45(5):1314–22.

112. Jakubowski JA, Utterback BG, Mais DE, Hardinger SA, Braish TF, Richard Nevill C, et al. Biochemical and pharmacological activity of arene-fused prostacyclin analogues on human platelets. Prostaglandins. 1994 Mar 1;47(3):189–201.

113. Clapp LH, Finney P, Turcato S, Tran S, Rubin LJ, Tinker A. Differential effects of stable prostacyclin analogs on smooth muscle proliferation and cyclic AMP generation in human pulmonary artery. Am J Respir Cell Mol Biol. 2002 Feb;26(2):194–201.

114. Christman BW, McPherson CD, Newman JH, King GA, Bernard GR, Groves BM, et al. An imbalance between the excretion of thromboxane and prostacyclin metabolites in pulmonary hypertension. N Engl J Med. 1992 Jul 9;327(2):70–5.

115. Tuder RM, Cool CD, Geraci MW, Wang J, Abman SH, Wright L, et al. Prostacyclin synthase expression is decreased in lungs from patients with severe pulmonary hypertension. Am J Respir Crit Care Med. 1999 Jun;159(6):1925–32.

116. Simonneau G, Barst RJ, Galie N, Naeije R, Rich S, Bourge RC, et al. Continuous subcutaneous infusion of treprostinil, a prostacyclin analogue, in patients with pulmonary arterial hypertension: a double-blind, randomized, placebo-controlled trial. Am J Respir Crit Care Med. 2002 Mar 15;165(6):800–4.

117. McLaughlin VV, Oudiz RJ, Frost A, Tapson VF, Murali S, Channick RN, et al. Randomized study of adding inhaled iloprost to existing bosentan in pulmonary arterial hypertension. Am J Respir Crit Care Med. 2006 Dec 1;174(11):1257–63.

118. Olschewski H, Simonneau G, Galiè N, Higenbottam T, Naeije R, Rubin LJ, et al. Inhaled iloprost for severe pulmonary hypertension. N Engl J Med. 2002 Aug 1;347(5):322–9.

119. Jing ZC, Parikh K, Pulido T, Jerjes-Sanchez C, White RJ, Allen R, et al. Efficacy and safety of oral treprostinil monotherapy for the treatment of pulmonary arterial hypertension: a randomized, controlled trial. Circulation. 2013 Feb 5;127(5):624–33.

120. Shao D, Park JES, Wort SJ. The role of endothelin-1 in the pathogenesis of pulmonary arterial hypertension. Pharmacol Res. 2011 Jun;63(6):504–11.

121. Chester AH, Yacoub MH. The role of endothelin-1 in pulmonary arterial hypertension. Glob Cardiol Sci Pract. 2014;2014(2):62–78.

122. Ben-Yehuda O, Pizzuti D, Brown A, Littman M, Gillies H, Henig N, et al. Long-term hepatic safety of ambrisentan in patients with pulmonary arterial hypertension. J Am Coll Cardiol. 2012 Jul 3;60(1):80–1.

123. Galiè N, Olschewski H, Oudiz RJ, Torres F, Frost A, Ghofrani HA, et al. Ambrisentan for the treatment of pulmonary arterial hypertension: results of the ambrisentan in pulmonary arterial hypertension, randomized, double-blind, placebo-controlled, multicenter, efficacy (ARIES) study 1 and 2. Circulation. 2008 Jun 10;117(23):3010–9.

124. Rubin LJ, Badesch DB, Barst RJ, Galie N, Black CM, Keogh A, et al. Bosentan therapy for pulmonary arterial hypertension. N Engl J Med. 2002 Mar 21;346(12):896–903.

125. Islam S, Masiakos P, Schnitzer JJ, Doody DP, Ryan DP. Diltiazem reduces pulmonary arterial pressures in recurrent pulmonary hypertension associated with pulmonary hypoplasia. J Pediatr Surg. 1999 May;34(5):712–4.

126. Rubin LJ, Nicod P, Hillis LD, Firth BG. Treatment of primary pulmonary hypertension with nifedipine. A hemodynamic and scintigraphic evaluation. Ann Intern Med. 1983 Oct;99(4):433–8.

127. Maron BA, Bhatt DL, Nykiel M, Kinlay S, Waxman AB. Protocol for vasoreactivity testing with epoprostenol in pulmonary hypertension. Crit Pathw Cardiol. 2012 Mar;11(1):40–2.

128. Oliveira EC, Ribeiro ALP, Amaral CFS. Adenosine for vasoreactivity testing in pulmonary hypertension: a head-to-head comparison with inhaled nitric oxide. Respir Med. 2010 Apr;104(4):606–11.

129. Sitbon O, Humbert M, Nunes H, Parent F, Garcia G, Hervé P, et al. Long-term intravenous epoprostenol infusion in primary pulmonary hypertension: prognostic factors and survival. J Am Coll Cardiol. 2002 Aug 21;40(4):780–8.

130. Sitbon O, Gomberg-Maitland M, Granton J, Lewis MI, Mathai SC, Rainisio M, et al. Clinical trial design and new therapies for pulmonary arterial hypertension. Eur Respir J. 2019 Jan;53(1):1801908.

131. Southgate L, Machado RD, Gräf S, Morrell NW. Molecular genetic framework underlying pulmonary arterial hypertension. Nat Rev Cardiol. 2020 Feb;17(2):85–95.

132. Deng Z, Morse JH, Slager SL, Cuervo N, Moore KJ, Venetos G, et al. Familial primary pulmonary hypertension (gene PPH1) is caused by mutations in the bone morphogenetic protein receptor-II gene. Am J Hum Genet. 2000 Sep;67(3):737–44.

133. Foletta VC, Lim MA, Soosairajah J, Kelly AP, Stanley EG, Shannon M, et al. Direct signaling by the BMP type II receptor via the cytoskeletal regulator LIMK1. J Cell Biol. 2003 Sep 15;162(6):1089–98.

134. Soubrier F, Chung WK, Machado R, Grünig E, Aldred M, Geraci M, et al. Genetics and genomics of pulmonary arterial hypertension. J Am Coll Cardiol. 2013 Dec 24;62(25 Suppl):D13-21.

135. Newman JH, Trembath RC, Morse JA, Grunig E, Loyd JE, Adnot S, et al. Genetic basis of pulmonary arterial hypertension: current understanding and future directions. J Am Coll Cardiol. 2004 Jun 16;43(12 Suppl S):33S-39S.

136. Trembath RC, Thomson JR, Machado RD, Morgan NV, Atkinson C, Winship I, et al. Clinical and molecular genetic features of pulmonary hypertension in patients with hereditary hemorrhagic telangiectasia. N Engl J Med. 2001 Aug 2;345(5):325–34.

137. Machado RD, Eickelberg O, Elliott CG, Geraci MW, Hanaoka M, Loyd JE, et al. Genetics and genomics of pulmonary arterial hypertension. J Am Coll Cardiol. 2009 Jun 30;54(1 Suppl):S32–42.

138. Koehler R, Grünig E, Pauciulo MW, Hoeper MM, Olschewski H, Wilkens H, et al. Low frequency of BMPR2 mutations in a German cohort of patients with sporadic idiopathic pulmonary arterial hypertension. J Med Genet. 2004 Dec;41(12):e127.

139. Kudryashova TV, Goncharov DA, Pena A, Ihida-Stansbury K, DeLisser H, Kawut SM, et al. Profiling the role of mammalian target of rapamycin in the vascular smooth muscle metabolome in pulmonary arterial hypertension. Pulm Circ. 2015 Dec;5(4):667–80.

140. Long L, Ormiston ML, Yang X, Southwood M, Gräf S, Machado RD, et al. Selective enhancement of endothelial BMPR-II with BMP9 reverses pulmonary arterial hypertension. Nat Med. 2015 Jul;21(7):777–85.

141. Ormiston ML, Godoy RS, Chaudhary KR, Stewart DJ. The Janus Faces of Bone Morphogenetic Protein 9 in Pulmonary Arterial Hypertension. Circ Res. 2019 Mar 15;124(6):822–4.

142. Cogan J, Austin E, Hedges L, Womack B, West J, Loyd J, et al. Role of BMPR2 alternative splicing in heritable pulmonary arterial hypertension penetrance. Circulation. 2012 Oct 9;126(15):1907–16.

143. Wang D, Chu M, Wang F, Zhou A, Ruan M, Chen Y. A Genetic Variant in FIGN Gene Reduces the Risk of Congenital Heart Disease in Han Chinese Populations. Pediatr Cardiol. 2017 Aug 1;38(6):1169–74.

144. Stearman RS, Cornelius AR, Lu X, Conklin DS, Del Rosario MJ, Lowe AM, et al. Functional Prostacyclin Synthase Promoter Polymorphisms. Impact in Pulmonary Arterial Hypertension. Am J Respir Crit Care Med. 2014 May 1;189(9):1110–20.

145. Hurst LA, Dunmore BJ, Long L, Crosby A, Al-Lamki R, Deighton J, et al. TNFα drives pulmonary arterial hypertension by suppressing the BMP type-II receptor and altering NOTCH signalling. Nat Commun. 2017 Jan 13;8:14079.

146. Miyagawa K, Shi M, Chen PI, Hennigs JK, Zhao Z, Wang M, et al. Smooth Muscle Contact Drives Endothelial Regeneration by BMPR2-Notch1-Mediated Metabolic and Epigenetic Changes. Circ Res. 2019 Jan 18;124(2):211–24.

147. Gräf S, Morrell NW. Towards a molecular classification of pulmonary arterial hypertension. Eur Respir J. 2016 Oct;48(4):987–9.

148. Kerstjens-Frederikse WS, Bongers EMHF, Roofthooft MTR, Leter EM, Douwes JM, Van Dijk A, et al. TBX4 mutations (small patella syndrome) are associated with childhood-onset pulmonary arterial hypertension. J Med Genet. 2013 Aug;50(8):500–6.

149. Eichstaedt CA, Song J, Viales RR, Pan Z, Benjamin N, Fischer C, et al. First identification of Krüppel-like factor 2 mutation in heritable pulmonary arterial hypertension. Clin Sci Lond Engl 1979. 2017 Apr 25;131(8):689–98.

150. Gräf S, Haimel M, Bleda M, Hadinnapola C, Southgate L, Li W, et al. Identification of rare sequence variation underlying heritable pulmonary arterial hypertension. Nat Commun. 2018 Apr 12;9(1):1416.

151. Remillard CV, Tigno DD, Platoshyn O, Burg ED, Brevnova EE, Conger D, et al. Function of Kv1.5 channels and genetic variations of KCNA5 in patients with idiopathic pulmonary arterial hypertension. Am J Physiol Cell Physiol. 2007 May;292(5):C1837-1853.

152. Ma L, Roman-Campos D, Austin ED, Eyries M, Sampson KS, Soubrier F, et al. A novel channelopathy in pulmonary arterial hypertension. N Engl J Med. 2013 Jul 25;369(4):351–61.

153. Eichstaedt CA, Belge C, Chung WK, Gräf S, Grünig E, Montani D, et al. Genetic counselling and testing in pulmonary arterial hypertension -A consensus statement on behalf of the International Consortium for Genetic Studies in PAH. Eur Respir J [Internet]. 2022 Jan 1 [cited 2022 Nov 2]; Available from: https://erj.ersjournals.com/content/early/2022/10/13/13993003.01471-2022

154. Gibson G. Rare and Common Variants: Twenty arguments. Nat Rev Genet. 2012 Jan 18;13(2):135–45.

155. Huston JH, Ryan JJ. The emerging role of epigenetics in pulmonary arterial hypertension: an important avenue for clinical trials (2015 Grover Conference Series). Pulm Circ. 2016 Sep;6(3):274–84.

156. Rhodes CJ, Batai K, Bleda M, Haimel M, Southgate L, Germain M, et al. Genetic determinants of risk in pulmonary arterial hypertension: international genome-wide association studies and meta-analysis. Lancet Respir Med. 2019 Mar;7(3):227–38.

157. Benza RL, Gomberg-Maitland M, Demarco T, Frost AE, Torbicki A, Langleben D, et al. Endothelin-1 Pathway Polymorphisms and Outcomes in Pulmonary Arterial Hypertension. Am J Respir Crit Care Med. 2015 Dec 1;192(11):1345–54.

158. Damico R, Kolb TM, Valera L, Wang L, Housten T, Tedford RJ, et al. Serum endostatin is a genetically determined predictor of survival in pulmonary arterial hypertension. Am J Respir Crit Care Med. 2015 Jan 15;191(2):208–18.

159. Rhodes CJ, Wharton J, Boon RA, Roexe T, Tsang H, Wojciak-Stothard B, et al. Reduced microRNA-150 is associated with poor survival in pulmonary arterial hypertension. Am J Respir Crit Care Med. 2013 Feb 1;187(3):294–302.

160. Boucherat O, Potus F, Bonnet S. microRNA and Pulmonary Hypertension. Adv Exp Med Biol. 2015;888:237–52.

161. Viales RR, Eichstaedt CA, Ehlken N, Fischer C, Lichtblau M, Grünig E, et al. Mutation in BMPR2 Promoter: A ‘Second Hit’ for Manifestation of Pulmonary Arterial Hypertension? PLOS ONE. 2015 Jul 13;10(7):e0133042.

162. Germain M, Eyries M, Montani D, Poirier O, Girerd B, Dorfmüller P, et al. Genome-wide association analysis identifies a susceptibility locus for pulmonary arterial hypertension. Nat Genet. 2013 May;45(5):518–21.

163. Conesa A, Beck S. Making multi-omics data accessible to researchers. Sci Data. 2019 Oct 31;6(1):251.

164. Rhodes CJ, Wharton J, Ghataorhe P, Watson G, Girerd B, Howard LS, et al. Plasma proteome analysis in patients with pulmonary arterial hypertension: an observational cohort study. Lancet Respir Med. 2017 Sep;5(9):717–26.

165. Rhodes CJ, Ghataorhe P, Wharton J, Rue-Albrecht KC, Hadinnapola C, Watson G, et al. Plasma Metabolomics Implicates Modified Transfer RNAs and Altered Bioenergetics in the Outcomes of Pulmonary Arterial Hypertension. Circulation. 2017 Jan 31;135(5):460–75.

166. Geraci MW, Moore M, Gesell T, Yeager ME, Alger L, Golpon H, et al. Gene expression patterns in the lungs of patients with primary pulmonary hypertension: a gene microarray analysis. Circ Res. 2001 Mar 30;88(6):555–62.

167. Rajkumar R, Konishi K, Richards TJ, Ishizawar DC, Wiechert AC, Kaminski N, et al. Genomewide RNA expression profiling in lung identifies distinct signatures in idiopathic pulmonary arterial hypertension and secondary pulmonary hypertension. Am J Physiol Heart Circ Physiol. 2010 Apr;298(4):H1235-1248.

168. Hsu E, Shi H, Jordan RM, Lyons-Weiler J, Pilewski JM, Feghali-Bostwick CA. Lung tissues in patients with systemic sclerosis have gene expression patterns unique to pulmonary fibrosis and pulmonary hypertension. Arthritis Rheum. 2011 Mar;63(3):783–94.

169. Mura M, Anraku M, Yun Z, McRae K, Liu M, Waddell TK, et al. Gene expression profiling in the lungs of patients with pulmonary hypertension associated with pulmonary fibrosis. Chest. 2012 Mar;141(3):661–73.

170. Shimodaira K, Okubo Y, Ochiai E, Nakayama H, Katano H, Wakayama M, et al. Gene expression analysis of a murine model with pulmonary vascular remodeling compared to end-stage IPAH lungs. Respir Res. 2012 Nov 17;13(1):103.

171. Liew CC, Ma J, Tang HC, Zheng R, Dempsey AA. The peripheral blood transcriptome dynamically reflects system wide biology: a potential diagnostic tool. J Lab Clin Med. 2006 Mar;147(3):126–32.

172. Pendergrass SA, Hayes E, Farina G, Lemaire R, Farber HW, Whitfield ML, et al. Limited Systemic Sclerosis Patients with Pulmonary Arterial Hypertension Show Biomarkers of Inflammation and Vascular Injury. PLoS ONE. 2010 Aug 17;5(8):e12106.

173. Risbano MG, Meadows CA, Coldren CD, Jenkins TJ, Edwards MG, Collier D, et al. Altered immune phenotype in peripheral blood cells of patients with scleroderma-associated pulmonary hypertension. Clin Transl Sci. 2010 Oct;3(5):210–8.

174. Bull TM, Coldren CD, Moore M, Sotto-Santiago SM, Pham DV, Nana-Sinkam SP, et al. Gene microarray analysis of peripheral blood cells in pulmonary arterial hypertension. Am J Respir Crit Care Med. 2004 Oct 15;170(8):911–9.

175. Cheadle C, Berger AE, Mathai SC, Grigoryev DN, Watkins TN, Sugawara Y, et al. Erythroid-specific transcriptional changes in PBMCs from pulmonary hypertension patients. PloS One. 2012;7(4):e34951.

176. Hemnes AR, Trammell AW, Archer SL, Rich S, Yu C, Nian H, et al. Peripheral blood signature of vasodilator-responsive pulmonary arterial hypertension. Circulation. 2015 Jan 27;131(4):401–9; discussion 409.

177. Sutendra G, Michelakis ED. Pulmonary arterial hypertension: challenges in translational research and a vision for change. Sci Transl Med. 2013 Oct 23;5(208):208sr5.

178. Harbaum L, Rhodes CJ, Otero-Núñez P, Wharton J, Wilkins MR. The application of 'omics' to pulmonary arterial hypertension. Br J Pharmacol. 2021 Jan;178(1):108–20.

179. Mohr S, Liew CC. The peripheral-blood transcriptome: new insights into disease and risk assessment. Trends Mol Med. 2007 Oct;13(10):422–32.

180. Soneson C, Yao Y, Bratus-Neuenschwander A, Patrignani A, Robinson MD, Hussain S. A comprehensive examination of Nanopore native RNA sequencing for characterization of complex transcriptomes. Nat Commun. 2019 Jul 31;10(1):3359.

181. Perrino C, Barabási AL, Condorelli G, Davidson SM, De Windt L, Dimmeler S, et al. Epigenomic and transcriptomic approaches in the post-genomic era: path to novel targets for diagnosis and therapy of the ischaemic heart? Position Paper of the European Society of Cardiology Working Group on Cellular Biology of the Heart. Cardiovasc Res. 2017 Jun 1;113(7):725–36.

182. Hoffmann J, Wilhelm J, Olschewski A, Kwapiszewska G. Microarray analysis in pulmonary hypertension. Eur Respir J. 2016 Jul;48(1):229–41.

183. Zhao M, Austin ED, Hemnes AR, Loyd JE, Zhao Z. An evidence-based knowledgebase of pulmonary arterial hypertension to identify genes and pathways relevant to pathogenesis. Mol Biosyst. 2014 Apr;10(4):732–40.

184. Stearman RS, Bui QM, Speyer G, Handen A, Cornelius AR, Graham BB, et al. Systems Analysis of the Human Pulmonary Arterial Hypertension Lung Transcriptome. Am J Respir Cell Mol Biol. 2019 Jun;60(6):637–49.

185. Yates LL, Dean CH. Planar polarity: A new player in both lung development and disease. Organogenesis. 2011 Sep;7(3):209–16.

186. Pongracz JE, Stockley RA. Wnt signalling in lung development and diseases. Respir Res. 2006 Jan 26;7:15.

187. de Jesus Perez VA, Alastalo TP, Wu JC, Axelrod JD, Cooke JP, Amieva M, et al. Bone morphogenetic protein 2 induces pulmonary angiogenesis via Wnt-beta-catenin and Wnt-RhoA-Rac1 pathways. J Cell Biol. 2009 Jan 12;184(1):83–99.

188. Laumanns IP, Fink L, Wilhelm J, Wolff JC, Mitnacht-Kraus R, Graef-Hoechst S, et al. The noncanonical WNT pathway is operative in idiopathic pulmonary arterial hypertension. Am J Respir Cell Mol Biol. 2009 Jun;40(6):683–91.

189. Rhodes CJ, Im H, Cao A, Hennigs JK, Wang L, Sa S, et al. RNA Sequencing Analysis Detection of a Novel Pathway of Endothelial Dysfunction in Pulmonary Arterial Hypertension. Am J Respir Crit Care Med. 2015 Aug 1;192(3):356–66.

190. Harigae H, Suwabe N, Weinstock PH, Nagai M, Fujita H, Yamamoto M, et al. Deficient heme and globin synthesis in embryonic stem cells lacking the erythroid-specific delta-aminolevulinate synthase gene. Blood. 1998 Feb 1;91(3):798–805.

191. Bult CJ, Eppig JT, Kadin JA, Richardson JE, Blake JA, Mouse Genome Database Group. The Mouse Genome Database (MGD): mouse biology and model systems. Nucleic Acids Res. 2008 Jan;36(Database issue):D724-728.

192. Abdul-Salam VB, Russomanno G, Chien-Nien C, Mahomed AS, Yates LA, Wilkins MR, et al. CLIC4/Arf6 Pathway. Circ Res. 2019 Jan 4;124(1):52–65.

193. Xu W, Comhair SAA, Chen R, Hu B, Hou Y, Zhou Y, et al. Integrative proteomics and phosphoproteomics in pulmonary arterial hypertension. Sci Rep. 2019 Dec 9;9(1):18623.

194. Harbaum L, Rhodes CJ, Wharton J, Lawrie A, Karnes JH, Desai AA, et al. Mining the Plasma Proteome for Insights into the Molecular Pathology of Pulmonary Arterial Hypertension. Am J Respir Crit Care Med. 2022 Jun 15;205(12):1449–60.

195. Suhre K, Gieger C. Genetic variation in metabolic phenotypes: study designs and applications. Nat Rev Genet. 2012 Nov;13(11):759–69.

196. Zhao YD, Chu L, Lin K, Granton E, Yin L, Peng J, et al. A Biochemical Approach to Understand the Pathogenesis of Advanced Pulmonary Arterial Hypertension: Metabolomic Profiles of Arginine, Sphingosine-1-Phosphate, and Heme of Human Lung. PloS One. 2015;10(8):e0134958.

197. Brittain EL, Talati M, Fessel JP, Zhu H, Penner N, Calcutt MW, et al. Fatty Acid Metabolic Defects and Right Ventricular Lipotoxicity in Human Pulmonary Arterial Hypertension. Circulation. 2016 May 17;133(20):1936–44.

198. Lewis GD, Ngo D, Hemnes AR, Farrell L, Domos C, Pappagianopoulos PP, et al. Metabolic Profiling of Right Ventricular-Pulmonary Vascular Function Reveals Circulating Biomarkers of Pulmonary Hypertension. J Am Coll Cardiol. 2016 Jan 19;67(2):174–89.

199. Harbaum L, Ghataorhe P, Wharton J, Jiménez B, Howard LSG, Gibbs JSR, et al. Reduced plasma levels of small HDL particles transporting fibrinolytic proteins in pulmonary arterial hypertension. Thorax. 2019 Apr;74(4):380–9.

200. Gamen E, Seeger W, Pullamsetti SS. The emerging role of epigenetics in pulmonary hypertension. Eur Respir J. 2016 Sep;48(3):903–17.

201. Liu D, Yan Y, Chen JW, Yuan P, Wang XJ, Jiang R, et al. Hypermethylation of BMPR2 Promoter Occurs in Patients with Heritable Pulmonary Arterial Hypertension and Inhibits BMPR2 Expression. Am J Respir Crit Care Med. 2017 Oct 1;196(7):925–8.

202. de Armas LR, Podack ER. Chapter Sixteen - Natural killer cytolytic activity. In: Lotze MT, Thomson AW, editors. Natural Killer Cells [Internet]. San Diego: Academic Press; 2010 [cited 2022 Aug 6]. p. 215–27. Available from: https://www.sciencedirect.com/science/article/pii/B9780123704542000168

203. Perros F, Cohen-Kaminsky S, Gambaryan N, Girerd B, Raymond N, Klingelschmitt I, et al. Cytotoxic cells and granulysin in pulmonary arterial hypertension and pulmonary veno-occlusive disease. Am J Respir Crit Care Med. 2013 Jan 15;187(2):189–96.

204. Chambers DC, Carew AM, Lukowski SW, Powell JE. Transcriptomics and single-cell RNA-sequencing. Respirology. 2019;24(1):29–36.

205. Wang Z, Gerstein M, Snyder M. RNA-Seq: a revolutionary tool for transcriptomics. Nat Rev Genet. 2009 Jan;10(1):57–63.

206. Hingorani AD, Kuan V, Finan C, Kruger FA, Gaulton A, Chopade S, et al. Improving the odds of drug development success through human genomics: modelling study. Sci Rep. 2019 Dec 11;9(1):18911.

207. Law BK. Rapamycin: an anti-cancer immunosuppressant? Crit Rev Oncol Hematol. 2005 Oct;56(1):47–60.

208. Bitto A, Ito TK, Pineda VV, LeTexier NJ, Huang HZ, Sutlief E, et al. Transient rapamycin treatment can increase lifespan and healthspan in middle-aged mice. eLife. 2016 Aug 23;5:e16351.

209. Panwalkar A, Verstovsek S, Giles FJ. Mammalian target of rapamycin inhibition as therapy for hematologic malignancies. Cancer. 2004 Feb 15;100(4):657–66.

210. Wagle N, Grabiner BC, Van Allen EM, Hodis E, Jacobus S, Supko JG, et al. Activating mTOR mutations in a patient with an extraordinary response on a phase I trial of everolimus and pazopanib. Cancer Discov. 2014 May;4(5):546–53.

211. Grabiner BC, Nardi V, Birsoy K, Possemato R, Shen K, Sinha S, et al. A diverse array of cancer-associated MTOR mutations are hyperactivating and can predict rapamycin sensitivity. Cancer Discov. 2014 May;4(5):554–63.

212. Aadi Bioscience, Inc. A Phase 1 Clinical Trial of ABI-009, an mTOR Inhibitor, for Patients With Severe Pulmonary Arterial Hypertension (PAH) [Internet]. clinicaltrials.gov; 2021 Oct [cited 2022 Aug 4]. Report No.: NCT02587325. Available from: https://clinicaltrials.gov/ct2/show/NCT02587325

213. Goldstein I, Lue TF, Padma-Nathan H, Rosen RC, Steers WD, Wicker PA. Oral sildenafil in the treatment of erectile dysfunction. Sildenafil Study Group. N Engl J Med. 1998 May 14;338(20):1397–404.

214. Wang R chun, Jiang F ming, Zheng Q ling, Li C tao, Peng X ying, He C yun, et al. Efficacy and safety of sildenafil treatment in pulmonary arterial hypertension: a systematic review. Respir Med. 2014 Mar;108(3):531–7.

215. Ahmad G, Amiji M. Use of CRISPR/Cas9 gene-editing tools for developing models in drug discovery. Drug Discov Today. 2018 Mar;23(3):519–33.

216. Lamb J, Crawford ED, Peck D, Modell JW, Blat IC, Wrobel MJ, et al. The Connectivity Map: using gene-expression signatures to connect small molecules, genes, and disease. Science. 2006 Sep 29;313(5795):1929–35.

217. Subramanian A, Narayan R, Corsello SM, Peck DD, Natoli TE, Lu X, et al. A Next Generation Connectivity Map: L1000 Platform and the First 1,000,000 Profiles. Cell. 2017 Nov 30;171(6):1437-1452.e17.

218. Gao Y, Kim S, Lee YI, Lee J. Cellular Stress-Modulating Drugs Can Potentially Be Identified by in Silico Screening with Connectivity Map (CMap). Int J Mol Sci. 2019 Nov 9;20(22):5601.

219. Rho SB, Kim BR, Kang S. A gene signature-based approach identifies thioridazine as an inhibitor of phosphatidylinositol-3’-kinase (PI3K)/AKT pathway in ovarian cancer cells. Gynecol Oncol. 2011 Jan;120(1):121–7.

220. Patro R, Duggal G, Love MI, Irizarry RA, Kingsford C. Salmon provides fast and bias-aware quantification of transcript expression. Nat Methods. 2017 Apr;14(4):417–9.

221. R Core Team. R: a language and environment for statistical computing [Internet]. 2018 [cited 2022 Jul 19]. Available from: https://www.r-project.org/

222. Finotello F, Mayer C, Plattner C, Laschober G, Rieder D, Hackl H, et al. Molecular and pharmacological modulators of the tumor immune contexture revealed by deconvolution of RNA-seq data. Genome Med. 2019 May 24;11(1):34.

223. Newman AM, Liu CL, Green MR, Gentles AJ, Feng W, Xu Y, et al. Robust enumeration of cell subsets from tissue expression profiles. Nat Methods. 2015 May;12(5):453–7.

224. Bozdogan H. Akaike’s Information Criterion and Recent Developments in Information Complexity. J Math Psychol. 2000 Mar;44(1):62–91.

225. Robinson MD, McCarthy DJ, Smyth GK. edgeR: a Bioconductor package for differential expression analysis of digital gene expression data. Bioinforma Oxf Engl. 2010 Jan 1;26(1):139–40.

226. Wang J, Wang Y, Wang H, Hao X, Wu Y, Guo J. Selection of Reference Genes for Gene Expression Studies in Porcine Whole Blood and Peripheral Blood Mononuclear Cells under Polyinosinic:Polycytidylic Acid Stimulation. Asian-Australas J Anim Sci. 2014 Apr;27(4):471–8.

227. Kosinová L, Cahová M, Fábryová E, Týcová I, Koblas T, Leontovyč I, et al. Unstable Expression of Commonly Used Reference Genes in Rat Pancreatic Islets Early after Isolation Affects Results of Gene Expression Studies. PloS One. 2016;11(4):e0152664.

228. Errico A, Ballabio A, Rugarli EI. Spastin, the protein mutated in autosomal dominant hereditary spastic paraplegia, is involved in microtubule dynamics. Hum Mol Genet. 2002 Jan 15;11(2):153–63.

229. Tibshirani R. Regression Shrinkage and Selection via the Lasso. J R Stat Soc Ser B Methodol. 1996;58(1):267–88.

230. Robin X, Turck N, Hainard A, Tiberti N, Lisacek F, Sanchez JC, et al. pROC: an open-source package for R and S+ to analyze and compare ROC curves. BMC Bioinformatics. 2011 Mar 17;12(1):77.

231. Burgess S, Dudbridge F, Thompson SG. Combining information on multiple instrumental variables in Mendelian randomization: comparison of allele score and summarized data methods. Stat Med. 2016 May 20;35(11):1880–906.

232. Joehanes R, Zhang X, Huan T, Yao C, Ying SX, Nguyen QT, et al. Integrated genome-wide analysis of expression quantitative trait loci aids interpretation of genomic association studies. Genome Biol. 2017 Jan 25;18(1):16.

233. Westra HJ, Peters MJ, Esko T, Yaghootkar H, Schurmann C, Kettunen J, et al. Systematic identification of trans eQTLs as putative drivers of known disease associations. Nat Genet. 2013 Oct;45(10):1238–43.

234. Rabinovitch M, Guignabert C, Humbert M, Nicolls MR. Inflammation and Immunity in the Pathogenesis of Pulmonary Arterial Hypertension. Circ Res. 2014 Jun 20;115(1):165–75.

235. Chabot-Richards DS, George TI. White blood cell counts: reference methodology. Clin Lab Med. 2015 Mar;35(1):11–24.

236. Palmer C, Diehn M, Alizadeh AA, Brown PO. Cell-type specific gene expression profiles of leukocytes in human peripheral blood. BMC Genomics. 2006 May 16;7:115.

237. Elinoff JM, Mazer AJ, Cai R, Lu M, Graninger G, Harper B, et al. Meta-analysis of blood genome-wide expression profiling studies in pulmonary arterial hypertension. Am J Physiol Lung Cell Mol Physiol. 2020 Jan 1;318(1):L98–111.

238. Lemmens K, Segers VFM, Demolder M, Keulenaer GWD. Role of Neuregulin-1/ErbB2 Signaling in Endothelium-Cardiomyocyte Cross-talk *. J Biol Chem. 2006 Jul 14;281(28):19469–77.

239. Lemmens K, Doggen K, De Keulenaer GW. Role of neuregulin-1/ErbB signaling in cardiovascular physiology and disease: implications for therapy of heart failure. Circulation. 2007 Aug 21;116(8):954–60.

240. Dennis G, Sherman BT, Hosack DA, Yang J, Gao W, Lane HC, et al. DAVID: Database for Annotation, Visualization, and Integrated Discovery. Genome Biol. 2003;4(5):P3.

241. Krämer A, Green J, Pollard J, Tugendreich S. Causal analysis approaches in Ingenuity Pathway Analysis. Bioinforma Oxf Engl. 2014 Feb 15;30(4):523–30.

242. Asghar MY, Magnusson M, Kemppainen K, Sukumaran P, Löf C, Pulli I, et al. Transient Receptor Potential Canonical 1 (TRPC1) Channels as Regulators of Sphingolipid and VEGF Receptor Expression: IMPLICATIONS FOR THYROID CANCER CELL MIGRATION AND PROLIFERATION. J Biol Chem. 2015 Jun 26;290(26):16116–31.

243. Formigli L, Sassoli C, Squecco R, Bini F, Martinesi M, Chellini F, et al. Regulation of transient receptor potential canonical channel 1 (TRPC1) by sphingosine 1-phosphate in C2C12 myoblasts and its relevance for a role of mechanotransduction in skeletal muscle differentiation. J Cell Sci. 2009 May 1;122(Pt 9):1322–33.

244. Özpelit E, Akdeniz B, Özpelit ME, Tas S, Bozkurt S, Tertemiz KC, et al. Prognostic value of neutrophil-to-lymphocyte ratio in pulmonary arterial hypertension. J Int Med Res. 2015 Oct;43(5):661–71.

245. Huertas A, Phan C, Bordenave J, Tu L, Thuillet R, Le Hiress M, et al. Regulatory T Cell Dysfunction in Idiopathic, Heritable and Connective Tissue-Associated Pulmonary Arterial Hypertension. Chest. 2016 Jun;149(6):1482–93.

246. Ulrich S, Nicolls MR, Taraseviciene L, Speich R, Voelkel N. Increased regulatory and decreased CD8+ cytotoxic T cells in the blood of patients with idiopathic pulmonary arterial hypertension. Respir Int Rev Thorac Dis. 2008;75(3):272–80.

247. Qiu H, He Y, Ouyang F, Jiang P, Guo S, Guo Y. The Role of Regulatory T Cells in Pulmonary Arterial Hypertension. J Am Heart Assoc. 2019 Dec 3;8(23):e014201.

248. Casero RA, Murray Stewart T, Pegg AE. Polyamine metabolism and cancer: treatments, challenges and opportunities. Nat Rev Cancer. 2018 Nov;18(11):681–95.

249. Weisel FC, Kloepping C, Pichl A, Sydykov A, Kojonazarov B, Wilhelm J, et al. Impact of S-adenosylmethionine decarboxylase 1 on pulmonary vascular remodeling. Circulation. 2014 Apr 8;129(14):1510–23.

250. Mumby S, Perros F, Hui C, Xu B l., Xu W, Elyasigomari V, et al. Extracellular matrix degradation pathways and fatty acid metabolism regulate distinct pulmonary vascular cell types in pulmonary arterial hypertension. Pulm Circ. 2021;11(1):2045894021996190.

251. Ellis DE, Hubbard RA, Willis AW, Zuppa AF, Zaoutis TE, Hennessy S. Comparing LASSO and random forest models for predicting neurological dysfunction among fluoroquinolone users. Pharmacoepidemiol Drug Saf. 2022 Apr;31(4):393–403.

252. Lu F, Petkova E. A comparative study of variable selection methods in the context of developing psychiatric screening instruments. Stat Med. 2014;33(3):401–21.

253. Kiselev VY, Andrews TS, Hemberg M. Challenges in unsupervised clustering of single-cell RNA-seq data. Nat Rev Genet. 2019 May;20(5):273–82.

254. Kariotis S, Jammeh E, Swietlik EM, Pickworth JA, Rhodes CJ, Otero P, et al. Biological heterogeneity in idiopathic pulmonary arterial hypertension identified through unsupervised transcriptomic profiling of whole blood. Nat Commun. 2021 Dec 7;12(1):7104.

255. Irizarry KA, Miller M, Freemark M, Haqq AM. Prader Willi Syndrome: genetics, metabolomics, hormonal function, and new approaches to therapy. Adv Pediatr. 2016 Aug;63(1):47–77.

256. Poulet M, Sirois J, Boyé K, Uetani N, Hardy S, Daubon T, et al. PRL-2 phosphatase is required for vascular morphogenesis and angiogenic signaling. Commun Biol. 2020 Oct 23;3:603.

257. Zhong S, Li L, Zhang YL, Zhang L, Lu J, Guo S, et al. Acetaldehyde dehydrogenase 2 interactions with LDLR and AMPK regulate foam cell formation. J Clin Invest. 129(1):252–67.

258. Fang Y, Liu Z, Chen Z, Xu X, Xiao M, Yu Y, et al. Smad5 acts as an intracellular pH messenger and maintains bioenergetic homeostasis. Cell Res. 2017 Sep;27(9):1083–99.

259. Wang C, Fang Z, Zhu Z, Liu J, Chen H. Reciprocal regulation between hepcidin and erythropoiesis and its therapeutic application in erythroid disorders. Exp Hematol. 2017 Aug;52:24–31.

260. Rhodes CJ, Howard LS, Busbridge M, Ashby D, Kondili E, Gibbs JSR, et al. Iron deficiency and raised hepcidin in idiopathic pulmonary arterial hypertension: clinical prevalence, outcomes, and mechanistic insights. J Am Coll Cardiol. 2011 Jul 12;58(3):300–9.

261. Humbert M, McLaughlin V, Gibbs JSR, Gomberg-Maitland M, Hoeper MM, Preston IR, et al. Sotatercept for the Treatment of Pulmonary Arterial Hypertension. N Engl J Med. 2021 Apr 1;384(13):1204–15.

262. Smits AJ, Arkani M, In ’t Veld SGJG, Huis In ’t Veld AE, Sol N, Groeneveldt JA, et al. Distinct Platelet RNA Signatures in Patients with Pulmonary Hypertension. Ann Am Thorac Soc. 2022 May 10;

263. Dufresne J, Bowden P, Thavarajah T, Florentinus-Mefailoski A, Chen ZZ, Tucholska M, et al. The plasma peptides of ovarian cancer. Clin Proteomics. 2018 Dec 21;15:41.

264. Zhu W, Jiang H, Xie S, Xiao H, Liu Q, Chen N, et al. Downregulation of PPA2 expression correlates with poor prognosis of kidney renal clear cell carcinoma. PeerJ. 2021 Sep 6;9:e12086.

265. Guimier A, Gordon CT, Godard F, Ravenscroft G, Oufadem M, Vasnier C, et al. Biallelic PPA2 Mutations Cause Sudden Unexpected Cardiac Arrest in Infancy. Am J Hum Genet. 2016 Sep 1;99(3):666–73.

266. Sun W, Tian BX, Wang SH, Liu PJ, Wang YC. The function of SEC22B and its role in human diseases. Cytoskeleton. 2020;77(8):303–12.

267. Haziza S, Magnani R, Lan D, Keinan O, Saada A, Hershkovitz E, et al. Calmodulin Methyltransferase Is Required for Growth, Muscle Strength, Somatosensory Development and Brain Function. PLoS Genet. 2015 Aug 6;11(8):e1005388.

268. Nowakowska-Gołacka J, Czapiewska J, Sominka H, Sowa-Rogozińska N, Słomińska-Wojewódzka M. EDEM1 Regulates Amyloid Precursor Protein (APP) Metabolism and Amyloid-β Production. Int J Mol Sci. 2021 Dec 23;23(1):117.

269. Papaioannou A, Higa A, Jégou G, Jouan F, Pineau R, Saas L, et al. Alterations of EDEM1 functions enhance ATF6 pro-survival signaling. FEBS J. 2018 Nov;285(22):4146–64.

270. Li C, Pan B, Liu X, Qin J, Wang X, He B, et al. Long intergenic non-coding RNA LINC00485 exerts tumor-suppressive activity by regulating miR-581/EDEM1 axis in colorectal cancer. Aging. 2021 Jan 10;13(3):3866–85.

271. FER FER tyrosine kinase [Homo sapiens (human)] - Gene - NCBI [Internet]. [cited 2022 Aug 1]. Available from: https://www.ncbi.nlm.nih.gov/gene?Db=gene&Cmd=ShowDetailView&TermToSearch=2241

272. Sehgal PB, Lee JE. Protein Trafficking Dysfunctions: Role in the Pathogenesis of Pulmonary Arterial Hypertension. Pulm Circ. 2011 Jan 1;1(1):17–32.

273. Robinson DR, Kalyana-Sundaram S, Wu YM, Shankar S, Cao X, Ateeq B, et al. Functionally recurrent rearrangements of the MAST kinase and Notch gene families in breast cancer. Nat Med. 2011 Nov 20;17(12):1646–51.

274. Wang Y, Lu P, Wu B, Morrow BE, Zhou B. NOTCH maintains developmental cardiac gene network through WNT5A. J Mol Cell Cardiol. 2018 Dec;125:98–105.

275. Nair JR, Carlson LM, Koorella C, Rozanski CH, Byrne GE, Bergsagel PL, et al. CD28 Expressed on Malignant Plasma Cells Induces A Pro-Survival and Immunosuppressive Microenvironment. J Immunol Baltim Md 1950. 2011 Aug 1;187(3):1243–53.

276. Kimura T, Jain A, Choi SW, Mandell MA, Johansen T, Deretic V. TRIM-directed selective autophagy regulates immune activation. Autophagy. 2017 May 4;13(5):989–90.

277. Li P, Ma Z, Yu Y, Hu X, Zhou Y, Song H. FER promotes cell migration via regulating JNK activity. Cell Prolif. 2019 Jul 1;52(5):e12656.

278. Karin M, Gallagher E. From JNK to pay dirt: jun kinases, their biochemistry, physiology and clinical importance. IUBMB Life. 2005 May;57(4–5):283–95.

279. Jin N, Hatton N, Swartz DR, Xia X l, Harrington MA, Larsen SH, et al. Hypoxia activates jun-N-terminal kinase, extracellular signal-regulated protein kinase, and p38 kinase in pulmonary arteries. Am J Respir Cell Mol Biol. 2000 Nov;23(5):593–601.

280. Henriques-Coelho T, Oliveira SM, Moura RS, Roncon-Albuquerque R, Neves AL, Santos M, et al. Thymulin inhibits monocrotaline-induced pulmonary hypertension modulating interleukin-6 expression and suppressing p38 pathway. Endocrinology. 2008 Sep;149(9):4367–73.

281. Wilson JL, Yu J, Taylor L, Polgar P. Hyperplastic Growth of Pulmonary Artery Smooth Muscle Cells from Subjects with Pulmonary Arterial Hypertension Is Activated through JNK and p38 MAPK. PloS One. 2015;10(4):e0123662.

282. Guma M, Rius J, Duong-Polk KX, Haddad GG, Lindsey JD, Karin M. Genetic and pharmacological inhibition of JNK ameliorates hypoxia-induced retinopathy through interference with VEGF expression. Proc Natl Acad Sci U S A. 2009 May 26;106(21):8760–5.

283. Sala MA, Chen C, Zhang Q, Do-Umehara HC, Wu W, Misharin AV, et al. JNK2 up-regulates hypoxia-inducible factors and contributes to hypoxia-induced erythropoiesis and pulmonary hypertension. J Biol Chem. 2018 Jan 5;293(1):271–84.

284. Das M, Zawada WM, West J, Stenmark KR. JNK2 regulates vascular remodeling in pulmonary hypertension. Pulm Circ. 2018 May 2;8(3):2045894018778156.

285. Wouters OJ, McKee M, Luyten J. Estimated Research and Development Investment Needed to Bring a New Medicine to Market, 2009-2018. JAMA. 2020 Mar 3;323(9):844–53.

286. California Biomedical Research Association. New Drug Development Process [Internet]. 2016. Available from: https://ca-biomed.org/wp-content/uploads/2020/08/FS-DrugDevelop.pdf

287. Voelkel NF, Gomez-Arroyo J. The role of vascular endothelial growth factor in pulmonary arterial hypertension. The angiogenesis paradox. Am J Respir Cell Mol Biol. 2014 Oct;51(4):474–84.

288. Taraseviciene-Stewart L, Kasahara Y, Alger L, Hirth P, Mc Mahon G, Waltenberger J, et al. Inhibition of the VEGF receptor 2 combined with chronic hypoxia causes cell death-dependent pulmonary endothelial cell proliferation and severe pulmonary hypertension. FASEB J Off Publ Fed Am Soc Exp Biol. 2001 Feb;15(2):427–38.

289. Sakao S, Tatsumi K, Voelkel NF. Endothelial cells and pulmonary arterial hypertension: apoptosis, proliferation, interaction and transdifferentiation. Respir Res. 2009;10(1):95.

290. Ando J, Kamiya A. Blood flow and vascular endothelial cell function. Front Med Biol Eng Int J Jpn Soc Med Electron Biol Eng. 1993;5(4):245–64.

291. Chatterjee S, Fisher AB. Shear Stress, Cell Signaling, and Pulmonary Vascular Remodeling. In: Yuan JXJ, Garcia JGN, West JB, Hales CA, Rich S, Archer SL, editors. Textbook of Pulmonary Vascular Disease [Internet]. Boston, MA: Springer US; 2011 [cited 2022 Aug 1]. p. 787–99. Available from: https://doi.org/10.1007/978-0-387-87429-6_54

292. Li M, Scott DE, Shandas R, Stenmark KR, Tan W. High pulsatility flow induces adhesion molecule and cytokine mRNA expression in distal pulmonary artery endothelial cells. Ann Biomed Eng. 2009 Jun;37(6):1082–92.

293. Tian J, Fratz S, Hou Y, Lu Q, Görlach A, Hess J, et al. Delineating the angiogenic gene expression profile before pulmonary vascular remodeling in a lamb model of congenital heart disease. Physiol Genomics. 2011 Jan 1;43(2):87–98.

294. Hoffman JI, Rudolph AM, Heymann MA. Pulmonary vascular disease with congenital heart lesions: pathologic features and causes. Circulation. 1981 Nov;64(5):873–7.

295. Small-Molecule Compound Libraries | High Throughput Analysis Laboratory [Internet]. [cited 2022 Aug 1]. Available from: https://sites.northwestern.edu/htal/libraries/small-molecule-compound-libraries/

296. Romanoski CE, Qi X, Sangam S, Vanderpool RR, Stearman RS, Conklin A, et al. Transcriptomic profiles in pulmonary arterial hypertension associate with disease severity and identify novel candidate genes. Pulm Circ. 2020 Dec 7;10(4):2045894020968531.

297. Zhang L, Chen S, Zeng X, Lin D, Li Y, Gui L, et al. Revealing the pathogenic changes of PAH based on multiomics characteristics. J Transl Med. 2019 Jul 22;17(1):231.

298. Asosingh K, Comhair S, Mavrakis L, Xu W, Horton D, Taylor I, et al. Single-cell transcriptomic profile of human pulmonary artery endothelial cells in health and pulmonary arterial hypertension. Sci Rep. 2021 Jul 19;11(1):14714.

299. Xiao G, Wang T, Zhuang W, Ye C, Luo L, Wang H, et al. RNA sequencing analysis of monocrotaline-induced PAH reveals dysregulated chemokine and neuroactive ligand receptor pathways. Aging. 2020 Mar 16;12(6):4953–69.

300. Zeng Y, Liu H, Kang K, Wang Z, Hui G, Zhang X, et al. Hypoxia inducible factor-1 mediates expression of miR-322: potential role in proliferation and migration of pulmonary arterial smooth muscle cells. Sci Rep. 2015 Jul 13;5(1):12098.

301. Wei F, Yang S, Guo Q, Zhang X, Ren D, Lv T, et al. MicroRNA-21 regulates Osteogenic Differentiation of Periodontal Ligament Stem Cells by targeting Smad5. Sci Rep. 2017 Nov 30;7(1):16608.

302. Liu T, Zou XZ, Huang N, Ge XY, Yao MZ, Liu H, et al. miR-27a promotes endothelial-mesenchymal transition in hypoxia-induced pulmonary arterial hypertension by suppressing BMP signaling. Life Sci. 2019 Jun 15;227:64–73.

303. Chang H, Huylebroeck D, Verschueren K, Guo Q, Matzuk MM, Zwijsen A. Smad5 knockout mice die at mid-gestation due to multiple embryonic and extraembryonic defects. Dev Camb Engl. 1999 Apr;126(8):1631–42.

304. Umans L, Cox L, Tjwa M, Bito V, Vermeire L, Laperre K, et al. Inactivation of Smad5 in Endothelial Cells and Smooth Muscle Cells Demonstrates that Smad5 Is Required for Cardiac Homeostasis. Am J Pathol. 2007 May;170(5):1460–72.

305. Sun CK, Zhen YY, Lu HI, Sung PH, Chang LT, Tsai TH, et al. Reducing TRPC1 Expression through Liposome-Mediated siRNA Delivery Markedly Attenuates Hypoxia-Induced Pulmonary Arterial Hypertension in a Murine Model. Stem Cells Int. 2014;2014:316214.

306. Xia Y, Yang XR, Fu Z, Paudel O, Abramowitz J, Birnbaumer L, et al. TRPC1 and TRPC6 Contribute to Hypoxic Pulmonary Hypertension through Differential Regulation of Pulmonary Vascular Functions RR. Hypertension. 2014 Jan;63(1):173–80.

307. Morita T, Mitsuyama K, Yamasaki H, Mori A, Yoshimura T, Araki T, et al. Gene Expression of Transient Receptor Potential Channels in Peripheral Blood Mononuclear Cells of Inflammatory Bowel Disease Patients. J Clin Med. 2020 Aug 14;9(8):2643.

308. Altamura C, Greco MR, Carratù MR, Cardone RA, Desaphy JF. Emerging Roles for Ion Channels in Ovarian Cancer: Pathomechanisms and Pharmacological Treatment. Cancers. 2021 Feb 7;13(4):668.

309. Hong J, Arneson D, Umar S, Ruffenach G, Cunningham CM, Ahn IS, et al. Single-Cell Study of Two Rat Models of Pulmonary Arterial Hypertension Reveals Connections to Human Pathobiology and Drug Repositioning. Am J Respir Crit Care Med. 2021 Apr 15;203(8):1006–22.

310. Dong H, Li X, Cai M, Zhang C, Mao W, Wang Y, et al. Integrated bioinformatic analysis reveals the underlying molecular mechanism of and potential drugs for pulmonary arterial hypertension. Aging. 2021 May 18;13(10):14234–57.

311. Hemnes AR, Zhao M, West J, Newman JH, Rich S, Archer SL, et al. Critical Genomic Networks and Vasoreactive Variants in Idiopathic Pulmonary Arterial Hypertension. Am J Respir Crit Care Med. 2016 Aug 15;194(4):464–75.

312. Kantarjian HM, Talpaz M, Santini V, Murgo A, Cheson B, O'Brien SM. Homoharringtonine. Cancer. 2001;92(6):1591–605.

313. O'Brien S, Kantarjian H, Keating M, Beran M, Koller C, Robertson LE, et al. Homoharringtonine therapy induces responses in patients with chronic myelogenous leukemia in late chronic phase. Blood. 1995 Nov 1;86(9):3322–6.

314. Lü S, Wang J. Homoharringtonine and omacetaxine for myeloid hematological malignancies. J Hematol OncolJ Hematol Oncol. 2014 Jan 3;7(1):2.

315. Ajani JA, Dimery I, Chawla SP, Pinnamaneni K, Benjamin RS, Legha SS, et al. Phase II studies of homoharringtonine in patients with advanced malignant melanoma; sarcoma; and head and neck, breast, and colorectal carcinomas. Cancer Treat Rep. 1986 Mar;70(3):375–9.

316. Nazha A, Kantarjian H, Cortes J, Quintás-Cardama A. Omacetaxine mepesuccinate (synribo) - newly launched in chronic myeloid leukemia. Expert Opin Pharmacother. 2013 Oct;14(14):1977–86.

317. Daver N, Vega-Ruiz A, Kantarjian HM, Estrov Z, Ferrajoli A, Kornblau S, et al. A phase II Open-label Study of the Intravenous Administration of Homoharringtonine in the treatment of Myelodysplastic syndrome. Eur J Cancer Care (Engl). 2013 Sep;22(5):605–11.

318. Walker ZJ, Idler BM, Davis LN, Stevens BM, VanWyngarden MJ, Ohlstrom D, et al. Exploiting Protein Translation Dependence in Multiple Myeloma with Omacetaxine-based Therapy. Clin Cancer Res Off J Am Assoc Cancer Res. 2021 Feb 1;27(3):819–30.

319. Weng TY, Wu HF, Li CY, Hung YH, Chang YW, Chen YL, et al. Homoharringtonine induced immune alteration for an Efficient Anti-tumor Response in Mouse Models of Non-small Cell Lung Adenocarcinoma Expressing Kras Mutation. Sci Rep. 2018 May 29;8:8216.

320. Beranova L, Pombinho AR, Spegarova J, Koc M, Klanova M, Molinsky J, et al. The plant alkaloid and anti-leukemia drug homoharringtonine sensitizes resistant human colorectal carcinoma cells to TRAIL-induced apoptosis via multiple mechanisms. Apoptosis Int J Program Cell Death. 2013 Jun;18(6):739–50.

321. Wolff NC, Pavía-Jiménez A, Tcheuyap VT, Alexander S, Vishwanath M, Christie A, et al. High-throughput simultaneous screen and counterscreen identifies homoharringtonine as synthetic lethal with von Hippel-Lindau loss in renal cell carcinoma. Oncotarget. 2015 Jul 3;6(19):16951–62.

322. Ye X jin, Lin M fang. Homoharringtonine induces apoptosis of endothelium and down-regulates VEGF expression of K562 cells. J Zhejiang Univ Sci. 2004 Feb;5(2):230–4.

323. Zhao S, Xia Y, Zhang F, Xiong Z, Li Y, Yan W, et al. Nucleostemin dysregulation contributes to ischemic vulnerability of diabetic hearts: Role of ribosomal biogenesis. J Mol Cell Cardiol. 2017 Jul;108:106–13.

324. Zhu M, Gong Z, Wu Q, Su Q, Yang T, Yu R, et al. Homoharringtonine suppresses tumor proliferation and migration by regulating EphB4-mediated β-catenin loss in hepatocellular carcinoma. Cell Death Dis. 2020 Aug 14;11(8):632.

325. Tan Y, Du B, Zhan Y, Wang K, Wang X, Chen B, et al. Antitumor effects of circ-EPHB4 in hepatocellular carcinoma via inhibition of HIF-1α. Mol Carcinog. 2019 Jun;58(6):875–86.

8 – Data Supplement

	RNA Discovery		RNA Validation		Combined Discovery and Validation		
GeneName	**logFC A**	**Sig. A**	**logFC B**	**Sig. B**	**logFC AB**	**Sig. AB**	**FDR AB**
RSRC2	-0.188	$3.00x10^{-07}$	-0.110	$8.64x10^{-04}$	-0.142	$4.85x10^{-09}$	$4.37x10^{-05}$
PTAR1	-0.197	$5.01x10^{-06}$	-0.140	$1.10x10^{-03}$	-0.164	$3.16x10^{-08}$	$1.90x10^{-04}$
RP11-379H18.1	0.155	$5.00x10^{-04}$	0.209	$2.88x10^{-05}$	0.177	$5.20x10^{-08}$	$2.34x10^{-04}$
C1orf27	-0.196	$1.39x10^{-05}$	-0.158	$1.23x10^{-03}$	-0.175	$8.08x10^{-08}$	$2.91x10^{-04}$
AP004289.1	0.321	$9.03x10^{-07}$	0.202	$4.61x10^{-03}$	0.255	$1.26x10^{-07}$	$3.16x10^{-04}$
BTAF1	-0.192	$2.75x10^{-05}$	-0.130	$1.26x10^{-03}$	-0.157	$1.76x10^{-07}$	$3.16x10^{-04}$
TEX10	-0.141	$5.52x10^{-06}$	-0.087	$5.53x10^{-03}$	-0.113	$1.39x10^{-07}$	$3.16x10^{-04}$
TLR5	-0.349	$2.18x10^{-04}$	-0.410	$2.23x10^{-04}$	-0.368	$1.49x10^{-07}$	$3.16x10^{-04}$
ARFGAP3	-0.160	$1.93x10^{-04}$	-0.150	$6.01x10^{-04}$	-0.155	$2.69x10^{-07}$	$3.24x10^{-04}$
HLTF	-0.212	$1.08x10^{-05}$	-0.150	$5.06x10^{-03}$	-0.179	$2.70x10^{-07}$	$3.24x10^{-04}$
RBM27	-0.136	$6.00x10^{-04}$	-0.135	$4.90x10^{-04}$	-0.140	$2.08x10^{-07}$	$3.24x10^{-04}$
SAMD8	-0.125	$2.76x10^{-03}$	-0.177	$2.46x10^{-05}$	-0.149	$2.23x10^{-07}$	$3.24x10^{-04}$
SCYL3	-0.142	$3.37x10^{-06}$	-0.085	$1.11x10^{-02}$	-0.113	$2.36x10^{-07}$	$3.24x10^{-04}$
SCFD2	-0.257	$3.63x10^{-05}$	-0.211	$5.53x10^{-04}$	-0.227	$2.99x10^{-07}$	$3.37x10^{-04}$
ZNF211	-0.182	$7.91x10^{-05}$	-0.154	$6.68x10^{-04}$	-0.163	$3.26x10^{-07}$	$3.45x10^{-04}$
DDX17	-0.159	$4.61x10^{-06}$	-0.083	$1.34x10^{-02}$	-0.118	$3.68x10^{-07}$	$3.68x10^{-04}$
AL844908.5	-0.300	$1.86x10^{-04}$	-0.280	$1.62x10^{-03}$	-0.297	$4.76x10^{-07}$	$4.29x10^{-04}$
RALA	0.160	$1.36x10^{-03}$	0.204	$1.33x10^{-04}$	0.181	$5.22x10^{-07}$	$4.48x10^{-04}$
PTEN	-0.181	$1.32x10^{-04}$	-0.176	$6.67x10^{-04}$	-0.171	$5.73x10^{-07}$	$4.69x10^{-04}$
CCNB1IP1	-0.148	$9.46x10^{-04}$	-0.150	$2.80x10^{-04}$	-0.149	$6.17x10^{-07}$	$4.84x10^{-04}$
AP000240.5	0.324	$2.64x10^{-03}$	0.400	$8.03x10^{-04}$	0.389	$6.86x10^{-07}$	$5.15x10^{-04}$
RBM5	-0.137	$2.28x10^{-06}$	-0.062	$4.48x10^{-02}$	-0.101	$7.51x10^{-07}$	$5.41x10^{-04}$
KCNQ1OT1	0.152	$1.41x10^{-04}$	0.132	$1.26x10^{-03}$	0.140	$9.24x10^{-07}$	$6.17x10^{-04}$
ZNF224	-0.135	$2.53x10^{-05}$	-0.090	$9.32x10^{-03}$	-0.112	$9.08x10^{-07}$	$6.17x10^{-04}$
RP11-138A9.2	0.223	$6.17x10^{-04}$	0.238	$3.59x10^{-04}$	0.225	$1.08x10^{-06}$	$6.72x10^{-04}$
ZFAND1	-0.151	$8.35x10^{-04}$	-0.167	$3.08x10^{-04}$	-0.157	$1.06x10^{-06}$	$6.72x10^{-04}$
AC010746.2	0.206	$3.04x10^{-04}$	0.213	$1.10x10^{-03}$	0.207	$1.33x10^{-06}$	$8.01x10^{-04}$
CCDC186	-0.153	$1.45x10^{-04}$	-0.109	$6.54x10^{-03}$	-0.132	$1.52x10^{-06}$	$8.24x10^{-04}$
CHD9	-0.157	$3.20x10^{-04}$	-0.178	$2.04x10^{-04}$	-0.155	$1.49x10^{-06}$	$8.24x10^{-04}$
RASA2	-0.145	$2.57x10^{-04}$	-0.113	$7.17x10^{-03}$	-0.135	$1.56x10^{-06}$	$8.24x10^{-04}$
UBR1	-0.150	$1.13x10^{-05}$	-0.089	$1.01x10^{-02}$	-0.114	$1.52x10^{-06}$	$8.24x10^{-04}$
ZNF141	-0.159	$1.49x10^{-04}$	-0.110	$2.62x10^{-03}$	-0.130	$1.64x10^{-06}$	$8.46x10^{-04}$
AC009299.4	1.414	$2.20x10^{-05}$	0.600	$3.22x10^{-02}$	1.048	$1.74x10^{-06}$	$8.69x10^{-04}$
ARHGAP12	-0.195	$1.89x10^{-05}$	-0.099	$3.39x10^{-02}$	-0.151	$1.84x10^{-06}$	$8.78x10^{-04}$
ZNF486	-0.229	$3.96x10^{-03}$	-0.321	$7.27x10^{-05}$	-0.266	$1.85x10^{-06}$	$8.78x10^{-04}$
BCLAF1	-0.166	$3.01x10^{-05}$	-0.092	$1.53x10^{-02}$	-0.127	$2.00x10^{-06}$	$9.25x10^{-04}$
SMARCD2	-0.158	$8.08x10^{-05}$	-0.114	$5.20x10^{-03}$	-0.132	$2.23x10^{-06}$	$1.00x10^{-03}$
RP11-158K1.3	-0.160	$5.37x10^{-04}$	-0.138	$3.47x10^{-03}$	-0.151	$2.30x10^{-06}$	$1.01x10^{-03}$

DENND4C	-0.176	2.52x10^{-05}	-0.094	1.63x10^{-02}	-0.132	2.48x10^{-06}	1.04x10^{-03}
RP11-154H23.1	0.279	2.47x10^{-05}	0.172	1.24x10^{-02}	0.221	2.48x10^{-06}	1.04x10^{-03}
PCF11	-0.136	2.21x10^{-04}	-0.118	2.46x10^{-03}	-0.122	2.74x10^{-06}	1.10x10^{-03}
ZNF397	-0.101	2.13x10^{-03}	-0.105	2.48x10^{-03}	-0.109	2.76x10^{-06}	1.10x10^{-03}
XKRX	-0.544	3.45x10^{-03}	-0.763	2.38x10^{-05}	-0.604	2.87x10^{-06}	1.12x10^{-03}
RP11-775J23.2	0.357	1.12x10^{-04}	0.279	2.52x10^{-03}	0.299	3.01x10^{-06}	1.15x10^{-03}
HECTD1	-0.133	1.93x10^{-05}	-0.088	7.92x10^{-03}	-0.103	3.10x10^{-06}	1.16x10^{-03}
CTD-2317K6.1	0.299	2.62x10^{-04}	0.253	2.63x10^{-03}	0.272	3.32x10^{-06}	1.22x10^{-03}
ZNF24	-0.126	6.16x10^{-04}	-0.107	3.45x10^{-03}	-0.116	3.48x10^{-06}	1.25x10^{-03}
RP11-426D19.1	0.205	9.97x10^{-05}	0.142	1.36x10^{-02}	0.177	3.65x10^{-06}	1.29x10^{-03}
DNAJB4	-0.266	5.60x10^{-05}	-0.179	1.30x10^{-02}	-0.228	3.80x10^{-06}	1.31x10^{-03}
ZNF432	-0.171	2.55x10^{-04}	-0.130	4.99x10^{-03}	-0.149	3.86x10^{-06}	1.31x10^{-03}
BROX	-0.107	4.75x10^{-03}	-0.150	2.14x10^{-04}	-0.123	4.06x10^{-06}	1.35x10^{-03}
RNASEL	-0.162	8.71x10^{-04}	-0.215	1.28x10^{-03}	-0.184	4.31x10^{-06}	1.41x10^{-03}
SEC23A	-0.125	1.61x10^{-04}	-0.081	1.74x10^{-02}	-0.104	4.90x10^{-06}	1.55x10^{-03}
ALG8	-0.139	1.40x10^{-04}	-0.086	1.33x10^{-02}	-0.111	5.06x10^{-06}	1.56x10^{-03}
RIF1	-0.143	8.11x10^{-05}	-0.103	7.88x10^{-03}	-0.117	5.20x10^{-06}	1.56x10^{-03}
SETX	-0.140	2.22x10^{-04}	-0.095	1.03x10^{-02}	-0.117	5.19x10^{-06}	1.56x10^{-03}
RLIM	-0.141	8.03x10^{-04}	-0.128	3.45x10^{-03}	-0.134	5.58x10^{-06}	1.62x10^{-03}
TCAIM	-0.154	1.89x10^{-04}	-0.108	1.17x10^{-02}	-0.130	5.54x10^{-06}	1.62x10^{-03}
RP11-43D4.2	0.300	4.10x10^{-04}	0.245	7.45x10^{-03}	0.280	5.81x10^{-06}	1.64x10^{-03}
ZMYM1	-0.144	2.21x10^{-03}	-0.169	1.40x10^{-03}	-0.156	5.78x10^{-06}	1.64x10^{-03}
PTPRC	-0.154	2.37x10^{-04}	-0.112	8.20x10^{-03}	-0.130	5.96x10^{-06}	1.65x10^{-03}
AC074092.1	0.260	2.29x10^{-03}	0.268	1.77x10^{-03}	0.273	6.28x10^{-06}	1.67x10^{-03}
CEP120	-0.134	1.15x10^{-03}	-0.129	9.59x10^{-04}	-0.126	6.30x10^{-06}	1.67x10^{-03}
ZNF763	-0.225	4.15x10^{-03}	-0.264	1.29x10^{-03}	-0.252	6.44x10^{-06}	1.67x10^{-03}
ZC3H11A	-0.142	3.38x10^{-05}	-0.068	4.12x10^{-02}	-0.104	6.82x10^{-06}	1.73x10^{-03}
PRKD3	-0.162	1.04x10^{-03}	-0.162	1.94x10^{-03}	-0.157	7.29x10^{-06}	1.75x10^{-03}
SLC16A10	-0.333	2.64x10^{-03}	-0.383	1.14x10^{-03}	-0.358	7.28x10^{-06}	1.75x10^{-03}
ATF6	-0.157	1.69x10^{-03}	-0.186	7.20x10^{-04}	-0.162	8.01x10^{-06}	1.90x10^{-03}
PTGR1	0.155	2.56x10^{-03}	0.188	1.13x10^{-03}	0.168	8.80x10^{-06}	2.03x10^{-03}
KIAA1551	-0.209	2.81x10^{-05}	-0.114	2.28x10^{-02}	-0.154	8.96x10^{-06}	2.04x10^{-03}
ATG12	-0.125	9.35x10^{-04}	-0.114	4.28x10^{-03}	-0.118	9.09x10^{-06}	2.05x10^{-03}
CTC-559E9.5	-0.199	9.20x10^{-04}	-0.182	4.81x10^{-03}	-0.190	9.72x10^{-06}	2.16x10^{-03}
TMTC3	-0.217	3.69x10^{-05}	-0.129	1.51x10^{-02}	-0.164	9.86x10^{-06}	2.17x10^{-03}
ZNF252P	-0.136	7.08x10^{-03}	-0.169	3.60x10^{-04}	-0.150	1.03x10^{-05}	2.23x10^{-03}
RP11-254B13.3	0.296	1.85x10^{-04}	0.249	1.44x10^{-02}	0.282	1.08x10^{-05}	2.28x10^{-03}
RP11-2J18.1	0.240	4.96x10^{-03}	0.356	2.17x10^{-04}	0.276	1.06x10^{-05}	2.28x10^{-03}
CTD-2303B20.1	0.293	4.05x10^{-03}	0.386	9.54x10^{-04}	0.333	1.13x10^{-05}	2.36x10^{-03}
KAT8	-0.127	1.27x10^{-03}	-0.123	5.78x10^{-03}	-0.128	1.14x10^{-05}	2.37x10^{-03}
AMD1	-0.151	2.59x10^{-03}	-0.186	4.74x10^{-04}	-0.159	1.16x10^{-05}	2.37x10^{-03}
BACE1	0.307	8.53x10^{-05}	0.194	3.08x10^{-02}	0.254	1.31x10^{-05}	2.63x10^{-03}
EIF4A2	-0.168	1.75x10^{-04}	-0.107	2.33x10^{-02}	-0.140	1.35x10^{-05}	2.68x10^{-03}
NAA35	-0.112	1.82x10^{-03}	-0.090	4.01x10^{-03}	-0.100	1.37x10^{-05}	2.68x10^{-03}
HELQ	-0.115	3.21x10^{-03}	-0.106	4.26x10^{-03}	-0.114	1.54x10^{-05}	2.87x10^{-03}
RP11-140I24.1	0.289	2.26x10^{-04}	0.227	1.25x10^{-02}	0.252	1.51x10^{-05}	2.87x10^{-03}

RP11-255H23.2	-0.354	8.93x10^{-04}	-0.317	5.61x10^{-03}	-0.331	1.49x10^{-05}	2.87x10^{-03}
ZNF33A	-0.121	3.41x10^{-03}	-0.132	2.03x10^{-03}	-0.126	1.52x10^{-05}	2.87x10^{-03}
RP11-135N5.3	0.189	3.01x10^{-03}	0.185	9.46x10^{-03}	0.200	1.60x10^{-05}	2.93x10^{-03}
SIKE1	-0.138	7.06x10^{-04}	-0.106	3.14x10^{-03}	-0.116	1.61x10^{-05}	2.93x10^{-03}
MAP3K7CL	-0.330	2.70x10^{-02}	-0.615	2.98x10^{-04}	-0.479	1.72x10^{-05}	3.04x10^{-03}
STAG2	-0.124	1.40x10^{-03}	-0.104	8.05x10^{-03}	-0.114	1.72x10^{-05}	3.04x10^{-03}
NR1D2	-0.142	6.69x10^{-03}	-0.145	1.99x10^{-03}	-0.147	1.80x10^{-05}	3.15x10^{-03}
PWWP2A	-0.117	8.80x10^{-04}	-0.081	1.52x10^{-02}	-0.101	1.82x10^{-05}	3.15x10^{-03}
EHBP1L1	-0.199	8.44x10^{-04}	-0.143	1.93x10^{-02}	-0.180	1.87x10^{-05}	3.21x10^{-03}
RP11-538D16.2	0.164	6.49x10^{-04}	0.099	1.57x10^{-02}	0.135	1.94x10^{-05}	3.29x10^{-03}
C12orf45	-0.160	7.02x10^{-03}	-0.167	5.87x10^{-03}	-0.180	1.99x10^{-05}	3.32x10^{-03}
FRRS1L	0.182	1.08x10^{-03}	0.151	9.28x10^{-03}	0.168	2.05x10^{-05}	3.32x10^{-03}
HOMER1	-0.272	3.46x10^{-03}	-0.256	4.02x10^{-03}	-0.274	2.04x10^{-05}	3.32x10^{-03}
KDM1A	-0.110	1.55x10^{-03}	-0.090	4.62x10^{-03}	-0.097	2.03x10^{-05}	3.32x10^{-03}
RP11-259P6.2	0.367	2.71x10^{-03}	0.367	2.88x10^{-03}	0.367	2.06x10^{-05}	3.32x10^{-03}
RP11-24J23.2	0.145	2.84x10^{-03}	0.150	1.46x10^{-03}	0.141	2.09x10^{-05}	3.33x10^{-03}
UHRF2	-0.164	2.16x10^{-04}	-0.108	2.04x10^{-02}	-0.133	2.21x10^{-05}	3.50x10^{-03}
ACAP2	-0.101	2.57x10^{-03}	-0.106	3.11x10^{-03}	-0.100	2.24x10^{-05}	3.50x10^{-03}
THAP2	-0.207	1.15x10^{-03}	-0.186	1.52x10^{-03}	-0.181	2.25x10^{-05}	3.50x10^{-03}
HIF1A	-0.209	1.50x10^{-04}	-0.162	1.28x10^{-02}	-0.175	2.28x10^{-05}	3.51x10^{-03}
C12orf29	-0.191	1.30x10^{-02}	-0.330	8.14x10^{-05}	-0.247	2.35x10^{-05}	3.56x10^{-03}
RP11-678G14.2	-0.362	5.11x10^{-03}	-0.437	2.29x10^{-03}	-0.404	2.35x10^{-05}	3.56x10^{-03}
ATM	-0.142	9.30x10^{-04}	-0.096	2.18x10^{-02}	-0.123	2.44x10^{-05}	3.66x10^{-03}
DEF6	-0.129	7.34x10^{-04}	-0.085	2.95x10^{-02}	-0.113	2.49x10^{-05}	3.68x10^{-03}
RP11-182I10.2	0.242	6.39x10^{-03}	0.264	2.72x10^{-03}	0.260	2.55x10^{-05}	3.68x10^{-03}
ZNF680	-0.106	1.52x10^{-02}	-0.151	8.49x10^{-04}	-0.128	2.54x10^{-05}	3.68x10^{-03}
ZNF627	-0.125	1.70x10^{-03}	-0.101	1.17x10^{-02}	-0.116	2.59x10^{-05}	3.70x10^{-03}
ZNF876P	-0.398	4.95x10^{-03}	-0.480	2.17x10^{-03}	-0.439	2.63x10^{-05}	3.73x10^{-03}
ZNF283	-0.133	3.55x10^{-03}	-0.131	2.64x10^{-03}	-0.129	2.66x10^{-05}	3.74x10^{-03}
CTD-2579N5.1	-1.227	1.72x10^{-03}	-1.221	4.56x10^{-03}	-1.221	2.93x10^{-05}	4.02x10^{-03}
KLHL28	-0.110	3.80x10^{-03}	-0.103	5.48x10^{-03}	-0.107	3.09x10^{-05}	4.20x10^{-03}
RIC8B	-0.169	2.36x10^{-04}	-0.103	4.02x10^{-02}	-0.139	3.15x10^{-05}	4.20x10^{-03}
RP11-349A22.5	-0.110	8.64x10^{-04}	-0.087	1.26x10^{-02}	-0.097	3.15x10^{-05}	4.20x10^{-03}
ITGA6	-0.199	1.79x10^{-03}	-0.213	4.58x10^{-03}	-0.199	3.32x10^{-05}	4.34x10^{-03}
ZNF160	-0.084	4.50x10^{-02}	-0.137	1.86x10^{-04}	-0.113	3.28x10^{-05}	4.34x10^{-03}
XRCC5	-0.133	2.75x10^{-04}	-0.082	2.42x10^{-02}	-0.104	3.38x10^{-05}	4.38x10^{-03}
DHX15	-0.131	3.79x10^{-04}	-0.083	2.05x10^{-02}	-0.103	3.49x10^{-05}	4.43x10^{-03}
PMS1	-0.179	5.85x10^{-05}	-0.100	4.18x10^{-02}	-0.135	3.49x10^{-05}	4.43x10^{-03}
SRSF10	-0.107	1.55x10^{-03}	-0.077	5.95x10^{-03}	-0.089	3.86x10^{-05}	4.77x10^{-03}
TWF1	-0.142	3.98x10^{-04}	-0.102	1.77x10^{-02}	-0.117	3.96x10^{-05}	4.77x10^{-03}
C2orf49	-0.095	1.08x10^{-02}	-0.119	1.34x10^{-03}	-0.106	4.07x10^{-05}	4.78x10^{-03}
KLF10	0.290	1.64x10^{-03}	0.281	6.08x10^{-03}	0.274	4.11x10^{-05}	4.78x10^{-03}
AC093642.3	0.185	9.06x10^{-04}	0.151	1.00x10^{-02}	0.163	4.25x10^{-05}	4.78x10^{-03}
IFT46	-0.118	2.07x10^{-03}	-0.097	1.45x10^{-02}	-0.109	4.20x10^{-05}	4.78x10^{-03}
RP11-480C16.1	0.227	1.47x10^{-02}	0.271	4.09x10^{-03}	0.268	4.23x10^{-05}	4.78x10^{-03}
SF3B1	-0.156	4.15x10^{-04}	-0.087	3.71x10^{-02}	-0.122	4.17x10^{-05}	4.78x10^{-03}

THAP5	-0.130	7.89x10^{-03}	-0.139	1.41x10^{-03}	-0.132	4.27x10^{-05}	4.78x10^{-03}
TMED4	-0.105	1.41x10^{-03}	-0.080	1.14x10^{-02}	-0.090	4.24x10^{-05}	4.78x10^{-03}
AC096921.2	0.209	4.32x10^{-03}	0.217	6.85x10^{-03}	0.217	4.30x10^{-05}	4.78x10^{-03}
CHPF	0.399	3.59x10^{-03}	0.358	8.21x10^{-03}	0.385	4.39x10^{-05}	4.85x10^{-03}
SNW1	-0.094	1.97x10^{-03}	-0.085	1.57x10^{-02}	-0.091	4.53x10^{-05}	4.93x10^{-03}
TNFSF4	-0.327	5.38x10^{-03}	-0.382	4.67x10^{-03}	-0.360	4.52x10^{-05}	4.93x10^{-03}
RP3-442L6.4	0.235	1.71x10^{-03}	0.179	1.27x10^{-02}	0.208	4.77x10^{-05}	5.11x10^{-03}
CREBRF	-0.142	8.80x10^{-04}	-0.109	1.76x10^{-02}	-0.123	5.05x10^{-05}	5.35x10^{-03}
PPP2R2D	-0.100	2.26x10^{-03}	-0.101	4.47x10^{-03}	-0.096	5.04x10^{-05}	5.35x10^{-03}
RYK	-0.117	1.31x10^{-03}	-0.088	3.07x10^{-02}	-0.107	5.33x10^{-05}	5.52x10^{-03}
GPRASP1	-0.243	2.80x10^{-03}	-0.198	1.56x10^{-02}	-0.226	5.36x10^{-05}	5.52x10^{-03}
ZNF790	-0.166	1.75x10^{-03}	-0.130	2.30x10^{-02}	-0.155	5.39x10^{-05}	5.52x10^{-03}
RP11-43D4.3	0.215	3.28x10^{-03}	0.263	6.00x10^{-04}	0.216	5.45x10^{-05}	5.54x10^{-03}
SESN1	-0.205	5.87x10^{-04}	-0.205	1.05x10^{-02}	-0.196	5.51x10^{-05}	5.58x10^{-03}
OPA1	-0.323	7.13x10^{-04}	-0.299	3.19x10^{-03}	-0.282	5.67x10^{-05}	5.64x10^{-03}
ARHGAP5	-0.187	1.67x10^{-03}	-0.176	4.46x10^{-03}	-0.169	5.88x10^{-05}	5.67x10^{-03}
ARRDC3	-0.219	2.49x10^{-03}	-0.192	9.89x10^{-03}	-0.205	5.89x10^{-05}	5.67x10^{-03}
CLTC	0.141	2.18x10^{-03}	0.126	7.59x10^{-03}	0.131	5.91x10^{-05}	5.67x10^{-03}
GOLGA2	-0.109	1.48x10^{-02}	-0.141	2.75x10^{-03}	-0.128	5.88x10^{-05}	5.67x10^{-03}
RP11-107E5.3	0.161	2.93x10^{-02}	0.275	7.84x10^{-04}	0.217	5.95x10^{-05}	5.67x10^{-03}
RP11-264L1.2	0.148	2.76x10^{-02}	0.262	5.66x10^{-04}	0.199	5.74x10^{-05}	5.67x10^{-03}
ATP5S	-0.193	2.14x10^{-02}	-0.345	5.92x10^{-04}	-0.262	6.12x10^{-05}	5.73x10^{-03}
CCND3	-0.190	2.27x10^{-03}	-0.215	4.83x10^{-03}	-0.190	6.23x10^{-05}	5.73x10^{-03}
HACD4	-0.185	1.47x10^{-03}	-0.150	8.10x10^{-03}	-0.159	6.07x10^{-05}	5.73x10^{-03}
MEFV	-0.213	9.71x10^{-04}	-0.199	9.28x10^{-03}	-0.199	6.27x10^{-05}	5.73x10^{-03}
NEK7	-0.115	5.44x10^{-03}	-0.122	4.35x10^{-03}	-0.115	6.20x10^{-05}	5.73x10^{-03}
TUBE1	-0.148	2.38x10^{-03}	-0.124	9.38x10^{-03}	-0.132	6.09x10^{-05}	5.73x10^{-03}
ZNF28	-0.140	8.64x10^{-03}	-0.162	3.11x10^{-03}	-0.150	6.29x10^{-05}	5.73x10^{-03}
ZNF506	-0.167	4.66x10^{-03}	-0.156	2.15x10^{-03}	-0.152	6.16x10^{-05}	5.73x10^{-03}
OR6Y1	0.176	3.18x10^{-03}	0.131	1.14x10^{-02}	0.156	6.37x10^{-05}	5.73x10^{-03}
TRIM65	-0.179	7.28x10^{-04}	-0.124	3.06x10^{-02}	-0.153	6.41x10^{-05}	5.73x10^{-03}
ZNF638	-0.102	3.59x10^{-03}	-0.114	2.66x10^{-03}	-0.100	6.46x10^{-05}	5.73x10^{-03}
ANKRD34A	-0.331	3.07x10^{-03}	-0.315	6.03x10^{-03}	-0.316	6.76x10^{-05}	5.79x10^{-03}
CSNK2A2	0.181	2.69x10^{-03}	0.175	6.52x10^{-03}	0.173	6.72x10^{-05}	5.79x10^{-03}
GPBP1	-0.125	1.17x10^{-03}	-0.109	1.46x10^{-02}	-0.113	6.77x10^{-05}	5.79x10^{-03}
OXNAD1	-0.153	9.99x10^{-03}	-0.196	2.61x10^{-03}	-0.174	6.65x10^{-05}	5.79x10^{-03}
ZNF845	-0.111	1.58x10^{-02}	-0.132	1.37x10^{-03}	-0.120	6.72x10^{-05}	5.79x10^{-03}
SENP7	-0.104	8.78x10^{-03}	-0.141	1.53x10^{-03}	-0.116	6.92x10^{-05}	5.86x10^{-03}
ALPK2	0.378	7.78x10^{-03}	0.426	2.46x10^{-03}	0.396	7.08x10^{-05}	5.92x10^{-03}
MBTD1	-0.091	1.11x10^{-02}	-0.101	1.76x10^{-03}	-0.092	7.13x10^{-05}	5.92x10^{-03}
SLC13A4	0.331	3.04x10^{-03}	0.333	1.58x10^{-03}	0.306	7.10x10^{-05}	5.92x10^{-03}
GOLGA4	-0.124	1.05x10^{-03}	-0.088	1.22x10^{-02}	-0.100	7.42x10^{-05}	6.04x10^{-03}
RP11-145P16.2	0.135	4.92x10^{-03}	0.153	3.56x10^{-03}	0.139	7.36x10^{-05}	6.04x10^{-03}
TOPORS	-0.148	6.65x10^{-03}	-0.161	3.70x10^{-03}	-0.151	7.47x10^{-05}	6.04x10^{-03}
ZNF841	-0.160	7.64x10^{-04}	-0.115	2.71x10^{-02}	-0.137	7.36x10^{-05}	6.04x10^{-03}
OR1A1	0.178	1.68x10^{-03}	0.131	8.25x10^{-03}	0.148	7.83x10^{-05}	6.24x10^{-03}

ZBTB14	-0.116	8.22x10^{-03}	-0.133	2.61x10^{-03}	-0.119	7.88x10^{-05}	6.26x10^{-03}
LA16c-60D12.1	0.173	1.40x10^{-03}	0.115	1.46x10^{-02}	0.138	8.10x10^{-05}	6.35x10^{-03}
ZNF417	-0.113	1.04x10^{-02}	-0.114	9.11x10^{-03}	-0.120	8.09x10^{-05}	6.35x10^{-03}
MIA3	-0.128	1.54x10^{-03}	-0.101	1.19x10^{-02}	-0.109	8.24x10^{-05}	6.37x10^{-03}
RANBP2	-0.136	1.62x10^{-03}	-0.100	1.65x10^{-02}	-0.115	8.22x10^{-05}	6.37x10^{-03}
KATNBL1	-0.213	9.76x10^{-04}	-0.216	8.53x10^{-03}	-0.203	8.44x10^{-05}	6.45x10^{-03}
TMEM154	-0.196	1.67x10^{-03}	-0.191	3.68x10^{-03}	-0.177	8.53x10^{-05}	6.48x10^{-03}
GLT8D1	-0.073	2.26x10^{-02}	-0.096	4.27x10^{-03}	-0.089	8.62x10^{-05}	6.52x10^{-03}
TXNDC11	0.199	2.98x10^{-03}	0.130	3.45x10^{-02}	0.177	8.69x10^{-05}	6.55x10^{-03}
CTB-47B11.3	0.244	5.98x10^{-03}	0.278	6.72x10^{-03}	0.258	8.78x10^{-05}	6.55x10^{-03}
OSBPL2	-0.116	7.79x10^{-03}	-0.124	1.04x10^{-02}	-0.124	8.80x10^{-05}	6.55x10^{-03}
SCARNA3	0.279	1.38x10^{-03}	0.199	3.12x10^{-02}	0.245	8.87x10^{-05}	6.58x10^{-03}
BBX	-0.128	8.13x10^{-04}	-0.074	4.49x10^{-02}	-0.100	8.96x10^{-05}	6.59x10^{-03}
SMAD5	-0.224	7.74x10^{-04}	-0.183	1.44x10^{-02}	-0.193	8.97x10^{-05}	6.59x10^{-03}
AC018890.6	0.334	2.34x10^{-04}	0.199	3.45x10^{-02}	0.251	9.05x10^{-05}	6.60x10^{-03}
FNTA	-0.093	2.03x10^{-03}	-0.058	3.09x10^{-02}	-0.076	9.09x10^{-05}	6.60x10^{-03}
ZBTB10	-0.171	5.85x10^{-03}	-0.177	6.74x10^{-03}	-0.173	9.08x10^{-05}	6.60x10^{-03}
APBB1	-0.181	6.49x10^{-03}	-0.184	1.09x10^{-02}	-0.186	9.29x10^{-05}	6.62x10^{-03}
RP11-452H21.2	0.383	2.64x10^{-03}	0.299	2.32x10^{-02}	0.352	9.36x10^{-05}	6.62x10^{-03}
STAU2	-0.111	1.52x10^{-03}	-0.084	2.26x10^{-02}	-0.096	9.23x10^{-05}	6.62x10^{-03}
TRIP10	-0.204	2.48x10^{-02}	-0.302	2.36x10^{-03}	-0.257	9.30x10^{-05}	6.62x10^{-03}
TTF1	-0.097	7.86x10^{-03}	-0.094	6.51x10^{-03}	-0.095	9.37x10^{-05}	6.62x10^{-03}
UBE2D3	-0.111	1.02x10^{-02}	-0.139	3.82x10^{-03}	-0.123	9.29x10^{-05}	6.62x10^{-03}
DOCK11	-0.144	7.51x10^{-04}	-0.089	4.65x10^{-02}	-0.117	9.57x10^{-05}	6.74x10^{-03}
NPIPB4	0.267	1.54x10^{-03}	0.216	7.04x10^{-03}	0.222	9.83x10^{-05}	6.80x10^{-03}
POTEI	0.304	1.38x10^{-03}	0.179	3.69x10^{-02}	0.246	9.83x10^{-05}	6.80x10^{-03}
RP11-438E5.1	-0.251	6.10x10^{-03}	-0.236	1.33x10^{-02}	-0.250	9.92x10^{-05}	6.80x10^{-03}
AF131215.4	0.272	1.13x10^{-02}	0.345	4.64x10^{-03}	0.303	1.03x10^{-04}	6.80x10^{-03}
C3orf17	-0.103	3.42x10^{-03}	-0.083	2.67x10^{-02}	-0.097	1.02x10^{-04}	6.80x10^{-03}
CTD-2006C1.2	-0.118	1.39x10^{-02}	-0.163	2.55x10^{-03}	-0.137	1.03x10^{-04}	6.80x10^{-03}
DNPH1	0.209	2.10x10^{-03}	0.164	2.12x10^{-02}	0.188	1.01x10^{-04}	6.80x10^{-03}
GPR15	0.853	6.45x10^{-03}	0.877	1.31x10^{-02}	0.904	1.05x10^{-04}	6.80x10^{-03}
LEMD3	-0.105	1.98x10^{-03}	-0.077	3.03x10^{-02}	-0.092	1.04x10^{-04}	6.80x10^{-03}
ZNF304	-0.152	9.29x10^{-03}	-0.157	4.75x10^{-03}	-0.153	1.05x10^{-04}	6.80x10^{-03}
DDB1	-0.133	1.63x10^{-03}	-0.116	1.46x10^{-02}	-0.121	1.07x10^{-04}	6.86x10^{-03}
EPC2	-0.103	6.26x10^{-03}	-0.095	8.31x10^{-03}	-0.098	1.07x10^{-04}	6.86x10^{-03}
TPR	-0.092	1.26x10^{-02}	-0.097	4.22x10^{-03}	-0.094	1.10x10^{-04}	6.93x10^{-03}
ZNF426	-0.131	4.89x10^{-03}	-0.098	1.76x10^{-02}	-0.118	1.10x10^{-04}	6.93x10^{-03}
RP11-64P12.3	0.265	8.81x10^{-03}	0.311	1.05x10^{-03}	0.263	1.14x10^{-04}	7.03x10^{-03}
RP11-689D3.4	0.258	3.59x10^{-03}	0.197	2.69x10^{-02}	0.238	1.14x10^{-04}	7.03x10^{-03}
TJP1	0.171	2.57x10^{-02}	0.247	1.07x10^{-03}	0.202	1.13x10^{-04}	7.03x10^{-03}
ZNF132	-0.318	5.98x10^{-04}	-0.140	4.43x10^{-02}	-0.222	1.13x10^{-04}	7.03x10^{-03}
RP11-701H24.6	-0.198	9.25x10^{-03}	-0.168	1.31x10^{-02}	-0.192	1.15x10^{-04}	7.03x10^{-03}
ZBTB8B	0.142	1.65x10^{-02}	0.179	2.17x10^{-03}	0.156	1.15x10^{-04}	7.03x10^{-03}
RP11-510H23.1	0.162	8.63x10^{-03}	0.144	1.44x10^{-02}	0.164	1.18x10^{-04}	7.18x10^{-03}
SLC25A16	-0.142	2.99x10^{-03}	-0.099	3.39x10^{-02}	-0.126	1.19x10^{-04}	7.20x10^{-03}

FBXL4	-0.095	1.97x10^{-02}	-0.144	1.33x10^{-03}	-0.115	1.19x10^{-04}	7.20x10^{-03}
MPV17L	0.200	6.86x10^{-03}	0.206	8.04x10^{-03}	0.202	1.25x10^{-04}	7.36x10^{-03}
TCP1	-0.106	6.25x10^{-03}	-0.090	1.36x10^{-02}	-0.099	1.26x10^{-04}	7.36x10^{-03}
ZNF485	-0.210	1.32x10^{-03}	-0.165	8.85x10^{-03}	-0.172	1.30x10^{-04}	7.53x10^{-03}
TMEM65	-0.083	1.22x10^{-02}	-0.098	3.73x10^{-03}	-0.089	1.32x10^{-04}	7.57x10^{-03}
TNPO1	-0.119	3.47x10^{-03}	-0.106	1.44x10^{-02}	-0.109	1.34x10^{-04}	7.60x10^{-03}
ZDHHC6	-0.111	1.31x10^{-03}	-0.066	4.78x10^{-02}	-0.090	1.33x10^{-04}	7.60x10^{-03}
PARP8	-0.133	8.13x10^{-04}	-0.090	4.20x10^{-02}	-0.110	1.35x10^{-04}	7.63x10^{-03}
LRCH1	0.126	7.86x10^{-03}	0.154	2.72x10^{-03}	0.131	1.36x10^{-04}	7.64x10^{-03}
TANK	-0.126	2.18x10^{-03}	-0.127	5.48x10^{-03}	-0.117	1.37x10^{-04}	7.64x10^{-03}
GPR37L1	0.233	4.79x10^{-03}	0.181	4.17x10^{-02}	0.223	1.38x10^{-04}	7.71x10^{-03}
RBPJ	-0.118	5.23x10^{-03}	-0.123	5.93x10^{-03}	-0.114	1.39x10^{-04}	7.72x10^{-03}
RP4-591N18.2	0.275	2.25x10^{-03}	0.191	2.74x10^{-02}	0.233	1.40x10^{-04}	7.72x10^{-03}
DEC1	0.159	5.20x10^{-03}	0.143	2.07x10^{-02}	0.156	1.42x10^{-04}	7.78x10^{-03}
SHOC2	-0.103	4.71x10^{-03}	-0.099	1.80x10^{-02}	-0.103	1.41x10^{-04}	7.78x10^{-03}
GATA3	0.401	7.96x10^{-04}	0.224	3.86x10^{-02}	0.299	1.44x10^{-04}	7.83x10^{-03}
ZNF548	-0.155	4.62x10^{-03}	-0.128	1.50x10^{-02}	-0.141	1.47x10^{-04}	7.91x10^{-03}
CTD-2246P4.1	0.168	1.61x10^{-02}	0.187	2.37x10^{-03}	0.173	1.47x10^{-04}	7.91x10^{-03}
C4BPB	0.193	7.06x10^{-03}	0.210	1.04x10^{-02}	0.200	1.50x10^{-04}	7.97x10^{-03}
PANK4	-0.124	8.45x10^{-03}	-0.113	2.06x10^{-02}	-0.124	1.53x10^{-04}	8.06x10^{-03}
CCNG1	-0.106	1.48x10^{-02}	-0.139	1.87x10^{-03}	-0.115	1.55x10^{-04}	8.09x10^{-03}
COG8	-0.103	9.78x10^{-03}	-0.119	8.31x10^{-03}	-0.111	1.55x10^{-04}	8.09x10^{-03}
RP4-751H13.6	-0.227	8.85x10^{-03}	-0.205	3.48x10^{-02}	-0.241	1.58x10^{-04}	8.18x10^{-03}
NUP107	-0.128	1.17x10^{-02}	-0.160	2.62x10^{-03}	-0.138	1.59x10^{-04}	8.22x10^{-03}
MBTPS2	0.123	3.29x10^{-03}	0.115	1.32x10^{-02}	0.117	1.61x10^{-04}	8.23x10^{-03}
RP11-486O12.2	0.143	8.48x10^{-03}	0.139	8.71x10^{-03}	0.139	1.60x10^{-04}	8.23x10^{-03}
MT-ND1	-0.104	6.30x10^{-03}	-0.090	2.74x10^{-02}	-0.102	1.63x10^{-04}	8.31x10^{-03}
PPP2R5E	0.139	1.42x10^{-02}	0.175	2.97x10^{-03}	0.151	1.66x10^{-04}	8.47x10^{-03}
ZNF587B	-0.097	1.16x10^{-02}	-0.116	7.09x10^{-03}	-0.106	1.68x10^{-04}	8.52x10^{-03}
NACC1	0.241	2.49x10^{-02}	0.320	6.08x10^{-04}	0.262	1.69x10^{-04}	8.55x10^{-03}
HLX	-0.215	1.30x10^{-02}	-0.301	2.59x10^{-03}	-0.242	1.73x10^{-04}	8.69x10^{-03}
INPP5A	-0.170	6.05x10^{-04}	-0.146	2.25x10^{-02}	-0.150	1.75x10^{-04}	8.71x10^{-03}
MIA2	-0.128	7.46x10^{-03}	-0.134	1.73x10^{-02}	-0.134	1.74x10^{-04}	8.71x10^{-03}
PEX1	-0.121	1.79x10^{-03}	-0.091	2.85x10^{-02}	-0.105	1.75x10^{-04}	8.71x10^{-03}
CEP85L	-0.111	4.14x10^{-03}	-0.086	2.96x10^{-02}	-0.101	1.76x10^{-04}	8.73x10^{-03}
TRMT11	-0.166	1.83x10^{-03}	-0.107	2.91x10^{-02}	-0.133	1.77x10^{-04}	8.75x10^{-03}
RP11-746L20.1	0.209	6.55x10^{-03}	0.216	5.03x10^{-03}	0.203	1.79x10^{-04}	8.83x10^{-03}
RP11-391L3.4	0.235	7.06x10^{-03}	0.276	3.58x10^{-03}	0.234	1.80x10^{-04}	8.83x10^{-03}
CWF19L2	-0.102	1.17x10^{-02}	-0.095	7.41x10^{-03}	-0.097	1.86x10^{-04}	8.97x10^{-03}
DIP2B	-0.173	1.55x10^{-03}	-0.124	2.88x10^{-02}	-0.143	1.86x10^{-04}	8.97x10^{-03}
ZNF235	-0.169	4.38x10^{-04}	-0.115	2.21x10^{-02}	-0.129	1.88x10^{-04}	9.02x10^{-03}
PGS1	-0.174	4.13x10^{-03}	-0.153	2.88x10^{-02}	-0.167	1.97x10^{-04}	9.27x10^{-03}
RP4-778K6.2	0.322	4.58x10^{-03}	0.274	1.07x10^{-02}	0.287	2.01x10^{-04}	9.37x10^{-03}
ZNF329	-0.140	1.50x10^{-02}	-0.150	1.06x10^{-02}	-0.152	2.03x10^{-04}	9.41x10^{-03}
SDCCAG3	-0.176	9.11x10^{-04}	-0.102	3.54x10^{-02}	-0.132	2.19x10^{-04}	1.00x10^{-02}
DENND6A	-0.093	2.32x10^{-02}	-0.121	1.16x10^{-02}	-0.113	2.22x10^{-04}	1.01x10^{-02}

LINC00582	0.113	7.77x10^{-03}	0.115	1.01x10^{-02}	0.112	2.23x10^{-04}	1.01x10^{-02}
STAT5A	-0.128	5.37x10^{-03}	-0.109	3.89x10^{-02}	-0.126	2.23x10^{-04}	1.01x10^{-02}
CTD-2024I7.13	0.239	3.18x10^{-03}	0.215	2.34x10^{-02}	0.230	2.26x10^{-04}	1.01x10^{-02}
HAP1	0.376	8.46x10^{-03}	0.368	1.10x10^{-02}	0.368	2.26x10^{-04}	1.01x10^{-02}
MIGA1	-0.075	2.16x10^{-02}	-0.080	1.53x10^{-02}	-0.082	2.28x10^{-04}	1.02x10^{-02}
PVT1	0.257	5.43x10^{-03}	0.323	3.06x10^{-03}	0.258	2.38x10^{-04}	1.03x10^{-02}
ZNF254	-0.130	3.68x10^{-02}	-0.163	4.07x10^{-03}	-0.152	2.40x10^{-04}	1.03x10^{-02}
ETS2	-0.177	8.92x10^{-03}	-0.215	5.95x10^{-03}	-0.186	2.44x10^{-04}	1.04x10^{-02}
MLH3	-0.217	3.40x10^{-02}	-0.336	6.13x10^{-03}	-0.287	2.45x10^{-04}	1.04x10^{-02}
WAPL	-0.105	6.19x10^{-03}	-0.085	3.00x10^{-02}	-0.097	2.45x10^{-04}	1.04x10^{-02}
XPC	-0.124	1.20x10^{-02}	-0.111	9.64x10^{-03}	-0.117	2.44x10^{-04}	1.04x10^{-02}
ANGEL2	-0.090	3.98x10^{-03}	-0.060	4.06x10^{-02}	-0.076	2.47x10^{-04}	1.04x10^{-02}
LL22NC03-79E2.1	0.212	3.76x10^{-03}	0.195	1.55x10^{-02}	0.195	2.56x10^{-04}	1.07x10^{-02}
RP11-241K18.1	0.468	1.69x10^{-02}	0.452	1.87x10^{-02}	0.489	2.57x10^{-04}	1.07x10^{-02}
SYNJ2BP	-0.132	2.67x10^{-03}	-0.096	3.85x10^{-02}	-0.114	2.59x10^{-04}	1.07x10^{-02}
ENPP6	0.257	1.05x10^{-02}	0.242	1.46x10^{-02}	0.253	2.61x10^{-04}	1.08x10^{-02}
ACAA2	0.167	5.25x10^{-03}	0.121	4.06x10^{-02}	0.150	2.64x10^{-04}	1.08x10^{-02}
PARG	-0.117	3.56x10^{-03}	-0.096	2.92x10^{-02}	-0.105	2.64x10^{-04}	1.08x10^{-02}
ZNF322	-0.151	1.58x10^{-03}	-0.114	2.50x10^{-02}	-0.124	2.63x10^{-04}	1.08x10^{-02}
ZNF418	-0.418	1.91x10^{-03}	-0.302	1.10x10^{-02}	-0.327	2.63x10^{-04}	1.08x10^{-02}
ZNF354B	-0.157	4.97x10^{-03}	-0.152	1.07x10^{-02}	-0.146	2.70x10^{-04}	1.10x10^{-02}
CH507-513H4.1	0.292	1.18x10^{-02}	0.258	4.60x10^{-03}	0.280	2.72x10^{-04}	1.10x10^{-02}
SIRT1	-0.096	1.57x10^{-02}	-0.102	6.07x10^{-03}	-0.096	2.73x10^{-04}	1.10x10^{-02}
TMEM68	-0.114	5.69x10^{-03}	-0.098	4.81x10^{-03}	-0.096	2.75x10^{-04}	1.10x10^{-02}
ZNF549	-0.105	1.49x10^{-02}	-0.096	1.80x10^{-02}	-0.105	2.74x10^{-04}	1.10x10^{-02}
ARGFXP2	0.266	9.02x10^{-03}	0.222	1.16x10^{-02}	0.238	2.82x10^{-04}	1.13x10^{-02}
RN7SL517P	0.227	3.34x10^{-03}	0.211	1.06x10^{-02}	0.201	2.82x10^{-04}	1.13x10^{-02}
MEPCE	-0.116	4.17x10^{-02}	-0.181	1.53x10^{-03}	-0.144	2.85x10^{-04}	1.14x10^{-02}
ZNF720	-0.171	2.51x10^{-03}	-0.115	4.06x10^{-02}	-0.142	2.86x10^{-04}	1.14x10^{-02}
AMN1	-0.127	2.36x10^{-03}	-0.086	3.06x10^{-02}	-0.103	2.92x10^{-04}	1.15x10^{-02}
CYP2R1	-0.133	1.28x10^{-03}	-0.093	4.89x10^{-02}	-0.110	2.94x10^{-04}	1.16x10^{-02}
MED13	-0.106	1.00x10^{-02}	-0.138	4.51x10^{-03}	-0.113	2.95x10^{-04}	1.16x10^{-02}
GNL3L	-0.152	3.04x10^{-03}	-0.114	2.84x10^{-02}	-0.130	2.99x10^{-04}	1.17x10^{-02}
RP11-165F24.3	0.136	3.00x10^{-02}	0.165	2.68x10^{-03}	0.150	3.03x10^{-04}	1.18x10^{-02}
AP000240.6	0.179	1.21x10^{-02}	0.198	1.09x10^{-02}	0.186	3.08x10^{-04}	1.19x10^{-02}
RP11-267M23.1	-0.263	7.49x10^{-03}	-0.194	4.12x10^{-02}	-0.240	3.07x10^{-04}	1.19x10^{-02}
RP11-472I20.4	-0.181	7.43x10^{-03}	-0.163	3.03x10^{-02}	-0.176	3.06x10^{-04}	1.19x10^{-02}
RP11-61L19.1	0.233	6.57x10^{-03}	0.295	7.98x10^{-03}	0.250	3.09x10^{-04}	1.19x10^{-02}
RP11-659P15.1	0.183	3.35x10^{-02}	0.217	9.96x10^{-03}	0.210	3.09x10^{-04}	1.19x10^{-02}
GGTA1P	-0.383	3.01x10^{-03}	-0.384	1.09x10^{-02}	-0.355	3.11x10^{-04}	1.19x10^{-02}
SOCS7	-0.161	8.42x10^{-03}	-0.159	9.27x10^{-03}	-0.153	3.15x10^{-04}	1.20x10^{-02}
HELLPAR	0.105	9.95x10^{-03}	0.090	1.10x10^{-02}	0.096	3.18x10^{-04}	1.21x10^{-02}
GRAP2	-0.179	8.68x10^{-03}	-0.177	1.52x10^{-02}	-0.176	3.20x10^{-04}	1.21x10^{-02}
ZNF816	-0.096	2.45x10^{-02}	-0.106	1.11x10^{-02}	-0.106	3.19x10^{-04}	1.21x10^{-02}
DDX47	-0.080	1.86x10^{-02}	-0.088	1.42x10^{-02}	-0.087	3.26x10^{-04}	1.22x10^{-02}
CSNK2A1	-0.100	1.62x10^{-03}	-0.073	2.63x10^{-02}	-0.079	3.29x10^{-04}	1.23x10^{-02}

B4GAT1	-0.163	7.22x10^{-03}	-0.158	1.62x10^{-02}	-0.157	3.36x10^{-04}	1.23x10^{-02}
EZH1	-0.148	1.37x10^{-03}	-0.102	4.44x10^{-02}	-0.121	3.33x10^{-04}	1.23x10^{-02}
INTS10	-0.094	1.45x10^{-02}	-0.068	1.71x10^{-02}	-0.083	3.34x10^{-04}	1.23x10^{-02}
RC3H2	-0.095	6.45x10^{-03}	-0.094	1.26x10^{-02}	-0.088	3.34x10^{-04}	1.23x10^{-02}
VPS39	0.071	4.08x10^{-02}	0.122	1.42x10^{-03}	0.092	3.32x10^{-04}	1.23x10^{-02}
ZNF829	-0.141	4.68x10^{-03}	-0.099	4.55x10^{-02}	-0.123	3.39x10^{-04}	1.24x10^{-02}
ZNF606	-0.116	2.02x10^{-02}	-0.137	1.16x10^{-02}	-0.129	3.42x10^{-04}	1.24x10^{-02}
ZNF320	-0.156	4.06x10^{-02}	-0.187	1.07x10^{-02}	-0.188	3.46x10^{-04}	1.25x10^{-02}
RP11-887P2.5	0.219	1.61x10^{-02}	0.264	7.63x10^{-03}	0.237	3.53x10^{-04}	1.26x10^{-02}
VPS37A	-0.129	3.36x10^{-03}	-0.103	1.72x10^{-02}	-0.107	3.53x10^{-04}	1.26x10^{-02}
RP11-138A9.1	0.180	8.63x10^{-03}	0.168	1.46x10^{-02}	0.173	3.58x10^{-04}	1.27x10^{-02}
SP3	-0.092	9.52x10^{-03}	-0.088	2.03x10^{-02}	-0.089	3.57x10^{-04}	1.27x10^{-02}
FAM129A	-0.184	1.84x10^{-02}	-0.211	6.26x10^{-03}	-0.193	3.64x10^{-04}	1.28x10^{-02}
RP1-102G20.3	0.180	7.13x10^{-03}	0.151	9.51x10^{-03}	0.155	3.66x10^{-04}	1.28x10^{-02}
RP11-34F20.4	0.234	1.49x10^{-02}	0.249	8.42x10^{-03}	0.232	3.66x10^{-04}	1.28x10^{-02}
DCAF7	0.135	1.53x10^{-02}	0.162	2.92x10^{-03}	0.137	3.79x10^{-04}	1.29x10^{-02}
KRIT1	-0.093	1.08x10^{-02}	-0.098	7.17x10^{-03}	-0.090	3.80x10^{-04}	1.29x10^{-02}
MTERF1	-0.303	1.83x10^{-02}	-0.336	1.59x10^{-02}	-0.332	3.80x10^{-04}	1.29x10^{-02}
ZNF233	0.157	1.62x10^{-02}	0.193	5.33x10^{-03}	0.166	3.75x10^{-04}	1.29x10^{-02}
ZNF430	-0.107	2.22x10^{-02}	-0.116	8.01x10^{-03}	-0.111	3.76x10^{-04}	1.29x10^{-02}
OLMALINC	0.138	5.12x10^{-03}	0.108	1.72x10^{-02}	0.119	3.89x10^{-04}	1.31x10^{-02}
TECPR1	-0.133	1.21x10^{-02}	-0.135	2.82x10^{-02}	-0.139	3.92x10^{-04}	1.31x10^{-02}
MFAP3	-0.116	1.53x10^{-02}	-0.126	6.75x10^{-03}	-0.116	3.93x10^{-04}	1.31x10^{-02}
AVL9	-0.092	9.44x10^{-03}	-0.094	5.45x10^{-03}	-0.084	3.98x10^{-04}	1.32x10^{-02}
ABHD2	-0.162	2.00x10^{-02}	-0.183	2.52x10^{-02}	-0.185	4.00x10^{-04}	1.33x10^{-02}
AP1AR	-0.119	5.45x10^{-03}	-0.093	4.33x10^{-02}	-0.109	4.18x10^{-04}	1.36x10^{-02}
ENKUR	-0.309	1.11x10^{-02}	-0.315	3.90x10^{-02}	-0.336	4.23x10^{-04}	1.37x10^{-02}
HSPD1	-0.100	8.19x10^{-03}	-0.081	1.80x10^{-02}	-0.087	4.28x10^{-04}	1.38x10^{-02}
PPP1R2	-0.096	2.59x10^{-02}	-0.115	8.57x10^{-03}	-0.107	4.28x10^{-04}	1.38x10^{-02}
PPA2	-0.106	1.75x10^{-02}	-0.092	1.18x10^{-02}	-0.101	4.31x10^{-04}	1.39x10^{-02}
CDA	0.371	2.79x10^{-03}	0.240	4.05x10^{-02}	0.297	4.36x10^{-04}	1.39x10^{-02}
DICER1	-0.114	6.50x10^{-03}	-0.122	1.32x10^{-02}	-0.110	4.36x10^{-04}	1.39x10^{-02}
PTPN14	0.212	1.29x10^{-02}	0.248	1.16x10^{-02}	0.223	4.35x10^{-04}	1.39x10^{-02}
L3MBTL3	-0.105	2.36x10^{-02}	-0.119	1.87x10^{-02}	-0.118	4.40x10^{-04}	1.39x10^{-02}
CSE1L	-0.131	5.38x10^{-03}	-0.123	7.03x10^{-03}	-0.114	4.42x10^{-04}	1.39x10^{-02}
UBE4A	-0.161	2.84x10^{-03}	-0.101	3.49x10^{-02}	-0.124	4.49x10^{-04}	1.41x10^{-02}
RP11-182I10.3	0.154	3.52x10^{-02}	0.195	7.83x10^{-03}	0.179	4.61x10^{-04}	1.44x10^{-02}
NRG1	0.439	3.47x10^{-02}	0.588	5.82x10^{-03}	0.508	4.67x10^{-04}	1.44x10^{-02}
PABPC1	0.242	3.62x10^{-03}	0.241	7.39x10^{-03}	0.220	4.66x10^{-04}	1.44x10^{-02}
UFM1	-0.124	1.97x10^{-03}	-0.075	4.93x10^{-02}	-0.096	4.64x10^{-04}	1.44x10^{-02}
ZNF765	-0.111	8.55x10^{-03}	-0.100	1.80x10^{-02}	-0.102	4.68x10^{-04}	1.44x10^{-02}
LINC-PINT	0.125	2.02x10^{-02}	0.157	4.12x10^{-03}	0.133	4.72x10^{-04}	1.45x10^{-02}
VPS37B	0.140	1.29x10^{-02}	0.166	3.99x10^{-03}	0.140	4.87x10^{-04}	1.49x10^{-02}
ATXN1	0.087	4.21x10^{-02}	0.118	1.46x10^{-02}	0.110	4.94x10^{-04}	1.49x10^{-02}
HSF2	-0.123	2.04x10^{-02}	-0.133	1.77x10^{-02}	-0.131	5.01x10^{-04}	1.50x10^{-02}
CTC-429P9.3	-0.111	2.33x10^{-02}	-0.103	3.12x10^{-02}	-0.116	5.08x10^{-04}	1.52x10^{-02}

TMEM41B	-0.108	3.51x10^{-02}	-0.120	1.48x10^{-02}	-0.121	5.09x10^{-04}	1.52x10^{-02}
OR7E94P	-0.195	4.22x10^{-02}	-0.278	1.37x10^{-02}	-0.255	5.12x10^{-04}	1.52x10^{-02}
RP11-484O2.1	0.125	1.45x10^{-02}	0.128	7.32x10^{-03}	0.121	5.12x10^{-04}	1.52x10^{-02}
PREP	0.174	6.59x10^{-03}	0.155	2.95x10^{-02}	0.162	5.24x10^{-04}	1.53x10^{-02}
ZNF525	-0.185	1.03x10^{-02}	-0.178	2.09x10^{-02}	-0.179	5.24x10^{-04}	1.53x10^{-02}
BEND2	-0.325	1.26x10^{-02}	-0.374	1.37x10^{-02}	-0.344	5.32x10^{-04}	1.54x10^{-02}
RP11-163O17.1	-0.165	3.65x10^{-03}	-0.106	3.89x10^{-02}	-0.130	5.33x10^{-04}	1.54x10^{-02}
ORC4	-0.116	1.35x10^{-02}	-0.127	2.22x10^{-02}	-0.124	5.36x10^{-04}	1.54x10^{-02}
ZNF585A	-0.147	2.37x10^{-02}	-0.160	1.90x10^{-02}	-0.159	5.37x10^{-04}	1.54x10^{-02}
CAMKMT	-0.178	8.80x10^{-03}	-0.139	3.08x10^{-02}	-0.159	5.66x10^{-04}	1.59x10^{-02}
RP11-10E18.7	0.224	1.13x10^{-02}	0.165	3.30x10^{-02}	0.200	5.67x10^{-04}	1.59x10^{-02}
PTTG2	0.194	2.91x10^{-02}	0.281	6.53x10^{-03}	0.231	5.86x10^{-04}	1.63x10^{-02}
ZNF91	-0.288	3.24x10^{-03}	-0.208	4.98x10^{-02}	-0.244	5.86x10^{-04}	1.63x10^{-02}
RSBN1L	-0.099	1.17x10^{-02}	-0.103	2.08x10^{-02}	-0.098	5.92x10^{-04}	1.64x10^{-02}
CEP350	-0.085	1.81x10^{-02}	-0.103	9.53x10^{-03}	-0.089	6.03x10^{-04}	1.66x10^{-02}
RP5-1022P6.3	0.225	2.04x10^{-02}	0.234	9.55x10^{-03}	0.226	6.12x10^{-04}	1.68x10^{-02}
ATP10B	0.190	2.01x10^{-02}	0.194	5.17x10^{-03}	0.184	6.19x10^{-04}	1.70x10^{-02}
ZFP36L2	0.231	3.40x10^{-03}	0.201	1.59x10^{-02}	0.194	6.22x10^{-04}	1.70x10^{-02}
CARNMT1	-0.113	3.87x10^{-02}	-0.165	1.58x10^{-02}	-0.145	6.29x10^{-04}	1.71x10^{-02}
CEP290	-0.160	2.36x10^{-03}	-0.111	4.31x10^{-02}	-0.127	6.26x10^{-04}	1.71x10^{-02}
TMEM220	-0.178	1.36x10^{-02}	-0.157	2.87x10^{-02}	-0.169	6.29x10^{-04}	1.71x10^{-02}
MINPP1	-0.223	1.19x10^{-02}	-0.253	1.10x10^{-02}	-0.225	6.36x10^{-04}	1.71x10^{-02}
ATF2	-0.108	1.60x10^{-03}	-0.081	3.26x10^{-02}	-0.085	6.45x10^{-04}	1.73x10^{-02}
CRLF3	-0.092	2.78x10^{-02}	-0.110	1.85x10^{-02}	-0.104	6.48x10^{-04}	1.73x10^{-02}
UPF2	-0.091	1.81x10^{-02}	-0.091	1.58x10^{-02}	-0.089	6.47x10^{-04}	1.73x10^{-02}
CASD1	-0.096	2.68x10^{-02}	-0.111	5.28x10^{-03}	-0.097	6.73x10^{-04}	1.78x10^{-02}
ZNF121	-0.133	6.60x10^{-03}	-0.099	3.60x10^{-02}	-0.113	6.83x10^{-04}	1.80x10^{-02}
GADL1	0.116	2.33x10^{-02}	0.106	2.53x10^{-02}	0.116	6.89x10^{-04}	1.81x10^{-02}
C7orf60	-0.151	8.46x10^{-03}	-0.127	2.42x10^{-02}	-0.133	7.21x10^{-04}	1.87x10^{-02}
GTF2H1	-0.091	1.15x10^{-02}	-0.076	1.24x10^{-02}	-0.078	7.23x10^{-04}	1.87x10^{-02}
CTD-2192J16.20	0.249	7.65x10^{-03}	0.212	9.51x10^{-03}	0.208	7.35x10^{-04}	1.89x10^{-02}
USP8	-0.093	3.01x10^{-03}	-0.062	3.88x10^{-02}	-0.071	7.40x10^{-04}	1.90x10^{-02}
OR1I1	0.127	2.88x10^{-02}	0.162	1.36x10^{-02}	0.144	7.49x10^{-04}	1.91x10^{-02}
TRUB1	-0.088	3.15x10^{-02}	-0.104	1.15x10^{-02}	-0.096	7.51x10^{-04}	1.92x10^{-02}
RP11-78J21.6	0.269	1.25x10^{-02}	0.271	1.45x10^{-02}	0.257	7.53x10^{-04}	1.92x10^{-02}
STK38L	-0.114	1.40x10^{-02}	-0.101	2.63x10^{-02}	-0.108	7.83x10^{-04}	1.95x10^{-02}
PPWD1	-0.108	3.03x10^{-02}	-0.159	1.17x10^{-02}	-0.131	7.95x10^{-04}	1.97x10^{-02}
ARHGAP1	0.163	1.66x10^{-02}	0.205	5.06x10^{-03}	0.164	8.00x10^{-04}	1.98x10^{-02}
NGLY1	-0.070	2.70x10^{-02}	-0.073	5.19x10^{-03}	-0.067	8.04x10^{-04}	1.98x10^{-02}
CHP1	0.211	2.43x10^{-03}	0.155	2.96x10^{-02}	0.169	8.19x10^{-04}	2.00x10^{-02}
RP11-651P23.6	0.216	2.17x10^{-02}	0.246	2.70x10^{-02}	0.240	8.19x10^{-04}	2.00x10^{-02}
ZNF268	-0.109	1.47x10^{-02}	-0.096	3.83x10^{-02}	-0.104	8.20x10^{-04}	2.00x10^{-02}
RP4-534N18.4	0.271	3.64x10^{-02}	0.339	1.27x10^{-02}	0.307	8.36x10^{-04}	2.01x10^{-02}
CEP295	-0.123	4.98x10^{-03}	-0.111	8.15x10^{-03}	-0.101	8.57x10^{-04}	2.03x10^{-02}
ZNF880	-0.143	8.64x10^{-03}	-0.113	4.17x10^{-02}	-0.126	8.80x10^{-04}	2.06x10^{-02}
RNF26	0.303	3.69x10^{-03}	0.276	1.87x10^{-02}	0.259	9.00x10^{-04}	2.09x10^{-02}

WFDC1	0.207	1.02x10^{-02}	0.181	4.42x10^{-02}	0.201	9.00x10^{-04}	2.09x10^{-02}
ZNF30	-0.208	7.95x10^{-03}	-0.176	3.65x10^{-02}	-0.186	9.03x10^{-04}	2.09x10^{-02}
RP11-930O11.2	-0.235	2.02x10^{-02}	-0.302	1.31x10^{-02}	-0.256	9.23x10^{-04}	2.11x10^{-02}
CRNDE	0.220	1.83x10^{-02}	0.221	1.70x10^{-02}	0.213	9.32x10^{-04}	2.12x10^{-02}
MBD1	-0.104	1.88x10^{-02}	-0.100	4.09x10^{-02}	-0.105	9.48x10^{-04}	2.13x10^{-02}
RIOX2	-0.113	1.00x10^{-02}	-0.101	2.67x10^{-02}	-0.101	9.77x10^{-04}	2.18x10^{-02}
ZCCHC7	-0.170	1.24x10^{-02}	-0.151	4.02x10^{-02}	-0.163	9.80x10^{-04}	2.18x10^{-02}
CCAR1	-0.138	3.53x10^{-03}	-0.103	4.35x10^{-02}	-0.112	9.88x10^{-04}	2.19x10^{-02}
ZNF649	-0.107	1.18x10^{-02}	-0.112	1.85x10^{-02}	-0.102	1.01x10^{-03}	2.22x10^{-02}
SLC38A1	-0.143	1.42x10^{-02}	-0.107	3.60x10^{-02}	-0.124	1.03x10^{-03}	2.25x10^{-02}
TTC17	-0.090	1.64x10^{-02}	-0.090	1.02x10^{-02}	-0.081	1.04x10^{-03}	2.27x10^{-02}
CEPT1	-0.073	3.27x10^{-02}	-0.089	1.08x10^{-02}	-0.078	1.07x10^{-03}	2.31x10^{-02}
TYW3	-0.094	3.81x10^{-02}	-0.094	1.59x10^{-02}	-0.096	1.08x10^{-03}	2.31x10^{-02}
RIMKLB	-0.127	2.16x10^{-02}	-0.160	1.38x10^{-02}	-0.137	1.08x10^{-03}	2.32x10^{-02}
SNRK	-0.107	1.71x10^{-02}	-0.093	4.82x10^{-02}	-0.102	1.15x10^{-03}	2.41x10^{-02}
NF2	0.148	1.46x10^{-02}	0.162	6.97x10^{-03}	0.136	1.16x10^{-03}	2.42x10^{-02}
RP11-346D14.1	0.124	1.99x10^{-02}	0.124	1.00x10^{-02}	0.116	1.19x10^{-03}	2.46x10^{-02}
ZBTB41	-0.113	1.62x10^{-02}	-0.100	3.13x10^{-02}	-0.105	1.19x10^{-03}	2.46x10^{-02}
PSME3	0.131	9.70x10^{-03}	0.113	2.46x10^{-02}	0.114	1.20x10^{-03}	2.47x10^{-02}
BET1	-0.104	2.40x10^{-02}	-0.110	1.98x10^{-02}	-0.104	1.25x10^{-03}	2.53x10^{-02}
EXOSC10	-0.093	1.91x10^{-02}	-0.096	2.42x10^{-02}	-0.092	1.25x10^{-03}	2.53x10^{-02}
ZNF737	-0.169	4.64x10^{-02}	-0.203	4.01x10^{-03}	-0.175	1.24x10^{-03}	2.53x10^{-02}
LIN52	-0.164	4.12x10^{-03}	-0.144	1.96x10^{-02}	-0.139	1.26x10^{-03}	2.53x10^{-02}
FAM213A	-0.205	1.76x10^{-02}	-0.194	3.07x10^{-02}	-0.195	1.32x10^{-03}	2.58x10^{-02}
NDUFV3	-0.174	8.11x10^{-03}	-0.153	1.26x10^{-02}	-0.143	1.38x10^{-03}	2.66x10^{-02}
NCK2	-0.121	2.35x10^{-02}	-0.153	1.80x10^{-02}	-0.130	1.44x10^{-03}	2.72x10^{-02}
ZNF131	-0.128	4.10x10^{-03}	-0.112	4.37x10^{-02}	-0.110	1.48x10^{-03}	2.77x10^{-02}
AC010127.3	0.221	3.94x10^{-02}	0.216	2.21x10^{-02}	0.221	1.51x10^{-03}	2.80x10^{-02}
ZNF264	-0.106	4.86x10^{-02}	-0.106	3.91x10^{-02}	-0.115	1.51x10^{-03}	2.80x10^{-02}
BRAP	-0.093	2.98x10^{-02}	-0.121	1.37x10^{-02}	-0.101	1.52x10^{-03}	2.80x10^{-02}
HIP1R	-0.167	3.33x10^{-02}	-0.149	3.53x10^{-02}	-0.163	1.55x10^{-03}	2.82x10^{-02}
RP5-968D22.3	0.162	2.21x10^{-02}	0.189	3.05x10^{-02}	0.171	1.55x10^{-03}	2.82x10^{-02}
CTC-340A15.2	0.187	1.49x10^{-02}	0.181	1.17x10^{-02}	0.165	1.56x10^{-03}	2.84x10^{-02}
PPIG	-0.096	2.98x10^{-02}	-0.100	1.51x10^{-02}	-0.093	1.58x10^{-03}	2.86x10^{-02}
PEX13	-0.071	3.11x10^{-02}	-0.069	4.99x10^{-02}	-0.075	1.60x10^{-03}	2.87x10^{-02}
PIGU	-0.162	5.62x10^{-03}	-0.140	3.51x10^{-02}	-0.136	1.62x10^{-03}	2.89x10^{-02}
CPT1A	0.217	2.66x10^{-02}	0.201	4.24x10^{-02}	0.213	1.67x10^{-03}	2.94x10^{-02}
MAP4	0.152	3.38x10^{-02}	0.205	1.18x10^{-02}	0.167	1.67x10^{-03}	2.94x10^{-02}
MMP28	-0.375	2.51x10^{-02}	-0.472	1.48x10^{-02}	-0.393	1.67x10^{-03}	2.94x10^{-02}
GPAM	-0.119	1.69x10^{-02}	-0.104	3.41x10^{-02}	-0.108	1.70x10^{-03}	2.96x10^{-02}
NEMF	-0.120	1.07x10^{-02}	-0.112	2.89x10^{-02}	-0.108	1.70x10^{-03}	2.97x10^{-02}
RP11-15H20.6	-0.105	4.88x10^{-02}	-0.120	4.50x10^{-02}	-0.123	1.72x10^{-03}	2.98x10^{-02}
ZNF382	-0.195	1.61x10^{-02}	-0.154	4.01x10^{-02}	-0.168	1.73x10^{-03}	3.00x10^{-02}
ZNF257	-0.418	2.45x10^{-02}	-0.419	3.12x10^{-02}	-0.421	1.74x10^{-03}	3.01x10^{-02}
TSR1	-0.116	1.79x10^{-02}	-0.087	4.44x10^{-02}	-0.100	1.76x10^{-03}	3.03x10^{-02}
DGCR11	0.131	3.84x10^{-02}	0.141	2.93x10^{-02}	0.140	1.77x10^{-03}	3.04x10^{-02}

RP11-701H24.5	-0.220	2.50x10^{-02}	-0.208	4.67x10^{-02}	-0.219	1.77x10^{-03}	3.04x10^{-02}
MARK2	0.144	1.91x10^{-02}	0.138	3.84x10^{-02}	0.139	1.79x10^{-03}	3.05x10^{-02}
ZNF589	-0.114	2.34x10^{-02}	-0.103	4.93x10^{-02}	-0.110	1.79x10^{-03}	3.05x10^{-02}
TRABD2A	-0.189	3.85x10^{-02}	-0.190	2.21x10^{-02}	-0.190	1.91x10^{-03}	3.17x10^{-02}
HDAC6	-0.092	2.96x10^{-02}	-0.092	3.12x10^{-02}	-0.090	1.93x10^{-03}	3.18x10^{-02}
CCDC18	-0.187	1.70x10^{-02}	-0.206	1.89x10^{-02}	-0.179	1.99x10^{-03}	3.24x10^{-02}
RP11-574K11.28	0.121	2.47x10^{-02}	0.129	4.63x10^{-02}	0.124	2.02x10^{-03}	3.28x10^{-02}
TSHZ3	0.248	2.22x10^{-02}	0.263	1.97x10^{-02}	0.235	2.04x10^{-03}	3.30x10^{-02}
SASH1	0.454	2.20x10^{-02}	0.440	3.43x10^{-02}	0.434	2.06x10^{-03}	3.32x10^{-02}
MAP2K4	-0.101	2.94x10^{-02}	-0.096	4.14x10^{-02}	-0.100	2.07x10^{-03}	3.33x10^{-02}
GIN1	-0.091	3.03x10^{-02}	-0.095	4.17x10^{-02}	-0.093	2.12x10^{-03}	3.37x10^{-02}
C22orf39	-0.086	2.99x10^{-02}	-0.085	4.47x10^{-02}	-0.086	2.15x10^{-03}	3.39x10^{-02}
TMX2	-0.103	5.64x10^{-03}	-0.091	3.05x10^{-02}	-0.084	2.15x10^{-03}	3.39x10^{-02}
ZNF273	-0.113	1.80x10^{-02}	-0.136	1.26x10^{-02}	-0.108	2.23x10^{-03}	3.48x10^{-02}
PCBP1	0.188	8.58x10^{-03}	0.164	2.90x10^{-02}	0.154	2.42x10^{-03}	3.61x10^{-02}
FAM20C	0.329	1.83x10^{-02}	0.300	3.59x10^{-02}	0.306	2.46x10^{-03}	3.66x10^{-02}
NDC1	-0.155	7.19x10^{-03}	-0.140	3.94x10^{-02}	-0.132	2.48x10^{-03}	3.67x10^{-02}
RP11-523H20.5	0.107	4.41x10^{-02}	0.109	3.19x10^{-02}	0.110	2.49x10^{-03}	3.68x10^{-02}
EPHX2	-0.113	2.44x10^{-02}	-0.127	4.92x10^{-02}	-0.123	2.52x10^{-03}	3.70x10^{-02}
CTPS2	-0.100	4.02x10^{-02}	-0.106	1.92x10^{-02}	-0.098	2.52x10^{-03}	3.70x10^{-02}
RP11-815J21.3	0.183	3.39x10^{-02}	0.201	4.03x10^{-02}	0.191	2.53x10^{-03}	3.72x10^{-02}
ZNF577	-0.219	3.55x10^{-02}	-0.248	3.99x10^{-02}	-0.235	2.56x10^{-03}	3.73x10^{-02}
CNOT7	-0.104	1.91x10^{-02}	-0.088	3.69x10^{-02}	-0.089	2.63x10^{-03}	3.77x10^{-02}
IL6ST	-0.145	3.37x10^{-02}	-0.169	2.43x10^{-02}	-0.148	2.68x10^{-03}	3.80x10^{-02}
NOM1	-0.113	2.21x10^{-02}	-0.105	3.27x10^{-02}	-0.102	2.72x10^{-03}	3.83x10^{-02}
GGNBP2	-0.074	2.60x10^{-02}	-0.061	4.59x10^{-02}	-0.066	2.76x10^{-03}	3.87x10^{-02}
WRN	-0.110	4.43x10^{-02}	-0.165	9.49x10^{-03}	-0.124	2.78x10^{-03}	3.89x10^{-02}
SMIM8	-0.100	4.17x10^{-02}	-0.114	2.98x10^{-02}	-0.104	2.84x10^{-03}	3.93x10^{-02}
AC007743.1	0.186	1.08x10^{-02}	0.135	4.16x10^{-02}	0.147	2.86x10^{-03}	3.94x10^{-02}
FSTL1	-0.450	1.56x10^{-02}	-0.501	3.14x10^{-02}	-0.428	3.09x10^{-03}	4.13x10^{-02}
RP11-391L3.3	0.174	4.79x10^{-02}	0.194	1.64x10^{-02}	0.174	3.29x10^{-03}	4.29x10^{-02}
ZNF350	-0.089	3.52x10^{-02}	-0.101	4.31x10^{-02}	-0.094	3.37x10^{-03}	4.34x10^{-02}
FAM132B	0.662	2.31x10^{-02}	0.656	3.01x10^{-02}	0.610	3.43x10^{-03}	4.38x10^{-02}
MFF	-0.100	1.63x10^{-02}	-0.077	4.44x10^{-02}	-0.080	3.46x10^{-03}	4.39x10^{-02}
NDUFB10	0.072	4.71x10^{-02}	0.092	3.28x10^{-02}	0.079	3.50x10^{-03}	4.41x10^{-02}
MALT1	-0.080	3.97x10^{-02}	-0.073	4.36x10^{-02}	-0.075	3.51x10^{-03}	4.41x10^{-02}
SLAIN2	-0.216	5.68x10^{-03}	-0.144	3.90x10^{-02}	-0.151	3.74x10^{-03}	4.56x10^{-02}
TAF6L	-0.134	2.10x10^{-02}	-0.128	4.70x10^{-02}	-0.123	3.80x10^{-03}	4.59x10^{-02}
PLCG1	-0.157	3.30x10^{-02}	-0.124	4.71x10^{-02}	-0.136	3.80x10^{-03}	4.59x10^{-02}
SRSF8	-0.126	2.70x10^{-02}	-0.126	4.82x10^{-02}	-0.122	3.96x10^{-03}	4.70x10^{-02}
DNAJC2	-0.112	1.12x10^{-02}	-0.089	4.84x10^{-02}	-0.089	4.18x10^{-03}	4.85x10^{-02}
FBLN2	-0.356	3.08x10^{-02}	-0.368	3.60x10^{-02}	-0.346	4.41x10^{-03}	5.00x10^{-02}
PAPD4	-0.079	1.96x10^{-02}	-0.068	4.15x10^{-02}	-0.066	4.51x10^{-03}	5.05x10^{-02}
TXK	-0.157	3.86x10^{-02}	-0.171	3.34x10^{-02}	-0.156	4.62x10^{-03}	5.12x10^{-02}
ZGRF1	-0.171	6.06x10^{-03}	-0.139	3.40x10^{-02}	-0.127	4.69x10^{-03}	5.15x10^{-02}
RP11-326C3.2	-0.257	1.98x10^{-02}	-0.256	3.75x10^{-02}	-0.227	4.98x10^{-03}	5.32x10^{-02}

ZNF528	-0.133	4.50x10^{-02}	-0.173	1.49x10^{-02}	-0.135	5.01x10^{-03}	5.34x10^{-02}
TRPC1	-0.206	3.00x10^{-02}	-0.217	4.64x10^{-02}	-0.199	5.06x10^{-03}	5.36x10^{-02}
CYTIP	-0.086	3.14x10^{-02}	-0.092	4.27x10^{-02}	-0.082	5.23x10^{-03}	5.46x10^{-02}
ALG10	-0.133	1.29x10^{-02}	-0.128	3.02x10^{-02}	-0.110	5.28x10^{-03}	5.49x10^{-02}
DLG1	-0.104	3.49x10^{-02}	-0.098	4.05x10^{-02}	-0.093	5.65x10^{-03}	5.71x10^{-02}
RP11-362F19.2	0.251	3.72x10^{-02}	0.260	3.98x10^{-02}	0.237	5.78x10^{-03}	5.75x10^{-02}
FAN1	-0.103	3.50x10^{-02}	-0.108	3.74x10^{-02}	-0.096	6.21x10^{-03}	5.94x10^{-02}
RP11-540A21.3	-0.175	3.62x10^{-02}	-0.219	4.12x10^{-02}	-0.181	6.70x10^{-03}	6.19x10^{-02}
EIF4G1	0.127	3.54x10^{-02}	0.165	2.15x10^{-02}	0.128	7.68x10^{-03}	6.70x10^{-02}

Supplementary Table 1: Top dysregulated RNAs in whole blood PAH RNAseq. List of 507 differentially expressed, overlapping and directionally consistent genes in differential expression analysis in the RNA Discovery and RNA Validation groups. $N_{controls}$= 24 per group; N_{PAH}= 120 per group. Genes listed by significance (weakest FDR first).

	PAH Cohort		PAH Meta-analysis			IPAH Meta-analysis	
Genes	**logFC AB**	**Sig. AB**	**log2(FC)**	**Sig.**	**FDR**	**log2(FC)**	**Sig.**
Same direction, significant, meeting FDR in both meta-analyses							
DDX17	-0.117	4.30x10^{-7}	-0.590	2.00x10^{-3}	2.30x10^{-2}	-0.817	2.00x10^{-3}
RASA2	-0.135	4.60x10^{-7}	-0.861	5.00x10^{-4}	8.00x10^{-3}	-0.597	5.00x10^{-4}
ATM	-0.131	3.40x10^{-6}	-0.767	7.00x10^{-8}	9.00x10^{-6}	-0.831	5.00x10^{-6}
UHRF2	-0.141	3.70x10^{-6}	-0.493	6.00x10^{-4}	1.00x10^{-2}	-0.586	2.00x10^{-3}
ITGA6	-0.204	9.50x10^{-6}	-1.137	1.00x10^{-4}	3.00x10^{-3}	-0.874	2.00x10^{-3}
OXNAD1	-0.183	1.00x10^{-5}	-1.118	9.00x10^{-7}	7.00x10^{-5}	-1.099	2.00x10^{-8}
ATG12	-0.118	1.00x10^{-5}	-0.634	7.00x10^{-4}	1.10x10^{-2}	-0.690	1.00x10^{-4}
SESN1	-0.205	2.00x10^{-5}	-1.194	7.00x10^{-5}	2.00x10^{-3}	-1.212	7.00x10^{-4}
ZNF160	-0.113	3.30x10^{-5}	-0.806	6.00x10^{-8}	8.00x10^{-6}	-0.717	1.00x10^{-4}
KLHL28	-0.105	3.50x10^{-5}	-0.501	3.00x10^{-3}	3.20x10^{-2}	-0.592	1.00x10^{-3}
GPRASP1	-0.230	3.70x10^{-5}	-0.952	4.00x10^{-4}	7.00x10^{-3}	-0.688	1.00x10^{-4}
ZNF506	-0.155	4.50x10^{-5}	-0.953	1.00x10^{-4}	2.00x10^{-3}	-1.200	9.00x10^{-6}
PEX1	-0.108	5.40x10^{-5}	-0.940	1.00x10^{-6}	9.00x10^{-5}	-0.915	2.00x10^{-7}
BBX	-0.102	5.90x10^{-5}	-1.115	2.00x10^{-5}	6.00x10^{-4}	-1.205	2.00x10^{-5}
PPP1R2	-0.104	5.90x10^{-5}	-0.822	3.00x10^{-5}	1.00x10^{-3}	-1.013	1.00x10^{-8}
TRMT11	-0.137	7.30x10^{-5}	-0.906	2.00x10^{-10}	8.00x10^{-8}	-0.934	3.00x10^{-7}
ZNF329	-0.152	1.40x10^{-4}	-1.047	6.00x10^{-12}	6.00x10^{-9}	-0.990	3.00x10^{-7}
HSF2	-0.137	1.90x10^{-4}	-1.207	2.00x10^{-6}	1.00x10^{-4}	-0.950	3.00x10^{-4}
CEP85L	-0.100	2.00x10^{-4}	-1.107	5.00x10^{-12}	5.00x10^{-9}	-1.100	1.00x10^{-7}
MIGA1	-0.081	2.20x10^{-4}	-0.430	3.00x10^{-3}	2.90x10^{-2}	-0.592	2.00x10^{-3}
ZNF549	-0.104	3.00x10^{-4}	-0.500	3.00x10^{-3}	3.30x10^{-2}	-0.578	2.00x10^{-3}
SYNJ2BP	-0.110	3.10x10^{-4}	-0.736	1.00x10^{-3}	1.40x10^{-2}	-0.820	6.00x10^{-4}
FAM213A	-0.206	3.30x10^{-4}	-0.769	2.00x10^{-7}	2.00x10^{-5}	-0.705	2.00x10^{-4}
UFM1	-0.099	3.30x10^{-4}	-0.502	2.00x10^{-4}	4.00x10^{-3}	-0.508	3.00x10^{-3}
L3MBTL3	-0.118	4.00x10^{-4}	-0.731	6.00x10^{-7}	5.00x10^{-5}	-0.816	3.00x10^{-4}
ATF2	-0.085	5.10x10^{-4}	-0.816	9.00x10^{-4}	1.30x10^{-2}	-1.297	2.00x10^{-4}
ZCCHC7	-0.164	5.20x10^{-4}	-0.888	2.00x10^{-3}	2.20x10^{-2}	-0.730	1.00x10^{-4}
SLC38A1	-0.125	9.40x10^{-4}	-1.299	2.00x10^{-5}	6.00x10^{-4}	-1.116	4.00x10^{-6}
PLCG1	-0.145	1.17x10^{-3}	-0.804	1.00x10^{-8}	2.00x10^{-6}	-0.826	2.00x10^{-6}
EPHX2	-0.127	1.65x10^{-3}	-0.874	8.00x10^{-10}	2.00x10^{-7}	-0.883	1.00x10^{-6}
IL6ST	-0.148	1.76x10^{-3}	-0.951	5.00x10^{-6}	3.00x10^{-4}	-1.013	3.00x10^{-7}
TSR1	-0.100	1.92x10^{-3}	-0.499	3.00x10^{-4}	6.00x10^{-3}	-0.579	1.00x10^{-3}
TXK	-0.159	3.51x10^{-3}	-0.636	3.00x10^{-5}	9.00x10^{-4}	-0.619	3.00x10^{-4}
MALT1	-0.074	4.18x10^{-3}	-0.662	2.00x10^{-5}	6.00x10^{-4}	-0.852	4.00x10^{-4}
Same direction, significant, meeting FDR in PAH meta-analysis							
PTAR1	-0.168	1.30x10^{-8}	-0.743	5.00x10^{-4}	8.00x10^{-3}	-0.713	1.03x10^{-1}
RBM27	-0.137	1.30x10^{-7}	-0.736	5.00x10^{-4}	9.00x10^{-3}	-0.589	4.80x10^{-2}
ZNF211	-0.166	1.70x10^{-7}	-0.438	1.00x10^{-3}	1.50x10^{-2}	-0.506	3.00x10^{-3}
UBR1	-0.119	4.50x10^{-7}	-0.399	5.00x10^{-3}	4.70x10^{-2}	-0.364	7.60x10^{-2}
CCNB1IP1	-0.150	5.60x10^{-7}	-0.715	4.00x10^{-5}	1.00x10^{-3}	-0.334	2.95x10^{-1}
AMD1	-0.160	2.00x10^{-6}	-0.614	1.00x10^{-5}	5.00x10^{-4}	-0.266	4.66x10^{-1}

ARHGAP12	-0.149	2.10x10^{-6}	-0.708	2.00x10^{-3}	2.30x10^{-2}	-0.657	3.30x10^{-2}
BCLAF1	-0.127	2.20x10^{-6}	-0.927	5.00x10^{-6}	2.00x10^{-4}	-0.706	3.20x10^{-2}
ZNF33A	-0.122	6.50x10^{-6}	-0.459	5.00x10^{-3}	4.60x10^{-2}	-0.594	4.80x10^{-2}
CEP120	-0.126	7.10x10^{-6}	-0.695	6.00x10^{-4}	1.00x10^{-2}	-0.627	1.90x10^{-2}
EIF4A2	-0.141	7.60x10^{-6}	-0.825	5.00x10^{-4}	8.00x10^{-3}	-0.698	1.10x10^{-2}
NR1D2	-0.150	9.80x10^{-6}	-0.870	9.00x10^{-5}	2.00x10^{-3}	-0.844	4.00x10^{-3}
C12orf45	-0.177	1.00x10^{-5}	-0.497	5.00x10^{-3}	4.40x10^{-2}	-0.224	3.89x10^{-1}
TUBE1	-0.136	1.70x10^{-5}	-0.409	4.00x10^{-3}	4.00x10^{-2}	-0.496	8.00x10^{-3}
CREBRF	-0.116	3.20x10^{-5}	-0.551	3.00x10^{-4}	6.00x10^{-3}	-0.338	8.30x10^{-2}
ZBTB14	-0.119	7.10x10^{-5}	-0.662	1.00x10^{-3}	1.40x10^{-2}	-0.604	8.00x10^{-3}
DENND6A	-0.114	1.90x10^{-4}	-0.613	1.00x10^{-3}	1.50x10^{-2}	-0.596	2.70x10^{-2}
CSE1L	-0.115	3.10x10^{-4}	-0.505	2.00x10^{-4}	3.00x10^{-3}	-0.490	4.00x10^{-3}
CDA	0.291	3.40x10^{-4}	0.721	1.00x10^{-3}	1.80x10^{-2}	0.320	5.70x10^{-2}
SNRK	-0.099	4.00x10^{-4}	-0.884	5.00x10^{-5}	1.00x10^{-3}	-0.724	3.20x10^{-2}
ZNF525	-0.181	4.40x10^{-4}	-0.499	1.00x10^{-3}	1.60x10^{-2}	-0.705	1.70x10^{-2}
CASD1	-0.097	5.60x10^{-4}	-0.427	2.00x10^{-3}	2.30x10^{-2}	-0.372	3.40x10^{-2}
ZNF121	-0.113	6.90x10^{-4}	-0.398	6.00x10^{-3}	4.80x10^{-2}	-0.281	1.26x10^{-1}
HIP1R	-0.170	9.10x10^{-4}	-0.745	1.00x10^{-4}	3.00x10^{-3}	-0.391	1.06x10^{-1}
ZNF589	-0.112	1.25x10^{-3}	-0.476	1.00x10^{-3}	1.50x10^{-2}	-0.490	1.00x10^{-2}
FAM20C	0.309	1.79x10^{-3}	0.700	1.00x10^{-3}	1.80x10^{-2}	0.679	6.20x10^{-2}
SASH1	0.437	1.98x10^{-3}	0.564	3.00x10^{-3}	3.30x10^{-2}	0.446	1.20x10^{-2}
CNOT7	-0.089	2.16x10^{-3}	-0.734	2.00x10^{-3}	2.20x10^{-2}	-0.302	2.72x10^{-1}
CYTIP	-0.080	2.85x10^{-3}	-0.474	5.00x10^{-3}	4.70x10^{-2}	-0.591	3.60x10^{-2}
FBLN2	-0.355	2.99x10^{-3}	-0.707	3.00x10^{-4}	6.00x10^{-3}	-0.493	5.00x10^{-3}
DLG1	-0.099	3.26x10^{-3}	-0.815	3.00x10^{-3}	2.80x10^{-2}	-0.600	1.00x10^{-2}
FAN1	-0.096	5.45x10^{-3}	-0.454	2.00x10^{-3}	2.10x10^{-2}	-0.504	5.70x10^{-2}
TRPC1	-0.197	5.71x10^{-3}	-0.691	8.00x10^{-4}	1.10x10^{-2}	-0.783	4.00x10^{-3}
Same direction and significant in PAH meta-analysis							
BTAF1	-0.160	5.70x10^{-08}	-0.350	1.10x10^{-02}	7.80x10^{-02}	-0.506	4.00x10^{-03}
RLIM	-0.129	3.10x10^{-07}	-0.491	3.80x10^{-02}	1.82x10^{-01}	-0.780	2.00x10^{-05}
ZFAND1	-0.157	5.30x10^{-07}	-0.766	2.10x10^{-02}	1.21x10^{-01}	-0.632	1.33x10^{-01}
ZNF24	-0.114	9.40x10^{-07}	-0.549	1.50x10^{-02}	9.50x10^{-02}	-0.510	9.60x10^{-02}
HECTD1	-0.106	1.10x10^{-06}	-0.342	2.70x10^{-02}	1.42x10^{-01}	-0.208	2.55x10^{-01}
STAG2	-0.112	2.50x10^{-06}	-0.669	1.90x10^{-02}	1.12x10^{-01}	-0.591	4.70x10^{-02}
PCF11	-0.121	3.00x10^{-06}	-0.591	2.70x10^{-02}	1.42x10^{-01}	-0.592	8.40x10^{-02}
RIF1	-0.120	3.50x10^{-06}	-0.337	1.10x10^{-02}	7.90x10^{-02}	-0.394	1.90x10^{-02}
ZC3H11A	-0.102	5.10x10^{-06}	-0.582	1.20x10^{-02}	8.50x10^{-02}	-0.724	1.70x10^{-02}
HELQ	-0.114	1.10x10^{-05}	-0.333	2.00x10^{-02}	1.18x10^{-01}	-0.502	8.40x10^{-02}
BACE1	0.255	1.20x10^{-05}	0.299	3.00x10^{-02}	1.53x10^{-01}	0.369	3.40x10^{-02}
TOPORS	-0.147	1.30x10^{-05}	-0.346	1.20x10^{-02}	8.30x10^{-02}	-0.405	1.15x10^{-01}
HOMER1	-0.277	1.60x10^{-05}	-0.481	3.10x10^{-02}	1.59x10^{-01}	-0.658	2.10x10^{-02}
TMED4	-0.087	1.90x10^{-05}	-0.389	1.00x10^{-02}	7.20x10^{-02}	-0.307	1.14x10^{-01}
SRSF10	-0.090	2.50x10^{-05}	-0.751	1.60x10^{-02}	1.03x10^{-01}	-0.620	1.28x10^{-01}
CRLF3	-0.102	2.60x10^{-05}	-0.690	3.90x10^{-02}	1.85x10^{-01}	-0.739	6.80x10^{-02}
RP4-751H13.6	-0.257	3.00x10^{-05}	-0.740	2.80x10^{-02}	1.47x10^{-01}	-0.512	1.35x10^{-01}
PPP2R2D	-0.097	3.10x10^{-05}	-0.452	2.80x10^{-02}	1.47x10^{-01}	-0.348	7.30x10^{-02}
SENP7	-0.120	3.30x10^{-05}	-0.593	8.00x10^{-03}	6.10x10^{-02}	-0.539	4.00x10^{-03}

ATP5S	-0.263	3.80x10^{-05}	-0.368	3.90x10^{-02}	1.85x10^{-01}	-0.480	1.70x10^{-02}
ACAA2	0.160	3.80x10^{-05}	0.366	6.00x10^{-03}	5.00x10^{-02}	0.152	3.60x10^{-01}
RYK	-0.109	4.00x10^{-05}	-0.450	1.50x10^{-02}	9.50x10^{-02}	-0.555	1.00x10^{-03}
SF3B1	-0.122	4.40x10^{-05}	-0.793	3.10x10^{-02}	1.57x10^{-01}	-1.050	9.00x10^{-04}
ARHGAP5	-0.165	5.50x10^{-05}	-0.524	1.30x10^{-02}	8.90x10^{-02}	-0.687	1.60x10^{-02}
APBB1	-0.190	5.90x10^{-05}	-0.659	1.50x10^{-02}	9.40x10^{-02}	-0.486	1.32x10^{-01}
MBTD1	-0.093	6.40x10^{-05}	-0.561	6.00x10^{-03}	5.10x10^{-02}	-0.634	1.80x10^{-02}
CEP290	-0.132	6.60x10^{-05}	-0.790	3.40x10^{-02}	1.67x10^{-01}	-0.537	2.15x10^{-01}
LEMD3	-0.090	9.00x10^{-05}	-0.694	2.40x10^{-02}	1.33x10^{-01}	-0.591	9.10x10^{-02}
PARP8	-0.111	1.40x10^{-04}	-0.425	4.00x10^{-02}	1.88x10^{-01}	-0.322	2.49x10^{-01}
SIRT1	-0.094	2.20x10^{-04}	-0.645	1.10x10^{-02}	8.00x10^{-02}	-0.690	9.00x10^{-03}
CYP2R1	-0.109	2.30x10^{-04}	-0.514	2.40x10^{-02}	1.34x10^{-01}	-0.299	8.80x10^{-02}
HSPD1	-0.088	2.40x10^{-04}	-0.485	4.10x10^{-02}	1.90x10^{-01}	-0.162	3.60x10^{-01}
TMEM41B	-0.119	2.40x10^{-04}	-0.434	1.60x10^{-02}	1.01x10^{-01}	-0.295	7.80x10^{-02}
ZNF430	-0.112	2.90x10^{-04}	-0.412	4.30x10^{-02}	1.95x10^{-01}	-0.536	3.00x10^{-03}
DDX47	-0.087	3.00x10^{-04}	-0.612	3.50x10^{-02}	1.71x10^{-01}	-0.198	6.47x10^{-01}
ZNF829	-0.122	3.70x10^{-04}	-0.593	1.50x10^{-02}	9.50x10^{-02}	-0.462	1.30x10^{-02}
PSME3	0.117	4.00x10^{-04}	0.366	6.00x10^{-03}	5.30x10^{-02}	0.303	1.29x10^{-01}
ZNF91	-0.247	4.50x10^{-04}	-0.631	1.50x10^{-02}	9.70x10^{-02}	-0.575	6.40x10^{-02}
NRG1	0.488	6.30x10^{-04}	0.392	2.00x10^{-02}	1.19x10^{-01}	-0.087	6.28x10^{-01}
WFDC1	0.205	6.30x10^{-04}	0.339	1.80x10^{-02}	1.08x10^{-01}	0.549	3.00x10^{-03}
CEP295	-0.102	8.10x10^{-04}	-0.471	1.50x10^{-02}	9.50x10^{-02}	-0.569	2.70x10^{-02}
ARHGAP1	0.163	8.80x10^{-04}	0.714	9.00x10^{-03}	6.70x10^{-02}	0.341	3.81x10^{-01}
ZNF131	-0.110	1.10x10^{-03}	-0.450	4.00x10^{-02}	1.87x10^{-01}	-0.409	1.10x10^{-01}
CPT1A	0.219	1.10x10^{-03}	0.478	3.20x10^{-02}	1.61x10^{-01}	0.064	7.80x10^{-01}
ZNF273	-0.114	1.11x10^{-03}	-0.495	4.50x10^{-02}	2.03x10^{-01}	-0.575	5.00x10^{-03}
TYW3	-0.096	1.13x10^{-03}	-0.353	1.40x10^{-02}	8.90x10^{-02}	-0.237	1.98x10^{-01}
ZNF264	-0.113	1.45x10^{-03}	-0.712	2.40x10^{-02}	1.33x10^{-01}	-0.787	3.90x10^{-02}
NDC1	-0.131	1.74x10^{-03}	-0.334	1.50x10^{-02}	9.80x10^{-02}	-0.255	1.48x10^{-01}
ZNF577	-0.232	1.78x10^{-03}	-0.445	1.50x10^{-02}	9.40x10^{-02}	-0.509	4.80x10^{-02}
TSHZ3	0.236	2.05x10^{-03}	0.389	4.90x10^{-02}	2.13x10^{-01}	0.033	8.92x10^{-01}
SLAIN2	-0.151	3.68x10^{-03}	-0.573	6.00x10^{-03}	5.30x10^{-02}	0.034	9.49x10^{-01}
Same direction in PAH meta-analysis							
SAMD8	-0.143	9.10x10^{-10}	-0.365	3.21x10^{-01}	6.37x10^{-01}	-0.644	1.62x10^{-01}
RSRC2	-0.144	2.70x10^{-09}	-0.284	2.33x10^{-01}	5.40x10^{-01}	-0.450	6.80x10^{-02}
SLC16A10	-0.381	5.00x10^{-08}	-0.335	2.87x10^{-01}	6.02x10^{-01}	-0.411	1.95x10^{-01}
TEX10	-0.116	5.10x10^{-08}	-0.292	9.00x10^{-02}	3.14x10^{-01}	-0.317	1.41x10^{-01}
HLTF	-0.186	6.70x10^{-08}	-0.571	1.24x10^{-01}	3.81x10^{-01}	-0.384	3.52x10^{-01}
RALA	0.181	2.70x10^{-07}	0.149	6.27x10^{-01}	8.52x10^{-01}	0.124	7.02x10^{-01}
SCFD2	-0.223	4.40x10^{-07}	-0.216	1.31x10^{-01}	3.92x10^{-01}	-0.138	4.51x10^{-01}
CHD9	-0.158	6.70x10^{-07}	-0.310	3.72x10^{-01}	6.84x10^{-01}	-0.347	4.94x10^{-01}
ZNF141	-0.132	7.80x10^{-07}	-0.292	1.33x10^{-01}	3.95x10^{-01}	-0.231	3.57x10^{-01}
RBM5	-0.101	8.50x10^{-07}	-0.216	3.03x10^{-01}	6.19x10^{-01}	-0.298	3.67x10^{-01}
ZNF397	-0.106	8.90x10^{-07}	-0.106	7.03x10^{-01}	8.92x10^{-01}	-0.293	4.50x10^{-01}
SEC23A	-0.101	1.30x10^{-06}	-0.228	4.45x10^{-01}	7.39x10^{-01}	-0.372	2.70x10^{-01}
KAT8	-0.123	1.30x10^{-06}	-0.414	1.25x10^{-01}	3.82x10^{-01}	-0.629	6.90x10^{-02}

ACAP2	-0.098	$1.70x10^{-06}$	-0.007	$9.82x10^{-01}$	$9.94x10^{-01}$	-0.366	$3.46x10^{-01}$
DENND4C	-0.132	$2.20x10^{-06}$	-0.298	$8.30x10^{-02}$	$2.98x10^{-01}$	-0.397	$6.10x10^{-02}$
PTPRC	-0.125	$2.40x10^{-06}$	-0.382	$1.22x10^{-01}$	$3.77x10^{-01}$	-0.690	$5.60x10^{-02}$
PTGR1	0.169	$4.20x10^{-06}$	0.146	$5.47x10^{-01}$	$8.07x10^{-01}$	0.275	$3.97x10^{-01}$
HIF1A	-0.170	$4.50x10^{-06}$	-0.161	$4.79x10^{-01}$	$7.62x10^{-01}$	-0.281	$3.28x10^{-01}$
ALG8	-0.111	$4.90x10^{-06}$	-0.336	$8.80x10^{-02}$	$3.09x10^{-01}$	-0.108	$5.37x10^{-01}$
SETX	-0.115	$5.10x10^{-06}$	-0.096	$6.75x10^{-01}$	$8.78x10^{-01}$	-0.325	$2.34x10^{-01}$
ZNF763	-0.251	$5.30x10^{-06}$	-0.142	$3.81x10^{-01}$	$6.92x10^{-01}$	-0.264	$1.52x10^{-01}$
ZNF627	-0.116	$5.80x10^{-06}$	-0.172	$2.27x10^{-01}$	$5.32x10^{-01}$	-0.087	$6.36x10^{-01}$
PRKD3	-0.158	$6.90x10^{-06}$	-0.259	$1.94x10^{-01}$	$4.89x10^{-01}$	-0.388	$3.60x10^{-02}$
ZMYM1	-0.154	$7.70x10^{-06}$	-0.129	$5.79x10^{-01}$	$8.25x10^{-01}$	-0.195	$4.66x10^{-01}$
TMTC3	-0.167	$7.70x10^{-06}$	-0.054	$8.76x10^{-01}$	$9.61x10^{-01}$	-0.439	$3.21x10^{-01}$
KDM1A	-0.098	$8.10x10^{-06}$	-0.225	$2.06x10^{-01}$	$5.05x10^{-01}$	-0.279	$3.43x10^{-01}$
NAA35	-0.102	$8.40x10^{-06}$	-0.147	$5.15x10^{-01}$	$7.87x10^{-01}$	-0.022	$9.19x10^{-01}$
KIAA1551	-0.148	$9.50x10^{-06}$	-0.294	$3.78x10^{-01}$	$6.89x10^{-01}$	-0.834	$1.68x10^{-01}$
DEF6	-0.111	$1.00x10^{-05}$	-0.137	$5.25x10^{-01}$	$7.94x10^{-01}$	-0.083	$6.52x10^{-01}$
ZNF283	-0.133	$1.10x10^{-05}$	-0.084	$5.76x10^{-01}$	$8.23x10^{-01}$	-0.131	$5.39x10^{-01}$
GPBP1	-0.112	$1.10x10^{-05}$	-0.412	$7.90x10^{-02}$	$2.89x10^{-01}$	-0.460	$1.99x10^{-01}$
PMS1	-0.141	$1.30x10^{-05}$	-0.439	$6.80x10^{-02}$	$2.63x10^{-01}$	-0.398	$1.70x10^{-01}$
SIKE1	-0.118	$1.30x10^{-05}$	-0.065	$8.20x10^{-01}$	$9.39x10^{-01}$	-0.408	$2.15x10^{-01}$
KLF10	0.280	$1.30x10^{-05}$	0.430	$2.15x10^{-01}$	$5.16x10^{-01}$	0.369	$3.57x10^{-01}$
ZNF680	-0.132	$1.50x10^{-05}$	-0.134	$6.13x10^{-01}$	$8.45x10^{-01}$	0.008	$9.83x10^{-01}$
MAP3K7CL	-0.482	$1.50x10^{-05}$	-0.134	$5.67x10^{-01}$	$8.19x10^{-01}$	-0.266	$1.49x10^{-01}$
RIC8B	-0.142	$1.60x10^{-05}$	-0.151	$4.88x10^{-01}$	$7.68x10^{-01}$	-0.139	$5.30x10^{-01}$
ZNF354B	-0.154	$2.00x10^{-05}$	-0.221	$2.68x10^{-01}$	$5.81x10^{-01}$	-0.257	$3.77x10^{-01}$
ARRDC3	-0.205	$2.20x10^{-05}$	-0.333	$2.22x10^{-01}$	$5.25x10^{-01}$	-0.058	$8.52x10^{-01}$
SNW1	-0.087	$2.30x10^{-05}$	-0.147	$2.66x10^{-01}$	$5.78x10^{-01}$	-0.222	$1.84x10^{-01}$
C12orf29	-0.246	$2.30x10^{-05}$	-0.702	$6.80x10^{-02}$	$2.64x10^{-01}$	-0.526	$2.07x10^{-01}$
DHX15	-0.105	$2.30x10^{-05}$	-0.153	$2.88x10^{-01}$	$6.03x10^{-01}$	-0.238	$1.96x10^{-01}$
NEK7	-0.113	$2.80x10^{-05}$	-0.030	$9.14x10^{-01}$	$9.75x10^{-01}$	-0.253	$4.98x10^{-01}$
CHPF	0.389	$3.10x10^{-05}$	0.112	$5.71x10^{-01}$	$8.21x10^{-01}$	0.213	$2.46x10^{-01}$
CLTC	0.134	$3.30x10^{-05}$	0.204	$3.21x10^{-01}$	$6.36x10^{-01}$	-0.159	$3.98x10^{-01}$
ZNF638	-0.103	$3.40x10^{-05}$	-0.440	$1.06x10^{-01}$	$3.47x10^{-01}$	-0.585	$1.80x10^{-02}$
TTF1	-0.091	$3.50x10^{-05}$	-0.061	$6.94x10^{-01}$	$8.88x10^{-01}$	-0.182	$3.42x10^{-01}$
FNTA	-0.076	$3.70x10^{-05}$	-0.278	$3.20x10^{-01}$	$6.36x10^{-01}$	-0.293	$1.68x10^{-01}$
STAU2	-0.095	$3.70x10^{-05}$	-0.233	$4.37x10^{-01}$	$7.34x10^{-01}$	-0.016	$9.57x10^{-01}$
SP3	-0.086	$3.70x10^{-05}$	-0.451	$3.04x10^{-01}$	$6.20x10^{-01}$	0.159	$7.47x10^{-01}$
TWF1	-0.117	$4.00x10^{-05}$	-0.007	$9.82x10^{-01}$	$9.94x10^{-01}$	0.165	$6.46x10^{-01}$
OR6Y1	0.155	$4.20x10^{-05}$	0.139	$5.30x10^{-01}$	$7.97x10^{-01}$	0.239	$6.03x10^{-01}$
ZNF876P	-0.427	$4.30x10^{-05}$	-0.437	$6.40x10^{-02}$	$2.56x10^{-01}$	-0.492	$3.10x10^{-02}$
IFT46	-0.108	$4.70x10^{-05}$	-0.003	$9.86x10^{-01}$	$9.95x10^{-01}$	0.139	$4.28x10^{-01}$
KATNBL1	-0.202	$4.70x10^{-05}$	-0.022	$9.30x10^{-01}$	$9.80x10^{-01}$	-0.144	$6.96x10^{-01}$
GOLGA4	-0.102	$4.80x10^{-05}$	-0.293	$3.07x10^{-01}$	$6.23x10^{-01}$	-0.173	$5.26x10^{-01}$
ZNF304	-0.155	$4.90x10^{-05}$	-0.221	$2.75x10^{-01}$	$5.88x10^{-01}$	-0.390	$1.56x10^{-01}$
OR1A1	0.147	$5.10x10^{-05}$	0.073	$6.05x10^{-01}$	$8.42x10^{-01}$	0.175	$3.39x10^{-01}$
ZNF845	-0.120	$5.20x10^{-05}$	-0.645	$8.70x10^{-02}$	$3.08x10^{-01}$	-0.636	$2.40x10^{-01}$

ZNF548	-0.146	5.20x10^{-05}	-0.788	6.40x10^{-02}	2.54x10^{-01}	-1.165	3.00x10^{-09}
DIP2B	-0.138	5.50x10^{-05}	-0.095	7.71x10^{-01}	9.20x10^{-01}	-0.504	1.10x10^{-02}
C3orf17	-0.099	6.30x10^{-05}	-0.500	1.08x10^{-01}	3.49x10^{-01}	-0.386	2.16x10^{-01}
ZNF841	-0.139	6.40x10^{-05}	-0.306	9.00x10^{-02}	3.14x10^{-01}	-0.466	2.84x10^{-01}
GPR15	0.930	6.40x10^{-05}	0.227	2.22x10^{-01}	5.26x10^{-01}	0.193	5.51x10^{-01}
NUP107	-0.145	6.50x10^{-05}	-0.263	2.81x10^{-01}	5.96x10^{-01}	0.000	9.98x10^{-01}
ZNF790	-0.153	6.60x10^{-05}	-0.046	8.19x10^{-01}	9.38x10^{-01}	-0.149	7.29x10^{-01}
DOCK11	-0.114	6.60x10^{-05}	-0.020	8.90x10^{-01}	9.67x10^{-01}	-0.076	6.76x10^{-01}
POTEI	0.249	6.60x10^{-05}	0.253	4.17x10^{-01}	7.19x10^{-01}	0.014	9.62x10^{-01}
ZNF426	-0.120	6.90x10^{-05}	-0.277	1.19x10^{-01}	3.72x10^{-01}	-0.364	3.80x10^{-02}
TNPO1	-0.111	7.20x10^{-05}	-0.363	1.99x10^{-01}	4.96x10^{-01}	-0.659	2.00x10^{-03}
ZNF417	-0.121	7.20x10^{-05}	-0.195	1.71x10^{-01}	4.58x10^{-01}	-0.237	1.97x10^{-01}
SLC13A4	0.302	7.30x10^{-05}	0.182	2.00x10^{-01}	4.97x10^{-01}	0.105	5.67x10^{-01}
ZBTB10	-0.174	7.30x10^{-05}	-0.407	3.70x10^{-01}	6.83x10^{-01}	-0.281	5.47x10^{-01}
WAPL	-0.096	7.30x10^{-05}	-0.380	1.73x10^{-01}	4.60x10^{-01}	-0.236	4.01x10^{-01}
TRIM65	-0.149	7.40x10^{-05}	-0.279	1.86x10^{-01}	4.79x10^{-01}	-0.246	3.65x10^{-01}
ZNF28	-0.147	8.40x10^{-05}	-0.309	3.62x10^{-01}	6.76x10^{-01}	-0.235	5.41x10^{-01}
CWF19L2	-0.102	9.30x10^{-05}	-0.375	2.93x10^{-01}	6.09x10^{-01}	-0.567	2.16x10^{-01}
RANBP2	-0.113	9.30x10^{-05}	-0.471	1.06x10^{-01}	3.45x10^{-01}	-0.519	7.50x10^{-02}
GLT8D1	-0.087	1.00x10^{-04}	-0.160	6.43x10^{-01}	8.60x10^{-01}	-0.032	9.39x10^{-01}
SLC25A16	-0.126	1.00x10^{-04}	-0.325	3.10x10^{-01}	6.26x10^{-01}	-0.355	3.93x10^{-01}
MIA3	-0.108	1.00x10^{-04}	-0.294	3.01x10^{-01}	6.17x10^{-01}	-0.740	6.60x10^{-02}
TCP1	-0.098	1.10x10^{-04}	-0.283	2.91x10^{-01}	6.07x10^{-01}	-0.610	6.00x10^{-02}
SMAD5	-0.187	1.10x10^{-04}	-0.230	4.52x10^{-01}	7.44x10^{-01}	-0.084	8.11x10^{-01}
ALPK2	0.387	1.10x10^{-04}	0.152	3.08x10^{-01}	6.24x10^{-01}	0.131	5.12x10^{-01}
TJP1	0.198	1.20x10^{-04}	0.009	9.65x10^{-01}	9.89x10^{-01}	0.327	1.92x10^{-01}
CCNG1	-0.114	1.20x10^{-04}	-0.374	1.33x10^{-01}	3.95x10^{-01}	-0.293	3.70x10^{-01}
GPR37L1	0.219	1.30x10^{-04}	0.305	9.70x10^{-02}	3.29x10^{-01}	0.427	2.10x10^{-02}
TPR	-0.092	1.40x10^{-04}	-0.268	3.05x10^{-01}	6.21x10^{-01}	-0.140	6.39x10^{-01}
MFAP3	-0.114	1.40x10^{-04}	-0.025	9.18x10^{-01}	9.76x10^{-01}	-0.118	6.87x10^{-01}
PANK4	-0.125	1.40x10^{-04}	-0.172	4.89x10^{-01}	7.69x10^{-01}	-0.097	6.75x10^{-01}
C4BPB	0.200	1.50x10^{-04}	0.146	3.08x10^{-01}	6.24x10^{-01}	0.002	9.92x10^{-01}
MTERF1	-0.101	1.70x10^{-04}	-0.228	9.70x10^{-02}	3.30x10^{-01}	-0.125	4.71x10^{-01}
EZH1	-0.126	1.80x10^{-04}	-0.142	5.24x10^{-01}	7.93x10^{-01}	-0.182	6.33x10^{-01}
ZDHHC6	-0.086	1.90x10^{-04}	-0.107	6.67x10^{-01}	8.73x10^{-01}	-0.441	8.20x10^{-02}
MLH3	-0.286	1.90x10^{-04}	-0.255	9.20x10^{-02}	3.19x10^{-01}	-0.266	1.12x10^{-01}
SDCCAG3	-0.133	2.10x10^{-04}	-0.289	6.10x10^{-02}	2.47x10^{-01}	-0.227	3.15x10^{-01}
ANGEL2	-0.075	2.10x10^{-04}	-0.575	1.02x10^{-01}	3.39x10^{-01}	-0.510	2.18x10^{-01}
COG8	-0.108	2.10x10^{-04}	-0.414	2.92x10^{-01}	6.07x10^{-01}	-0.164	6.70x10^{-01}
ZNF254	-0.152	2.10x10^{-04}	-0.336	3.72x10^{-01}	6.85x10^{-01}	-0.344	4.32x10^{-01}
AMN1	-0.100	2.20x10^{-04}	-0.177	2.14x10^{-01}	5.16x10^{-01}	-0.274	1.35x10^{-01}
MED13	-0.114	2.20x10^{-04}	-0.617	1.68x10^{-01}	4.53x10^{-01}	-0.872	2.30x10^{-02}
KRIT1	-0.093	2.20x10^{-04}	-0.448	2.78x10^{-01}	5.93x10^{-01}	-0.554	3.18x10^{-01}
CAMKMT	-0.168	2.30x10^{-04}	-0.340	2.18x10^{-01}	5.21x10^{-01}	-0.264	6.27x10^{-01}
MEPCE	-0.141	2.40x10^{-04}	-0.207	2.35x10^{-01}	5.42x10^{-01}	-0.029	8.68x10^{-01}
ZNF585A	-0.156	2.40x10^{-04}	-0.100	8.21x10^{-01}	9.40x10^{-01}	-0.024	9.67x10^{-01}

ZNF606	-0.132	2.60x10^{-04}	-0.029	9.13x10^{-01}	9.75x10^{-01}	-0.038	9.26x10^{-01}
UPF2	-0.087	2.60x10^{-04}	-0.278	1.57x10^{-01}	4.36x10^{-01}	-0.475	4.20x10^{-02}
PPA2	-0.097	2.80x10^{-04}	-0.078	7.80x10^{-01}	9.25x10^{-01}	-0.155	6.25x10^{-01}
VPS39	0.092	2.90x10^{-04}	0.217	2.15x10^{-01}	5.17x10^{-01}	-0.077	6.82x10^{-01}
XPC	-0.109	3.00x10^{-04}	-0.062	6.38x10^{-01}	8.58x10^{-01}	-0.174	2.96x10^{-01}
CSNK2A1	-0.079	3.00x10^{-04}	-0.138	5.36x10^{-01}	8.02x10^{-01}	-0.143	6.27x10^{-01}
INTS10	-0.084	3.10x10^{-04}	-0.366	5.50x10^{-02}	2.30x10^{-01}	-0.590	5.00x10^{-03}
B4GAT1	-0.153	3.10x10^{-04}	-0.417	5.90x10^{-02}	2.41x10^{-01}	-0.490	8.20x10^{-02}
MBD1	-0.109	3.10x10^{-04}	-0.140	6.48x10^{-01}	8.63x10^{-01}	-0.288	3.58x10^{-01}
ZNF320	-0.189	3.20x10^{-04}	-0.357	1.08x10^{-01}	3.49x10^{-01}	-0.393	2.48x10^{-01}
ZNF816	-0.106	3.30x10^{-04}	-0.239	7.05x10^{-01}	8.92x10^{-01}	-0.081	8.88x10^{-01}
ENPP6	0.244	3.30x10^{-04}	0.104	4.63x10^{-01}	7.52x10^{-01}	0.025	8.90x10^{-01}
DCAF7	0.138	3.40x10^{-04}	0.241	4.60x10^{-01}	7.50x10^{-01}	0.310	3.10x10^{-01}
GNL3L	-0.127	3.60x10^{-04}	-0.114	5.18x10^{-01}	7.90x10^{-01}	-0.020	9.07x10^{-01}
ZNF765	-0.103	3.60x10^{-04}	-0.150	5.10x10^{-01}	7.84x10^{-01}	-0.181	6.02x10^{-01}
CHP1	0.172	3.60x10^{-04}	0.468	6.50x10^{-02}	2.58x10^{-01}	0.171	4.55x10^{-01}
ATXN1	0.112	3.70x10^{-04}	0.021	9.28x10^{-01}	9.79x10^{-01}	-0.267	2.69x10^{-01}
PPWD1	-0.138	3.70x10^{-04}	-0.352	5.10x10^{-02}	2.19x10^{-01}	-0.227	1.75x10^{-01}
TECPR1	-0.136	3.90x10^{-04}	-0.385	9.30x10^{-02}	3.20x10^{-01}	-0.407	2.00x10^{-01}
RC3H2	-0.086	4.30x10^{-04}	-0.074	6.20x10^{-01}	8.49x10^{-01}	0.268	1.45x10^{-01}
C7orf60	-0.128	4.60x10^{-04}	-0.052	7.28x10^{-01}	9.03x10^{-01}	-0.146	4.27x10^{-01}
NDUFB10	0.086	4.70x10^{-04}	0.107	6.97x10^{-01}	8.89x10^{-01}	-0.256	1.88x10^{-01}
TMEM220	-0.173	4.80x10^{-04}	-0.244	2.69x10^{-01}	5.82x10^{-01}	-0.129	6.18x10^{-01}
NGLY1	-0.069	5.00x10^{-04}	-0.259	2.29x10^{-01}	5.34x10^{-01}	0.032	9.04x10^{-01}
CEP350	-0.089	5.00x10^{-04}	-0.408	1.09x10^{-01}	3.51x10^{-01}	-0.699	1.30x10^{-02}
ZNF880	-0.129	5.20x10^{-04}	-0.327	1.29x10^{-01}	3.89x10^{-01}	-0.518	8.00x10^{-03}
OR1I1	0.144	5.70x10^{-04}	0.090	5.50x10^{-01}	8.09x10^{-01}	0.001	9.96x10^{-01}
RIMKLB	-0.142	6.40x10^{-04}	-0.292	5.29x10^{-01}	7.96x10^{-01}	-0.765	1.35x10^{-01}
BRAP	-0.100	6.40x10^{-04}	-0.159	2.45x10^{-01}	5.55x10^{-01}	-0.112	5.17x10^{-01}
CCAR1	-0.116	6.40x10^{-04}	-0.167	5.28x10^{-01}	7.96x10^{-01}	-0.415	3.24x10^{-01}
ZNF30	-0.190	7.40x10^{-04}	-0.163	4.27x10^{-01}	7.26x10^{-01}	0.092	6.13x10^{-01}
ZNF649	-0.105	7.70x10^{-04}	-0.007	9.80x10^{-01}	9.93x10^{-01}	-0.086	8.21x10^{-01}
NEMF	-0.114	7.80x10^{-04}	-0.412	1.55x10^{-01}	4.32x10^{-01}	-0.379	2.92x10^{-01}
ZNF268	-0.104	8.10x10^{-04}	-0.214	4.15x10^{-01}	7.17x10^{-01}	-0.164	5.71x10^{-01}
EXOSC10	-0.092	8.70x10^{-04}	-0.167	3.25x10^{-01}	6.40x10^{-01}	-0.163	4.84x10^{-01}
MAP4	0.166	9.30x10^{-04}	0.111	6.96x10^{-01}	8.89x10^{-01}	0.028	9.33x10^{-01}
PIGU	-0.141	1.17x10^{-03}	-0.227	4.38x10^{-01}	7.35x10^{-01}	-0.111	7.39x10^{-01}
GIN1	-0.098	1.18x10^{-03}	-0.207	6.19x10^{-01}	8.49x10^{-01}	-0.391	4.63x10^{-01}
ZBTB41	-0.105	1.26x10^{-03}	-0.096	5.00x10^{-01}	7.76x10^{-01}	-0.140	4.44x10^{-01}
RIOX2	-0.098	1.37x10^{-03}	-0.466	3.48x10^{-01}	6.63x10^{-01}	-1.246	1.80x10^{-02}
NCK2	-0.123	1.39x10^{-03}	-0.339	7.60x10^{-02}	2.83x10^{-01}	-0.436	1.80x10^{-02}
WRN	-0.131	1.47x10^{-03}	-0.339	1.06x10^{-01}	3.46x10^{-01}	-0.289	2.94x10^{-01}
MARK2	0.141	1.51x10^{-03}	0.211	3.84x10^{-01}	6.94x10^{-01}	-0.225	2.78x10^{-01}
ZNF382	-0.168	1.63x10^{-03}	-0.264	2.50x10^{-01}	5.61x10^{-01}	-0.177	5.06x10^{-01}
PEX13	-0.074	1.63x10^{-03}	-0.308	2.13x10^{-01}	5.13x10^{-01}	-0.371	2.56x10^{-01}
PPIG	-0.090	1.64x10^{-03}	-0.544	1.24x10^{-01}	3.81x10^{-01}	-0.257	5.12x10^{-01}

TAF6L	-0.131	1.77x10^{-03}	-0.213	3.18x10^{-01}	6.33x10^{-01}	-0.023	9.35x10^{-01}
PCBP1	0.158	1.85x10^{-03}	0.151	2.69x10^{-01}	5.82x10^{-01}	0.007	9.68x10^{-01}
SMIM8	-0.108	2.05x10^{-03}	-0.310	1.18x10^{-01}	3.71x10^{-01}	-0.187	2.85x10^{-01}
ZNF257	-0.403	2.26x10^{-03}	-0.431	9.40x10^{-02}	3.22x10^{-01}	-0.496	1.39x10^{-01}
ZGRF1	-0.135	2.40x10^{-03}	-0.491	9.50x10^{-02}	3.24x10^{-01}	-0.538	1.94x10^{-01}
MFF	-0.080	2.66x10^{-03}	-0.139	5.29x10^{-01}	7.96x10^{-01}	-0.056	8.35x10^{-01}
DNAJC2	-0.093	2.77x10^{-03}	-0.325	2.13x10^{-01}	5.13x10^{-01}	-0.192	4.15x10^{-01}
CTPS2	-0.096	2.79x10^{-03}	-0.177	4.19x10^{-01}	7.20x10^{-01}	-0.374	3.30x10^{-02}
EIF4G1	0.129	6.64x10^{-03}	0.407	5.00x10^{-02}	2.18x10^{-01}	0.482	1.78x10^{-01}
Not validated by meta-analysis							
TLR5	-0.350	1.90x10^{-08}	0.596	5.00x10^{-05}	1.00x10^{-03}	0.366	4.90x10^{-02}
C1orf27	-0.175	6.80x10^{-08}	0.120	5.27x10^{-01}	7.95x10^{-01}	-0.051	8.46x10^{-01}
PTEN	-0.170	7.70x10^{-08}	0.267	2.64x10^{-01}	5.77x10^{-01}	-0.040	8.58x10^{-01}
RNASEL	-0.174	1.50x10^{-07}	0.380	2.64x10^{-01}	5.76x10^{-01}	0.152	7.47x10^{-01}
SCYL3	-0.112	1.70x10^{-07}	0.076	7.17x10^{-01}	8.97x10^{-01}	0.019	9.45x10^{-01}
BROX	-0.119	8.00x10^{-07}	0.049	7.29x10^{-01}	9.03x10^{-01}	-0.053	7.71x10^{-01}
SMARCD2	-0.126	1.00x10^{-06}	0.131	3.40x10^{-01}	6.56x10^{-01}	0.039	8.71x10^{-01}
ATF6	-0.156	1.10x10^{-06}	0.037	8.93x10^{-01}	9.68x10^{-01}	-0.343	3.22x10^{-01}
DNAJB4	-0.237	1.30x10^{-06}	0.098	5.41x10^{-01}	8.05x10^{-01}	0.116	5.52x10^{-01}
XKRX	-0.587	2.70x10^{-06}	0.100	5.66x10^{-01}	8.18x10^{-01}	0.174	4.38x10^{-01}
TCAIM	-0.127	3.80x10^{-06}	0.398	3.10x10^{-02}	1.58x10^{-01}	0.435	2.70x10^{-02}
DNPH1	0.197	4.70x10^{-06}	-0.222	1.06x10^{-01}	3.46x10^{-01}	-0.196	2.63x10^{-01}
MEFV	-0.193	5.40x10^{-06}	0.581	1.00x10^{-03}	1.50x10^{-02}	0.311	1.12x10^{-01}
ZNF252P	-0.146	6.70x10^{-06}	0.225	4.68x10^{-01}	7.55x10^{-01}	0.033	9.65x10^{-01}
OSBPL2	-0.117	7.20x10^{-06}	0.287	1.46x10^{-01}	4.20x10^{-01}	0.068	8.45x10^{-01}
THAP2	-0.186	7.90x10^{-06}	0.095	7.95x10^{-01}	9.30x10^{-01}	-0.037	9.41x10^{-01}
TMEM154	-0.175	9.70x10^{-06}	0.552	2.00x10^{-04}	3.00x10^{-03}	0.303	9.80x10^{-02}
XRCC5	-0.102	1.10x10^{-05}	0.035	8.51x10^{-01}	9.52x10^{-01}	0.026	9.23x10^{-01}
PWWP2A	-0.100	1.20x10^{-05}	0.068	8.26x10^{-01}	9.42x10^{-01}	-0.148	7.03x10^{-01}
C2orf49	-0.105	1.40x10^{-05}	0.326	1.80x10^{-02}	1.09x10^{-01}	0.130	4.92x10^{-01}
EHBP1L1	-0.174	2.30x10^{-05}	1.246	5.00x10^{-02}	2.18x10^{-01}	1.337	1.87x10^{-01}
NPIPB4	0.216	2.50x10^{-05}	-0.223	6.44x10^{-01}	8.62x10^{-01}	-0.379	4.54x10^{-01}
OPA1	-0.293	2.60x10^{-05}	0.171	5.67x10^{-01}	8.19x10^{-01}	-0.204	5.40x10^{-01}
UBE2D3	-0.124	3.10x10^{-05}	0.484	2.31x10^{-01}	5.37x10^{-01}	0.375	4.99x10^{-01}
THAP5	-0.130	3.10x10^{-05}	0.008	9.64x10^{-01}	9.89x10^{-01}	0.080	7.41x10^{-01}
SHOC2	-0.099	3.10x10^{-05}	0.419	1.30x10^{-02}	8.60x10^{-02}	0.247	1.57x10^{-01}
MPV17L	0.201	3.40x10^{-05}	-0.360	1.20x10^{-02}	8.30x10^{-02}	-0.244	2.71x10^{-01}
RBPJ	-0.112	3.50x10^{-05}	0.424	1.54x10^{-01}	4.31x10^{-01}	0.155	6.51x10^{-01}
TNFSF4	-0.360	3.90x10^{-05}	0.050	8.53x10^{-01}	9.53x10^{-01}	0.154	5.95x10^{-01}
HACD4	-0.156	4.30x10^{-05}	0.288	2.20x10^{-01}	5.24x10^{-01}	0.246	4.54x10^{-01}
FBXL4	-0.119	4.90x10^{-05}	0.351	1.10x10^{-02}	7.80x10^{-02}	0.270	1.23x10^{-01}
ETS2	-0.168	5.00x10^{-05}	0.454	2.00x10^{-03}	2.00x10^{-02}	0.176	2.90x10^{-01}
GOLGA2	-0.121	5.10x10^{-05}	0.073	8.11x10^{-01}	9.35x10^{-01}	0.199	5.15x10^{-01}
INPP5A	-0.148	5.70x10^{-05}	0.498	6.00x10^{-04}	1.00x10^{-02}	0.412	3.30x10^{-02}
DDB1	-0.119	5.80x10^{-05}	0.050	8.77x10^{-01}	9.62x10^{-01}	0.055	8.69x10^{-01}
CSNK2A2	0.174	6.00x10^{-05}	-0.203	1.24x10^{-01}	3.81x10^{-01}	-0.301	7.10x10^{-02}

dic-01	0.157	6.50x10^{-05}	-0.023	8.72x10^{-01}	9.59x10^{-01}	0.021	9.11x10^{-01}
CCND3	-0.188	7.60x10^{-05}	0.288	1.10x10^{-01}	3.55x10^{-01}	-0.001	9.95x10^{-01}
ZNF132	-0.228	7.60x10^{-05}	0.021	8.96x10^{-01}	9.69x10^{-01}	0.000	9.98x10^{-01}
GATA3	0.305	8.20x10^{-05}	-0.674	4.00x10^{-03}	3.80x10^{-02}	-0.528	3.10x10^{-02}
TMEM65	-0.090	8.40x10^{-05}	0.046	8.09x10^{-01}	9.34x10^{-01}	0.032	8.81x10^{-01}
TTC17	-0.085	9.00x10^{-05}	0.153	7.51x10^{-01}	9.12x10^{-01}	0.125	8.20x10^{-01}
STK38L	-0.106	9.90x10^{-05}	0.438	1.05x10^{-01}	3.45x10^{-01}	0.278	4.12x10^{-01}
PGS1	-0.152	1.00x10^{-04}	0.141	4.65x10^{-01}	7.53x10^{-01}	-0.035	8.89x10^{-01}
TXNDC11	0.174	1.10x10^{-04}	-0.592	8.00x10^{-03}	6.30x10^{-02}	-0.401	3.04x10^{-01}
EPC2	-0.096	1.20x10^{-04}	0.012	9.34x10^{-01}	9.81x10^{-01}	0.060	7.52x10^{-01}
FAM129A	-0.179	1.20x10^{-04}	0.297	5.00x10^{-02}	2.18x10^{-01}	0.034	8.46x10^{-01}
STAT5A	-0.118	1.20x10^{-04}	0.171	3.51x10^{-01}	6.66x10^{-01}	-0.103	5.38x10^{-01}
MIA2	-0.133	1.20x10^{-04}	0.034	9.13x10^{-01}	9.75x10^{-01}	0.013	9.73x10^{-01}
TRIP10	-0.250	1.20x10^{-04}	0.348	8.80x10^{-02}	3.09x10^{-01}	0.365	1.57x10^{-01}
LRCH1	0.131	1.20x10^{-04}	-0.713	6.00x10^{-05}	2.00x10^{-03}	-0.575	6.70x10^{-02}
ABHD2	-0.179	1.30x10^{-04}	0.687	1.30x10^{-02}	8.80x10^{-02}	0.476	2.03x10^{-01}
HLX	-0.229	1.30x10^{-04}	0.716	3.00x10^{-03}	2.80x10^{-02}	0.458	1.23x10^{-01}
ZNF485	-0.172	1.30x10^{-04}	0.045	8.83x10^{-01}	9.65x10^{-01}	-0.016	9.66x10^{-01}
TANK	-0.116	1.40x10^{-04}	0.321	3.74x10^{-01}	6.86x10^{-01}	-0.050	9.14x10^{-01}
PPP2R5E	0.152	1.50x10^{-04}	-0.656	2.00x10^{-03}	2.10x10^{-02}	-0.710	1.20x10^{-02}
NACC1	0.263	1.50x10^{-04}	-0.283	1.23x10^{-01}	3.79x10^{-01}	-0.497	7.00x10^{-03}
ZNF235	-0.131	1.50x10^{-04}	0.005	9.82x10^{-01}	9.94x10^{-01}	-0.590	1.53x10^{-01}
AVL9	-0.081	1.50x10^{-04}	0.569	5.40x10^{-02}	2.26x10^{-01}	0.381	2.94x10^{-01}
MBTPS2	0.117	1.50x10^{-04}	-0.222	3.45x10^{-01}	6.60x10^{-01}	-0.304	3.32x10^{-01}
ZNF418	-0.327	1.50x10^{-04}	0.016	9.25x10^{-01}	9.79x10^{-01}	-0.049	8.59x10^{-01}
TMEM68	-0.098	1.80x10^{-04}	0.159	5.91x10^{-01}	8.33x10^{-01}	0.112	7.54x10^{-01}
MINPP1	-0.240	1.90x10^{-04}	0.048	9.08x10^{-01}	9.73x10^{-01}	-0.217	6.91x10^{-01}
ZNF322	-0.125	2.00x10^{-04}	0.204	3.31x10^{-01}	6.47x10^{-01}	0.142	6.62x10^{-01}
ORC4	-0.127	2.20x10^{-04}	0.239	4.02x10^{-01}	7.08x10^{-01}	0.343	3.33x10^{-01}
HAP1	0.369	2.30x10^{-04}	-0.018	9.01x10^{-01}	9.71x10^{-01}	0.149	4.17x10^{-01}
GGTA1P	-0.355	2.30x10^{-04}	0.159	4.30x10^{-01}	7.29x10^{-01}	0.409	2.70x10^{-02}
GADL1	0.116	2.70x10^{-04}	-0.035	8.17x10^{-01}	9.37x10^{-01}	-0.071	6.99x10^{-01}
AP1AR	-0.110	2.80x10^{-04}	0.017	9.53x10^{-01}	9.85x10^{-01}	-0.130	7.12x10^{-01}
DICER1	-0.110	2.80x10^{-04}	0.720	3.00x10^{-03}	2.70x10^{-02}	0.479	1.34x10^{-01}
PTPN14	0.224	3.00x10^{-04}	-0.096	5.10x10^{-01}	7.84x10^{-01}	-0.126	4.94x10^{-01}
GRAP2	-0.176	3.00x10^{-04}	0.078	8.10x10^{-01}	9.35x10^{-01}	0.437	8.90x10^{-02}
ZFP36L2	0.200	3.10x10^{-04}	-1.029	4.00x10^{-08}	6.00x10^{-06}	-1.101	6.00x10^{-09}
VPS37A	-0.106	3.30x10^{-04}	0.496	1.56x10^{-01}	4.34x10^{-01}	0.326	5.24x10^{-01}
PREP	0.166	3.30x10^{-04}	-0.040	8.71x10^{-01}	9.59x10^{-01}	-0.203	5.38x10^{-01}
CARNMT1	-0.147	3.50x10^{-04}	0.127	4.88x10^{-01}	7.68x10^{-01}	0.397	3.10x10^{-02}
BEND2	-0.350	4.00x10^{-04}	0.282	3.81x10^{-01}	6.92x10^{-01}	0.628	1.50x10^{-02}
ENKUR	-0.337	4.10x10^{-04}	0.103	7.37x10^{-01}	9.06x10^{-01}	0.358	5.20x10^{-02}
RSBN1L	-0.095	4.20x10^{-04}	0.110	6.97x10^{-01}	8.89x10^{-01}	-0.060	8.84x10^{-01}
MT-ND1	-0.330	4.30x10^{-04}	0.085	7.60x10^{-01}	9.15x10^{-01}	0.231	5.07x10^{-01}
UBE4A	-0.123	4.90x10^{-04}	0.145	4.18x10^{-01}	7.19x10^{-01}	-0.130	5.97x10^{-01}
ZNF233	0.161	5.10x10^{-04}	-0.240	4.22x10^{-01}	7.23x10^{-01}	0.082	6.73x10^{-01}

USP8	-0.070	5.30x10^{-04}	0.132	5.74x10^{-01}	8.22x10^{-01}	-0.136	6.00x10^{-01}
VPS37B	0.140	5.40x10^{-04}	-0.189	4.12x10^{-01}	7.15x10^{-01}	-0.066	8.42x10^{-01}
ATP10B	0.182	5.90x10^{-04}	-0.279	2.36x10^{-01}	5.44x10^{-01}	-0.147	5.23x10^{-01}
TRUB1	-0.097	6.40x10^{-04}	0.051	7.75x10^{-01}	9.23x10^{-01}	0.065	7.78x10^{-01}
RNF26	0.261	7.60x10^{-04}	-0.439	2.10x10^{-02}	1.22x10^{-01}	-0.508	7.00x10^{-03}
CEPT1	-0.080	7.70x10^{-04}	0.345	1.47x10^{-01}	4.21x10^{-01}	0.486	7.30x10^{-02}
LIN52	-0.142	8.10x10^{-04}	0.111	4.37x10^{-01}	7.34x10^{-01}	0.025	8.93x10^{-01}
BET1	-0.106	8.40x10^{-04}	0.084	8.33x10^{-01}	9.45x10^{-01}	-0.062	9.04x10^{-01}
GTF2H1	-0.076	9.40x10^{-04}	0.197	5.09x10^{-01}	7.84x10^{-01}	-0.024	9.42x10^{-01}
NF2	0.138	9.80x10^{-04}	-0.264	4.35x10^{-01}	7.33x10^{-01}	-0.123	7.61x10^{-01}
MAP2K4	-0.100	1.12x10^{-03}	0.332	1.20x10^{-02}	8.50x10^{-02}	0.340	4.20x10^{-02}
CCDC18	-0.187	1.21x10^{-03}	0.076	6.82x10^{-01}	8.82x10^{-01}	-0.104	7.29x10^{-01}
NDUFV3	-0.142	1.59x10^{-03}	0.780	1.00x10^{-07}	2.00x10^{-05}	0.739	1.00x10^{-04}
PAPD4	-0.071	1.65x10^{-03}	0.102	6.58x10^{-01}	8.69x10^{-01}	-0.010	9.67x10^{-01}
FSTL1	-0.442	1.87x10^{-03}	0.377	1.60x10^{-02}	1.02x10^{-01}	0.464	6.00x10^{-03}
HDAC6	-0.089	1.91x10^{-03}	0.199	3.68x10^{-01}	6.81x10^{-01}	-0.006	9.77x10^{-01}
NOM1	-0.105	1.98x10^{-03}	0.027	8.91x10^{-01}	9.68x10^{-01}	-0.108	7.60x10^{-01}
TMX2	-0.083	2.05x10^{-03}	0.131	5.37x10^{-01}	8.03x10^{-01}	-0.018	9.36x10^{-01}
GPAM	-0.106	2.15x10^{-03}	0.039	7.89x10^{-01}	9.27x10^{-01}	0.042	8.61x10^{-01}
RP11-523H20.5	0.108	2.57x10^{-03}	-0.096	5.25x10^{-01}	7.94x10^{-01}	0.248	1.77x10^{-01}
FAM132B	0.615	3.24x10^{-03}	-0.035	9.09x10^{-01}	9.73x10^{-01}	0.164	6.63x10^{-01}
ZNF528	-0.137	3.99x10^{-03}	0.089	5.54x10^{-01}	8.11x10^{-01}	-0.394	4.40x10^{-02}
ALG10	-0.107	6.83x10^{-03}	0.265	2.01x10^{-01}	4.99x10^{-01}	0.062	8.24x10^{-01}
ARFGAP3	-0.153	5.80x10^{-08}	-0.411	1.32x10^{-01}	3.94x10^{-01}	-0.427	2.23x10^{-01}
KCNQ1OT1	0.138	2.00x10^{-07}	-0.102	7.78x10^{-01}	9.24x10^{-01}	-0.087	8.86x10^{-01}
AL844908.5	-0.302	3.50x10^{-07}	-0.166	5.59x10^{-01}	8.14x10^{-01}		
ZNF486	-0.271	5.50x10^{-07}	-0.349	1.50x10^{-02}	9.60x10^{-02}	-0.416	2.70x10^{-02}
ZNF224	-0.114	6.40x10^{-07}	-0.234	2.51x10^{-01}	5.61x10^{-01}	-0.320	1.77x10^{-01}
CTD-2303B20.1	0.331	2.40x10^{-06}	-0.040	7.81x10^{-01}	9.25x10^{-01}	-0.183	4.82x10^{-01}
ZNF432	-0.145	6.00x10^{-06}	-0.617	3.00x10^{-05}	9.00x10^{-04}	-0.626	9.00x10^{-04}
FRRS1L	0.162	6.40x10^{-06}	0.133	4.92x10^{-01}	7.71x10^{-01}	0.350	5.70x10^{-02}
ANKRD34A	-0.338	9.30x10^{-06}	-0.106	5.54x10^{-01}	8.12x10^{-01}	-0.203	4.74x10^{-01}
RP11-349A22.5	-0.098	2.30x10^{-05}	-0.590	1.30x10^{-02}	8.60x10^{-02}	-0.774	3.30x10^{-02}
RP11-438E5.1	-0.258	5.40x10^{-05}	0.143	7.15x10^{-01}	8.97x10^{-01}	0.614	9.00x10^{-02}
ZBTB8B	0.153	5.50x10^{-05}	-0.045	8.61x10^{-01}	9.56x10^{-01}	-0.023	9.30x10^{-01}
RP11-701H24.6	-0.194	1.10x10^{-04}	-0.568	1.20x10^{-02}	8.30x10^{-02}	-0.645	1.20x10^{-02}
RP11-510H23.1	0.165	1.10x10^{-04}	0.089	7.52x10^{-01}	9.13x10^{-01}	0.462	1.61x10^{-01}
LINC-PINT	0.113	1.10x10^{-04}	-1.027	3.20x10^{-02}	1.61x10^{-01}	-0.553	5.13x10^{-01}
ZNF587B	-0.105	1.70x10^{-04}	-0.639	1.00x10^{-03}	1.80x10^{-02}	-0.822	2.00x10^{-03}
LL22NC03-79E2.1	0.191	1.80x10^{-04}	0.245	8.50x10^{-02}	3.04x10^{-01}	0.209	4.59x10^{-01}
PARG	-0.105	2.20x10^{-04}	-0.303	3.10x10^{-02}	1.58x10^{-01}	-0.287	1.11x10^{-01}
OLMALINC	0.117	2.50x10^{-04}	-0.365	2.78x10^{-01}	5.92x10^{-01}	-0.250	4.49x10^{-01}
PVT1	0.254	2.90x10^{-04}	-0.183	7.63x10^{-01}	9.17x10^{-01}	-0.102	7.88x10^{-01}
SOCS7	-0.151	3.80x10^{-04}	-0.712	1.00x10^{-06}	8.00x10^{-05}	-0.662	4.00x10^{-04}
RP11-163O17.1	-0.131	3.80x10^{-04}	0.035	8.71x10^{-01}	9.59x10^{-01}	-0.038	8.82x10^{-01}
MMP28	-0.411	4.10x10^{-04}	-0.133	7.96x10^{-01}	9.30x10^{-01}	-0.447	5.33x10^{-01}

PTTG2	0.230	6.50x10^{-04}	0.136	3.40x10^{-01}	6.56x10^{-01}	0.041	8.55x10^{-01}
C22orf39	-0.080	7.00x10^{-04}	0.049	8.08x10^{-01}	9.34x10^{-01}	0.094	6.98x10^{-01}
ZNF737	-0.178	1.02x10^{-03}	-0.224	3.68x10^{-01}	6.81x10^{-01}	-0.144	7.35x10^{-01}
DGCR11	0.138	2.18x10^{-03}	-0.480	2.70x10^{-02}	1.44x10^{-01}	-0.536	3.60x10^{-02}
AC007743.1	0.141	2.64x10^{-03}	0.366	1.85x10^{-01}	4.78x10^{-01}	0.521	4.24x10^{-01}
ZNF350	-0.091	2.91x10^{-03}	-0.242	7.90x10^{-02}	2.89x10^{-01}	-0.316	7.10x10^{-02}
RP11-574K11.28	0.119	2.94x10^{-03}	-0.073	8.06x10^{-01}	9.33x10^{-01}	-0.261	3.85x10^{-01}
GGNBP2	-0.063	3.73x10^{-03}	-0.302	3.60x10^{-02}	1.75x10^{-01}	-0.534	3.90x10^{-02}
SRSF8	-0.119	4.97x10^{-03}	-0.425	9.70x10^{-02}	3.29x10^{-01}	-0.134	6.68x10^{-01}
RP11-540A21.3	-0.188	5.01x10^{-03}	-0.097	5.79x10^{-01}	8.25x10^{-01}	0.146	4.97x10^{-01}

Supplementary Table 2: Results of meta-analysis of PAH transcriptomic studies in blood samples for RNAs associated with PAH in RNAseq. Table shows 416/507 genes from the PAH RNAseq analysis present in the meta-analysis of whole blood PAH. Data ordered based on dysregulation significance (p-value) in current PAH RNAseq analysis.

	PAH Cohort		PAH Meta-analysis		
Genes	**logFC AB**	**Sig. AB**	**Average FC**	**Sig.**	**FDR**
Same direction, significant, meeting FDR					
TLR5	-0.350	1.90x10^{-08}	0.810	<1.00x10^{-04}	2.00x10^{-03}
PTEN	-0.170	7.70x10^{-08}	0.889	7.00x10^{-03}	3.20x10^{-02}
BROX	-0.119	8.00x10^{-07}	0.886	1.00x10^{-03}	7.00x10^{-03}
AMD1	-0.160	2.00x10^{-06}	0.813	<1.00x10^{-04}	<1.00x10^{-04}
XKRX	-0.587	2.70x10^{-06}	0.709	<1.00x10^{-04}	<1.00x10^{-04}
MEFV	-0.193	5.40x10^{-06}	0.783	<1.00x10^{-04}	<1.00x10^{-04}
ZNF252P	-0.146	6.70x10^{-06}	0.849	<1.00x10^{-04}	3.00x10^{-03}
RP11-43D4.3	0.217	3.20x10^{-05}	1.255	6.00x10^{-03}	3.00x10^{-02}
TWF1	-0.117	4.00x10^{-05}	0.861	1.00x10^{-03}	8.00x10^{-03}
SLC25A16	-0.126	1.00x10^{-04}	0.875	1.00x10^{-03}	9.00x10^{-03}
STAT5A	-0.118	1.20x10^{-04}	0.860	2.00x10^{-03}	1.60x10^{-02}
LRCH1	0.131	1.20x10^{-04}	1.285	<1.00x10^{-04}	4.00x10^{-03}
SDCCAG3	-0.133	2.10x10^{-04}	0.872	<1.00x10^{-04}	3.00x10^{-03}
CYP2R1	-0.109	2.30x10^{-04}	0.828	<1.00x10^{-04}	2.00x10^{-03}
ZFP36L2	0.200	3.10x10^{-04}	1.263	<1.00x10^{-04}	2.00x10^{-03}
ATXN1	0.112	3.70x10^{-04}	1.164	<1.00x10^{-04}	<1.00x10^{-04}
TECPR1	-0.136	3.90x10^{-04}	0.929	8.00x10^{-03}	3.80x10^{-02}
UBE4A	-0.123	4.90x10^{-04}	0.893	<1.00x10^{-04}	<1.00x10^{-04}
ZNF233	0.161	5.10x10^{-04}	1.040	6.00x10^{-03}	3.00x10^{-02}
CEPT1	-0.080	7.70x10^{-04}	0.875	1.00x10^{-03}	6.00x10^{-03}
LIN52	-0.142	8.10x10^{-04}	0.855	2.00x10^{-03}	1.10x10^{-02}
GTF2H1	-0.076	9.40x10^{-04}	0.890	8.00x10^{-03}	3.70x10^{-02}
TYW3	-0.096	1.10x10^{-03}	0.918	1.00x10^{-02}	4.20x10^{-02}
CCDC18	-0.187	1.20x10^{-03}	0.927	<1.00x10^{-04}	2.00x10^{-03}
NDC1	-0.131	1.70x10^{-03}	0.872	7.00x10^{-03}	3.20x10^{-02}
TAF6L	-0.131	1.80x10^{-03}	0.891	1.00x10^{-03}	7.00x10^{-03}
Same direction, significant					
RNASEL	-0.174	1.50x10^{-07}	0.918	4.30x10^{-02}	1.12x10^{-01}
RALA	0.182	2.70x10^{-07}	1.132	3.60x10^{-02}	1.00x10^{-01}
ALG8	-0.111	4.90x10^{-06}	0.909	3.30x10^{-02}	9.40x10^{-02}
CRLF3	-0.102	2.60x10^{-05}	0.905	3.30x10^{-02}	9.50x10^{-02}
SHOC2	-0.099	3.10x10^{-05}	0.926	2.10x10^{-02}	7.00x10^{-02}
ZNF845	-0.120	5.20x10^{-05}	0.858	4.20x10^{-02}	1.10x10^{-01}
TRIM65	-0.149	7.40x10^{-05}	0.950	2.80x10^{-02}	8.40x10^{-02}
FAM129A	-0.179	1.20x10^{-04}	0.860	1.30x10^{-02}	5.00x10^{-02}
CSNK2A1	-0.079	3.00x10^{-04}	0.941	3.10x10^{-02}	9.10x10^{-02}
ZNF30	-0.190	7.40x10^{-04}	0.960	4.20x10^{-02}	1.11x10^{-01}
ZNF589	-0.112	1.30x10^{-03}	0.859	1.80x10^{-02}	6.20x10^{-02}
NDUFV3	-0.142	1.60x10^{-03}	0.930	3.50x10^{-02}	9.90x10^{-02}
IL6ST	-0.148	1.80x10^{-03}	0.917	1.40x10^{-02}	5.40x10^{-02}
GPAM	-0.106	2.20x10^{-03}	0.783	2.40x10^{-02}	7.80x10^{-02}

SRSF8	-0.119	5.00x10^{-03}	0.929	1.30x10^{-02}	5.20x10^{-02}
Same direction					
SLC16A10	-0.381	5.00x10^{-08}	0.934	4.68x10^{-01}	4.51x10^{-01}
RBM27	-0.137	1.30x10^{-07}	0.983	4.91x10^{-01}	4.62x10^{-01}
SCYL3	-0.112	1.70x10^{-07}	0.957	3.12x10^{-01}	3.68x10^{-01}
RLIM	-0.129	3.10x10^{-07}	0.940	1.08x10^{-01}	2.02x10^{-01}
SCFD2	-0.223	4.40x10^{-07}	0.912	2.06x10^{-01}	2.94x10^{-01}
ZFAND1	-0.157	5.30x10^{-07}	0.982	7.06x10^{-01}	5.45x10^{-01}
CCNB1IP1	-0.150	5.60x10^{-07}	0.990	8.26x10^{-01}	5.82x10^{-01}
SMARCD2	-0.126	1.00x10^{-06}	0.935	5.20x10^{-02}	1.28x10^{-01}
ATF6	-0.156	1.10x10^{-06}	0.995	8.68x10^{-01}	5.94x10^{-01}
SEC23A	-0.101	1.30x10^{-06}	0.986	6.99x10^{-01}	5.42x10^{-01}
ACAP2	-0.098	1.70x10^{-06}	0.990	7.22x10^{-01}	5.50x10^{-01}
ARHGAP12	-0.149	2.10x10^{-06}	0.998	9.63x10^{-01}	6.19x10^{-01}
PTPRC	-0.125	2.40x10^{-06}	0.957	5.43x10^{-01}	4.85x10^{-01}
TCAIM	-0.127	3.80x10^{-06}	0.936	9.70x10^{-02}	1.88x10^{-01}
ZNF763	-0.251	5.30x10^{-06}	0.935	1.04x10^{-01}	1.97x10^{-01}
ZNF33A	-0.122	6.50x10^{-06}	0.980	6.66x10^{-01}	5.31x10^{-01}
OSBPL2	-0.117	7.20x10^{-06}	0.972	3.21x10^{-01}	3.73x10^{-01}
TMTC3	-0.167	7.70x10^{-06}	0.987	7.57x10^{-01}	5.61x10^{-01}
KIAA1551	-0.148	9.50x10^{-06}	0.928	1.86x10^{-01}	2.78x10^{-01}
ITGA6	-0.204	9.50x10^{-06}	0.995	9.48x10^{-01}	6.16x10^{-01}
TMEM154	-0.175	9.70x10^{-06}	0.898	8.80x10^{-02}	1.77x10^{-01}
OXNAD1	-0.183	1.00x10^{-05}	0.949	3.67x10^{-01}	3.99x10^{-01}
ATG12	-0.118	1.00x10^{-05}	0.995	8.43x10^{-01}	5.87x10^{-01}
DEF6	-0.111	1.00x10^{-05}	0.987	7.03x10^{-01}	5.44x10^{-01}
HELQ	-0.114	1.10x10^{-05}	0.997	9.32x10^{-01}	6.12x10^{-01}
XRCC5	-0.102	1.10x10^{-05}	0.957	1.12x10^{-01}	2.07x10^{-01}
BACE1	0.255	1.20x10^{-05}	1.050	2.19x10^{-01}	3.05x10^{-01}
PMS1	-0.141	1.30x10^{-05}	0.985	7.53x10^{-01}	5.59x10^{-01}
SIKE1	-0.118	1.30x10^{-05}	0.980	6.31x10^{-01}	5.19x10^{-01}
C2orf49	-0.105	1.40x10^{-05}	0.981	5.42x10^{-01}	4.85x10^{-01}
SNW1	-0.087	2.30x10^{-05}	0.978	4.76x10^{-01}	4.55x10^{-01}
EHBP1L1	-0.174	2.30x10^{-05}	0.989	5.70x10^{-01}	4.96x10^{-01}
OPA1	-0.293	2.60x10^{-05}	0.968	4.02x10^{-01}	4.19x10^{-01}
CHPF	0.389	3.10x10^{-05}	1.034	3.72x10^{-01}	4.02x10^{-01}
RBPJ	-0.112	3.50x10^{-05}	0.973	4.77x10^{-01}	4.55x10^{-01}
TTF1	-0.091	3.50x10^{-05}	0.975	4.38x10^{-01}	4.37x10^{-01}
OR6Y1	0.156	4.20x10^{-05}	1.006	6.11x10^{-01}	5.11x10^{-01}
ZNF506	-0.155	4.50x10^{-05}	0.993	8.11x10^{-01}	5.77x10^{-01}
IFT46	-0.108	4.70x10^{-05}	0.917	6.10x10^{-02}	1.41x10^{-01}
GOLGA4	-0.102	4.80x10^{-05}	0.995	9.14x10^{-01}	6.07x10^{-01}
ZNF304	-0.155	4.90x10^{-05}	0.985	7.45x10^{-01}	5.57x10^{-01}
ETS2	-0.168	5.00x10^{-05}	0.987	8.37x10^{-01}	5.85x10^{-01}
GOLGA2	-0.121	5.10x10^{-05}	0.965	3.06x10^{-01}	3.64x10^{-01}
OR1A1	0.147	5.10x10^{-05}	1.004	7.56x10^{-01}	5.60x10^{-01}

DIP2B	-0.138	$5.50x10^{-05}$	0.995	$8.76x10^{-01}$	$5.96x10^{-01}$
DDB1	-0.119	$5.80x10^{-05}$	0.966	$4.15x10^{-01}$	$4.25x10^{-01}$
APBB1	-0.190	$5.90x10^{-05}$	0.984	$5.84x10^{-01}$	$5.01x10^{-01}$
C3orf17	-0.099	$6.30x10^{-05}$	0.981	$5.67x10^{-01}$	$4.95x10^{-01}$
DEC1	0.157	$6.50x10^{-05}$	1.015	$2.46x10^{-01}$	$3.24x10^{-01}$
ZNF790	-0.153	$6.60x10^{-05}$	0.970	$5.34x10^{-01}$	$4.81x10^{-01}$
ZBTB14	-0.119	$7.10x10^{-05}$	0.987	$7.26x10^{-01}$	$5.51x10^{-01}$
GATA3	0.305	$8.20x10^{-05}$	1.064	$1.88x10^{-01}$	$2.79x10^{-01}$
ZNF28	-0.147	$8.40x10^{-05}$	0.946	$2.36x10^{-01}$	$3.17x10^{-01}$
PGS1	-0.152	$1.00x10^{-04}$	0.963	$4.45x10^{-01}$	$4.40x10^{-01}$
MIA3	-0.108	$1.00x10^{-04}$	0.946	$1.17x10^{-01}$	$2.11x10^{-01}$
TXNDC11	0.174	$1.10x10^{-04}$	1.003	$9.23x10^{-01}$	$6.09x10^{-01}$
TJP1	0.198	$1.20x10^{-04}$	1.039	$5.10x10^{-01}$	$4.70x10^{-01}$
CCNG1	-0.114	$1.20x10^{-04}$	0.943	$1.90x10^{-01}$	$2.81x10^{-01}$
ZNF485	-0.172	$1.30x10^{-04}$	0.962	$2.79x10^{-01}$	$3.47x10^{-01}$
ABHD2	-0.179	$1.30x10^{-04}$	0.951	$2.67x10^{-01}$	$3.38x10^{-01}$
HLX	-0.229	$1.30x10^{-04}$	0.957	$2.31x10^{-01}$	$3.14x10^{-01}$
MFAP3	-0.114	$1.40x10^{-04}$	0.947	$2.41x10^{-01}$	$3.20x10^{-01}$
PANK4	-0.125	$1.40x10^{-04}$	0.981	$5.13x10^{-01}$	$4.72x10^{-01}$
MBTPS2	0.117	$1.50x10^{-04}$	1.055	$9.00x10^{-02}$	$1.80x10^{-01}$
EZH1	-0.126	$1.80x10^{-04}$	0.934	$1.39x10^{-01}$	$2.35x10^{-01}$
ZDHHC6	-0.086	$1.90x10^{-04}$	0.995	$8.63x10^{-01}$	$5.92x10^{-01}$
MINPP1	-0.240	$1.90x10^{-04}$	0.963	$4.52x10^{-01}$	$4.43x10^{-01}$
ANGEL2	-0.075	$2.10x10^{-04}$	0.934	$1.12x10^{-01}$	$2.06x10^{-01}$
COG8	-0.108	$2.10x10^{-04}$	0.977	$3.78x10^{-01}$	$4.06x10^{-01}$
ORC4	-0.127	$2.20x10^{-04}$	0.969	$4.82x10^{-01}$	$4.57x10^{-01}$
PARG	-0.105	$2.20x10^{-04}$	0.918	$1.13x10^{-01}$	$2.08x10^{-01}$
AMN1	-0.100	$2.20x10^{-04}$	0.953	$1.93x10^{-01}$	$2.83x10^{-01}$
KRIT1	-0.093	$2.20x10^{-04}$	0.993	$8.06x10^{-01}$	$5.76x10^{-01}$
MEPCE	-0.141	$2.40x10^{-04}$	0.957	$3.73x10^{-01}$	$4.03x10^{-01}$
HSPD1	-0.088	$2.40x10^{-04}$	0.915	$1.87x10^{-01}$	$2.79x10^{-01}$
TMEM41B	-0.119	$2.40x10^{-04}$	0.951	$2.77x10^{-01}$	$3.46x10^{-01}$
UPF2	-0.087	$2.60x10^{-04}$	0.963	$2.13x10^{-01}$	$3.00x10^{-01}$
GADL1	0.116	$2.70x10^{-04}$	1.004	$6.70x10^{-01}$	$5.33x10^{-01}$
AP1AR	-0.110	$2.80x10^{-04}$	0.941	$1.83x10^{-01}$	$2.76x10^{-01}$
DICER1	-0.110	$2.80x10^{-04}$	0.993	$8.20x10^{-01}$	$5.80x10^{-01}$
VPS39	0.092	$2.90x10^{-04}$	1.034	$3.25x10^{-01}$	$3.76x10^{-01}$
PTPN14	0.224	$3.00x10^{-04}$	1.087	$8.10x10^{-02}$	$1.68x10^{-01}$
CSE1L	-0.115	$3.10x10^{-04}$	0.947	$1.46x10^{-01}$	$2.41x10^{-01}$
MBD1	-0.109	$3.10x10^{-04}$	0.994	$8.63x10^{-01}$	$5.93x10^{-01}$
VPS37A	-0.106	$3.30x10^{-04}$	0.964	$3.72x10^{-01}$	$4.02x10^{-01}$
FAM213A	-0.206	$3.30x10^{-04}$	0.965	$5.52x10^{-01}$	$4.89x10^{-01}$
UFM1	-0.099	$3.30x10^{-04}$	0.923	$5.60x10^{-02}$	$1.34x10^{-01}$
ZNF816	-0.106	$3.30x10^{-04}$	0.991	$8.07x10^{-01}$	$5.76x10^{-01}$
ENPP6	0.244	$3.30x10^{-04}$	1.001	$9.20x10^{-01}$	$6.09x10^{-01}$
DCAF7	0.138	$3.40x10^{-04}$	1.001	$9.85x10^{-01}$	$6.24x10^{-01}$

GNL3L	-0.127	3.60x10^{-04}	0.947	2.69x10^{-01}	3.40x10^{-01}
ZNF829	-0.122	3.70x10^{-04}	0.997	8.74x10^{-01}	5.96x10^{-01}
BEND2	-0.350	4.00x10^{-04}	1.000	9.81x10^{-01}	6.23x10^{-01}
SNRK	-0.099	4.00x10^{-04}	0.942	3.13x10^{-01}	3.68x10^{-01}
ENKUR	-0.337	4.10x10^{-04}	0.885	2.95x10^{-01}	3.57x10^{-01}
CEP350	-0.089	5.00x10^{-04}	0.969	2.98x10^{-01}	3.59x10^{-01}
USP8	-0.070	5.30x10^{-04}	0.970	3.88x10^{-01}	4.11x10^{-01}
VPS37B	0.140	5.40x10^{-04}	1.038	5.03x10^{-01}	4.67x10^{-01}
BRAP	-0.100	6.40x10^{-04}	0.942	8.80x10^{-02}	1.78x10^{-01}
TRUB1	-0.097	6.40x10^{-04}	0.972	5.13x10^{-01}	4.72x10^{-01}
PTTG2	0.230	6.50x10^{-04}	1.072	5.20x10^{-02}	1.28x10^{-01}
C22orf39	-0.080	7.00x10^{-04}	0.948	8.70x10^{-02}	1.76x10^{-01}
ZNF268	-0.104	8.10x10^{-04}	0.974	4.72x10^{-01}	4.53x10^{-01}
EXOSC10	-0.092	8.70x10^{-04}	0.967	1.26x10^{-01}	2.21x10^{-01}
GIN1	-0.098	1.20x10^{-03}	0.949	1.83x10^{-01}	2.75x10^{-01}
PAPD4	-0.071	1.70x10^{-03}	0.987	6.40x10^{-01}	5.23x10^{-01}
HDAC6	-0.089	1.90x10^{-03}	0.956	7.10x10^{-02}	1.55x10^{-01}
TSR1	-0.100	1.90x10^{-03}	0.912	1.69x10^{-01}	2.63x10^{-01}
NOM1	-0.105	2.00x10^{-03}	0.975	4.79x10^{-01}	4.56x10^{-01}
SASH1	0.437	2.00x10^{-03}	1.010	9.03x10^{-01}	6.04x10^{-01}
TMX2	-0.083	2.00x10^{-03}	0.958	3.57x10^{-01}	3.94x10^{-01}
TSHZ3	0.236	2.00x10^{-03}	1.042	2.51x10^{-01}	3.28x10^{-01}
SMIM8	-0.108	2.10x10^{-03}	0.973	6.29x10^{-01}	5.19x10^{-01}
CNOT7	-0.089	2.20x10^{-03}	0.949	9.50x10^{-02}	1.86x10^{-01}
ZNF257	-0.403	2.30x10^{-03}	0.965	3.18x10^{-01}	3.71x10^{-01}
MFF	-0.080	2.70x10^{-03}	0.969	3.31x10^{-01}	3.79x10^{-01}
ZNF350	-0.091	2.90x10^{-03}	0.948	1.80x10^{-01}	2.73x10^{-01}
SLAIN2	-0.151	3.70x10^{-03}	0.996	8.74x10^{-01}	5.96x10^{-01}
FAN1	-0.096	5.40x10^{-03}	0.991	7.94x10^{-01}	5.73x10^{-01}
ALG10	-0.107	6.80x10^{-03}	0.993	8.58x10^{-01}	5.91x10^{-01}
Not validated by meta-analysis					
BTAF1	-0.160	5.70x10^{-08}	1.140	<1.00x10^{-04}	2.00x10^{-03}
DDX17	-0.117	4.30x10^{-07}	1.135	<1.00x10^{-04}	2.00x10^{-03}
ZNF486	-0.271	5.50x10^{-07}	1.201	4.00x10^{-03}	2.10x10^{-02}
ZNF141	-0.132	7.80x10^{-07}	1.160	2.00x10^{-03}	1.40x10^{-02}
RBM5	-0.101	8.50x10^{-07}	1.104	5.00x10^{-03}	2.70x10^{-02}
DNAJB4	-0.237	1.30x10^{-06}	1.227	6.00x10^{-03}	3.10x10^{-02}
RP11-254B13.3	0.286	1.80x10^{-06}	0.819	<1.00x10^{-04}	<1.00x10^{-04}
RIF1	-0.120	3.50x10^{-06}	1.102	1.00x10^{-03}	1.10x10^{-02}
UHRF2	-0.141	3.70x10^{-06}	1.186	<1.00x10^{-04}	<1.00x10^{-04}
PTGR1	0.169	4.20x10^{-06}	0.824	2.00x10^{-03}	1.20x10^{-02}
ZC3H11A	-0.102	5.10x10^{-06}	1.115	1.00x10^{-03}	5.00x10^{-03}
KDM1A	-0.098	8.10x10^{-06}	1.112	<1.00x10^{-04}	2.00x10^{-03}
NR1D2	-0.150	9.80x10^{-06}	1.404	4.00x10^{-03}	2.20x10^{-02}
ZNF283	-0.133	1.10x10^{-05}	1.155	5.00x10^{-03}	2.80x10^{-02}
GPBP1	-0.112	1.10x10^{-05}	1.130	4.00x10^{-03}	2.40x10^{-02}

ZNF680	-0.132	1.50x10^{-05}	1.164	3.00x10^{-03}	2.00x10^{-02}
TMED4	-0.087	1.90x10^{-05}	1.151	<1.00x10^{-04}	<1.00x10^{-04}
ZNF354B	-0.154	2.00x10^{-05}	1.123	2.00x10^{-03}	1.30x10^{-02}
SESN1	-0.205	2.00x10^{-05}	1.281	3.00x10^{-03}	1.70x10^{-02}
ARRDC3	-0.205	2.20x10^{-05}	1.219	2.00x10^{-03}	1.20x10^{-02}
PPP2R2D	-0.097	3.10x10^{-05}	1.182	<1.00x10^{-04}	<1.00x10^{-04}
CLTC	0.134	3.30x10^{-05}	0.890	<1.00x10^{-04}	5.00x10^{-03}
GPRASP1	-0.230	3.70x10^{-05}	1.301	<1.00x10^{-04}	<1.00x10^{-04}
RYK	-0.109	4.00x10^{-05}	1.136	<1.00x10^{-04}	1.00x10^{-03}
ZNF876P	-0.427	4.30x10^{-05}	1.116	1.00x10^{-03}	8.00x10^{-03}
SF3B1	-0.122	4.40x10^{-05}	1.087	3.00x10^{-03}	1.80x10^{-02}
ZNF548	-0.146	5.20x10^{-05}	1.086	1.30x10^{-02}	5.00x10^{-02}
MBTD1	-0.093	6.40x10^{-05}	1.206	<1.00x10^{-04}	4.00x10^{-03}
GPR15	0.931	6.40x10^{-05}	0.915	2.00x10^{-03}	1.40x10^{-02}
ZNF426	-0.120	6.90x10^{-05}	1.103	3.00x10^{-03}	1.90x10^{-02}
ZBTB10	-0.174	7.30x10^{-05}	1.166	<1.00x10^{-04}	<1.00x10^{-04}
TTC17	-0.085	9.00x10^{-05}	1.106	1.00x10^{-03}	1.00x10^{-02}
STK38L	-0.106	9.90x10^{-05}	1.133	5.00x10^{-03}	2.70x10^{-02}
C4BPB	0.200	1.50x10^{-04}	0.855	<1.00x10^{-04}	<1.00x10^{-04}
ZNF418	-0.327	1.50x10^{-04}	1.175	<1.00x10^{-04}	1.00x10^{-03}
HSF2	-0.137	1.90x10^{-04}	1.119	2.00x10^{-03}	1.60x10^{-02}
MED13	-0.114	2.20x10^{-04}	1.115	<1.00x10^{-04}	1.00x10^{-03}
GGTA1P	-0.355	2.30x10^{-04}	1.757	<1.00x10^{-04}	<1.00x10^{-04}
ZNF720	-0.141	2.40x10^{-04}	1.192	1.00x10^{-03}	1.10x10^{-02}
ZNF585A	-0.156	2.40x10^{-04}	1.083	1.00x10^{-03}	7.00x10^{-03}
GRAP2	-0.176	3.00x10^{-04}	1.238	1.20x10^{-02}	4.90x10^{-02}
CDA	0.291	3.40x10^{-04}	0.884	5.00x10^{-03}	2.80x10^{-02}
PABPC1	0.221	3.60x10^{-04}	0.870	<1.00x10^{-04}	2.00x10^{-03}
PSME3	0.117	4.00x10^{-04}	0.858	3.00x10^{-03}	1.60x10^{-02}
C7orf60	-0.128	4.60x10^{-04}	1.152	1.00x10^{-03}	5.00x10^{-03}
ZCCHC7	-0.164	5.20x10^{-04}	1.083	7.00x10^{-03}	3.40x10^{-02}
ZNF880	-0.129	5.20x10^{-04}	1.109	1.00x10^{-03}	1.00x10^{-02}
CASD1	-0.097	5.60x10^{-04}	1.178	<1.00x10^{-04}	3.00x10^{-03}
ZNF649	-0.105	7.70x10^{-04}	1.098	1.20x10^{-02}	4.70x10^{-02}
ZNF737	-0.178	1.00x10^{-03}	1.254	4.00x10^{-03}	2.20x10^{-02}
NCK2	-0.123	1.40x10^{-03}	1.111	6.00x10^{-03}	2.80x10^{-02}
WRN	-0.131	1.50x10^{-03}	1.144	4.00x10^{-03}	2.20x10^{-02}
EPHX2	-0.127	1.60x10^{-03}	1.252	<1.00x10^{-04}	4.00x10^{-03}
ZNF577	-0.232	1.80x10^{-03}	1.167	2.00x10^{-03}	1.20x10^{-02}
DGCR11	0.138	2.20x10^{-03}	0.953	3.00x10^{-03}	1.80x10^{-02}
CTPS2	-0.096	2.80x10^{-03}	1.203	<1.00x10^{-04}	1.00x10^{-03}
FBLN2	-0.355	3.00x10^{-03}	1.297	<1.00x10^{-04}	1.00x10^{-03}
ZNF528	-0.137	4.00x10^{-03}	1.321	<1.00x10^{-04}	<1.00x10^{-04}
TRPC1	-0.197	5.70x10^{-03}	1.349	<1.00x10^{-04}	<1.00x10^{-04}
EIF4G1	0.130	6.60x10^{-03}	0.855	2.00x10^{-03}	1.60x10^{-02}
UBR1	-0.119	4.50x10^{-07}	1.073	2.10x10^{-02}	7.10x10^{-02}

RASA2	-0.135	4.60x10^{-07}	1.111	1.80x10^{-02}	6.40x10^{-02}
ZNF224	-0.114	6.40x10^{-07}	1.115	3.20x10^{-02}	9.30x10^{-02}
EIF4A2	-0.141	7.60x10^{-06}	1.098	1.30x10^{-02}	5.10x10^{-02}
MPV17L	0.201	3.40x10^{-05}	0.939	2.90x10^{-02}	8.60x10^{-02}
ARHGAP5	-0.165	5.50x10^{-05}	1.103	4.40x10^{-02}	1.14x10^{-01}
BBX	-0.102	5.90x10^{-05}	1.066	3.00x10^{-02}	8.80x10^{-02}
CCND3	-0.188	7.60x10^{-05}	1.150	2.90x10^{-02}	8.70x10^{-02}
TMEM65	-0.090	8.40x10^{-05}	1.126	1.80x10^{-02}	6.30x10^{-02}
LEMD3	-0.090	9.00x10^{-05}	1.094	1.50x10^{-02}	5.60x10^{-02}
EPC2	-0.096	1.20x10^{-04}	1.092	1.80x10^{-02}	6.30x10^{-02}
NACC1	0.263	1.50x10^{-04}	0.907	1.50x10^{-02}	5.70x10^{-02}
CEP85L	-0.100	2.00x10^{-04}	1.103	1.30x10^{-02}	5.20x10^{-02}
ZNF91	-0.247	4.50x10^{-04}	1.127	1.50x10^{-02}	5.70x10^{-02}
TMEM220	-0.173	4.80x10^{-04}	1.080	2.10x10^{-02}	7.00x10^{-02}
CCAR1	-0.116	6.40x10^{-04}	1.067	3.50x10^{-02}	9.90x10^{-02}
RNF26	0.261	7.60x10^{-04}	0.929	2.20x10^{-02}	7.30x10^{-02}
MAP2K4	-0.100	1.10x10^{-03}	1.063	4.10x10^{-02}	1.10x10^{-01}
TRABD2A	-0.190	1.60x10^{-03}	1.072	3.30x10^{-02}	9.40x10^{-02}
PEX13	-0.074	1.60x10^{-03}	1.062	3.60x10^{-02}	1.00x10^{-01}
PCBP1	0.158	1.90x10^{-03}	0.924	2.40x10^{-02}	7.70x10^{-02}
SAMD8	-0.143	9.10x10^{-10}	1.040	2.66x10^{-01}	3.38x10^{-01}
RSRC2	-0.144	2.70x10^{-09}	1.082	6.70x10^{-02}	1.49x10^{-01}
PTAR1	-0.168	1.30x10^{-08}	1.051	1.99x10^{-01}	2.89x10^{-01}
TEX10	-0.116	5.10x10^{-08}	1.085	8.40x10^{-02}	1.72x10^{-01}
ARFGAP3	-0.153	5.80x10^{-08}	1.046	3.47x10^{-01}	3.89x10^{-01}
HLTF	-0.186	6.70x10^{-08}	1.098	1.77x10^{-01}	2.70x10^{-01}
C1orf27	-0.175	6.80x10^{-08}	1.005	8.92x10^{-01}	6.02x10^{-01}
ZNF211	-0.166	1.70x10^{-07}	1.045	2.58x10^{-01}	3.33x10^{-01}
CHD9	-0.158	6.70x10^{-07}	1.027	4.05x10^{-01}	4.20x10^{-01}
ZNF24	-0.114	9.40x10^{-07}	1.001	9.81x10^{-01}	6.23x10^{-01}
HECTD1	-0.106	1.10x10^{-06}	1.001	9.82x10^{-01}	6.23x10^{-01}
KAT8	-0.123	1.30x10^{-06}	1.016	6.51x10^{-01}	5.27x10^{-01}
BCLAF1	-0.127	2.20x10^{-06}	1.006	8.63x10^{-01}	5.93x10^{-01}
DENND4C	-0.132	2.20x10^{-06}	1.071	1.23x10^{-01}	2.18x10^{-01}
STAG2	-0.112	2.50x10^{-06}	1.046	2.19x10^{-01}	3.05x10^{-01}
PCF11	-0.121	3.00x10^{-06}	1.003	9.51x10^{-01}	6.16x10^{-01}
ATM	-0.131	3.40x10^{-06}	1.039	4.78x10^{-01}	4.56x10^{-01}
HIF1A	-0.170	4.50x10^{-06}	1.157	9.00x10^{-02}	1.80x10^{-01}
DNPH1	0.197	4.70x10^{-06}	0.913	6.10x10^{-02}	1.40x10^{-01}
SETX	-0.115	5.10x10^{-06}	1.014	6.54x10^{-01}	5.28x10^{-01}
ZNF627	-0.116	5.80x10^{-06}	1.077	6.30x10^{-02}	1.43x10^{-01}
ZNF432	-0.145	6.00x10^{-06}	1.054	1.49x10^{-01}	2.44x10^{-01}
FRRS1L	0.162	6.40x10^{-06}	0.994	7.23x10^{-01}	5.50x10^{-01}
CEP120	-0.126	7.10x10^{-06}	1.057	1.45x10^{-01}	2.41x10^{-01}
ZMYM1	-0.154	7.70x10^{-06}	1.022	6.38x10^{-01}	5.22x10^{-01}
RP11-264L1.2	0.192	7.80x10^{-06}	0.987	3.83x10^{-01}	4.08x10^{-01}

THAP2	-0.186	7.90x10^{-06}	1.023	3.66x10^{-01}	3.99x10^{-01}
NAA35	-0.102	8.40x10^{-06}	1.009	7.70x10^{-01}	5.65x10^{-01}
ANKRD34A	-0.338	9.30x10^{-06}	1.003	8.17x10^{-01}	5.80x10^{-01}
C12orf45	-0.177	1.00x10^{-05}	1.051	2.83x10^{-01}	3.50x10^{-01}
PWWP2A	-0.100	1.20x10^{-05}	1.014	5.99x10^{-01}	5.07x10^{-01}
TOPORS	-0.147	1.30x10^{-05}	1.022	5.05x10^{-01}	4.68x10^{-01}
KLF10	0.281	1.30x10^{-05}	0.932	4.63x10^{-01}	4.48x10^{-01}
MAP3K7CL	-0.482	1.50x10^{-05}	1.057	1.28x10^{-01}	2.24x10^{-01}
HOMER1	-0.277	1.60x10^{-05}	1.016	8.23x10^{-01}	5.81x10^{-01}
TUBE1	-0.136	1.70x10^{-05}	1.016	7.44x10^{-01}	5.57x10^{-01}
C12orf29	-0.246	2.30x10^{-05}	1.001	9.91x10^{-01}	6.26x10^{-01}
DHX15	-0.105	2.30x10^{-05}	1.049	1.36x10^{-01}	2.32x10^{-01}
NEK7	-0.113	2.80x10^{-05}	1.056	2.30x10^{-01}	3.13x10^{-01}
CREBRF	-0.116	3.20x10^{-05}	1.070	3.03x10^{-01}	3.62x10^{-01}
SENP7	-0.120	3.30x10^{-05}	1.083	1.60x10^{-01}	2.55x10^{-01}
ZNF160	-0.113	3.30x10^{-05}	1.068	1.65x10^{-01}	2.58x10^{-01}
KLHL28	-0.105	3.50x10^{-05}	1.068	2.16x10^{-01}	3.03x10^{-01}
FNTA	-0.076	3.70x10^{-05}	1.053	1.25x10^{-01}	2.21x10^{-01}
STAU2	-0.095	3.70x10^{-05}	1.036	2.84x10^{-01}	3.50x10^{-01}
SP3	-0.086	3.70x10^{-05}	1.009	7.30x10^{-01}	5.52x10^{-01}
ACAA2	0.160	3.80x10^{-05}	0.944	7.90x10^{-02}	1.66x10^{-01}
TNFSF4	-0.360	3.90x10^{-05}	1.036	3.66x10^{-01}	3.99x10^{-01}
KATNBL1	-0.202	4.70x10^{-05}	1.023	4.87x10^{-01}	4.60x10^{-01}
FBXL4	-0.119	4.90x10^{-05}	1.044	3.22x10^{-01}	3.74x10^{-01}
PEX1	-0.108	5.40x10^{-05}	1.005	9.17x10^{-01}	6.08x10^{-01}
PPP1R2	-0.104	5.90x10^{-05}	1.019	5.67x10^{-01}	4.95x10^{-01}
CSNK2A2	0.174	6.00x10^{-05}	0.991	7.58x10^{-01}	5.61x10^{-01}
ZNF841	-0.139	6.40x10^{-05}	1.102	6.10x10^{-02}	1.40x10^{-01}
NUP107	-0.145	6.50x10^{-05}	1.024	5.96x10^{-01}	5.05x10^{-01}
CEP290	-0.132	6.60x10^{-05}	1.069	2.66x10^{-01}	3.38x10^{-01}
DOCK11	-0.114	6.60x10^{-05}	1.010	7.82x10^{-01}	5.69x10^{-01}
POTEI	0.249	6.60x10^{-05}	0.949	1.25x10^{-01}	2.20x10^{-01}
TNPO1	-0.111	7.20x10^{-05}	1.035	3.35x10^{-01}	3.81x10^{-01}
ZNF417	-0.121	7.20x10^{-05}	1.076	1.12x10^{-01}	2.06x10^{-01}
SLC13A4	0.302	7.30x10^{-05}	0.984	2.19x10^{-01}	3.05x10^{-01}
TRMT11	-0.137	7.30x10^{-05}	1.010	8.00x10^{-01}	5.74x10^{-01}
ZNF132	-0.228	7.60x10^{-05}	1.051	8.80x10^{-02}	1.78x10^{-01}
CWF19L2	-0.102	9.30x10^{-05}	1.030	5.24x10^{-01}	4.77x10^{-01}
RANBP2	-0.113	9.30x10^{-05}	1.059	1.87x10^{-01}	2.79x10^{-01}
GLT8D1	-0.087	1.00x10^{-04}	1.026	3.69x10^{-01}	4.01x10^{-01}
TCP1	-0.098	1.10x10^{-04}	1.010	8.00x10^{-01}	5.74x10^{-01}
SMAD5	-0.187	1.10x10^{-04}	1.027	4.97x10^{-01}	4.64x10^{-01}
ALPK2	0.387	1.10x10^{-04}	1.000	9.85x10^{-01}	6.24x10^{-01}
MIA2	-0.133	1.20x10^{-04}	1.012	5.68x10^{-01}	4.95x10^{-01}
TRIP10	-0.250	1.20x10^{-04}	1.003	9.57x10^{-01}	6.18x10^{-01}
GPR37L1	0.219	1.30x10^{-04}	0.982	2.38x10^{-01}	3.19x10^{-01}

TPR	-0.092	1.40x10^{-04}	1.000	9.90x10^{-01}	6.25x10^{-01}
PARP8	-0.111	1.40x10^{-04}	1.065	2.66x10^{-01}	3.38x10^{-01}
ZNF329	-0.152	1.40x10^{-04}	1.043	7.50x10^{-02}	1.61x10^{-01}
TANK	-0.116	1.40x10^{-04}	1.021	5.66x10^{-01}	4.94x10^{-01}
ZNF235	-0.131	1.50x10^{-04}	1.056	1.80x10^{-01}	2.72x10^{-01}
AVL9	-0.081	1.50x10^{-04}	1.004	8.72x10^{-01}	5.95x10^{-01}
PPP2R5E	0.152	1.50x10^{-04}	0.978	4.27x10^{-01}	4.31x10^{-01}
HELLPAR	0.094	1.70x10^{-04}	0.991	4.89x10^{-01}	4.61x10^{-01}
TMEM68	-0.098	1.80x10^{-04}	1.002	8.82x10^{-01}	5.98x10^{-01}
DENND6A	-0.114	1.90x10^{-04}	1.032	4.09x10^{-01}	4.22x10^{-01}
MLH3	-0.286	1.90x10^{-04}	1.004	9.40x10^{-01}	6.14x10^{-01}
ZNF322	-0.125	2.00x10^{-04}	1.047	2.70x10^{-01}	3.41x10^{-01}
ZNF254	-0.152	2.10x10^{-04}	1.057	3.31x10^{-01}	3.79x10^{-01}
SIRT1	-0.094	2.20x10^{-04}	1.078	7.30x10^{-02}	1.58x10^{-01}
HAP1	0.369	2.30x10^{-04}	0.998	9.02x10^{-01}	6.04x10^{-01}
CAMKMT	-0.168	2.30x10^{-04}	1.025	4.61x10^{-01}	4.47x10^{-01}
ZNF606	-0.132	2.60x10^{-04}	1.028	4.80x10^{-01}	4.57x10^{-01}
PPA2	-0.097	2.80x10^{-04}	1.039	1.88x10^{-01}	2.80x10^{-01}
ZNF430	-0.112	2.90x10^{-04}	1.025	3.85x10^{-01}	4.10x10^{-01}
ZNF549	-0.104	3.00x10^{-04}	1.023	4.76x10^{-01}	4.55x10^{-01}
XPC	-0.109	3.00x10^{-04}	1.024	4.97x10^{-01}	4.64x10^{-01}
SYNJ2BP	-0.110	3.10x10^{-04}	1.033	3.09x10^{-01}	3.65x10^{-01}
INTS10	-0.084	3.10x10^{-04}	1.042	1.92x10^{-01}	2.83x10^{-01}
ZNF320	-0.189	3.20x10^{-04}	1.044	1.92x10^{-01}	2.83x10^{-01}
PREP	0.166	3.30x10^{-04}	0.952	2.02x10^{-01}	2.92x10^{-01}
ZNF765	-0.103	3.60x10^{-04}	1.001	9.68x10^{-01}	6.20x10^{-01}
CHP1	0.172	3.60x10^{-04}	0.943	1.23x10^{-01}	2.18x10^{-01}
PPWD1	-0.138	3.70x10^{-04}	1.046	2.87x10^{-01}	3.52x10^{-01}
SOCS7	-0.151	3.80x10^{-04}	1.024	2.78x10^{-01}	3.47x10^{-01}
L3MBTL3	-0.118	4.00x10^{-04}	1.090	1.25x10^{-01}	2.20x10^{-01}
RSBN1L	-0.095	4.20x10^{-04}	1.064	9.50x10^{-02}	1.87x10^{-01}
NGLY1	-0.069	5.00x10^{-04}	1.029	5.09x10^{-01}	4.70x10^{-01}
ATF2	-0.085	5.10x10^{-04}	1.046	1.24x10^{-01}	2.19x10^{-01}
OR1I1	0.144	5.70x10^{-04}	0.994	6.81x10^{-01}	5.37x10^{-01}
ATP10B	0.182	5.90x10^{-04}	0.959	6.10x10^{-02}	1.41x10^{-01}
NRG1	0.488	6.30x10^{-04}	0.938	4.39x10^{-01}	4.37x10^{-01}
WFDC1	0.206	6.30x10^{-04}	0.904	1.80x10^{-01}	2.73x10^{-01}
ZNF121	-0.113	6.90x10^{-04}	1.056	1.91x10^{-01}	2.82x10^{-01}
BET1	-0.106	8.40x10^{-04}	1.041	3.56x10^{-01}	3.93x10^{-01}
ARHGAP1	0.163	8.80x10^{-04}	0.962	5.18x10^{-01}	4.74x10^{-01}
HIP1R	-0.170	9.10x10^{-04}	1.031	3.17x10^{-01}	3.70x10^{-01}
SLC38A1	-0.125	9.40x10^{-04}	1.012	8.10x10^{-01}	5.77x10^{-01}
ZNF131	-0.110	1.10x10^{-03}	1.012	8.14x10^{-01}	5.78x10^{-01}
CPT1A	0.219	1.10x10^{-03}	0.889	5.10x10^{-02}	1.25x10^{-01}
ZNF273	-0.114	1.10x10^{-03}	1.007	8.78x10^{-01}	5.97x10^{-01}
PIGU	-0.141	1.20x10^{-03}	1.045	3.48x10^{-01}	3.89x10^{-01}

PLCG1	-0.145	1.20x10^{-03}	1.111	5.70x10^{-02}	1.35x10^{-01}
ZBTB41	-0.105	1.30x10^{-03}	1.040	4.64x10^{-01}	4.49x10^{-01}
ZNF264	-0.113	1.50x10^{-03}	1.042	1.93x10^{-01}	2.83x10^{-01}
MARK2	0.142	1.50x10^{-03}	0.982	6.44x10^{-01}	5.24x10^{-01}
ZNF382	-0.168	1.60x10^{-03}	1.072	5.70x10^{-02}	1.36x10^{-01}
PPIG	-0.090	1.60x10^{-03}	1.066	7.40x10^{-02}	1.59x10^{-01}
FAM20C	0.309	1.80x10^{-03}	0.951	5.18x10^{-01}	4.74x10^{-01}
FSTL1	-0.442	1.90x10^{-03}	1.066	2.95x10^{-01}	3.57x10^{-01}
CYTIP	-0.080	2.80x10^{-03}	1.082	3.56x10^{-01}	3.93x10^{-01}
DLG1	-0.099	3.30x10^{-03}	1.031	2.99x10^{-01}	3.60x10^{-01}
TXK	-0.159	3.50x10^{-03}	1.038	6.43x10^{-01}	5.24x10^{-01}
MALT1	-0.074	4.20x10^{-03}	1.095	5.70x10^{-02}	1.35x10^{-01}

Supplementary Table 3: Results of meta-analysis of PAH transcriptomic studies in lung tissue for RNAs associated with PAH in RNAseq. Table shows 372/507 genes from the PAH RNAseq analysis present in the PAH lung study. Data ordered based on dysregulation significance (p-value) in current PAH RNAseq analysis.

	PAH Meta-analysis			PAH Cohort		
Gene	**log2FC**	**Sig.**	**FDR**	**logFC**	**Sig.**	**FDR**
Same direction, significant, meeting FDR						
YTHDC1	-1.039	7.34x10^{-13}	1.64x10^{-09}	-0.118	7.82x10^{-05}	4.39x10^{-03}
NCR3	-1.084	1.32x10^{-12}	2.15x10^{-09}	-0.201	1.49x10^{-03}	2.35x10^{-02}
CEP85L	-1.107	4.52x10^{-12}	5.14x10^{-09}	-0.100	2.00x10^{-04}	7.55x10^{-03}
ZNF329	-1.047	6.31x10^{-12}	6.24x10^{-09}	-0.152	1.41x10^{-04}	6.16x10^{-03}
EPC1	-0.952	1.92x10^{-10}	7.80x10^{-08}	-0.062	1.04x10^{-03}	1.93x10^{-02}
TRMT11	-0.906	2.12x10^{-10}	8.32x10^{-08}	-0.137	7.33x10^{-05}	4.23x10^{-03}
GON4L	-0.885	5.56x10^{-10}	1.83x10^{-07}	-0.119	2.76x10^{-03}	3.36x10^{-02}
EPHX2	-0.874	7.98x10^{-10}	2.42x10^{-07}	-0.127	1.65x10^{-03}	2.48x10^{-02}
TMIGD2	-1.071	1.27x10^{-09}	3.66x10^{-07}	-0.249	1.28x10^{-03}	2.17x10^{-02}
BRWD1	-0.872	5.15x10^{-09}	1.23x10^{-06}	-0.108	3.80x10^{-04}	1.05x10^{-02}
PLCG1	-0.804	1.16x10^{-08}	2.26x10^{-06}	-0.145	1.17x10^{-03}	2.07x10^{-02}
IFI27	0.829	2.23x10^{-08}	3.65x10^{-06}	1.240	1.89x10^{-03}	2.70x10^{-02}
HIST2H3C	1.065	2.41x10^{-08}	3.81x10^{-06}	0.501	1.60x10^{-04}	6.50x10^{-03}
ZNF14	-0.949	3.72x10^{-08}	5.43x10^{-06}	-0.118	4.07x10^{-03}	4.22x10^{-02}
ZNF160	-0.806	6.32x10^{-08}	7.86x10^{-06}	-0.113	3.30x10^{-05}	2.86x10^{-03}
ATM	-0.767	7.01x10^{-08}	8.53x10^{-06}	-0.131	3.41x10^{-06}	8.29x10^{-04}
MTX3	-0.791	7.96x10^{-08}	9.38x10^{-06}	-0.101	1.45x10^{-03}	2.32x10^{-02}
URI1	-0.774	1.74x10^{-07}	1.78x10^{-05}	-0.090	9.44x10^{-04}	1.81x10^{-02}
DHX9	-0.695	2.71x10^{-07}	2.52x10^{-05}	-0.083	3.74x10^{-04}	1.04x10^{-02}
NR2C1	-0.708	5.70x10^{-07}	4.57x10^{-05}	-0.099	1.36x10^{-03}	2.25x10^{-02}
L3MBTL3	-0.731	5.91x10^{-07}	4.65x10^{-05}	-0.118	3.96x10^{-04}	1.08x10^{-02}
ATF7IP2	-0.862	6.10x10^{-07}	4.72x10^{-05}	-0.185	2.19x10^{-04}	7.96x10^{-03}
SOCS7	-0.712	1.13x10^{-06}	7.72x10^{-05}	-0.151	3.78x10^{-04}	1.05x10^{-02}
RPS25	-0.682	1.24x10^{-06}	8.42x10^{-05}	-0.112	3.27x10^{-03}	3.72x10^{-02}
ARGLU1	-0.707	1.30x10^{-06}	8.75x10^{-05}	-0.121	3.81x10^{-03}	4.08x10^{-02}
PEX1	-0.940	1.33x10^{-06}	8.87x10^{-05}	-0.108	5.43x10^{-05}	3.72x10^{-03}
ZMYM5	-0.860	1.43x10^{-06}	9.38x10^{-05}	-0.087	2.48x10^{-03}	3.15x10^{-02}
UTP23	-0.796	1.46x10^{-06}	9.52x10^{-05}	-0.078	2.89x10^{-03}	3.45x10^{-02}
NOG	-0.702	1.47x10^{-06}	9.56x10^{-05}	-0.357	1.79x10^{-03}	2.60x10^{-02}
JADE1	-0.848	2.26x10^{-06}	1.35x10^{-04}	-0.086	5.32x10^{-03}	4.92x10^{-02}
PDE6B	-0.762	2.42x10^{-06}	1.42x10^{-04}	-0.118	3.05x10^{-03}	3.57x10^{-02}
HNRNPK	-0.657	2.69x10^{-06}	1.55x10^{-04}	-0.102	2.40x10^{-05}	2.43x10^{-03}
MS4A4A	0.825	3.23x10^{-06}	1.79x10^{-04}	0.264	5.28x10^{-03}	4.89x10^{-02}
ANAPC16	-0.678	3.25x10^{-06}	1.79x10^{-04}	-0.088	1.57x10^{-03}	2.42x10^{-02}
NT5E	-0.657	3.24x10^{-06}	1.79x10^{-04}	-0.286	2.44x10^{-03}	3.13x10^{-02}
DBP	-0.618	4.43x10^{-06}	2.28x10^{-04}	-0.133	5.40x10^{-03}	4.97x10^{-02}
RABGGTB	-0.782	4.39x10^{-06}	2.28x10^{-04}	-0.094	1.59x10^{-03}	2.44x10^{-02}

FAM185A	-0.652	7.15x10^{-06}	3.31x10^{-04}	-0.168	2.49x10^{-03}	3.15x10^{-02}
SNHG1	-1.154	8.20x10^{-06}	3.64x10^{-04}	-0.124	7.89x10^{-04}	1.64x10^{-02}
ACAP1	-0.621	9.97x10^{-06}	4.19x10^{-04}	-0.117	2.28x10^{-03}	3.02x10^{-02}
ARHGEF18	-0.646	1.07x10^{-05}	4.37x10^{-04}	-0.111	3.39x10^{-03}	3.79x10^{-02}
INTS6	-0.832	1.17x10^{-05}	4.65x10^{-04}	-0.087	9.21x10^{-05}	4.82x10^{-03}
TMEM45A	0.638	1.31x10^{-05}	5.12x10^{-04}	0.124	4.64x10^{-04}	1.18x10^{-02}
AMD1	-0.614	1.33x10^{-05}	5.17x10^{-04}	-0.160	1.96x10^{-06}	6.42x10^{-04}
EIF4A2	-0.667	1.47x10^{-05}	5.58x10^{-04}	-0.141	7.62x10^{-06}	1.32x10^{-03}
TSGA10	-0.663	1.53x10^{-05}	5.71x10^{-04}	-0.140	3.47x10^{-03}	3.84x10^{-02}
COQ10A	-0.663	1.55x10^{-05}	5.75x10^{-04}	-0.096	3.79x10^{-03}	4.07x10^{-02}
MALT1	-0.662	1.75x10^{-05}	6.31x10^{-04}	-0.073	4.18x10^{-03}	4.28x10^{-02}
SLC30A4	-0.613	2.41x10^{-05}	8.15x10^{-04}	-0.097	4.34x10^{-03}	4.37x10^{-02}
TXK	-0.636	2.66x10^{-05}	8.78x10^{-04}	-0.159	3.51x10^{-03}	3.88x10^{-02}
ZNF432	-0.617	2.66x10^{-05}	8.78x10^{-04}	-0.145	6.03x10^{-06}	1.17x10^{-03}
ELANE	0.560	3.00x10^{-05}	9.75x10^{-04}	0.835	4.41x10^{-04}	1.16x10^{-02}
GALNT11	-0.768	3.18x10^{-05}	1.01x10^{-03}	-0.066	4.37x10^{-03}	4.38x10^{-02}
RAPH1	0.635	3.41x10^{-05}	1.07x10^{-03}	0.290	1.63x10^{-03}	2.47x10^{-02}
CAPN10	-0.635	3.40x10^{-05}	1.07x10^{-03}	-0.110	4.97x10^{-04}	1.24x10^{-02}
CCNB1IP1	-0.715	3.63x10^{-05}	1.13x10^{-03}	-0.150	5.61x10^{-07}	3.06x10^{-04}
ING3	-0.783	4.83x10^{-05}	1.41x10^{-03}	-0.087	8.18x10^{-04}	1.67x10^{-02}
MITF	0.558	6.26x10^{-05}	1.73x10^{-03}	0.155	1.82x10^{-03}	2.63x10^{-02}
UBASH3B	0.767	6.43x10^{-05}	1.77x10^{-03}	0.145	5.60x10^{-04}	1.33x10^{-02}
ANKRD44	-0.605	7.27x10^{-05}	1.94x10^{-03}	-0.067	4.46x10^{-03}	4.42x10^{-02}
ZNF506	-0.953	9.53x10^{-05}	2.38x10^{-03}	-0.155	4.51x10^{-05}	3.35x10^{-03}
CREBZF	-0.736	1.11x10^{-04}	2.66x10^{-03}	-0.138	1.85x10^{-04}	7.18x10^{-03}
HIP1R	-0.745	1.20x10^{-04}	2.80x10^{-03}	-0.169	9.14x10^{-04}	1.79x10^{-02}
TRABD2A	-0.976	1.20x10^{-04}	2.80x10^{-03}	-0.190	1.55x10^{-03}	2.40x10^{-02}
SUPT20H	-0.526	1.52x10^{-04}	3.37x10^{-03}	-0.076	1.96x10^{-03}	2.75x10^{-02}
CSE1L	-0.505	1.56x10^{-04}	3.42x10^{-03}	-0.115	3.10x10^{-04}	9.55x10^{-03}
ZNF626	-0.546	1.59x10^{-04}	3.49x10^{-03}	-0.181	1.94x10^{-03}	2.73x10^{-02}
UFM1	-0.502	1.70x10^{-04}	3.65x10^{-03}	-0.099	3.26x10^{-04}	9.81x10^{-03}
ZNF75A	-0.585	1.70x10^{-04}	3.65x10^{-03}	-0.101	5.72x10^{-04}	1.35x10^{-02}
ESYT2	-0.781	1.81x10^{-04}	3.83x10^{-03}	-0.131	9.19x10^{-05}	4.82x10^{-03}
CTNNB1	-0.668	2.00x10^{-04}	4.13x10^{-03}	-0.096	3.09x10^{-05}	2.80x10^{-03}
HAUS6	-0.515	2.11x10^{-04}	4.31x10^{-03}	-0.115	2.62x10^{-04}	8.77x10^{-03}
TMEM200A	0.564	2.23x10^{-04}	4.50x10^{-03}	0.328	9.51x10^{-04}	1.82x10^{-02}
LONP1	-0.510	2.37x10^{-04}	4.72x10^{-03}	-0.079	3.90x10^{-03}	4.13x10^{-02}
POLE3	-0.583	2.45x10^{-04}	4.84x10^{-03}	-0.085	1.28x10^{-03}	2.17x10^{-02}
MRI1	-0.557	2.58x10^{-04}	5.04x10^{-03}	-0.163	1.17x10^{-04}	5.58x10^{-03}
MAOB	0.504	2.73x10^{-04}	5.28x10^{-03}	0.282	4.38x10^{-03}	4.39x10^{-02}
RSAD1	-0.502	2.98x10^{-04}	5.65x10^{-03}	-0.100	3.84x10^{-03}	4.10x10^{-02}

CREBRF	-0.551	3.05x10^{-04}	5.75x10^{-03}	-0.116	3.23x10^{-05}	2.85x10^{-03}
TSR1	-0.499	3.16x10^{-04}	5.91x10^{-03}	-0.100	1.92x10^{-03}	2.72x10^{-02}
CYP20A1	-0.499	3.20x10^{-04}	5.95x10^{-03}	-0.077	3.91x10^{-03}	4.14x10^{-02}
FBLN2	-0.707	3.37x10^{-04}	6.21x10^{-03}	-0.355	2.99x10^{-03}	3.52x10^{-02}
DFFA	-0.477	3.62x10^{-04}	6.55x10^{-03}	-0.069	5.40x10^{-03}	4.97x10^{-02}
ZNF766	-0.539	4.02x10^{-04}	7.05x10^{-03}	-0.082	3.79x10^{-03}	4.07x10^{-02}
WTAP	-0.603	4.19x10^{-04}	7.24x10^{-03}	-0.060	4.12x10^{-03}	4.24x10^{-02}
HORMAD1	0.508	4.28x10^{-04}	7.32x10^{-03}	0.271	1.63x10^{-03}	2.47x10^{-02}
PRKRIP1	-0.487	4.54x10^{-04}	7.64x10^{-03}	-0.073	3.85x10^{-03}	4.10x10^{-02}
ZNF518B	-0.505	4.67x10^{-04}	7.79x10^{-03}	-0.149	2.67x10^{-05}	2.57x10^{-03}
PTAR1	-0.743	5.09x10^{-04}	8.33x10^{-03}	-0.168	1.35x10^{-08}	4.48x10^{-05}
RBM27	-0.736	5.29x10^{-04}	8.59x10^{-03}	-0.137	1.33x10^{-07}	1.49x10^{-04}
CCNB2	0.480	5.37x10^{-04}	8.70x10^{-03}	0.370	2.05x10^{-03}	2.83x10^{-02}
LCN2	0.548	5.57x10^{-04}	8.96x10^{-03}	0.435	3.29x10^{-03}	3.74x10^{-02}
URGCP	-0.482	5.67x10^{-04}	9.08x10^{-03}	-0.097	1.08x10^{-03}	1.97x10^{-02}
UHRF2	-0.493	6.05x10^{-04}	9.51x10^{-03}	-0.141	3.70x10^{-06}	8.70x10^{-04}
CEP120	-0.695	6.12x10^{-04}	9.58x10^{-03}	-0.126	7.14x10^{-06}	1.28x10^{-03}
MFNG	-0.473	6.16x10^{-04}	9.61x10^{-03}	-0.096	5.42x10^{-03}	4.97x10^{-02}
Same direction, significant						
BCKDHB	-1.054	5.41x10^{-13}	1.37x10^{-09}	-0.089	2.44x10^{-02}	1.21x10^{-01}
EIF4B	-0.989	1.01x10^{-12}	1.92x10^{-09}	-0.065	4.30x10^{-02}	1.67x10^{-01}
OBSCN	-1.131	1.79x10^{-12}	2.55x10^{-09}	-0.121	8.82x10^{-03}	6.61x10^{-02}
FOXP1	-1.047	4.65x10^{-11}	2.54x10^{-08}	-0.080	6.04x10^{-03}	5.31x10^{-02}
YWHAH	0.903	1.50x10^{-10}	6.69x10^{-08}	0.139	2.99x10^{-02}	1.36x10^{-01}
VWA5A	0.919	1.59x10^{-10}	6.96x10^{-08}	0.119	3.33x10^{-02}	1.44x10^{-01}
AK5	-0.99	3.88x10^{-10}	1.38x10^{-07}	-0.157	3.18x10^{-02}	1.40x10^{-01}
SUPV3L1	-0.891	4.07x10^{-10}	1.40x10^{-07}	-0.070	7.39x10^{-03}	5.91x10^{-02}
ABCB1	-0.901	3.50x10^{-09}	8.95x10^{-07}	-0.161	2.73x10^{-02}	1.29x10^{-01}
ATG16L1	-0.839	3.65x10^{-09}	9.23x10^{-07}	-0.056	1.90x10^{-02}	1.03x10^{-01}
ZNF551	-0.901	3.87x10^{-09}	9.68x10^{-07}	-0.105	8.13x10^{-03}	6.26x10^{-02}
AHSP	0.86	1.18x10^{-08}	2.28x10^{-06}	0.242	2.79x10^{-02}	1.30x10^{-01}
PLEKHG4	-0.798	5.82x10^{-08}	7.33x10^{-06}	-0.127	2.90x10^{-02}	1.34x10^{-01}
RAP1GAP	0.794	7.99x10^{-08}	9.38x10^{-06}	0.688	3.07x10^{-02}	1.38x10^{-01}
UBTF	-0.745	1.31x10^{-07}	1.43x10^{-05}	-0.081	6.46x10^{-03}	5.52x10^{-02}
STXBP5	-0.815	1.61x10^{-07}	1.67x10^{-05}	-0.080	1.48x10^{-02}	8.95x10^{-02}
CARD6	0.815	1.66x10^{-07}	1.72x10^{-05}	0.093	2.96x10^{-02}	1.35x10^{-01}
EIF2D	-0.737	1.68x10^{-07}	1.73x10^{-05}	-0.066	4.99x10^{-02}	1.82x10^{-01}
LAS1L	-0.733	1.98x10^{-07}	1.96x10^{-05}	-0.070	1.22x10^{-02}	8.03x10^{-02}
KPNA5	-0.732	2.47x10^{-07}	2.34x10^{-05}	-0.116	2.95x10^{-02}	1.35x10^{-01}
CTSL	0.732	3.03x10^{-07}	2.77x10^{-05}	0.211	3.09x10^{-02}	1.38x10^{-01}
CDC34	0.685	3.81x10^{-07}	3.33x10^{-05}	0.151	1.41x10^{-02}	8.72x10^{-02}
C3AR1	0.835	4.04x10^{-07}	3.50x10^{-05}	0.233	1.46x10^{-02}	8.89x10^{-02}
UXT	-0.711	4.21x10^{-07}	3.60x10^{-05}	-0.064	4.78x10^{-02}	1.77x10^{-01}

SPINK2	-0.883	$5.09x10^{-07}$	$4.20x10^{-05}$	-0.295	$6.03x10^{-03}$	$5.31x10^{-02}$
DHRS3	-1.009	$7.26x10^{-07}$	$5.40x10^{-05}$	-0.112	$3.84x10^{-02}$	$1.57x10^{-01}$
MYBL1	-0.962	$8.66x10^{-07}$	$6.30x10^{-05}$	-0.179	$1.21x10^{-02}$	$7.99x10^{-02}$
ASB3	-0.867	$8.88x10^{-07}$	$6.43x10^{-05}$	-0.059	$7.21x10^{-03}$	$5.79x10^{-02}$
ZIK1	-0.755	$9.94x10^{-07}$	$7.05x10^{-05}$	-0.106	$4.70x10^{-02}$	$1.76x10^{-01}$
TAF1D	-0.682	$1.13x10^{-06}$	$7.72x10^{-05}$	-0.090	$1.84x10^{-02}$	$1.01x10^{-01}$
EIF3D	-0.669	$1.78x10^{-06}$	$1.11x10^{-04}$	-0.074	$5.96x10^{-03}$	$5.28x10^{-02}$
TMEM243	-0.667	$2.06x10^{-06}$	$1.26x10^{-04}$	-0.051	$3.10x10^{-02}$	$1.38x10^{-01}$
NLE1	-0.684	$2.75x10^{-06}$	$1.57x10^{-04}$	-0.092	$2.87x10^{-02}$	$1.33x10^{-01}$
HIST1H2AE	0.657	$2.90x10^{-06}$	$1.64x10^{-04}$	0.101	$2.31x10^{-02}$	$1.17x10^{-01}$
TMC6	-0.69	$2.89x10^{-06}$	$1.64x10^{-04}$	-0.078	$1.80x10^{-02}$	$1.00x10^{-01}$
RAB11FIP4	-0.677	$3.36x10^{-06}$	$1.85x10^{-04}$	-0.085	$1.15x10^{-02}$	$7.75x10^{-02}$
SMARCC1	-0.624	$3.54x10^{-06}$	$1.92x10^{-04}$	-0.063	$3.78x10^{-02}$	$1.55x10^{-01}$
RNF185	0.673	$3.76x10^{-06}$	$2.01x10^{-04}$	0.097	$1.24x10^{-02}$	$8.12x10^{-02}$
CD320	-0.646	$3.93x10^{-06}$	$2.08x10^{-04}$	-0.118	$1.68x10^{-02}$	$9.63x10^{-02}$
MPP5	-0.647	$4.10x10^{-06}$	$2.16x10^{-04}$	-0.060	$3.04x10^{-02}$	$1.37x10^{-01}$
DPH5	-0.947	$4.15x10^{-06}$	$2.18x10^{-04}$	-0.068	$4.70x10^{-02}$	$1.76x10^{-01}$
POLR2E	0.975	$6.47x10^{-06}$	$3.06x10^{-04}$	0.117	$1.70x10^{-02}$	$9.66x10^{-02}$
CAMTA1	-0.652	$7.56x10^{-06}$	$3.43x10^{-04}$	-0.100	$1.03x10^{-02}$	$7.23x10^{-02}$
HOOK1	-0.651	$7.65x10^{-06}$	$3.45x10^{-04}$	-0.179	$1.38x10^{-02}$	$8.65x10^{-02}$
TCERG1	-0.771	$8.79x10^{-06}$	$3.82x10^{-04}$	-0.070	$1.69x10^{-02}$	$9.65x10^{-02}$
DNMT3A	-0.926	$9.33x10^{-06}$	$4.01x10^{-04}$	-0.067	$3.56x10^{-02}$	$1.50x10^{-01}$
PPIP5K1	-0.642	$9.61x10^{-06}$	$4.08x10^{-04}$	-0.105	$1.27x10^{-02}$	$8.25x10^{-02}$
KIF5C	-0.813	$1.02x10^{-05}$	$4.24x10^{-04}$	-0.196	$1.12x10^{-02}$	$7.62x10^{-02}$
LYAR	-0.639	$1.15x10^{-05}$	$4.59x10^{-04}$	-0.129	$1.60x10^{-02}$	$9.39x10^{-02}$
FILIP1L	0.588	$1.20x10^{-05}$	$4.73x10^{-04}$	0.155	$4.42x10^{-02}$	$1.69x10^{-01}$
KLRK1	-0.583	$1.47x10^{-05}$	$5.58x10^{-04}$	-0.138	$3.65x10^{-02}$	$1.53x10^{-01}$
PPM1B	-0.936	$1.50x10^{-05}$	$5.63x10^{-04}$	-0.055	$1.19x10^{-02}$	$7.93x10^{-02}$
TMEM170A	-0.755	$1.66x10^{-05}$	$6.05x10^{-04}$	-0.055	$4.12x10^{-02}$	$1.63x10^{-01}$
DNAJC9	-0.633	$1.73x10^{-05}$	$6.25x10^{-04}$	-0.055	$4.49x10^{-02}$	$1.71x10^{-01}$
YWHAG	0.622	$1.86x10^{-05}$	$6.58x10^{-04}$	0.094	$2.71x10^{-02}$	$1.28x10^{-01}$
VPS13A	-0.812	$2.04x10^{-05}$	$7.12x10^{-04}$	-0.072	$1.79x10^{-02}$	$1.00x10^{-01}$
DDHD2	-0.622	$2.18x10^{-05}$	$7.52x10^{-04}$	-0.079	$5.97x10^{-03}$	$5.28x10^{-02}$
DDX6	-0.588	$2.41x10^{-05}$	$8.15x10^{-04}$	-0.072	$9.68x10^{-03}$	$6.98x10^{-02}$
GKAP1	-0.698	$2.47x10^{-05}$	$8.30x10^{-04}$	-0.128	$1.43x10^{-02}$	$8.80x10^{-02}$
TMEM97	-0.564	$2.55x10^{-05}$	$8.53x10^{-04}$	-0.169	$6.12x10^{-03}$	$5.36x10^{-02}$
TMEM116	-0.611	$2.61x10^{-05}$	$8.66x10^{-04}$	-0.119	$9.79x10^{-03}$	$7.02x10^{-02}$
TRMT2B	-0.617	$2.64x10^{-05}$	$8.74x10^{-04}$	-0.070	$9.37x10^{-03}$	$6.87x10^{-02}$
TRMO	-0.613	$2.74x10^{-05}$	$9.04x10^{-04}$	-0.064	$8.61x10^{-03}$	$6.50x10^{-02}$
C7orf26	-0.571	$4.04x10^{-05}$	$1.23x10^{-03}$	-0.075	$2.63x10^{-02}$	$1.26x10^{-01}$
LETMD1	-0.572	$4.09x10^{-05}$	$1.24x10^{-03}$	-0.053	$2.49x10^{-02}$	$1.22x10^{-01}$
ZNF600	-0.58	$6.19x10^{-05}$	$1.72x10^{-03}$	-0.192	$6.18x10^{-03}$	$5.38x10^{-02}$
DCUN1D4	-0.533	$6.77x10^{-05}$	$1.84x10^{-03}$	-0.110	$4.54x10^{-02}$	$1.72x10^{-01}$
HMGB1	-0.771	$7.52x10^{-05}$	$1.99x10^{-03}$	-0.067	$1.25x10^{-02}$	$8.15x10^{-02}$
RORC	-0.574	$7.74x10^{-05}$	$2.03x10^{-03}$	-0.142	$2.74x10^{-02}$	$1.29x10^{-01}$
TARSL2	-0.646	$8.24x10^{-05}$	$2.13x10^{-03}$	-0.066	$2.79x10^{-02}$	$1.30x10^{-01}$

SIAH2	0.545	8.95x10^{-05}	2.27x10^{-03}	0.138	4.40x10^{-02}	1.69x10^{-01}
RAB3IP	-0.565	9.01x10^{-05}	2.28x10^{-03}	-0.158	5.78x10^{-03}	5.17x10^{-02}
PRDX1	0.567	9.44x10^{-05}	2.36x10^{-03}	0.060	4.41x10^{-02}	1.69x10^{-01}
NRCAM	-0.566	1.02x10^{-04}	2.50x10^{-03}	-0.488	1.33x10^{-02}	8.47x10^{-02}
MYO9A	-0.54	1.06x10^{-04}	2.58x10^{-03}	-0.070	1.90x10^{-02}	1.03x10^{-01}
PDK1	-0.566	1.09x10^{-04}	2.63x10^{-03}	-0.103	7.17x10^{-03}	5.78x10^{-02}
USP7	-0.537	1.13x10^{-04}	2.69x10^{-03}	-0.053	4.58x10^{-02}	1.73x10^{-01}
KLC3	0.588	1.14x10^{-04}	2.71x10^{-03}	0.231	3.28x10^{-02}	1.43x10^{-01}
SYTL1	-0.558	1.14x10^{-04}	2.71x10^{-03}	-0.072	4.11x10^{-02}	1.62x10^{-01}
SYTL2	-0.564	1.15x10^{-04}	2.72x10^{-03}	-0.177	1.83x10^{-02}	1.01x10^{-01}
HOPX	-0.564	1.16x10^{-04}	2.73x10^{-03}	-0.159	4.01x10^{-02}	1.60x10^{-01}
TRIM37	-0.536	1.18x10^{-04}	2.77x10^{-03}	-0.083	1.98x10^{-02}	1.06x10^{-01}
TMC8	-0.73	1.24x10^{-04}	2.89x10^{-03}	-0.088	2.66x10^{-02}	1.27x10^{-01}
TFAM	-0.608	1.28x10^{-04}	2.95x10^{-03}	-0.066	2.99x10^{-02}	1.36x10^{-01}
ZNHIT3	-0.622	1.34x10^{-04}	3.05x10^{-03}	-0.054	4.52x10^{-02}	1.72x10^{-01}
CAMLG	-0.542	1.35x10^{-04}	3.09x10^{-03}	-0.061	4.27x10^{-02}	1.66x10^{-01}
LRRC6	0.507	1.44x10^{-04}	3.24x10^{-03}	0.230	2.08x10^{-02}	1.09x10^{-01}
PCK2	0.686	1.65x10^{-04}	3.57x10^{-03}	0.128	2.25x10^{-02}	1.15x10^{-01}
LPL	0.521	1.71x10^{-04}	3.67x10^{-03}	0.412	3.42x10^{-02}	1.47x10^{-01}
PTPN4	-0.716	1.80x10^{-04}	3.81x10^{-03}	-0.110	7.05x10^{-03}	5.74x10^{-02}
ZNF93	-0.66	1.80x10^{-04}	3.81x10^{-03}	-0.109	1.06x10^{-02}	7.38x10^{-02}
SIGLEC5	0.519	1.86x10^{-04}	3.91x10^{-03}	0.174	4.60x10^{-02}	1.73x10^{-01}
TSEN54	-0.754	1.93x10^{-04}	4.02x10^{-03}	-0.127	1.44x10^{-02}	8.83x10^{-02}
ZNF154	-0.516	1.95x10^{-04}	4.06x10^{-03}	-0.201	2.04x10^{-02}	1.08x10^{-01}
PRKRA	-0.517	1.97x10^{-04}	4.08x10^{-03}	-0.058	3.41x10^{-02}	1.46x10^{-01}
CAPN7	-0.51	2.40x10^{-04}	4.77x10^{-03}	-0.045	3.56x10^{-02}	1.50x10^{-01}
INO80E	-0.524	2.80x10^{-04}	5.38x10^{-03}	-0.127	1.07x10^{-02}	7.42x10^{-02}
RAB11FIP2	-0.583	3.04x10^{-04}	5.73x10^{-03}	-0.072	2.10x10^{-02}	1.10x10^{-01}
MYO10	0.547	3.19x10^{-04}	5.94x10^{-03}	0.229	6.54x10^{-03}	5.55x10^{-02}
NID1	0.48	3.23x10^{-04}	6.00x10^{-03}	0.253	2.30x10^{-02}	1.17x10^{-01}
SMYD3	-0.525	3.25x10^{-04}	6.00x10^{-03}	-0.077	3.76x10^{-02}	1.55x10^{-01}
GID4	0.515	3.59x10^{-04}	6.54x10^{-03}	0.106	1.79x10^{-02}	1.00x10^{-01}
DUS1L	-0.604	3.66x10^{-04}	6.59x10^{-03}	-0.064	3.45x10^{-02}	1.47x10^{-01}
LYSMD4	-0.541	3.81x10^{-04}	6.79x10^{-03}	-0.095	3.59x10^{-02}	1.51x10^{-01}
SRI	0.496	3.84x10^{-04}	6.84x10^{-03}	0.060	4.86x10^{-02}	1.80x10^{-01}
SH3YL1	-0.558	4.55x10^{-04}	7.64x10^{-03}	-0.174	9.13x10^{-03}	6.74x10^{-02}
FAHD2A	-0.482	4.96x10^{-04}	8.18x10^{-03}	-0.071	4.56x10^{-02}	1.72x10^{-01}
TBC1D10C	-0.678	4.98x10^{-04}	8.19x10^{-03}	-0.095	1.20x10^{-02}	7.95x10^{-02}
GPRASP2	-0.499	5.48x10^{-04}	8.84x10^{-03}	-0.161	2.79x10^{-02}	1.30x10^{-01}
DHODH	-0.541	5.57x10^{-04}	8.96x10^{-03}	-0.074	4.24x10^{-02}	1.65x10^{-01}
Same direction						
PDE4D	-1.353			-0.047	3.73X10^{-01}	5.95X10^{-01}
RGPD8	-1.319	4.44X10^{-16}	5.05X10^{-12}	-0.072	3.84X10^{-01}	6.05X10^{-01}
LYL1	1.042	9.59X10^{-14}	4.36X10^{-10}	0.071	3.09X10^{-01}	5.33X10^{-01}
PITPNC1	-1.066	2.44X10^{-13}	9.13X10^{-10}	-0.035	3.92X10^{-01}	6.13X10^{-01}
TOP1MT	-1.071	1.47X10^{-12}	2.23X10^{-09}	-0.028	6.03X10^{-01}	7.76X10^{-01}

OSBP2	1.053	2.99X10^{-12}	3.64X10^{-09}	0.007	9.22X10^{-01}	9.65X10^{-01}
LTBP3	-1.007	3.04X10^{-12}	3.64X10^{-09}	-0.063	2.28X10^{-01}	4.47X10^{-01}
NR3C2	-1.181	5.03X10^{-12}	5.45X10^{-09}	-0.101	9.89X10^{-02}	2.72X10^{-01}
LY9	-0.995	7.67X10^{-12}	6.98X10^{-09}	-0.020	6.63X10^{-01}	8.14X10^{-01}
E2F2	1.027	8.17X10^{-12}	7.00X10^{-09}	0.001	9.85X10^{-01}	9.94X10^{-01}
PRKCH	-0.947	8.31X10^{-12}	7.00X10^{-09}	-0.019	5.80X10^{-01}	7.60X10^{-01}
FBL	-0.942	1.01X10^{-11}	8.21X10^{-09}	-0.084	1.28X10^{-01}	3.17X10^{-01}
ANAPC1	-1.014	1.58X10^{-11}	1.20X10^{-08}	-0.049	1.11X10^{-01}	2.92X10^{-01}
IFIT3	0.973	1.76X10^{-11}	1.25X10^{-08}	0.069	7.26X10^{-01}	8.54X10^{-01}
PATJ	-1.013	2.42X10^{-11}	1.67X10^{-08}	-0.028	4.98X10^{-01}	6.99X10^{-01}
RPL3	-0.92	2.62X10^{-11}	1.75X10^{-08}	-0.033	4.85X10^{-01}	6.89X10^{-01}
MTHFD2	0.952	3.65X10^{-11}	2.21X10^{-08}	0.040	3.67X10^{-01}	5.89X10^{-01}
IFIT1	0.913	3.77X10^{-11}	2.21X10^{-08}	0.198	4.59X10^{-01}	6.68X10^{-01}
MID2	-1.151	4.01X10^{-11}	2.28X10^{-08}	-0.145	7.98X10^{-02}	2.41X10^{-01}
TNFAIP6	0.907	4.91X10^{-11}	2.54X10^{-08}	0.127	3.17X10^{-01}	5.42X10^{-01}
EDAR	-0.941	6.01X10^{-11}	3.04X10^{-08}	-0.132	1.69X10^{-01}	3.75X10^{-01}
GMPR	0.892	8.46X10^{-11}	4.01X10^{-08}	0.152	5.05X10^{-02}	1.84X10^{-01}
SNRPN	-0.884	1.37X10^{-10}	6.23X10^{-08}	-0.035	3.28X10^{-01}	5.52X10^{-01}
BMPR1A	-0.904	2.42X10^{-10}	9.33X10^{-08}	-0.057	3.59X10^{-01}	5.82X10^{-01}
CCNT1	-0.929	4.01X10^{-10}	1.40X10^{-07}	-0.046	8.99X10^{-02}	2.58X10^{-01}
FAM153B	-0.881	5.93X10^{-10}	1.90X10^{-07}	-0.118	3.31X10^{-01}	5.55X10^{-01}
SLC25A36	-0.882	6.74X10^{-10}	2.10X10^{-07}	-0.013	6.52X10^{-01}	8.07X10^{-01}
MT2A	0.841	7.49X10^{-10}	2.30X10^{-07}	0.152	2.62X10^{-01}	4.84X10^{-01}
NEO1	-0.908	8.76X10^{-10}	2.62X10^{-07}	-0.049	5.81X10^{-01}	7.61X10^{-01}
MRPL9	-0.845	2.93X10^{-09}	7.84X10^{-07}	-0.005	8.57X10^{-01}	9.32X10^{-01}
EPSTI1	0.879	3.23X10^{-09}	8.35X10^{-07}	0.032	8.37X10^{-01}	9.21X10^{-01}
EPB42	0.832	4.38X10^{-09}	1.08X10^{-06}	0.020	8.21X10^{-01}	9.12X10^{-01}
SLC1A5	0.794	5.17X10^{-09}	1.23X10^{-06}	0.084	2.13X10^{-01}	4.29X10^{-01}
C12orf57	-0.919	5.21X10^{-09}	1.23X10^{-06}	-0.024	6.19X10^{-01}	7.86X10^{-01}
SLC2A4RG	-0.829	5.31X10^{-09}	1.23X10^{-06}	-0.018	7.17X10^{-01}	8.49X10^{-01}
PEBP1	-0.827	6.10X10^{-09}	1.37X10^{-06}	-0.015	6.24X10^{-01}	7.89X10^{-01}
PHLDB3	-0.857	7.02X10^{-09}	1.54X10^{-06}	-0.069	1.63X10^{-01}	3.66X10^{-01}
ACBD6	-0.857	7.06X10^{-09}	1.54X10^{-06}	-0.040	7.14X10^{-02}	2.26X10^{-01}
RPL22	-1.014	7.54X10^{-09}	1.62X10^{-06}	-0.039	3.03X10^{-01}	5.26X10^{-01}
CTSF	-0.954	8.18X10^{-09}	1.71X10^{-06}	-0.032	6.23X10^{-01}	7.89X10^{-01}
RSAD2	0.816	8.19X10^{-09}	1.71X10^{-06}	0.173	5.17X10^{-01}	7.14X10^{-01}
ZEB1	-0.861	8.20X10^{-09}	1.71X10^{-06}	-0.030	3.45X10^{-01}	5.69X10^{-01}
AGO3	-0.852	1.10X10^{-08}	2.18X10^{-06}	0.000	9.95X10^{-01}	9.97X10^{-01}
IGF2BP2	0.808	1.12X10^{-08}	2.20X10^{-06}	0.109	7.39X10^{-02}	2.29X10^{-01}
RHOH	-0.777	1.19X10^{-08}	2.28X10^{-06}	-0.011	7.50X10^{-01}	8.68X10^{-01}
WIPI2	0.809	1.21X10^{-08}	2.29X10^{-06}	0.008	7.68X10^{-01}	8.79X10^{-01}
DDX24	-0.806	1.22X10^{-08}	2.29X10^{-06}	-0.043	1.46X10^{-01}	3.43X10^{-01}
RPS3	-0.776	1.31X10^{-08}	2.44X10^{-06}	-0.028	5.53X10^{-01}	7.41X10^{-01}
MX2	0.771	1.43X10^{-08}	2.65X10^{-06}	0.019	7.70X10^{-01}	8.80X10^{-01}
PNP	0.768	1.56X10^{-08}	2.82X10^{-06}	0.055	2.90X10^{-01}	5.12X10^{-01}
ELK4	-0.84	1.72X10^{-08}	3.03X10^{-06}	-0.001	9.78X10^{-01}	9.91X10^{-01}

FPR3	0.833	1.73X10^{-08}	3.03X10^{-06}	0.206	8.52X10^{-02}	2.50X10^{-01}
CBFA2T2	-0.91	1.75X10^{-08}	3.04X10^{-06}	-0.050	2.88X10^{-01}	5.10X10^{-01}
LCK	-1.007	1.78X10^{-08}	3.07X10^{-06}	-0.039	3.32X10^{-01}	5.56X10^{-01}
CFAP36	-0.827	1.94X10^{-08}	3.29X10^{-06}	-0.001	9.87X10^{-01}	9.94X10^{-01}
OAS2	0.801	2.08X10^{-08}	3.45X10^{-06}	0.022	8.71X10^{-01}	9.39X10^{-01}
ARL4C	-1.145	2.08X10^{-08}	3.45X10^{-06}	-0.039	3.98X10^{-01}	6.18X10^{-01}
IL15	0.799	2.11X10^{-08}	3.48X10^{-06}	0.023	6.70X10^{-01}	8.19X10^{-01}
ANKRD23	-0.824	2.26X10^{-08}	3.67X10^{-06}	-0.087	1.47X10^{-01}	3.45X10^{-01}
PINK1	0.79	2.28X10^{-08}	3.68X10^{-06}	0.025	5.74X10^{-01}	7.55X10^{-01}
ATP6V0E2	-0.789	2.43X10^{-08}	3.81X10^{-06}	-0.072	1.98X10^{-01}	4.10X10^{-01}
HNRNPA1L2	-0.83	2.62X10^{-08}	4.06X10^{-06}	-0.053	1.59X10^{-01}	3.61X10^{-01}
RRAS2	-0.784	3.07X10^{-08}	4.61X10^{-06}	-0.044	4.15X10^{-01}	6.32X10^{-01}
PCTP	0.823	3.08X10^{-08}	4.61X10^{-06}	0.072	2.43X10^{-01}	4.64X10^{-01}
OAS1	0.824	3.28X10^{-08}	4.85X10^{-06}	0.136	3.63X10^{-01}	5.86X10^{-01}
SLC25A37	0.776	3.87X10^{-08}	5.57X10^{-06}	0.016	8.02X10^{-01}	9.00X10^{-01}
STOM	0.775	3.95X10^{-08}	5.62X10^{-06}	0.007	8.97X10^{-01}	9.53X10^{-01}
TCEAL3	-0.872	4.00X10^{-08}	5.65X10^{-06}	-0.075	1.19X10^{-01}	3.03X10^{-01}
FAM98C	-0.807	4.39X10^{-08}	6.09X10^{-06}	-0.066	7.12X10^{-02}	2.25X10^{-01}
RPS6	-0.74	4.60X10^{-08}	6.27X10^{-06}	-0.094	5.35X10^{-02}	1.90X10^{-01}
OAS3	0.771	4.95X10^{-08}	6.55X10^{-06}	0.159	4.69X10^{-01}	6.76X10^{-01}
SLC7A6	-0.742	5.03X10^{-08}	6.62X10^{-06}	-0.025	5.12X10^{-01}	7.11X10^{-01}
RPS5	-0.814	5.71X10^{-08}	7.33X10^{-06}	-0.035	4.57X10^{-01}	6.66X10^{-01}
TMCC2	0.797	5.81X10^{-08}	7.33X10^{-06}	0.119	2.03X10^{-01}	4.17X10^{-01}
NOSIP	-0.766	5.83X10^{-08}	7.33X10^{-06}	-0.042	2.56X10^{-01}	4.77X10^{-01}
HNMT	0.84	5.91X10^{-08}	7.39X10^{-06}	0.005	9.12X10^{-01}	9.60X10^{-01}
DRAM1	0.804	6.84X10^{-08}	8.41X10^{-06}	0.002	9.43X10^{-01}	9.75X10^{-01}
WDR89	-0.832	6.90X10^{-08}	8.44X10^{-06}	-0.042	1.95X10^{-01}	4.07X10^{-01}
SNX25	-0.832	8.28X10^{-08}	9.61X10^{-06}	-0.019	7.13X10^{-01}	8.46X10^{-01}
ODF2	-0.785	9.29X10^{-08}	1.06X10^{-05}	-0.037	2.01X10^{-01}	4.15X10^{-01}
SMIM11A	-0.832	9.39X10^{-08}	1.07X10^{-05}	-0.188	2.50X10^{-01}	4.71X10^{-01}
HK1	0.781	1.18X10^{-07}	1.32X10^{-05}	0.098	8.76X10^{-02}	2.54X10^{-01}
CD247	-0.717	1.33X10^{-07}	1.45X10^{-05}	-0.058	2.47X10^{-01}	4.68X10^{-01}
SNURF	-0.911	1.50X10^{-07}	1.58X10^{-05}	-0.006	9.32X10^{-01}	9.70X10^{-01}
DHRS7B	0.739	1.55X10^{-07}	1.62X10^{-05}	0.008	7.90X10^{-01}	8.92X10^{-01}
PDLIM7	0.741	1.75X10^{-07}	1.78X10^{-05}	0.026	5.84X10^{-01}	7.63X10^{-01}
KLHL3	-0.735	1.78X10^{-07}	1.78X10^{-05}	-0.010	8.57X10^{-01}	9.32X10^{-01}
RUNX2	-0.733	1.78X10^{-07}	1.78X10^{-05}	-0.083	1.11X10^{-01}	2.92X10^{-01}
IFIT1B	0.888	1.97X10^{-07}	1.96X10^{-05}	0.154	5.74X10^{-02}	1.98X10^{-01}
ECHDC2	-0.802	2.25X10^{-07}	2.19X10^{-05}	-0.034	4.52X10^{-01}	6.63X10^{-01}
MAP2K3	0.861	2.32X10^{-07}	2.24X10^{-05}	0.023	7.12X10^{-01}	8.45X10^{-01}
TRAFD1	0.725	2.41X10^{-07}	2.30X10^{-05}	0.005	9.23X10^{-01}	9.65X10^{-01}
VPS51	-0.725	2.45X10^{-07}	2.33X10^{-05}	-0.024	3.84X10^{-01}	6.05X10^{-01}
RPL4	-0.768	2.57X10^{-07}	2.43X10^{-05}	-0.022	4.99X10^{-01}	6.99X10^{-01}
SAFB2	-0.697	2.63X10^{-07}	2.47X10^{-05}	-0.033	1.65X10^{-01}	3.69X10^{-01}
MIB2	-0.753	2.64X10^{-07}	2.47X10^{-05}	-0.076	7.07X10^{-02}	2.24X10^{-01}
MPP6	-0.796	2.83X10^{-07}	2.62X10^{-05}	-0.113	8.11X10^{-02}	2.43X10^{-01}

PPME1	0.758	$3.01X10^{-07}$	$2.76X10^{-05}$	0.014	$7.64X10^{-01}$	$8.77X10^{-01}$
SERGEF	-0.75	$3.06X10^{-07}$	$2.78X10^{-05}$	-0.037	$2.81X10^{-01}$	$5.02X10^{-01}$
LMF1	-0.772	$3.30X10^{-07}$	$2.97X10^{-05}$	-0.038	$4.58X10^{-01}$	$6.67X10^{-01}$
RNF213	0.746	$3.67X10^{-07}$	$3.25X10^{-05}$	0.053	$5.13X10^{-01}$	$7.11X10^{-01}$
GATA1	0.712	$3.70X10^{-07}$	$3.26X10^{-05}$	0.058	$4.54X10^{-01}$	$6.64X10^{-01}$
PRPF4B	-0.741	$3.92X10^{-07}$	$3.42X10^{-05}$	-0.036	$6.50X10^{-02}$	$2.13X10^{-01}$
IMPDH2	-0.679	$4.89X10^{-07}$	$4.11X10^{-05}$	-0.031	$3.21X10^{-01}$	$5.45X10^{-01}$
POLR1E	-0.825	$4.99X10^{-07}$	$4.14X10^{-05}$	-0.062	$8.69X10^{-02}$	$2.53X10^{-01}$
B3GLCT	-0.868	$5.62X10^{-07}$	$4.55X10^{-05}$	-0.062	$1.13X10^{-01}$	$2.95X10^{-01}$
HNRNPA3	-0.825	$5.66X10^{-07}$	$4.57X10^{-05}$	0.000	$9.95X10^{-01}$	$9.98X10^{-01}$
BLVRB	0.795	$5.84X10^{-07}$	$4.65X10^{-05}$	0.011	$8.82X10^{-01}$	$9.44X10^{-01}$
KMT2E	-0.775	$5.85X10^{-07}$	$4.65X10^{-05}$	-0.016	$4.53X10^{-01}$	$6.63X10^{-01}$
RTN2	0.74	$5.89X10^{-07}$	$4.65X10^{-05}$	0.009	$8.88X10^{-01}$	$9.48X10^{-01}$
SERF1B	-0.739	$5.91X10^{-07}$	$4.65X10^{-05}$	-0.085	$1.22X10^{-01}$	$3.08X10^{-01}$
EEF2	-0.7	$5.99X10^{-07}$	$4.67X10^{-05}$	-0.011	$7.91X10^{-01}$	$8.92X10^{-01}$
NIPSNAP1	-0.701	$5.99X10^{-07}$	$4.67X10^{-05}$	-0.078	$9.83X10^{-02}$	$2.72X10^{-01}$
MLX	0.836	$6.06X10^{-07}$	$4.71X10^{-05}$	0.002	$9.55X10^{-01}$	$9.81X10^{-01}$
DMXL2	0.828	$6.49X10^{-07}$	$4.96X10^{-05}$	0.006	$8.86X10^{-01}$	$9.47X10^{-01}$
RIN2	0.71	$7.00X10^{-07}$	$5.25X10^{-05}$	0.121	$5.86X10^{-02}$	$2.01X10^{-01}$
PAK1	0.67	$7.10X10^{-07}$	$5.30X10^{-05}$	0.031	$3.80X10^{-01}$	$6.01X10^{-01}$
ZNF8	-0.688	$9.05X10^{-07}$	$6.54X10^{-05}$	-0.036	$2.65X10^{-01}$	$4.87X10^{-01}$
CHIC1	-0.984	$9.15X10^{-07}$	$6.57X10^{-05}$	-0.069	$8.21X10^{-02}$	$2.45X10^{-01}$
EPHB2	0.692	$9.56X10^{-07}$	$6.82X10^{-05}$	0.080	$5.31X10^{-01}$	$7.25X10^{-01}$
WDR86	-0.818	$9.69X10^{-07}$	$6.89X10^{-05}$	-0.159	$6.75X10^{-02}$	$2.18X10^{-01}$
SPTB	0.719	$1.02X10^{-06}$	$7.19X10^{-05}$	0.038	$6.51X10^{-01}$	$8.06X10^{-01}$
ZCWPW1	-0.715	$1.05X10^{-06}$	$7.35X10^{-05}$	-0.001	$9.73X10^{-01}$	$9.88X10^{-01}$
TNS1	0.774	$1.06X10^{-06}$	$7.38X10^{-05}$	0.048	$5.52X10^{-01}$	$7.40X10^{-01}$
ZNF529	-0.68	$1.27X10^{-06}$	$8.60X10^{-05}$	-0.046	$7.90X10^{-02}$	$2.40X10^{-01}$
KEL	0.676	$1.32X10^{-06}$	$8.83X10^{-05}$	0.037	$6.63X10^{-01}$	$8.14X10^{-01}$
MICAL2	0.679	$1.32X10^{-06}$	$8.83X10^{-05}$	0.007	$8.73X10^{-01}$	$9.40X10^{-01}$
IFI44	0.652	$1.36X10^{-06}$	$9.00X10^{-05}$	0.125	$5.70X10^{-01}$	$7.52X10^{-01}$
RPL36	-0.676	$1.36X10^{-06}$	$9.00X10^{-05}$	-0.023	$5.70X10^{-01}$	$7.52X10^{-01}$
HP1BP3	-0.744	$1.38X10^{-06}$	$9.10X10^{-05}$	-0.068	$1.74X10^{-01}$	$3.82X10^{-01}$
ANK1	0.709	$1.45X10^{-06}$	$9.48X10^{-05}$	0.009	$9.36X10^{-01}$	$9.71X10^{-01}$
MRPL55	-0.704	$1.51X10^{-06}$	$9.73X10^{-05}$	-0.018	$5.71X10^{-01}$	$7.53X10^{-01}$
EIF3L	-0.675	$1.52X10^{-06}$	$9.77X10^{-05}$	-0.057	$1.94X10^{-01}$	$4.06X10^{-01}$
VWA8	-0.994	$1.57X10^{-06}$	$1.01X10^{-04}$	-0.040	$3.74X10^{-01}$	$5.95X10^{-01}$
RPS13	-0.673	$1.63X10^{-06}$	$1.04X10^{-04}$	-0.062	$1.03X10^{-01}$	$2.80X10^{-01}$
COX19	-0.699	$1.64X10^{-06}$	$1.05X10^{-04}$	-0.006	$8.36X10^{-01}$	$9.21X10^{-01}$
ATP8B4	0.67	$1.66X10^{-06}$	$1.06X10^{-04}$	0.046	$3.93X10^{-01}$	$6.13X10^{-01}$
ADIPOR1	0.671	$1.76X10^{-06}$	$1.11X10^{-04}$	0.007	$8.94X10^{-01}$	$9.51X10^{-01}$
TMTC1	0.736	$1.77X10^{-06}$	$1.11X10^{-04}$	0.158	$3.80X10^{-01}$	$6.02X10^{-01}$
PLCD1	-0.668	$1.79X10^{-06}$	$1.12X10^{-04}$	-0.069	$1.18X10^{-01}$	$3.03X10^{-01}$
LRIG1	-0.829	$1.89X10^{-06}$	$1.17X10^{-04}$	-0.029	$5.38X10^{-01}$	$7.30X10^{-01}$
RPL14	-0.952	$1.90X10^{-06}$	$1.17X10^{-04}$	-0.042	$2.00X10^{-01}$	$4.14X10^{-01}$
C11orf80	-0.694	$1.97X10^{-06}$	$1.21X10^{-04}$	-0.026	$6.53X10^{-01}$	$8.07X10^{-01}$

RPS20	-0.665	2.09X10^{-06}	1.27X10^{-04}	-0.032	4.24X10^{-01}	6.40X10^{-01}
SQLE	0.668	2.10X10^{-06}	1.27X10^{-04}	0.049	3.75X10^{-01}	5.97X10^{-01}
PRKAR2A	-0.664	2.12X10^{-06}	1.28X10^{-04}	-0.027	3.41X10^{-01}	5.64X10^{-01}
EIF3H	-0.664	2.14X10^{-06}	1.29X10^{-04}	-0.022	3.49X10^{-01}	5.73X10^{-01}
LRRC14	-0.744	2.14X10^{-06}	1.29X10^{-04}	-0.049	3.54X10^{-01}	5.78X10^{-01}
P4HTM	-0.663	2.29X10^{-06}	1.36X10^{-04}	-0.054	1.19X10^{-01}	3.04X10^{-01}
BEX4	-0.737	2.35X10^{-06}	1.38X10^{-04}	-0.083	6.78X10^{-02}	2.19X10^{-01}
RPS29	-0.633	2.58X10^{-06}	1.51X10^{-04}	-0.039	4.19X10^{-01}	6.36X10^{-01}
C1QTNF6	-0.684	2.64X10^{-06}	1.52X10^{-04}	-0.091	9.28X10^{-02}	2.63X10^{-01}
ANO9	-0.682	2.73X10^{-06}	1.56X10^{-04}	-0.084	1.25X10^{-01}	3.13X10^{-01}
SRSF3	-0.63	2.73X10^{-06}	1.56X10^{-04}	-0.018	5.04X10^{-01}	7.04X10^{-01}
BEST1	0.9	2.77X10^{-06}	1.58X10^{-04}	0.015	7.22X10^{-01}	8.51X10^{-01}
SEMA4F	-0.655	2.80X10^{-06}	1.59X10^{-04}	-0.012	8.39X10^{-01}	9.23X10^{-01}
CDC42SE2	-0.746	2.91X10^{-06}	1.64X10^{-04}	-0.040	1.21X10^{-01}	3.06X10^{-01}
TTC32	-0.683	3.02X10^{-06}	1.70X10^{-04}	-0.077	6.46X10^{-02}	2.12X10^{-01}
RPUSD2	-0.65	3.49X10^{-06}	1.90X10^{-04}	-0.045	2.24X10^{-01}	4.42X10^{-01}
MAN1C1	-0.836	3.65X10^{-06}	1.96X10^{-04}	-0.045	3.92X10^{-01}	6.13X10^{-01}
WBP2	0.648	3.78X10^{-06}	2.01X10^{-04}	0.027	6.56X10^{-01}	8.09X10^{-01}
EPHB6	-0.648	3.78X10^{-06}	2.01X10^{-04}	-0.003	9.73X10^{-01}	9.89X10^{-01}
NDUFAF1	0.647	3.93X10^{-06}	2.08X10^{-04}	0.056	9.00X10^{-02}	2.58X10^{-01}
EIF2A	-0.707	4.21X10^{-06}	2.20X10^{-04}	-0.052	9.77X10^{-02}	2.71X10^{-01}
PML	0.693	4.26X10^{-06}	2.22X10^{-04}	0.022	8.30X10^{-01}	9.17X10^{-01}
SFXN1	-0.643	4.41X10^{-06}	2.28X10^{-04}	-0.004	9.17X10^{-01}	9.62X10^{-01}
MX1	0.617	4.42X10^{-06}	2.28X10^{-04}	0.075	6.63X10^{-01}	8.14X10^{-01}
RTTN	-0.874	4.56X10^{-06}	2.34X10^{-04}	-0.008	7.30X10^{-01}	8.56X10^{-01}
ACVR1C	-0.722	4.62X10^{-06}	2.37X10^{-04}	-0.098	2.12X10^{-01}	4.28X10^{-01}
YBX3	0.615	4.90X10^{-06}	2.46X10^{-04}	0.068	2.88X10^{-01}	5.10X10^{-01}
FHL2	0.671	5.07X10^{-06}	2.51X10^{-04}	0.099	1.50X10^{-01}	3.49X10^{-01}
TSR2	-0.639	5.07X10^{-06}	2.51X10^{-04}	-0.008	8.10X10^{-01}	9.05X10^{-01}
NCL	-0.614	5.12X10^{-06}	2.52X10^{-04}	-0.056	2.62X10^{-01}	4.84X10^{-01}
RPS10	-0.613	5.42X10^{-06}	2.65X10^{-04}	-0.005	9.18X10^{-01}	9.63X10^{-01}
RAD51C	-0.77	5.45X10^{-06}	2.66X10^{-04}	-0.064	2.18X10^{-01}	4.36X10^{-01}
ILK	0.778	5.85X10^{-06}	2.84X10^{-04}	0.034	5.33X10^{-01}	7.27X10^{-01}
NCEH1	0.66	6.17X10^{-06}	2.96X10^{-04}	0.010	8.42X10^{-01}	9.24X10^{-01}
HMBS	0.663	6.49X10^{-06}	3.06X10^{-04}	0.097	2.16X10^{-01}	4.33X10^{-01}
RPL37	-0.628	7.12X10^{-06}	3.30X10^{-04}	-0.056	1.61X10^{-01}	3.64X10^{-01}
VILL	-0.688	7.21X10^{-06}	3.32X10^{-04}	-0.054	1.37X10^{-01}	3.29X10^{-01}
SP110	0.632	7.29X10^{-06}	3.35X10^{-04}	0.079	1.30X10^{-01}	3.19X10^{-01}
WDR41	0.627	7.34X10^{-06}	3.37X10^{-04}	0.006	8.72X10^{-01}	9.40X10^{-01}
GP1BA	0.603	7.46X10^{-06}	3.39X10^{-04}	0.090	3.85X10^{-01}	6.06X10^{-01}
CCDC136	-0.65	7.51X10^{-06}	3.41X10^{-04}	0.000	1.00E+00	1.00E+00
WDR33	-0.625	7.61X10^{-06}	3.44X10^{-04}	-0.022	2.30X10^{-01}	4.49X10^{-01}
NOTCH2	0.754	8.02X10^{-06}	3.59X10^{-04}	0.066	7.66X10^{-02}	2.34X10^{-01}
TUBGCP6	-0.685	8.09X10^{-06}	3.61X10^{-04}	-0.023	4.79X10^{-01}	6.83X10^{-01}
PARVB	0.624	8.17X10^{-06}	3.63X10^{-04}	0.099	1.47X10^{-01}	3.45X10^{-01}
PARP2	-0.623	8.27X10^{-06}	3.65X10^{-04}	-0.021	4.92X10^{-01}	6.95X10^{-01}

ZNF862	-0.799	8.42X10^{-06}	3.69X10^{-04}	-0.022	5.26X10^{-01}	7.21X10^{-01}
SLC6A8	0.596	8.81X10^{-06}	3.83X10^{-04}	0.116	2.18X10^{-01}	4.35X10^{-01}
AGAP1	-0.952	9.46X10^{-06}	4.05X10^{-04}	-0.120	2.66X10^{-01}	4.89X10^{-01}
TMEM8B	-0.652	9.62X10^{-06}	4.08X10^{-04}	-0.028	6.51X10^{-01}	8.07X10^{-01}
PRKCD	0.778	1.02X10^{-05}	4.24X10^{-04}	0.030	6.13X10^{-01}	7.82X10^{-01}
GNLY	-0.592	1.03X10^{-05}	4.25X10^{-04}	-0.177	1.05X10^{-01}	2.82X10^{-01}
ZGPAT	-0.615	1.04X10^{-05}	4.27X10^{-04}	-0.060	1.05X10^{-01}	2.82X10^{-01}
MRPL10	-0.64	1.06X10^{-05}	4.34X10^{-04}	-0.007	8.89X10^{-01}	9.48X10^{-01}
TDP1	-0.643	1.15X10^{-05}	4.59X10^{-04}	-0.049	6.84X10^{-02}	2.20X10^{-01}
TMEM25	-0.637	1.19X10^{-05}	4.70X10^{-04}	-0.061	2.28X10^{-01}	4.47X10^{-01}
PCYOX1	-0.608	1.33X10^{-05}	5.17X10^{-04}	-0.075	7.22X10^{-02}	2.27X10^{-01}
RSL1D1	-0.605	1.38X10^{-05}	5.29X10^{-04}	-0.045	2.37X10^{-01}	4.57X10^{-01}
BBS9	-0.637	1.39X10^{-05}	5.32X10^{-04}	-0.080	6.20X10^{-02}	2.08X10^{-01}
CHD3	-0.604	1.48X10^{-05}	5.60X10^{-04}	-0.073	6.81X10^{-02}	2.19X10^{-01}
RPL30	-0.604	1.50X10^{-05}	5.63X10^{-04}	-0.029	3.38X10^{-01}	5.62X10^{-01}
DGCR6	-0.702	1.51X10^{-05}	5.66X10^{-04}	-0.039	5.93X10^{-01}	7.69X10^{-01}
NKTR	-0.722	1.52X10^{-05}	5.69X10^{-04}	-0.046	8.89X10^{-02}	2.57X10^{-01}
SSR2	-0.603	1.55X10^{-05}	5.75X10^{-04}	-0.004	8.59X10^{-01}	9.34X10^{-01}
GAS2L1	0.606	1.63X10^{-05}	5.99X10^{-04}	0.122	2.05X10^{-01}	4.20X10^{-01}
CNNM3	-0.661	1.64X10^{-05}	6.00X10^{-04}	-0.058	1.59X10^{-01}	3.61X10^{-01}
IL23A	-0.603	1.64X10^{-05}	6.00X10^{-04}	-0.012	8.35X10^{-01}	9.20X10^{-01}
EIF3G	-0.599	1.68X10^{-05}	6.11X10^{-04}	-0.031	2.10X10^{-01}	4.25X10^{-01}
ALAS2	0.679	1.82X10^{-05}	6.48X10^{-04}	0.178	1.55X10^{-01}	3.56X10^{-01}
ISYNA1	-0.599	1.82X10^{-05}	6.48X10^{-04}	-0.087	2.66X10^{-01}	4.88X10^{-01}
USP13	-0.574	1.87X10^{-05}	6.61X10^{-04}	-0.048	3.49X10^{-01}	5.72X10^{-01}
SGO2	0.655	1.92X10^{-05}	6.74X10^{-04}	0.070	7.49X10^{-02}	2.31X10^{-01}
KRT18	-0.595	1.92X10^{-05}	6.74X10^{-04}	-0.078	2.07X10^{-01}	4.22X10^{-01}
MRPS30	-0.852	2.02X10^{-05}	7.06X10^{-04}	-0.055	7.22X10^{-02}	2.27X10^{-01}
OTUD4	-0.635	2.05X10^{-05}	7.13X10^{-04}	-0.060	8.20X10^{-02}	2.45X10^{-01}
MTMR3	0.788	2.09X10^{-05}	7.23X10^{-04}	0.001	9.75X10^{-01}	9.90X10^{-01}
HERC5	0.591	2.22X10^{-05}	7.63X10^{-04}	0.010	9.61X10^{-01}	9.84X10^{-01}
H1F0	0.668	2.32X10^{-05}	7.93X10^{-04}	0.161	2.76X10^{-01}	4.98X10^{-01}
MAPK13	-0.591	2.34X10^{-05}	7.98X10^{-04}	-0.023	6.55X10^{-01}	8.09X10^{-01}
ZNF365	-0.649	2.35X10^{-05}	7.99X10^{-04}	-0.114	2.35X10^{-01}	4.55X10^{-01}
TGFBR2	-0.669	2.42X10^{-05}	8.17X10^{-04}	-0.071	7.24X10^{-02}	2.27X10^{-01}
SH2D3A	-0.586	2.58X10^{-05}	8.62X10^{-04}	-0.046	2.80X10^{-01}	5.02X10^{-01}
MERTK	0.563	2.60X10^{-05}	8.65X10^{-04}	0.091	4.48X10^{-01}	6.59X10^{-01}
ATAD3A	-0.585	2.60X10^{-05}	8.65X10^{-04}	-0.058	2.06X10^{-01}	4.21X10^{-01}
SREK1	-0.588	2.61X10^{-05}	8.66X10^{-04}	-0.061	5.42X10^{-02}	1.92X10^{-01}
DHCR7	-0.608	2.80X10^{-05}	9.21X10^{-04}	-0.062	3.36X10^{-01}	5.60X10^{-01}
KCTD11	0.606	3.00X10^{-05}	9.75X10^{-04}	0.037	4.37X10^{-01}	6.51X10^{-01}
PHB2	-0.559	3.02X10^{-05}	9.77X10^{-04}	-0.033	1.96X10^{-01}	4.09X10^{-01}
DUS3L	-0.605	3.05X10^{-05}	9.83X10^{-04}	-0.035	4.08X10^{-01}	6.27X10^{-01}
ULK3	-0.604	3.05X10^{-05}	9.83X10^{-04}	-0.116	1.76X10^{-01}	3.83X10^{-01}
RACK1	-0.557	3.17X10^{-05}	1.01X10^{-03}	-0.018	5.59X10^{-01}	7.45X10^{-01}
BBS4	-0.579	3.22X10^{-05}	1.02X10^{-03}	-0.027	4.51X10^{-01}	6.62X10^{-01}

LRRC23	-0.556	3.37X10^{-05}	1.07X10^{-03}	-0.089	1.81X10^{-01}	3.90X10^{-01}
SIGLEC1	0.577	3.38X10^{-05}	1.07X10^{-03}	0.320	2.55X10^{-01}	4.76X10^{-01}
NHP2	-0.576	3.44X10^{-05}	1.08X10^{-03}	-0.029	2.59X10^{-01}	4.80X10^{-01}
PPRC1	-0.576	3.66X10^{-05}	1.13X10^{-03}	-0.065	3.87X10^{-01}	6.08X10^{-01}
NOL11	-0.64	3.78X10^{-05}	1.16X10^{-03}	-0.030	2.20X10^{-01}	4.37X10^{-01}
COLQ	-0.841	3.83X10^{-05}	1.17X10^{-03}	-0.110	3.11X10^{-01}	5.35X10^{-01}
PIKFYVE	-0.573	3.96X10^{-05}	1.21X10^{-03}	-0.048	5.45X10^{-02}	1.93X10^{-01}
ABHD17A	-0.573	4.07X10^{-05}	1.24X10^{-03}	-0.036	2.34X10^{-01}	4.53X10^{-01}
RPL19	-0.55	4.09X10^{-05}	1.24X10^{-03}	-0.081	5.31X10^{-02}	1.90X10^{-01}
DAZAP1	-0.571	4.16X10^{-05}	1.26X10^{-03}	-0.028	2.50X10^{-01}	4.71X10^{-01}
ENO3	-0.69	4.19X10^{-05}	1.26X10^{-03}	-0.049	3.56X10^{-01}	5.80X10^{-01}
RIPK3	0.593	4.20X10^{-05}	1.26X10^{-03}	0.010	8.10X10^{-01}	9.05X10^{-01}
CTNNAL1	0.569	4.29X10^{-05}	1.28X10^{-03}	0.007	9.35X10^{-01}	9.71X10^{-01}
RUNDC3A	0.592	4.29X10^{-05}	1.28X10^{-03}	0.162	1.44X10^{-01}	3.40X10^{-01}
ELP2	-0.651	4.53X10^{-05}	1.35X10^{-03}	-0.051	9.24X10^{-02}	2.62X10^{-01}
RPL23A	-0.573	4.53X10^{-05}	1.35X10^{-03}	-0.004	9.03X10^{-01}	9.55X10^{-01}
ZBTB49	-0.59	4.71X10^{-05}	1.39X10^{-03}	-0.083	6.07X10^{-02}	2.05X10^{-01}
OPRL1	0.571	4.76X10^{-05}	1.40X10^{-03}	0.054	3.85X10^{-01}	6.06X10^{-01}
WDR59	-0.693	5.03X10^{-05}	1.46X10^{-03}	-0.007	8.43X10^{-01}	9.25X10^{-01}
IFI44L	0.567	5.17X10^{-05}	1.50X10^{-03}	0.218	4.77X10^{-01}	6.82X10^{-01}
PCNX2	-0.836	5.18X10^{-05}	1.50X10^{-03}	-0.073	7.46X10^{-02}	2.30X10^{-01}
SNPH	-0.712	5.19X10^{-05}	1.50X10^{-03}	-0.024	6.84X10^{-01}	8.27X10^{-01}
SOX6	0.561	5.46X10^{-05}	1.56X10^{-03}	0.041	6.24X10^{-01}	7.90X10^{-01}
TRIM6	0.585	5.49X10^{-05}	1.57X10^{-03}	0.059	6.37X10^{-01}	7.98X10^{-01}
DLGAP5	0.586	5.52X10^{-05}	1.57X10^{-03}	0.058	5.08X10^{-01}	7.08X10^{-01}
HSD17B8	-0.539	5.59X10^{-05}	1.59X10^{-03}	-0.073	1.92X10^{-01}	4.04X10^{-01}
IFI6	0.538	5.78X10^{-05}	1.63X10^{-03}	0.110	5.87X10^{-01}	7.65X10^{-01}
KLF13	-0.558	6.04X10^{-05}	1.69X10^{-03}	-0.003	9.50X10^{-01}	9.79X10^{-01}
RPL9	-0.724	6.05X10^{-05}	1.69X10^{-03}	-0.045	5.57X10^{-01}	7.44X10^{-01}
BEX1	0.557	6.27X10^{-05}	1.74X10^{-03}	0.137	4.52X10^{-01}	6.63X10^{-01}
MYL9	0.658	6.34X10^{-05}	1.75X10^{-03}	0.219	1.33X10^{-01}	3.25X10^{-01}
CCDC65	-0.611	6.36X10^{-05}	1.75X10^{-03}	-0.051	3.54X10^{-01}	5.76X10^{-01}
ANKRD36C	-0.713	6.51X10^{-05}	1.79X10^{-03}	-0.030	3.85X10^{-01}	6.06X10^{-01}
ARG1	0.535	6.62X10^{-05}	1.81X10^{-03}	0.081	4.32X10^{-01}	6.46X10^{-01}
NSUN5	-0.555	6.76X10^{-05}	1.84X10^{-03}	-0.056	1.20X10^{-01}	3.06X10^{-01}
SIDT1	-0.555	6.83X10^{-05}	1.86X10^{-03}	-0.063	7.33X10^{-02}	2.29X10^{-01}
GIGYF1	-0.575	6.92X10^{-05}	1.87X10^{-03}	-0.090	9.87X10^{-02}	2.72X10^{-01}
S1PR1	-0.562	7.26X10^{-05}	1.94X10^{-03}	-0.016	7.85X10^{-01}	8.89X10^{-01}
CRCP	-0.551	7.39X10^{-05}	1.97X10^{-03}	-0.057	3.29X10^{-01}	5.53X10^{-01}
FBXO2	-0.55	7.41X10^{-05}	1.97X10^{-03}	-0.002	9.84X10^{-01}	9.94X10^{-01}
NDRG3	-0.551	7.43X10^{-05}	1.97X10^{-03}	-0.035	2.87X10^{-01}	5.09X10^{-01}
D2HGDH	-0.571	7.66X10^{-05}	2.01X10^{-03}	-0.023	6.68X10^{-01}	8.18X10^{-01}
PYROXD2	-0.573	7.73X10^{-05}	2.03X10^{-03}	-0.099	1.28X10^{-01}	3.17X10^{-01}
ATP8B2	-0.549	7.82X10^{-05}	2.05X10^{-03}	-0.008	8.30X10^{-01}	9.17X10^{-01}
KBTBD4	-0.727	7.84X10^{-05}	2.05X10^{-03}	-0.040	1.38X10^{-01}	3.32X10^{-01}
C15orf41	-0.603	7.89X10^{-05}	2.06X10^{-03}	-0.002	9.77X10^{-01}	9.90X10^{-01}

SLC48A1	0.577	7.94X10^{-05}	2.07X10^{-03}	0.085	2.96X10^{-01}	5.18X10^{-01}
NOD2	0.767	8.23X10^{-05}	2.13X10^{-03}	0.044	6.07X10^{-01}	7.78X10^{-01}
NOL7	-0.752	8.31X10^{-05}	2.15X10^{-03}	-0.002	9.39X10^{-01}	9.73X10^{-01}
NSUN4	0.569	8.36X10^{-05}	2.15X10^{-03}	0.000	9.93X10^{-01}	9.97X10^{-01}
STARD8	0.527	8.52X10^{-05}	2.19X10^{-03}	0.039	4.93X10^{-01}	6.95X10^{-01}
SLC25A44	0.546	8.59X10^{-05}	2.20X10^{-03}	0.026	5.99X10^{-01}	7.73X10^{-01}
MBIP	-0.546	8.61X10^{-05}	2.20X10^{-03}	-0.032	3.10X10^{-01}	5.33X10^{-01}
IKZF2	-0.673	8.74X10^{-05}	2.23X10^{-03}	-0.094	1.59X10^{-01}	3.62X10^{-01}
ABHD14A	-0.751	8.84X10^{-05}	2.25X10^{-03}	-0.066	9.85X10^{-02}	2.72X10^{-01}
ITGA2B	0.674	8.93X10^{-05}	2.27X10^{-03}	0.043	7.42X10^{-01}	8.63X10^{-01}
TCTN1	-0.598	8.95X10^{-05}	2.27X10^{-03}	-0.052	2.98X10^{-01}	5.20X10^{-01}
DIDO1	-0.571	9.07X10^{-05}	2.29X10^{-03}	-0.044	6.41X10^{-02}	2.12X10^{-01}
RAB1B	0.546	9.13X10^{-05}	2.30X10^{-03}	0.046	3.48X10^{-01}	5.72X10^{-01}
UBALD1	0.565	9.21X10^{-05}	2.31X10^{-03}	0.024	6.64X10^{-01}	8.15X10^{-01}
ALMS1	-0.543	9.37X10^{-05}	2.35X10^{-03}	-0.067	1.13X10^{-01}	2.95X10^{-01}
ZNF587	-0.721	9.49X10^{-05}	2.37X10^{-03}	-0.027	3.19X10^{-01}	5.43X10^{-01}
SYTL3	-0.564	9.71X10^{-05}	2.41X10^{-03}	-0.101	5.35X10^{-02}	1.90X10^{-01}
KDSR	-0.552	9.73X10^{-05}	2.41X10^{-03}	-0.039	4.01X10^{-01}	6.21X10^{-01}
SCAF8	-0.542	9.87X10^{-05}	2.44X10^{-03}	-0.029	2.75X10^{-01}	4.97X10^{-01}
PI4K2B	0.562	1.04X10^{-04}	2.53X10^{-03}	0.001	9.85X10^{-01}	9.94X10^{-01}
FCER1G	0.542	1.06X10^{-04}	2.58X10^{-03}	0.001	9.86X10^{-01}	9.94X10^{-01}
CFAP44	-0.603	1.08X10^{-04}	2.62X10^{-03}	-0.085	1.12X10^{-01}	2.95X10^{-01}
PSMD12	-0.541	1.09X10^{-04}	2.63X10^{-03}	-0.009	7.48X10^{-01}	8.67X10^{-01}
NUDT16L1	-0.734	1.09X10^{-04}	2.63X10^{-03}	-0.026	4.11X10^{-01}	6.29X10^{-01}
CNN1	0.535	1.12X10^{-04}	2.69X10^{-03}	0.124	1.42X10^{-01}	3.38X10^{-01}
MMP1	0.557	1.14X10^{-04}	2.71X10^{-03}	0.166	4.75X10^{-01}	6.80X10^{-01}
OSBPL11	0.759	1.15X10^{-04}	2.71X10^{-03}	0.005	8.48X10^{-01}	9.28X10^{-01}
ZBTB16	-0.541	1.15X10^{-04}	2.72X10^{-03}	-0.125	1.86X10^{-01}	3.96X10^{-01}
CDK5	0.516	1.16X10^{-04}	2.73X10^{-03}	0.013	7.47X10^{-01}	8.67X10^{-01}
TTC9	-0.706	1.18X10^{-04}	2.77X10^{-03}	-0.098	1.51X10^{-01}	3.50X10^{-01}
GRAP	-0.534	1.19X10^{-04}	2.79X10^{-03}	-0.023	6.33X10^{-01}	7.96X10^{-01}
GLRX5	0.533	1.23X10^{-04}	2.85X10^{-03}	0.016	7.92X10^{-01}	8.93X10^{-01}
ACAD11	-0.555	1.25X10^{-04}	2.89X10^{-03}	-0.060	1.43X10^{-01}	3.40X10^{-01}
RPS28	-0.513	1.26X10^{-04}	2.91X10^{-03}	-0.025	5.28X10^{-01}	7.23X10^{-01}
RHCE	0.676	1.27X10^{-04}	2.94X10^{-03}	0.042	6.29X10^{-01}	7.93X10^{-01}
RPL27	-0.512	1.29X10^{-04}	2.96X10^{-03}	-0.025	6.26X10^{-01}	7.91X10^{-01}
GNL1	-0.532	1.31X10^{-04}	3.00X10^{-03}	-0.038	1.74X10^{-01}	3.82X10^{-01}
HELB	-0.552	1.32X10^{-04}	3.01X10^{-03}	-0.043	1.61X10^{-01}	3.64X10^{-01}
ILF3	-0.764	1.32X10^{-04}	3.02X10^{-03}	-0.054	6.03X10^{-02}	2.04X10^{-01}
PIGB	0.507	1.42X10^{-04}	3.21X10^{-03}	0.032	4.51X10^{-01}	6.61X10^{-01}
LGALSL	0.684	1.42X10^{-04}	3.22X10^{-03}	0.017	8.59X10^{-01}	9.34X10^{-01}
MACF1	-0.611	1.44X10^{-04}	3.23X10^{-03}	-0.053	1.02X10^{-01}	2.78X10^{-01}
RPL13A	-0.725	1.44X10^{-04}	3.24X10^{-03}	-0.018	6.01X10^{-01}	7.74X10^{-01}
XAF1	0.596	1.46X10^{-04}	3.27X10^{-03}	0.062	6.63X10^{-01}	8.14X10^{-01}
ALOX12	0.507	1.52X10^{-04}	3.37X10^{-03}	0.003	9.44X10^{-01}	9.76X10^{-01}
MZT2A	-0.6	1.52X10^{-04}	3.37X10^{-03}	-0.053	3.43X10^{-01}	5.67X10^{-01}

IL21R	-0.552	$1.55X10^{-04}$	$3.42X10^{-03}$	-0.014	$7.67X10^{-01}$	$8.79X10^{-01}$
HBM	0.728	$1.57X10^{-04}$	$3.44X10^{-03}$	0.103	$3.46X10^{-01}$	$5.70X10^{-01}$
ZNF598	-0.546	$1.59X10^{-04}$	$3.48X10^{-03}$	-0.004	$9.35X10^{-01}$	$9.71X10^{-01}$
R3HDM4	0.524	$1.61X10^{-04}$	$3.51X10^{-03}$	0.090	$1.60X10^{-01}$	$3.63X10^{-01}$
CHD2	-0.76	$1.63X10^{-04}$	$3.54X10^{-03}$	-0.027	$3.61X10^{-01}$	$5.84X10^{-01}$
EID3	-0.783	$1.64X10^{-04}$	$3.57X10^{-03}$	-0.053	$1.82X10^{-01}$	$3.92X10^{-01}$
TTC39B	-0.573	$1.74X10^{-04}$	$3.72X10^{-03}$	-0.078	$8.86X10^{-02}$	$2.56X10^{-01}$
MDS2	-0.801	$1.78X10^{-04}$	$3.78X10^{-03}$	-0.056	$4.74X10^{-01}$	$6.79X10^{-01}$
ARHGEF37	0.542	$1.78X10^{-04}$	$3.78X10^{-03}$	0.019	$8.25X10^{-01}$	$9.15X10^{-01}$
SLC25A39	0.54	$1.79X10^{-04}$	$3.80X10^{-03}$	0.069	$3.53X10^{-01}$	$5.76X10^{-01}$
KCNA3	-0.519	$1.83X10^{-04}$	$3.86X10^{-03}$	-0.010	$8.64X10^{-01}$	$9.36X10^{-01}$
PGBD4	-0.64	$1.83X10^{-04}$	$3.86X10^{-03}$	-0.062	$5.55X10^{-02}$	$1.95X10^{-01}$
CAPN12	-0.671	$1.83X10^{-04}$	$3.86X10^{-03}$	-0.127	$1.72X10^{-01}$	$3.79X10^{-01}$
LRRC8A	-0.54	$1.85X10^{-04}$	$3.89X10^{-03}$	-0.012	$8.35X10^{-01}$	$9.20X10^{-01}$
RPL35	-0.562	$1.87X10^{-04}$	$3.93X10^{-03}$	-0.012	$7.63X10^{-01}$	$8.77X10^{-01}$
PRMT2	-0.631	$1.90X10^{-04}$	$3.97X10^{-03}$	-0.046	$2.52X10^{-01}$	$4.73X10^{-01}$
ANXA4	0.63	$1.91X10^{-04}$	$3.99X10^{-03}$	0.038	$3.88X10^{-01}$	$6.09X10^{-01}$
BCL7C	-0.694	$1.97X10^{-04}$	$4.08X10^{-03}$	-0.017	$5.56X10^{-01}$	$7.44X10^{-01}$
ZNF416	-0.536	$2.01X10^{-04}$	$4.14X10^{-03}$	-0.055	$1.13X10^{-01}$	$2.96X10^{-01}$
ZSCAN25	-0.536	$2.05X10^{-04}$	$4.21X10^{-03}$	-0.025	$4.48X10^{-01}$	$6.59X10^{-01}$
BLK	-0.496	$2.06X10^{-04}$	$4.23X10^{-03}$	-0.077	$4.38X10^{-01}$	$6.51X10^{-01}$
DCAF10	0.725	$2.11X10^{-04}$	$4.31X10^{-03}$	0.026	$5.61X10^{-01}$	$7.46X10^{-01}$
POP5	-0.514	$2.11X10^{-04}$	$4.31X10^{-03}$	-0.042	$1.05X10^{-01}$	$2.82X10^{-01}$
SMIM1	0.565	$2.14X10^{-04}$	$4.37X10^{-03}$	0.119	$6.08X10^{-01}$	$7.79X10^{-01}$
RPS17	-0.494	$2.17X10^{-04}$	$4.42X10^{-03}$	-0.043	$3.43X10^{-01}$	$5.67X10^{-01}$
IRF2	0.513	$2.21X10^{-04}$	$4.48X10^{-03}$	0.050	$1.20X10^{-01}$	$3.06X10^{-01}$
BTBD11	-0.532	$2.34X10^{-04}$	$4.67X10^{-03}$	-0.052	$3.62X10^{-01}$	$5.85X10^{-01}$
NUBPL	-0.509	$2.36X10^{-04}$	$4.71X10^{-03}$	-0.031	$3.01X10^{-01}$	$5.24X10^{-01}$
ZNF805	-0.564	$2.46X10^{-04}$	$4.87X10^{-03}$	-0.032	$2.84X10^{-01}$	$5.05X10^{-01}$
CXCR5	-0.511	$2.52X10^{-04}$	$4.96X10^{-03}$	-0.038	$6.70X10^{-01}$	$8.19X10^{-01}$
SCMH1	-0.535	$2.52X10^{-04}$	$4.96X10^{-03}$	-0.050	$2.86X10^{-01}$	$5.08X10^{-01}$
LLGL2	-0.534	$2.53X10^{-04}$	$4.96X10^{-03}$	-0.021	$7.06X10^{-01}$	$8.42X10^{-01}$
GNE	-0.506	$2.58X10^{-04}$	$5.04X10^{-03}$	-0.058	$8.13X10^{-02}$	$2.44X10^{-01}$
KLF1	0.486	$2.62X10^{-04}$	$5.09X10^{-03}$	0.058	$5.18X10^{-01}$	$7.14X10^{-01}$
CLEC4D	0.627	$2.71X10^{-04}$	$5.25X10^{-03}$	0.015	$8.57X10^{-01}$	$9.33X10^{-01}$
DAP3	-0.572	$2.71X10^{-04}$	$5.25X10^{-03}$	-0.029	$1.73X10^{-01}$	$3.80X10^{-01}$
MUTYH	-0.485	$2.76X10^{-04}$	$5.33X10^{-03}$	-0.046	$1.17X10^{-01}$	$3.01X10^{-01}$
MAML2	-0.525	$2.78X10^{-04}$	$5.35X10^{-03}$	-0.024	$6.21X10^{-01}$	$7.88X10^{-01}$
PLEK	0.504	$2.81X10^{-04}$	$5.40X10^{-03}$	0.113	$1.26X10^{-01}$	$3.15X10^{-01}$
USP34	-0.636	$2.89X10^{-04}$	$5.52X10^{-03}$	-0.008	$7.15X10^{-01}$	$8.47X10^{-01}$
PMPCB	-0.669	$2.89X10^{-04}$	$5.52X10^{-03}$	-0.032	$1.44X10^{-01}$	$3.40X10^{-01}$
ZNF786	-0.562	$2.89X10^{-04}$	$5.52X10^{-03}$	-0.043	$1.09X10^{-01}$	$2.90X10^{-01}$
CTTNBP2NL	0.552	$2.92X10^{-04}$	$5.57X10^{-03}$	0.065	$2.36X10^{-01}$	$4.56X10^{-01}$
CSTF1	-0.505	$2.97X10^{-04}$	$5.63X10^{-03}$	-0.035	$1.85X10^{-01}$	$3.95X10^{-01}$
TFDP1	0.613	$3.01X10^{-04}$	$5.68X10^{-03}$	0.014	$8.12X10^{-01}$	$9.07X10^{-01}$
M1AP	-0.55	$3.11X10^{-04}$	$5.83X10^{-03}$	-0.033	$7.23X10^{-01}$	$8.52X10^{-01}$

STRBP	-0.668	3.15X10^{-04}	5.90X10^{-03}	-0.062	1.90X10^{-01}	4.01X10^{-01}
RTN3	0.678	3.16X10^{-04}	5.91X10^{-03}	0.073	1.10X10^{-01}	2.90X10^{-01}
CYTOR	0.519	3.24X10^{-04}	6.00X10^{-03}	0.013	7.94X10^{-01}	8.94X10^{-01}
ILKAP	-0.499	3.26X10^{-04}	6.02X10^{-03}	-0.011	8.10X10^{-01}	9.05X10^{-01}
SRA1	0.629	3.40X10^{-04}	6.25X10^{-03}	0.027	4.83X10^{-01}	6.87X10^{-01}
LSM4	-0.497	3.40X10^{-04}	6.25X10^{-03}	-0.023	3.83X10^{-01}	6.04X10^{-01}
TAX1BP3	0.543	3.41X10^{-04}	6.25X10^{-03}	0.037	6.26X10^{-01}	7.91X10^{-01}
NDRG2	-0.544	3.47X10^{-04}	6.35X10^{-03}	-0.078	1.02X10^{-01}	2.78X10^{-01}
QTRT1	-0.516	3.48X10^{-04}	6.36X10^{-03}	-0.012	7.77X10^{-01}	8.85X10^{-01}
ZNF516	0.536	3.50X10^{-04}	6.38X10^{-03}	0.017	6.71X10^{-01}	8.20X10^{-01}
EXOSC2	-0.495	3.59X10^{-04}	6.54X10^{-03}	-0.030	2.31X10^{-01}	4.51X10^{-01}
OXSR1	0.495	3.62X10^{-04}	6.55X10^{-03}	0.013	6.47X10^{-01}	8.04X10^{-01}
DNAH1	-0.494	3.66X10^{-04}	6.60X10^{-03}	-0.005	9.11X10^{-01}	9.60X10^{-01}
POLR1C	-0.519	3.69X10^{-04}	6.64X10^{-03}	-0.052	9.13X10^{-02}	2.60X10^{-01}
MMAB	-0.513	3.83X10^{-04}	6.82X10^{-03}	-0.068	8.44X10^{-02}	2.49X10^{-01}
ZNF280D	-0.609	3.87X10^{-04}	6.87X10^{-03}	-0.055	6.60X10^{-02}	2.15X10^{-01}
LANCL1	-0.621	3.88X10^{-04}	6.89X10^{-03}	-0.013	6.35X10^{-01}	7.96X10^{-01}
GOLGA8R	-1.083	3.90X10^{-04}	6.89X10^{-03}	0.000	9.97X10^{-01}	9.98X10^{-01}
ID3	-0.51	3.95X10^{-04}	6.96X10^{-03}	-0.092	2.41X10^{-01}	4.61X10^{-01}
DNTTIP1	0.64	4.06X10^{-04}	7.11X10^{-03}	0.006	9.10X10^{-01}	9.59X10^{-01}
HEPACAM2	0.538	4.07X10^{-04}	7.13X10^{-03}	0.010	8.99X10^{-01}	9.54X10^{-01}
DNAH2	0.509	4.08X10^{-04}	7.14X10^{-03}	0.036	5.27X10^{-01}	7.22X10^{-01}
SPATS2L	0.49	4.12X10^{-04}	7.16X10^{-03}	0.060	6.39X10^{-01}	7.99X10^{-01}
KIZ	-0.523	4.14X10^{-04}	7.19X10^{-03}	-0.060	6.92X10^{-02}	2.21X10^{-01}
SDSL	0.51	4.17X10^{-04}	7.22X10^{-03}	0.097	2.17X10^{-01}	4.34X10^{-01}
DSC1	-0.51	4.17X10^{-04}	7.22X10^{-03}	-0.017	9.01X10^{-01}	9.54X10^{-01}
ITSN1	0.671	4.19X10^{-04}	7.25X10^{-03}	0.057	3.15X10^{-01}	5.39X10^{-01}
DTD1	-0.509	4.23X10^{-04}	7.28X10^{-03}	-0.005	8.72X10^{-01}	9.39X10^{-01}
SPA17	0.555	4.24X10^{-04}	7.28X10^{-03}	0.116	9.68X10^{-02}	2.69X10^{-01}
SLC25A42	-0.509	4.25X10^{-04}	7.28X10^{-03}	-0.037	4.56X10^{-01}	6.65X10^{-01}
NAP1L3	-0.63	4.27X10^{-04}	7.32X10^{-03}	-0.066	3.50X10^{-01}	5.73X10^{-01}
RPSA	-0.609	4.31X10^{-04}	7.36X10^{-03}	-0.028	5.29X10^{-01}	7.23X10^{-01}
HARS	-0.469	4.32X10^{-04}	7.36X10^{-03}	-0.029	2.48X10^{-01}	4.69X10^{-01}
SPATA13	-0.648	4.38X10^{-04}	7.45X10^{-03}	-0.064	7.78X10^{-02}	2.37X10^{-01}
RP9	-0.506	4.38X10^{-04}	7.45X10^{-03}	-0.015	6.94X10^{-01}	8.33X10^{-01}
MKI67	0.498	4.45X10^{-04}	7.54X10^{-03}	0.050	5.90X10^{-01}	7.67X10^{-01}
MKNK2	-0.486	4.54X10^{-04}	7.64X10^{-03}	-0.032	4.65X10^{-01}	6.73X10^{-01}
TSN	-0.668	4.54X10^{-04}	7.64X10^{-03}	-0.031	2.20X10^{-01}	4.37X10^{-01}
MPI	-0.486	4.56X10^{-04}	7.65X10^{-03}	-0.029	3.92X10^{-01}	6.13X10^{-01}
RRS1	-0.466	4.88X10^{-04}	8.08X10^{-03}	-0.023	5.91X10^{-01}	7.67X10^{-01}
KANK2	0.529	4.92X10^{-04}	8.14X10^{-03}	0.059	4.13X10^{-01}	6.30X10^{-01}
TUFM	-0.464	5.03X10^{-04}	8.26X10^{-03}	-0.050	1.70X10^{-01}	3.76X10^{-01}
PRPF38A	-0.502	5.09X10^{-04}	8.33X10^{-03}	-0.034	2.41X10^{-01}	4.61X10^{-01}
CD1A	0.486	5.12X10^{-04}	8.37X10^{-03}	0.066	4.36X10^{-01}	6.50X10^{-01}
CD8A	-0.663	5.17X10^{-04}	8.44X10^{-03}	-0.024	8.26X10^{-01}	9.15X10^{-01}
PI16	-0.5	5.27X10^{-04}	8.57X10^{-03}	-0.055	6.05X10^{-01}	7.77X10^{-01}

FGFBP3	-0.669	$5.31X10^{-04}$	$8.62X10^{-03}$	-0.112	$8.89X10^{-02}$	$2.57X10^{-01}$
SCRN2	-0.498	$5.42X10^{-04}$	$8.77X10^{-03}$	-0.063	$2.19X10^{-01}$	$4.36X10^{-01}$
UBAP2	-0.525	$5.47X10^{-04}$	$8.83X10^{-03}$	-0.074	$1.81X10^{-01}$	$3.90X10^{-01}$
ZAP70	-0.635	$5.61X10^{-04}$	$9.01X10^{-03}$	-0.091	$5.39X10^{-02}$	$1.91X10^{-01}$
KLRF1	-0.645	$5.66X10^{-04}$	$9.07X10^{-03}$	-0.184	$5.70X10^{-02}$	$1.98X10^{-01}$
OTUD3	-0.478	$5.68X10^{-04}$	$9.09X10^{-03}$	-0.019	$7.29X10^{-01}$	$8.56X10^{-01}$
TNFRSF13B	-0.496	$5.91X10^{-04}$	$9.35X10^{-03}$	-0.019	$8.84X10^{-01}$	$9.45X10^{-01}$
P2RY13	0.713	$6.15X10^{-04}$	$9.61X10^{-03}$	0.038	$4.71X10^{-01}$	$6.78X10^{-01}$
OSBPL7	-0.52	$6.16X10^{-04}$	$9.62X10^{-03}$	-0.063	$2.73X10^{-01}$	$4.95X10^{-01}$
FBXW8	-0.531	$6.24X10^{-04}$	$9.72X10^{-03}$	-0.018	$7.09X10^{-01}$	$8.43X10^{-01}$
KDM4B	0.502	$6.27X10^{-04}$	$9.74X10^{-03}$	0.085	$1.15X10^{-01}$	$2.99X10^{-01}$
GRB10	0.578	$6.38X10^{-04}$	$9.86X10^{-03}$	0.050	$4.75X10^{-01}$	$6.80X10^{-01}$
RPS27	-0.455	$6.44X10^{-04}$	$9.94X10^{-03}$	-0.028	$4.88X10^{-01}$	$6.91X10^{-01}$
CACYBP	-0.639	$6.49X10^{-04}$	$9.99X10^{-03}$	-0.046	$6.89X10^{-02}$	$2.21X10^{-01}$
Not validated						
CD6	-1.062	$2.81X10^{-13}$	$9.13X10^{-10}$	0.015	$7.26X10^{-01}$	$8.54X10^{-01}$
RCAN3	-1.113	$1.11X10^{-12}$	$1.94X10^{-09}$	0.022	$7.04X10^{-01}$	$8.40X10^{-01}$
EVL	-1.049	$5.49X10^{-12}$	$5.68X10^{-09}$	0.007	$8.26X10^{-01}$	$9.15X10^{-01}$
PARP9	1.018	$1.25X10^{-11}$	$9.81X10^{-09}$	-0.004	$9.69X10^{-01}$	$9.87X10^{-01}$
KMO	0.929	$1.70X10^{-11}$	$1.25X10^{-08}$	-0.037	$6.32X10^{-01}$	$7.94X10^{-01}$
MPP1	0.916	$3.24X10^{-11}$	$2.11X10^{-08}$	-0.063	$2.14X10^{-01}$	$4.30X10^{-01}$
P2RY8	-0.993	$3.43X10^{-11}$	$2.17X10^{-08}$	0.090	$7.77X10^{-02}$	$2.37X10^{-01}$
ZBTB20	-1	$3.79X10^{-11}$	$2.21X10^{-08}$	0.032	$2.85X10^{-01}$	$5.07X10^{-01}$
PLSCR1	0.951	$4.71X10^{-11}$	$2.54X10^{-08}$	-0.045	$6.67X10^{-01}$	$8.17X10^{-01}$
CD5	-0.985	$4.92X10^{-11}$	$2.54X10^{-08}$	0.105	$1.50X10^{-01}$	$3.49X10^{-01}$
CBLB	-0.897	$6.66X10^{-11}$	$3.29X10^{-08}$	0.043	$2.19X10^{-01}$	$4.36X10^{-01}$
CA1	0.929	$8.06X10^{-11}$	$3.90X10^{-08}$	-0.200	$4.49X10^{-02}$	$1.71X10^{-01}$
IFIT2	0.893	$9.34X10^{-11}$	$4.34X10^{-08}$	-0.019	$8.93X10^{-01}$	$9.50X10^{-01}$
NABP1	0.916	$1.68X10^{-10}$	$7.21X10^{-08}$	-0.085	$2.84X10^{-02}$	$1.32X10^{-01}$
RPL13	-0.909	$1.91X10^{-10}$	$7.80X10^{-08}$	0.028	$4.57X10^{-01}$	$6.66X10^{-01}$
KANSL1	-1.006	$1.92X10^{-10}$	$7.80X10^{-08}$	0.021	$7.11X10^{-01}$	$8.44X10^{-01}$
DDX58	0.909	$2.04X10^{-10}$	$8.14X10^{-08}$	-0.084	$3.81X10^{-01}$	$6.02X10^{-01}$
MLLT6	-1.03	$2.87X10^{-10}$	$1.07X10^{-07}$	0.007	$8.59X10^{-01}$	$9.34X10^{-01}$
PIP5K1B	0.861	$3.08X10^{-10}$	$1.13X10^{-07}$	-0.065	$1.63X10^{-01}$	$3.67X10^{-01}$
BCL9L	-0.934	$3.68X10^{-10}$	$1.33X10^{-07}$	0.000	$9.98X10^{-01}$	$9.99X10^{-01}$
BMP2K	0.937	$4.67X10^{-10}$	$1.59X10^{-07}$	-0.035	$3.74X10^{-01}$	$5.96X10^{-01}$
ATP6V1D	0.884	$5.40X10^{-10}$	$1.81X10^{-07}$	-0.064	$6.29X10^{-02}$	$2.10X10^{-01}$
FAR2	0.882	$6.28X10^{-10}$	$1.98X10^{-07}$	-0.009	$8.51X10^{-01}$	$9.29X10^{-01}$
GK	1.068	$1.02X10^{-09}$	$3.01X10^{-07}$	-0.081	$9.87X10^{-02}$	$2.72X10^{-01}$
TCF7	-0.995	$1.42X10^{-09}$	$4.04X10^{-07}$	0.064	$2.71X10^{-01}$	$4.93X10^{-01}$
TPM1	0.864	$1.59X10^{-09}$	$4.47X10^{-07}$	-0.069	$3.18X10^{-01}$	$5.42X10^{-01}$
CXCL10	0.855	$1.85X10^{-09}$	$5.13X10^{-07}$	-0.322	$8.59X10^{-02}$	$2.52X10^{-01}$
EPHA4	-0.851	$2.11X10^{-09}$	$5.72X10^{-07}$	0.070	$2.81X10^{-01}$	$5.02X10^{-01}$
GDF11	-0.877	$3.02X10^{-09}$	$7.99X10^{-07}$	0.004	$9.28X10^{-01}$	$9.68X10^{-01}$
FMNL3	-0.929	$3.17X10^{-09}$	$8.29X10^{-07}$	0.118	$3.55X10^{-02}$	$1.50X10^{-01}$
AXIN2	-0.913	$5.42X10^{-09}$	$1.25X10^{-06}$	0.051	$5.11X10^{-01}$	$7.10X10^{-01}$

LHFPL2	0.795	5.58X10^{-09}	1.27X10^{-06}	-0.015	8.21X10^{-01}	9.12X10^{-01}
SYNE2	-0.867	6.56X10^{-09}	1.46X10^{-06}	0.082	4.49X10^{-02}	1.71X10^{-01}
VAMP2	-0.83	7.47X10^{-09}	1.62X10^{-06}	0.057	2.58X10^{-01}	4.79X10^{-01}
YIPF6	0.781	9.02X10^{-09}	1.87X10^{-06}	-0.192	4.59X10^{-04}	1.18X10^{-02}
FHIT	-0.783	9.98X10^{-09}	2.05X10^{-06}	0.095	3.69X10^{-01}	5.91X10^{-01}
ATP6V1C1	0.78	1.03X10^{-08}	2.09X10^{-06}	-0.048	1.18X10^{-01}	3.02X10^{-01}
TLR6	0.812	1.05X10^{-08}	2.11X10^{-06}	-0.069	1.26X10^{-01}	3.15X10^{-01}
SEC14L1	0.778	1.06X10^{-08}	2.12X10^{-06}	-0.003	9.32X10^{-01}	9.70X10^{-01}
TRIM10	0.801	1.45X10^{-08}	2.66X10^{-06}	-0.045	5.80X10^{-01}	7.60X10^{-01}
GYPA	0.798	1.53X10^{-08}	2.78X10^{-06}	-0.314	1.89X10^{-04}	7.25X10^{-03}
CELF2	-0.808	1.68X10^{-08}	3.01X10^{-06}	0.028	3.03X10^{-01}	5.25X10^{-01}
FBXO11	-1.015	1.73X10^{-08}	3.03X10^{-06}	0.023	3.14X10^{-01}	5.38X10^{-01}
STX7	0.796	1.94X10^{-08}	3.29X10^{-06}	-0.022	5.78X10^{-01}	7.59X10^{-01}
OTUD7A	-0.829	2.08X10^{-08}	3.45X10^{-06}	0.045	6.94X10^{-01}	8.33X10^{-01}
PTGIR	0.792	2.32X10^{-08}	3.72X10^{-06}	-0.095	1.13X10^{-01}	2.95X10^{-01}
CUTA	-0.789	2.38X10^{-08}	3.79X10^{-06}	0.002	9.59X10^{-01}	9.83X10^{-01}
EPOR	0.758	2.49X10^{-08}	3.88X10^{-06}	-0.023	6.97X10^{-01}	8.35X10^{-01}
TNRC6B	-0.827	3.03X10^{-08}	4.61X10^{-06}	0.031	1.39X10^{-01}	3.34X10^{-01}
XK	0.785	3.08X10^{-08}	4.61X10^{-06}	-0.050	5.50X10^{-01}	7.39X10^{-01}
TCEAL9	0.782	3.24X10^{-08}	4.82X10^{-06}	-0.068	4.27X10^{-01}	6.43X10^{-01}
PPP1R16B	-0.852	3.57X10^{-08}	5.24X10^{-06}	0.095	7.13X10^{-02}	2.25X10^{-01}
ZFP36L2	-1.029	3.95X10^{-08}	5.62X10^{-06}	0.200	3.08X10^{-04}	9.53X10^{-03}
IRF9	0.781	4.44X10^{-08}	6.12X10^{-06}	-0.054	3.53X10^{-01}	5.76X10^{-01}
SLC41A1	-0.805	4.58X10^{-08}	6.27X10^{-06}	0.124	1.29X10^{-01}	3.19X10^{-01}
SAMD9L	0.977	4.68X10^{-08}	6.34X10^{-06}	-0.029	7.87X10^{-01}	8.90X10^{-01}
MGLL	0.742	4.76X10^{-08}	6.40X10^{-06}	-0.020	8.52X10^{-01}	9.29X10^{-01}
GYPB	0.767	4.78X10^{-08}	6.40X10^{-06}	-0.271	2.35X10^{-03}	3.06X10^{-02}
GOLGA8A	-0.77	4.93X10^{-08}	6.55X10^{-06}	0.090	1.97X10^{-01}	4.10X10^{-01}
TLR1	0.741	5.14X10^{-08}	6.72X10^{-06}	-0.117	6.36X10^{-04}	1.44X10^{-02}
CD7	-0.738	5.36X10^{-08}	6.97X10^{-06}	0.089	2.46X10^{-01}	4.67X10^{-01}
TAF3	-0.801	5.45X10^{-08}	7.05X10^{-06}	0.081	5.63X10^{-02}	1.96X10^{-01}
CASP5	0.738	5.76X10^{-08}	7.33X10^{-06}	-0.243	4.45X10^{-02}	1.70X10^{-01}
EEF1G	-0.731	6.84X10^{-08}	8.41X10^{-06}	0.012	7.02X10^{-01}	8.38X10^{-01}
SRRM1	-0.761	7.18X10^{-08}	8.69X10^{-06}	0.036	1.06X10^{-01}	2.83X10^{-01}
SCAI	-0.939	7.28X10^{-08}	8.76X10^{-06}	0.023	5.65X10^{-01}	7.49X10^{-01}
IL10RB	0.73	7.87X10^{-08}	9.38X10^{-06}	-0.003	9.28X10^{-01}	9.68X10^{-01}
DIP2A	-0.798	8.12X10^{-08}	9.47X10^{-06}	0.035	5.32X10^{-01}	7.25X10^{-01}
MAP3K20	0.907	1.01X10^{-07}	1.14X10^{-05}	-0.039	4.83X10^{-01}	6.87X10^{-01}
MORC4	-0.75	1.01X10^{-07}	1.14X10^{-05}	0.003	9.29X10^{-01}	9.68X10^{-01}
HEMGN	0.819	1.28X10^{-07}	1.41X10^{-05}	-0.332	8.83X10^{-04}	1.74X10^{-02}
ZNF395	-0.992	1.35X10^{-07}	1.46X10^{-05}	0.054	2.78X10^{-01}	5.00X10^{-01}
ARHGEF12	0.716	1.38X10^{-07}	1.47X10^{-05}	-0.010	8.31X10^{-01}	9.18X10^{-01}
NDUFV3	0.78	1.42X10^{-07}	1.51X10^{-05}	-0.142	1.59X10^{-03}	2.44X10^{-02}
ZNF346	-0.817	1.47X10^{-07}	1.56X10^{-05}	0.008	8.74X10^{-01}	9.40X10^{-01}
TLR4	0.948	1.72X10^{-07}	1.76X10^{-05}	-0.143	1.61X10^{-03}	2.46X10^{-02}
RABL2A	-0.736	1.77X10^{-07}	1.78X10^{-05}	0.035	5.29X10^{-01}	7.23X10^{-01}

SLFN13	-0.763	$2.12X10^{-07}$	$2.09X10^{-05}$	0.111	$2.92X10^{-02}$	$1.34X10^{-01}$
PCMTD1	0.761	$2.17X10^{-07}$	$2.12X10^{-05}$	-0.213	$1.02X10^{-03}$	$1.91X10^{-02}$
TJP2	0.733	$2.32X10^{-07}$	$2.24X10^{-05}$	-0.036	$5.01X10^{-01}$	$7.01X10^{-01}$
ST3GAL2	0.701	$2.39X10^{-07}$	$2.29X10^{-05}$	-0.099	$4.51X10^{-03}$	$4.45X10^{-02}$
NEXN	0.753	$2.70X10^{-07}$	$2.52X10^{-05}$	-0.126	$1.44X10^{-02}$	$8.82X10^{-02}$
TRERF1	-0.993	$3.22X10^{-07}$	$2.92X10^{-05}$	0.103	$2.48X10^{-02}$	$1.22X10^{-01}$
SELENBP1	0.691	$3.29X10^{-07}$	$2.97X10^{-05}$	-0.021	$8.00X10^{-01}$	$8.98X10^{-01}$
RABL2B	-0.764	$3.37X10^{-07}$	$3.02X10^{-05}$	0.088	$8.08X10^{-02}$	$2.43X10^{-01}$
SKAP1	-1	$3.49X10^{-07}$	$3.11X10^{-05}$	0.129	$5.34X10^{-03}$	$4.94X10^{-02}$
CARD16	0.816	$3.76X10^{-07}$	$3.30X10^{-05}$	-0.073	$1.32X10^{-01}$	$3.23X10^{-01}$
TSG101	0.742	$3.97X10^{-07}$	$3.45X10^{-05}$	-0.052	$5.77X10^{-02}$	$1.99X10^{-01}$
RAB11FIP1	0.753	$4.08X10^{-07}$	$3.52X10^{-05}$	-0.095	$6.14X10^{-03}$	$5.37X10^{-02}$
FKBP11	-0.735	$4.21X10^{-07}$	$3.60X10^{-05}$	0.092	$9.29X10^{-02}$	$2.63X10^{-01}$
ABCF2	-0.744	$4.54X10^{-07}$	$3.87X10^{-05}$	0.048	$4.06X10^{-01}$	$6.24X10^{-01}$
CASP1	0.775	$4.58X10^{-07}$	$3.89X10^{-05}$	-0.098	$2.51X10^{-02}$	$1.23X10^{-01}$
SLC6A16	-0.781	$4.63X10^{-07}$	$3.92X10^{-05}$	0.089	$2.55X10^{-01}$	$4.76X10^{-01}$
UNC93B1	0.709	$4.90X10^{-07}$	$4.11X10^{-05}$	-0.088	$1.11X10^{-01}$	$2.92X10^{-01}$
LXN	0.71	$5.08X10^{-07}$	$4.20X10^{-05}$	-0.032	$5.52X10^{-01}$	$7.40X10^{-01}$
B4GALT5	0.705	$5.56X10^{-07}$	$4.55X10^{-05}$	-0.059	$2.21X10^{-01}$	$4.40X10^{-01}$
STAM2	0.756	$5.61X10^{-07}$	$4.55X10^{-05}$	-0.076	$1.25X10^{-03}$	$2.14X10^{-02}$
CD58	0.858	$5.61X10^{-07}$	$4.55X10^{-05}$	-0.038	$1.74X10^{-01}$	$3.81X10^{-01}$
RNF216	-0.704	$5.68X10^{-07}$	$4.57X10^{-05}$	0.009	$7.06X10^{-01}$	$8.42X10^{-01}$
PACSIN2	0.83	$5.97X10^{-07}$	$4.67X10^{-05}$	-0.116	$1.49X10^{-04}$	$6.30X10^{-03}$
TOR1B	0.701	$6.15X10^{-07}$	$4.74X10^{-05}$	-0.108	$8.13X10^{-02}$	$2.44X10^{-01}$
SYNJ2	-0.889	$6.19X10^{-07}$	$4.76X10^{-05}$	0.046	$2.88X10^{-01}$	$5.10X10^{-01}$
SCRN3	0.699	$6.44X10^{-07}$	$4.93X10^{-05}$	-0.057	$3.25X10^{-02}$	$1.42X10^{-01}$
MEI1	-0.768	$6.87X10^{-07}$	$5.21X10^{-05}$	0.075	$1.23X10^{-01}$	$3.10X10^{-01}$
STRADB	0.722	$8.01X10^{-07}$	$5.93X10^{-05}$	-0.116	$8.02X10^{-02}$	$2.42X10^{-01}$
ANKRD11	-0.692	$8.13X10^{-07}$	$5.97X10^{-05}$	0.040	$2.44X10^{-01}$	$4.66X10^{-01}$
KIAA1328	-0.72	$8.16X10^{-07}$	$5.97X10^{-05}$	0.029	$2.89X10^{-01}$	$5.11X10^{-01}$
FOXK1	-0.72	$8.35X10^{-07}$	$6.09X10^{-05}$	0.079	$5.74X10^{-02}$	$1.98X10^{-01}$
TAF6	-0.693	$9.38X10^{-07}$	$6.71X10^{-05}$	0.113	$3.48X10^{-02}$	$1.48X10^{-01}$
RNF144B	0.717	$1.00X10^{-06}$	$7.07X10^{-05}$	-0.116	$4.52X10^{-02}$	$1.72X10^{-01}$
HERC2	-0.686	$1.04X10^{-06}$	$7.30X10^{-05}$	0.071	$3.13X10^{-02}$	$1.39X10^{-01}$
DSE	0.753	$1.06X10^{-06}$	$7.38X10^{-05}$	-0.091	$2.09X10^{-02}$	$1.10X10^{-01}$
FAS	0.658	$1.07X10^{-06}$	$7.42X10^{-05}$	-0.088	$7.56X10^{-02}$	$2.32X10^{-01}$
ST6GALNAC6	-0.714	$1.10X10^{-06}$	$7.58X10^{-05}$	0.025	$5.55X10^{-01}$	$7.42X10^{-01}$
PCSK6	0.689	$1.13X10^{-06}$	$7.72X10^{-05}$	-0.062	$5.60X10^{-01}$	$7.46X10^{-01}$
AUTS2	-1.003	$1.24X10^{-06}$	$8.42X10^{-05}$	0.054	$3.78X10^{-01}$	$6.00X10^{-01}$
ZNF213	0.709	$1.28X10^{-06}$	$8.64X10^{-05}$	-0.010	$8.42X10^{-01}$	$9.25X10^{-01}$
AQP10	0.774	$1.34X10^{-06}$	$8.91X10^{-05}$	-0.171	$2.34X10^{-01}$	$4.53X10^{-01}$
TDRD7	0.675	$1.42X10^{-06}$	$9.34X10^{-05}$	-0.063	$2.93X10^{-01}$	$5.15X10^{-01}$
DIS3L2	-0.741	$1.51X10^{-06}$	$9.73X10^{-05}$	0.014	$7.25X10^{-01}$	$8.53X10^{-01}$
TARDBP	-0.756	$1.51X10^{-06}$	$9.73X10^{-05}$	0.002	$9.33X10^{-01}$	$9.70X10^{-01}$
HMGA1	-0.712	$1.70X10^{-06}$	$1.08X10^{-04}$	0.150	$1.67X10^{-02}$	$9.61X10^{-02}$
MPRIP	-0.811	$1.73X10^{-06}$	$1.09X10^{-04}$	0.070	$6.10X10^{-02}$	$2.06X10^{-01}$

UNKL	-0.67	1.75X10^{-06}	1.10X10^{-04}	0.021	6.28X10^{-01}	7.92X10^{-01}
UBTD2	0.697	1.80X10^{-06}	1.12X10^{-04}	-0.017	5.94X10^{-01}	7.69X10^{-01}
AQP3	-0.643	1.91X10^{-06}	1.18X10^{-04}	0.056	3.75X10^{-01}	5.97X10^{-01}
ARHGEF9	-0.668	1.92X10^{-06}	1.18X10^{-04}	0.045	4.60X10^{-01}	6.68X10^{-01}
ZNF831	-0.95	2.08X10^{-06}	1.27X10^{-04}	0.059	2.71X10^{-01}	4.93X10^{-01}
GALNT7	0.665	2.18X10^{-06}	1.31X10^{-04}	-0.050	8.00X10^{-02}	2.42X10^{-01}
MFSD1	0.664	2.27X10^{-06}	1.35X10^{-04}	-0.137	1.68X10^{-04}	6.76X10^{-03}
HSP90AB1	-0.633	2.59X10^{-06}	1.51X10^{-04}	0.065	1.61X10^{-01}	3.64X10^{-01}
CDC25B	-0.691	2.64X10^{-06}	1.52X10^{-04}	0.116	2.26X10^{-02}	1.15X10^{-01}
ARG2	0.633	2.81X10^{-06}	1.59X10^{-04}	-0.116	2.22X10^{-01}	4.40X10^{-01}
SLC14A1	0.628	3.05X10^{-06}	1.71X10^{-04}	-0.070	3.78X10^{-01}	6.00X10^{-01}
ASPM	0.68	3.08X10^{-06}	1.72X10^{-04}	-0.116	7.43X10^{-02}	2.30X10^{-01}
ZNF512B	-0.652	3.17X10^{-06}	1.76X10^{-04}	0.024	6.99X10^{-01}	8.37X10^{-01}
ABHD4	0.65	3.37X10^{-06}	1.85X10^{-04}	-0.011	8.32X10^{-01}	9.18X10^{-01}
FBXO32	-0.958	3.47X10^{-06}	1.89X10^{-04}	0.078	2.21X10^{-01}	4.39X10^{-01}
C12orf76	0.676	3.59X10^{-06}	1.94X10^{-04}	-0.056	8.02X10^{-02}	2.42X10^{-01}
MAGED1	-0.683	3.60X10^{-06}	1.95X10^{-04}	0.110	4.09X10^{-02}	1.62X10^{-01}
LMNB1	0.625	3.62X10^{-06}	1.95X10^{-04}	-0.026	6.94X10^{-01}	8.33X10^{-01}
MAK	0.681	3.68X10^{-06}	1.97X10^{-04}	-0.211	2.48X10^{-03}	3.15X10^{-02}
SFMBT1	-0.647	3.74X10^{-06}	2.00X10^{-04}	0.039	3.44X10^{-01}	5.67X10^{-01}
WDR54	-0.672	4.04X10^{-06}	2.13X10^{-04}	0.043	2.88X10^{-01}	5.10X10^{-01}
ZNF331	-0.704	4.14X10^{-06}	2.18X10^{-04}	0.041	2.02X10^{-01}	4.16X10^{-01}
GPD2	0.648	4.29X10^{-06}	2.23X10^{-04}	-0.065	1.42X10^{-01}	3.38X10^{-01}
JAK2	0.826	4.68X10^{-06}	2.39X10^{-04}	-0.019	6.23X10^{-01}	7.89X10^{-01}
XKR6	-0.771	4.72X10^{-06}	2.40X10^{-04}	0.036	4.72X10^{-01}	6.78X10^{-01}
PSRC1	0.64	4.76X10^{-06}	2.41X10^{-04}	-0.123	6.80X10^{-02}	2.19X10^{-01}
STX3	0.768	4.80X10^{-06}	2.42X10^{-04}	-0.076	1.84X10^{-02}	1.01X10^{-01}
NCOA4	0.677	5.04X10^{-06}	2.51X10^{-04}	-0.058	1.99X10^{-01}	4.12X10^{-01}
MBOAT2	0.666	5.09X10^{-06}	2.52X10^{-04}	-0.162	3.74X10^{-02}	1.54X10^{-01}
GCH1	0.671	5.10X10^{-06}	2.52X10^{-04}	-0.086	1.83X10^{-01}	3.93X10^{-01}
CR1	0.742	5.22X10^{-06}	2.57X10^{-04}	-0.026	6.17X10^{-01}	7.84X10^{-01}
MRPS24	-0.662	5.31X10^{-06}	2.60X10^{-04}	0.032	2.35X10^{-01}	4.55X10^{-01}
FNBP1L	0.635	5.75X10^{-06}	2.80X10^{-04}	-0.030	7.50X10^{-01}	8.68X10^{-01}
PARP14	0.661	5.94X10^{-06}	2.87X10^{-04}	-0.136	1.44X10^{-01}	3.40X10^{-01}
PCSK5	-0.636	6.27X10^{-06}	3.00X10^{-04}	0.533	7.52X10^{-05}	4.30X10^{-03}
TRAF3IP2	-0.631	6.30X10^{-06}	3.01X10^{-04}	0.177	4.35X10^{-03}	4.37X10^{-02}
CTNS	0.668	6.47X10^{-06}	3.06X10^{-04}	-0.081	6.50X10^{-02}	2.13X10^{-01}
GAMT	-0.661	6.50X10^{-06}	3.06X10^{-04}	0.013	7.84X10^{-01}	8.88X10^{-01}
UBIAD1	-0.63	6.69X10^{-06}	3.14X10^{-04}	0.011	7.71X10^{-01}	8.81X10^{-01}
MDM4	-0.604	6.88X10^{-06}	3.21X10^{-04}	0.016	5.35X10^{-01}	7.28X10^{-01}
RPL12	-0.605	6.92X10^{-06}	3.22X10^{-04}	0.045	2.77X10^{-01}	4.99X10^{-01}
TGM2	0.658	7.09X10^{-06}	3.29X10^{-04}	-0.048	4.68X10^{-01}	6.75X10^{-01}
CHMP5	0.668	7.17X10^{-06}	3.31X10^{-04}	-0.039	4.65X10^{-01}	6.72X10^{-01}
NMI	0.603	7.39X10^{-06}	3.38X10^{-04}	-0.087	9.68X10^{-02}	2.69X10^{-01}
TICAM2	0.918	7.46X10^{-06}	3.39X10^{-04}	-0.043	4.16X10^{-01}	6.33X10^{-01}
ZNF438	0.688	7.68X10^{-06}	3.45X10^{-04}	-0.105	2.22X10^{-02}	1.14X10^{-01}

SPTA1	0.624	7.96X10^{-06}	3.57X10^{-04}	-0.081	2.44X10^{-01}	4.65X10^{-01}
PARP16	-0.625	8.16X10^{-06}	3.63X10^{-04}	0.041	4.70X10^{-01}	6.77X10^{-01}
GOLGA8B	-0.712	8.23X10^{-06}	3.64X10^{-04}	0.067	2.19X10^{-01}	4.36X10^{-01}
SERF1A	-0.657	8.27X10^{-06}	3.65X10^{-04}	0.312	6.06X10^{-02}	2.05X10^{-01}
C16orf74	-0.685	8.29X10^{-06}	3.65X10^{-04}	0.054	3.78X10^{-01}	6.00X10^{-01}
MGAT1	0.626	8.50X10^{-06}	3.72X10^{-04}	-0.049	1.46X10^{-01}	3.44X10^{-01}
PHC1	-0.647	8.71X10^{-06}	3.80X10^{-04}	0.007	8.91X10^{-01}	9.49X10^{-01}
SPX	0.646	9.03X10^{-06}	3.91X10^{-04}	-0.367	3.12X10^{-03}	3.62X10^{-02}
TANGO2	0.646	9.26X10^{-06}	3.99X10^{-04}	-0.044	4.48X10^{-01}	6.59X10^{-01}
SUPT3H	-0.747	9.27X10^{-06}	3.99X10^{-04}	0.006	8.84X10^{-01}	9.45X10^{-01}
APEX1	-0.594	9.46X10^{-06}	4.05X10^{-04}	0.043	3.57X10^{-01}	5.80X10^{-01}
MAL	-0.625	9.69X10^{-06}	4.11X10^{-04}	0.059	3.49X10^{-01}	5.73X10^{-01}
RPS9	-0.594	9.87X10^{-06}	4.17X10^{-04}	0.003	9.46X10^{-01}	9.77X10^{-01}
APOBEC3A	1.22	9.90X10^{-06}	4.18X10^{-04}	-0.020	7.41X10^{-01}	8.63X10^{-01}
CCDC120	-0.641	9.96X10^{-06}	4.19X10^{-04}	0.076	3.59X10^{-01}	5.82X10^{-01}
LYST	0.621	1.02X10^{-05}	4.24X10^{-04}	-0.031	3.23X10^{-01}	5.46X10^{-01}
SH3KBP1	-0.678	1.02X10^{-05}	4.24X10^{-04}	0.032	3.23X10^{-01}	5.47X10^{-01}
CSGALNACT1	-0.648	1.03X10^{-05}	4.25X10^{-04}	0.006	9.35X10^{-01}	9.71X10^{-01}
ERLIN1	0.615	1.10X10^{-05}	4.46X10^{-04}	-0.067	2.55X10^{-01}	4.76X10^{-01}
EIF5A2	-0.688	1.11X10^{-05}	4.49X10^{-04}	0.100	1.27X10^{-01}	3.16X10^{-01}
ENDOD1	0.612	1.14X10^{-05}	4.57X10^{-04}	-0.118	4.63X10^{-02}	1.74X10^{-01}
TMEM33	0.83	1.15X10^{-05}	4.59X10^{-04}	-0.067	9.67X10^{-03}	6.98X10^{-02}
MNDA	0.825	1.19X10^{-05}	4.70X10^{-04}	-0.111	7.50X10^{-03}	5.95X10^{-02}
OASL	0.586	1.23X10^{-05}	4.83X10^{-04}	-0.003	9.86X10^{-01}	9.94X10^{-01}
WIPI1	0.612	1.24X10^{-05}	4.86X10^{-04}	-0.050	2.61X10^{-01}	4.82X10^{-01}
TTC39C	-0.633	1.32X10^{-05}	5.15X10^{-04}	0.037	3.25X10^{-01}	5.49X10^{-01}
ATG4C	0.632	1.35X10^{-05}	5.21X10^{-04}	-0.078	2.34X10^{-02}	1.18X10^{-01}
AQP9	0.862	1.35X10^{-05}	5.21X10^{-04}	-0.071	1.15X10^{-01}	2.99X10^{-01}
NLK	0.609	1.35X10^{-05}	5.21X10^{-04}	-0.073	5.64X10^{-02}	1.96X10^{-01}
ARHGEF40	0.607	1.36X10^{-05}	5.23X10^{-04}	-0.009	8.73X10^{-01}	9.40X10^{-01}
RPLP0	-0.584	1.36X10^{-05}	5.23X10^{-04}	0.028	4.31X10^{-01}	6.45X10^{-01}
USP32	0.608	1.40X10^{-05}	5.35X10^{-04}	-0.070	4.10X10^{-03}	4.23X10^{-02}
RNF13	0.607	1.42X10^{-05}	5.41X10^{-04}	-0.056	8.52X10^{-02}	2.50X10^{-01}
IFI35	0.756	1.48X10^{-05}	5.60X10^{-04}	-0.012	8.96X10^{-01}	9.52X10^{-01}
DGKA	-0.608	1.49X10^{-05}	5.62X10^{-04}	0.005	8.77X10^{-01}	9.42X10^{-01}
TFEB	0.635	1.50X10^{-05}	5.63X10^{-04}	-0.088	7.56X10^{-02}	2.32X10^{-01}
OR2W3	0.673	1.56X10^{-05}	5.78X10^{-04}	-0.033	7.46X10^{-01}	8.66X10^{-01}
SERPING1	0.775	1.58X10^{-05}	5.84X10^{-04}	-0.037	8.57X10^{-01}	9.33X10^{-01}
SEC63	-0.602	1.58X10^{-05}	5.84X10^{-04}	0.023	4.08X10^{-01}	6.26X10^{-01}
RNF157	-0.625	1.63X10^{-05}	5.99X10^{-04}	0.046	4.41X10^{-01}	6.54X10^{-01}
CCDC57	-0.911	1.68X10^{-05}	6.11X10^{-04}	0.028	3.74X10^{-01}	5.95X10^{-01}
RAB1A	0.578	1.70X10^{-05}	6.17X10^{-04}	-0.019	4.77X10^{-01}	6.83X10^{-01}
FAM200B	0.624	1.73X10^{-05}	6.25X10^{-04}	-0.113	6.74X10^{-04}	1.49X10^{-02}
C11orf1	-0.624	1.80X10^{-05}	6.46X10^{-04}	0.013	8.27X10^{-01}	9.15X10^{-01}
FBXO7	0.636	1.81X10^{-05}	6.48X10^{-04}	-0.197	4.66X10^{-03}	4.54X10^{-02}
SNU13	-0.597	1.81X10^{-05}	6.48X10^{-04}	0.049	3.45X10^{-02}	1.47X10^{-01}

ZHX2	-0.67	1.82X10^{-05}	6.48X10^{-04}	0.119	1.03X10^{-01}	2.79X10^{-01}
ANKRD39	-0.621	1.83X10^{-05}	6.50X10^{-04}	0.038	2.98X10^{-01}	5.20X10^{-01}
TMEM143	-0.622	1.88X10^{-05}	6.62X10^{-04}	0.032	5.57X10^{-01}	7.44X10^{-01}
IRF7	0.755	1.96X10^{-05}	6.87X10^{-04}	-0.098	3.04X10^{-01}	5.27X10^{-01}
SERAC1	0.655	2.01X10^{-05}	7.04X10^{-04}	-0.041	3.09X10^{-01}	5.33X10^{-01}
PROS1	0.596	2.05X10^{-05}	7.13X10^{-04}	-0.157	1.76X10^{-01}	3.84X10^{-01}
KLHDC8B	0.724	2.06X10^{-05}	7.16X10^{-04}	-0.061	4.84X10^{-01}	6.88X10^{-01}
CHST7	0.647	2.07X10^{-05}	7.17X10^{-04}	-0.037	5.70X10^{-01}	7.52X10^{-01}
PSEN1	0.826	2.22X10^{-05}	7.63X10^{-04}	-0.011	6.71X10^{-01}	8.20X10^{-01}
CCR1	0.825	2.25X10^{-05}	7.72X10^{-04}	-0.144	9.49X10^{-02}	2.66X10^{-01}
FKBP1B	0.568	2.27X10^{-05}	7.78X10^{-04}	-0.032	6.45X10^{-01}	8.02X10^{-01}
EIF2AK1	0.592	2.29X10^{-05}	7.84X10^{-04}	-0.027	6.19X10^{-01}	7.86X10^{-01}
RAB32	0.769	2.37X10^{-05}	8.05X10^{-04}	-0.013	7.62X10^{-01}	8.76X10^{-01}
RHD	0.626	2.40X10^{-05}	8.14X10^{-04}	-0.050	7.50X10^{-01}	8.68X10^{-01}
FOXO4	0.565	2.45X10^{-05}	8.25X10^{-04}	-0.137	6.76X10^{-02}	2.19X10^{-01}
REPS2	0.754	2.51X10^{-05}	8.41X10^{-04}	-0.045	2.94X10^{-01}	5.17X10^{-01}
STX12	0.586	2.77X10^{-05}	9.12X10^{-04}	-0.079	8.74X10^{-04}	1.74X10^{-02}
ATP6V1E1	0.584	2.88X10^{-05}	9.43X10^{-04}	-0.026	2.44X10^{-01}	4.66X10^{-01}
PRDX3	0.56	2.97X10^{-05}	9.71X10^{-04}	-0.034	2.04X10^{-01}	4.19X10^{-01}
ZNF324	-0.654	3.01X10^{-05}	9.76X10^{-04}	0.005	8.87X10^{-01}	9.47X10^{-01}
ADORA2B	0.671	3.04X10^{-05}	9.83X10^{-04}	-0.019	7.85X10^{-01}	8.89X10^{-01}
PGM2	0.606	3.09X10^{-05}	9.93X10^{-04}	-0.053	1.26X10^{-01}	3.14X10^{-01}
NUP210	-0.579	3.13X10^{-05}	1.00X10^{-03}	0.105	3.80X10^{-03}	4.08X10^{-02}
DYNC1LI1	0.58	3.13X10^{-05}	1.00X10^{-03}	-0.080	1.75X10^{-02}	9.81X10^{-02}
SLC25A23	-0.637	3.14X10^{-05}	1.00X10^{-03}	0.140	5.16X10^{-02}	1.86X10^{-01}
KLHL12	0.581	3.20X10^{-05}	1.02X10^{-03}	-0.050	2.76X10^{-02}	1.30X10^{-01}
TM9SF1	0.673	3.20X10^{-05}	1.02X10^{-03}	-0.027	3.66X10^{-01}	5.89X10^{-01}
FBXO6	0.637	3.44X10^{-05}	1.08X10^{-03}	-0.058	4.57X10^{-01}	6.66X10^{-01}
SLC19A1	0.693	3.44X10^{-05}	1.08X10^{-03}	-0.026	5.79X10^{-01}	7.59X10^{-01}
ALKBH7	-0.599	3.52X10^{-05}	1.10X10^{-03}	0.057	1.29X10^{-01}	3.18X10^{-01}
TMEM165	0.698	3.55X10^{-05}	1.11X10^{-03}	-0.045	4.81X10^{-02}	1.78X10^{-01}
EMC3	0.814	3.62X10^{-05}	1.13X10^{-03}	-0.079	1.72X10^{-01}	3.78X10^{-01}
UHRF1BP1	-0.631	3.64X10^{-05}	1.13X10^{-03}	0.062	1.94X10^{-01}	4.06X10^{-01}
CLASP1	-0.574	3.65X10^{-05}	1.13X10^{-03}	0.072	3.10X10^{-03}	3.61X10^{-02}
KRT1	0.59	3.65X10^{-05}	1.13X10^{-03}	-0.291	6.12X10^{-02}	2.06X10^{-01}
SDK2	-0.725	3.68X10^{-05}	1.13X10^{-03}	0.166	3.50X10^{-01}	5.73X10^{-01}
HECW2	0.599	3.75X10^{-05}	1.15X10^{-03}	-0.100	1.77X10^{-01}	3.85X10^{-01}
DPP7	-0.594	4.02X10^{-05}	1.23X10^{-03}	0.078	6.96X10^{-02}	2.22X10^{-01}
LIMK2	0.819	4.07X10^{-05}	1.24X10^{-03}	-0.062	1.67X10^{-01}	3.73X10^{-01}
IPP	-0.6	4.10X10^{-05}	1.24X10^{-03}	0.025	5.34X10^{-01}	7.27X10^{-01}
GLA	0.734	4.12X10^{-05}	1.24X10^{-03}	-0.063	1.74X10^{-01}	3.81X10^{-01}
IL1RL1	-0.599	4.12X10^{-05}	1.24X10^{-03}	0.022	8.77X10^{-01}	9.42X10^{-01}
ZBTB4	-0.696	4.20X10^{-05}	1.26X10^{-03}	0.039	3.86X10^{-01}	6.07X10^{-01}
EBPL	-0.594	4.27X10^{-05}	1.28X10^{-03}	0.038	4.46X10^{-01}	6.58X10^{-01}
IFITM3	0.567	4.43X10^{-05}	1.32X10^{-03}	-0.176	2.23X10^{-01}	4.42X10^{-01}
FCHO2	0.592	4.44X10^{-05}	1.32X10^{-03}	-0.071	2.92X10^{-01}	5.14X10^{-01}

CCDC84	-0.591	4.60X10^{-05}	1.36X10^{-03}	0.020	5.64X10^{-01}	7.48X10^{-01}
TLR5	0.596	4.74X10^{-05}	1.40X10^{-03}	-0.350	1.85X10^{-08}	4.77X10^{-05}
RUNX3	-0.786	4.78X10^{-05}	1.41X10^{-03}	0.010	8.66X10^{-01}	9.37X10^{-01}
HIST1H1D	-0.588	4.79X10^{-05}	1.41X10^{-03}	0.006	9.08X10^{-01}	9.58X10^{-01}
EGFL8	-0.572	4.84X10^{-05}	1.42X10^{-03}	0.006	9.39X10^{-01}	9.73X10^{-01}
METRN	-0.589	4.91X10^{-05}	1.43X10^{-03}	0.152	1.94X10^{-02}	1.05X10^{-01}
MGME1	0.604	4.91X10^{-05}	1.43X10^{-03}	-0.022	6.57X10^{-01}	8.10X10^{-01}
AURKA	0.565	5.12X10^{-05}	1.49X10^{-03}	-0.014	8.63X10^{-01}	9.35X10^{-01}
CDHR3	-0.585	5.16X10^{-05}	1.50X10^{-03}	0.079	1.34X10^{-01}	3.26X10^{-01}
CEP162	0.564	5.19X10^{-05}	1.50X10^{-03}	-0.114	1.01X10^{-02}	7.14X10^{-02}
IL2RB	-0.583	5.24X10^{-05}	1.51X10^{-03}	0.073	2.88X10^{-01}	5.10X10^{-01}
NCF4	0.773	5.25X10^{-05}	1.51X10^{-03}	-0.071	1.13X10^{-01}	2.95X10^{-01}
BAZ2B	0.672	5.33X10^{-05}	1.53X10^{-03}	-0.031	3.63X10^{-01}	5.86X10^{-01}
SUMF2	-0.584	5.33X10^{-05}	1.53X10^{-03}	0.035	1.77X10^{-01}	3.85X10^{-01}
CASK	-0.641	5.37X10^{-05}	1.54X10^{-03}	0.033	3.53X10^{-01}	5.76X10^{-01}
MRPS18C	0.586	5.40X10^{-05}	1.54X10^{-03}	-0.025	4.79X10^{-01}	6.84X10^{-01}
KIAA0232	0.626	5.54X10^{-05}	1.57X10^{-03}	-0.077	1.98X10^{-03}	2.77X10^{-02}
FLCN	0.589	5.60X10^{-05}	1.59X10^{-03}	-0.052	3.59X10^{-01}	5.82X10^{-01}
LRCH1	-0.713	5.65X10^{-05}	1.60X10^{-03}	0.131	1.24X10^{-04}	5.72X10^{-03}
RPS2	-0.772	5.82X10^{-05}	1.64X10^{-03}	0.032	3.98X10^{-01}	6.18X10^{-01}
THAP4	-0.588	5.83X10^{-05}	1.64X10^{-03}	0.011	8.17X10^{-01}	9.10X10^{-01}
FAH	0.538	5.87X10^{-05}	1.65X10^{-03}	0.000	9.94X10^{-01}	9.97X10^{-01}
GPATCH8	-0.559	5.87X10^{-05}	1.65X10^{-03}	0.049	7.34X10^{-02}	2.29X10^{-01}
GCHFR	-0.666	6.02X10^{-05}	1.68X10^{-03}	0.076	1.15X10^{-01}	2.99X10^{-01}
PLEK2	0.579	6.09X10^{-05}	1.70X10^{-03}	-0.021	7.90X10^{-01}	8.92X10^{-01}
RNF123	0.558	6.12X10^{-05}	1.70X10^{-03}	-0.044	2.95X10^{-01}	5.17X10^{-01}
RPL38	-0.537	6.22X10^{-05}	1.73X10^{-03}	0.004	9.01X10^{-01}	9.54X10^{-01}
YDJC	-0.71	6.33X10^{-05}	1.75X10^{-03}	0.001	9.77X10^{-01}	9.90X10^{-01}
IFITM2	0.556	6.50X10^{-05}	1.79X10^{-03}	-0.034	6.80X10^{-01}	8.25X10^{-01}
PLOD2	0.676	6.57X10^{-05}	1.80X10^{-03}	-0.128	2.19X10^{-01}	4.36X10^{-01}
CASP10	0.558	6.59X10^{-05}	1.81X10^{-03}	-0.080	2.29X10^{-02}	1.16X10^{-01}
CELSR3	-0.554	6.65X10^{-05}	1.82X10^{-03}	0.231	3.02X10^{-02}	1.36X10^{-01}
ZBED6CL	-0.578	6.71X10^{-05}	1.83X10^{-03}	0.017	8.01X10^{-01}	8.99X10^{-01}
STEAP4	0.603	6.86X10^{-05}	1.86X10^{-03}	-0.065	2.73X10^{-01}	4.95X10^{-01}
PRRC2B	-0.787	6.89X10^{-05}	1.86X10^{-03}	0.064	1.57X10^{-01}	3.58X10^{-01}
RNF126	-0.675	6.92X10^{-05}	1.87X10^{-03}	0.023	5.18X10^{-01}	7.14X10^{-01}
CA13	0.577	7.02X10^{-05}	1.89X10^{-03}	-0.045	3.48X10^{-01}	5.72X10^{-01}
IFNGR2	0.607	7.20X10^{-05}	1.93X10^{-03}	-0.023	4.80X10^{-01}	6.84X10^{-01}
ECHDC3	0.554	7.21X10^{-05}	1.93X10^{-03}	-0.080	4.23X10^{-01}	6.38X10^{-01}
PLA2G6	-0.58	7.56X10^{-05}	2.00X10^{-03}	0.008	8.59X10^{-01}	9.33X10^{-01}
FCGR3B	0.606	7.60X10^{-05}	2.00X10^{-03}	-0.123	1.33X10^{-01}	3.25X10^{-01}
KCNJ15	0.702	7.62X10^{-05}	2.01X10^{-03}	-0.082	2.28X10^{-01}	4.47X10^{-01}
ABCC4	0.654	7.89X10^{-05}	2.06X10^{-03}	-0.105	1.66X10^{-01}	3.71X10^{-01}
FAM160B2	-0.547	8.76X10^{-05}	2.24X10^{-03}	0.011	7.85X10^{-01}	8.89X10^{-01}
LTB	-0.525	8.83X10^{-05}	2.25X10^{-03}	0.048	3.57X10^{-01}	5.80X10^{-01}
SETD2	-0.546	8.83X10^{-05}	2.25X10^{-03}	0.013	6.96X10^{-01}	8.34X10^{-01}

TBC1D2B	0.546	8.85X10^{-05}	2.25X10^{-03}	-0.017	6.59X10^{-01}	8.12X10^{-01}
TATDN3	0.598	9.06X10^{-05}	2.29X10^{-03}	-0.046	1.35X10^{-01}	3.27X10^{-01}
SAP30	0.545	9.17X10^{-05}	2.31X10^{-03}	-0.055	3.74X10^{-01}	5.96X10^{-01}
CMPK2	0.642	9.31X10^{-05}	2.34X10^{-03}	-0.005	9.74X10^{-01}	9.89X10^{-01}
GSKIP	0.566	9.57X10^{-05}	2.38X10^{-03}	-0.075	5.40X10^{-02}	1.92X10^{-01}
RNF38	-0.542	9.68X10^{-05}	2.40X10^{-03}	0.007	8.90X10^{-01}	9.49X10^{-01}
WDPCP	-0.563	1.00X10^{-04}	2.47X10^{-03}	0.002	9.17X10^{-01}	9.62X10^{-01}
CD300C	0.627	1.02X10^{-04}	2.51X10^{-03}	-0.012	8.52X10^{-01}	9.29X10^{-01}
ENOSF1	-0.531	1.04X10^{-04}	2.54X10^{-03}	0.019	7.23X10^{-01}	8.52X10^{-01}
UNC119B	-0.537	1.07X10^{-04}	2.61X10^{-03}	0.070	1.01X10^{-01}	2.76X10^{-01}
BCAP29	0.565	1.10X10^{-04}	2.64X10^{-03}	-0.078	1.81X10^{-02}	1.01X10^{-01}
MFSD2B	0.78	1.10X10^{-04}	2.64X10^{-03}	-0.065	3.85X10^{-01}	6.06X10^{-01}
MRVI1	0.591	1.12X10^{-04}	2.67X10^{-03}	-0.130	1.63X10^{-02}	9.50X10^{-02}
DMAP1	-0.737	1.13X10^{-04}	2.69X10^{-03}	0.011	8.07X10^{-01}	9.03X10^{-01}
TSPAN2	0.537	1.13X10^{-04}	2.70X10^{-03}	-0.002	9.80X10^{-01}	9.92X10^{-01}
OSBPL3	-0.535	1.13X10^{-04}	2.70X10^{-03}	0.000	9.97X10^{-01}	9.98X10^{-01}
PACS1	-0.718	1.21X10^{-04}	2.82X10^{-03}	0.117	4.59X10^{-03}	4.48X10^{-02}
PDCD10	0.561	1.22X10^{-04}	2.85X10^{-03}	-0.082	1.03X10^{-02}	7.22X10^{-02}
QPCTL	-0.593	1.25X10^{-04}	2.90X10^{-03}	0.038	5.31X10^{-01}	7.25X10^{-01}
EIF3K	-0.533	1.28X10^{-04}	2.94X10^{-03}	0.026	3.49X10^{-01}	5.73X10^{-01}
ALDOC	-0.682	1.28X10^{-04}	2.94X10^{-03}	0.153	4.31X10^{-02}	1.67X10^{-01}
TRIM25	0.612	1.30X10^{-04}	2.99X10^{-03}	-0.025	5.81X10^{-01}	7.61X10^{-01}
RFESD	0.633	1.33X10^{-04}	3.04X10^{-03}	-0.148	6.89X10^{-03}	5.69X10^{-02}
NRF1	-0.533	1.37X10^{-04}	3.13X10^{-03}	0.007	7.87X10^{-01}	8.90X10^{-01}
ETFA	0.51	1.40X10^{-04}	3.18X10^{-03}	-0.048	1.46X10^{-01}	3.44X10^{-01}
AKR1B1	-0.68	1.42X10^{-04}	3.21X10^{-03}	0.023	5.16X10^{-01}	7.13X10^{-01}
MS4A6A	0.556	1.43X10^{-04}	3.23X10^{-03}	-0.086	9.85X10^{-02}	2.72X10^{-01}
KCNK6	0.578	1.49X10^{-04}	3.32X10^{-03}	0.000	9.98X10^{-01}	9.99X10^{-01}
HMBOX1	-0.553	1.50X10^{-04}	3.33X10^{-03}	0.064	5.96X10^{-02}	2.03X10^{-01}
TMEM154	0.552	1.50X10^{-04}	3.35X10^{-03}	-0.175	9.66X10^{-06}	1.50X10^{-03}
FBXO30	0.548	1.52X10^{-04}	3.37X10^{-03}	-0.056	7.60X10^{-02}	2.33X10^{-01}
MRPS15	-0.527	1.53X10^{-04}	3.38X10^{-03}	0.013	6.53X10^{-01}	8.08X10^{-01}
CLEC1B	0.553	1.56X10^{-04}	3.42X10^{-03}	-0.216	2.07X10^{-02}	1.09X10^{-01}
CLSTN1	-0.525	1.57X10^{-04}	3.44X10^{-03}	0.159	4.40X10^{-03}	4.39X10^{-02}
CCPG1	0.734	1.60X10^{-04}	3.49X10^{-03}	-0.091	4.30X10^{-03}	4.36X10^{-02}
WNT5B	0.575	1.62X10^{-04}	3.53X10^{-03}	-0.166	1.64X10^{-01}	3.68X10^{-01}
CXorf21	0.524	1.64X10^{-04}	3.57X10^{-03}	-0.019	6.66X10^{-01}	8.17X10^{-01}
SERPINB2	0.524	1.64X10^{-04}	3.57X10^{-03}	-0.006	9.53X10^{-01}	9.80X10^{-01}
ECHDC1	0.524	1.65X10^{-04}	3.57X10^{-03}	-0.014	5.72X10^{-01}	7.53X10^{-01}
IL1R2	0.528	1.67X10^{-04}	3.60X10^{-03}	-0.163	2.19X10^{-02}	1.13X10^{-01}
NDUFB8	-0.549	1.69X10^{-04}	3.64X10^{-03}	0.028	1.73X10^{-01}	3.80X10^{-01}
SMARCD1	-0.499	1.82X10^{-04}	3.84X10^{-03}	0.113	2.79X10^{-03}	3.38X10^{-02}
FAM161A	-0.538	1.90X10^{-04}	3.97X10^{-03}	0.040	5.39X10^{-01}	7.30X10^{-01}
SLAMF8	0.527	1.92X10^{-04}	3.99X10^{-03}	-0.021	8.72X10^{-01}	9.39X10^{-01}
TECR	-0.566	1.92X10^{-04}	3.99X10^{-03}	0.059	1.50X10^{-01}	3.48X10^{-01}
METTL16	-0.695	1.93X10^{-04}	4.02X10^{-03}	0.053	2.32X10^{-01}	4.52X10^{-01}

IL32	-0.496	2.02X10^{-04}	4.16X10^{-03}	0.106	9.06X10^{-02}	2.59X10^{-01}
DNLZ	-0.565	2.06X10^{-04}	4.23X10^{-03}	0.082	2.76X10^{-01}	4.98X10^{-01}
AFTPH	0.514	2.11X10^{-04}	4.32X10^{-03}	-0.085	2.36X10^{-04}	8.21X10^{-03}
ZBTB34	0.534	2.14X10^{-04}	4.37X10^{-03}	-0.077	1.59X10^{-02}	9.36X10^{-02}
PCYT1B	0.563	2.17X10^{-04}	4.42X10^{-03}	-0.090	3.84X10^{-01}	6.05X10^{-01}
SARM1	-0.513	2.19X10^{-04}	4.45X10^{-03}	0.153	2.26X10^{-02}	1.15X10^{-01}
EGF	0.513	2.20X10^{-04}	4.45X10^{-03}	-0.347	3.90X10^{-04}	1.07X10^{-02}
TMEM40	0.626	2.21X10^{-04}	4.48X10^{-03}	-0.074	3.63X10^{-01}	5.86X10^{-01}
ATG3	0.685	2.22X10^{-04}	4.48X10^{-03}	-0.063	2.17X10^{-02}	1.12X10^{-01}
YLPM1	-0.67	2.29X10^{-04}	4.62X10^{-03}	0.051	5.93X10^{-02}	2.03X10^{-01}
ZDHHC16	0.53	2.30X10^{-04}	4.63X10^{-03}	-0.016	5.70X10^{-01}	7.52X10^{-01}
PHLPP2	-0.536	2.35X10^{-04}	4.68X10^{-03}	0.012	8.94X10^{-01}	9.51X10^{-01}
THADA	-0.536	2.37X10^{-04}	4.71X10^{-03}	0.018	4.35X10^{-01}	6.49X10^{-01}
NUDT6	0.559	2.47X10^{-04}	4.87X10^{-03}	-0.027	6.81X10^{-01}	8.25X10^{-01}
GABARAPL2	0.508	2.47X10^{-04}	4.87X10^{-03}	-0.123	1.86X10^{-02}	1.02X10^{-01}
KIAA1841	0.557	2.50X10^{-04}	4.93X10^{-03}	-0.005	9.48X10^{-01}	9.78X10^{-01}
FBXL17	-0.558	2.53X10^{-04}	4.96X10^{-03}	0.060	3.81X10^{-01}	6.02X10^{-01}
HERPUD2	-0.528	2.57X10^{-04}	5.03X10^{-03}	0.015	6.38X10^{-01}	7.98X10^{-01}
ETS1	-0.738	2.58X10^{-04}	5.04X10^{-03}	0.052	1.82X10^{-01}	3.91X10^{-01}
UBE2H	0.527	2.61X10^{-04}	5.08X10^{-03}	-0.062	1.57X10^{-01}	3.58X10^{-01}
IKZF1	-0.486	2.77X10^{-04}	5.33X10^{-03}	0.007	7.88X10^{-01}	8.90X10^{-01}
RALB	0.626	2.77X10^{-04}	5.34X10^{-03}	-0.061	1.41X10^{-01}	3.37X10^{-01}
NDUFB3	0.504	2.82X10^{-04}	5.40X10^{-03}	-0.030	4.09X10^{-01}	6.27X10^{-01}
LSM7	-0.503	2.96X10^{-04}	5.63X10^{-03}	0.072	1.91X10^{-02}	1.04X10^{-01}
TSPYL5	-0.502	3.02X10^{-04}	5.71X10^{-03}	0.030	7.17X10^{-01}	8.49X10^{-01}
DCAF4	-0.521	3.05X10^{-04}	5.74X10^{-03}	0.007	9.07X10^{-01}	9.58X10^{-01}
TREML2	0.522	3.07X10^{-04}	5.77X10^{-03}	-0.163	1.31X10^{-03}	2.20X10^{-02}
ASH2L	0.732	3.08X10^{-04}	5.78X10^{-03}	-0.070	3.03X10^{-01}	5.26X10^{-01}
PSD3	0.519	3.20X10^{-04}	5.95X10^{-03}	-0.154	8.89X10^{-02}	2.57X10^{-01}
BBOF1	0.607	3.20X10^{-04}	5.95X10^{-03}	-0.041	4.80X10^{-01}	6.84X10^{-01}
GRIN3A	0.643	3.24X10^{-04}	6.00X10^{-03}	-0.066	1.49X10^{-01}	3.48X10^{-01}
TMEM109	-0.54	3.24X10^{-04}	6.00X10^{-03}	0.006	9.06X10^{-01}	9.57X10^{-01}
USE1	-0.498	3.24X10^{-04}	6.00X10^{-03}	0.025	5.47X10^{-01}	7.37X10^{-01}
CD160	-0.497	3.50X10^{-04}	6.39X10^{-03}	0.023	8.39X10^{-01}	9.23X10^{-01}
TESC	0.496	3.60X10^{-04}	6.55X10^{-03}	-0.029	7.16X10^{-01}	8.48X10^{-01}
ERGIC3	-0.495	3.60X10^{-04}	6.55X10^{-03}	0.069	6.95X10^{-02}	2.22X10^{-01}
FAXDC2	0.585	3.64X10^{-04}	6.58X10^{-03}	-0.093	3.47X10^{-01}	5.71X10^{-01}
CATSPER2	-0.512	3.68X10^{-04}	6.62X10^{-03}	0.035	5.41X10^{-01}	7.32X10^{-01}
NFU1	-0.519	3.70X10^{-04}	6.65X10^{-03}	0.001	9.74X10^{-01}	9.89X10^{-01}
RPRD2	-0.494	3.75X10^{-04}	6.71X10^{-03}	0.093	4.16X10^{-03}	4.26X10^{-02}
CLEC12B	0.601	3.77X10^{-04}	6.72X10^{-03}	-0.080	6.32X10^{-01}	7.95X10^{-01}
NOL9	-0.521	3.84X10^{-04}	6.84X10^{-03}	0.011	7.37X10^{-01}	8.61X10^{-01}
TSR3	-0.492	3.89X10^{-04}	6.89X10^{-03}	0.017	5.11X10^{-01}	7.10X10^{-01}
NREP	0.474	3.90X10^{-04}	6.89X10^{-03}	-0.034	3.75X10^{-01}	5.96X10^{-01}
PLXNA3	-0.492	3.90X10^{-04}	6.89X10^{-03}	0.077	4.87X10^{-01}	6.91X10^{-01}
GIPC1	-0.492	3.90X10^{-04}	6.89X10^{-03}	0.083	8.01X10^{-02}	2.42X10^{-01}

SCLT1	0.511	3.91X10^{-04}	6.90X10^{-03}	-0.120	3.22X10^{-03}	3.69X10^{-02}
YIPF3	0.508	3.98X10^{-04}	7.00X10^{-03}	-0.021	6.56X10^{-01}	8.10X10^{-01}
FCGR2B	0.49	4.00X10^{-04}	7.03X10^{-03}	-0.239	4.33X10^{-03}	4.37X10^{-02}
PODXL	-0.511	4.03X10^{-04}	7.06X10^{-03}	0.031	5.85X10^{-01}	7.63X10^{-01}
COPS7B	-0.489	4.11X10^{-04}	7.16X10^{-03}	0.015	6.68X10^{-01}	8.18X10^{-01}
TRIM59	-0.509	4.11X10^{-04}	7.16X10^{-03}	0.024	5.07X10^{-01}	7.06X10^{-01}
MAP7	0.583	4.16X10^{-04}	7.22X10^{-03}	-0.076	2.49X10^{-01}	4.70X10^{-01}
RNPS1	-0.47	4.23X10^{-04}	7.28X10^{-03}	0.011	7.06X10^{-01}	8.42X10^{-01}
RASGRP4	0.715	4.23X10^{-04}	7.28X10^{-03}	-0.021	6.84X10^{-01}	8.28X10^{-01}
IDO1	0.488	4.28X10^{-04}	7.32X10^{-03}	-0.083	5.99X10^{-01}	7.73X10^{-01}
SETD1A	-0.585	4.32X10^{-04}	7.36X10^{-03}	0.040	7.36X10^{-01}	8.60X10^{-01}
SPG11	0.487	4.35X10^{-04}	7.42X10^{-03}	-0.050	1.83X10^{-02}	1.01X10^{-01}
NT5DC1	-0.507	4.39X10^{-04}	7.45X10^{-03}	0.000	9.96X10^{-01}	9.98X10^{-01}
POLR2I	-0.487	4.39X10^{-04}	7.45X10^{-03}	0.047	2.50X10^{-01}	4.71X10^{-01}
CELSR1	-0.504	4.57X10^{-04}	7.67X10^{-03}	0.013	9.19X10^{-01}	9.63X10^{-01}
SEC31B	-0.505	4.70X10^{-04}	7.84X10^{-03}	0.092	1.90X10^{-01}	4.01X10^{-01}
PUS10	0.622	4.74X10^{-04}	7.89X10^{-03}	-0.039	2.01X10^{-01}	4.15X10^{-01}
RHOU	0.744	4.76X10^{-04}	7.91X10^{-03}	-0.064	2.76X10^{-01}	4.98X10^{-01}
BRF2	-0.567	4.85X10^{-04}	8.04X10^{-03}	0.006	8.45X10^{-01}	9.27X10^{-01}
VSIG4	0.502	4.95X10^{-04}	8.17X10^{-03}	-0.093	1.32X10^{-01}	3.23X10^{-01}
ZDHHC8	-0.501	4.95X10^{-04}	8.17X10^{-03}	0.067	3.67X10^{-01}	5.90X10^{-01}
MBNL3	0.529	4.96X10^{-04}	8.18X10^{-03}	-0.115	3.43X10^{-02}	1.47X10^{-01}
NIPSNAP3A	0.501	5.02X10^{-04}	8.25X10^{-03}	-0.025	5.17X10^{-01}	7.14X10^{-01}
LAMA5	-0.528	5.04X10^{-04}	8.27X10^{-03}	0.104	2.16X10^{-01}	4.33X10^{-01}
RNF166	-0.501	5.06X10^{-04}	8.29X10^{-03}	0.000	9.95X10^{-01}	9.97X10^{-01}
UBASH3A	-0.566	5.10X10^{-04}	8.33X10^{-03}	0.006	9.18X10^{-01}	9.63X10^{-01}
DCAF6	0.569	5.27X10^{-04}	8.57X10^{-03}	-0.039	4.11X10^{-01}	6.29X10^{-01}
PLPP1	-0.504	5.37X10^{-04}	8.70X10^{-03}	0.040	5.41X10^{-01}	7.32X10^{-01}
ZFYVE21	0.668	5.54X10^{-04}	8.93X10^{-03}	-0.059	7.38X10^{-02}	2.29X10^{-01}
IDH1	0.685	5.58X10^{-04}	8.96X10^{-03}	-0.030	3.93X10^{-01}	6.13X10^{-01}
WSB1	0.694	5.69X10^{-04}	9.09X10^{-03}	-0.080	1.31X10^{-02}	8.37X10^{-02}
TSHZ1	-0.497	5.69X10^{-04}	9.09X10^{-03}	0.118	3.39X10^{-02}	1.46X10^{-01}
UBE2L6	0.544	5.72X10^{-04}	9.11X10^{-03}	-0.009	9.28X10^{-01}	9.68X10^{-01}
SLFN12	0.477	5.72X10^{-04}	9.11X10^{-03}	-0.142	1.17X10^{-02}	7.80X10^{-02}
CREBBP	-0.463	5.74X10^{-04}	9.13X10^{-03}	0.125	4.76X10^{-02}	1.77X10^{-01}
MOB3C	0.738	5.82X10^{-04}	9.24X10^{-03}	-0.053	1.78X10^{-01}	3.87X10^{-01}
AFF4	-0.522	5.90X10^{-04}	9.34X10^{-03}	0.054	6.31X10^{-02}	2.10X10^{-01}
TBK1	0.474	5.97X10^{-04}	9.42X10^{-03}	-0.067	1.22X10^{-02}	8.03X10^{-02}
TAP1	0.475	6.00X10^{-04}	9.45X10^{-03}	-0.098	8.54X10^{-02}	2.51X10^{-01}
RPTOR	-0.493	6.02X10^{-04}	9.48X10^{-03}	0.035	5.39X10^{-01}	7.30X10^{-01}
KIF18A	0.528	6.02X10^{-04}	9.48X10^{-03}	-0.083	1.58X10^{-01}	3.59X10^{-01}
MELK	0.586	6.06X10^{-04}	9.51X10^{-03}	-0.098	1.99X10^{-01}	4.13X10^{-01}
CUL4B	-0.479	6.06X10^{-04}	9.51X10^{-03}	0.050	6.44X10^{-02}	2.12X10^{-01}
TM6SF1	0.548	6.07X10^{-04}	9.51X10^{-03}	-0.082	5.04X10^{-02}	1.84X10^{-01}
INPP5A	0.498	6.10X10^{-04}	9.55X10^{-03}	-0.148	5.72X10^{-05}	3.80X10^{-03}
MST1L	-0.495	6.30X10^{-04}	9.78X10^{-03}	0.044	6.86X10^{-01}	8.29X10^{-01}

PLXNC1	0.563	$6.36X10^{-04}$	$9.84X10^{-03}$	-0.149	$1.06X10^{-05}$	$1.54X10^{-03}$
TAL1	0.545	$6.37X10^{-04}$	$9.85X10^{-03}$	-0.087	$1.46X10^{-01}$	$3.44X10^{-01}$
LYSMD2	0.578	$6.47X10^{-04}$	$9.97X10^{-03}$	-0.043	$3.75X10^{-01}$	$5.96X10^{-01}$

Supplementary Table 4: Results of whole blood PAH RNA signature in the meta-analysis of PAH transcriptomic studies in blood samples. Table shows results for 1087/1267 genes from the meta-analysis present in the current PAH RNAseq. Data ordered based on dysregulation significance (p-value) in meta-analysis of PAH transcriptomic studies in blood samples.

	PAH Meta-analysis			**PAH Cohort**		
Gene	**Average FC**	**Sig.**	**FDR**	**logFC AB**	**Sig. AB**	**FDR AB**
Same direction, significant, meeting FDR						
TLR8	-0.451	8.37x10^{-14}	2.50x10^{-10}	-0.166	2.60x10^{-04}	8.76x10^{-03}
TALDO1	-0.349	1.25x10^{-13}	2.90x10^{-10}	-0.099	4.04x10^{-03}	4.21x10^{-02}
TXNRD1	-0.416	7.09x10^{-13}	8.24x10^{-10}	-0.099	2.04x10^{-03}	2.82x10^{-02}
TLR1	-0.421	7.36x10^{-11}	3.14x10^{-08}	-0.117	6.36x10^{-04}	1.44x10^{-02}
FAM45A	-0.209	8.86x10^{-11}	3.56x10^{-08}	-0.097	1.36x10^{-04}	6.03x10^{-03}
ACOT13	-0.266	1.16x10^{-10}	4.25x10^{-08}	-0.077	3.29x10^{-03}	3.73x10^{-02}
MAOB	0.533	8.01x10^{-10}	2.09x10^{-07}	0.282	4.38x10^{-03}	4.39x10^{-02}
DSEL	-0.383	8.82x10^{-10}	2.25x10^{-07}	-0.252	3.22x10^{-03}	3.69x10^{-02}
LILRB3	-0.476	1.07x10^{-09}	2.57x10^{-07}	-0.186	3.93x10^{-03}	4.14x10^{-02}
MMP25	-0.248	1.51x10^{-09}	3.35x10^{-07}	-0.261	8.42x10^{-04}	1.70x10^{-02}
TMEM184C	-0.176	5.20x10^{-09}	8.43x10^{-07}	-0.085	1.90x10^{-03}	2.70x10^{-02}
TLR4	-0.334	5.86x10^{-09}	9.01x10^{-07}	-0.143	1.61x10^{-03}	2.46x10^{-02}
MEG3	0.507	1.97x10^{-08}	2.34x10^{-06}	0.492	3.25x10^{-03}	3.71x10^{-02}
PFKFB4	-0.158	4.95x10^{-08}	4.81x10^{-06}	-0.123	2.58x10^{-04}	8.75x10^{-03}
TNKS	0.180	6.30x10^{-08}	5.77x10^{-06}	0.092	4.26x10^{-03}	4.32x10^{-02}
GSR	-0.248	8.27x10^{-08}	7.21x10^{-06}	-0.100	1.30x10^{-03}	2.19x10^{-02}
C6orf89	-0.118	1.08x10^{-07}	8.72x10^{-06}	-0.081	4.04x10^{-03}	4.21x10^{-02}
SMAD3	0.334	2.31x10^{-07}	1.55x10^{-05}	0.165	1.41x10^{-03}	2.29x10^{-02}
PLXNC1	-0.384	3.20x10^{-07}	1.98x10^{-05}	-0.149	1.06x10^{-05}	1.54x10^{-03}
INHBA	0.780	4.25x10^{-07}	2.44x10^{-05}	0.579	2.24x10^{-03}	2.98x10^{-02}
CXCR1	-0.528	4.77x10^{-07}	2.67x10^{-05}	-0.196	2.69x10^{-03}	3.31x10^{-02}
MEFV	-0.217	5.59x10^{-07}	3.05x10^{-05}	-0.193	5.37x10^{-06}	1.06x10^{-03}
FLT3	-0.251	7.54x10^{-07}	3.90x10^{-05}	-0.323	3.13x10^{-03}	3.62x10^{-02}
ATP6V1B2	-0.194	1.17x10^{-06}	5.47x10^{-05}	-0.104	9.20x10^{-04}	1.80x10^{-02}
RNF141	-0.214	2.99x10^{-06}	1.12x10^{-04}	-0.132	1.49x10^{-04}	6.30x10^{-03}
TLR2	-0.331	3.02x10^{-06}	1.12x10^{-04}	-0.168	1.59x10^{-03}	2.44x10^{-02}
XKRX	-0.291	3.39x10^{-06}	1.24x10^{-04}	-0.587	2.66x10^{-06}	7.45x10^{-04}
MAPKAP1	-0.131	4.39x10^{-06}	1.50x10^{-04}	-0.065	1.19x10^{-03}	2.10x10^{-02}
MBD2	-0.098	4.49x10^{-06}	1.53x10^{-04}	-0.084	3.19x10^{-03}	3.68x10^{-02}
DUSP4	0.154	5.13x10^{-06}	1.69x10^{-04}	0.353	5.02x10^{-04}	1.24x10^{-02}
MED11	-0.159	5.12x10^{-06}	1.69x10^{-04}	-0.080	1.53x10^{-03}	2.38x10^{-02}
HCK	-0.423	5.69x10^{-06}	1.82x10^{-04}	-0.137	2.08x10^{-04}	7.68x10^{-03}
TBC1D14	-0.162	6.42x10^{-06}	1.99x10^{-04}	-0.091	2.14x10^{-03}	2.91x10^{-02}
MCOLN3	0.560	6.93x10^{-06}	2.11x10^{-04}	0.162	5.00x10^{-04}	1.24x10^{-02}
IRAK4	-0.181	9.40x10^{-06}	2.64x10^{-04}	-0.075	1.08x10^{-03}	1.97x10^{-02}
NCF2	-0.306	1.04x10^{-05}	2.84x10^{-04}	-0.111	3.97x10^{-04}	1.08x10^{-02}
UBE4A	-0.107	1.36x10^{-05}	3.45x10^{-04}	-0.123	4.92x10^{-04}	1.23x10^{-02}

CYTH4	-0.341	1.47x10^{-05}	3.66x10^{-04}	-0.119	7.67x10^{-04}	1.61x10^{-02}
GMPR2	-0.140	1.54x10^{-05}	3.78x10^{-04}	-0.099	3.27x10^{-04}	9.84x10^{-03}
AMD1	-0.187	1.90x10^{-05}	4.48x10^{-04}	-0.160	1.96x10^{-06}	6.42x10^{-04}
ATXN1	0.164	2.05x10^{-05}	4.76x10^{-04}	0.112	3.67x10^{-04}	1.03x10^{-02}
YIPF1	-0.154	2.08x10^{-05}	4.82x10^{-04}	-0.123	1.81x10^{-04}	7.14x10^{-03}
NUCB2	-0.248	2.54x10^{-05}	5.65x10^{-04}	-0.109	2.24x10^{-03}	2.98x10^{-02}
GOLGA5	-0.125	3.82x10^{-05}	7.63x10^{-04}	-0.081	8.96x10^{-05}	4.80x10^{-03}
SLC25A45	0.126	5.32x10^{-05}	9.79x10^{-04}	0.106	5.07x10^{-03}	4.78x10^{-02}
ALG13	0.185	5.40x10^{-05}	9.92x10^{-04}	0.136	3.97x10^{-03}	4.17x10^{-02}
Same direction, significant						
CSF3R	0.489	6.14x10^{-16}	6.42x10^{-12}	-0.094	1.59x10^{-02}	9.35x10^{-02}
HBB	5.500	4.81x10^{-13}	6.26x10^{-10}	1.255	1.84x10^{-02}	1.01x10^{-01}
FGR	0.548	3.23x10^{-11}	1.69x10^{-08}	-0.094	1.05x10^{-02}	7.32x10^{-02}
IL1R2	0.201	1.18x10^{-10}	4.25x10^{-08}	-0.163	2.19x10^{-02}	1.13x10^{-01}
NADK	0.788	4.26x10^{-10}	1.25x10^{-07}	-0.081	1.65x10^{-02}	9.54x10^{-02}
GCA	0.629	7.25x10^{-10}	1.97x10^{-07}	-0.106	1.75x10^{-02}	9.81x10^{-02}
MKNK1	0.778	2.74x10^{-09}	5.34x10^{-07}	-0.097	1.30x10^{-02}	8.35x10^{-02}
MNDA	0.593	2.85x10^{-09}	5.43x10^{-07}	-0.111	7.50x10^{-03}	5.95x10^{-02}
TBXAS1	0.667	4.21x10^{-09}	7.21x10^{-07}	-0.063	4.40x10^{-02}	1.69x10^{-01}
WNK1	1.408	8.15x10^{-09}	1.19x10^{-06}	0.137	2.58x10^{-02}	1.25x10^{-01}
SIGLEC9	0.609	1.20x10^{-08}	1.59x10^{-06}	-0.112	1.10x10^{-02}	7.53x10^{-02}
SDK1	0.780	1.72x10^{-08}	2.11x10^{-06}	-0.475	2.98x10^{-02}	1.36x10^{-01}
AFF2	0.594	2.75x10^{-08}	3.03x10^{-06}	-0.113	4.58x10^{-02}	1.73x10^{-01}
RGS1	2.654	4.79x10^{-08}	4.71x10^{-06}	0.218	1.75x10^{-02}	9.81x10^{-02}
HGSNAT	1.219	5.18x10^{-08}	4.97x10^{-06}	0.084	4.03x10^{-02}	1.61x10^{-01}
DSE	0.728	6.68x10^{-08}	6.04x10^{-06}	-0.091	2.09x10^{-02}	1.10x10^{-01}
KCNE1	0.668	6.88x10^{-08}	6.15x10^{-06}	-0.163	1.15x10^{-02}	7.75x10^{-02}
ZNF438	0.805	8.47x10^{-08}	7.31x10^{-06}	-0.105	2.22x10^{-02}	1.14x10^{-01}
ARID2	1.188	8.57x10^{-08}	7.32x10^{-06}	0.059	1.73x10^{-02}	9.78x10^{-02}
ABCC9	1.583	1.19x10^{-07}	9.33x10^{-06}	0.104	9.70x10^{-03}	6.99x10^{-02}
CDC123	0.819	1.52x10^{-07}	1.14x10^{-05}	-0.065	2.03x10^{-02}	1.08x10^{-01}
ITGA9	1.495	2.37x10^{-07}	1.56x10^{-05}	0.249	2.96x10^{-02}	1.35x10^{-01}
TMEM97	0.712	3.41x10^{-07}	2.06x10^{-05}	-0.169	6.12x10^{-03}	5.36x10^{-02}
ZDHHC15	1.181	5.46x10^{-07}	3.00x10^{-05}	0.066	4.29x10^{-02}	1.67x10^{-01}
DNAJC14	0.853	7.59x10^{-07}	3.92x10^{-05}	-0.051	3.23x10^{-02}	1.42x10^{-01}
SNX18	0.865	8.21x10^{-07}	4.15x10^{-05}	-0.088	2.42x10^{-02}	1.20x10^{-01}
TAF12	0.852	1.17x10^{-06}	5.47x10^{-05}	-0.063	1.43x10^{-02}	8.80x10^{-02}
ESR1	1.122	1.35x10^{-06}	6.16x10^{-05}	0.291	9.36x10^{-03}	6.86x10^{-02}
PRKAG1	0.855	1.41x10^{-06}	6.35x10^{-05}	-0.044	3.12x10^{-02}	1.39x10^{-01}
CEP68	1.279	1.74x10^{-06}	7.40x10^{-05}	0.093	5.65x10^{-03}	5.11x10^{-02}
LGALS8	0.886	2.26x10^{-06}	8.96x10^{-05}	-0.087	1.15x10^{-02}	7.75x10^{-02}
TDP2	0.826	2.33x10^{-06}	9.16x10^{-05}	-0.107	7.17x10^{-03}	5.78x10^{-02}
ATP6V1A	0.814	2.34x10^{-06}	9.16x10^{-05}	-0.065	2.53x10^{-02}	1.23x10^{-01}
HTRA1	1.317	2.37x10^{-06}	9.26x10^{-05}	0.300	2.71x10^{-02}	1.29x10^{-01}
GHITM	0.832	2.58x10^{-06}	9.91x10^{-05}	-0.069	3.23x10^{-02}	1.42x10^{-01}

KDM6A	1.181	3.19x10^{-06}	1.17x10^{-04}	0.055	3.83x10^{-02}	1.56x10^{-01}
DPYD	0.865	3.29x10^{-06}	1.20x10^{-04}	-0.086	1.33x10^{-02}	8.45x10^{-02}
CRTC3	1.247	3.40x10^{-06}	1.24x10^{-04}	0.084	8.69x10^{-03}	6.54x10^{-02}
GREM2	1.126	3.61x10^{-06}	1.30x10^{-04}	0.216	7.02x10^{-03}	5.73x10^{-02}
EPRS	0.766	3.98x10^{-06}	1.39x10^{-04}	-0.057	3.32x10^{-02}	1.44x10^{-01}
HAL	0.817	4.11x10^{-06}	1.43x10^{-04}	-0.119	2.40x10^{-02}	1.19x10^{-01}
LIMD1	1.365	4.15x10^{-06}	1.44x10^{-04}	0.090	1.24x10^{-02}	8.11x10^{-02}
RAP1GAP	1.276	4.16x10^{-06}	1.44x10^{-04}	0.688	3.07x10^{-02}	1.38x10^{-01}
TCEAL4	0.797	4.64x10^{-06}	1.57x10^{-04}	-0.106	3.70x10^{-02}	1.54x10^{-01}
AGTPBP1	0.807	4.73x10^{-06}	1.59x10^{-04}	-0.071	1.15x10^{-02}	7.75x10^{-02}
RPS6KA1	0.806	5.10x10^{-06}	1.68x10^{-04}	-0.054	4.51x10^{-02}	1.72x10^{-01}
GRB2	0.813	5.80x10^{-06}	1.85x10^{-04}	-0.060	1.66x10^{-02}	9.56x10^{-02}
HERC2	1.296	5.81x10^{-06}	1.85x10^{-04}	0.071	3.13x10^{-02}	1.39x10^{-01}
SIK3	1.235	6.79x10^{-06}	2.08x10^{-04}	0.069	2.98x10^{-02}	1.36x10^{-01}
FILIP1L	1.298	9.53x10^{-06}	2.67x10^{-04}	0.155	4.42x10^{-02}	1.69x10^{-01}
PIK3AP1	0.618	9.81x10^{-06}	2.72x10^{-04}	-0.125	2.59x10^{-02}	1.25x10^{-01}
NBL1	1.287	1.04x10^{-05}	2.84x10^{-04}	0.248	1.96x10^{-02}	1.05x10^{-01}
ARPC5	0.912	1.04x10^{-05}	2.84x10^{-04}	-0.087	2.17x10^{-02}	1.12x10^{-01}
STX10	0.828	1.08x10^{-05}	2.92x10^{-04}	-0.071	3.11x10^{-02}	1.38x10^{-01}
RILPL2	0.813	1.15x10^{-05}	3.05x10^{-04}	-0.060	3.69x10^{-02}	1.54x10^{-01}
CYB5R4	0.778	1.17x10^{-05}	3.10x10^{-04}	-0.072	8.09x10^{-03}	6.25x10^{-02}
RYR3	1.072	1.23x10^{-05}	3.21x10^{-04}	0.406	2.04x10^{-02}	1.08x10^{-01}
TDRKH	0.852	1.27x10^{-05}	3.27x10^{-04}	-0.108	2.91x10^{-02}	1.34x10^{-01}
HSD17B12	0.861	1.52x10^{-05}	3.76x10^{-04}	-0.123	3.04x10^{-02}	1.37x10^{-01}
HSD17B4	0.837	1.64x10^{-05}	3.96x10^{-04}	-0.105	6.54x10^{-03}	5.55x10^{-02}
CACNB3	1.206	1.75x10^{-05}	4.18x10^{-04}	0.119	4.91x10^{-02}	1.81x10^{-01}
MOCS3	0.881	2.02x10^{-05}	4.72x10^{-04}	-0.050	4.95x10^{-02}	1.82x10^{-01}
DARS2	0.841	2.11x10^{-05}	4.89x10^{-04}	-0.091	1.12x10^{-02}	7.64x10^{-02}
RNF130	0.867	2.16x10^{-05}	4.98x10^{-04}	-0.074	3.02x10^{-02}	1.36x10^{-01}
SUN2	0.742	2.34x10^{-05}	5.31x10^{-04}	-0.093	6.67x10^{-03}	5.59x10^{-02}
CHST15	0.788	2.61x10^{-05}	5.77x10^{-04}	-0.083	3.42x10^{-02}	1.47x10^{-01}
MRPL35	0.795	2.79x10^{-05}	6.04x10^{-04}	-0.056	4.75x10^{-02}	1.77x10^{-01}
PPP1R11	0.822	2.89x10^{-05}	6.21x10^{-04}	-0.079	1.06x10^{-02}	7.37x10^{-02}
ITGB2	0.689	3.14x10^{-05}	6.60x10^{-04}	-0.102	1.52x10^{-02}	9.11x10^{-02}
GCLM	0.746	3.51x10^{-05}	7.16x10^{-04}	-0.130	6.40x10^{-03}	5.50x10^{-02}
GALNT16	1.118	5.04x10^{-05}	9.36x10^{-04}	0.124	1.95x10^{-02}	1.05x10^{-01}
TOR1AIP2	0.828	5.17x10^{-05}	9.56x10^{-04}	-0.066	3.39x10^{-02}	1.46x10^{-01}
Same direction						
ACSS2	0.613	2.25x10^{-13}	3.91x10^{-10}	-0.063	1.38x10^{-01}	3.31x10^{-01}
S100A9	0.282	5.09x10^{-13}	6.26x10^{-10}	-0.036	5.28x10^{-01}	7.23x10^{-01}
CBS	0.562	1.33x10^{-12}	1.46x10^{-09}	-0.178	2.33x10^{-01}	4.52x10^{-01}
GLT1D1	0.532	1.98x10^{-12}	1.97x10^{-09}	-0.023	5.34x10^{-01}	7.27x10^{-01}
NQO1	0.439	4.00x10^{-12}	3.09x10^{-09}	-0.007	9.02x10^{-01}	9.55x10^{-01}
SIRPB2	0.676	6.85x10^{-12}	4.94x10^{-09}	-0.012	8.45x10^{-01}	9.26x10^{-01}
CR1	0.417	8.17x10^{-12}	5.34x10^{-09}	-0.026	6.17x10^{-01}	7.84x10^{-01}
HBA2	4.232	1.41x10^{-11}	8.42x10^{-09}	0.948	5.73x10^{-02}	1.98x10^{-01}

H2AFY	0.736	1.71x10^{-11}	9.94x10^{-09}	-0.033	2.67x10^{-01}	4.89x10^{-01}
PYGL	0.640	2.19x10^{-11}	1.21x10^{-08}	-0.077	6.17x10^{-02}	2.07x10^{-01}
LILRA2	0.705	3.54x10^{-11}	1.76x10^{-08}	-0.022	6.37x10^{-01}	7.98x10^{-01}
NLRP12	0.739	5.02x10^{-11}	2.23x10^{-08}	-0.039	3.15x10^{-01}	5.39x10^{-01}
CIDEB	0.804	5.16x10^{-11}	2.25x10^{-08}	-0.088	1.05x10^{-01}	2.82x10^{-01}
SIGLEC10	0.454	7.91x10^{-11}	3.26x10^{-08}	-0.050	4.71x10^{-01}	6.78x10^{-01}
CUBN	1.328	9.67x10^{-11}	3.81x10^{-08}	0.048	4.91x10^{-01}	6.94x10^{-01}
ADORA3	0.477	1.03x10^{-10}	3.98x10^{-08}	-0.021	8.78x10^{-01}	9.42x10^{-01}
APBB1IP	0.630	1.29x10^{-10}	4.44x10^{-08}	0.000	1.00e+00	1.00e+00
NLRC4	0.574	1.40x10^{-10}	4.72x10^{-08}	-0.039	4.05x10^{-01}	6.23x10^{-01}
ABCB6	0.734	1.93x10^{-10}	6.32x10^{-08}	-0.085	1.35x10^{-01}	3.27x10^{-01}
PGD	0.595	2.48x10^{-10}	7.86x10^{-08}	-0.004	9.21x10^{-01}	9.65x10^{-01}
PCYT2	0.696	2.96x10^{-10}	9.25x10^{-08}	-0.071	7.53x10^{-02}	2.32x10^{-01}
ITGAM	0.544	3.41x10^{-10}	1.03x10^{-07}	-0.014	7.64x10^{-01}	8.77x10^{-01}
TLR6	0.624	3.92x10^{-10}	1.17x10^{-07}	-0.069	1.26x10^{-01}	3.15x10^{-01}
HRH2	0.728	5.59x10^{-10}	1.60x10^{-07}	-0.063	2.53x10^{-01}	4.74x10^{-01}
ACAT2	0.579	8.11x10^{-10}	2.09x10^{-07}	-0.034	3.22x10^{-01}	5.46x10^{-01}
TLE4	0.747	9.58x10^{-10}	2.38x10^{-07}	-0.012	6.59x10^{-01}	8.12x10^{-01}
ACPP	0.663	1.33x10^{-09}	3.09x10^{-07}	-0.024	6.52x10^{-01}	8.07x10^{-01}
S100A12	0.264	1.45x10^{-09}	3.30x10^{-07}	-0.024	7.87x10^{-01}	8.89x10^{-01}
AQP9	0.339	1.69x10^{-09}	3.68x10^{-07}	-0.071	1.15x10^{-01}	2.99x10^{-01}
SSPN	1.450	2.54x10^{-09}	5.21x10^{-07}	0.128	2.77x10^{-01}	4.99x10^{-01}
PADI2	0.789	2.66x10^{-09}	5.34x10^{-07}	-0.024	7.86x10^{-01}	8.89x10^{-01}
NKD1	0.550	2.69x10^{-09}	5.34x10^{-07}	-0.048	7.18x10^{-01}	8.49x10^{-01}
FAM217B	0.776	2.73x10^{-09}	5.34x10^{-07}	-0.046	2.49x10^{-01}	4.70x10^{-01}
DCBLD1	1.425	2.90x10^{-09}	5.46x10^{-07}	0.121	1.02x10^{-01}	2.78x10^{-01}
SFRP2	3.108	3.88x10^{-09}	6.76x10^{-07}	0.229	7.90x10^{-02}	2.40x10^{-01}
IDH1	0.609	4.61x10^{-09}	7.77x10^{-07}	-0.030	3.93x10^{-01}	6.13x10^{-01}
NCF4	0.649	5.01x10^{-09}	8.26x10^{-07}	-0.071	1.13x10^{-01}	2.95x10^{-01}
CNIH4	0.762	5.69x10^{-09}	8.87x10^{-07}	-0.027	4.94x10^{-01}	6.97x10^{-01}
AIFM2	0.816	6.30x10^{-09}	9.54x10^{-07}	-0.025	6.22x10^{-01}	7.88x10^{-01}
ARRB2	0.695	8.67x10^{-09}	1.24x10^{-06}	-0.032	2.99x10^{-01}	5.21x10^{-01}
HIVEP2	1.780	9.58x10^{-09}	1.34x10^{-06}	0.088	7.43x10^{-02}	2.30x10^{-01}
RASGRP1	1.906	1.27x10^{-08}	1.67x10^{-06}	0.036	3.94x10^{-01}	6.14x10^{-01}
FADS1	0.622	1.39x10^{-08}	1.79x10^{-06}	-0.083	1.85x10^{-01}	3.96x10^{-01}
MSRB1	0.695	1.48x10^{-08}	1.88x10^{-06}	-0.021	6.58x10^{-01}	8.11x10^{-01}
SHKBP1	0.760	1.60x10^{-08}	1.99x10^{-06}	-0.039	3.95x10^{-01}	6.15x10^{-01}
SLC25A24	0.821	1.85x10^{-08}	2.22x10^{-06}	-0.021	6.21x10^{-01}	7.87x10^{-01}
SARS	0.770	2.06x10^{-08}	2.42x10^{-06}	-0.024	3.24x10^{-01}	5.47x10^{-01}
IMPDH1	0.857	2.14x10^{-08}	2.48x10^{-06}	-0.017	6.89x10^{-01}	8.31x10^{-01}
QPCT	0.684	2.21x10^{-08}	2.53x10^{-06}	-0.038	5.00x10^{-01}	7.00x10^{-01}
LSS	0.697	2.47x10^{-08}	2.79x10^{-06}	-0.066	2.52x10^{-01}	4.73x10^{-01}
HK3	0.641	2.51x10^{-08}	2.80x10^{-06}	-0.034	5.44x10^{-01}	7.35x10^{-01}
HTATIP2	0.763	2.80x10^{-08}	3.04x10^{-06}	-0.017	6.89x10^{-01}	8.31x10^{-01}
ARHGEF7	1.249	2.82x10^{-08}	3.04x10^{-06}	0.024	4.54x10^{-01}	6.64x10^{-01}
VCAM1	3.076	3.83x10^{-08}	4.02x10^{-06}	0.002	9.91x10^{-01}	9.96x10^{-01}

LRRC25	0.676	3.96x10^{-08}	4.11x10^{-06}	-0.022	6.90x10^{-01}	8.31x10^{-01}
ADCY6	1.225	4.05x10^{-08}	4.19x10^{-06}	0.123	3.10x10^{-01}	5.34x10^{-01}
PROK2	0.508	4.37x10^{-08}	4.46x10^{-06}	-0.058	4.13x10^{-01}	6.30x10^{-01}
NPL	0.533	4.94x10^{-08}	4.81x10^{-06}	-0.029	4.44x10^{-01}	6.56x10^{-01}
VSIG4	0.505	5.17x10^{-08}	4.97x10^{-06}	-0.093	1.32x10^{-01}	3.23x10^{-01}
MYO1F	0.616	5.28x10^{-08}	5.01x10^{-06}	-0.044	1.40x10^{-01}	3.34x10^{-01}
CLEC7A	0.688	5.76x10^{-08}	5.42x10^{-06}	-0.031	5.00x10^{-01}	7.00x10^{-01}
DUSP18	0.775	5.85x10^{-08}	5.48x10^{-06}	-0.003	9.40x10^{-01}	9.73x10^{-01}
TBC1D8	0.698	5.99x10^{-08}	5.59x10^{-06}	-0.045	2.68x10^{-01}	4.90x10^{-01}
CFD	1.646	6.08x10^{-08}	5.65x10^{-06}	0.054	6.97x10^{-01}	8.35x10^{-01}
SLC26A8	0.900	8.03x10^{-08}	7.02x10^{-06}	-0.029	6.65x10^{-01}	8.16x10^{-01}
KDM5B	1.238	8.58x10^{-08}	7.32x10^{-06}	0.014	6.76x10^{-01}	8.22x10^{-01}
CTNS	0.754	9.20x10^{-08}	7.70x10^{-06}	-0.081	6.50x10^{-02}	2.13x10^{-01}
MTCH2	0.778	9.50x10^{-08}	7.81x10^{-06}	-0.023	3.73x10^{-01}	5.95x10^{-01}
TNXB	1.566	1.09x10^{-07}	8.79x10^{-06}	0.041	7.18x10^{-01}	8.49x10^{-01}
LTBP2	1.916	1.12x10^{-07}	8.96x10^{-06}	0.006	9.48x10^{-01}	9.78x10^{-01}
ZHX2	1.350	1.17x10^{-07}	9.23x10^{-06}	0.119	1.03x10^{-01}	2.79x10^{-01}
BCL2	1.233	1.39x10^{-07}	1.06x10^{-05}	0.062	2.08x10^{-01}	4.23x10^{-01}
HLA-DRA	1.297	1.41x10^{-07}	1.07x10^{-05}	0.058	3.13x10^{-01}	5.37x10^{-01}
SFXN2	0.764	1.45x10^{-07}	1.10x10^{-05}	-0.019	6.81x10^{-01}	8.25x10^{-01}
MS4A2	2.036	1.57x10^{-07}	1.15x10^{-05}	0.046	6.86x10^{-01}	8.29x10^{-01}
PRKAR2A	0.860	1.65x10^{-07}	1.18x10^{-05}	-0.027	3.41x10^{-01}	5.64x10^{-01}
TSHZ2	1.686	1.69x10^{-07}	1.20x10^{-05}	0.120	2.59x10^{-01}	4.81x10^{-01}
MOB3B	1.269	1.77x10^{-07}	1.25x10^{-05}	0.039	4.81x10^{-01}	6.85x10^{-01}
BICC1	1.593	1.98x10^{-07}	1.37x10^{-05}	0.013	8.99x10^{-01}	9.54x10^{-01}
FGD2	0.708	2.10x10^{-07}	1.44x10^{-05}	-0.063	2.72x10^{-01}	4.94x10^{-01}
SLC22A23	1.344	2.13x10^{-07}	1.44x10^{-05}	0.089	2.57x10^{-01}	4.78x10^{-01}
ITSN1	1.156	2.32x10^{-07}	1.55x10^{-05}	0.057	3.15x10^{-01}	5.39x10^{-01}
CRIP1	1.281	2.33x10^{-07}	1.55x10^{-05}	0.035	4.22x10^{-01}	6.38x10^{-01}
SLC37A2	0.737	2.36x10^{-07}	1.56x10^{-05}	-0.024	7.17x10^{-01}	8.48x10^{-01}
OGN	2.219	2.42x10^{-07}	1.59x10^{-05}	0.145	1.86x10^{-01}	3.97x10^{-01}
ZBTB20	1.423	2.53x10^{-07}	1.65x10^{-05}	0.032	2.85x10^{-01}	5.07x10^{-01}
PON2	0.758	2.70x10^{-07}	1.74x10^{-05}	-0.078	1.10x10^{-01}	2.90x10^{-01}
MT-TS1	0.679	2.93x10^{-07}	1.87x10^{-05}	-0.067	6.29x10^{-01}	7.93x10^{-01}
THOC5	0.769	2.99x10^{-07}	1.89x10^{-05}	-0.032	3.43x10^{-01}	5.66x10^{-01}
HDC	1.856	3.03x10^{-07}	1.91x10^{-05}	0.103	3.95x10^{-01}	6.15x10^{-01}
ORMDL2	0.781	3.17x10^{-07}	1.97x10^{-05}	-0.022	4.36x10^{-01}	6.49x10^{-01}
NICN1	1.227	3.27x10^{-07}	2.00x10^{-05}	0.001	9.81x10^{-01}	9.93x10^{-01}
NQO2	0.679	3.27x10^{-07}	2.00x10^{-05}	-0.099	2.81x10^{-01}	5.02x10^{-01}
AKR1C3	0.641	3.59x10^{-07}	2.16x10^{-05}	-0.124	2.27x10^{-01}	4.46x10^{-01}
PGM5	1.571	3.71x10^{-07}	2.21x10^{-05}	0.237	7.66x10^{-02}	2.34x10^{-01}
RNF13	0.837	3.77x10^{-07}	2.24x10^{-05}	-0.056	8.52x10^{-02}	2.50x10^{-01}
MTRF1L	0.786	3.93x10^{-07}	2.32x10^{-05}	-0.053	8.64x10^{-02}	2.53x10^{-01}
DSCR3	0.867	4.17x10^{-07}	2.42x10^{-05}	-0.009	6.55x10^{-01}	8.09x10^{-01}
CNOT6L	1.290	4.60x10^{-07}	2.60x10^{-05}	0.010	6.96x10^{-01}	8.35x10^{-01}
TMEM69	0.839	4.60x10^{-07}	2.60x10^{-05}	-0.078	2.07x10^{-01}	4.22x10^{-01}

CXCR2	0.536	4.73x10^{-07}	2.66x10^{-05}	-0.096	1.18x10^{-01}	3.02x10^{-01}
CHFR	0.833	4.75x10^{-07}	2.66x10^{-05}	-0.012	5.88x10^{-01}	7.66x10^{-01}
DOK6	1.310	4.82x10^{-07}	2.69x10^{-05}	0.131	3.09x10^{-01}	5.33x10^{-01}
SERINC5	1.280	5.64x10^{-07}	3.06x10^{-05}	0.014	6.85x10^{-01}	8.29x10^{-01}
TMED8	0.841	5.96x10^{-07}	3.21x10^{-05}	-0.045	3.19x10^{-01}	5.43x10^{-01}
RPS6KA5	1.324	6.06x10^{-07}	3.25x10^{-05}	0.016	6.49x10^{-01}	8.05x10^{-01}
RASGRP4	0.810	6.70x10^{-07}	3.53x10^{-05}	-0.021	6.84x10^{-01}	8.28x10^{-01}
HCLS1	0.662	6.92x10^{-07}	3.61x10^{-05}	-0.049	2.42x10^{-01}	4.63x10^{-01}
VNN2	0.447	8.24x10^{-07}	4.15x10^{-05}	-0.020	7.34x10^{-01}	8.59x10^{-01}
FAH	0.706	8.49x10^{-07}	4.26x10^{-05}	0.000	9.94x10^{-01}	9.97x10^{-01}
TKT	0.727	8.58x10^{-07}	4.30x10^{-05}	-0.061	1.19x10^{-01}	3.04x10^{-01}
YBX1	0.878	9.42x10^{-07}	4.66x10^{-05}	-0.069	2.45x10^{-01}	4.66x10^{-01}
AHCYL2	1.444	9.51x10^{-07}	4.68x10^{-05}	0.008	7.82x10^{-01}	8.87x10^{-01}
XAF1	1.629	9.74x10^{-07}	4.74x10^{-05}	0.062	6.63x10^{-01}	8.14x10^{-01}
PREX1	0.683	1.03x10^{-06}	4.95x10^{-05}	-0.074	6.89x10^{-02}	2.21x10^{-01}
PNRC1	1.311	1.04x10^{-06}	5.02x10^{-05}	0.039	3.78x10^{-01}	6.00x10^{-01}
CPPED1	0.734	1.06x10^{-06}	5.09x10^{-05}	-0.044	4.03x10^{-01}	6.22x10^{-01}
CCR2	0.648	1.09x10^{-06}	5.19x10^{-05}	-0.039	4.67x10^{-01}	6.75x10^{-01}
FPR1	0.544	1.12x10^{-06}	5.31x10^{-05}	-0.062	3.05x10^{-01}	5.28x10^{-01}
SOAT1	0.730	1.15x10^{-06}	5.42x10^{-05}	-0.043	2.00x10^{-01}	4.14x10^{-01}
FKBP15	0.774	1.41x10^{-06}	6.36x10^{-05}	-0.045	2.45x10^{-01}	4.66x10^{-01}
RPN1	0.820	1.43x10^{-06}	6.42x10^{-05}	-0.049	6.45x10^{-02}	2.12x10^{-01}
ENTPD5	0.860	1.47x10^{-06}	6.57x10^{-05}	-0.013	7.89x10^{-01}	8.91x10^{-01}
SH3BP5L	0.897	1.47x10^{-06}	6.55x10^{-05}	-0.003	9.46x10^{-01}	9.76x10^{-01}
CDRT4	1.200	1.56x10^{-06}	6.87x10^{-05}	0.090	3.40x10^{-01}	5.63x10^{-01}
NAIP	0.701	1.57x10^{-06}	6.87x10^{-05}	-0.144	1.11x10^{-01}	2.93x10^{-01}
LGALSL	1.604	1.62x10^{-06}	7.04x10^{-05}	0.017	8.59x10^{-01}	9.34x10^{-01}
HLA-DQA1	1.648	1.67x10^{-06}	7.16x10^{-05}	0.053	5.98x10^{-01}	7.73x10^{-01}
CD53	0.732	1.70x10^{-06}	7.26x10^{-05}	-0.031	3.26x10^{-01}	5.49x10^{-01}
CCR1	0.535	1.72x10^{-06}	7.34x10^{-05}	-0.144	9.49x10^{-02}	2.66x10^{-01}
RGS13	1.586	1.78x10^{-06}	7.52x10^{-05}	0.216	6.16x10^{-02}	2.07x10^{-01}
LILRA1	0.599	1.82x10^{-06}	7.64x10^{-05}	-0.051	3.13x10^{-01}	5.37x10^{-01}
ABI2	1.219	1.85x10^{-06}	7.73x10^{-05}	0.012	7.81x10^{-01}	8.87x10^{-01}
MFGE8	0.702	1.91x10^{-06}	7.88x10^{-05}	-0.101	1.64x10^{-01}	3.68x10^{-01}
SIK2	1.379	1.95x10^{-06}	8.01x10^{-05}	0.052	2.06x10^{-01}	4.21x10^{-01}
ESM1	2.324	1.96x10^{-06}	8.05x10^{-05}	0.073	6.24x10^{-01}	7.90x10^{-01}
FBXL2	1.238	2.02x10^{-06}	8.21x10^{-05}	0.060	1.17x10^{-01}	3.01x10^{-01}
KIAA0040	0.707	2.02x10^{-06}	8.21x10^{-05}	-0.083	1.18x10^{-01}	3.02x10^{-01}
PPP1R7	0.849	2.08x10^{-06}	8.38x10^{-05}	-0.018	5.22x10^{-01}	7.18x10^{-01}
EIF2B2	0.790	2.11x10^{-06}	8.45x10^{-05}	-0.024	3.93x10^{-01}	6.13x10^{-01}
S1PR1	0.777	2.28x10^{-06}	9.01x10^{-05}	-0.016	7.85x10^{-01}	8.89x10^{-01}
GSTA4	0.696	2.32x10^{-06}	9.12x10^{-05}	-0.003	9.61x10^{-01}	9.83x10^{-01}
VIM	1.199	2.41x10^{-06}	9.36x10^{-05}	0.012	7.91x10^{-01}	8.92x10^{-01}
TRANK1	1.339	2.50x10^{-06}	9.69x10^{-05}	0.043	4.14x10^{-01}	6.31x10^{-01}
REV3L	1.180	2.58x10^{-06}	9.91x10^{-05}	0.012	6.77x10^{-01}	8.23x10^{-01}
VPS33B	0.847	2.58x10^{-06}	9.91x10^{-05}	-0.070	9.11x10^{-02}	2.60x10^{-01}

KCNAB2	0.696	2.69x10^{-06}	1.02x10^{-04}	-0.004	9.31x10^{-01}	9.69x10^{-01}
MANSC1	0.803	2.69x10^{-06}	1.02x10^{-04}	-0.153	5.25x10^{-02}	1.88x10^{-01}
UBE2D1	0.762	2.74x10^{-06}	1.04x10^{-04}	-0.094	7.44x10^{-02}	2.30x10^{-01}
ASPH	0.837	2.83x10^{-06}	1.07x10^{-04}	-0.076	1.97x10^{-01}	4.10x10^{-01}
CNOT11	0.888	2.92x10^{-06}	1.10x10^{-04}	-0.027	4.06x10^{-01}	6.25x10^{-01}
GAPT	0.759	3.00x10^{-06}	1.12x10^{-04}	-0.053	3.69x10^{-01}	5.91x10^{-01}
SCAMP3	0.827	3.24x10^{-06}	1.19x10^{-04}	-0.037	4.08x10^{-01}	6.26x10^{-01}
SPIN1	1.196	3.29x10^{-06}	1.20x10^{-04}	0.040	2.03x10^{-01}	4.17x10^{-01}
AREL1	0.829	3.63x10^{-06}	1.30x10^{-04}	-0.034	1.66x10^{-01}	3.70x10^{-01}
PPP1R12B	1.222	3.74x10^{-06}	1.33x10^{-04}	0.009	8.34x10^{-01}	9.20x10^{-01}
BASP1	0.721	3.78x10^{-06}	1.34x10^{-04}	-0.106	9.50x10^{-02}	2.66x10^{-01}
GABBR1	1.282	3.86x10^{-06}	1.36x10^{-04}	0.003	9.54x10^{-01}	9.81x10^{-01}
WEE1	1.421	3.90x10^{-06}	1.38x10^{-04}	0.016	7.70x10^{-01}	8.80x10^{-01}
SNX11	0.842	3.98x10^{-06}	1.39x10^{-04}	-0.059	5.09x10^{-02}	1.85x10^{-01}
SLC3A2	0.768	4.01x10^{-06}	1.40x10^{-04}	-0.034	2.62x10^{-01}	4.84x10^{-01}
COPE	0.775	4.11x10^{-06}	1.43x10^{-04}	-0.017	4.99x10^{-01}	6.99x10^{-01}
SPI1	0.755	4.19x10^{-06}	1.44x10^{-04}	-0.064	1.48x10^{-01}	3.47x10^{-01}
FAM171B	1.314	4.59x10^{-06}	1.56x10^{-04}	0.060	4.87x10^{-01}	6.91x10^{-01}
RPL22L1	0.741	4.67x10^{-06}	1.58x10^{-04}	-0.020	6.14x10^{-01}	7.82x10^{-01}
C7orf49	0.823	4.87x10^{-06}	1.63x10^{-04}	-0.041	4.46x10^{-01}	6.58x10^{-01}
SEMA5A	1.481	5.09x10^{-06}	1.68x10^{-04}	0.175	1.65x10^{-01}	3.70x10^{-01}
CASK	1.167	5.27x10^{-06}	1.72x10^{-04}	0.033	3.53x10^{-01}	5.76x10^{-01}
GOLGA8B	1.312	5.52x10^{-06}	1.79x10^{-04}	0.067	2.19x10^{-01}	4.36x10^{-01}
MKL1	1.167	5.53x10^{-06}	1.79x10^{-04}	0.034	2.66x10^{-01}	4.89x10^{-01}
FARP2	1.196	5.59x10^{-06}	1.80x10^{-04}	0.004	9.33x10^{-01}	9.70x10^{-01}
SIRPD	0.877	5.61x10^{-06}	1.80x10^{-04}	-0.133	7.31x10^{-02}	2.28x10^{-01}
POLR3B	0.768	5.80x10^{-06}	1.85x10^{-04}	-0.020	5.90x10^{-01}	7.67x10^{-01}
RNF150	1.222	5.84x10^{-06}	1.85x10^{-04}	0.064	8.37x10^{-01}	9.21x10^{-01}
EIF4EBP1	0.781	5.89x10^{-06}	1.86x10^{-04}	-0.019	7.73x10^{-01}	8.82x10^{-01}
GMIP	0.805	6.21x10^{-06}	1.95x10^{-04}	-0.026	4.93x10^{-01}	6.96x10^{-01}
CALML4	0.826	6.24x10^{-06}	1.95x10^{-04}	-0.109	1.24x10^{-01}	3.11x10^{-01}
RENBP	0.780	6.33x10^{-06}	1.98x10^{-04}	-0.038	4.02x10^{-01}	6.22x10^{-01}
TMEM138	0.851	6.37x10^{-06}	1.98x10^{-04}	-0.034	5.62x10^{-01}	7.47x10^{-01}
IRF5	0.858	6.38x10^{-06}	1.98x10^{-04}	-0.046	3.63x10^{-01}	5.86x10^{-01}
CDON	1.512	6.47x10^{-06}	2.00x10^{-04}	0.017	8.27x10^{-01}	9.16x10^{-01}
PLXDC1	1.333	6.56x10^{-06}	2.02x10^{-04}	0.012	8.69x10^{-01}	9.38x10^{-01}
FGFR2	1.667	6.72x10^{-06}	2.06x10^{-04}	0.034	8.05x10^{-01}	9.02x10^{-01}
OSBPL10	1.247	7.05x10^{-06}	2.14x10^{-04}	0.025	8.35x10^{-01}	9.20x10^{-01}
GNPDA1	0.687	7.10x10^{-06}	2.15x10^{-04}	-0.015	6.62x10^{-01}	8.14x10^{-01}
ZNF622	0.834	7.13x10^{-06}	2.16x10^{-04}	-0.018	4.66x10^{-01}	6.74x10^{-01}
SMAD9	1.354	7.20x10^{-06}	2.17x10^{-04}	0.045	3.08x10^{-01}	5.31x10^{-01}
EIF2A	0.870	7.37x10^{-06}	2.20x10^{-04}	-0.052	9.77x10^{-02}	2.71x10^{-01}
MIER2	0.816	7.37x10^{-06}	2.20x10^{-04}	-0.060	3.46x10^{-01}	5.69x10^{-01}
TCF4	1.300	7.69x10^{-06}	2.26x10^{-04}	0.060	3.95x10^{-01}	6.15x10^{-01}
EFNB1	0.774	7.77x10^{-06}	2.27x10^{-04}	-0.044	3.57x10^{-01}	5.80x10^{-01}
CD14	0.579	7.93x10^{-06}	2.31x10^{-04}	-0.035	5.42x10^{-01}	7.33x10^{-01}

BCAT2	0.738	8.19x10^{-06}	2.37x10^{-04}	-0.005	9.19x10^{-01}	9.64x10^{-01}
NUDT4	1.216	8.22x10^{-06}	2.38x10^{-04}	0.017	7.86x10^{-01}	8.89x10^{-01}
VASH2	1.113	8.53x10^{-06}	2.44x10^{-04}	0.008	8.82x10^{-01}	9.44x10^{-01}
GIMAP6	0.689	8.95x10^{-06}	2.55x10^{-04}	-0.028	3.77x10^{-01}	5.99x10^{-01}
SLC16A6	0.532	9.70x10^{-06}	2.70x10^{-04}	-0.059	1.52x10^{-01}	3.52x10^{-01}
SELL	0.587	1.01x10^{-05}	2.77x10^{-04}	-0.040	4.21x10^{-01}	6.37x10^{-01}
CPT2	0.802	1.02x10^{-05}	2.81x10^{-04}	-0.018	5.65x10^{-01}	7.49x10^{-01}
MICAL3	1.278	1.05x10^{-05}	2.86x10^{-04}	0.011	8.39x10^{-01}	9.23x10^{-01}
INIP	0.862	1.06x10^{-05}	2.88x10^{-04}	-0.049	5.17x10^{-02}	1.86x10^{-01}
TRIM25	0.794	1.08x10^{-05}	2.91x10^{-04}	-0.025	5.81x10^{-01}	7.61x10^{-01}
ITIH5	1.394	1.10x10^{-05}	2.95x10^{-04}	0.089	2.26x10^{-01}	4.45x10^{-01}
UBR5	1.106	1.10x10^{-05}	2.96x10^{-04}	0.000	9.99x10^{-01}	1.00e+00
BLOC1S2	0.822	1.10x10^{-05}	2.96x10^{-04}	-0.035	2.45x10^{-01}	4.66x10^{-01}
ENO1	0.740	1.12x10^{-05}	3.00x10^{-04}	-0.015	6.24x10^{-01}	7.90x10^{-01}
TVP23A	1.091	1.14x10^{-05}	3.05x10^{-04}	0.046	4.02x10^{-01}	6.21x10^{-01}
SYT11	1.310	1.40x10^{-05}	3.52x10^{-04}	0.084	1.43x10^{-01}	3.40x10^{-01}
RRAGD	0.720	1.41x10^{-05}	3.54x10^{-04}	-0.032	4.47x10^{-01}	6.58x10^{-01}
MTIF2	0.789	1.45x10^{-05}	3.63x10^{-04}	-0.032	2.38x10^{-01}	4.58x10^{-01}
IL18RAP	0.554	1.46x10^{-05}	3.65x10^{-04}	-0.123	2.66x10^{-01}	4.89x10^{-01}
SEC14L4	0.568	1.46x10^{-05}	3.65x10^{-04}	-0.094	2.26x10^{-01}	4.45x10^{-01}
C1D	0.800	1.52x10^{-05}	3.75x10^{-04}	-0.108	4.33x10^{-01}	6.47x10^{-01}
PTPRJ	0.768	1.53x10^{-05}	3.77x10^{-04}	-0.019	6.36x10^{-01}	7.98x10^{-01}
ZMAT2	0.856	1.54x10^{-05}	3.78x10^{-04}	-0.082	7.47x10^{-02}	2.31x10^{-01}
MVK	0.853	1.56x10^{-05}	3.81x10^{-04}	-0.024	6.70x10^{-01}	8.19x10^{-01}
MAPK13	0.804	1.58x10^{-05}	3.86x10^{-04}	-0.023	6.55x10^{-01}	8.09x10^{-01}
GCSH	0.831	1.60x10^{-05}	3.89x10^{-04}	-0.079	1.71x10^{-01}	3.78x10^{-01}
RBBP8	0.801	1.63x10^{-05}	3.96x10^{-04}	-0.035	4.80x10^{-01}	6.84x10^{-01}
DONSON	1.146	1.67x10^{-05}	4.02x10^{-04}	0.006	8.63x10^{-01}	9.36x10^{-01}
GLB1L2	0.838	1.72x10^{-05}	4.12x10^{-04}	-0.057	7.27x10^{-01}	8.54x10^{-01}
NCR3LG1	0.740	1.76x10^{-05}	4.21x10^{-04}	-0.099	1.62x10^{-01}	3.65x10^{-01}
CD82	0.760	1.78x10^{-05}	4.23x10^{-04}	-0.097	7.32x10^{-02}	2.28x10^{-01}
CPNE8	0.844	1.78x10^{-05}	4.23x10^{-04}	-0.074	1.54x10^{-01}	3.54x10^{-01}
RASAL2	1.281	1.83x10^{-05}	4.33x10^{-04}	0.035	7.42x10^{-01}	8.63x10^{-01}
DNM1	1.110	1.86x10^{-05}	4.37x10^{-04}	0.150	5.34x10^{-01}	7.27x10^{-01}
ATP5SL	0.806	1.94x10^{-05}	4.55x10^{-04}	-0.036	4.26x10^{-01}	6.41x10^{-01}
C1orf162	0.736	2.04x10^{-05}	4.76x10^{-04}	-0.072	2.95x10^{-01}	5.17x10^{-01}
SYK	0.767	2.12x10^{-05}	4.91x10^{-04}	-0.055	1.43x10^{-01}	3.39x10^{-01}
TST	0.756	2.13x10^{-05}	4.91x10^{-04}	-0.079	1.22x10^{-01}	3.08x10^{-01}
SCIMP	0.702	2.17x10^{-05}	4.98x10^{-04}	-0.030	6.16x10^{-01}	7.84x10^{-01}
SDHB	0.869	2.18x10^{-05}	5.00x10^{-04}	-0.036	1.97x10^{-01}	4.10x10^{-01}
GPR155	1.294	2.39x10^{-05}	5.40x10^{-04}	0.005	9.11x10^{-01}	9.59x10^{-01}
LDLRAD4	1.178	2.44x10^{-05}	5.49x10^{-04}	0.019	5.80x10^{-01}	7.60x10^{-01}
LACTB2	0.850	2.51x10^{-05}	5.61x10^{-04}	-0.007	8.46x10^{-01}	9.27x10^{-01}
ZNF445	1.152	2.53x10^{-05}	5.65x10^{-04}	0.046	1.94x10^{-01}	4.06x10^{-01}
SNRPC	0.868	2.54x10^{-05}	5.65x10^{-04}	-0.054	3.82x10^{-01}	6.04x10^{-01}
BRAF	1.160	2.58x10^{-05}	5.72x10^{-04}	0.014	5.36x10^{-01}	7.28x10^{-01}

SGCD	1.292	2.61x10^{-05}	5.76x10^{-04}	0.196	3.97x10^{-01}	6.17x10^{-01}
SPTLC2	0.868	2.61x10^{-05}	5.77x10^{-04}	-0.045	2.96x10^{-01}	5.18x10^{-01}
MPP1	0.695	2.64x10^{-05}	5.80x10^{-04}	-0.063	2.14x10^{-01}	4.30x10^{-01}
NOP10	0.777	2.65x10^{-05}	5.81x10^{-04}	-0.055	1.61x10^{-01}	3.64x10^{-01}
SLIT3	1.429	2.73x10^{-05}	5.97x10^{-04}	0.123	1.54x10^{-01}	3.55x10^{-01}
TDRD9	0.728	2.81x10^{-05}	6.08x10^{-04}	-0.016	8.74x10^{-01}	9.40x10^{-01}
CEP85	0.890	2.82x10^{-05}	6.09x10^{-04}	-0.009	8.07x10^{-01}	9.03x10^{-01}
PDSS1	0.718	2.93x10^{-05}	6.27x10^{-04}	-0.002	9.62x10^{-01}	9.84x10^{-01}
C1QTNF3	1.291	2.96x10^{-05}	6.30x10^{-04}	0.067	2.15x10^{-01}	4.31x10^{-01}
LAT2	0.844	2.96x10^{-05}	6.31x10^{-04}	-0.059	1.19x10^{-01}	3.03x10^{-01}
TRIO	1.155	2.99x10^{-05}	6.35x10^{-04}	0.074	1.12x10^{-01}	2.95x10^{-01}
STAMBPL1	1.312	3.00x10^{-05}	6.38x10^{-04}	0.029	4.86x10^{-01}	6.89x10^{-01}
HLA-DQA2	1.362	3.05x10^{-05}	6.46x10^{-04}	0.372	3.25x10^{-01}	5.49x10^{-01}
CCRL2	0.759	3.12x10^{-05}	6.57x10^{-04}	-0.050	3.21x10^{-01}	5.45x10^{-01}
PI3	0.605	3.13x10^{-05}	6.59x10^{-04}	-0.222	1.71x10^{-01}	3.78x10^{-01}
SPP1	0.322	3.14x10^{-05}	6.60x10^{-04}	-0.181	3.69x10^{-01}	5.91x10^{-01}
COL6A6	2.138	3.16x10^{-05}	6.62x10^{-04}	0.013	7.97x10^{-01}	8.97x10^{-01}
FMN1	0.671	3.17x10^{-05}	6.62x10^{-04}	-0.153	3.83x10^{-01}	6.04x10^{-01}
ARL8A	0.857	3.19x10^{-05}	6.64x10^{-04}	-0.046	2.44x10^{-01}	4.65x10^{-01}
TRAF7	0.827	3.19x10^{-05}	6.65x10^{-04}	-0.065	2.73x10^{-01}	4.95x10^{-01}
LILRB1	0.656	3.20x10^{-05}	6.66x10^{-04}	-0.081	2.26x10^{-01}	4.45x10^{-01}
UEVLD	0.836	3.27x10^{-05}	6.78x10^{-04}	-0.043	9.52x10^{-02}	2.66x10^{-01}
FAHD1	0.856	3.34x10^{-05}	6.89x10^{-04}	-0.024	5.59x10^{-01}	7.45x10^{-01}
ACSL1	0.710	3.35x10^{-05}	6.90x10^{-04}	-0.115	6.33x10^{-02}	2.10x10^{-01}
MS4A6A	0.729	3.36x10^{-05}	6.92x10^{-04}	-0.086	9.85x10^{-02}	2.72x10^{-01}
CMKLR1	0.757	3.43x10^{-05}	7.02x10^{-04}	-0.036	6.61x10^{-01}	8.14x10^{-01}
ARL11	0.911	3.47x10^{-05}	7.09x10^{-04}	-0.011	8.45x10^{-01}	9.26x10^{-01}
PLSCR4	1.316	3.57x10^{-05}	7.25x10^{-04}	0.031	7.22x10^{-01}	8.51x10^{-01}
RN7SL683P	1.343	3.65x10^{-05}	7.38x10^{-04}	0.081	2.45x10^{-01}	4.66x10^{-01}
KIAA0100	0.850	3.67x10^{-05}	7.41x10^{-04}	-0.029	3.05x10^{-01}	5.28x10^{-01}
COMMD8	0.824	3.77x10^{-05}	7.56x10^{-04}	-0.027	3.93x10^{-01}	6.14x10^{-01}
CCZ1	0.906	3.99x10^{-05}	7.92x10^{-04}	-0.004	8.81x10^{-01}	9.44x10^{-01}
IFITM2	0.847	4.00x10^{-05}	7.93x10^{-04}	-0.034	6.80x10^{-01}	8.25x10^{-01}
PSEN2	0.835	4.08x10^{-05}	8.07x10^{-04}	-0.066	2.06x10^{-01}	4.21x10^{-01}
NDUFS2	0.880	4.10x10^{-05}	8.09x10^{-04}	-0.028	2.49x10^{-01}	4.70x10^{-01}
HERC3	0.828	4.11x10^{-05}	8.10x10^{-04}	-0.016	5.75x10^{-01}	7.56x10^{-01}
KNSTRN	0.777	4.16x10^{-05}	8.17x10^{-04}	-0.016	7.72x10^{-01}	8.81x10^{-01}
CDC42EP2	0.824	4.21x10^{-05}	8.24x10^{-04}	-0.034	6.45x10^{-01}	8.02x10^{-01}
TM7SF2	0.844	4.22x10^{-05}	8.25x10^{-04}	-0.015	7.68x10^{-01}	8.79x10^{-01}
SH3BP2	0.857	4.31x10^{-05}	8.38x10^{-04}	-0.027	4.60x10^{-01}	6.68x10^{-01}
KCNE4	1.258	4.39x10^{-05}	8.50x10^{-04}	0.067	5.56x10^{-02}	1.95x10^{-01}
PCCB	0.849	4.39x10^{-05}	8.50x10^{-04}	-0.019	4.93x10^{-01}	6.96x10^{-01}
CTSB	0.750	4.47x10^{-05}	8.60x10^{-04}	-0.019	7.43x10^{-01}	8.64x10^{-01}
S100A4	0.747	4.48x10^{-05}	8.60x10^{-04}	-0.003	9.22x10^{-01}	9.65x10^{-01}
IL10RB	0.853	4.65x10^{-05}	8.83x10^{-04}	-0.003	9.28x10^{-01}	9.68x10^{-01}
TGIF2	1.169	4.72x10^{-05}	8.92x10^{-04}	0.026	6.01x10^{-01}	7.74x10^{-01}

MAP10	0.909	4.72x10^{-05}	8.93x10^{-04}	-0.077	2.07x10^{-01}	4.22x10^{-01}
MEGF11	1.098	4.74x10^{-05}	8.94x10^{-04}	0.072	9.31x10^{-02}	2.63x10^{-01}
JMY	1.273	4.88x10^{-05}	9.15x10^{-04}	0.063	1.73x10^{-01}	3.79x10^{-01}
UBE2E2	1.188	4.88x10^{-05}	9.15x10^{-04}	0.048	4.41x10^{-01}	6.54x10^{-01}
CD163L1	1.479	4.92x10^{-05}	9.18x10^{-04}	0.008	9.51x10^{-01}	9.79x10^{-01}
IQCE	0.880	4.95x10^{-05}	9.23x10^{-04}	-0.034	4.25x10^{-01}	6.40x10^{-01}
RABIF	0.899	5.03x10^{-05}	9.35x10^{-04}	-0.050	1.51x10^{-01}	3.50x10^{-01}
DENND2A	1.341	5.07x10^{-05}	9.41x10^{-04}	0.107	6.93x10^{-02}	2.21x10^{-01}
TTC28	1.209	5.21x10^{-05}	9.62x10^{-04}	0.072	5.01x10^{-01}	7.01x10^{-01}
Not validated						
LTBP1	2.015	9.12x10^{-17}	1.91x10^{-12}	-0.089	2.92x10^{-01}	5.14x10^{-01}
RNASE2	0.285	1.41x10^{-15}	9.84x10^{-12}	0.247	1.03x10^{-01}	2.80x10^{-01}
PDE3A	2.293	3.52x10^{-14}	1.23x10^{-10}	-0.247	1.89x10^{-02}	1.03x10^{-01}
SULT1B1	0.424	1.23x10^{-13}	2.90x10^{-10}	0.009	8.45x10^{-01}	9.27x10^{-01}
PDE7B	1.985	2.10x10^{-13}	3.91x10^{-10}	-0.104	2.56x10^{-01}	4.77x10^{-01}
SGSM2	1.277	1.41x10^{-12}	1.47x10^{-09}	-0.095	6.92x10^{-03}	5.70x10^{-02}
DLAT	0.759	2.12x10^{-12}	1.98x10^{-09}	0.042	1.92x10^{-01}	4.04x10^{-01}
PDE8A	1.346	2.18x10^{-12}	1.98x10^{-09}	-0.037	3.36x10^{-01}	5.60x10^{-01}
MGAM	0.312	3.45x10^{-12}	2.87x10^{-09}	0.137	2.01x10^{-02}	1.07x10^{-01}
GGTA1P	1.757	3.57x10^{-12}	2.87x10^{-09}	-0.355	2.32x10^{-04}	8.19x10^{-03}
SLC36A1	0.534	7.54x10^{-12}	5.09x10^{-09}	0.037	4.79x10^{-01}	6.83x10^{-01}
PTGDS	1.478	2.15x10^{-11}	1.21x10^{-08}	-0.354	3.63x10^{-03}	3.96x10^{-02}
ZNF483	1.458	3.51x10^{-11}	1.76x10^{-08}	-0.059	1.34x10^{-01}	3.25x10^{-01}
EVI2B	0.668	3.83x10^{-11}	1.86x10^{-08}	0.067	2.74x10^{-01}	4.96x10^{-01}
MEGF9	0.677	4.57x10^{-11}	2.08x10^{-08}	0.103	4.87x10^{-02}	1.80x10^{-01}
LARGE	1.339	1.51x10^{-10}	5.02x10^{-08}	-0.044	6.44x10^{-01}	8.02x10^{-01}
MEX3C	1.256	3.02x10^{-10}	9.28x10^{-08}	-0.055	1.54x10^{-01}	3.54x10^{-01}
ANKRD36C	1.474	5.32x10^{-10}	1.54x10^{-07}	-0.030	3.85x10^{-01}	6.06x10^{-01}
PDE4D	1.591	5.82x10^{-10}	1.64x10^{-07}	-0.047	3.73x10^{-01}	5.95x10^{-01}
S100A8	0.337	8.05x10^{-10}	2.09x10^{-07}	0.000	1.00e+00	1.00e+00
H1F0	0.668	1.01x10^{-09}	2.49x10^{-07}	0.161	2.76x10^{-01}	4.98x10^{-01}
TMEM45B	0.543	1.05x10^{-09}	2.56x10^{-07}	0.035	6.84x10^{-01}	8.28x10^{-01}
SLC6A9	0.716	1.15x10^{-09}	2.73x10^{-07}	0.182	6.39x10^{-02}	2.11x10^{-01}
PMEPA1	1.504	1.20x10^{-09}	2.82x10^{-07}	-0.029	8.17x10^{-01}	9.10x10^{-01}
HLA-DPB1	1.543	1.39x10^{-09}	3.19x10^{-07}	-0.023	6.84x10^{-01}	8.28x10^{-01}
TMEM98	1.383	1.47x10^{-09}	3.30x10^{-07}	-0.124	3.38x10^{-01}	5.62x10^{-01}
IL17RA	0.700	1.66x10^{-09}	3.66x10^{-07}	0.021	5.89x10^{-01}	7.66x10^{-01}
PROCR	1.268	1.74x10^{-09}	3.76x10^{-07}	-0.082	1.74x10^{-01}	3.81x10^{-01}
PHGDH	0.522	2.23x10^{-09}	4.70x10^{-07}	0.037	6.56x10^{-01}	8.10x10^{-01}
MGST1	0.688	2.38x10^{-09}	4.97x10^{-07}	0.118	5.53x10^{-02}	1.94x10^{-01}
BMP6	2.133	2.48x10^{-09}	5.14x10^{-07}	-0.290	4.54x10^{-04}	1.18x10^{-02}
PRDX1	0.842	3.00x10^{-09}	5.60x10^{-07}	0.060	4.41x10^{-02}	1.69x10^{-01}
CD163	0.367	3.65x10^{-09}	6.46x10^{-07}	0.053	3.60x10^{-01}	5.83x10^{-01}
C1orf54	1.523	3.93x10^{-09}	6.79x10^{-07}	-0.148	8.88x10^{-02}	2.57x10^{-01}
PSD3	1.686	4.77x10^{-09}	7.98x10^{-07}	-0.154	8.89x10^{-02}	2.57x10^{-01}
SCARNA17	1.381	5.30x10^{-09}	8.45x10^{-07}	-0.076	2.66x10^{-01}	4.88x10^{-01}

MOB3A	0.755	5.33x10^{-09}	8.45x10^{-07}	0.093	7.12x10^{-02}	2.25x10^{-01}
G6PD	0.707	5.59x10^{-09}	8.79x10^{-07}	0.061	1.92x10^{-01}	4.03x10^{-01}
CCL5	2.112	6.03x10^{-09}	9.19x10^{-07}	-0.119	1.03x10^{-01}	2.80x10^{-01}
LUC7L	1.252	7.15x10^{-09}	1.07x10^{-06}	-0.030	3.73x10^{-01}	5.95x10^{-01}
PRTFDC1	1.243	7.51x10^{-09}	1.11x10^{-06}	-0.201	3.86x10^{-02}	1.57x10^{-01}
LAMP5	1.466	7.51x10^{-09}	1.11x10^{-06}	-0.011	9.22x10^{-01}	9.65x10^{-01}
FZR1	1.224	7.58x10^{-09}	1.12x10^{-06}	-0.023	5.15x10^{-01}	7.12x10^{-01}
SLC18A2	2.079	8.23x10^{-09}	1.19x10^{-06}	-0.150	3.74x10^{-02}	1.55x10^{-01}
ARMCX3	1.236	9.44x10^{-09}	1.32x10^{-06}	-0.061	3.48x10^{-02}	1.48x10^{-01}
DHDDS	0.769	9.91x10^{-09}	1.37x10^{-06}	0.088	5.87x10^{-03}	5.23x10^{-02}
SIGLEC5	0.757	1.15x10^{-08}	1.55x10^{-06}	0.174	4.60x10^{-02}	1.73x10^{-01}
NT5E	1.621	1.19x10^{-08}	1.59x10^{-06}	-0.286	2.44x10^{-03}	3.13x10^{-02}
PCYT1A	0.832	1.20x10^{-08}	1.59x10^{-06}	0.002	9.37x10^{-01}	9.72x10^{-01}
RBM33	1.239	1.28x10^{-08}	1.67x10^{-06}	-0.073	2.70x10^{-01}	4.92x10^{-01}
STAT4	1.581	1.32x10^{-08}	1.70x10^{-06}	-0.113	4.75x10^{-03}	4.58x10^{-02}
ANKRD10	1.270	1.50x10^{-08}	1.88x10^{-06}	-0.065	5.60x10^{-02}	1.95x10^{-01}
CARD6	0.799	1.52x10^{-08}	1.90x10^{-06}	0.093	2.96x10^{-02}	1.35x10^{-01}
FDPS	0.750	1.64x10^{-08}	2.02x10^{-06}	0.017	4.53x10^{-01}	6.63x10^{-01}
LCN2	0.361	1.77x10^{-08}	2.16x10^{-06}	0.435	3.29x10^{-03}	3.74x10^{-02}
GPRASP1	1.301	2.28x10^{-08}	2.61x10^{-06}	-0.230	3.74x10^{-05}	3.02x10^{-03}
ZNF460	1.222	2.50x10^{-08}	2.80x10^{-06}	-0.037	2.68x10^{-01}	4.90x10^{-01}
MATN2	1.477	2.66x10^{-08}	2.96x10^{-06}	-0.228	4.40x10^{-03}	4.39x10^{-02}
PITPNC1	1.597	2.76x10^{-08}	3.03x10^{-06}	-0.035	3.92x10^{-01}	6.13x10^{-01}
FAT3	1.921	2.77x10^{-08}	3.04x10^{-06}	-0.174	6.78x10^{-02}	2.19x10^{-01}
LTBP3	1.421	2.92x10^{-08}	3.13x10^{-06}	-0.063	2.28x10^{-01}	4.47x10^{-01}
SLC7A7	0.673	4.18x10^{-08}	4.31x10^{-06}	0.005	9.15x10^{-01}	9.61x10^{-01}
AIG1	1.205	4.21x10^{-08}	4.31x10^{-06}	-0.085	1.14x10^{-01}	2.97x10^{-01}
IL12RB2	1.178	4.56x10^{-08}	4.61x10^{-06}	-0.205	3.30x10^{-02}	1.44x10^{-01}
NF1	1.152	4.59x10^{-08}	4.61x10^{-06}	-0.016	6.37x10^{-01}	7.98x10^{-01}
ZSCAN18	1.266	4.61x10^{-08}	4.62x10^{-06}	-0.193	8.84x10^{-04}	1.74x10^{-02}
CAP1	0.835	4.65x10^{-08}	4.63x10^{-06}	0.014	6.61x10^{-01}	8.14x10^{-01}
C4BPB	0.855	4.74x10^{-08}	4.69x10^{-06}	0.200	1.47x10^{-04}	6.26x10^{-03}
SIGLEC14	0.701	4.98x10^{-08}	4.82x10^{-06}	0.123	4.21x10^{-01}	6.37x10^{-01}
SHMT2	0.607	6.28x10^{-08}	5.77x10^{-06}	0.018	6.46x10^{-01}	8.04x10^{-01}
OGT	1.219	6.87x10^{-08}	6.15x10^{-06}	-0.031	8.88x10^{-02}	2.57x10^{-01}
FOXJ3	1.134	7.37x10^{-08}	6.53x10^{-06}	-0.017	6.55x10^{-01}	8.09x10^{-01}
FABP5	0.683	8.34x10^{-08}	7.23x10^{-06}	0.151	7.28x10^{-03}	5.85x10^{-02}
MLX	0.792	8.52x10^{-08}	7.32x10^{-06}	0.002	9.55x10^{-01}	9.81x10^{-01}
MAPK8	1.220	9.09x10^{-08}	7.66x10^{-06}	-0.137	1.26x10^{-03}	2.15x10^{-02}
TRPC6	1.789	9.12x10^{-08}	7.66x10^{-06}	-0.111	3.44x10^{-01}	5.67x10^{-01}
SEPHS2	0.837	9.39x10^{-08}	7.79x10^{-06}	0.094	7.74x10^{-02}	2.36x10^{-01}
CTSF	1.474	9.40x10^{-08}	7.79x10^{-06}	-0.032	6.23x10^{-01}	7.89x10^{-01}
CNTF	0.883	9.54x10^{-08}	7.82x10^{-06}	0.016	7.70x10^{-01}	8.80x10^{-01}
C3AR1	0.568	1.11x10^{-07}	8.92x10^{-06}	0.233	1.46x10^{-02}	8.89x10^{-02}
RFTN1	1.383	1.14x10^{-07}	9.06x10^{-06}	-0.015	6.14x10^{-01}	7.83x10^{-01}
MDGA1	1.188	1.16x10^{-07}	9.15x10^{-06}	-0.012	9.67x10^{-01}	9.86x10^{-01}

MYBL1	1.456	$1.18x10^{-07}$	$9.23x10^{-06}$	-0.179	$1.21x10^{-02}$	$7.99x10^{-02}$
EBP	0.692	$1.26x10^{-07}$	$9.86x10^{-06}$	0.074	$2.89x10^{-02}$	$1.34x10^{-01}$
MTF1	0.752	$1.27x10^{-07}$	$9.91x10^{-06}$	0.133	$1.40x10^{-02}$	$8.67x10^{-02}$
KLF12	1.376	$1.29x10^{-07}$	$1.00x10^{-05}$	-0.063	$1.96x10^{-01}$	$4.09x10^{-01}$
TRPC1	1.349	$1.47x10^{-07}$	$1.11x10^{-05}$	-0.197	$5.71x10^{-03}$	$5.12x10^{-02}$
FBXW11	1.156	$1.49x10^{-07}$	$1.13x10^{-05}$	-0.082	$7.23x10^{-04}$	$1.56x10^{-02}$
SEPW1	1.323	$1.55x10^{-07}$	$1.15x10^{-05}$	-0.082	$1.10x10^{-02}$	$7.52x10^{-02}$
SLC38A7	0.822	$1.57x10^{-07}$	$1.15x10^{-05}$	0.029	$5.89x10^{-01}$	$7.66x10^{-01}$
F5	0.749	$1.65x10^{-07}$	$1.18x10^{-05}$	0.178	$6.43x10^{-03}$	$5.51x10^{-02}$
SNAP29	0.801	$1.77x10^{-07}$	$1.25x10^{-05}$	0.001	$9.80x10^{-01}$	$9.92x10^{-01}$
FCGBP	0.733	$1.85x10^{-07}$	$1.29x10^{-05}$	0.018	$8.76x10^{-01}$	$9.41x10^{-01}$
MAP3K4	1.214	$1.92x10^{-07}$	$1.34x10^{-05}$	-0.085	$1.70x10^{-02}$	$9.67x10^{-02}$
MTR	1.154	$2.07x10^{-07}$	$1.42x10^{-05}$	-0.081	$1.29x10^{-03}$	$2.19x10^{-02}$
SPATS2	1.302	$2.11x10^{-07}$	$1.44x10^{-05}$	-0.028	$5.07x10^{-01}$	$7.07x10^{-01}$
ABCG2	1.915	$2.21x10^{-07}$	$1.50x10^{-05}$	-0.075	$3.34x10^{-01}$	$5.58x10^{-01}$
BNC2	1.375	$2.25x10^{-07}$	$1.52x10^{-05}$	-0.100	$4.64x10^{-01}$	$6.72x10^{-01}$
DNASE1L1	0.830	$2.33x10^{-07}$	$1.55x10^{-05}$	0.010	$8.23x10^{-01}$	$9.13x10^{-01}$
ZNF711	1.390	$2.34x10^{-07}$	$1.55x10^{-05}$	-0.280	$1.29x10^{-04}$	$5.85x10^{-03}$
HIVEP1	1.435	$2.39x10^{-07}$	$1.57x10^{-05}$	-0.037	$3.86x10^{-01}$	$6.07x10^{-01}$
UHRF2	1.186	$2.86x10^{-07}$	$1.84x10^{-05}$	-0.141	$3.70x10^{-06}$	$8.70x10^{-04}$
STXBP2	0.745	$2.94x10^{-07}$	$1.87x10^{-05}$	0.031	$4.32x10^{-01}$	$6.46x10^{-01}$
MTOR	0.846	$3.04x10^{-07}$	$1.91x10^{-05}$	0.050	$7.74x10^{-02}$	$2.36x10^{-01}$
BLVRA	0.800	$3.18x10^{-07}$	$1.97x10^{-05}$	0.114	$5.30x10^{-02}$	$1.89x10^{-01}$
CD69	2.127	$3.36x10^{-07}$	$2.05x10^{-05}$	-0.117	$1.70x10^{-02}$	$9.66x10^{-02}$
IGFBP7	1.430	$3.41x10^{-07}$	$2.06x10^{-05}$	-0.029	$6.39x10^{-01}$	$7.99x10^{-01}$
RORA	1.450	$3.59x10^{-07}$	$2.16x10^{-05}$	-0.064	$1.85x10^{-01}$	$3.95x10^{-01}$
HLA-DOA	1.562	$3.61x10^{-07}$	$2.16x10^{-05}$	-0.088	$2.52x10^{-01}$	$4.73x10^{-01}$
EFEMP2	1.362	$4.11x10^{-07}$	$2.40x10^{-05}$	-0.108	$1.35x10^{-01}$	$3.27x10^{-01}$
ADAP2	0.628	$4.14x10^{-07}$	$2.41x10^{-05}$	0.160	$3.42x10^{-02}$	$1.47x10^{-01}$
ANPEP	0.479	$4.21x10^{-07}$	$2.43x10^{-05}$	0.243	$4.15x10^{-03}$	$4.26x10^{-02}$
GNB5	1.122	$4.23x10^{-07}$	$2.43x10^{-05}$	-0.012	$8.30x10^{-01}$	$9.17x10^{-01}$
NHEJ1	0.805	$4.23x10^{-07}$	$2.43x10^{-05}$	0.001	$9.75x10^{-01}$	$9.90x10^{-01}$
PDGFA	1.424	$4.38x10^{-07}$	$2.50x10^{-05}$	-0.286	$1.03x10^{-03}$	$1.92x10^{-02}$
RAB23	1.347	$4.50x10^{-07}$	$2.56x10^{-05}$	-0.190	$1.70x10^{-02}$	$9.67x10^{-02}$
FUBP1	1.213	$4.63x10^{-07}$	$2.61x10^{-05}$	-0.091	$1.06x10^{-03}$	$1.95x10^{-02}$
PCNA	0.792	$5.63x10^{-07}$	$3.06x10^{-05}$	0.080	$2.09x10^{-02}$	$1.09x10^{-01}$
WDR59	1.195	$5.87x10^{-07}$	$3.17x10^{-05}$	-0.007	$8.43x10^{-01}$	$9.25x10^{-01}$
NOD1	1.283	$6.14x10^{-07}$	$3.29x10^{-05}$	-0.018	$6.91x10^{-01}$	$8.32x10^{-01}$
ENPP2	2.479	$6.16x10^{-07}$	$3.29x10^{-05}$	-0.085	$2.71x10^{-01}$	$4.93x10^{-01}$
MCU	1.351	$6.42x10^{-07}$	$3.41x10^{-05}$	-0.016	$5.82x10^{-01}$	$7.61x10^{-01}$
KIT	1.993	$6.50x10^{-07}$	$3.44x10^{-05}$	-0.192	$2.14x10^{-02}$	$1.11x10^{-01}$
ANKRD36B	1.497	$6.87x10^{-07}$	$3.59x10^{-05}$	-0.051	$3.78x10^{-01}$	$5.99x10^{-01}$
C2CD2	1.235	$7.43x10^{-07}$	$3.85x10^{-05}$	-0.075	$2.12x10^{-01}$	$4.28x10^{-01}$
COMMD9	0.805	$7.68x10^{-07}$	$3.96x10^{-05}$	0.008	$8.25x10^{-01}$	$9.14x10^{-01}$
PPFIA1	0.855	$7.73x10^{-07}$	$3.97x10^{-05}$	0.099	$1.75x10^{-02}$	$9.83x10^{-02}$
SCARNA9	1.451	$7.81x10^{-07}$	$4.00x10^{-05}$	-0.104	$4.63x10^{-02}$	$1.74x10^{-01}$

COL18A1	1.218	$8.00x10^{-07}$	$4.08x10^{-05}$	-0.169	$7.42x10^{-02}$	$2.30x10^{-01}$
ZCCHC11	1.190	$8.66x10^{-07}$	$4.33x10^{-05}$	-0.064	$1.69x10^{-02}$	$9.64x10^{-02}$
ELOF1	0.855	$8.68x10^{-07}$	$4.33x10^{-05}$	0.088	$1.24x10^{-01}$	$3.12x10^{-01}$
ATP5H	0.857	$8.89x10^{-07}$	$4.42x10^{-05}$	0.013	$5.77x10^{-01}$	$7.58x10^{-01}$
PCID2	1.319	$9.17x10^{-07}$	$4.54x10^{-05}$	-0.052	$5.01x10^{-02}$	$1.83x10^{-01}$
CPA3	2.222	$9.54x10^{-07}$	$4.68x10^{-05}$	-0.004	$9.75x10^{-01}$	$9.90x10^{-01}$
RUFY3	1.338	$9.72x10^{-07}$	$4.74x10^{-05}$	-0.097	$1.95x10^{-03}$	$2.75x10^{-02}$
PKD2	1.271	$9.95x10^{-07}$	$4.84x10^{-05}$	-0.041	$2.89x10^{-01}$	$5.11x10^{-01}$
RLF	1.208	$1.02x10^{-06}$	$4.95x10^{-05}$	-0.086	$2.18x10^{-03}$	$2.94x10^{-02}$
SCAMP2	0.833	$1.08x10^{-06}$	$5.17x10^{-05}$	0.067	$2.02x10^{-01}$	$4.17x10^{-01}$
MYH10	1.529	$1.10x10^{-06}$	$5.25x10^{-05}$	-0.058	$3.95x10^{-01}$	$6.15x10^{-01}$
ZNF337	1.185	$1.12x10^{-06}$	$5.31x10^{-05}$	-0.055	$3.68x10^{-02}$	$1.53x10^{-01}$
AQP1	0.719	$1.17x10^{-06}$	$5.47x10^{-05}$	0.008	$9.40x10^{-01}$	$9.73x10^{-01}$
CDC25B	0.707	$1.18x10^{-06}$	$5.48x10^{-05}$	0.116	$2.26x10^{-02}$	$1.15x10^{-01}$
DNM2	0.792	$1.18x10^{-06}$	$5.47x10^{-05}$	0.021	$4.32x10^{-01}$	$6.46x10^{-01}$
HMOX1	0.431	$1.18x10^{-06}$	$5.47x10^{-05}$	0.043	$4.78x10^{-01}$	$6.83x10^{-01}$
KIAA1147	1.379	$1.37x10^{-06}$	$6.23x10^{-05}$	-0.066	$5.32x10^{-02}$	$1.90x10^{-01}$
EPOR	1.202	$1.39x10^{-06}$	$6.30x10^{-05}$	-0.023	$6.97x10^{-01}$	$8.35x10^{-01}$
PAK2	0.846	$1.51x10^{-06}$	$6.69x10^{-05}$	0.118	$5.41x10^{-02}$	$1.92x10^{-01}$
ADAMTS17	1.131	$1.55x10^{-06}$	$6.82x10^{-05}$	-0.051	$5.74x10^{-01}$	$7.56x10^{-01}$
FRMD6	1.465	$1.58x10^{-06}$	$6.92x10^{-05}$	-0.025	$7.87x10^{-01}$	$8.89x10^{-01}$
BOD1	1.169	$1.62x10^{-06}$	$7.02x10^{-05}$	-0.085	$7.58x10^{-03}$	$5.99x10^{-02}$
TWSG1	1.222	$1.63x10^{-06}$	$7.06x10^{-05}$	-0.020	$7.20x10^{-01}$	$8.51x10^{-01}$
RPS6KA2	0.716	$1.69x10^{-06}$	$7.26x10^{-05}$	0.013	$8.79x10^{-01}$	$9.43x10^{-01}$
CD9	1.257	$1.71x10^{-06}$	$7.30x10^{-05}$	-0.083	$4.45x10^{-01}$	$6.57x10^{-01}$
TSPAN14	0.806	$1.74x10^{-06}$	$7.40x10^{-05}$	0.023	$6.48x10^{-01}$	$8.04x10^{-01}$
PDCD4	1.375	$1.75x10^{-06}$	$7.42x10^{-05}$	-0.037	$2.56x10^{-01}$	$4.77x10^{-01}$
SGIP1	1.626	$1.84x10^{-06}$	$7.71x10^{-05}$	-0.015	$8.99x10^{-01}$	$9.54x10^{-01}$
LYRM2	0.730	$1.88x10^{-06}$	$7.81x10^{-05}$	0.009	$7.30x10^{-01}$	$8.56x10^{-01}$
FUT1	0.812	$1.91x10^{-06}$	$7.89x10^{-05}$	0.144	$5.37x10^{-03}$	$4.95x10^{-02}$
LUC7L3	1.258	$2.00x10^{-06}$	$8.15x10^{-05}$	-0.132	$2.95x10^{-04}$	$9.43x10^{-03}$
RTN3	0.838	$2.07x10^{-06}$	$8.37x10^{-05}$	0.073	$1.10x10^{-01}$	$2.90x10^{-01}$
TCN2	0.628	$2.13x10^{-06}$	$8.51x10^{-05}$	0.114	$2.68x10^{-01}$	$4.90x10^{-01}$
SAMD4A	1.519	$2.17x10^{-06}$	$8.67x10^{-05}$	-0.054	$5.34x10^{-01}$	$7.27x10^{-01}$
NUPR1	0.759	$2.18x10^{-06}$	$8.67x10^{-05}$	0.037	$4.27x10^{-01}$	$6.43x10^{-01}$
GZMK	2.409	$2.29x10^{-06}$	$9.01x10^{-05}$	-0.030	$7.79x10^{-01}$	$8.86x10^{-01}$
PHIP	1.176	$2.39x10^{-06}$	$9.29x10^{-05}$	-0.072	$2.08x10^{-03}$	$2.86x10^{-02}$
NREP	1.920	$2.47x10^{-06}$	$9.59x10^{-05}$	-0.034	$3.75x10^{-01}$	$5.96x10^{-01}$
CHKA	1.279	$2.53x10^{-06}$	$9.77x10^{-05}$	-0.033	$4.30x10^{-01}$	$6.45x10^{-01}$
DERA	0.837	$2.59x10^{-06}$	$9.91x10^{-05}$	0.025	$4.28x10^{-01}$	$6.43x10^{-01}$
MAPK7	0.875	$2.70x10^{-06}$	$1.02x10^{-04}$	0.068	$3.40x10^{-01}$	$5.64x10^{-01}$
PRR14L	0.899	$2.92x10^{-06}$	$1.10x10^{-04}$	0.025	$4.73x10^{-01}$	$6.79x10^{-01}$
CLPB	0.773	$3.02x10^{-06}$	$1.12x10^{-04}$	0.004	$9.19x10^{-01}$	$9.63x10^{-01}$
COL4A3	1.380	$3.24x10^{-06}$	$1.19x10^{-04}$	-0.165	$1.61x10^{-01}$	$3.64x10^{-01}$
TPT1	1.126	$3.25x10^{-06}$	$1.19x10^{-04}$	-0.027	$5.69x10^{-01}$	$7.52x10^{-01}$
CBR1	0.813	$3.42x10^{-06}$	$1.24x10^{-04}$	0.013	$7.98x10^{-01}$	$8.97x10^{-01}$

BDH1	0.897	3.43x10^{-06}	1.24x10^{-04}	0.016	7.36x10^{-01}	8.60x10^{-01}
PPP2R2D	1.182	3.58x10^{-06}	1.29x10^{-04}	-0.097	3.07x10^{-05}	2.80x10^{-03}
SYTL2	1.275	3.69x10^{-06}	1.32x10^{-04}	-0.177	1.83x10^{-02}	1.01x10^{-01}
SGPP1	1.199	3.80x10^{-06}	1.35x10^{-04}	-0.018	6.77x10^{-01}	8.23x10^{-01}
ATXN10	1.105	3.96x10^{-06}	1.39x10^{-04}	-0.050	9.52x10^{-02}	2.66x10^{-01}
ACP2	0.746	4.00x10^{-06}	1.40x10^{-04}	0.059	2.36x10^{-01}	4.57x10^{-01}
PBXIP1	1.205	4.14x10^{-06}	1.44x10^{-04}	-0.083	3.87x10^{-02}	1.57x10^{-01}
MTMR14	0.817	4.20x10^{-06}	1.45x10^{-04}	0.003	9.04x10^{-01}	9.56x10^{-01}
SLC24A3	1.292	4.24x10^{-06}	1.46x10^{-04}	-0.059	5.32x10^{-01}	7.25x10^{-01}
PIK3CB	0.857	4.29x10^{-06}	1.47x10^{-04}	0.053	1.02x10^{-01}	2.77x10^{-01}
GPA33	1.254	4.33x10^{-06}	1.48x10^{-04}	-0.014	8.52x10^{-01}	9.29x10^{-01}
SELP	1.748	4.37x10^{-06}	1.49x10^{-04}	-0.207	4.87x10^{-02}	1.80x10^{-01}
NBEAL1	1.278	4.62x10^{-06}	1.57x10^{-04}	-0.108	4.03x10^{-03}	4.20x10^{-02}
F2R	1.666	4.68x10^{-06}	1.58x10^{-04}	-0.095	2.08x10^{-01}	4.23x10^{-01}
ZNF846	1.304	4.73x10^{-06}	1.59x10^{-04}	-0.109	6.98x10^{-03}	5.72x10^{-02}
CTSO	1.266	4.77x10^{-06}	1.60x10^{-04}	-0.068	6.15x10^{-02}	2.07x10^{-01}
CD1C	1.512	4.87x10^{-06}	1.63x10^{-04}	-0.071	3.91x10^{-01}	6.13x10^{-01}
PYGO1	1.222	4.95x10^{-06}	1.65x10^{-04}	-0.121	2.94x10^{-01}	5.17x10^{-01}
PRSS35	1.096	5.04x10^{-06}	1.68x10^{-04}	-0.454	3.46x10^{-02}	1.48x10^{-01}
SPAG9	1.183	5.06x10^{-06}	1.68x10^{-04}	-0.087	1.17x10^{-03}	2.07x10^{-02}
MIEN1	0.857	5.09x10^{-06}	1.68x10^{-04}	0.051	3.69x10^{-01}	5.91x10^{-01}
AHI1	1.249	5.17x10^{-06}	1.70x10^{-04}	-0.011	9.01x10^{-01}	9.54x10^{-01}
UACA	1.516	5.31x10^{-06}	1.73x10^{-04}	-0.004	9.54x10^{-01}	9.81x10^{-01}
ALDH4A1	0.901	5.36x10^{-06}	1.74x10^{-04}	0.025	7.67x10^{-01}	8.78x10^{-01}
GYG1	0.791	5.52x10^{-06}	1.79x10^{-04}	0.098	7.32x10^{-02}	2.28x10^{-01}
PLEKHO2	0.800	5.92x10^{-06}	1.87x10^{-04}	0.031	6.16x10^{-01}	7.83x10^{-01}
LILRB4	0.624	6.38x10^{-06}	1.98x10^{-04}	0.068	2.73x10^{-01}	4.95x10^{-01}
SHPRH	1.202	6.41x10^{-06}	1.99x10^{-04}	-0.108	3.40x10^{-05}	2.90x10^{-03}
LILRB2	0.613	6.68x10^{-06}	2.05x10^{-04}	0.042	4.62x10^{-01}	6.70x10^{-01}
VEGFA	1.372	6.78x10^{-06}	2.07x10^{-04}	-0.004	9.53x10^{-01}	9.80x10^{-01}
UBE2J1	0.803	6.90x10^{-06}	2.10x10^{-04}	0.012	8.32x10^{-01}	9.18x10^{-01}
ELP2	1.182	7.26x10^{-06}	2.19x10^{-04}	-0.051	9.24x10^{-02}	2.62x10^{-01}
NSDHL	0.783	7.28x10^{-06}	2.19x10^{-04}	0.041	2.80x10^{-01}	5.01x10^{-01}
FOXP1	1.169	7.32x10^{-06}	2.19x10^{-04}	-0.080	6.04x10^{-03}	5.31x10^{-02}
NMT1	0.805	7.33x10^{-06}	2.20x10^{-04}	0.005	8.37x10^{-01}	9.21x10^{-01}
MACC1	1.594	7.55x10^{-06}	2.24x10^{-04}	-0.065	4.24x10^{-01}	6.40x10^{-01}
KCNA3	1.553	7.63x10^{-06}	2.26x10^{-04}	-0.010	8.64x10^{-01}	9.36x10^{-01}
ZBTB10	1.166	7.66x10^{-06}	2.26x10^{-04}	-0.174	7.26x10^{-05}	4.22x10^{-03}
ANKRD36	1.301	7.67x10^{-06}	2.26x10^{-04}	-0.010	7.70x10^{-01}	8.80x10^{-01}
TRIM16L	0.791	7.72x10^{-06}	2.27x10^{-04}	0.062	2.49x10^{-01}	4.70x10^{-01}
FRS2	1.161	7.74x10^{-06}	2.27x10^{-04}	-0.024	4.34x10^{-01}	6.48x10^{-01}
GLE1	0.827	7.74x10^{-06}	2.27x10^{-04}	0.012	6.52x10^{-01}	8.07x10^{-01}
FCER1G	0.707	7.84x10^{-06}	2.29x10^{-04}	0.001	9.86x10^{-01}	9.94x10^{-01}
SNED1	1.316	8.08x10^{-06}	2.34x10^{-04}	-0.074	6.91x10^{-01}	8.32x10^{-01}
PSAT1	0.573	8.37x10^{-06}	2.41x10^{-04}	0.153	5.95x10^{-02}	2.03x10^{-01}
YWHAE	0.866	8.40x10^{-06}	2.42x10^{-04}	0.111	9.78x10^{-03}	7.01x10^{-02}

ARG1	0.695	$8.43x10^{-06}$	$2.43x10^{-04}$	0.081	$4.32x10^{-01}$	$6.46x10^{-01}$
ZNF154	1.341	$8.46x10^{-06}$	$2.43x10^{-04}$	-0.201	$2.04x10^{-02}$	$1.08x10^{-01}$
CYSLTR2	1.211	$8.55x10^{-06}$	$2.45x10^{-04}$	-0.115	$1.27x10^{-01}$	$3.16x10^{-01}$
NMT2	1.206	$8.57x10^{-06}$	$2.45x10^{-04}$	-0.084	$5.02x10^{-02}$	$1.83x10^{-01}$
AKAP5	1.156	$9.18x10^{-06}$	$2.61x10^{-04}$	-0.085	$1.87x10^{-01}$	$3.97x10^{-01}$
LACC1	0.770	$9.21x10^{-06}$	$2.61x10^{-04}$	0.022	$6.91x10^{-01}$	$8.32x10^{-01}$
HRASLS2	0.826	$9.29x10^{-06}$	$2.63x10^{-04}$	0.011	$9.54x10^{-01}$	$9.81x10^{-01}$
CBFA2T3	0.916	$9.46x10^{-06}$	$2.65x10^{-04}$	0.197	$1.17x10^{-02}$	$7.83x10^{-02}$
HMBS	0.807	$9.56x10^{-06}$	$2.67x10^{-04}$	0.097	$2.16x10^{-01}$	$4.33x10^{-01}$
IRF2BP2	1.171	$9.60x10^{-06}$	$2.68x10^{-04}$	-0.064	$8.34x10^{-02}$	$2.48x10^{-01}$
SRSF5	1.202	$9.82x10^{-06}$	$2.72x10^{-04}$	-0.072	$4.97x10^{-02}$	$1.82x10^{-01}$
PNISR	1.219	$9.93x10^{-06}$	$2.74x10^{-04}$	-0.124	$1.69x10^{-05}$	$1.96x10^{-03}$
CTTNBP2NL	0.794	$1.04x10^{-05}$	$2.84x10^{-04}$	0.065	$2.36x10^{-01}$	$4.56x10^{-01}$
POLR2D	0.889	$1.04x10^{-05}$	$2.84x10^{-04}$	0.017	$6.22x10^{-01}$	$7.88x10^{-01}$
GCLC	0.706	$1.05x10^{-05}$	$2.87x10^{-04}$	0.036	$4.46x10^{-01}$	$6.58x10^{-01}$
HLA-DPA1	1.364	$1.06x10^{-05}$	$2.89x10^{-04}$	-0.074	$3.00x10^{-01}$	$5.22x10^{-01}$
AZIN2	1.104	$1.12x10^{-05}$	$3.01x10^{-04}$	-0.175	$2.54x10^{-02}$	$1.24x10^{-01}$
CSAD	1.188	$1.13x10^{-05}$	$3.01x10^{-04}$	-0.021	$6.11x10^{-01}$	$7.81x10^{-01}$
GOPC	1.170	$1.14x10^{-05}$	$3.05x10^{-04}$	-0.070	$5.68x10^{-03}$	$5.11x10^{-02}$
THRB	1.229	$1.16x10^{-05}$	$3.07x10^{-04}$	-0.192	$7.74x10^{-02}$	$2.36x10^{-01}$
ATP2B1	1.305	$1.17x10^{-05}$	$3.09x10^{-04}$	-0.012	$6.82x10^{-01}$	$8.26x10^{-01}$
TMED4	1.151	$1.18x10^{-05}$	$3.12x10^{-04}$	-0.087	$1.93x10^{-05}$	$2.16x10^{-03}$
MIB1	1.215	$1.19x10^{-05}$	$3.14x10^{-04}$	-0.104	$1.71x10^{-04}$	$6.85x10^{-03}$
MS4A4A	0.664	$1.19x10^{-05}$	$3.13x10^{-04}$	0.264	$5.28x10^{-03}$	$4.89x10^{-02}$
DOCK1	1.178	$1.19x10^{-05}$	$3.13x10^{-04}$	-0.017	$8.76x10^{-01}$	$9.41x10^{-01}$
CHAMP1	0.825	$1.20x10^{-05}$	$3.16x10^{-04}$	0.137	$9.28x10^{-03}$	$6.82x10^{-02}$
LTBP4	1.449	$1.21x10^{-05}$	$3.16x10^{-04}$	-0.016	$8.01x10^{-01}$	$8.99x10^{-01}$
TSEN54	1.149	$1.23x10^{-05}$	$3.22x10^{-04}$	-0.127	$1.44x10^{-02}$	$8.83x10^{-02}$
ROBO1	1.322	$1.23x10^{-05}$	$3.22x10^{-04}$	-0.140	$2.34x10^{-01}$	$4.54x10^{-01}$
ZNRF2	1.152	$1.24x10^{-05}$	$3.22x10^{-04}$	-0.001	$9.71x10^{-01}$	$9.88x10^{-01}$
TNFRSF25	1.140	$1.25x10^{-05}$	$3.25x10^{-04}$	-0.072	$2.30x10^{-01}$	$4.49x10^{-01}$
SH2D2A	1.182	$1.27x10^{-05}$	$3.28x10^{-04}$	-0.045	$6.22x10^{-01}$	$7.89x10^{-01}$
HNRNPLL	1.262	$1.28x10^{-05}$	$3.29x10^{-04}$	-0.012	$7.40x10^{-01}$	$8.62x10^{-01}$
CIITA	1.291	$1.33x10^{-05}$	$3.39x10^{-04}$	-0.034	$5.29x10^{-01}$	$7.23x10^{-01}$
ZMAT1	1.319	$1.33x10^{-05}$	$3.39x10^{-04}$	-0.011	$7.78x10^{-01}$	$8.85x10^{-01}$
SERPINB8	0.717	$1.33x10^{-05}$	$3.40x10^{-04}$	0.055	$2.67x10^{-01}$	$4.89x10^{-01}$
DCUN1D4	1.186	$1.34x10^{-05}$	$3.40x10^{-04}$	-0.110	$4.54x10^{-02}$	$1.72x10^{-01}$
ZNF528	1.321	$1.35x10^{-05}$	$3.44x10^{-04}$	-0.137	$3.99x10^{-03}$	$4.19x10^{-02}$
CAPRIN2	1.178	$1.37x10^{-05}$	$3.48x10^{-04}$	-0.105	$8.94x10^{-02}$	$2.57x10^{-01}$
SMPD1	0.823	$1.37x10^{-05}$	$3.48x10^{-04}$	0.038	$5.84x10^{-01}$	$7.63x10^{-01}$
ABI3	0.815	$1.38x10^{-05}$	$3.49x10^{-04}$	0.018	$7.34x10^{-01}$	$8.59x10^{-01}$
NDUFAF1	0.796	$1.40x10^{-05}$	$3.52x10^{-04}$	0.056	$9.00x10^{-02}$	$2.58x10^{-01}$
MYO15B	1.344	$1.42x10^{-05}$	$3.58x10^{-04}$	-0.106	$3.69x10^{-02}$	$1.54x10^{-01}$
SZRD1	0.844	$1.44x10^{-05}$	$3.62x10^{-04}$	0.131	$1.91x10^{-03}$	$2.70x10^{-02}$
AP1B1	0.747	$1.44x10^{-05}$	$3.62x10^{-04}$	0.046	$4.05x10^{-01}$	$6.24x10^{-01}$
PRKCQ	1.378	$1.45x10^{-05}$	$3.63x10^{-04}$	-0.007	$8.73x10^{-01}$	$9.40x10^{-01}$

CA2	1.674	$1.47x10^{-05}$	$3.67x10^{-04}$	-0.227	$1.44x10^{-02}$	$8.83x10^{-02}$
AEBP2	1.171	$1.49x10^{-05}$	$3.71x10^{-04}$	-0.009	$7.28x10^{-01}$	$8.55x10^{-01}$
ZFYVE26	0.848	$1.49x10^{-05}$	$3.71x10^{-04}$	0.031	$3.41x10^{-01}$	$5.64x10^{-01}$
CD177	0.567	$1.50x10^{-05}$	$3.71x10^{-04}$	0.126	$6.57x10^{-01}$	$8.10x10^{-01}$
SLC12A6	0.847	$1.50x10^{-05}$	$3.73x10^{-04}$	0.043	$1.78x10^{-01}$	$3.86x10^{-01}$
RAB5C	0.846	$1.51x10^{-05}$	$3.74x10^{-04}$	0.009	$8.03x10^{-01}$	$9.00x10^{-01}$
RAB7A	0.864	$1.53x10^{-05}$	$3.77x10^{-04}$	0.087	$9.65x10^{-02}$	$2.69x10^{-01}$
FARS2	1.166	$1.58x10^{-05}$	$3.86x10^{-04}$	-0.090	$2.00x10^{-03}$	$2.79x10^{-02}$
TP53INP1	1.356	$1.62x10^{-05}$	$3.93x10^{-04}$	0.000	$9.95x10^{-01}$	$9.97x10^{-01}$
TP53BP1	1.168	$1.63x10^{-05}$	$3.96x10^{-04}$	-0.011	$7.43x10^{-01}$	$8.64x10^{-01}$
MMP8	0.508	$1.64x10^{-05}$	$3.96x10^{-04}$	0.722	$3.90x10^{-03}$	$4.13x10^{-02}$
GBGT1	0.778	$1.64x10^{-05}$	$3.97x10^{-04}$	0.054	$3.12x10^{-01}$	$5.36x10^{-01}$
GSAP	1.272	$1.71x10^{-05}$	$4.10x10^{-04}$	-0.166	$2.02x10^{-04}$	$7.56x10^{-03}$
NAP1L4	1.133	$1.78x10^{-05}$	$4.23x10^{-04}$	-0.044	$1.95x10^{-01}$	$4.07x10^{-01}$
ZDHHC3	1.385	$1.81x10^{-05}$	$4.28x10^{-04}$	-0.006	$8.71x10^{-01}$	$9.39x10^{-01}$
POP4	0.854	$1.82x10^{-05}$	$4.30x10^{-04}$	0.040	$1.62x10^{-01}$	$3.65x10^{-01}$
ARHGEF11	0.874	$1.85x10^{-05}$	$4.36x10^{-04}$	0.113	$2.05x10^{-02}$	$1.08x10^{-01}$
MACF1	1.277	$1.91x10^{-05}$	$4.48x10^{-04}$	-0.053	$1.02x10^{-01}$	$2.78x10^{-01}$
MPDU1	0.827	$1.93x10^{-05}$	$4.53x10^{-04}$	0.043	$2.16x10^{-01}$	$4.33x10^{-01}$
CLCN7	0.767	$2.03x10^{-05}$	$4.73x10^{-04}$	0.104	$6.75x10^{-02}$	$2.18x10^{-01}$
RAPGEFL1	0.893	$2.10x10^{-05}$	$4.88x10^{-04}$	0.204	$4.30x10^{-02}$	$1.67x10^{-01}$
P2RY13	0.722	$2.14x10^{-05}$	$4.94x10^{-04}$	0.038	$4.71x10^{-01}$	$6.78x10^{-01}$
OLFM4	0.557	$2.22x10^{-05}$	$5.09x10^{-04}$	1.004	$2.86x10^{-03}$	$3.42x10^{-02}$
GABARAPL2	1.166	$2.23x10^{-05}$	$5.12x10^{-04}$	-0.123	$1.86x10^{-02}$	$1.02x10^{-01}$
HERC2P2	1.279	$2.27x10^{-05}$	$5.20x10^{-04}$	-0.042	$5.59x10^{-01}$	$7.45x10^{-01}$
LONRF1	1.330	$2.27x10^{-05}$	$5.19x10^{-04}$	-0.005	$8.93x10^{-01}$	$9.50x10^{-01}$
SLC35F6	0.816	$2.30x10^{-05}$	$5.24x10^{-04}$	0.118	$1.66x10^{-02}$	$9.56x10^{-02}$
ST8SIA1	1.308	$2.30x10^{-05}$	$5.24x10^{-04}$	-0.235	$1.49x10^{-01}$	$3.47x10^{-01}$
RYK	1.136	$2.32x10^{-05}$	$5.27x10^{-04}$	-0.109	$4.00x10^{-05}$	$3.12x10^{-03}$
SRXN1	0.739	$2.36x10^{-05}$	$5.35x10^{-04}$	0.080	$3.03x10^{-01}$	$5.25x10^{-01}$
CAMK4	1.406	$2.41x10^{-05}$	$5.43x10^{-04}$	-0.126	$2.65x10^{-02}$	$1.27x10^{-01}$
CNKSR3	1.566	$2.71x10^{-05}$	$5.93x10^{-04}$	-0.039	$4.85x10^{-01}$	$6.88x10^{-01}$
LYPD5	0.861	$2.73x10^{-05}$	$5.96x10^{-04}$	0.202	$1.39x10^{-03}$	$2.27x10^{-02}$
COX5A	0.835	$2.75x10^{-05}$	$5.98x10^{-04}$	0.051	$2.27x10^{-01}$	$4.46x10^{-01}$
CLK1	1.311	$2.76x10^{-05}$	$6.00x10^{-04}$	-0.102	$4.83x10^{-03}$	$4.64x10^{-02}$
KIAA0930	0.808	$2.80x10^{-05}$	$6.05x10^{-04}$	0.076	$2.60x10^{-01}$	$4.82x10^{-01}$
FLOT2	0.808	$2.82x10^{-05}$	$6.09x10^{-04}$	0.081	$2.29x10^{-01}$	$4.48x10^{-01}$
SLC4A4	1.400	$2.83x10^{-05}$	$6.10x10^{-04}$	-0.010	$9.10x10^{-01}$	$9.59x10^{-01}$
RWDD2A	1.194	$2.89x10^{-05}$	$6.21x10^{-04}$	-0.003	$9.38x10^{-01}$	$9.72x10^{-01}$
VPS25	0.847	$2.89x10^{-05}$	$6.21x10^{-04}$	0.040	$7.96x10^{-02}$	$2.41x10^{-01}$
NRBF2	0.837	$2.91x10^{-05}$	$6.24x10^{-04}$	0.007	$8.55x10^{-01}$	$9.31x10^{-01}$
PSMC2	0.858	$3.05x10^{-05}$	$6.46x10^{-04}$	0.033	$1.84x10^{-01}$	$3.95x10^{-01}$
RXRB	1.158	$3.06x10^{-05}$	$6.46x10^{-04}$	-0.031	$3.45x10^{-01}$	$5.68x10^{-01}$
BRWD1	1.237	$3.08x10^{-05}$	$6.49x10^{-04}$	-0.108	$3.80x10^{-04}$	$1.05x10^{-02}$
SCARNA7	1.266	$3.23x10^{-05}$	$6.71x10^{-04}$	-0.162	$4.22x10^{-03}$	$4.30x10^{-02}$
MME	1.741	$3.29x10^{-05}$	$6.80x10^{-04}$	-0.137	$3.49x10^{-02}$	$1.49x10^{-01}$

PRAM1	0.875	3.34x10^{-05}	6.89x10^{-04}	0.113	6.27x10^{-02}	2.09x10^{-01}
AGO3	1.135	3.38x10^{-05}	6.95x10^{-04}	0.000	9.95x10^{-01}	9.97x10^{-01}
CASC3	0.876	3.41x10^{-05}	6.99x10^{-04}	0.026	4.34x10^{-01}	6.48x10^{-01}
DNTTIP1	0.842	3.41x10^{-05}	6.99x10^{-04}	0.006	9.10x10^{-01}	9.59x10^{-01}
ZNF418	1.175	3.43x10^{-05}	7.02x10^{-04}	-0.327	1.55x10^{-04}	6.39x10^{-03}
METRNL	1.210	3.45x10^{-05}	7.06x10^{-04}	-0.011	8.36x10^{-01}	9.21x10^{-01}
PEPD	0.815	3.55x10^{-05}	7.21x10^{-04}	0.011	7.55x10^{-01}	8.71x10^{-01}
WISP2	0.636	3.62x10^{-05}	7.34x10^{-04}	0.087	3.66x10^{-01}	5.88x10^{-01}
PLXDC2	1.189	3.63x10^{-05}	7.34x10^{-04}	-0.066	7.14x10^{-02}	2.26x10^{-01}
CSTF2	0.890	3.63x10^{-05}	7.34x10^{-04}	0.014	6.43x10^{-01}	8.01x10^{-01}
TRMT1	0.810	3.67x10^{-05}	7.41x10^{-04}	0.074	2.65x10^{-01}	4.87x10^{-01}
MAP4K5	1.147	3.69x10^{-05}	7.43x10^{-04}	-0.044	2.24x10^{-01}	4.42x10^{-01}
AHCY	0.759	3.70x10^{-05}	7.46x10^{-04}	0.055	2.07x10^{-01}	4.22x10^{-01}
EBPL	0.848	3.71x10^{-05}	7.46x10^{-04}	0.038	4.46x10^{-01}	6.58x10^{-01}
STXBP5	1.158	3.76x10^{-05}	7.56x10^{-04}	-0.080	1.48x10^{-02}	8.95x10^{-02}
MPEG1	0.650	3.77x10^{-05}	7.56x10^{-04}	0.014	8.26x10^{-01}	9.15x10^{-01}
RAPGEF6	1.144	3.85x10^{-05}	7.68x10^{-04}	-0.040	2.79x10^{-01}	5.01x10^{-01}
ATP10A	1.189	3.91x10^{-05}	7.80x10^{-04}	-0.040	4.91x10^{-01}	6.94x10^{-01}
TRPM2	0.875	3.91x10^{-05}	7.80x10^{-04}	0.061	4.09x10^{-01}	6.27x10^{-01}
TRIM26	0.860	3.93x10^{-05}	7.82x10^{-04}	0.089	5.56x10^{-02}	1.95x10^{-01}
NAALADL2	1.277	3.94x10^{-05}	7.85x10^{-04}	-0.166	5.93x10^{-02}	2.03x10^{-01}
MSRB2	1.241	4.02x10^{-05}	7.97x10^{-04}	-0.028	6.04x10^{-01}	7.76x10^{-01}
CNST	1.278	4.11x10^{-05}	8.10x10^{-04}	-0.191	9.73x10^{-05}	5.01x10^{-03}
APEX1	0.840	4.16x10^{-05}	8.17x10^{-04}	0.043	3.57x10^{-01}	5.80x10^{-01}
PKM	0.780	4.17x10^{-05}	8.18x10^{-04}	0.160	3.83x10^{-03}	4.09x10^{-02}
BLVRB	0.787	4.18x10^{-05}	8.18x10^{-04}	0.011	8.82x10^{-01}	9.44x10^{-01}
CBX6	0.829	4.33x10^{-05}	8.41x10^{-04}	0.066	8.42x10^{-02}	2.49x10^{-01}
DYRK2	1.128	4.34x10^{-05}	8.41x10^{-04}	-0.088	1.54x10^{-02}	9.17x10^{-02}
GAPDH	0.786	4.36x10^{-05}	8.44x10^{-04}	0.027	5.39x10^{-01}	7.31x10^{-01}
ESYT2	1.155	4.42x10^{-05}	8.53x10^{-04}	-0.131	9.19x10^{-05}	4.82x10^{-03}
GOLGA1	0.877	4.42x10^{-05}	8.52x10^{-04}	0.004	9.50x10^{-01}	9.79x10^{-01}
WDR33	1.125	4.47x10^{-05}	8.60x10^{-04}	-0.022	2.30x10^{-01}	4.49x10^{-01}
SMCHD1	1.183	4.58x10^{-05}	8.74x10^{-04}	-0.049	2.10x10^{-01}	4.25x10^{-01}
SORBS3	0.837	4.58x10^{-05}	8.74x10^{-04}	0.045	5.64x10^{-01}	7.48x10^{-01}
YPEL2	1.249	4.59x10^{-05}	8.75x10^{-04}	-0.028	3.99x10^{-01}	6.18x10^{-01}
BTBD11	1.062	4.62x10^{-05}	8.80x10^{-04}	-0.052	3.62x10^{-01}	5.85x10^{-01}
URM1	0.886	4.63x10^{-05}	8.81x10^{-04}	0.048	4.92x10^{-01}	6.95x10^{-01}
CYLD	1.187	4.64x10^{-05}	8.82x10^{-04}	-0.025	3.46x10^{-01}	5.70x10^{-01}
NIPSNAP3B	1.171	4.66x10^{-05}	8.85x10^{-04}	-0.034	6.30x10^{-01}	7.93x10^{-01}
RHOG	0.833	4.70x10^{-05}	8.90x10^{-04}	0.031	5.92x10^{-01}	7.68x10^{-01}
SLC25A28	1.180	4.72x10^{-05}	8.92x10^{-04}	-0.108	5.13x10^{-03}	4.81x10^{-02}
VAV2	1.261	4.74x10^{-05}	8.94x10^{-04}	-0.125	1.41x10^{-01}	3.36x10^{-01}
ZNF571	1.133	4.76x10^{-05}	8.98x10^{-04}	-0.024	5.61x10^{-01}	7.46x10^{-01}
LILRA5	0.681	4.80x10^{-05}	9.04x10^{-04}	0.041	5.24x10^{-01}	7.19x10^{-01}
FAM65C	0.872	4.84x10^{-05}	9.09x10^{-04}	0.040	4.48x10^{-01}	6.59x10^{-01}
STAB1	0.686	4.84x10^{-05}	9.09x10^{-04}	0.138	6.05x10^{-02}	2.05x10^{-01}

SPRY1	1.394	4.89x10^{-05}	9.17x10^{-04}	-0.214	3.27x10^{-02}	1.43x10^{-01}
SLFN12L	1.439	4.92x10^{-05}	9.18x10^{-04}	-0.054	1.24x10^{-01}	3.11x10^{-01}
N6AMT1	1.242	5.01x10^{-05}	9.33x10^{-04}	-0.110	8.30x10^{-03}	6.33x10^{-02}
LSAMP	1.272	5.28x10^{-05}	9.73x10^{-04}	-0.008	9.58x10^{-01}	9.82x10^{-01}
CHL1	0.662	5.28x10^{-05}	9.73x10^{-04}	0.237	1.55x10^{-01}	3.55x10^{-01}
MAB21L3	0.911	5.32x10^{-05}	9.79x10^{-04}	0.121	5.98x10^{-02}	2.03x10^{-01}
CD180	0.638	5.42x10^{-05}	9.95x10^{-04}	0.138	1.18x10^{-01}	3.02x10^{-01}
RNF19A	1.203	5.43x10^{-05}	9.95x10^{-04}	-0.084	3.53x10^{-03}	3.89x10^{-02}

Supplementary Table 5: Results of whole blood PAH RNA signature in the PAH lung tissue microarray study. Table shows results for 777/1140 genes from the PAH lung tissue microarray study present in the current PAH RNAseq. Data ordered based on dysregulation significance (p-value) in lung tissue microarray.

RNAseq gene	Study 1 Gene(s) tested	N SNPs	OR	Sig.	Study 2 Gene(s) tested	N SNPs	OR	Sig.	Max p-value
STAT5A	STAT5A STAT5B	1	16.04	0.016					**0.02**
TYW3	TYW3 CRYZ	1	3.856	0.023					**0.02**
C1orf27	C1orf27	1	0.123	0.023					**0.02**
SESN1	SESN1	2	0.222	0.02	SESN1	1	0.819	0.025	**0.02**
SMAD5	SMAD5	1	0.317	0.012	SMAD5	1	0.883	0.028	**0.03**
ZNF430	ZNF100 ZNF430 LOC400682	5	0.679	0.031					**0.03**
ZNF638	ZNF638	1	8.019	0.032					**0.03**
ZNF577	ZNF577	1	0.123	0.032					**0.03**
LRCH1	LRCH1	1	0.066	0.036					**0.04**
CHP1	CHP1	1	0.111	0.037					**0.04**
SCFD2	SCFD2	1	16.8	0.038					**0.04**
FBLN2					FBLN2	1	1.727	0.039	**0.04**
ZNF28	ZNF468 ZNF28	1	0.565	0.042					**0.04**
NR1D2	NR1D2	1	0.126	0.052					**0.05**
SF3B1	SF3B1	1	0.059	0.052	SF3B1	1	0.544	0.042	**0.05**
FBXL4	FBXL4	1	10.94	0.059					**0.06**
TYW3	CRYZ TYW3	5	1.47	0.062					**0.06**
PTPRC					PTPRC	1	0.636	0.063	**0.06**
BBX	BBX	1	0.07	0.066					**0.07**
ZNF765	ZNF765 ZNF761 ZNF525	1	0.095	0.067					**0.07**
OPA1	OPA1	1	63.18	0.067					**0.07**
ZNF397					ZNF397	1	0.646	0.083	**0.08**
CCAR1	CCAR1	1	36.13	0.091					**0.09**
CHD9	CHD9	2	0.026	0.002	CHD9	1	1.463	0.094	**0.09**
SENP7	SENP7	3	2.434	0.097	SENP7	1	1.23	0.029	**0.1**
EIF4A2	EIF4A2 MIR1248 SNORA81 SNORA4 SNORD2 SNORA63 LOC730139	1	2.413	0.099					**0.1**
NRG1	NRG1	3	2.784	0.054	NRG1	1	1.094	0.107	**0.11**
RBM5	RBM5 LUST LOC100129060	1	0.047	0.111					**0.11**
MED13	MED13	1	107.9	0.111					**0.11**

	LOC100129112								
GLT8D1	GLT8D1 SPCS1	1	17.93	0.113					**0.11**
SLC13A4	SLC13A4	2	0.125	0.114					**0.11**
DENND4C	DENND4C	2	7.945	0.036	DENND4C	1	1.401	0.115	**0.11**
ZNF816	ZNF816-ZNF321P ZNF321P ZNF816	1	0.392	0.122					**0.12**
TSHZ3	TSHZ3	2	0.401	0.122					**0.12**
FAM129A	FAM129A	1	0.066	0.133					**0.13**
ZNF264	ZNF264 ZNF805 ZNF543	1	3.276	0.136	ZNF264	1	0.734	0.033	**0.14**
ACAA2	ACAA2 SCARNA17	1	0.253	0.138					**0.14**
CEP85L	CEP85L	2	0.366	0.141					**0.14**
TMEM68	TMEM68	1	7.862	0.143					**0.14**
NGLY1	NGLY1	1	23.03	0.147					**0.15**
CSNK2A2	CSNK2A2	1	0.076	0.154					**0.15**
SNRK					SNRK	1	0.731	0.165	**0.17**
EXOSC10	EXOSC10	1	6.179	0.166					**0.17**
C3orf17	C3orf17	2	0.445	0.166					**0.17**
SLC38A1	SLC38A1	1	0.003	0.041	SLC38A1	3	1.073	0.168	**0.17**
ZNF268	ZNF10 ZNF268 RPL23AP67	1	0.219	0.17					**0.17**
UBE4A	UBE4A	1	0.232	0.175	UBE4A	1	0.68	0.171	**0.18**
ZNF418	ZNF418	2	0.397	0.177	ZNF418	1	0.807	0.119	**0.18**
MINPP1	MINPP1	1	0.136	0.182					**0.18**
ANGEL2	ANGEL2	1	0.376	0.199					**0.2**
FAM213A	FAM213A	1	1.8	0.207					**0.21**
UBE2D3	UBE2D3	2	0.534	0.214					**0.21**
AMD1	AMD1	1	0.02	0.218					**0.22**
ALG8	ALG8	1	2.805	0.219					**0.22**
ZNF257	ZNF729 ZNF257 ZNF492 ZNF98 ZNF99	2	0.565	0.22					**0.22**
RIF1	RIF1	3	0.353	0.224					**0.22**
SYNJ2BP	SYNJ2BP SYNJ2BP-COX16	1	0.288	0.225					**0.22**
MAP4	MAP4	1	7.233	0.226					**0.23**
AVL9	AVL9	2	4.504	0.237					**0.24**
ZNF587B	ZNF552 ZNF814	1	1.814	0.239					**0.24**

	ZNF587B ZNF587								
GPAM	GPAM	1	4.235	0.242					**0.24**
IFT46	IFT46	1	2.661	0.248					**0.25**
CAMKMT	CAMKMT	2	0.387	0.251					**0.25**
ZNF30	ZNF30	1	3.406	0.079	ZNF30	1	1.176	0.257	**0.26**
TMEM220	TMEM220 C17orf48 MAGOH2	1	0.596	0.259	TMEM220	1	0.716	0.242	**0.26**
XRCC5	XRCC5 PKI55	1	5.723	0.268					**0.27**
C2orf49	C2orf49	1	4.351	0.273					**0.27**
DCAF7	DCAF7	1	12.22	0.276					**0.28**
KRIT1					KRIT1	2	0.847	0.279	**0.28**
TNFSF4	TNFSF4 LOC100506023 LOC100631377	1	0.698	0.282	TNFSF4	1	0.844	0.282	**0.28**
GPBP1	GPBP1	1	48.85	0.041	GPBP1	1	1.219	0.285	**0.28**
ZNF304	ZNF304	1	0.385	0.292					**0.29**
PTGR1	PTGR1	1	0.236	0.295					**0.3**
GGTA1P	GGTA1P	4	1.181	0.296					**0.3**
ZNF790	ZNF850 ZNF260 ZNF790	1	1.752	0.302					**0.3**
ZNF141	ZNF141	1	3.412	0.307					**0.31**
ZNF350	ZNF350	1	4.666	0.326					**0.33**
SLC25A16	SLC25A16	1	0.173	0.33					**0.33**
TRIM65					TRIM65	1	1.294	0.332	**0.33**
CLTCL1					CLTCL1	1	1.077	0.335	**0.33**
CCNB1IP1	CCNB1IP1	1	0.473	0.335	CCNB1IP1	1	0.776	0.177	**0.34**
BET1	BET1 GNG11	1	2.115	0.248	BET1	1	1.272	0.337	**0.34**
DGCR11	DGCR2 DGCR11 DGCR12	1	0.177	0.339					**0.34**
ZNF211	ZNF134 ZNF211	1	3.384	0.12	ZNF211	1	0.91	0.343	**0.34**
PEX1	PEX1	1	4.38	0.344					**0.34**
ZNF354B	ZNF354A ZNF354B	5	1.227	0.357					**0.36**
UBR1	UBR1	1	0.24	0.358					**0.36**
ORC4	ORC4	1	5.68	0.361					**0.36**
MFF	MFF	1	2.309	0.181	MFF	3	0.951	0.364	**0.36**
INTS10	INTS10	1	0.548	0.369					**0.37**
RASA2	RASA2	1	0.163	0.371					**0.37**
OSBPL2	OSBPL2	2	2.602	0.221	OSBPL2	2	1.066	0.378	**0.38**
DNAJC2	DNAJC21	1	2.478	0.386					**0.39**

KDM1A	LUZP1 KDM1A	1	0.192	0.39					**0.39**
ABHD2	ABHD2	4	2.765	0.39					**0.39**
BTAF1	BTAF1	1	0.195	0.397					**0.4**
HECTD1	HECTD1	1	0.064	0.403					**0.4**
TPR	TPR PRG4	1	6.07	0.404					**0.4**
FAN1	MTMR10 FAN1	1	0.21	0.404					**0.4**
PIGU	PIGU	1	2.815	0.405					**0.4**
TPR	PRG4 TPR	1	3.268	0.39	TPR	1	1.102	0.406	**0.41**
ATP5S	ATP5SL	1	0.316	0.185	ATP5S	1	1.086	0.406	**0.41**
ARFGAP3					ARFGAP3	1	0.878	0.416	**0.42**
PCBP1	PCBP1	1	7.423	0.417					**0.42**
ZNF121					ZNF121	1	1.121	0.421	**0.42**
AMN1	METTL20 AMN1	1	0.375	0.426					**0.43**
ZNF525	ZNF525 ZNF845 ZNF813 ZNF611	1	1.386	0.441					**0.44**
ZNF845	ZNF525 ZNF845 ZNF813 ZNF611	1	1.386	0.441					**0.44**
ZNF876P	ZNF595 ZNF876P	2	1.73	0.441					**0.44**
TUBE1	TUBE1 WISP3	1	3.385	0.444					**0.44**
OXNAD1	OXNAD1 RFTN1	1	0.318	0.446					**0.45**
ZNF131	ZNF131 LOC100506639	1	1.615	0.453					**0.45**
SASH1	SASH1	1	3.702	0.319	SASH1	1	1.182	0.455	**0.45**
DEF6					DEF6	1	1.06	0.458	**0.46**
ZNF24	ZNF271 ZNF24	1	0.671	0.459					**0.46**
PPA2	PPA2	1	1.79	0.47					**0.47**
TCP1	MRPL18 TCP1 SNORA29	3	0.692	0.47					**0.47**
NOM1					NOM1	1	0.813	0.473	**0.47**
SDCCAG3	SDCCAG3	1	0.648	0.477	SDCCAG3	1	0.897	0.375	**0.48**
KDM1A	KDM1A	1	0.183	0.481					**0.48**
ARHGAP5	ARHGAP5	3	0.657	0.482					**0.48**
PMS1	ORMDL1 PMS1	1	0.665	0.482					**0.48**

LEMD3	LEMD3	1	0.195	0.483	LEMD3	2	1.105	0.048	**0.48**
ZNF763	ZNF700 ZNF763 ZNF833P	1	2.148	0.49					**0.49**
TEX10	TEX10	1	2.925	0.268	TEX10	1	1.242	0.497	**0.5**
RALA	RALA	1	1.715	0.498					**0.5**
ARFGAP3	ARFGAP3 RPL5 SNORD21	1	0.534	0.499					**0.5**
TCP1	ACAT2 TCP1 SNORA29 LOC100129518 SOD2	1	0.428	0.502					**0.5**
TANK	TANK	3	0.684	0.502	TANK	1	0.843	0.504	**0.5**
SMARCD2	PSMC5 SMARCD2	1	2.411	0.509	SMARCD2	1	0.849	0.246	**0.51**
PAPD4	PAPD4	1	17.29	0.323	PAPD4	1	0.82	0.514	**0.51**
RIMKLB	RIMKLB	1	0.65	0.514					**0.51**
CLTC	CLTC	1	7.645	0.515					**0.52**
ZMYM1					ZMYM1	1	0.891	0.523	**0.52**
CEPT1	CEPT1 DRAM2	1	0.32	0.524					**0.52**
DDX47	DDX47	1	0.401	0.527	DDX47	1	0.791	0.339	**0.53**
PMS1	PMS1	2	0.635	0.53					**0.53**
CWF19L2	CWF19L2	1	0.634	0.534	CWF19L2	1	0.858	0.109	**0.53**
RC3H2	RC3H2	1	0.196	0.54					**0.54**
FNTA	FNTA	1	2.826	0.542					**0.54**
CASD1	CASD1	1	0.342	0.545					**0.54**
RYK	RYK	3	0.532	0.557	RYK	1	0.768	0.388	**0.56**
PLCG1	PLCG1	1	9.951	0.563					**0.56**
ZNF91	ZNF91	1	1.18	0.578					**0.58**
SCYL3	SCYL3 C1orf112	1	0.552	0.551	SCYL3	1	0.835	0.579	**0.58**
ZNF273	ZNF273	1	1.635	0.583					**0.58**
PPP2R2D	PPP2R2D	1	0.499	0.588	PPP2R2D	1	0.752	0.147	**0.59**
PGS1	PGS1 DNAH17	1	0.375	0.146	PGS1	1	0.914	0.59	**0.59**
CRLF3	CRLF3	2	0.614	0.528	CRLF3	1	0.908	0.594	**0.59**
ZNF211	ZNF211	1	1.579	0.595					**0.59**
ZNF417	ZNF587 ZNF417 ZNF587B	3	1.193	0.596	ZNF417	1	1.834	0.014	**0.6**
ZNF587B	ZNF587 ZNF417 ZNF587B	3	1.193	0.596					**0.6**
AMN1	AMN1 METTL20	1	0.354	0.603					**0.6**

TTC17	TTC17	1	0.459	0.605					**0.61**
TRABD2A	TMSB10 TRABD2A	1	0.547	0.606					**0.61**
ETS2	ETS2	2	2.999	0.361	ETS2	1	0.959	0.609	**0.61**
TMTC3	TMTC3	1	1.865	0.609					**0.61**
AP1AR	AP1AR	1	2.857	0.61					**0.61**
ZFP36L2	ZFP36L2	1	2.846	0.612					**0.61**
HLX	HLX	1	4.79	0.629	HLX	1	0.682	0.023	**0.63**
PCF11					PCF11	1	1.159	0.63	**0.63**
USP8	USP8	3	0.732	0.631					**0.63**
RBPJ	RBPJ	2	3.176	0.478	RBPJ	1	1.04	0.632	**0.63**
ZNF585A					ZNF585A	1	0.903	0.633	**0.63**
CEP350	CEP350	1	63.52	0.066	CEP350	1	0.935	0.634	**0.63**
TECPR1	TECPR1	1	2.242	0.641					**0.64**
DDX17	DDX17	1	2.248	0.644					**0.64**
GLT8D1	SNORD19B GNL3 GLT8D1	1	1.955	0.648					**0.65**
ZNF649	ZNF649 ZNF615	1	0.627	0.649					**0.65**
UFM1	UFM1	1	1.364	0.662					**0.66**
ZNF548	ZNF548	1	1.453	0.665					**0.66**
PTTG2	PTTG2	1	0.934	0.668					**0.67**
CEPT1	DRAM2 CEPT1	3	1.496	0.67					**0.67**
BACE1	BACE1	1	2.336	0.673					**0.67**
GATA3	GATA3	1	2.002	0.681					**0.68**
ZDHHC6	ZDHHC6	1	1.541	0.686	ZDHHC6	1	1.067	0.611	**0.69**
TXK	TXK	2	1.234	0.688	TXK	1	0.922	0.464	**0.69**
DDX17	KDELR3 DDX17	1	0.732	0.692	DDX17	2	1.125	0.431	**0.69**
ZNF525	ZNF765 ZNF761 ZNF525	1	0.095	0.067	ZNF525	1	1.085	0.692	**0.69**
HELQ	HELQ	1	0.555	0.694					**0.69**
PRKD3	PRKD3	2	0.782	0.695					**0.69**
GIN1	GIN1	1	1.22	0.695					**0.7**
ZNF417	ZNF417 ZNF587 ZNF587B	1	1.275	0.696					**0.7**
ZNF587B	ZNF417 ZNF587 ZNF587B	1	1.275	0.696					**0.7**
TXNDC11	SNN TXNDC11	1	0.281	0.651	TXNDC11	1	1.104	0.7	**0.7**
KLF10	KLF10	1	1.466	0.701	KLF10	1	1.191	0.592	**0.7**
HLTF	HLTF	1	0.74	0.704					**0.7**

VPS37B	VPS37B	1	0.489	0.705	VPS37B	1	0.955	0.705	**0.7**
ZNF160	ZNF160	2	0.52	0.247	ZNF160	2	1.07	0.705	**0.7**
SMARCD2	SMARCD2 PTCRA	1	1.7	0.705					**0.71**
ZNF549	ZNF550 ZNF549	1	0.671	0.707					**0.71**
TRPC1	TRPC1	1	1.451	0.711					**0.71**
HIF1A	HIF1A HIF1A-AS2	2	1.439	0.715					**0.72**
ZNF589	ZNF589	1	0.841	0.717					**0.72**
LIN52					LIN52	1	0.951	0.719	**0.72**
MEPCE	MEPCE	1	2.182	0.721					**0.72**
CCDC18	CCDC18	3	1.191	0.727					**0.73**
FSTL1					FSTL1	1	1.115	0.73	**0.73**
ZNF528	ZNF528	1	1.209	0.738					**0.74**
RSRC2	RSRC2	1	0.492	0.746	RSRC2	1	1.107	0.747	**0.75**
EPHX2	EPHX2	2	0.649	0.748	EPHX2	2	1.075	0.243	**0.75**
PREP	PREP	1	0.528	0.75					**0.75**
HAP1	HADHA HADHAP1	2	0.742	0.755					**0.75**
HSPD1	MYCT1 HSPD1	2	1.173	0.757					**0.76**
ARHGAP1	ARHGAP1	1	1.939	0.757					**0.76**
ZNF24	ZNF24 ZNF396	1	0.816	0.765					**0.77**
UPF2	UPF2	1	8.97	0.019	UPF2	1	0.952	0.765	**0.77**
CCDC18	TMED5 CCDC18	1	3.485	0.444	CCDC18	1	1.098	0.767	**0.77**
LRCH1	LRCH1 ESD	1	0.74	0.773					**0.77**
DIP2B	DIP2B	1	0.742	0.78	DIP2B	1	0.969	0.647	**0.78**
ZNF432	ZNF841 ZNF432 ZNF836	1	0.632	0.786					**0.79**
ZNF841	ZNF841 ZNF432 ZNF836	1	0.632	0.786					**0.79**
ARHGAP12	ARHGAP12	2	0.834	0.786					**0.79**
SLAIN2	SLAIN2	1	1.268	0.792					**0.79**
NDUFB10	NDUFB10	2	1.208	0.792	NDUFB10	1	0.89	0.563	**0.79**
ZNF224	ZNF155 ZNF224	3	1.222	0.552	ZNF224	1	1.045	0.794	**0.79**
IL6ST	IL6ST	2	0.567	0.797					**0.8**
C12orf29	CEP290 C12orf29	1	0.658	0.798					**0.8**
CEP290	CEP290 C12orf29	1	0.658	0.798					**0.8**
FAN1	FAN1	5	1.082	0.8					**0.8**

	MTMR10								
VPS39	VPS39	1	0.509	0.802					**0.8**
CNOT7	CNOT7 ZDHHC2	4	1.099	0.802					**0.8**
NUP107	NUP107	1	1.601	0.42	NUP107	1	1.039	0.808	**0.81**
ZNF485	ZNF485 ZNF487P	1	0.783	0.808					**0.81**
ATF6	ATF6	2	0.796	0.811	ATF6	1	0.95	0.647	**0.81**
ZCCHC7	ZCCHC7	1	1.35	0.725	ZCCHC7	1	1.038	0.814	**0.81**
CDA	CDA	3	1.074	0.816	CDA	3	0.975	0.661	**0.82**
NEMF	NEMF	1	0.55	0.819					**0.82**
SEC23A	SEC23A	1	0.668	0.82					**0.82**
ENKUR	ENKUR	1	0.742	0.821					**0.82**
CCND3	CCND3	1	0.588	0.821	CCND3	1	0.573	0.014	**0.82**
PARP8	PARP8	2	1.263	0.825					**0.83**
HSF2	HSF2	1	0.841	0.826	HSF2	1	1.044	0.759	**0.83**
DICER1	DICER1	2	2.076	0.827	DICER1	1	2.382	4.00E-04	**0.83**
EZH1	EZH1	1	1.974	0.827					**0.83**
CEP120	CEP120 KRT8	1	0.816	0.832					**0.83**
ACAP2	ACAP2	1	0.422	0.835					**0.83**
ZNF737	ZNF737 ZNF626 ZNF826P	2	0.909	0.835					**0.84**
ZNF329	ZNF329	1	1.238	0.841	ZNF329	2	0.869	0.261	**0.84**
ATP5S	ATP5S CDKL1	1	0.814	0.843					**0.84**
GTF2H1	GTF2H1	1	0.723	0.756	GTF2H1	1	1.054	0.844	**0.84**
ZNF680	ZNF680	1	0.813	0.847					**0.85**
ZNF589	NME6 ZNF589	1	1.305	0.852					**0.85**
SETX	SETX	2	1.416	0.86					**0.86**
ZNF606	ZNF606 LOC100128398	1	0.71	0.861					**0.86**
TWF1	TWF1	1	1.226	0.864					**0.86**
TMEM65	TMEM65	2	0.805	0.865					**0.86**
PPP1R2	PPP1R2 PPP1R2P3	1	1.038	0.866					**0.87**
TOPORS	TOPORS LOC100129250	1	0.772	0.867	TOPORS	1	0.844	0.582	**0.87**
CSE1L	CSE1L	1	6.973	0.445	CSE1L	1	0.977	0.875	**0.87**
NDUFV3	NDUFV3	2	0.883	0.875					**0.87**
XPC	XPC	1	0.263	0.648	XPC	1	0.979	0.878	**0.88**
WRN	WRN	1	1.25	0.881	WRN	1	0.893	0.52	**0.88**
APBB1	APBB1IP	4	1.111	0.887					**0.89**
ZFAND1	ZFAND1	1	1.134	0.889	ZFAND1	1	1.054	0.748	**0.89**

PPIG	PPIG	1	1.178	0.895					**0.9**
SIRT1	SIRT1	3	1.068	0.897					**0.9**
COG8	COG8 PDF VPS4A LOC100506031	1	1.177	0.898					**0.9**
ZNF132	ZNF132	1	0.936	0.9	ZNF132	1	0.802	0.225	**0.9**
MLH3	MLH3	1	0.942	0.9	MLH3	1	0.976	0.845	**0.9**
INPP5A	INPP5A	1	0.853	0.902					**0.9**
ZNF720	ZNF720	1	1.225	0.729	ZNF720	1	1.034	0.909	**0.91**
NAA35	NAA35	1	0.813	0.911					**0.91**
C4BPB	C4BPB	1	0.91	0.912					**0.91**
TMEM154	TMEM154	1	0.859	0.912					**0.91**
RNASEL	RNASEL RGSL1	1	11.34	0.243	RNASEL	2	0.982	0.918	**0.92**
ZNF354B	ZNF354B ZNF879 ZNF354A	1	1.196	0.918					**0.92**
HELQ	MRPS18C FAM175A HELQ LOC100509751	1	0.987	0.928					**0.93**
PANK4	PANK4	2	1.268	0.929	PANK4	1	1.041	0.876	**0.93**
CPT1A	CPT1A	1	0.166	0.318	CPT1A	1	0.987	0.931	**0.93**
CEPT1	DENND2D CEPT1	2	1.168	0.931	CEPT1	1	0.88	0.378	**0.93**
ATG12	SLC39A11 ATG12	3	0.929	0.934	ATG12	1	1.474	0.16	**0.93**
GGNBP2	GGNBP2	2	0.945	0.936	GGNBP2	1	0.984	0.848	**0.94**
MFAP3	MFAP3	1	0.885	0.944					**0.94**
ZNF33A	ZNF33A ZNF33B	1	0.949	0.944					**0.94**
VPS37A					VPS37A	1	1.018	0.948	**0.95**
SNW1	SLIRP SNW1	1	1.042	0.949	SNW1	1	1.567	0.19	**0.95**
PPWD1	PPWD1	1	0.916	0.9	PPWD1	1	0.984	0.951	**0.95**
STK38L	STK38L	3	1.066	0.954					**0.95**
L3MBTL3	L3MBTL3	4	0.409	0.049	L3MBTL3	2	0.996	0.955	**0.96**
ATXN1	ATXN1 GMPR	1	1.058	0.957					**0.96**
DLG1	DLG1	1	0.9	0.958					**0.96**
MEFV	MEFV	2	0.941	0.962	MEFV	1	0.944	0.794	**0.96**
TLR5	TLR5	1	1.02	0.964	TLR5	1	1.236	0.421	**0.96**
SNW1	SNW1	1	1.043	0.968					**0.97**
C7orf60	C7orf60	1	1.031	0.98					**0.98**
C22ORF39	C12orf29	1	1.033	0.98					**0.98**
TMED4	TMED4	1	1.336	0.874	TMED4	1	0.998	0.98	**0.98**

COG8	NIP7 TMED6 COG8	1	1.015	0.984					**0.98**
CREBRF	CREBRF CDC42	1	1.051	0.984					**0.98**
NCK2	NCK2 LOC285000	3	1.023	0.987	NCK2	1	0.94	0.735	**0.99**
ITGA6	ITGA6 LOC100287375	1	1.056	0.988					**0.99**
MALT1	MALT1	1	510.3	0.005	MALT1	1	1	0.998	**1**

Supplementary Table 6: Mendelian randomisation analysis for eQTLs associated with PAH development. Results from 2 separate analyses using eQTLs from different studies. N SNPs: number of relevant single nucleotide polymorphisms within that locus. OR: odds ratio for that SNP. Sig.: significance. Max p-value: highest p-value reached for that eQTL in either of the studies.

Gene	Study	SNP	Effect allele	Other allele	Sig.	St. Error
NCK2 **LOC285000**	Joehanes	rs6711659	T	A	$1.28\text{x}10^{-03}$	0.054
DICER1	Westra	rs1054195	A	C	$2.46\text{x}10^{-03}$	0.033
CHD9	Joehanes	rs7195476	A	G	$3.77\text{x}10^{-03}$	0.035
CCND3	Westra	rs4130023	T	C	$7.94\text{x}10^{-03}$	0.047
ABHD2	Joehanes	rs16942644	G	A	0.010	0.048
HLX	Westra	rs11578466	G	C	0.015	0.053
MALT1	Joehanes	rs7243374	T	C	0.017	0.040
ZNF577	Joehanes	rs75647161	T	C	0.021	0.059
ZNF264	Westra	rs11879048	A	G	0.025	0.042
ZNF638	Joehanes	rs12613800	A	T	0.025	0.038
IL6ST	Joehanes	rs6875155	G	A	0.025	0.059
LRCH1	Joehanes	rs2794661	C	T	0.025	0.053
CRYZ **TYW3**	Joehanes	rs7522428	T	C	0.026	0.036
SMAD5	Joehanes	rs10064147	G	A	0.027	0.035
SCFD2 **LOC100506387**	Joehanes	rs76941389	T	A	0.028	0.052
ZNF417	Westra	rs3745134	G	C	0.029	0.034
CHP1	Joehanes	rs11857726	G	A	0.029	0.039
TANK	Joehanes	rs17705608	A	G	0.033	0.038
SF3B1	Westra	rs4685	T	C	0.034	0.041
DICER1	Joehanes	rs8005908	T	C	0.036	0.041
CRYZ **TYW3**	Joehanes	rs12748990	G	A	0.037	0.061
STAT5A **STAT5B**	Joehanes	rs8074524	C	T	0.037	0.040
UPF2	Joehanes	rs10906056	G	T	0.037	0.034
ZNF155 **ZNF224**	Joehanes	rs8100059	T	C	0.037	0.149
SLC13A4	Joehanes	rs3110823	A	C	0.038	0.043
TYW3 **CRYZ**	Joehanes	rs28767547	A	G	0.041	0.032
C1orf27	Joehanes	rs2026189	C	G	0.042	0.033
SF3B1	Joehanes	rs788018	G	A	0.043	0.041
ZNF100 **ZNF430** **LOC400682**	Joehanes	rs11085488	A	G	0.043	0.046
SENP7	Joehanes	rs508537	C	T	0.048	0.039
SENP7	Westra	rs7631506	A	C	0.050	0.033
SMAD5	Westra	rs2548979	A	G	0.050	0.035
APBB1IP	Joehanes	rs787041	A	T	0.052	0.039
BBX	Joehanes	rs595176	G	A	0.053	0.057
SESN1	Westra	rs12197912	T	C	0.057	0.048
DRAM2 **CEPT1**	Joehanes	rs78068836	C	T	0.058	0.142

FBLN2	Westra	rs2167197	C	G	0.063	0.033
GPBP1	Joehanes	rs13189573	T	A	0.066	0.034
MEFV	Joehanes	rs12921606	G	A	0.067	0.040
ZNF30	Joehanes	rs2546030	A	G	0.070	0.038
ZNF468 **ZNF28**	Joehanes	rs4803014	G	A	0.072	0.039
CCAR1	Joehanes	rs1163195	C	T	0.078	0.054
DENND4C	Joehanes	rs10757034	A	C	0.083	0.033
OSBPL2	Westra	rs6142990	G	A	0.086	0.040
DENND2D **CEPT1**	Joehanes	rs600430	G	T	0.088	0.038
MRPL18 **TCP1** **SNORA29**	Joehanes	rs748897	C	G	0.090	0.042
DICER1	Joehanes	rs78322855	A	G	0.090	0.078
SLC38A1	Joehanes	rs10880936	T	C	0.093	0.060
PTPRC	Westra	rs16843742	C	T	0.097	0.039
FBXL4	Joehanes	rs7743033	G	A	0.098	0.044
MED13 **LOC100129112**	Joehanes	rs72843781	A	C	0.098	0.055
RNASEL	Westra	rs12729828	T	C	0.100	0.054
NR1D2	Joehanes	rs4858556	T	A	0.100	0.054
L3MBTL3	Joehanes	rs1415700	A	G	0.102	0.041
RBM5 **LUST** **LOC100129060**	Joehanes	rs2624848	C	T	0.102	0.037
OPA1	Joehanes	rs6444726	C	T	0.104	0.041
SESN1	Joehanes	rs2492975	C	G	0.109	0.066
ZNF765 **ZNF761** **ZNF525**	Joehanes	rs112833827	G	A	0.111	0.048
AVL9	Joehanes	rs1993051	C	T	0.113	0.041
GGTA1P	Joehanes	rs425398	T	C	0.115	0.036
TANK	Joehanes	rs1064576	G	A	0.117	0.062
CAMKMT	Joehanes	rs73924764	C	A	0.124	0.073
FAM129A	Joehanes	rs234103	G	T	0.125	0.037
CEP350	Joehanes	rs113256141	A	T	0.126	0.061
APBB1IP	Joehanes	rs3006773	T	C	0.126	0.045
LEMD3	Westra	rs7398513	G	T	0.127	0.036
CHD9	Westra	rs8050947	T	C	0.128	0.035
ZNF264 **ZNF805** **ZNF543**	Joehanes	rs9304792	G	C	0.128	0.039
MFF	Westra	rs12623665	C	A	0.130	0.048
ACAA2 **SCARNA17**	Joehanes	rs7505997	G	A	0.131	0.038
DRAM2	Joehanes	rs72691222	A	G	0.133	0.076

CEPT1						
TMEM68	Joehanes	rs1823504	A	G	0.134	0.043
ZNF397	Westra	rs1549051	A	T	0.136	0.053
EIF4A2 **MIR1248** **SNORA81** **SNORA4** **SNORD2** **SNORA63** **LOC730139**	Joehanes	rs62294445	C	T	0.138	0.038
PPP2R2D	Westra	rs7915610	T	C	0.138	0.044
CSNK2A2	Joehanes	rs111234535	G	A	0.140	0.071
NRG1	Westra	rs7005606	G	T	0.141	0.033
NRG1	Joehanes	rs7005606	T	G	0.141	0.033
GLT8D1 **SPCS1**	Joehanes	rs11130318	G	C	0.148	0.034
ZNF160	Westra	rs4801949	T	A	0.148	0.050
ATG12	Westra	rs1058600	T	C	0.151	0.044
SLC39A11 **ATG12**	Joehanes	rs903107	T	C	0.151	0.037
CWF19L2	Westra	rs12284352	C	T	0.153	0.043
UBE2D3	Joehanes	rs4239763	T	G	0.155	0.037
SNRK	Westra	rs1018175	C	T	0.158	0.041
ZNF816-ZNF321P **ZNF321P** **ZNF816**	Joehanes	rs10408667	G	A	0.161	0.038
ZNF10 **ZNF268** **RPL23AP67**	Joehanes	rs61960667	G	A	0.162	0.042
ABHD2	Joehanes	rs979171	A	C	0.162	0.038
DENND4C	Westra	rs2383093	T	C	0.163	0.046
CCNB1IP1	Westra	rs6575132	C	A	0.170	0.037
ZNF134 **ZNF211**	Joehanes	rs2885007	G	A	0.173	0.050
ZNF329	Westra	rs2554970	G	A	0.175	0.049
MINPP1	Joehanes	rs2077871	T	G	0.176	0.037
ATP5SL	Joehanes	rs10420556	G	A	0.179	0.038
SESN1	Joehanes	rs1407241	G	A	0.181	0.063
SNW1	Westra	rs10151830	A	G	0.183	0.046
PGS1 **DNAH17**	Joehanes	rs12942811	C	T	0.184	0.036
ZNF595 **ZNF876P**	Joehanes	rs144012347	G	C	0.185	0.091
ZNF418	Westra	rs9630883	C	G	0.186	0.061
ZNF587 **ZNF417** **ZNF587B**	Joehanes	rs9630883	G	C	0.186	0.061

NGLY1	Joehanes	rs6786520	T	C	0.187	0.037
SIRT1	Joehanes	rs16923897	T	A	0.193	0.062
ZNF418	Joehanes	rs150953181	T	G	0.196	0.060
LEMD3	Westra	rs7397906	T	C	0.202	0.037
FAM213A	Joehanes	rs4934165	C	A	0.202	0.037
EXOSC10	Joehanes	rs2791655	A	G	0.206	0.037
AMD1	Joehanes	rs802669	G	A	0.212	0.054
OSBPL2	Joehanes	rs6062146	A	G	0.212	0.051
SYNJ2BP **SYNJ2BP-COX16**	Joehanes	rs11627313	C	T	0.213	0.094
ZNF160	Joehanes	rs329719	C	T	0.214	0.048
ZNF132	Westra	rs4801583	G	A	0.220	0.037
MAP4	Joehanes	rs4858882	A	G	0.222	0.040
TSHZ3	Joehanes	rs13345671	G	A	0.224	0.040
UBE4A	Westra	rs3212262	T	G	0.228	0.052
UBE4A	Joehanes	rs2276419	C	T	0.233	0.052
ZNF160	Westra	rs329706	C	G	0.237	0.048
ANGEL2	Joehanes	rs3002284	T	C	0.238	0.036
TMEM220	Westra	rs368141	T	C	0.238	0.036
GGTA1P	Joehanes	rs145702693	C	T	0.240	0.107
MFF	Joehanes	rs148839567	C	T	0.246	0.058
EPHX2	Westra	rs13262930	C	G	0.246	0.041
ZNF100 **ZNF430** **LOC400682**	Joehanes	rs2435034	G	C	0.247	0.047
SLC39A11 **ATG12**	Joehanes	rs9912666	A	G	0.253	0.046
RIF1	Joehanes	rs12617724	C	T	0.253	0.034
CRYZ **TYW3**	Joehanes	rs11161851	T	C	0.255	0.037
TMEM220 **C17orf48** **MAGOH2**	Joehanes	rs387142	C	T	0.256	0.036
ALG8	Joehanes	rs624350	A	G	0.257	0.036
NRG1	Joehanes	rs6983748	C	T	0.258	0.103
C22ORF39	Westra	rs7575	A	G	0.259	0.049
L3MBTL3	Joehanes	rs12202273	G	C	0.261	0.086
HADHA **HADHAP1**	Joehanes	rs6734307	T	A	0.263	0.106
TEX10	Joehanes	rs7874710	C	T	0.265	0.039
CRYZ **TYW3**	Joehanes	rs72675369	T	G	0.266	0.089
C2orf49	Joehanes	rs115810418	A	T	0.268	0.085

ZNF354A **ZNF354B**	Joehanes	rs115070202	G	A	0.268	0.089
IL6ST	Joehanes	rs7731626	G	A	0.268	0.035
MRPL18 **TCP1** **SNORA29**	Joehanes	rs1033915	C	T	0.273	0.039
ZNF552 **ZNF814** **ZNF587B** **ZNF587**	Joehanes	rs10419004	A	G	0.276	0.035
GPAM	Joehanes	rs3824627	C	T	0.279	0.034
RNASEL **RGSL1**	Joehanes	rs942436	G	A	0.280	0.035
TNFSF4	Westra	rs10489268	C	T	0.280	0.045
TNFSF4 **LOC100506023** **LOC100631377**	Joehanes	rs10489268	T	C	0.280	0.045
GPBP1	Westra	rs10940534	G	T	0.283	0.040
BET1 **GNG11**	Joehanes	rs114584463	C	T	0.285	0.035
SMARCD2	Westra	rs7225092	T	G	0.286	0.037
SLC38A1	Westra	rs2241960	G	A	0.287	0.038
CEP85L	Joehanes	rs9489520	G	A	0.290	0.040
ZNF304	Joehanes	rs55789053	C	T	0.290	0.042
PTGR1	Joehanes	rs2418173	A	G	0.294	0.039
ZNF30	Westra	rs10518287	T	C	0.295	0.036
IFT46	Joehanes	rs11216902	A	G	0.301	0.049
ZNF850 **ZNF260** **ZNF790**	Joehanes	rs1148400	C	G	0.301	0.040
XRCC5 **PKI55**	Joehanes	rs828907	G	T	0.303	0.034
ZNF155 **ZNF224**	Joehanes	rs10415593	G	T	0.307	0.047
APBB1IP	Joehanes	rs150481075	G	T	0.309	0.101
ZNF100 **ZNF430** **LOC400682**	Joehanes	rs62108418	C	G	0.313	0.042
RIF1	Joehanes	rs193197864	A	G	0.316	0.125
CPT1A	Joehanes	rs2123869	A	G	0.318	0.050
SASH1	Joehanes	rs55857426	A	C	0.319	0.043
C3orf17	Joehanes	rs78804736	G	A	0.325	0.086
CCNB1IP1	Joehanes	rs12888870	A	G	0.335	0.038
ARHGAP5	Joehanes	rs1278924	A	G	0.338	0.034
DGCR2 **DGCR11** **DGCR12**	Joehanes	rs5993533	A	G	0.339	0.041

ARHGAP12	Joehanes	rs118076480	G	C	0.341	0.124
PEX1	Joehanes	rs55683154	C	T	0.345	0.108
DCAF7	Joehanes	rs75646162	G	A	0.353	0.072
CEP85L	Joehanes	rs544160	T	C	0.355	0.076
TSHZ3	Joehanes	rs4805622	A	G	0.362	0.034
ORC4	Joehanes	rs115004792	C	T	0.364	0.081
PANK4	Joehanes	rs58974156	C	T	0.368	0.042
INTS10	Joehanes	rs4268139	C	G	0.370	0.046
BET1	Westra	rs9641129	C	A	0.370	0.035
RASA2	Joehanes	rs10513140	T	C	0.372	0.040
ZNF141	Joehanes	rs58500057	C	T	0.373	0.064
TRIM65	Westra	rs8074216	T	C	0.375	0.045
DDX47	Westra	rs1010878	A	G	0.376	0.038
SDCCAG3	Westra	rs10870165	T	C	0.376	0.036
USP8	Joehanes	rs2414045	T	C	0.377	0.047
EPHX2	Joehanes	rs876891	A	G	0.377	0.065
ZNF350	Joehanes	rs7251478	G	A	0.378	0.053
FAN1 **MTMR10**	Joehanes	rs10775137	C	T	0.379	0.128
PAPD4	Joehanes	rs35776641	A	G	0.381	0.057
KRIT1	Westra	rs17756839	C	T	0.383	0.049
ZNF587 **ZNF417** **ZNF587B**	Joehanes	rs73068515	G	C	0.383	0.070
PMS1	Joehanes	rs62184268	A	G	0.383	0.047
NCK2 **LOC285000**	Joehanes	rs35677272	C	T	0.387	0.035
DNAJC21	Joehanes	rs37440	C	T	0.388	0.036
LUZP1 **KDM1A**	Joehanes	rs7527518	A	T	0.392	0.041
UBR1	Joehanes	rs12050604	C	A	0.393	0.037
ZNF211	Westra	rs12104224	T	C	0.394	0.052
ZNF729 **ZNF257** **ZNF492** **ZNF98** **ZNF99**	Joehanes	rs7253490	C	A	0.394	0.037
NDUFB10	Joehanes	rs30252	T	C	0.397	0.040
DENND4C	Joehanes	rs74648766	C	G	0.398	0.067
FAN1 **MTMR10**	Joehanes	rs11633433	T	G	0.401	0.136
SLC25A16	Joehanes	rs4564216	G	A	0.401	0.071
HECTD1	Joehanes	rs7147179	T	C	0.406	0.041
MTMR10 **FAN1**	Joehanes	rs2949576	T	C	0.407	0.043
TXK	Joehanes	rs10517217	G	A	0.408	0.060

ZNF155 **ZNF224**	Joehanes	rs62116613	G	A	0.410	0.056
ZNF354A **ZNF354B**	Joehanes	rs114565401	C	T	0.415	0.090
ZNF729 **ZNF257** **ZNF492** **ZNF98** **ZNF99**	Joehanes	rs7253881	G	A	0.419	0.077
ARFGAP3	Westra	rs6002985	C	T	0.419	0.036
DDX17	Westra	rs5750597	A	C	0.420	0.052
PCBP1	Joehanes	rs35266443	G	A	0.421	0.042
CEPT1	Westra	rs817580	A	C	0.421	0.047
FAN1 **MTMR10**	Joehanes	rs9672645	T	A	0.422	0.051
DENND2D **CEPT1**	Joehanes	rs626339	T	C	0.423	0.037
ZNF121	Westra	rs8102702	C	T	0.426	0.066
RBPJ	Joehanes	rs12651502	G	A	0.428	0.060
BTAF1	Joehanes	rs12416560	A	G	0.429	0.036
PRG4 **TPR**	Joehanes	rs111903500	G	A	0.431	0.045
RYK	Westra	rs4339087	T	C	0.432	0.049
ATP5S	Westra	rs2275592	C	T	0.436	0.034
PIGU	Joehanes	rs6088547	G	A	0.436	0.036
NDUFV3	Joehanes	rs71320571	G	A	0.438	0.071
TPR **PRG4**	Joehanes	rs77583019	T	C	0.443	0.045
TPR	Westra	rs3820182	A	G	0.445	0.045
NUP107	Joehanes	rs2431655	T	C	0.451	0.037
TLR5	Westra	rs9442041	T	C	0.456	0.041
CDA	Westra	rs10916851	A	G	0.457	0.047
SASH1	Westra	rs7739567	A	C	0.459	0.039
ZNF131 **LOC100506639**	Joehanes	rs71627581	G	A	0.459	0.059
DEF6	Westra	rs1888825	G	T	0.463	0.046
METTL20 **AMN1**	Joehanes	rs4931535	G	A	0.464	0.045
MRPL18 **TCP1** **SNORA29**	Joehanes	rs662138	C	G	0.465	0.044
NDUFB10	Joehanes	rs1122949	G	C	0.470	0.038
NDUFV3	Joehanes	rs4148974	C	T	0.470	0.076
ZNF525 **ZNF845** **ZNF813** **ZNF611**	Joehanes	rs2617680	T	A	0.472	0.038
CSE1L	Joehanes	rs2426132	G	C	0.472	0.034
TUBE1	Joehanes	rs7757296	A	G	0.475	0.038

WISP3						
NOM1	Westra	rs2969114	C	T	0.477	0.040
RYK	Joehanes	rs7355922	G	A	0.480	0.054
TMED5 **CCDC18**	Joehanes	rs12067005	A	G	0.481	0.045
SDCCAG3	Joehanes	rs10870166	G	C	0.482	0.039
CRYZ **TYW3**	Joehanes	rs116814216	C	T	0.483	0.104
GGNBP2	Joehanes	rs116916625	T	G	0.483	0.107
OXNAD1 **RFTN1**	Joehanes	rs28639712	C	A	0.485	0.048
ZNF587 **ZNF417** **ZNF587B**	Joehanes	rs113390133	C	T	0.486	0.073
ZNF271 **ZNF24**	Joehanes	rs1131709	A	G	0.486	0.034
SLC38A1	Westra	rs2242355	G	C	0.487	0.037
KDM1A	Joehanes	rs146670573	G	A	0.487	0.051
PANK4	Joehanes	rs147023904	C	T	0.494	0.111
PPA2	Joehanes	rs2726511	C	T	0.496	0.034
ETS2	Joehanes	rs445593	G	A	0.501	0.036
RALA	Joehanes	rs12701757	C	T	0.502	0.036
TEX10	Westra	rs875522	A	C	0.503	0.040
ARFGAP3 **RPL5** **SNORD21**	Joehanes	rs5758943	A	G	0.504	0.036
TXK	Westra	rs4695345	T	C	0.507	0.054
ACAT2 **TCP1** **SNORA29** **LOC100129518** **SOD2**	Joehanes	rs4709368	C	T	0.507	0.042
ETS2	Joehanes	rs711	G	A	0.508	0.036
C3orf17	Joehanes	rs2293560	T	C	0.508	0.042
TANK	Westra	rs1921310	G	A	0.510	0.043
ORMDL1 **PMS1**	Joehanes	rs1233265	G	T	0.511	0.039
LEMD3	Joehanes	rs11612097	A	G	0.511	0.037
PSMC5 **SMARCD2**	Joehanes	rs2854217	G	C	0.514	0.038
MEFV	Joehanes	rs450021	A	C	0.516	0.035
CLTC	Joehanes	rs7207419	T	G	0.520	0.037
PAPD4	Westra	rs7712162	T	C	0.521	0.046
DDX47	Joehanes	rs34323	A	G	0.532	0.037
ZMYM1	Westra	rs2971408	G	A	0.533	0.071

ZNF737 **ZNF626** **ZNF826P**	Joehanes	rs2336616	G	A	0.536	0.041
CWF19L2	Joehanes	rs7358296	T	C	0.541	0.050
ZNF354A **ZNF354B**	Joehanes	rs116283781	T	A	0.545	0.078
ARHGAP5	Joehanes	rs73268969	A	G	0.546	0.045
SETX	Joehanes	rs2296866	A	C	0.546	0.100
CRLF3	Joehanes	rs178843	C	T	0.549	0.045
WRN	Westra	rs4733225	C	T	0.550	0.043
CASD1	Joehanes	rs13227924	T	C	0.555	0.067
NRG1	Joehanes	rs7846169	T	C	0.556	0.037
USP8	Joehanes	rs7169770	G	A	0.557	0.037
ZNF700 **ZNF763** **ZNF833P**	Joehanes	rs10414934	G	A	0.558	0.089
ARHGAP12	Joehanes	rs2799035	G	A	0.559	0.044
CEPT1 **DRAM2**	Joehanes	rs7552535	T	A	0.561	0.054
PRKD3	Joehanes	rs7577041	A	C	0.565	0.053
RIMKLB	Joehanes	rs113505320	G	A	0.568	0.075
L3MBTL3	Westra	rs9492414	C	T	0.569	0.039
PMS1	Joehanes	rs4920657	T	A	0.574	0.075
FNTA	Joehanes	rs2692077	C	G	0.575	0.051
PLCG1	Joehanes	rs753381	C	T	0.584	0.035
RC3H2	Joehanes	rs1868590	A	C	0.584	0.066
SCYL3	Westra	rs10753798	G	T	0.585	0.036
CNOT7 **ZDHHC2**	Joehanes	rs62502370	C	T	0.585	0.062
ZNF91	Joehanes	rs56230498	C	A	0.585	0.043
SCYL3 **C1orf112**	Joehanes	rs12132222	A	G	0.587	0.056
TOPORS	Westra	rs12348918	G	A	0.588	0.041
NDUFB10	Westra	rs6366	C	G	0.589	0.042
ZNF273	Joehanes	rs658360	A	G	0.589	0.036
SETX	Joehanes	rs566069	C	G	0.590	0.063
SIRT1	Joehanes	rs7080662	T	C	0.592	0.036
PPP2R2D	Joehanes	rs7084062	G	A	0.594	0.036
KLF10	Westra	rs4734654	G	A	0.598	0.037
MFF	Westra	rs10933175	G	A	0.600	0.041
CRLF3	Westra	rs9891166	A	G	0.603	0.055
MYCT1 **HSPD1**	Joehanes	rs17710008	G	A	0.605	0.045
CNOT7 **ZDHHC2**	Joehanes	rs2952125	C	T	0.605	0.101
AMN1 **METTL20**	Joehanes	rs10771864	T	C	0.610	0.037

PGS1	Westra	rs4969170	A	G	0.610	0.036
TTC17	Joehanes	rs7934094	T	G	0.613	0.043
SIRT1	Joehanes	rs12358016	T	A	0.616	0.078
TMSB10 **TRABD2A**	Joehanes	rs76496318	A	T	0.616	0.060
AP1AR	Joehanes	rs28585013	A	G	0.619	0.048
ZNF211	Joehanes	rs11880986	C	T	0.621	0.047
TMTC3	Joehanes	rs59522735	G	A	0.624	0.084
ZFP36L2	Joehanes	rs75454372	G	T	0.624	0.071
ETS2	Westra	rs7282723	T	C	0.628	0.036
KRIT1	Westra	rs10281972	G	T	0.631	0.077
RIF1	Joehanes	rs6733645	T	C	0.633	0.038
HIF1A **HIF1A-AS2**	Joehanes	rs10459517	T	C	0.634	0.047
OSBPL2	Joehanes	rs6062166	T	A	0.637	0.075
ARHGAP5	Joehanes	rs78039640	A	G	0.639	0.115
ZDHHC6	Westra	rs3736946	G	A	0.639	0.053
ZNF585A	Westra	rs7257135	A	G	0.639	0.038
PCF11	Westra	rs11530859	G	C	0.643	0.072
OSBPL2	Westra	rs1739592	A	G	0.649	0.035
RBPJ	Westra	rs13133397	C	G	0.650	0.035
DDX17	Joehanes	rs12004	T	G	0.650	0.039
CEP350	Westra	rs2501611	T	A	0.651	0.036
HLX	Joehanes	rs3738182	G	A	0.652	0.044
DIP2B	Westra	rs1047912	T	C	0.654	0.039
SNORD19B **GNL3** **GLT8D1**	Joehanes	rs7612511	T	C	0.654	0.035
XPC	Joehanes	rs2607741	T	C	0.657	0.049
TECPR1	Joehanes	rs62479822	G	A	0.658	0.035
ATF6	Joehanes	rs2298019	G	A	0.662	0.051
ZNF649 **ZNF615**	Joehanes	rs10423027	G	A	0.666	0.036
GGTA1P	Joehanes	rs868043	C	G	0.668	0.052
ZNF548	Joehanes	rs35743706	A	G	0.674	0.051
PTTG2	Joehanes	rs6811863	C	G	0.674	0.036
DDX17	Westra	rs2267390	T	C	0.677	0.039
TANK	Joehanes	rs114692895	T	C	0.678	0.094
NCK2 **LOC285000**	Joehanes	rs56375303	A	T	0.679	0.053
BACE1	Joehanes	rs3017608	A	G	0.680	0.035
ATF6	Westra	rs12025202	C	T	0.681	0.070
ZNF100 **ZNF430** **LOC400682**	Joehanes	rs1510964	T	C	0.681	0.081
SNN **TXNDC11**	Joehanes	rs8191352	C	G	0.683	0.067

SLC13A4	Joehanes	rs73160740	T	C	0.688	0.047
GATA3	Joehanes	rs10905275	G	A	0.688	0.040
CNOT7 **ZDHHC2**	Joehanes	rs141417288	A	T	0.688	0.110
ZNF354A **ZNF354B**	Joehanes	rs13189523	T	C	0.689	0.041
CRLF3	Joehanes	rs8070182	A	C	0.690	0.054
KDELR3 **DDX17**	Joehanes	rs1043402	G	A	0.698	0.038
CHD9	Joehanes	rs1833206	T	C	0.702	0.041
ZNF417 **ZNF587** **ZNF587B**	Joehanes	rs28566599	T	G	0.702	0.036
APBB1IP	Joehanes	rs7098710	C	T	0.707	0.035
SLC38A1	Westra	rs2099984	G	A	0.707	0.038
KLF10	Joehanes	rs3191333	G	A	0.708	0.036
ZDHHC6	Joehanes	rs11195955	C	T	0.708	0.053
HELQ	Joehanes	rs34803094	T	C	0.709	0.037
UFM1	Joehanes	rs2485788	A	T	0.709	0.102
GIN1	Joehanes	rs34812	A	G	0.710	0.037
ZNF525	Westra	rs7259646	A	C	0.711	0.045
HLTF	Joehanes	rs9864549	A	C	0.711	0.038
DRAM2 **CEPT1**	Joehanes	rs3818797	T	C	0.714	0.039
VPS37B	Westra	rs3852537	T	C	0.714	0.054
VPS37B	Joehanes	rs3852537	C	T	0.714	0.054
TXNDC11	Westra	rs12919035	G	A	0.714	0.035
RNASEL	Westra	rs12041623	C	T	0.717	0.037
SMARCD2 **PTCRA**	Joehanes	rs2727295	C	T	0.719	0.035
USP8	Joehanes	rs3131569	G	C	0.722	0.085
ZNF550 **ZNF549**	Joehanes	rs75946741	C	T	0.724	0.043
LIN52	Westra	rs11622838	A	G	0.725	0.038
ZNF589	Joehanes	rs11720622	G	A	0.730	0.036
TRPC1	Joehanes	rs9754885	T	C	0.732	0.055
MEPCE	Joehanes	rs6967277	A	G	0.736	0.043
FSTL1	Westra	rs1270209	T	A	0.736	0.039
ZCCHC7	Joehanes	rs10116283	A	G	0.738	0.035
RYK	Joehanes	rs7649910	T	A	0.741	0.038
L3MBTL3	Joehanes	rs12193819	G	C	0.741	0.035
ZNF720	Joehanes	rs28427454	G	C	0.743	0.041
NCK2	Westra	rs6726571	C	T	0.747	0.035
RSRC2	Joehanes	rs7307867	C	T	0.752	0.035
STK38L	Joehanes	rs10842858	G	T	0.754	0.068
PARP8	Joehanes	rs12652962	C	T	0.755	0.037
PARP8	Joehanes	rs1823262	C	T	0.756	0.057
ZNF528	Joehanes	rs72483958	C	T	0.756	0.054

CDA	Joehanes	rs76594585	G	A	0.757	0.071
PREP	Joehanes	rs12210271	C	T	0.757	0.043
RSRC2	Westra	rs1473553	G	T	0.760	0.039
ZFAND1	Westra	rs2955005	C	A	0.760	0.038
CCDC18	Joehanes	rs142826897	G	A	0.762	0.103
HSF2	Westra	rs556439	A	G	0.765	0.038
ARHGAP1	Joehanes	rs72912177	T	C	0.765	0.051
ABHD2	Joehanes	rs77972530	A	G	0.766	0.081
GTF2H1	Joehanes	rs10832918	A	G	0.767	0.035
ZNF24 **ZNF396**	Joehanes	rs4291985	C	T	0.771	0.035
CCDC18	Westra	rs2433279	T	G	0.775	0.053
LRCH1 **ESD**	Joehanes	rs8192889	T	C	0.778	0.035
UPF2	Westra	rs11257438	T	G	0.780	0.048
SLC39A11 **ATG12**	Joehanes	rs9898137	C	A	0.781	0.047
DIP2B	Joehanes	rs11614785	C	G	0.785	0.037
ABHD2	Joehanes	rs62020268	A	G	0.791	0.102
ZNF841 **ZNF432** **ZNF836**	Joehanes	rs6509606	A	T	0.795	0.063
SLAIN2	Joehanes	rs9884339	A	T	0.802	0.038
MEFV	Westra	rs6501166	G	C	0.803	0.035
TMEM65	Joehanes	rs41327151	G	T	0.803	0.044
CNOT7 **ZDHHC2**	Joehanes	rs3808645	T	C	0.805	0.049
ZNF224	Westra	rs4508518	A	G	0.806	0.046
VPS39	Joehanes	rs8033080	G	A	0.810	0.052
ZNF160	Joehanes	rs12609697	G	A	0.813	0.036
NUP107	Westra	rs2439759	T	A	0.814	0.038
ZNF485 **ZNF487P**	Joehanes	rs7919223	T	C	0.815	0.048
CEP290 **C12orf29**	Joehanes	rs113132803	A	T	0.821	0.090
ZCCHC7	Westra	rs308495	T	G	0.822	0.036
L3MBTL3	Westra	rs7740107	T	A	0.822	0.040
SEC23A	Joehanes	rs8022510	C	G	0.826	0.046
CDA	Westra	rs657624	A	G	0.828	0.037
STK38L	Joehanes	rs12830757	T	C	0.829	0.045
CCND3	Joehanes	rs10947995	G	A	0.831	0.045
ENKUR	Joehanes	rs12769388	A	G	0.832	0.050
HSF2	Joehanes	rs1741820	G	A	0.833	0.035
EZH1	Joehanes	rs9895635	T	C	0.833	0.047
NEMF	Joehanes	rs76279626	C	T	0.835	0.113
PRKD3	Joehanes	rs2110962	C	T	0.837	0.036
CEP120	Joehanes	rs13154356	T	C	0.841	0.046

KRT8						
ACAP2	Joehanes	rs111581175	C	T	0.842	0.056
GGTA1P	Joehanes	rs145916505	G	A	0.845	0.087
ZNF329	Joehanes	rs76603935	G	A	0.847	0.048
GTF2H1	Westra	rs2305564	T	A	0.848	0.035
ATP5S **CDKL1**	Joehanes	rs7155405	G	A	0.849	0.047
EPHX2	Westra	rs733078	A	G	0.850	0.047
MLH3	Westra	rs13712	T	C	0.851	0.035
GGNBP2	Westra	rs9906189	G	A	0.852	0.035
CCDC18	Joehanes	rs72717352	C	T	0.852	0.066
ZNF680	Joehanes	rs77213048	T	C	0.855	0.065
ATF6	Joehanes	rs9729115	C	T	0.856	0.080
ZNF737 **ZNF626** **ZNF826P**	Joehanes	rs116995809	C	G	0.857	0.113
NME6 **ZNF589**	Joehanes	rs11718350	T	G	0.859	0.037
CDA	Joehanes	rs72649191	A	G	0.861	0.052
ZNF595 **ZNF876P**	Joehanes	rs6839041	T	G	0.863	0.041
MYCT1 **HSPD1**	Joehanes	rs80249508	C	A	0.870	0.101
ZNF606 **LOC100128398**	Joehanes	rs112235175	C	T	0.870	0.060
ZNF354A **ZNF354B**	Joehanes	rs12514827	T	C	0.870	0.038
TWF1	Joehanes	rs12829856	G	A	0.870	0.058
MFF	Westra	rs6707977	T	G	0.872	0.051
PPP1R2 **PPP1R2P3**	Joehanes	rs823509	C	T	0.872	0.035
TOPORS **LOC100129250**	Joehanes	rs72712924	A	T	0.872	0.047
SENP7	Joehanes	rs13099833	G	A	0.873	0.035
TMED4	Joehanes	rs1434961	T	C	0.878	0.035
AVL9	Joehanes	rs76226443	G	T	0.878	0.091
CSE1L	Westra	rs1997854	G	A	0.878	0.038
L3MBTL3	Joehanes	rs78404212	T	C	0.879	0.059
CDA	Joehanes	rs10916837	A	C	0.880	0.071
GGNBP2	Joehanes	rs8882	G	A	0.881	0.035
XPC	Westra	rs2733533	A	C	0.882	0.035
PANK4	Westra	rs2477703	C	T	0.882	0.039
HADHA **HADHAP1**	Joehanes	rs4665320	G	T	0.882	0.043
EPHX2	Joehanes	rs62504268	G	A	0.885	0.055
WRN	Joehanes	rs2737327	G	A	0.886	0.045

CAMKMT	Joehanes	rs13393132	T	A	0.891	0.081
ZFAND1	Joehanes	rs2932223	C	T	0.894	0.040
COG8 **PDF** **VPS4A** **LOC100506031**	Joehanes	rs7186635	A	G	0.901	0.037
PPIG	Joehanes	rs2044506	C	T	0.901	0.052
ZNF132	Joehanes	rs7408188	G	T	0.903	0.035
MLH3	Joehanes	rs175074	G	A	0.903	0.035
PPWD1	Joehanes	rs152061	T	C	0.903	0.036
INPP5A	Joehanes	rs2767458	C	T	0.907	0.061
RYK	Joehanes	rs12487646	A	G	0.913	0.095
ZNF720	Westra	rs6565286	T	C	0.913	0.043
CCDC18	Joehanes	rs61780648	C	T	0.914	0.081
NAA35	Joehanes	rs640731	A	G	0.915	0.042
C4BPB	Joehanes	rs2353545	A	G	0.915	0.035
HIF1A **HIF1A-AS2**	Joehanes	rs111522409	A	G	0.917	0.082
ZNF100 **ZNF430** **LOC400682**	Joehanes	rs72995861	A	G	0.918	0.040
ZNF354B **ZNF879** **ZNF354A**	Joehanes	rs111910613	T	C	0.922	0.054
TMEM154	Joehanes	rs9884317	A	G	0.922	0.124
SENP7	Joehanes	rs75519555	C	T	0.925	0.072
MRPS18C **FAM175A** **HELQ** **LOC100509751**	Joehanes	rs1908449	A	T	0.930	0.035
CPT1A	Westra	rs3136547	C	G	0.934	0.038
FAN1 **MTMR10**	Joehanes	rs140942239	C	T	0.938	0.131
MFAP3	Joehanes	rs72804696	A	G	0.946	0.043
UBE2D3	Joehanes	rs9994654	A	C	0.946	0.044
ZNF33A **ZNF33B**	Joehanes	rs615974	G	A	0.947	0.050
TMEM65	Joehanes	rs72722876	C	T	0.949	0.072
VPS37A	Westra	rs3213601	G	A	0.950	0.035
RBPJ	Joehanes	rs73243877	A	G	0.950	0.046
PPWD1	Westra	rs27137	C	G	0.953	0.036
SLIRP **SNW1**	Joehanes	rs10133987	G	A	0.954	0.092
TXK	Joehanes	rs1567218	T	A	0.954	0.036
ATXN1 **GMPR**	Joehanes	rs6924861	A	T	0.959	0.046
DLG1	Joehanes	rs9840527	T	C	0.960	0.035
TLR5	Joehanes	rs851136	T	C	0.966	0.036

SNW1	Joehanes	rs78617489	G	A	0.970	0.076
STK38L	Joehanes	rs841651	G	A	0.971	0.071
C12orf29	Joehanes	rs9262	C	G	0.980	0.035
TMED4	Westra	rs217373	A	C	0.980	0.035
CDA	Westra	rs17412543	T	G	0.981	0.054
C7orf60	Joehanes	rs28546198	A	T	0.981	0.080
FAN1 **MTMR10**	Joehanes	rs278355	C	G	0.982	0.087
ZNF329	Westra	rs260461	A	G	0.983	0.049
NIP7 **TMED6** **COG8**	Joehanes	rs2062547	G	C	0.984	0.037
CREBRF **CDC42**	Joehanes	rs4992808	T	C	0.985	0.047
ZNF418	Joehanes	rs260418	G	A	0.986	0.039
ITGA6 **LOC100287375**	Joehanes	rs7575468	C	A	0.988	0.046
MALT1	Westra	rs4940745	G	A	0.998	0.074

Supplementary Table 7: SNPs used for Mendelian randomisation analysis for RNAs associated with PAH. eQTLs originate from 2 different studies. N SNPs: number of relevant single nucleotide polymorphisms within that locus.

	RNA Discovery		RNA Validation		Combined Discovery and Validation		
Gene	**logFC**	**Sig**	**logFC**	**Sig**	**logFC**	**Sig**	**FDR**
EGR1	2.808	6.23x10^{-11}	0.444	4.94x10^{-02}	2.441	2.64x10^{-15}	6.06x10^{-11}
SNORD3A	-2.063	5.90x10^{-07}	-1.737	1.92x10^{-03}	-2.039	1.21x10^{-09}	6.94x10^{-06}
SNORD17	-1.931	3.21x10^{-07}	-1.609	7.65x10^{-03}	-1.905	5.38x10^{-09}	2.06x10^{-05}
SNORA53	-2.811	3.01x10^{-06}	-3.044	7.31x10^{-04}	-2.995	6.34x10^{-09}	2.08x10^{-05}
SCARNA10	-2.174	3.14x10^{-06}	-1.972	3.71x10^{-03}	-2.169	2.42x10^{-08}	4.64x10^{-05}
SNORA23	-1.740	8.70x10^{-06}	-1.627	3.38x10^{-03}	-1.756	3.42x10^{-08}	6.05x10^{-05}
POLDIP3	0.166	2.02x10^{-06}	0.118	3.78x10^{-02}	0.155	4.51x10^{-08}	7.40x10^{-05}
SNORA12	-1.433	3.33x10^{-06}	-0.930	2.64x10^{-02}	-1.333	7.06x10^{-08}	1.08x10^{-04}
RPPH1	-1.928	1.73x10^{-05}	-1.791	4.32x10^{-03}	-1.971	8.74x10^{-08}	1.25x10^{-04}
SCARNA6	-1.667	8.29x10^{-06}	-1.413	1.09x10^{-02}	-1.662	1.08x10^{-07}	1.31x10^{-04}
RNU12	-2.324	3.51x10^{-05}	-2.841	1.59x10^{-03}	-2.671	1.05x10^{-07}	1.31x10^{-04}
SCARNA5	-1.680	1.97x10^{-05}	-1.553	6.13x10^{-03}	-1.734	1.25x10^{-07}	1.43x10^{-04}
IFI27	1.788	6.95x10^{-03}	2.557	5.91x10^{-03}	2.671	1.67x10^{-07}	1.75x10^{-04}
RNU2-2P	-1.511	2.10x10^{-05}	-1.509	6.47x10^{-03}	-1.578	1.83x10^{-07}	1.83x10^{-04}
SNORA74B	-1.165	9.89x10^{-05}	-1.568	2.29x10^{-03}	-1.367	2.85x10^{-07}	2.45x10^{-04}
SNORD97	-1.271	5.78x10^{-05}	-1.271	4.83x10^{-03}	-1.298	4.28x10^{-07}	3.51x10^{-04}
RP11-734I18.1	1.522	4.71x10^{-06}	0.919	2.38x10^{-02}	1.326	6.09x10^{-07}	4.00x10^{-04}
SNORA57	-1.573	4.19x10^{-06}	-1.094	3.01x10^{-02}	-1.401	7.07x10^{-07}	4.28x10^{-04}
RNU4-2	-1.614	1.88x10^{-05}	-1.421	1.80x10^{-02}	-1.629	7.26x10^{-07}	4.28x10^{-04}
RP11-206L10.9	-0.165	2.32x10^{-05}	-0.139	4.37x10^{-02}	-0.160	1.23x10^{-06}	5.24x10^{-04}
GPKOW	0.238	1.24x10^{-04}	0.183	1.41x10^{-02}	0.230	1.18x10^{-06}	5.24x10^{-04}
NATD1	0.511	2.54x10^{-04}	0.650	8.24x10^{-03}	0.616	1.23x10^{-06}	5.24x10^{-04}
NAPA	0.501	6.27x10^{-04}	0.634	5.93x10^{-04}	0.559	1.13x10^{-06}	5.24x10^{-04}
RP11-85G21.3	0.788	2.07x10^{-04}	0.978	6.69x10^{-03}	0.898	1.41x10^{-06}	5.63x10^{-04}
UNC45A	0.192	3.70x10^{-04}	0.281	4.98x10^{-03}	0.229	1.47x10^{-06}	5.64x10^{-04}
SNORA38B	-1.161	1.60x10^{-04}	-1.217	1.30x10^{-02}	-1.251	1.88x10^{-06}	6.98x10^{-04}
RNU4-1	-1.392	4.43x10^{-05}	-1.190	2.10x10^{-02}	-1.371	2.16x10^{-06}	7.66x10^{-04}
FOXO4	0.651	3.61x10^{-04}	0.593	3.39x10^{-02}	0.732	2.23x10^{-06}	7.68x10^{-04}
OTOF	1.457	7.04x10^{-03}	2.680	9.38x10^{-04}	2.093	2.24x10^{-06}	7.68x10^{-04}
RNU1-1	-1.227	4.80x10^{-05}	-1.192	3.44x10^{-02}	-1.290	2.77x10^{-06}	9.09x10^{-04}
SCARNA1	-1.409	6.12x10^{-05}	-1.139	4.61x10^{-02}	-1.455	2.87x10^{-06}	9.30x10^{-04}
SNORA73B	-1.139	6.66x10^{-05}	-0.842	4.26x10^{-02}	-1.093	3.88x10^{-06}	1.17x10^{-03}
KHNYN	0.165	2.30x10^{-04}	0.210	2.58x10^{-02}	0.197	4.75x10^{-06}	1.36x10^{-03}
CHMP4B	0.361	1.51x10^{-04}	0.390	2.62x10^{-02}	0.400	4.94x10^{-06}	1.37x10^{-03}
E2F2	0.676	2.35x10^{-03}	1.114	8.45x10^{-03}	0.967	5.00x10^{-06}	1.37x10^{-03}
SNORD94	-1.270	4.48x10^{-05}	-1.064	4.58x10^{-02}	-1.238	5.07x10^{-06}	1.37x10^{-03}
SCARNA2	-1.255	1.75x10^{-04}	-1.215	1.72x10^{-02}	-1.257	5.65x10^{-06}	1.46x10^{-03}
DCAF11	0.287	8.36x10^{-04}	0.421	7.45x10^{-03}	0.352	5.64x10^{-06}	1.46x10^{-03}
KDELR1	0.194	1.12x10^{-04}	0.187	4.41x10^{-02}	0.195	8.69x10^{-06}	1.83x10^{-03}
WDTC1	0.350	8.15x10^{-04}	0.389	2.45x10^{-02}	0.404	8.64x10^{-06}	1.83x10^{-03}
KIAA0430	0.311	8.43x10^{-05}	0.350	1.89x10^{-02}	0.328	8.49x10^{-06}	1.83x10^{-03}
APOBEC3C	0.358	3.79x10^{-04}	0.352	3.93x10^{-02}	0.382	9.10x10^{-06}	1.85x10^{-03}
B3GALT2	-0.223	6.19x10^{-04}	-0.257	5.80x10^{-03}	-0.229	1.02x10^{-05}	2.02x10^{-03}
SCARNA12	-1.147	1.21x10^{-04}	-0.851	4.16x10^{-02}	-1.057	1.05x10^{-05}	2.05x10^{-03}

SDE2	0.214	7.43x10^{-05}	0.294	1.39x10^{-02}	0.234	1.06x10^{-05}	2.05x10^{-03}
SNORD15B	-1.193	7.30x10^{-04}	-1.407	2.15x10^{-02}	-1.385	1.11x10^{-05}	2.07x10^{-03}
CMBL	0.546	5.47x10^{-04}	0.529	8.53x10^{-03}	0.556	1.30x10^{-05}	2.28x10^{-03}
RNF40	0.245	6.07x10^{-04}	0.257	3.96x10^{-02}	0.270	1.59x10^{-05}	2.62x10^{-03}
MINK1	0.253	7.32x10^{-04}	0.227	2.57x10^{-02}	0.254	1.77x10^{-05}	2.74x10^{-03}
CAPN1	0.190	5.05x10^{-04}	0.149	3.01x10^{-02}	0.184	1.91x10^{-05}	2.93x10^{-03}
EPN1	0.290	6.82x10^{-04}	0.267	4.96x10^{-02}	0.310	1.95x10^{-05}	2.97x10^{-03}
ABCB6	0.270	5.76x10^{-03}	0.723	3.97x10^{-03}	0.456	2.08x10^{-05}	3.04x10^{-03}
SLFN14	0.537	6.16x10^{-03}	1.063	5.82x10^{-03}	0.797	2.34x10^{-05}	3.29x10^{-03}
CCDC171	-0.173	1.06x10^{-03}	-0.161	2.61x10^{-02}	-0.174	2.43x10^{-05}	3.39x10^{-03}
METTL7A	0.320	7.41x10^{-04}	0.344	2.29x10^{-02}	0.341	2.53x10^{-05}	3.48x10^{-03}
ZNF213	0.151	3.98x10^{-03}	0.298	3.03x10^{-03}	0.195	2.70x10^{-05}	3.59x10^{-03}
RP11-789C7.1	-0.131	7.00x10^{-03}	-0.218	6.76x10^{-03}	-0.172	2.78x10^{-05}	3.67x10^{-03}
WFDC11	-0.253	9.47x10^{-04}	-0.207	1.44x10^{-02}	-0.239	2.86x10^{-05}	3.69x10^{-03}
LY6E	0.613	2.17x10^{-02}	1.211	1.25x10^{-03}	0.902	2.87x10^{-05}	3.69x10^{-03}
ZNF23	0.325	6.07x10^{-03}	0.749	6.39x10^{-03}	0.524	3.30x10^{-05}	4.07x10^{-03}
GATAD2A	0.219	8.24x10^{-04}	0.210	4.86x10^{-02}	0.231	3.54x10^{-05}	4.30x10^{-03}
BECN1	0.181	4.79x10^{-04}	0.290	4.01x10^{-02}	0.243	3.97x10^{-05}	4.62x10^{-03}
KCNIP4	-0.320	9.92x10^{-04}	-0.303	3.51x10^{-02}	-0.320	4.10x10^{-05}	4.67x10^{-03}
ORMDL3	0.341	3.49x10^{-03}	0.439	1.90x10^{-02}	0.401	4.13x10^{-05}	4.68x10^{-03}
JHDM1D-AS1	0.320	1.95x10^{-02}	0.795	6.81x10^{-03}	0.558	4.27x10^{-05}	4.71x10^{-03}
PSMD2	0.208	4.14x10^{-03}	0.306	1.27x10^{-02}	0.255	4.48x10^{-05}	4.81x10^{-03}
RF00322	-0.403	2.91x10^{-03}	-0.377	3.37x10^{-02}	-0.437	4.63x10^{-05}	4.88x10^{-03}
MGLL	0.461	6.29x10^{-04}	0.370	4.51x10^{-02}	0.439	4.76x10^{-05}	4.99x10^{-03}
RP11-98I9.4	-0.217	1.67x10^{-03}	-0.233	1.55x10^{-02}	-0.221	5.54x10^{-05}	5.66x10^{-03}
RNU6ATAC	-1.003	1.29x10^{-03}	-1.032	3.73x10^{-02}	-1.087	5.79x10^{-05}	5.81x10^{-03}
ECHDC1	-0.115	4.45x10^{-03}	-0.181	8.23x10^{-03}	-0.135	5.88x10^{-05}	5.88x10^{-03}
SNORA71B	-1.001	1.14x10^{-03}	-1.223	3.89x10^{-02}	-1.160	6.10x10^{-05}	6.01x10^{-03}
HEXIM1	0.192	2.83x10^{-03}	0.340	1.61x10^{-02}	0.260	6.19x10^{-05}	6.02x10^{-03}
PPA2	-0.276	1.39x10^{-03}	-0.269	4.09x10^{-02}	-0.282	6.33x10^{-05}	6.09x10^{-03}
DNASE2	0.257	1.45x10^{-03}	0.323	2.85x10^{-02}	0.284	6.50x10^{-05}	6.18x10^{-03}
LRRC75A	0.328	7.56x10^{-03}	0.554	8.95x10^{-03}	0.436	6.53x10^{-05}	6.18x10^{-03}
RP11-888D10.4	-0.237	5.12x10^{-03}	-0.346	7.76x10^{-03}	-0.276	6.52x10^{-05}	6.18x10^{-03}
PPP6R1	0.228	3.68x10^{-03}	0.243	3.47x10^{-02}	0.256	6.60x10^{-05}	6.22x10^{-03}
EML4	-0.153	4.50x10^{-03}	-0.293	3.33x10^{-03}	-0.186	6.96x10^{-05}	6.40x10^{-03}
SNORD118	-1.339	1.54x10^{-03}	-1.535	3.80x10^{-02}	-1.607	7.07x10^{-05}	6.40x10^{-03}
MON2	-0.122	8.57x10^{-03}	-0.189	6.83x10^{-03}	-0.148	7.11x10^{-05}	6.40x10^{-03}
GPATCH2L	-0.105	7.66x10^{-03}	-0.172	8.72x10^{-03}	-0.131	7.13x10^{-05}	6.40x10^{-03}
UBAP1	0.355	2.75x10^{-03}	0.428	2.67x10^{-02}	0.422	7.28x10^{-05}	6.46x10^{-03}
RELA	0.106	4.09x10^{-03}	0.164	1.39x10^{-02}	0.124	7.80x10^{-05}	6.76x10^{-03}
MT-TL1	0.452	2.57x10^{-03}	0.599	7.99x10^{-03}	0.485	7.91x10^{-05}	6.83x10^{-03}
ARRDC2	0.208	4.14x10^{-03}	0.319	1.55x10^{-02}	0.251	7.97x10^{-05}	6.85x10^{-03}
RP11-804L24.1	-0.294	2.03x10^{-03}	-0.268	3.20x10^{-02}	-0.293	8.32x10^{-05}	6.96x10^{-03}
CTSB	0.351	8.89x10^{-03}	0.578	1.17x10^{-02}	0.467	8.28x10^{-05}	6.96x10^{-03}
ALAD	0.180	5.51x10^{-03}	0.302	1.95x10^{-02}	0.235	8.75x10^{-05}	7.16x10^{-03}
SLC10A3	0.226	1.97x10^{-03}	0.277	4.78x10^{-02}	0.257	9.21x10^{-05}	7.35x10^{-03}

COL6A6	-0.181	1.58×10^{-03}	-0.237	3.67×10^{-02}	-0.201	9.51×10^{-05}	7.47×10^{-03}
HIST2H2AB	-0.744	2.26×10^{-03}	-0.757	1.67×10^{-02}	-0.743	9.52×10^{-05}	7.47×10^{-03}
AC006042.8	-0.275	1.46×10^{-03}	-0.312	2.33×10^{-02}	-0.278	9.61×10^{-05}	7.49×10^{-03}
LARP1	0.220	6.77×10^{-03}	0.330	1.18×10^{-02}	0.269	9.61×10^{-05}	7.49×10^{-03}
SLC25A38	0.370	3.37×10^{-03}	0.500	2.59×10^{-02}	0.435	9.68×10^{-05}	7.51×10^{-03}
RNU5A-1	-1.128	6.15×10^{-03}	-1.948	9.54×10^{-03}	-1.534	1.00×10^{-04}	7.59×10^{-03}
RP11-504P24.3	-0.203	3.47×10^{-03}	-0.257	3.32×10^{-02}	-0.230	1.02×10^{-04}	7.63×10^{-03}
ZMAT2	0.355	1.46×10^{-02}	0.624	2.04×10^{-02}	0.526	1.07×10^{-04}	7.82×10^{-03}
DNAJB2	0.371	7.50×10^{-03}	0.535	2.92×10^{-02}	0.480	1.08×10^{-04}	7.83×10^{-03}
VAT1	0.201	6.00×10^{-03}	0.336	9.05×10^{-03}	0.246	1.10×10^{-04}	7.96×10^{-03}
OAS1	0.521	3.67×10^{-02}	1.135	2.20×10^{-03}	0.789	1.16×10^{-04}	8.31×10^{-03}
BAP1	0.119	5.15×10^{-03}	0.183	3.06×10^{-02}	0.148	1.20×10^{-04}	8.51×10^{-03}
YPEL4	0.415	3.11×10^{-02}	1.115	1.98×10^{-03}	0.699	1.21×10^{-04}	8.51×10^{-03}
FBXO22	-0.172	3.82×10^{-03}	-0.196	1.72×10^{-02}	-0.179	1.26×10^{-04}	8.75×10^{-03}
NUB1	0.154	1.96×10^{-02}	0.333	1.10×10^{-03}	0.208	1.26×10^{-04}	8.75×10^{-03}
CLCN3	0.222	1.73×10^{-03}	0.310	3.27×10^{-02}	0.254	1.27×10^{-04}	8.76×10^{-03}
TTLL12	0.183	3.21×10^{-03}	0.188	4.42×10^{-02}	0.192	1.32×10^{-04}	9.00×10^{-03}
AC124944.2	0.250	5.17×10^{-03}	0.325	1.27×10^{-02}	0.274	1.36×10^{-04}	9.15×10^{-03}
RP11-268I9.2	-0.288	1.94×10^{-03}	-0.232	3.22×10^{-02}	-0.276	1.38×10^{-04}	9.26×10^{-03}
PTPRF	0.446	4.01×10^{-03}	0.656	4.60×10^{-02}	0.597	1.52×10^{-04}	9.87×10^{-03}
RP11-3J10.4	0.169	1.92×10^{-02}	0.583	8.02×10^{-03}	0.335	1.56×10^{-04}	1.00×10^{-02}
MSH3	-0.189	2.90×10^{-03}	-0.275	3.29×10^{-02}	-0.220	1.63×10^{-04}	1.03×10^{-02}
PIM1	0.362	1.49×10^{-02}	0.688	9.58×10^{-03}	0.517	1.63×10^{-04}	1.03×10^{-02}
FNBP1L	0.326	9.53×10^{-03}	0.712	1.81×10^{-02}	0.481	1.65×10^{-04}	1.03×10^{-02}
MED16	0.192	2.76×10^{-02}	0.422	3.11×10^{-03}	0.286	1.67×10^{-04}	1.04×10^{-02}
ASCC2	0.375	7.76×10^{-03}	0.464	4.31×10^{-02}	0.456	1.70×10^{-04}	1.04×10^{-02}
ST3GAL1	0.134	5.27×10^{-03}	0.183	3.54×10^{-02}	0.159	1.70×10^{-04}	1.04×10^{-02}
BAG6	0.280	1.31×10^{-02}	0.430	2.77×10^{-02}	0.377	1.72×10^{-04}	1.05×10^{-02}
RNPS1	0.118	7.19×10^{-03}	0.159	3.21×10^{-02}	0.139	1.73×10^{-04}	1.05×10^{-02}
RP11-169E6.1	-0.201	6.20×10^{-03}	-0.280	1.60×10^{-02}	-0.228	1.74×10^{-04}	1.05×10^{-02}
USP18	0.694	3.23×10^{-02}	1.409	2.47×10^{-03}	0.988	1.75×10^{-04}	1.05×10^{-02}
TBC1D22B	0.401	8.22×10^{-03}	0.660	3.68×10^{-02}	0.555	1.76×10^{-04}	1.05×10^{-02}
TSPAN17	0.239	4.28×10^{-03}	0.271	4.83×10^{-02}	0.268	1.80×10^{-04}	1.06×10^{-02}
FRMD4A	0.362	6.53×10^{-03}	0.469	4.07×10^{-02}	0.441	1.80×10^{-04}	1.06×10^{-02}
RP11-504P24.9	-0.137	1.24×10^{-02}	-0.260	9.69×10^{-03}	-0.177	1.95×10^{-04}	1.11×10^{-02}
RP4-814D15.1	-0.194	6.62×10^{-03}	-0.288	2.10×10^{-02}	-0.227	1.97×10^{-04}	1.12×10^{-02}
DNMBP	0.200	3.34×10^{-03}	0.254	1.00×10^{-02}	0.206	2.11×10^{-04}	1.17×10^{-02}
FUCA1	0.218	2.47×10^{-02}	0.609	1.81×10^{-02}	0.408	2.14×10^{-04}	1.17×10^{-02}
OAS2	0.423	3.68×10^{-02}	0.923	3.07×10^{-03}	0.627	2.19×10^{-04}	1.19×10^{-02}
RP11-342D11.3	-0.343	1.14×10^{-02}	-0.813	1.50×10^{-03}	-0.447	2.27×10^{-04}	1.22×10^{-02}
ADRM1	0.117	8.92×10^{-03}	0.170	3.21×10^{-02}	0.144	2.30×10^{-04}	1.22×10^{-02}
KIF1C	0.194	5.28×10^{-03}	0.230	2.90×10^{-02}	0.208	2.30×10^{-04}	1.22×10^{-02}
TRIM26	0.187	3.02×10^{-03}	0.205	4.32×10^{-02}	0.195	2.32×10^{-04}	1.23×10^{-02}
TMEM57	0.294	9.11×10^{-03}	0.642	1.92×10^{-02}	0.434	2.35×10^{-04}	1.24×10^{-02}
FAM172A	-0.235	4.30×10^{-03}	-0.372	1.90×10^{-02}	-0.279	2.34×10^{-04}	1.24×10^{-02}
MFSD8	-0.110	4.60×10^{-03}	-0.161	4.51×10^{-02}	-0.130	2.42×10^{-04}	1.27×10^{-02}

SIGLEC1	0.811	3.90x10^{-02}	1.545	4.80x10^{-03}	1.155	2.54x10^{-04}	1.30x10^{-02}
DYRK3	0.594	1.70x10^{-02}	0.864	3.51x10^{-02}	0.799	2.59x10^{-04}	1.31x10^{-02}
SUMO4	-0.298	4.42x10^{-03}	-0.217	2.87x10^{-02}	-0.278	2.60x10^{-04}	1.31x10^{-02}
ENTPD5	0.175	2.37x10^{-02}	0.481	9.94x10^{-03}	0.295	2.63x10^{-04}	1.32x10^{-02}
PLBD2	0.271	8.82x10^{-03}	0.427	2.63x10^{-02}	0.332	2.79x10^{-04}	1.39x10^{-02}
MRFAP1	0.202	1.50x10^{-02}	0.396	3.12x10^{-02}	0.312	2.83x10^{-04}	1.39x10^{-02}
RN7SL3	-0.500	3.26x10^{-02}	-1.434	1.04x10^{-02}	-0.937	3.12x10^{-04}	1.49x10^{-02}
EEF1AL1	-0.275	3.80x10^{-03}	-0.241	3.02x10^{-02}	-0.261	3.15x10^{-04}	1.49x10^{-02}
RP5-1069C8.2	-0.198	3.58x10^{-03}	-0.137	4.12x10^{-02}	-0.178	3.30x10^{-04}	1.54x10^{-02}
NFE2L3	-0.143	1.89x10^{-02}	-0.219	8.85x10^{-03}	-0.172	3.33x10^{-04}	1.54x10^{-02}
RP11-872J21.5	-0.195	5.82x10^{-03}	-0.196	2.73x10^{-02}	-0.194	3.34x10^{-04}	1.54x10^{-02}
GLUL	0.416	8.82x10^{-03}	0.480	2.60x10^{-02}	0.469	3.48x10^{-04}	1.58x10^{-02}
PSMA3	-0.116	1.02x10^{-02}	-0.127	2.40x10^{-02}	-0.122	3.52x10^{-04}	1.58x10^{-02}
FRA10AC1	-0.159	1.31x10^{-02}	-0.338	1.91x10^{-02}	-0.232	3.52x10^{-04}	1.58x10^{-02}
PGBD4	-0.100	7.53x10^{-03}	-0.157	2.63x10^{-02}	-0.115	3.56x10^{-04}	1.59x10^{-02}
MARCH8	0.499	1.38x10^{-02}	0.611	3.95x10^{-02}	0.619	3.58x10^{-04}	1.59x10^{-02}
RNU5B-1	-0.841	2.31x10^{-02}	-2.225	6.84x10^{-03}	-1.473	3.67x10^{-04}	1.61x10^{-02}
TRPC5	-0.300	9.33x10^{-03}	-0.415	3.55x10^{-02}	-0.350	3.74x10^{-04}	1.63x10^{-02}
AKT2	0.116	3.24x10^{-02}	0.278	2.09x10^{-02}	0.189	3.83x10^{-04}	1.65x10^{-02}
RP11-43F13.3	-0.115	5.50x10^{-03}	-0.121	4.92x10^{-02}	-0.116	3.98x10^{-04}	1.69x10^{-02}
SOX2	-0.212	1.21x10^{-02}	-0.330	3.31x10^{-02}	-0.258	3.99x10^{-04}	1.69x10^{-02}
PRPF38B	-0.124	8.01x10^{-03}	-0.129	2.47x10^{-02}	-0.124	4.16x10^{-04}	1.72x10^{-02}
RP11-554D14.6	-0.203	1.02x10^{-02}	-0.236	2.62x10^{-02}	-0.217	4.18x10^{-04}	1.72x10^{-02}
XX-CR54.1	-0.213	8.55x10^{-03}	-0.321	2.54x10^{-02}	-0.244	4.20x10^{-04}	1.72x10^{-02}
FZR1	0.182	3.34x10^{-02}	0.391	1.15x10^{-02}	0.268	4.21x10^{-04}	1.72x10^{-02}
RP11-43N16.4	0.213	7.58x10^{-03}	0.296	2.58x10^{-02}	0.242	4.32x10^{-04}	1.75x10^{-02}
CLTB	0.252	1.04x10^{-02}	0.274	4.60x10^{-02}	0.276	4.38x10^{-04}	1.76x10^{-02}
LRRC41	0.110	1.12x10^{-02}	0.116	4.84x10^{-02}	0.119	4.61x10^{-04}	1.81x10^{-02}
TBXA2R	0.276	8.11x10^{-03}	0.243	3.27x10^{-02}	0.280	4.63x10^{-04}	1.81x10^{-02}
HSF1	0.118	1.74x10^{-02}	0.163	1.98x10^{-02}	0.139	4.62x10^{-04}	1.81x10^{-02}
RARRES2P2	-0.545	1.07x10^{-02}	-0.580	1.84x10^{-02}	-0.576	4.64x10^{-04}	1.81x10^{-02}
CCDC157	0.113	1.39x10^{-02}	0.202	2.18x10^{-02}	0.141	4.74x10^{-04}	1.83x10^{-02}
STEAP3	0.327	2.10x10^{-02}	0.522	1.50x10^{-02}	0.408	4.75x10^{-04}	1.83x10^{-02}
STX4	0.106	1.78x10^{-02}	0.168	3.09x10^{-02}	0.135	4.77x10^{-04}	1.84x10^{-02}
CH17-189H20.1	-0.126	3.53x10^{-02}	-0.278	2.94x10^{-03}	-0.170	5.04x10^{-04}	1.90x10^{-02}
AC017076.5	0.520	3.76x10^{-02}	1.052	4.03x10^{-03}	0.713	5.06x10^{-04}	1.91x10^{-02}
TTC32	-0.259	6.23x10^{-03}	-0.282	3.02x10^{-02}	-0.260	5.07x10^{-04}	1.91x10^{-02}
FAM225A	1.057	9.10x10^{-03}	1.429	1.99x10^{-02}	1.201	5.38x10^{-04}	1.98x10^{-02}
IQCF3	-0.155	1.14x10^{-02}	-0.167	4.79x10^{-02}	-0.166	5.45x10^{-04}	1.99x10^{-02}
ENSA	0.107	1.25x10^{-02}	0.144	3.62x10^{-02}	0.123	5.53x10^{-04}	2.00x10^{-02}
TCN2	0.434	1.11x10^{-02}	0.656	2.34x10^{-02}	0.508	5.93x10^{-04}	2.09x10^{-02}
FBXO6	0.318	8.44x10^{-03}	0.301	4.73x10^{-02}	0.323	6.13x10^{-04}	2.13x10^{-02}
TANGO2	0.264	1.76x10^{-02}	0.351	4.65x10^{-02}	0.323	6.48x10^{-04}	2.22x10^{-02}
TUBB4B	0.237	2.80x10^{-02}	0.417	3.30x10^{-02}	0.334	6.53x10^{-04}	2.23x10^{-02}
TMEM168	-0.129	3.40x10^{-02}	-0.252	1.15x10^{-02}	-0.173	6.54x10^{-04}	2.23x10^{-02}
KIAA1468	-0.114	2.27x10^{-02}	-0.160	3.19x10^{-02}	-0.137	6.63x10^{-04}	2.25x10^{-02}

RP4-547C10.1	-0.284	6.16x10^{-03}	-0.498	1.47x10^{-02}	-0.334	6.63x10^{-04}	2.25x10^{-02}
TEX35	-0.116	1.45x10^{-02}	-0.154	2.93x10^{-02}	-0.129	6.74x10^{-04}	2.28x10^{-02}
EIF5	0.119	3.92x10^{-02}	0.306	1.91x10^{-02}	0.199	6.86x10^{-04}	2.31x10^{-02}
SIGLEC16	0.193	2.59x10^{-02}	0.279	1.69x10^{-02}	0.231	6.98x10^{-04}	2.31x10^{-02}
ACO2	0.139	1.27x10^{-02}	0.207	4.90x10^{-02}	0.166	7.12x10^{-04}	2.35x10^{-02}
KLRB1	-0.537	7.92x10^{-03}	-0.602	2.50x10^{-02}	-0.540	7.17x10^{-04}	2.36x10^{-02}
AC092652.1	-0.174	3.81x10^{-02}	-0.333	1.72x10^{-03}	-0.218	7.23x10^{-04}	2.37x10^{-02}
CTSE	0.619	2.22x10^{-02}	0.983	1.30x10^{-02}	0.760	7.29x10^{-04}	2.38x10^{-02}
FBXO46	0.125	2.49x10^{-02}	0.180	3.99x10^{-02}	0.156	7.63x10^{-04}	2.45x10^{-02}
PINK1	0.324	4.73x10^{-02}	0.562	3.67x10^{-02}	0.482	7.62x10^{-04}	2.45x10^{-02}
TMEM5	-0.148	1.19x10^{-02}	-0.164	4.37x10^{-02}	-0.156	7.86x10^{-04}	2.51x10^{-02}
CTD-2311B13.7	-0.209	1.54x10^{-02}	-0.322	1.43x10^{-02}	-0.238	7.97x10^{-04}	2.53x10^{-02}
UBE2L6	0.344	1.18x10^{-02}	0.377	3.80x10^{-02}	0.359	8.13x10^{-04}	2.55x10^{-02}
TMEM106B	-0.191	1.08x10^{-02}	-0.231	4.64x10^{-02}	-0.206	8.50x10^{-04}	2.63x10^{-02}
POU5F1P5	-0.153	2.45x10^{-02}	-0.215	1.39x10^{-02}	-0.173	8.67x10^{-04}	2.65x10^{-02}
RP11-649A18.12	-0.285	5.64x10^{-03}	-0.362	4.84x10^{-02}	-0.301	8.97x10^{-04}	2.69x10^{-02}
RNF146	-0.188	3.36x10^{-02}	-0.353	7.43x10^{-03}	-0.242	9.49x10^{-04}	2.80x10^{-02}
ICAM4	0.254	2.66x10^{-02}	0.381	6.05x10^{-03}	0.302	9.62x10^{-04}	2.81x10^{-02}
MTERFD3	-0.210	1.11x10^{-02}	-0.337	2.50x10^{-02}	-0.239	9.65x10^{-04}	2.82x10^{-02}
RNY4	-0.756	9.17x10^{-03}	-1.848	4.54x10^{-02}	-1.516	9.88x10^{-04}	2.86x10^{-02}
RP3-508I15.20	0.178	2.21x10^{-02}	0.254	4.65x10^{-02}	0.213	1.06x10^{-03}	2.96x10^{-02}
WASHC2C	0.143	3.17x10^{-02}	0.238	1.27x10^{-02}	0.175	1.06x10^{-03}	2.96x10^{-02}
TPRG1L	0.211	3.93x10^{-02}	0.385	3.55x10^{-02}	0.297	1.07x10^{-03}	2.97x10^{-02}
HDAC5	0.142	2.47x10^{-02}	0.234	3.58x10^{-02}	0.179	1.07x10^{-03}	2.98x10^{-02}
CLK3	0.149	2.63x10^{-02}	0.198	4.28x10^{-02}	0.180	1.13x10^{-03}	3.08x10^{-02}
RP11-402J7.2	-0.360	1.04x10^{-02}	-0.461	4.62x10^{-02}	-0.386	1.15x10^{-03}	3.11x10^{-02}
SLC35G1	-0.159	3.03x10^{-02}	-0.370	1.42x10^{-03}	-0.200	1.17x10^{-03}	3.13x10^{-02}
MAN1A1	0.269	1.63x10^{-02}	0.371	2.93x10^{-02}	0.313	1.19x10^{-03}	3.15x10^{-02}
CDK12	0.109	1.90x10^{-02}	0.162	4.23x10^{-02}	0.127	1.20x10^{-03}	3.16x10^{-02}
GLCCI1	-0.127	4.76x10^{-02}	-0.306	1.37x10^{-02}	-0.183	1.22x10^{-03}	3.19x10^{-02}
GOLPH3L	0.159	3.87x10^{-02}	0.331	1.43x10^{-02}	0.218	1.27x10^{-03}	3.26x10^{-02}
IL31RA	0.284	4.66x10^{-02}	0.694	1.66x10^{-03}	0.390	1.28x10^{-03}	3.28x10^{-02}
VPS4A	0.110	2.27x10^{-02}	0.126	4.40x10^{-02}	0.120	1.29x10^{-03}	3.29x10^{-02}
CTC-457L16.1	0.389	1.25x10^{-02}	0.548	2.35x10^{-02}	0.423	1.32x10^{-03}	3.34x10^{-02}
EPC1	-0.125	3.63x10^{-02}	-0.243	2.15x10^{-02}	-0.163	1.38x10^{-03}	3.43x10^{-02}
RASGEF1B	0.133	4.10x10^{-02}	0.306	1.06x10^{-02}	0.184	1.38x10^{-03}	3.43x10^{-02}
RP11-1000B6.8	-0.238	2.50x10^{-02}	-0.335	3.07x10^{-02}	-0.275	1.40x10^{-03}	3.43x10^{-02}
LIPA	0.289	2.47x10^{-02}	0.419	2.73x10^{-02}	0.337	1.39x10^{-03}	3.43x10^{-02}
SMAD9	-0.106	4.30x10^{-02}	-0.218	2.10x10^{-02}	-0.144	1.39x10^{-03}	3.43x10^{-02}
FASTKD3	-0.235	1.53x10^{-02}	-0.345	2.57x10^{-02}	-0.257	1.41x10^{-03}	3.44x10^{-02}
PLEKHA2	0.135	2.22x10^{-02}	0.185	4.89x10^{-02}	0.154	1.51x10^{-03}	3.62x10^{-02}
NUCKS1	0.165	2.58x10^{-02}	0.305	2.07x10^{-02}	0.203	1.53x10^{-03}	3.63x10^{-02}
THAP6	-0.076	3.45x10^{-02}	-0.154	1.89x10^{-02}	-0.097	1.56x10^{-03}	3.68x10^{-02}
CTAGE4	-0.639	1.09x10^{-02}	-0.710	4.31x10^{-02}	-0.634	1.58x10^{-03}	3.70x10^{-02}
RP11-296I10.6	0.100	2.88x10^{-02}	0.218	3.43x10^{-02}	0.137	1.58x10^{-03}	3.70x10^{-02}
TMEM117	-0.291	9.36x10^{-03}	-0.395	4.41x10^{-02}	-0.302	1.60x10^{-03}	3.72x10^{-02}

TNKS	-0.082	3.32x10^{-02}	-0.132	3.75x10^{-02}	-0.102	1.60x10^{-03}	3.72x10^{-02}
MFSD12	0.116	3.35x10^{-02}	0.177	3.42x10^{-02}	0.140	1.65x10^{-03}	3.79x10^{-02}
RAPGEF6	-0.144	3.56x10^{-02}	-0.274	1.56x10^{-02}	-0.179	1.76x10^{-03}	3.91x10^{-02}
TPK1	-0.203	1.69x10^{-02}	-0.256	4.40x10^{-02}	-0.219	1.76x10^{-03}	3.92x10^{-02}
ODC1	0.335	4.90x10^{-02}	0.639	3.28x10^{-02}	0.478	1.81x10^{-03}	3.97x10^{-02}
HECTD4	0.161	4.94x10^{-02}	0.320	4.06x10^{-02}	0.234	1.81x10^{-03}	3.98x10^{-02}
RBM12B	-0.212	1.82x10^{-02}	-0.226	3.50x10^{-02}	-0.212	1.87x10^{-03}	4.07x10^{-02}
RP5-1142A6.3	0.150	4.46x10^{-02}	0.327	7.73x10^{-03}	0.194	1.91x10^{-03}	4.13x10^{-02}
SEC22B	-0.117	3.25x10^{-02}	-0.166	2.66x10^{-02}	-0.132	1.96x10^{-03}	4.18x10^{-02}
XRCC1	0.086	4.93x10^{-02}	0.182	3.27x10^{-02}	0.122	1.97x10^{-03}	4.19x10^{-02}
CMB9-75A1.1	0.427	3.63x10^{-02}	0.872	3.92x10^{-02}	0.603	1.99x10^{-03}	4.22x10^{-02}
ACTR3B	0.185	2.04x10^{-02}	0.259	2.23x10^{-02}	0.196	2.06x10^{-03}	4.27x10^{-02}
SMTNL1	0.459	4.24x10^{-02}	0.633	2.65x10^{-02}	0.540	2.20x10^{-03}	4.46x10^{-02}
CDC14A	-0.168	2.89x10^{-02}	-0.256	4.07x10^{-02}	-0.197	2.24x10^{-03}	4.50x10^{-02}
SYCP2	-0.219	4.91x10^{-02}	-0.462	1.21x10^{-02}	-0.286	2.29x10^{-03}	4.54x10^{-02}
CC2D1A	0.133	2.71x10^{-02}	0.164	4.87x10^{-02}	0.143	2.46x10^{-03}	4.70x10^{-02}
ZNF254	-0.214	4.44x10^{-02}	-0.469	3.47x10^{-03}	-0.267	2.46x10^{-03}	4.70x10^{-02}
COPS6	0.102	3.98x10^{-02}	0.141	4.08x10^{-02}	0.120	2.47x10^{-03}	4.71x10^{-02}
HPGD	-0.316	3.57x10^{-02}	-0.962	2.57x10^{-03}	-0.455	2.51x10^{-03}	4.75x10^{-02}
CDKN2B-AS1	-0.120	2.37x10^{-02}	-0.118	4.87x10^{-02}	-0.122	2.70x10^{-03}	4.91x10^{-02}
CTD-2521M24.13	0.242	3.59x10^{-02}	0.410	2.87x10^{-02}	0.291	2.70x10^{-03}	4.91x10^{-02}
AGPAT3	0.180	3.41x10^{-02}	0.266	4.69x10^{-02}	0.212	2.71x10^{-03}	4.94x10^{-02}
RP11-488L18.10	-0.208	3.82x10^{-02}	-0.348	2.58x10^{-02}	-0.247	2.73x10^{-03}	4.94x10^{-02}
RP11-33B1.1	-0.237	2.82x10^{-02}	-0.311	3.79x10^{-02}	-0.256	2.75x10^{-03}	4.95x10^{-02}
IL23R	-0.342	1.82x10^{-02}	-0.440	4.72x10^{-02}	-0.356	2.77x10^{-03}	4.96x10^{-02}

Supplementary Table 8: Dysregulated RNAs in whole blood RNAseq comparing PAH and other PH patients. List of 253 differentially expressed ($p< 0.05$), directionally consistent genes between PAH (PH Group I) and other PH (PH Groups II-IV) patients from Discovery (2/3 samples) and Validation (1/3 samples) analyses which also met FDR corrected significance ($q< 0.05$) in combined Discovery and Validation analysis (all samples). Genes listed by significance (lowest FDR q first).

	RNA Discovery		RNA Validation		Combined Discovery and Validation		
Gene	**logFC**	**Sig**	**logFC**	**Sig**	**logFC**	**Sig**	**FDR**
RSRC2	-0.188	3.00x10^{-07}	-0.110	8.64x10^{-04}	-0.142	4.85x10^{-09}	4.37x10^{-05}
PTAR1	-0.197	5.01x10^{-06}	-0.140	1.10x10^{-03}	-0.164	3.16x10^{-08}	1.90x10^{-04}
RP11-379H18.1	0.155	5.00x10^{-04}	0.209	2.88x10^{-05}	0.177	5.20x10^{-08}	2.34x10^{-04}
C1orf27	-0.196	1.39x10^{-05}	-0.158	1.23x10^{-03}	-0.175	8.08x10^{-08}	2.91x10^{-04}
AP004289.1	0.321	9.03x10^{-07}	0.202	4.61x10^{-03}	0.255	1.26x10^{-07}	3.16x10^{-04}
BTAF1	-0.192	2.75x10^{-05}	-0.130	1.26x10^{-03}	-0.157	1.76x10^{-07}	3.16x10^{-04}
TEX10	-0.141	5.52x10^{-06}	-0.087	5.53x10^{-03}	-0.113	1.39x10^{-07}	3.16x10^{-04}
TLR5	-0.349	2.18x10^{-04}	-0.410	2.23x10^{-04}	-0.368	1.49x10^{-07}	3.16x10^{-04}
ARFGAP3	-0.160	1.93x10^{-04}	-0.150	6.01x10^{-04}	-0.155	2.69x10^{-07}	3.24x10^{-04}
HLTF	-0.212	1.08x10^{-05}	-0.150	5.06x10^{-03}	-0.179	2.70x10^{-07}	3.24x10^{-04}
RBM27	-0.136	6.00x10^{-04}	-0.135	4.90x10^{-04}	-0.140	2.08x10^{-07}	3.24x10^{-04}
SAMD8	-0.125	2.76x10^{-03}	-0.177	2.46x10^{-05}	-0.149	2.23x10^{-07}	3.24x10^{-04}
SCYL3	-0.142	3.37x10^{-06}	-0.085	1.11x10^{-02}	-0.113	2.36x10^{-07}	3.24x10^{-04}
SCFD2	-0.257	3.63x10^{-05}	-0.211	5.53x10^{-04}	-0.227	2.99x10^{-07}	3.37x10^{-04}
ZNF211	-0.182	7.91x10^{-05}	-0.154	6.68x10^{-04}	-0.163	3.26x10^{-07}	3.45x10^{-04}
DDX17	-0.159	4.61x10^{-06}	-0.083	1.34x10^{-02}	-0.118	3.68x10^{-07}	3.68x10^{-04}
AL844908.5	-0.300	1.86x10^{-04}	-0.280	1.62x10^{-03}	-0.297	4.76x10^{-07}	4.29x10^{-04}
ZNF702P	-0.261	2.45x10^{-02}	-0.505	2.63x10^{-06}	-0.406	4.56x10^{-07}	4.29x10^{-04}
RALA	0.160	1.36x10^{-03}	0.204	1.33x10^{-04}	0.181	5.22x10^{-07}	4.48x10^{-04}
PTEN	-0.181	1.32x10^{-04}	-0.176	6.67x10^{-04}	-0.171	5.73x10^{-07}	4.69x10^{-04}
CCNB1IP1	-0.148	9.46x10^{-04}	-0.150	2.80x10^{-04}	-0.149	6.17x10^{-07}	4.84x10^{-04}
AP000240.5	0.324	2.64x10^{-03}	0.400	8.03x10^{-04}	0.389	6.86x10^{-07}	5.15x10^{-04}
RBM5	-0.137	2.28x10^{-06}	-0.062	4.48x10^{-02}	-0.101	7.51x10^{-07}	5.41x10^{-04}
KCNQ1OT1	0.152	1.41x10^{-04}	0.132	1.26x10^{-03}	0.140	9.24x10^{-07}	6.17x10^{-04}
ZNF224	-0.135	2.53x10^{-05}	-0.090	9.32x10^{-03}	-0.112	9.08x10^{-07}	6.17x10^{-04}
RP11-138A9.2	0.223	6.17x10^{-04}	0.238	3.59x10^{-04}	0.225	1.08x10^{-06}	6.72x10^{-04}
ZFAND1	-0.151	8.35x10^{-04}	-0.167	3.08x10^{-04}	-0.157	1.06x10^{-06}	6.72x10^{-04}
AC010746.2	0.206	3.04x10^{-04}	0.213	1.10x10^{-03}	0.207	1.33x10^{-06}	8.01x10^{-04}
CCDC186	-0.153	1.45x10^{-04}	-0.109	6.54x10^{-03}	-0.132	1.52x10^{-06}	8.24x10^{-04}
CHD9	-0.157	3.20x10^{-04}	-0.178	2.04x10^{-04}	-0.155	1.49x10^{-06}	8.24x10^{-04}
RASA2	-0.145	2.57x10^{-04}	-0.113	7.17x10^{-03}	-0.135	1.56x10^{-06}	8.24x10^{-04}
UBR1	-0.150	1.13x10^{-05}	-0.089	1.01x10^{-02}	-0.114	1.52x10^{-06}	8.24x10^{-04}
ZNF141	-0.159	1.49x10^{-04}	-0.110	2.62x10^{-03}	-0.130	1.64x10^{-06}	8.46x10^{-04}
AC009299.4	1.414	2.20x10^{-05}	0.600	3.22x10^{-02}	1.048	1.74x10^{-06}	8.69x10^{-04}
ARHGAP12	-0.195	1.89x10^{-05}	-0.099	3.39x10^{-02}	-0.151	1.84x10^{-06}	8.78x10^{-04}
ZNF486	-0.229	3.96x10^{-03}	-0.321	7.27x10^{-05}	-0.266	1.85x10^{-06}	8.78x10^{-04}
BCLAF1	-0.166	3.01x10^{-05}	-0.092	1.53x10^{-02}	-0.127	2.00x10^{-06}	9.25x10^{-04}
SMARCD2	-0.158	8.08x10^{-05}	-0.114	5.20x10^{-03}	-0.132	2.23x10^{-06}	1.00x10^{-03}
RP11-158K1.3	-0.160	5.37x10^{-04}	-0.138	3.47x10^{-03}	-0.151	2.30x10^{-06}	1.01x10^{-03}
DENND4C	-0.176	2.52x10^{-05}	-0.094	1.63x10^{-02}	-0.132	2.48x10^{-06}	1.04x10^{-03}
RP11-154H23.1	0.279	2.47x10^{-05}	0.172	1.24x10^{-02}	0.221	2.48x10^{-06}	1.04x10^{-03}
PCF11	-0.136	2.21x10^{-04}	-0.118	2.46x10^{-03}	-0.122	2.74x10^{-06}	1.10x10^{-03}
ZNF397	-0.101	2.13x10^{-03}	-0.105	2.48x10^{-03}	-0.109	2.76x10^{-06}	1.10x10^{-03}
XKRX	-0.544	3.45x10^{-03}	-0.763	2.38x10^{-05}	-0.604	2.87x10^{-06}	1.12x10^{-03}

RP11-775J23.2	0.357	1.12x10^{-04}	0.279	2.52x10^{-03}	0.299	3.01x10^{-06}	1.15x10^{-03}
HECTD1	-0.133	1.93x10^{-05}	-0.088	7.92x10^{-03}	-0.103	3.10x10^{-06}	1.16x10^{-03}
CTD-2317K6.1	0.299	2.62x10^{-04}	0.253	2.63x10^{-03}	0.272	3.32x10^{-06}	1.22x10^{-03}
ZNF24	-0.126	6.16x10^{-04}	-0.107	3.45x10^{-03}	-0.116	3.48x10^{-06}	1.25x10^{-03}
RP11-426D19.1	0.205	9.97x10^{-05}	0.142	1.36x10^{-02}	0.177	3.65x10^{-06}	1.29x10^{-03}
DNAJB4	-0.266	5.60x10^{-05}	-0.179	1.30x10^{-02}	-0.228	3.80x10^{-06}	1.31x10^{-03}
ZNF432	-0.171	2.55x10^{-04}	-0.130	4.99x10^{-03}	-0.149	3.86x10^{-06}	1.31x10^{-03}
BROX	-0.107	4.75x10^{-03}	-0.150	2.14x10^{-04}	-0.123	4.06x10^{-06}	1.35x10^{-03}
RNASEL	-0.162	8.71x10^{-04}	-0.215	1.28x10^{-03}	-0.184	4.31x10^{-06}	1.41x10^{-03}
SEC23A	-0.125	1.61x10^{-04}	-0.081	1.74x10^{-02}	-0.104	4.90x10^{-06}	1.55x10^{-03}
ALG8	-0.139	1.40x10^{-04}	-0.086	1.33x10^{-02}	-0.111	5.06x10^{-06}	1.56x10^{-03}
RIF1	-0.143	8.11x10^{-05}	-0.103	7.88x10^{-03}	-0.117	5.20x10^{-06}	1.56x10^{-03}
SETX	-0.140	2.22x10^{-04}	-0.095	1.03x10^{-02}	-0.117	5.19x10^{-06}	1.56x10^{-03}
RLIM	-0.141	8.03x10^{-04}	-0.128	3.45x10^{-03}	-0.134	5.58x10^{-06}	1.62x10^{-03}
TCAIM	-0.154	1.89x10^{-04}	-0.108	1.17x10^{-02}	-0.130	5.54x10^{-06}	1.62x10^{-03}
RP11-43D4.2	0.300	4.10x10^{-04}	0.245	7.45x10^{-03}	0.280	5.81x10^{-06}	1.64x10^{-03}
ZMYM1	-0.144	2.21x10^{-03}	-0.169	1.40x10^{-03}	-0.156	5.78x10^{-06}	1.64x10^{-03}
PTPRC	-0.154	2.37x10^{-04}	-0.112	8.20x10^{-03}	-0.130	5.96x10^{-06}	1.65x10^{-03}
AC074092.1	0.260	2.29x10^{-03}	0.268	1.77x10^{-03}	0.273	6.28x10^{-06}	1.67x10^{-03}
CEP120	-0.134	1.15x10^{-03}	-0.129	9.59x10^{-04}	-0.126	6.30x10^{-06}	1.67x10^{-03}
RP11-1086F11.1	0.245	1.84x10^{-04}	0.160	1.92x10^{-02}	0.212	6.32x10^{-06}	1.67x10^{-03}
ZNF763	-0.225	4.15x10^{-03}	-0.264	1.29x10^{-03}	-0.252	6.44x10^{-06}	1.67x10^{-03}
ZC3H11A	-0.142	3.38x10^{-05}	-0.068	4.12x10^{-02}	-0.104	6.82x10^{-06}	1.73x10^{-03}
PRKD3	-0.162	1.04x10^{-03}	-0.162	1.94x10^{-03}	-0.157	7.29x10^{-06}	1.75x10^{-03}
SLC16A10	-0.333	2.64x10^{-03}	-0.383	1.14x10^{-03}	-0.358	7.28x10^{-06}	1.75x10^{-03}
ATF6	-0.157	1.69x10^{-03}	-0.186	7.20x10^{-04}	-0.162	8.01x10^{-06}	1.90x10^{-03}
ITCH	-0.143	1.47x10^{-04}	-0.092	2.07x10^{-02}	-0.118	8.30x10^{-06}	1.94x10^{-03}
PTGR1	0.155	2.56x10^{-03}	0.188	1.13x10^{-03}	0.168	8.80x10^{-06}	2.03x10^{-03}
KIAA1551	-0.209	2.81x10^{-05}	-0.114	2.28x10^{-02}	-0.154	8.96x10^{-06}	2.04x10^{-03}
ATG12	-0.125	9.35x10^{-04}	-0.114	4.28x10^{-03}	-0.118	9.09x10^{-06}	2.05x10^{-03}
CTC-559E9.5	-0.199	9.20x10^{-04}	-0.182	4.81x10^{-03}	-0.190	9.72x10^{-06}	2.16x10^{-03}
TMTC3	-0.217	3.69x10^{-05}	-0.129	1.51x10^{-02}	-0.164	9.86x10^{-06}	2.17x10^{-03}
ZNF252P	-0.136	7.08x10^{-03}	-0.169	3.60x10^{-04}	-0.150	1.03x10^{-05}	2.23x10^{-03}
RP11-254B13.3	0.296	1.85x10^{-04}	0.249	1.44x10^{-02}	0.282	1.08x10^{-05}	2.28x10^{-03}
RP11-2J18.1	0.240	4.96x10^{-03}	0.356	2.17x10^{-04}	0.276	1.06x10^{-05}	2.28x10^{-03}
CTD-2303B20.1	0.293	4.05x10^{-03}	0.386	9.54x10^{-04}	0.333	1.13x10^{-05}	2.36x10^{-03}
KAT8	-0.127	1.27x10^{-03}	-0.123	5.78x10^{-03}	-0.128	1.14x10^{-05}	2.37x10^{-03}
AMD1	-0.151	2.59x10^{-03}	-0.186	4.74x10^{-04}	-0.159	1.16x10^{-05}	2.37x10^{-03}
BACE1	0.307	8.53x10^{-05}	0.194	3.08x10^{-02}	0.254	1.31x10^{-05}	2.63x10^{-03}
EIF4A2	-0.168	1.75x10^{-04}	-0.107	2.33x10^{-02}	-0.140	1.35x10^{-05}	2.68x10^{-03}
NAA35	-0.112	1.82x10^{-03}	-0.090	4.01x10^{-03}	-0.100	1.37x10^{-05}	2.68x10^{-03}
HELQ	-0.115	3.21x10^{-03}	-0.106	4.26x10^{-03}	-0.114	1.54x10^{-05}	2.87x10^{-03}
RP11-140I24.1	0.289	2.26x10^{-04}	0.227	1.25x10^{-02}	0.252	1.51x10^{-05}	2.87x10^{-03}
RP11-255H23.2	-0.354	8.93x10^{-04}	-0.317	5.61x10^{-03}	-0.331	1.49x10^{-05}	2.87x10^{-03}
ZNF33A	-0.121	3.41x10^{-03}	-0.132	2.03x10^{-03}	-0.126	1.52x10^{-05}	2.87x10^{-03}
RP11-135N5.3	0.189	3.01x10^{-03}	0.185	9.46x10^{-03}	0.200	1.60x10^{-05}	2.93x10^{-03}

SIKE1	-0.138	7.06x10^{-04}	-0.106	3.14x10^{-03}	-0.116	1.61x10^{-05}	2.93x10^{-03}
MAP3K7CL	-0.330	2.70x10^{-02}	-0.615	2.98x10^{-04}	-0.479	1.72x10^{-05}	3.04x10^{-03}
STAG2	-0.124	1.40x10^{-03}	-0.104	8.05x10^{-03}	-0.114	1.72x10^{-05}	3.04x10^{-03}
NR1D2	-0.142	6.69x10^{-03}	-0.145	1.99x10^{-03}	-0.147	1.80x10^{-05}	3.15x10^{-03}
PWWP2A	-0.117	8.80x10^{-04}	-0.081	1.52x10^{-02}	-0.101	1.82x10^{-05}	3.15x10^{-03}
EHBP1L1	-0.199	8.44x10^{-04}	-0.143	1.93x10^{-02}	-0.180	1.87x10^{-05}	3.21x10^{-03}
RP11-538D16.2	0.164	6.49x10^{-04}	0.099	1.57x10^{-02}	0.135	1.94x10^{-05}	3.29x10^{-03}
C12orf45	-0.160	7.02x10^{-03}	-0.167	5.87x10^{-03}	-0.180	1.99x10^{-05}	3.32x10^{-03}
FRRS1L	0.182	1.08x10^{-03}	0.151	9.28x10^{-03}	0.168	2.05x10^{-05}	3.32x10^{-03}
HOMER1	-0.272	3.46x10^{-03}	-0.256	4.02x10^{-03}	-0.274	2.04x10^{-05}	3.32x10^{-03}
KDM1A	-0.110	1.55x10^{-03}	-0.090	4.62x10^{-03}	-0.097	2.03x10^{-05}	3.32x10^{-03}
RP11-259P6.2	0.367	2.71x10^{-03}	0.367	2.88x10^{-03}	0.367	2.06x10^{-05}	3.32x10^{-03}
RP11-24J23.2	0.145	2.84x10^{-03}	0.150	1.46x10^{-03}	0.141	2.09x10^{-05}	3.33x10^{-03}
UHRF2	-0.164	2.16x10^{-04}	-0.108	2.04x10^{-02}	-0.133	2.21x10^{-05}	3.50x10^{-03}
ACAP2	-0.101	2.57x10^{-03}	-0.106	3.11x10^{-03}	-0.100	2.24x10^{-05}	3.50x10^{-03}
THAP2	-0.207	1.15x10^{-03}	-0.186	1.52x10^{-03}	-0.181	2.25x10^{-05}	3.50x10^{-03}
HIF1A	-0.209	1.50x10^{-04}	-0.162	1.28x10^{-02}	-0.175	2.28x10^{-05}	3.51x10^{-03}
C12orf29	-0.191	1.30x10^{-02}	-0.330	8.14x10^{-05}	-0.247	2.35x10^{-05}	3.56x10^{-03}
RP11-678G14.2	-0.362	5.11x10^{-03}	-0.437	2.29x10^{-03}	-0.404	2.35x10^{-05}	3.56x10^{-03}
ATM	-0.142	9.30x10^{-04}	-0.096	2.18x10^{-02}	-0.123	2.44x10^{-05}	3.66x10^{-03}
DEF6	-0.129	7.34x10^{-04}	-0.085	2.95x10^{-02}	-0.113	2.49x10^{-05}	3.68x10^{-03}
RP11-53B2.2	0.240	1.38x10^{-04}	0.179	1.39x10^{-02}	0.201	2.51x10^{-05}	3.68x10^{-03}
RP11-182I10.2	0.242	6.39x10^{-03}	0.264	2.72x10^{-03}	0.260	2.55x10^{-05}	3.68x10^{-03}
ZNF680	-0.106	1.52x10^{-02}	-0.151	8.49x10^{-04}	-0.128	2.54x10^{-05}	3.68x10^{-03}
ZNF627	-0.125	1.70x10^{-03}	-0.101	1.17x10^{-02}	-0.116	2.59x10^{-05}	3.70x10^{-03}
ZNF876P	-0.398	4.95x10^{-03}	-0.480	2.17x10^{-03}	-0.439	2.63x10^{-05}	3.73x10^{-03}
ZNF283	-0.133	3.55x10^{-03}	-0.131	2.64x10^{-03}	-0.129	2.66x10^{-05}	3.74x10^{-03}
CTD-2579N5.1	-1.227	1.72x10^{-03}	-1.221	4.56x10^{-03}	-1.221	2.93x10^{-05}	4.02x10^{-03}
KLHL28	-0.110	3.80x10^{-03}	-0.103	5.48x10^{-03}	-0.107	3.09x10^{-05}	4.20x10^{-03}
RIC8B	-0.169	2.36x10^{-04}	-0.103	4.02x10^{-02}	-0.139	3.15x10^{-05}	4.20x10^{-03}
RP11-349A22.5	-0.110	8.64x10^{-04}	-0.087	1.26x10^{-02}	-0.097	3.15x10^{-05}	4.20x10^{-03}
HAND2-AS1	0.177	9.84x10^{-04}	0.131	8.57x10^{-03}	0.150	3.31x10^{-05}	4.34x10^{-03}
ITGA6	-0.199	1.79x10^{-03}	-0.213	4.58x10^{-03}	-0.199	3.32x10^{-05}	4.34x10^{-03}
ZNF160	-0.084	4.50x10^{-02}	-0.137	1.86x10^{-04}	-0.113	3.28x10^{-05}	4.34x10^{-03}
XRCC5	-0.133	2.75x10^{-04}	-0.082	2.42x10^{-02}	-0.104	3.38x10^{-05}	4.38x10^{-03}
DHX15	-0.131	3.79x10^{-04}	-0.083	2.05x10^{-02}	-0.103	3.49x10^{-05}	4.43x10^{-03}
PMS1	-0.179	5.85x10^{-05}	-0.100	4.18x10^{-02}	-0.135	3.49x10^{-05}	4.43x10^{-03}
SRSF10	-0.107	1.55x10^{-03}	-0.077	5.95x10^{-03}	-0.089	3.86x10^{-05}	4.77x10^{-03}
HSP90AB4P	0.342	4.62x10^{-05}	0.195	3.92x10^{-02}	0.254	4.00x10^{-05}	4.77x10^{-03}
JKAMP	-0.117	3.62x10^{-03}	-0.117	1.78x10^{-03}	-0.111	3.99x10^{-05}	4.77x10^{-03}
TWF1	-0.142	3.98x10^{-04}	-0.102	1.77x10^{-02}	-0.117	3.96x10^{-05}	4.77x10^{-03}
C2orf49	-0.095	1.08x10^{-02}	-0.119	1.34x10^{-03}	-0.106	4.07x10^{-05}	4.78x10^{-03}
KLF10	0.290	1.64x10^{-03}	0.281	6.08x10^{-03}	0.274	4.11x10^{-05}	4.78x10^{-03}
AC093642.3	0.185	9.06x10^{-04}	0.151	1.00x10^{-02}	0.163	4.25x10^{-05}	4.78x10^{-03}
IFT46	-0.118	2.07x10^{-03}	-0.097	1.45x10^{-02}	-0.109	4.20x10^{-05}	4.78x10^{-03}
RP11-480C16.1	0.227	1.47x10^{-02}	0.271	4.09x10^{-03}	0.268	4.23x10^{-05}	4.78x10^{-03}

SF3B1	-0.156	4.15x10^{-04}	-0.087	3.71x10^{-02}	-0.122	4.17x10^{-05}	4.78x10^{-03}
THAP5	-0.130	7.89x10^{-03}	-0.139	1.41x10^{-03}	-0.132	4.27x10^{-05}	4.78x10^{-03}
TMED4	-0.105	1.41x10^{-03}	-0.080	1.14x10^{-02}	-0.090	4.24x10^{-05}	4.78x10^{-03}
AC096921.2	0.209	4.32x10^{-03}	0.217	6.85x10^{-03}	0.217	4.30x10^{-05}	4.78x10^{-03}
CHPF	0.399	3.59x10^{-03}	0.358	8.21x10^{-03}	0.385	4.39x10^{-05}	4.85x10^{-03}
PANK3	-0.203	2.63x10^{-05}	-0.100	4.78x10^{-02}	-0.141	4.54x10^{-05}	4.93x10^{-03}
SNW1	-0.094	1.97x10^{-03}	-0.085	1.57x10^{-02}	-0.091	4.53x10^{-05}	4.93x10^{-03}
TNFSF4	-0.327	5.38x10^{-03}	-0.382	4.67x10^{-03}	-0.360	4.52x10^{-05}	4.93x10^{-03}
RP3-442L6.4	0.235	1.71x10^{-03}	0.179	1.27x10^{-02}	0.208	4.77x10^{-05}	5.11x10^{-03}
CREBRF	-0.142	8.80x10^{-04}	-0.109	1.76x10^{-02}	-0.123	5.05x10^{-05}	5.35x10^{-03}
PPP2R2D	-0.100	2.26x10^{-03}	-0.101	4.47x10^{-03}	-0.096	5.04x10^{-05}	5.35x10^{-03}
CHUK	-0.129	3.63x10^{-04}	-0.079	4.70x10^{-02}	-0.105	5.33x10^{-05}	5.52x10^{-03}
RYK	-0.117	1.31x10^{-03}	-0.088	3.07x10^{-02}	-0.107	5.33x10^{-05}	5.52x10^{-03}
GPRASP1	-0.243	2.80x10^{-03}	-0.198	1.56x10^{-02}	-0.226	5.36x10^{-05}	5.52x10^{-03}
ZNF790	-0.166	1.75x10^{-03}	-0.130	2.30x10^{-02}	-0.155	5.39x10^{-05}	5.52x10^{-03}
RP11-43D4.3	0.215	3.28x10^{-03}	0.263	6.00x10^{-04}	0.216	5.45x10^{-05}	5.54x10^{-03}
SESN1	-0.205	5.87x10^{-04}	-0.205	1.05x10^{-02}	-0.196	5.51x10^{-05}	5.58x10^{-03}
OPA1	-0.323	7.13x10^{-04}	-0.299	3.19x10^{-03}	-0.282	5.67x10^{-05}	5.64x10^{-03}
XIAP	-0.147	1.12x10^{-03}	-0.115	3.07x10^{-02}	-0.137	5.67x10^{-05}	5.64x10^{-03}
ARHGAP5	-0.187	1.67x10^{-03}	-0.176	4.46x10^{-03}	-0.169	5.88x10^{-05}	5.67x10^{-03}
ARRDC3	-0.219	2.49x10^{-03}	-0.192	9.89x10^{-03}	-0.205	5.89x10^{-05}	5.67x10^{-03}
CLTC	0.141	2.18x10^{-03}	0.126	7.59x10^{-03}	0.131	5.91x10^{-05}	5.67x10^{-03}
GOLGA2	-0.109	1.48x10^{-02}	-0.141	2.75x10^{-03}	-0.128	5.88x10^{-05}	5.67x10^{-03}
RP11-107E5.3	0.161	2.93x10^{-02}	0.275	7.84x10^{-04}	0.217	5.95x10^{-05}	5.67x10^{-03}
RP11-264L1.2	0.148	2.76x10^{-02}	0.262	5.66x10^{-04}	0.199	5.74x10^{-05}	5.67x10^{-03}
SLC15A3	-0.219	7.92x10^{-04}	-0.178	1.56x10^{-02}	-0.198	5.93x10^{-05}	5.67x10^{-03}
ATP5S	-0.193	2.14x10^{-02}	-0.345	5.92x10^{-04}	-0.262	6.12x10^{-05}	5.73x10^{-03}
CCND3	-0.190	2.27x10^{-03}	-0.215	4.83x10^{-03}	-0.190	6.23x10^{-05}	5.73x10^{-03}
CTNNB1	-0.114	1.88x10^{-03}	-0.081	2.58x10^{-02}	-0.101	6.21x10^{-05}	5.73x10^{-03}
HACD4	-0.185	1.47x10^{-03}	-0.150	8.10x10^{-03}	-0.159	6.07x10^{-05}	5.73x10^{-03}
MEFV	-0.213	9.71x10^{-04}	-0.199	9.28x10^{-03}	-0.199	6.27x10^{-05}	5.73x10^{-03}
NEK7	-0.115	5.44x10^{-03}	-0.122	4.35x10^{-03}	-0.115	6.20x10^{-05}	5.73x10^{-03}
TUBE1	-0.148	2.38x10^{-03}	-0.124	9.38x10^{-03}	-0.132	6.09x10^{-05}	5.73x10^{-03}
ZNF28	-0.140	8.64x10^{-03}	-0.162	3.11x10^{-03}	-0.150	6.29x10^{-05}	5.73x10^{-03}
ZNF506	-0.167	4.66x10^{-03}	-0.156	2.15x10^{-03}	-0.152	6.16x10^{-05}	5.73x10^{-03}
OR6Y1	0.176	3.18x10^{-03}	0.131	1.14x10^{-02}	0.156	6.37x10^{-05}	5.73x10^{-03}
SCYL2	-0.092	7.24x10^{-03}	-0.125	1.87x10^{-03}	-0.102	6.37x10^{-05}	5.73x10^{-03}
TRIM65	-0.179	7.28x10^{-04}	-0.124	3.06x10^{-02}	-0.153	6.41x10^{-05}	5.73x10^{-03}
ZNF638	-0.102	3.59x10^{-03}	-0.114	2.66x10^{-03}	-0.100	6.46x10^{-05}	5.73x10^{-03}
ANKRD34A	-0.331	3.07x10^{-03}	-0.315	6.03x10^{-03}	-0.316	6.76x10^{-05}	5.79x10^{-03}
CSNK2A2	0.181	2.69x10^{-03}	0.175	6.52x10^{-03}	0.173	6.72x10^{-05}	5.79x10^{-03}
GPBP1	-0.125	1.17x10^{-03}	-0.109	1.46x10^{-02}	-0.113	6.77x10^{-05}	5.79x10^{-03}
OXNAD1	-0.153	9.99x10^{-03}	-0.196	2.61x10^{-03}	-0.174	6.65x10^{-05}	5.79x10^{-03}
SLC15A4	-0.156	2.92x10^{-03}	-0.117	2.25x10^{-02}	-0.144	6.78x10^{-05}	5.79x10^{-03}
ZNF845	-0.111	1.58x10^{-02}	-0.132	1.37x10^{-03}	-0.120	6.72x10^{-05}	5.79x10^{-03}
SENP7	-0.104	8.78x10^{-03}	-0.141	1.53x10^{-03}	-0.116	6.92x10^{-05}	5.86x10^{-03}

ALPK2	0.378	7.78x10^{-03}	0.426	2.46x10^{-03}	0.396	7.08x10^{-05}	5.92x10^{-03}
MBTD1	-0.091	1.11x10^{-02}	-0.101	1.76x10^{-03}	-0.092	7.13x10^{-05}	5.92x10^{-03}
SLC13A4	0.331	3.04x10^{-03}	0.333	1.58x10^{-03}	0.306	7.10x10^{-05}	5.92x10^{-03}
AKT3	-0.200	5.88x10^{-04}	-0.145	4.09x10^{-02}	-0.177	7.43x10^{-05}	6.04x10^{-03}
GOLGA4	-0.124	1.05x10^{-03}	-0.088	1.22x10^{-02}	-0.100	7.42x10^{-05}	6.04x10^{-03}
RP11-145P16.2	0.135	4.92x10^{-03}	0.153	3.56x10^{-03}	0.139	7.36x10^{-05}	6.04x10^{-03}
SH3TC2	-0.270	4.50x10^{-02}	-0.567	1.36x10^{-04}	-0.395	7.46x10^{-05}	6.04x10^{-03}
TOPORS	-0.148	6.65x10^{-03}	-0.161	3.70x10^{-03}	-0.151	7.47x10^{-05}	6.04x10^{-03}
ZNF841	-0.160	7.64x10^{-04}	-0.115	2.71x10^{-02}	-0.137	7.36x10^{-05}	6.04x10^{-03}
RP11-14N9.2	0.164	1.81x10^{-03}	0.142	1.47x10^{-02}	0.150	7.54x10^{-05}	6.04x10^{-03}
OR1A1	0.178	1.68x10^{-03}	0.131	8.25x10^{-03}	0.148	7.83x10^{-05}	6.24x10^{-03}
ZBTB14	-0.116	8.22x10^{-03}	-0.133	2.61x10^{-03}	-0.119	7.88x10^{-05}	6.26x10^{-03}
AC013402.2	0.236	3.38x10^{-03}	0.187	1.95x10^{-02}	0.219	8.06x10^{-05}	6.35x10^{-03}
LA16c-60D12.1	0.173	1.40x10^{-03}	0.115	1.46x10^{-02}	0.138	8.10x10^{-05}	6.35x10^{-03}
ZNF417	-0.113	1.04x10^{-02}	-0.114	9.11x10^{-03}	-0.120	8.09x10^{-05}	6.35x10^{-03}
MIA3	-0.128	1.54x10^{-03}	-0.101	1.19x10^{-02}	-0.109	8.24x10^{-05}	6.37x10^{-03}
RANBP2	-0.136	1.62x10^{-03}	-0.100	1.65x10^{-02}	-0.115	8.22x10^{-05}	6.37x10^{-03}
ADAM32	0.156	1.49x10^{-03}	0.083	2.87x10^{-02}	0.120	8.44x10^{-05}	6.45x10^{-03}
ANXA13	0.202	1.02x10^{-02}	0.194	3.00x10^{-03}	0.200	8.40x10^{-05}	6.45x10^{-03}
KATNBL1	-0.213	9.76x10^{-04}	-0.216	8.53x10^{-03}	-0.203	8.44x10^{-05}	6.45x10^{-03}
TMEM154	-0.196	1.67x10^{-03}	-0.191	3.68x10^{-03}	-0.177	8.53x10^{-05}	6.48x10^{-03}
GLT8D1	-0.073	2.26x10^{-02}	-0.096	4.27x10^{-03}	-0.089	8.62x10^{-05}	6.52x10^{-03}
TXNDC11	0.199	2.98x10^{-03}	0.130	3.45x10^{-02}	0.177	8.69x10^{-05}	6.55x10^{-03}
CTB-47B11.3	0.244	5.98x10^{-03}	0.278	6.72x10^{-03}	0.258	8.78x10^{-05}	6.55x10^{-03}
OSBPL2	-0.116	7.79x10^{-03}	-0.124	1.04x10^{-02}	-0.124	8.80x10^{-05}	6.55x10^{-03}
SCARNA3	0.279	1.38x10^{-03}	0.199	3.12x10^{-02}	0.245	8.87x10^{-05}	6.58x10^{-03}
BBX	-0.128	8.13x10^{-04}	-0.074	4.49x10^{-02}	-0.100	8.96x10^{-05}	6.59x10^{-03}
SMAD5	-0.224	7.74x10^{-04}	-0.183	1.44x10^{-02}	-0.193	8.97x10^{-05}	6.59x10^{-03}
AC018890.6	0.334	2.34x10^{-04}	0.199	3.45x10^{-02}	0.251	9.05x10^{-05}	6.60x10^{-03}
FNTA	-0.093	2.03x10^{-03}	-0.058	3.09x10^{-02}	-0.076	9.09x10^{-05}	6.60x10^{-03}
ZBTB10	-0.171	5.85x10^{-03}	-0.177	6.74x10^{-03}	-0.173	9.08x10^{-05}	6.60x10^{-03}
MED13L	-0.131	3.33x10^{-02}	-0.230	2.23x10^{-03}	-0.188	9.14x10^{-05}	6.61x10^{-03}
APBB1	-0.181	6.49x10^{-03}	-0.184	1.09x10^{-02}	-0.186	9.29x10^{-05}	6.62x10^{-03}
RP11-452H21.2	0.383	2.64x10^{-03}	0.299	2.32x10^{-02}	0.352	9.36x10^{-05}	6.62x10^{-03}
STAU2	-0.111	1.52x10^{-03}	-0.084	2.26x10^{-02}	-0.096	9.23x10^{-05}	6.62x10^{-03}
TRIP10	-0.204	2.48x10^{-02}	-0.302	2.36x10^{-03}	-0.257	9.30x10^{-05}	6.62x10^{-03}
TTF1	-0.097	7.86x10^{-03}	-0.094	6.51x10^{-03}	-0.095	9.37x10^{-05}	6.62x10^{-03}
UBE2D3	-0.111	1.02x10^{-02}	-0.139	3.82x10^{-03}	-0.123	9.29x10^{-05}	6.62x10^{-03}
DOCK11	-0.144	7.51x10^{-04}	-0.089	4.65x10^{-02}	-0.117	9.57x10^{-05}	6.74x10^{-03}
GNAI3	-0.104	6.91x10^{-03}	-0.101	9.78x10^{-03}	-0.104	9.85x10^{-05}	6.80x10^{-03}
NPIPB4	0.267	1.54x10^{-03}	0.216	7.04x10^{-03}	0.222	9.83x10^{-05}	6.80x10^{-03}
POTEI	0.304	1.38x10^{-03}	0.179	3.69x10^{-02}	0.246	9.83x10^{-05}	6.80x10^{-03}
RP11-438E5.1	-0.251	6.10x10^{-03}	-0.236	1.33x10^{-02}	-0.250	9.92x10^{-05}	6.80x10^{-03}
ZNF468	-0.129	3.83x10^{-02}	-0.186	1.53x10^{-03}	-0.165	9.91x10^{-05}	6.80x10^{-03}
AF131215.4	0.272	1.13x10^{-02}	0.345	4.64x10^{-03}	0.303	1.03x10^{-04}	6.80x10^{-03}
C3orf17	-0.103	3.42x10^{-03}	-0.083	2.67x10^{-02}	-0.097	1.02x10^{-04}	6.80x10^{-03}

CTD-2006C1.2	-0.118	1.39x10^{-02}	-0.163	2.55x10^{-03}	-0.137	1.03x10^{-04}	6.80x10^{-03}
DNPH1	0.209	2.10x10^{-03}	0.164	2.12x10^{-02}	0.188	1.01x10^{-04}	6.80x10^{-03}
GPR15	0.853	6.45x10^{-03}	0.877	1.31x10^{-02}	0.904	1.05x10^{-04}	6.80x10^{-03}
HNRNPK	-0.120	1.95x10^{-03}	-0.091	3.19x10^{-02}	-0.107	1.04x10^{-04}	6.80x10^{-03}
LEMD3	-0.105	1.98x10^{-03}	-0.077	3.03x10^{-02}	-0.092	1.04x10^{-04}	6.80x10^{-03}
MFSD14A	-0.124	3.21x10^{-03}	-0.113	1.37x10^{-02}	-0.117	1.03x10^{-04}	6.80x10^{-03}
RCHY1	-0.145	4.43x10^{-03}	-0.094	2.24x10^{-02}	-0.125	9.96x10^{-05}	6.80x10^{-03}
TMEM260	-0.153	2.36x10^{-04}	-0.093	4.29x10^{-02}	-0.118	1.01x10^{-04}	6.80x10^{-03}
ZNF304	-0.152	9.29x10^{-03}	-0.157	4.75x10^{-03}	-0.153	1.05x10^{-04}	6.80x10^{-03}
DDB1	-0.133	1.63x10^{-03}	-0.116	1.46x10^{-02}	-0.121	1.07x10^{-04}	6.86x10^{-03}
EPC2	-0.103	6.26x10^{-03}	-0.095	8.31x10^{-03}	-0.098	1.07x10^{-04}	6.86x10^{-03}
TPR	-0.092	1.26x10^{-02}	-0.097	4.22x10^{-03}	-0.094	1.10x10^{-04}	6.93x10^{-03}
ZNF426	-0.131	4.89x10^{-03}	-0.098	1.76x10^{-02}	-0.118	1.10x10^{-04}	6.93x10^{-03}
CTA-941F9.10	0.150	2.02x10^{-03}	0.127	1.95x10^{-02}	0.137	1.11x10^{-04}	7.00x10^{-03}
NPIPB5	0.223	3.45x10^{-03}	0.199	9.64x10^{-03}	0.205	1.14x10^{-04}	7.03x10^{-03}
RP11-64P12.3	0.265	8.81x10^{-03}	0.311	1.05x10^{-03}	0.263	1.14x10^{-04}	7.03x10^{-03}
RP11-689D3.4	0.258	3.59x10^{-03}	0.197	2.69x10^{-02}	0.238	1.14x10^{-04}	7.03x10^{-03}
TJP1	0.171	2.57x10^{-02}	0.247	1.07x10^{-03}	0.202	1.13x10^{-04}	7.03x10^{-03}
USO1	-0.102	3.96x10^{-03}	-0.080	1.99x10^{-02}	-0.092	1.13x10^{-04}	7.03x10^{-03}
ZNF132	-0.318	5.98x10^{-04}	-0.140	4.43x10^{-02}	-0.222	1.13x10^{-04}	7.03x10^{-03}
RP11-701H24.6	-0.198	9.25x10^{-03}	-0.168	1.31x10^{-02}	-0.192	1.15x10^{-04}	7.03x10^{-03}
ZBTB8B	0.142	1.65x10^{-02}	0.179	2.17x10^{-03}	0.156	1.15x10^{-04}	7.03x10^{-03}
RP11-510H23.1	0.162	8.63x10^{-03}	0.144	1.44x10^{-02}	0.164	1.18x10^{-04}	7.18x10^{-03}
SLC25A16	-0.142	2.99x10^{-03}	-0.099	3.39x10^{-02}	-0.126	1.19x10^{-04}	7.20x10^{-03}
FBXL4	-0.095	1.97x10^{-02}	-0.144	1.33x10^{-03}	-0.115	1.19x10^{-04}	7.20x10^{-03}
ZC3H7A	0.148	1.62x10^{-04}	0.099	2.67x10^{-02}	0.113	1.20x10^{-04}	7.23x10^{-03}
MFAP3L	-0.231	2.90x10^{-02}	-0.412	1.82x10^{-03}	-0.321	1.25x10^{-04}	7.36x10^{-03}
MPV17L	0.200	6.86x10^{-03}	0.206	8.04x10^{-03}	0.202	1.25x10^{-04}	7.36x10^{-03}
TCP1	-0.106	6.25x10^{-03}	-0.090	1.36x10^{-02}	-0.099	1.26x10^{-04}	7.36x10^{-03}
ZNF485	-0.210	1.32x10^{-03}	-0.165	8.85x10^{-03}	-0.172	1.30x10^{-04}	7.53x10^{-03}
TMEM65	-0.083	1.22x10^{-02}	-0.098	3.73x10^{-03}	-0.089	1.32x10^{-04}	7.57x10^{-03}
GOLGA5	-0.072	1.89x10^{-02}	-0.080	1.79x10^{-02}	-0.084	1.34x10^{-04}	7.60x10^{-03}
TNPO1	-0.119	3.47x10^{-03}	-0.106	1.44x10^{-02}	-0.109	1.34x10^{-04}	7.60x10^{-03}
ZDHHC6	-0.111	1.31x10^{-03}	-0.066	4.78x10^{-02}	-0.090	1.33x10^{-04}	7.60x10^{-03}
PARP8	-0.133	8.13x10^{-04}	-0.090	4.20x10^{-02}	-0.110	1.35x10^{-04}	7.63x10^{-03}
LRCH1	0.126	7.86x10^{-03}	0.154	2.72x10^{-03}	0.131	1.36x10^{-04}	7.64x10^{-03}
TANK	-0.126	2.18x10^{-03}	-0.127	5.48x10^{-03}	-0.117	1.37x10^{-04}	7.64x10^{-03}
GPR37L1	0.233	4.79x10^{-03}	0.181	4.17x10^{-02}	0.223	1.38x10^{-04}	7.71x10^{-03}
RBPJ	-0.118	5.23x10^{-03}	-0.123	5.93x10^{-03}	-0.114	1.39x10^{-04}	7.72x10^{-03}
RP4-591N18.2	0.275	2.25x10^{-03}	0.191	2.74x10^{-02}	0.233	1.40x10^{-04}	7.72x10^{-03}
DEC1	0.159	5.20x10^{-03}	0.143	2.07x10^{-02}	0.156	1.42x10^{-04}	7.78x10^{-03}
SHOC2	-0.103	4.71x10^{-03}	-0.099	1.80x10^{-02}	-0.103	1.41x10^{-04}	7.78x10^{-03}
GATA3	0.401	7.96x10^{-04}	0.224	3.86x10^{-02}	0.299	1.44x10^{-04}	7.83x10^{-03}
TIGD1L	0.136	2.38x10^{-03}	0.085	4.34x10^{-02}	0.114	1.45x10^{-04}	7.84x10^{-03}
ZNF548	-0.155	4.62x10^{-03}	-0.128	1.50x10^{-02}	-0.141	1.47x10^{-04}	7.91x10^{-03}
CTD-2246P4.1	0.168	1.61x10^{-02}	0.187	2.37x10^{-03}	0.173	1.47x10^{-04}	7.91x10^{-03}

ATP11B	-0.125	1.42x10^{-03}	-0.087	4.93x10^{-02}	-0.107	1.48x10^{-04}	7.93x10^{-03}
POLR2B	-0.112	2.00x10^{-03}	-0.069	4.57x10^{-02}	-0.092	1.48x10^{-04}	7.93x10^{-03}
C4BPB	0.193	7.06x10^{-03}	0.210	1.04x10^{-02}	0.200	1.50x10^{-04}	7.97x10^{-03}
PANK4	-0.124	8.45x10^{-03}	-0.113	2.06x10^{-02}	-0.124	1.53x10^{-04}	8.06x10^{-03}
CCNG1	-0.106	1.48x10^{-02}	-0.139	1.87x10^{-03}	-0.115	1.55x10^{-04}	8.09x10^{-03}
COG8	-0.103	9.78x10^{-03}	-0.119	8.31x10^{-03}	-0.111	1.55x10^{-04}	8.09x10^{-03}
RP4-751H13.6	-0.227	8.85x10^{-03}	-0.205	3.48x10^{-02}	-0.241	1.58x10^{-04}	8.18x10^{-03}
VSIR	-0.130	1.65x10^{-02}	-0.184	4.92x10^{-03}	-0.157	1.58x10^{-04}	8.19x10^{-03}
NUP107	-0.128	1.17x10^{-02}	-0.160	2.62x10^{-03}	-0.138	1.59x10^{-04}	8.22x10^{-03}
MBTPS2	0.123	3.29x10^{-03}	0.115	1.32x10^{-02}	0.117	1.61x10^{-04}	8.23x10^{-03}
RP11-486O12.2	0.143	8.48x10^{-03}	0.139	8.71x10^{-03}	0.139	1.60x10^{-04}	8.23x10^{-03}
MTERF1	-0.104	6.30x10^{-03}	-0.090	2.74x10^{-02}	-0.102	1.63x10^{-04}	8.31x10^{-03}
PPP2R5E	0.139	1.42x10^{-02}	0.175	2.97x10^{-03}	0.151	1.66x10^{-04}	8.47x10^{-03}
CCDC175	-0.483	3.71x10^{-03}	-0.347	1.76x10^{-02}	-0.408	1.67x10^{-04}	8.50x10^{-03}
ZNF587B	-0.097	1.16x10^{-02}	-0.116	7.09x10^{-03}	-0.106	1.68x10^{-04}	8.52x10^{-03}
NACC1	0.241	2.49x10^{-02}	0.320	6.08x10^{-04}	0.262	1.69x10^{-04}	8.55x10^{-03}
HLX	-0.215	1.30x10^{-02}	-0.301	2.59x10^{-03}	-0.242	1.73x10^{-04}	8.69x10^{-03}
ABI1	-0.101	3.73x10^{-03}	-0.093	1.50x10^{-02}	-0.094	1.75x10^{-04}	8.71x10^{-03}
INPP5A	-0.170	6.05x10^{-04}	-0.146	2.25x10^{-02}	-0.150	1.75x10^{-04}	8.71x10^{-03}
MIA2	-0.128	7.46x10^{-03}	-0.134	1.73x10^{-02}	-0.134	1.74x10^{-04}	8.71x10^{-03}
PEX1	-0.121	1.79x10^{-03}	-0.091	2.85x10^{-02}	-0.105	1.75x10^{-04}	8.71x10^{-03}
CEP85L	-0.111	4.14x10^{-03}	-0.086	2.96x10^{-02}	-0.101	1.76x10^{-04}	8.73x10^{-03}
TRMT11	-0.166	1.83x10^{-03}	-0.107	2.91x10^{-02}	-0.133	1.77x10^{-04}	8.75x10^{-03}
RP11-746L20.1	0.209	6.55x10^{-03}	0.216	5.03x10^{-03}	0.203	1.79x10^{-04}	8.83x10^{-03}
RP11-391L3.4	0.235	7.06x10^{-03}	0.276	3.58x10^{-03}	0.234	1.80x10^{-04}	8.83x10^{-03}
POMT1	-0.148	4.35x10^{-03}	-0.131	2.58x10^{-02}	-0.145	1.81x10^{-04}	8.85x10^{-03}
NUPL2	-0.080	2.69x10^{-02}	-0.105	3.26x10^{-03}	-0.093	1.82x10^{-04}	8.89x10^{-03}
CWF19L2	-0.102	1.17x10^{-02}	-0.095	7.41x10^{-03}	-0.097	1.86x10^{-04}	8.97x10^{-03}
DIP2B	-0.173	1.55x10^{-03}	-0.124	2.88x10^{-02}	-0.143	1.86x10^{-04}	8.97x10^{-03}
MB21D1	-0.173	9.92x10^{-04}	-0.131	2.84x10^{-02}	-0.145	1.85x10^{-04}	8.97x10^{-03}
ZNF235	-0.169	4.38x10^{-04}	-0.115	2.21x10^{-02}	-0.129	1.88x10^{-04}	9.02x10^{-03}
CYP3A5	0.131	4.21x10^{-03}	0.131	1.53x10^{-02}	0.129	1.89x10^{-04}	9.07x10^{-03}
HTN1	0.129	2.06x10^{-02}	0.196	9.00x10^{-04}	0.150	1.93x10^{-04}	9.18x10^{-03}
RP11-436I24.1	0.203	4.46x10^{-02}	0.320	4.87x10^{-03}	0.278	1.94x10^{-04}	9.23x10^{-03}
TTC30A	-0.170	2.22x10^{-02}	-0.233	1.44x10^{-03}	-0.191	1.95x10^{-04}	9.24x10^{-03}
PGS1	-0.174	4.13x10^{-03}	-0.153	2.88x10^{-02}	-0.167	1.97x10^{-04}	9.27x10^{-03}
CTC-242N15.1	0.104	3.58x10^{-02}	0.149	1.52x10^{-03}	0.125	1.99x10^{-04}	9.29x10^{-03}
RP4-778K6.2	0.322	4.58x10^{-03}	0.274	1.07x10^{-02}	0.287	2.01x10^{-04}	9.37x10^{-03}
ZNF329	-0.140	1.50x10^{-02}	-0.150	1.06x10^{-02}	-0.152	2.03x10^{-04}	9.41x10^{-03}
RIT1	-0.105	3.12x10^{-02}	-0.170	1.86x10^{-03}	-0.133	2.08x10^{-04}	9.64x10^{-03}
OR7D4	0.270	6.37x10^{-04}	0.179	2.88x10^{-02}	0.208	2.10x10^{-04}	9.71x10^{-03}
SDCCAG3	-0.176	9.11x10^{-04}	-0.102	3.54x10^{-02}	-0.132	2.19x10^{-04}	1.00x10^{-02}
DENND6A	-0.093	2.32x10^{-02}	-0.121	1.16x10^{-02}	-0.113	2.22x10^{-04}	1.01x10^{-02}
LINC-PINT	0.113	7.77x10^{-03}	0.115	1.01x10^{-02}	0.112	2.23x10^{-04}	1.01x10^{-02}
STAT5A	-0.128	5.37x10^{-03}	-0.109	3.89x10^{-02}	-0.126	2.23x10^{-04}	1.01x10^{-02}
CTD-2024I7.13	0.239	3.18x10^{-03}	0.215	2.34x10^{-02}	0.230	2.26x10^{-04}	1.01x10^{-02}

HAP1	0.376	8.46x10^{-03}	0.368	1.10x10^{-02}	0.368	2.26x10^{-04}	1.01x10^{-02}
ZNF711	-0.299	2.93x10^{-03}	-0.241	3.28x10^{-02}	-0.270	2.27x10^{-04}	1.01x10^{-02}
MIGA1	-0.075	2.16x10^{-02}	-0.080	1.53x10^{-02}	-0.082	2.28x10^{-04}	1.02x10^{-02}
RP3-412A9.17	0.146	4.65x10^{-03}	0.106	3.73x10^{-02}	0.130	2.28x10^{-04}	1.02x10^{-02}
FER	-0.110	1.76x10^{-02}	-0.160	2.74x10^{-03}	-0.128	2.30x10^{-04}	1.02x10^{-02}
BAZ1A	-0.143	6.60x10^{-04}	-0.102	4.06x10^{-02}	-0.115	2.32x10^{-04}	1.02x10^{-02}
CASC4	-0.101	2.37x10^{-02}	-0.126	6.64x10^{-03}	-0.115	2.35x10^{-04}	1.03x10^{-02}
KLHL29	0.255	1.03x10^{-02}	0.282	5.58x10^{-04}	0.234	2.38x10^{-04}	1.03x10^{-02}
PVT1	0.257	5.43x10^{-03}	0.323	3.06x10^{-03}	0.258	2.38x10^{-04}	1.03x10^{-02}
TROVE2	-0.121	5.46x10^{-03}	-0.092	3.18x10^{-02}	-0.110	2.39x10^{-04}	1.03x10^{-02}
ZNF254	-0.130	3.68x10^{-02}	-0.163	4.07x10^{-03}	-0.152	2.40x10^{-04}	1.03x10^{-02}
CRK	-0.122	5.94x10^{-03}	-0.125	9.45x10^{-03}	-0.118	2.44x10^{-04}	1.04x10^{-02}
ETS2	-0.177	8.92x10^{-03}	-0.215	5.95x10^{-03}	-0.186	2.44x10^{-04}	1.04x10^{-02}
MLH3	-0.217	3.40x10^{-02}	-0.336	6.13x10^{-03}	-0.287	2.45x10^{-04}	1.04x10^{-02}
RNF111	0.125	2.48x10^{-03}	0.094	3.99x10^{-02}	0.110	2.45x10^{-04}	1.04x10^{-02}
WAPL	-0.105	6.19x10^{-03}	-0.085	3.00x10^{-02}	-0.097	2.45x10^{-04}	1.04x10^{-02}
XPC	-0.124	1.20x10^{-02}	-0.111	9.64x10^{-03}	-0.117	2.44x10^{-04}	1.04x10^{-02}
ANGEL2	-0.090	3.98x10^{-03}	-0.060	4.06x10^{-02}	-0.076	2.47x10^{-04}	1.04x10^{-02}
LL22NC03-79E2.1	0.212	3.76x10^{-03}	0.195	1.55x10^{-02}	0.195	2.56x10^{-04}	1.07x10^{-02}
RP11-241K18.1	0.468	1.69x10^{-02}	0.452	1.87x10^{-02}	0.489	2.57x10^{-04}	1.07x10^{-02}
SYNJ2BP	-0.132	2.67x10^{-03}	-0.096	3.85x10^{-02}	-0.114	2.59x10^{-04}	1.07x10^{-02}
ENPP6	0.257	1.05x10^{-02}	0.242	1.46x10^{-02}	0.253	2.61x10^{-04}	1.08x10^{-02}
ACAA2	0.167	5.25x10^{-03}	0.121	4.06x10^{-02}	0.150	2.64x10^{-04}	1.08x10^{-02}
IGSF6	-0.189	4.43x10^{-03}	-0.188	9.21x10^{-03}	-0.178	2.64x10^{-04}	1.08x10^{-02}
PARG	-0.117	3.56x10^{-03}	-0.096	2.92x10^{-02}	-0.105	2.64x10^{-04}	1.08x10^{-02}
ZNF322	-0.151	1.58x10^{-03}	-0.114	2.50x10^{-02}	-0.124	2.63x10^{-04}	1.08x10^{-02}
ZNF418	-0.418	1.91x10^{-03}	-0.302	1.10x10^{-02}	-0.327	2.63x10^{-04}	1.08x10^{-02}
ZNF354B	-0.157	4.97x10^{-03}	-0.152	1.07x10^{-02}	-0.146	2.70x10^{-04}	1.10x10^{-02}
CH507-513H4.1	0.292	1.18x10^{-02}	0.258	4.60x10^{-03}	0.280	2.72x10^{-04}	1.10x10^{-02}
SIRT1	-0.096	1.57x10^{-02}	-0.102	6.07x10^{-03}	-0.096	2.73x10^{-04}	1.10x10^{-02}
TMEM68	-0.114	5.69x10^{-03}	-0.098	4.81x10^{-03}	-0.096	2.75x10^{-04}	1.10x10^{-02}
ZNF549	-0.105	1.49x10^{-02}	-0.096	1.80x10^{-02}	-0.105	2.74x10^{-04}	1.10x10^{-02}
ARGFXP2	0.266	9.02x10^{-03}	0.222	1.16x10^{-02}	0.238	2.82x10^{-04}	1.13x10^{-02}
RN7SL517P	0.227	3.34x10^{-03}	0.211	1.06x10^{-02}	0.201	2.82x10^{-04}	1.13x10^{-02}
MEPCE	-0.116	4.17x10^{-02}	-0.181	1.53x10^{-03}	-0.144	2.85x10^{-04}	1.14x10^{-02}
ZNF720	-0.171	2.51x10^{-03}	-0.115	4.06x10^{-02}	-0.142	2.86x10^{-04}	1.14x10^{-02}
AMN1	-0.127	2.36x10^{-03}	-0.086	3.06x10^{-02}	-0.103	2.92x10^{-04}	1.15x10^{-02}
CYP2R1	-0.133	1.28x10^{-03}	-0.093	4.89x10^{-02}	-0.110	2.94x10^{-04}	1.16x10^{-02}
MED13	-0.106	1.00x10^{-02}	-0.138	4.51x10^{-03}	-0.113	2.95x10^{-04}	1.16x10^{-02}
GNL3L	-0.152	3.04x10^{-03}	-0.114	2.84x10^{-02}	-0.130	2.99x10^{-04}	1.17x10^{-02}
RP11-165F24.3	0.136	3.00x10^{-02}	0.165	2.68x10^{-03}	0.150	3.03x10^{-04}	1.18x10^{-02}
RP11-63B13.1	0.118	2.32x10^{-02}	0.149	5.52x10^{-03}	0.132	3.03x10^{-04}	1.18x10^{-02}
RP11-356K23.1	0.288	1.43x10^{-03}	0.213	2.77x10^{-02}	0.235	3.05x10^{-04}	1.18x10^{-02}
AP000240.6	0.179	1.21x10^{-02}	0.198	1.09x10^{-02}	0.186	3.08x10^{-04}	1.19x10^{-02}
RP11-267M23.1	-0.263	7.49x10^{-03}	-0.194	4.12x10^{-02}	-0.240	3.07x10^{-04}	1.19x10^{-02}
RP11-472I20.4	-0.181	7.43x10^{-03}	-0.163	3.03x10^{-02}	-0.176	3.06x10^{-04}	1.19x10^{-02}

RP11-61L19.1	0.233	$6.57x10^{-03}$	0.295	$7.98x10^{-03}$	0.250	$3.09x10^{-04}$	$1.19x10^{-02}$
RP11-659P15.1	0.183	$3.35x10^{-02}$	0.217	$9.96x10^{-03}$	0.210	$3.09x10^{-04}$	$1.19x10^{-02}$
GGTA1P	-0.383	$3.01x10^{-03}$	-0.384	$1.09x10^{-02}$	-0.355	$3.11x10^{-04}$	$1.19x10^{-02}$
SOCS7	-0.161	$8.42x10^{-03}$	-0.159	$9.27x10^{-03}$	-0.153	$3.15x10^{-04}$	$1.20x10^{-02}$
HELLPAR	0.105	$9.95x10^{-03}$	0.090	$1.10x10^{-02}$	0.096	$3.18x10^{-04}$	$1.21x10^{-02}$
GRAP2	-0.179	$8.68x10^{-03}$	-0.177	$1.52x10^{-02}$	-0.176	$3.20x10^{-04}$	$1.21x10^{-02}$
ZNF816	-0.096	$2.45x10^{-02}$	-0.106	$1.11x10^{-02}$	-0.106	$3.19x10^{-04}$	$1.21x10^{-02}$
DDX47	-0.080	$1.86x10^{-02}$	-0.088	$1.42x10^{-02}$	-0.087	$3.26x10^{-04}$	$1.22x10^{-02}$
CSNK2A1	-0.100	$1.62x10^{-03}$	-0.073	$2.63x10^{-02}$	-0.079	$3.29x10^{-04}$	$1.23x10^{-02}$
B4GAT1	-0.163	$7.22x10^{-03}$	-0.158	$1.62x10^{-02}$	-0.157	$3.36x10^{-04}$	$1.23x10^{-02}$
EZH1	-0.148	$1.37x10^{-03}$	-0.102	$4.44x10^{-02}$	-0.121	$3.33x10^{-04}$	$1.23x10^{-02}$
INTS10	-0.094	$1.45x10^{-02}$	-0.068	$1.71x10^{-02}$	-0.083	$3.34x10^{-04}$	$1.23x10^{-02}$
RC3H2	-0.095	$6.45x10^{-03}$	-0.094	$1.26x10^{-02}$	-0.088	$3.34x10^{-04}$	$1.23x10^{-02}$
VPS39	0.071	$4.08x10^{-02}$	0.122	$1.42x10^{-03}$	0.092	$3.32x10^{-04}$	$1.23x10^{-02}$
ZNF829	-0.141	$4.68x10^{-03}$	-0.099	$4.55x10^{-02}$	-0.123	$3.39x10^{-04}$	$1.24x10^{-02}$
MXRA7	-0.404	$2.18x10^{-02}$	-0.610	$1.53x10^{-03}$	-0.460	$3.41x10^{-04}$	$1.24x10^{-02}$
NAB1	-0.141	$2.97x10^{-03}$	-0.089	$4.75x10^{-02}$	-0.114	$3.40x10^{-04}$	$1.24x10^{-02}$
ZNF606	-0.116	$2.02x10^{-02}$	-0.137	$1.16x10^{-02}$	-0.129	$3.42x10^{-04}$	$1.24x10^{-02}$
FEM1B	-0.111	$1.82x10^{-02}$	-0.118	$7.22x10^{-03}$	-0.112	$3.43x10^{-04}$	$1.24x10^{-02}$
OR2AT4	0.121	$1.65x10^{-02}$	0.114	$1.47x10^{-02}$	0.121	$3.44x10^{-04}$	$1.24x10^{-02}$
ZNF320	-0.156	$4.06x10^{-02}$	-0.187	$1.07x10^{-02}$	-0.188	$3.46x10^{-04}$	$1.25x10^{-02}$
SNAP23	-0.117	$2.07x10^{-02}$	-0.152	$8.08x10^{-03}$	-0.133	$3.51x10^{-04}$	$1.26x10^{-02}$
RP11-887P2.5	0.219	$1.61x10^{-02}$	0.264	$7.63x10^{-03}$	0.237	$3.53x10^{-04}$	$1.26x10^{-02}$
VPS37A	-0.129	$3.36x10^{-03}$	-0.103	$1.72x10^{-02}$	-0.107	$3.53x10^{-04}$	$1.26x10^{-02}$
RP11-138A9.1	0.180	$8.63x10^{-03}$	0.168	$1.46x10^{-02}$	0.173	$3.58x10^{-04}$	$1.27x10^{-02}$
SP3	-0.092	$9.52x10^{-03}$	-0.088	$2.03x10^{-02}$	-0.089	$3.57x10^{-04}$	$1.27x10^{-02}$
MORF4L2	-0.078	$3.88x10^{-02}$	-0.136	$1.50x10^{-03}$	-0.100	$3.60x10^{-04}$	$1.27x10^{-02}$
AL035610.2	0.125	$1.62x10^{-02}$	0.108	$2.83x10^{-02}$	0.128	$3.61x10^{-04}$	$1.27x10^{-02}$
FAM129A	-0.184	$1.84x10^{-02}$	-0.211	$6.26x10^{-03}$	-0.193	$3.64x10^{-04}$	$1.28x10^{-02}$
RP1-102G20.3	0.180	$7.13x10^{-03}$	0.151	$9.51x10^{-03}$	0.155	$3.66x10^{-04}$	$1.28x10^{-02}$
RP11-34F20.4	0.234	$1.49x10^{-02}$	0.249	$8.42x10^{-03}$	0.232	$3.66x10^{-04}$	$1.28x10^{-02}$
AC016831.7	0.185	$2.54x10^{-03}$	0.136	$4.52x10^{-02}$	0.159	$3.77x10^{-04}$	$1.29x10^{-02}$
DCAF7	0.135	$1.53x10^{-02}$	0.162	$2.92x10^{-03}$	0.137	$3.79x10^{-04}$	$1.29x10^{-02}$
GNAQ	-0.115	$2.63x10^{-02}$	-0.191	$1.37x10^{-03}$	-0.138	$3.73x10^{-04}$	$1.29x10^{-02}$
KRIT1	-0.093	$1.08x10^{-02}$	-0.098	$7.17x10^{-03}$	-0.090	$3.80x10^{-04}$	$1.29x10^{-02}$
MT-ND1	-0.303	$1.83x10^{-02}$	-0.336	$1.59x10^{-02}$	-0.332	$3.80x10^{-04}$	$1.29x10^{-02}$
sep-07	-0.116	$6.72x10^{-03}$	-0.081	$4.21x10^{-02}$	-0.101	$3.78x10^{-04}$	$1.29x10^{-02}$
ZNF233	0.157	$1.62x10^{-02}$	0.193	$5.33x10^{-03}$	0.166	$3.75x10^{-04}$	$1.29x10^{-02}$
ZNF430	-0.107	$2.22x10^{-02}$	-0.116	$8.01x10^{-03}$	-0.111	$3.76x10^{-04}$	$1.29x10^{-02}$
OLMALINC	0.138	$5.12x10^{-03}$	0.108	$1.72x10^{-02}$	0.119	$3.89x10^{-04}$	$1.31x10^{-02}$
TECPR1	-0.133	$1.21x10^{-02}$	-0.135	$2.82x10^{-02}$	-0.139	$3.92x10^{-04}$	$1.31x10^{-02}$
MFAP3	-0.116	$1.53x10^{-02}$	-0.126	$6.75x10^{-03}$	-0.116	$3.93x10^{-04}$	$1.31x10^{-02}$
PDE5A	-0.163	$4.64x10^{-02}$	-0.273	$3.83x10^{-03}$	-0.218	$3.93x10^{-04}$	$1.31x10^{-02}$
AVL9	-0.092	$9.44x10^{-03}$	-0.094	$5.45x10^{-03}$	-0.084	$3.98x10^{-04}$	$1.32x10^{-02}$
ABHD2	-0.162	$2.00x10^{-02}$	-0.183	$2.52x10^{-02}$	-0.185	$4.00x10^{-04}$	$1.33x10^{-02}$
CASP4	-0.181	$1.84x10^{-03}$	-0.156	$3.68x10^{-02}$	-0.163	$4.06x10^{-04}$	$1.34x10^{-02}$

AP1AR	-0.119	5.45x10^{-03}	-0.093	4.33x10^{-02}	-0.109	4.18x10^{-04}	1.36x10^{-02}
ENKUR	-0.309	1.11x10^{-02}	-0.315	3.90x10^{-02}	-0.336	4.23x10^{-04}	1.37x10^{-02}
HSPD1	-0.100	8.19x10^{-03}	-0.081	1.80x10^{-02}	-0.087	4.28x10^{-04}	1.38x10^{-02}
PPP1R2	-0.096	2.59x10^{-02}	-0.115	8.57x10^{-03}	-0.107	4.28x10^{-04}	1.38x10^{-02}
PPA2	-0.106	1.75x10^{-02}	-0.092	1.18x10^{-02}	-0.101	4.31x10^{-04}	1.39x10^{-02}
CDA	0.371	2.79x10^{-03}	0.240	4.05x10^{-02}	0.297	4.36x10^{-04}	1.39x10^{-02}
DICER1	-0.114	6.50x10^{-03}	-0.122	1.32x10^{-02}	-0.110	4.36x10^{-04}	1.39x10^{-02}
PTPN14	0.212	1.29x10^{-02}	0.248	1.16x10^{-02}	0.223	4.35x10^{-04}	1.39x10^{-02}
L3MBTL3	-0.105	2.36x10^{-02}	-0.119	1.87x10^{-02}	-0.118	4.40x10^{-04}	1.39x10^{-02}
KCNIP4-IT1	0.234	5.01x10^{-03}	0.174	2.28x10^{-02}	0.194	4.41x10^{-04}	1.39x10^{-02}
CSE1L	-0.131	5.38x10^{-03}	-0.123	7.03x10^{-03}	-0.114	4.42x10^{-04}	1.39x10^{-02}
UBE4A	-0.161	2.84x10^{-03}	-0.101	3.49x10^{-02}	-0.124	4.49x10^{-04}	1.41x10^{-02}
RP11-182I10.3	0.154	3.52x10^{-02}	0.195	7.83x10^{-03}	0.179	4.61x10^{-04}	1.44x10^{-02}
NRG1	0.439	3.47x10^{-02}	0.588	5.82x10^{-03}	0.508	4.67x10^{-04}	1.44x10^{-02}
PABPC1	0.242	3.62x10^{-03}	0.241	7.39x10^{-03}	0.220	4.66x10^{-04}	1.44x10^{-02}
SSTR2	0.124	4.72x10^{-02}	0.170	3.64x10^{-03}	0.146	4.67x10^{-04}	1.44x10^{-02}
UFM1	-0.124	1.97x10^{-03}	-0.075	4.93x10^{-02}	-0.096	4.64x10^{-04}	1.44x10^{-02}
ZNF765	-0.111	8.55x10^{-03}	-0.100	1.80x10^{-02}	-0.102	4.68x10^{-04}	1.44x10^{-02}
LINC00582	0.125	2.02x10^{-02}	0.157	4.12x10^{-03}	0.133	4.72x10^{-04}	1.45x10^{-02}
AC015849.16	0.158	4.76x10^{-02}	0.247	8.37x10^{-03}	0.213	4.79x10^{-04}	1.47x10^{-02}
VPS37B	0.140	1.29x10^{-02}	0.166	3.99x10^{-03}	0.140	4.87x10^{-04}	1.49x10^{-02}
ATXN1	0.087	4.21x10^{-02}	0.118	1.46x10^{-02}	0.110	4.94x10^{-04}	1.49x10^{-02}
ANAPC7	-0.069	1.66x10^{-02}	-0.088	8.70x10^{-03}	-0.075	4.98x10^{-04}	1.50x10^{-02}
HSF2	-0.123	2.04x10^{-02}	-0.133	1.77x10^{-02}	-0.131	5.01x10^{-04}	1.50x10^{-02}
CTC-429P9.3	-0.111	2.33x10^{-02}	-0.103	3.12x10^{-02}	-0.116	5.08x10^{-04}	1.52x10^{-02}
TMEM41B	-0.108	3.51x10^{-02}	-0.120	1.48x10^{-02}	-0.121	5.09x10^{-04}	1.52x10^{-02}
OR7E94P	-0.195	4.22x10^{-02}	-0.278	1.37x10^{-02}	-0.255	5.12x10^{-04}	1.52x10^{-02}
RP11-484O2.1	0.125	1.45x10^{-02}	0.128	7.32x10^{-03}	0.121	5.12x10^{-04}	1.52x10^{-02}
FES	-0.189	7.77x10^{-03}	-0.174	3.26x10^{-02}	-0.184	5.16x10^{-04}	1.53x10^{-02}
PREP	0.174	6.59x10^{-03}	0.155	2.95x10^{-02}	0.162	5.24x10^{-04}	1.53x10^{-02}
ZNF525	-0.185	1.03x10^{-02}	-0.178	2.09x10^{-02}	-0.179	5.24x10^{-04}	1.53x10^{-02}
BAIAP2L1	0.347	1.07x10^{-03}	0.187	3.81x10^{-02}	0.244	5.28x10^{-04}	1.54x10^{-02}
BEND2	-0.325	1.26x10^{-02}	-0.374	1.37x10^{-02}	-0.344	5.32x10^{-04}	1.54x10^{-02}
RP11-163O17.1	-0.165	3.65x10^{-03}	-0.106	3.89x10^{-02}	-0.130	5.33x10^{-04}	1.54x10^{-02}
LMAN2L	-0.131	9.07x10^{-03}	-0.100	3.06x10^{-02}	-0.115	5.34x10^{-04}	1.54x10^{-02}
ORC4	-0.116	1.35x10^{-02}	-0.127	2.22x10^{-02}	-0.124	5.36x10^{-04}	1.54x10^{-02}
ZNF585A	-0.147	2.37x10^{-02}	-0.160	1.90x10^{-02}	-0.159	5.37x10^{-04}	1.54x10^{-02}
ZBED3-AS1	0.106	4.40x10^{-02}	0.128	4.86x10^{-03}	0.118	5.54x10^{-04}	1.57x10^{-02}
MFSD1	-0.112	4.00x10^{-02}	-0.175	2.67x10^{-03}	-0.138	5.60x10^{-04}	1.58x10^{-02}
RP11-212D3.4	0.186	8.20x10^{-03}	0.176	3.06x10^{-02}	0.179	5.59x10^{-04}	1.58x10^{-02}
CAMKMT	-0.178	8.80x10^{-03}	-0.139	3.08x10^{-02}	-0.159	5.66x10^{-04}	1.59x10^{-02}
RP11-10E18.7	0.224	1.13x10^{-02}	0.165	3.30x10^{-02}	0.200	5.67x10^{-04}	1.59x10^{-02}
RP11-374N7.2	0.118	1.93x10^{-02}	0.118	1.69x10^{-02}	0.118	5.67x10^{-04}	1.59x10^{-02}
PTTG2	0.194	2.91x10^{-02}	0.281	6.53x10^{-03}	0.231	5.86x10^{-04}	1.63x10^{-02}
ZNF91	-0.288	3.24x10^{-03}	-0.208	4.98x10^{-02}	-0.244	5.86x10^{-04}	1.63x10^{-02}
PTAFR	-0.182	1.85x10^{-02}	-0.229	5.89x10^{-03}	-0.192	5.90x10^{-04}	1.64x10^{-02}

RSBN1L	-0.099	1.17x10^{-02}	-0.103	2.08x10^{-02}	-0.098	5.92x10^{-04}	1.64x10^{-02}
ATP13A1	0.195	1.30x10^{-02}	0.165	2.26x10^{-02}	0.182	5.97x10^{-04}	1.65x10^{-02}
CEP350	-0.085	1.81x10^{-02}	-0.103	9.53x10^{-03}	-0.089	6.03x10^{-04}	1.66x10^{-02}
RP5-1022P6.3	0.225	2.04x10^{-02}	0.234	9.55x10^{-03}	0.226	6.12x10^{-04}	1.68x10^{-02}
ATP10B	0.190	2.01x10^{-02}	0.194	5.17x10^{-03}	0.184	6.19x10^{-04}	1.70x10^{-02}
ZFP36L2	0.231	3.40x10^{-03}	0.201	1.59x10^{-02}	0.194	6.22x10^{-04}	1.70x10^{-02}
CARNMT1	-0.113	3.87x10^{-02}	-0.165	1.58x10^{-02}	-0.145	6.29x10^{-04}	1.71x10^{-02}
CEP290	-0.160	2.36x10^{-03}	-0.111	4.31x10^{-02}	-0.127	6.26x10^{-04}	1.71x10^{-02}
TMEM220	-0.178	1.36x10^{-02}	-0.157	2.87x10^{-02}	-0.169	6.29x10^{-04}	1.71x10^{-02}
MINPP1	-0.223	1.19x10^{-02}	-0.253	1.10x10^{-02}	-0.225	6.36x10^{-04}	1.71x10^{-02}
ATF2	-0.108	1.60x10^{-03}	-0.081	3.26x10^{-02}	-0.085	6.45x10^{-04}	1.73x10^{-02}
CRLF3	-0.092	2.78x10^{-02}	-0.110	1.85x10^{-02}	-0.104	6.48x10^{-04}	1.73x10^{-02}
UPF2	-0.091	1.81x10^{-02}	-0.091	1.58x10^{-02}	-0.089	6.47x10^{-04}	1.73x10^{-02}
YIPF1	-0.148	7.36x10^{-03}	-0.118	3.82x10^{-02}	-0.131	6.50x10^{-04}	1.73x10^{-02}
RP11-274G22.1	0.202	3.57x10^{-02}	0.259	4.28x10^{-03}	0.219	6.55x10^{-04}	1.74x10^{-02}
CASD1	-0.096	2.68x10^{-02}	-0.111	5.28x10^{-03}	-0.097	6.73x10^{-04}	1.78x10^{-02}
ZNF121	-0.133	6.60x10^{-03}	-0.099	3.60x10^{-02}	-0.113	6.83x10^{-04}	1.80x10^{-02}
GADL1	0.116	2.33x10^{-02}	0.106	2.53x10^{-02}	0.116	6.89x10^{-04}	1.81x10^{-02}
C7orf60	-0.151	8.46x10^{-03}	-0.127	2.42x10^{-02}	-0.133	7.21x10^{-04}	1.87x10^{-02}
GTF2H1	-0.091	1.15x10^{-02}	-0.076	1.24x10^{-02}	-0.078	7.23x10^{-04}	1.87x10^{-02}
SNRNP70	-0.098	1.85x10^{-02}	-0.100	2.78x10^{-02}	-0.101	7.26x10^{-04}	1.87x10^{-02}
RP6-159A1.4	-0.228	3.10x10^{-03}	-0.169	4.29x10^{-02}	-0.189	7.28x10^{-04}	1.87x10^{-02}
CTD-2192J16.20	0.249	7.65x10^{-03}	0.212	9.51x10^{-03}	0.208	7.35x10^{-04}	1.89x10^{-02}
USP8	-0.093	3.01x10^{-03}	-0.062	3.88x10^{-02}	-0.071	7.40x10^{-04}	1.90x10^{-02}
OR1I1	0.127	2.88x10^{-02}	0.162	1.36x10^{-02}	0.144	7.49x10^{-04}	1.91x10^{-02}
TRUB1	-0.088	3.15x10^{-02}	-0.104	1.15x10^{-02}	-0.096	7.51x10^{-04}	1.92x10^{-02}
RP11-78J21.6	0.269	1.25x10^{-02}	0.271	1.45x10^{-02}	0.257	7.53x10^{-04}	1.92x10^{-02}
TSIX	0.121	1.45x10^{-02}	0.101	2.00x10^{-02}	0.109	7.63x10^{-04}	1.94x10^{-02}
PPP4R1	-0.112	2.99x10^{-02}	-0.117	2.68x10^{-02}	-0.121	7.69x10^{-04}	1.95x10^{-02}
OSBPL9	-0.077	2.95x10^{-02}	-0.075	3.12x10^{-02}	-0.081	7.74x10^{-04}	1.95x10^{-02}
RSF1	-0.127	2.77x10^{-03}	-0.086	4.44x10^{-02}	-0.099	7.79x10^{-04}	1.95x10^{-02}
STK38L	-0.114	1.40x10^{-02}	-0.101	2.63x10^{-02}	-0.108	7.83x10^{-04}	1.95x10^{-02}
TMEM43	-0.120	4.34x10^{-02}	-0.150	1.06x10^{-02}	-0.137	7.80x10^{-04}	1.95x10^{-02}
NPIPB3	0.191	6.63x10^{-03}	0.162	2.33x10^{-02}	0.165	7.91x10^{-04}	1.97x10^{-02}
PPWD1	-0.108	3.03x10^{-02}	-0.159	1.17x10^{-02}	-0.131	7.95x10^{-04}	1.97x10^{-02}
ARHGAP1	0.163	1.66x10^{-02}	0.205	5.06x10^{-03}	0.164	8.00x10^{-04}	1.98x10^{-02}
NGLY1	-0.070	2.70x10^{-02}	-0.073	5.19x10^{-03}	-0.067	8.04x10^{-04}	1.98x10^{-02}
SMEK1	-0.089	1.52x10^{-02}	-0.066	4.40x10^{-02}	-0.080	8.05x10^{-04}	1.98x10^{-02}
TSPAN10	0.131	2.42x10^{-02}	0.162	9.54x10^{-03}	0.139	8.03x10^{-04}	1.98x10^{-02}
CHP1	0.211	2.43x10^{-03}	0.155	2.96x10^{-02}	0.169	8.19x10^{-04}	2.00x10^{-02}
RP11-651P23.6	0.216	2.17x10^{-02}	0.246	2.70x10^{-02}	0.240	8.19x10^{-04}	2.00x10^{-02}
YME1L1	-0.087	1.46x10^{-02}	-0.082	2.09x10^{-02}	-0.081	8.21x10^{-04}	2.00x10^{-02}
ZNF268	-0.109	1.47x10^{-02}	-0.096	3.83x10^{-02}	-0.104	8.20x10^{-04}	2.00x10^{-02}
GZF1	-0.116	3.12x10^{-02}	-0.141	3.10x10^{-03}	-0.117	8.30x10^{-04}	2.01x10^{-02}
AL035610.1	0.146	2.57x10^{-02}	0.153	3.77x10^{-02}	0.161	8.32x10^{-04}	2.01x10^{-02}
RP4-534N18.4	0.271	3.64x10^{-02}	0.339	1.27x10^{-02}	0.307	8.36x10^{-04}	2.01x10^{-02}

RP11-573D15.8	0.167	5.04x10^{-03}	0.133	3.81x10^{-02}	0.143	8.47x10^{-04}	2.02x10^{-02}
AP000459.7	0.228	1.84x10^{-02}	0.236	6.69x10^{-03}	0.215	8.52x10^{-04}	2.03x10^{-02}
AC018648.5	-0.322	2.63x10^{-02}	-0.415	1.21x10^{-02}	-0.363	8.55x10^{-04}	2.03x10^{-02}
CEP295	-0.123	4.98x10^{-03}	-0.111	8.15x10^{-03}	-0.101	8.57x10^{-04}	2.03x10^{-02}
MCOLN3	0.142	4.85x10^{-02}	0.181	7.72x10^{-03}	0.161	8.78x10^{-04}	2.06x10^{-02}
ZNF880	-0.143	8.64x10^{-03}	-0.113	4.17x10^{-02}	-0.126	8.80x10^{-04}	2.06x10^{-02}
ABHD10	-0.100	8.51x10^{-03}	-0.088	2.08x10^{-02}	-0.089	8.89x10^{-04}	2.07x10^{-02}
RNF26	0.303	3.69x10^{-03}	0.276	1.87x10^{-02}	0.259	9.00x10^{-04}	2.09x10^{-02}
WFDC1	0.207	1.02x10^{-02}	0.181	4.42x10^{-02}	0.201	9.00x10^{-04}	2.09x10^{-02}
SEC22B	-0.075	3.33x10^{-02}	-0.097	9.30x10^{-03}	-0.082	9.02x10^{-04}	2.09x10^{-02}
ZNF30	-0.208	7.95x10^{-03}	-0.176	3.65x10^{-02}	-0.186	9.03x10^{-04}	2.09x10^{-02}
SLC9A6	-0.092	4.29x10^{-02}	-0.092	3.87x10^{-02}	-0.105	9.10x10^{-04}	2.10x10^{-02}
PDGFA	-0.357	3.11x10^{-03}	-0.284	2.41x10^{-02}	-0.290	9.11x10^{-04}	2.10x10^{-02}
LAMB1	0.148	2.86x10^{-02}	0.140	3.82x10^{-02}	0.155	9.23x10^{-04}	2.11x10^{-02}
RP11-206L10.9	0.141	1.88x10^{-02}	0.119	4.82x10^{-02}	0.136	9.22x10^{-04}	2.11x10^{-02}
RP11-930O11.2	-0.235	2.02x10^{-02}	-0.302	1.31x10^{-02}	-0.256	9.23x10^{-04}	2.11x10^{-02}
ZC3H6	-0.217	1.48x10^{-03}	-0.140	4.97x10^{-02}	-0.161	9.26x10^{-04}	2.11x10^{-02}
CRNDE	0.220	1.83x10^{-02}	0.221	1.70x10^{-02}	0.213	9.32x10^{-04}	2.12x10^{-02}
MBD1	-0.104	1.88x10^{-02}	-0.100	4.09x10^{-02}	-0.105	9.48x10^{-04}	2.13x10^{-02}
RP13-507I23.1	0.175	4.11x10^{-02}	0.249	8.78x10^{-03}	0.205	9.43x10^{-04}	2.13x10^{-02}
PNPLA8	-0.099	1.01x10^{-02}	-0.085	3.51x10^{-02}	-0.090	9.51x10^{-04}	2.14x10^{-02}
ZNF267	-0.106	1.46x10^{-02}	-0.116	1.80x10^{-02}	-0.105	9.65x10^{-04}	2.16x10^{-02}
RIOX2	-0.113	1.00x10^{-02}	-0.101	2.67x10^{-02}	-0.101	9.77x10^{-04}	2.18x10^{-02}
ZCCHC7	-0.170	1.24x10^{-02}	-0.151	4.02x10^{-02}	-0.163	9.80x10^{-04}	2.18x10^{-02}
CCAR1	-0.138	3.53x10^{-03}	-0.103	4.35x10^{-02}	-0.112	9.88x10^{-04}	2.19x10^{-02}
SLC35A4	0.291	2.19x10^{-03}	0.180	3.32x10^{-02}	0.210	9.95x10^{-04}	2.20x10^{-02}
SLK	-0.121	2.25x10^{-02}	-0.150	2.08x10^{-02}	-0.134	1.01x10^{-03}	2.22x10^{-02}
ZNF649	-0.107	1.18x10^{-02}	-0.112	1.85x10^{-02}	-0.102	1.01x10^{-03}	2.22x10^{-02}
SLC38A1	-0.143	1.42x10^{-02}	-0.107	3.60x10^{-02}	-0.124	1.03x10^{-03}	2.25x10^{-02}
RP4-604K5.3	0.246	7.26x10^{-03}	0.192	4.66x10^{-02}	0.211	1.04x10^{-03}	2.26x10^{-02}
PRUNE	-0.124	3.14x10^{-02}	-0.163	1.65x10^{-02}	-0.144	1.04x10^{-03}	2.27x10^{-02}
TTC17	-0.090	1.64x10^{-02}	-0.090	1.02x10^{-02}	-0.081	1.04x10^{-03}	2.27x10^{-02}
LINC00506	0.123	1.43x10^{-02}	0.108	1.49x10^{-02}	0.109	1.05x10^{-03}	2.28x10^{-02}
MSANTD3-TMEFF1	-0.215	2.52x10^{-02}	-0.224	2.28x10^{-02}	-0.223	1.05x10^{-03}	2.28x10^{-02}
GPD1L	-0.091	3.01x10^{-02}	-0.119	7.89x10^{-03}	-0.097	1.06x10^{-03}	2.29x10^{-02}
CEPT1	-0.073	3.27x10^{-02}	-0.089	1.08x10^{-02}	-0.078	1.07x10^{-03}	2.31x10^{-02}
TYW3	-0.094	3.81x10^{-02}	-0.094	1.59x10^{-02}	-0.096	1.08x10^{-03}	2.31x10^{-02}
RIMKLB	-0.127	2.16x10^{-02}	-0.160	1.38x10^{-02}	-0.137	1.08x10^{-03}	2.32x10^{-02}
RP11-814P23.1	0.171	5.05x10^{-03}	0.103	3.41x10^{-02}	0.126	1.11x10^{-03}	2.37x10^{-02}
ZXDB	0.159	3.58x10^{-02}	0.227	5.64x10^{-03}	0.179	1.11x10^{-03}	2.37x10^{-02}
SNRK	-0.107	1.71x10^{-02}	-0.093	4.82x10^{-02}	-0.102	1.15x10^{-03}	2.41x10^{-02}
LINC00346	0.115	1.76x10^{-02}	0.097	4.04x10^{-02}	0.107	1.16x10^{-03}	2.42x10^{-02}
NF2	0.148	1.46x10^{-02}	0.162	6.97x10^{-03}	0.136	1.16x10^{-03}	2.42x10^{-02}
RAB8B	-0.120	8.73x10^{-03}	-0.108	3.70x10^{-02}	-0.109	1.17x10^{-03}	2.43x10^{-02}
AFTPH	-0.098	1.54x10^{-02}	-0.092	2.17x10^{-02}	-0.090	1.18x10^{-03}	2.44x10^{-02}
RP11-346D14.1	0.124	1.99x10^{-02}	0.124	1.00x10^{-02}	0.116	1.19x10^{-03}	2.46x10^{-02}

ZBTB41	-0.113	1.62x10^{-02}	-0.100	3.13x10^{-02}	-0.105	1.19x10^{-03}	2.46x10^{-02}
BNIP2	-0.092	4.01x10^{-02}	-0.110	1.56x10^{-02}	-0.100	1.20x10^{-03}	2.47x10^{-02}
PSME3	0.131	9.70x10^{-03}	0.113	2.46x10^{-02}	0.114	1.20x10^{-03}	2.47x10^{-02}
BLOC1S6	-0.115	4.72x10^{-02}	-0.167	8.65x10^{-03}	-0.141	1.23x10^{-03}	2.51x10^{-02}
AC092652.1	0.170	2.86x10^{-02}	0.197	1.38x10^{-02}	0.176	1.25x10^{-03}	2.53x10^{-02}
BET1	-0.104	2.40x10^{-02}	-0.110	1.98x10^{-02}	-0.104	1.25x10^{-03}	2.53x10^{-02}
EXOSC10	-0.093	1.91x10^{-02}	-0.096	2.42x10^{-02}	-0.092	1.25x10^{-03}	2.53x10^{-02}
FAM188A	-0.162	1.44x10^{-02}	-0.146	4.60x10^{-02}	-0.156	1.26x10^{-03}	2.53x10^{-02}
MAGT1	-0.103	1.11x10^{-02}	-0.084	4.18x10^{-02}	-0.090	1.26x10^{-03}	2.53x10^{-02}
PCBP2	0.192	9.85x10^{-03}	0.145	4.22x10^{-02}	0.163	1.26x10^{-03}	2.53x10^{-02}
ZNF737	-0.169	4.64x10^{-02}	-0.203	4.01x10^{-03}	-0.175	1.24x10^{-03}	2.53x10^{-02}
LIN52	-0.164	4.12x10^{-03}	-0.144	1.96x10^{-02}	-0.139	1.26x10^{-03}	2.53x10^{-02}
MAPKAP1	-0.074	1.48x10^{-02}	-0.068	1.49x10^{-02}	-0.065	1.27x10^{-03}	2.53x10^{-02}
RP11-573D15.2	0.182	1.82x10^{-02}	0.184	1.69x10^{-02}	0.171	1.27x10^{-03}	2.53x10^{-02}
FRK	0.095	3.85x10^{-02}	0.119	4.22x10^{-03}	0.099	1.28x10^{-03}	2.53x10^{-02}
SLC35A3	-0.087	1.66x10^{-02}	-0.089	1.45x10^{-02}	-0.082	1.28x10^{-03}	2.53x10^{-02}
XPNPEP1	-0.128	2.31x10^{-02}	-0.165	1.13x10^{-02}	-0.136	1.29x10^{-03}	2.54x10^{-02}
PELI1	-0.105	3.70x10^{-02}	-0.203	2.13x10^{-03}	-0.132	1.31x10^{-03}	2.57x10^{-02}
TLR8	-0.188	1.46x10^{-02}	-0.198	1.90x10^{-02}	-0.180	1.31x10^{-03}	2.57x10^{-02}
ZNF81	-0.102	2.37x10^{-02}	-0.102	4.19x10^{-02}	-0.106	1.31x10^{-03}	2.57x10^{-02}
FAM213A	-0.205	1.76x10^{-02}	-0.194	3.07x10^{-02}	-0.195	1.32x10^{-03}	2.58x10^{-02}
SUPT6H	0.096	2.35x10^{-02}	0.118	1.29x10^{-02}	0.103	1.32x10^{-03}	2.58x10^{-02}
ZUFSP	-0.155	2.04x10^{-03}	-0.136	3.68x10^{-02}	-0.130	1.32x10^{-03}	2.58x10^{-02}
RMND5A	-0.146	1.25x10^{-02}	-0.143	2.18x10^{-02}	-0.138	1.35x10^{-03}	2.61x10^{-02}
NDUFV3	-0.174	8.11x10^{-03}	-0.153	1.26x10^{-02}	-0.143	1.38x10^{-03}	2.66x10^{-02}
RP11-47I22.3	0.125	2.91x10^{-02}	0.120	2.65x10^{-02}	0.126	1.40x10^{-03}	2.69x10^{-02}
LRRTM2	0.321	1.80x10^{-02}	0.268	4.25x10^{-02}	0.293	1.42x10^{-03}	2.71x10^{-02}
SLC35A5	-0.126	1.06x10^{-02}	-0.114	3.58x10^{-02}	-0.114	1.42x10^{-03}	2.71x10^{-02}
CBR3	0.389	5.02x10^{-03}	0.286	3.85x10^{-02}	0.310	1.43x10^{-03}	2.72x10^{-02}
RAB20	-0.251	9.51x10^{-03}	-0.275	4.24x10^{-02}	-0.259	1.44x10^{-03}	2.72x10^{-02}
TRAPPC8	-0.062	2.14x10^{-02}	-0.056	2.90x10^{-02}	-0.057	1.43x10^{-03}	2.72x10^{-02}
RP11-946L20.4	0.181	4.41x10^{-02}	0.268	4.59x10^{-03}	0.206	1.44x10^{-03}	2.72x10^{-02}
NCK2	-0.121	2.35x10^{-02}	-0.153	1.80x10^{-02}	-0.130	1.44x10^{-03}	2.72x10^{-02}
AC092669.3	0.133	2.42x10^{-02}	0.116	1.38x10^{-02}	0.120	1.47x10^{-03}	2.76x10^{-02}
ZNF131	-0.128	4.10x10^{-03}	-0.112	4.37x10^{-02}	-0.110	1.48x10^{-03}	2.77x10^{-02}
PCMTD1	-0.176	4.38x10^{-02}	-0.244	1.34x10^{-02}	-0.208	1.50x10^{-03}	2.79x10^{-02}
AC010127.3	0.221	3.94x10^{-02}	0.216	2.21x10^{-02}	0.221	1.51x10^{-03}	2.80x10^{-02}
ZNF264	-0.106	4.86x10^{-02}	-0.106	3.91x10^{-02}	-0.115	1.51x10^{-03}	2.80x10^{-02}
BRAP	-0.093	2.98x10^{-02}	-0.121	1.37x10^{-02}	-0.101	1.52x10^{-03}	2.80x10^{-02}
CYB5R1	-0.103	3.85x10^{-02}	-0.147	1.25x10^{-02}	-0.118	1.52x10^{-03}	2.80x10^{-02}
METTL14	-0.090	3.54x10^{-02}	-0.089	2.82x10^{-02}	-0.091	1.52x10^{-03}	2.80x10^{-02}
RB1CC1	-0.096	1.39x10^{-02}	-0.086	4.90x10^{-02}	-0.091	1.52x10^{-03}	2.80x10^{-02}
SCN8A	0.683	1.15x10^{-02}	1.182	1.77x10^{-03}	0.721	1.54x10^{-03}	2.81x10^{-02}
HIP1R	-0.167	3.33x10^{-02}	-0.149	3.53x10^{-02}	-0.163	1.55x10^{-03}	2.82x10^{-02}
RP5-968D22.3	0.162	2.21x10^{-02}	0.189	3.05x10^{-02}	0.171	1.55x10^{-03}	2.82x10^{-02}
CTC-340A15.2	0.187	1.49x10^{-02}	0.181	1.17x10^{-02}	0.165	1.56x10^{-03}	2.84x10^{-02}

SCHLAP1	0.172	3.95x10^{-02}	0.217	1.59x10^{-02}	0.191	1.57x10^{-03}	2.85x10^{-02}
LAMP1	-0.133	2.03x10^{-02}	-0.133	3.82x10^{-02}	-0.132	1.58x10^{-03}	2.86x10^{-02}
PPIG	-0.096	2.98x10^{-02}	-0.100	1.51x10^{-02}	-0.093	1.58x10^{-03}	2.86x10^{-02}
PEX13	-0.071	3.11x10^{-02}	-0.069	4.99x10^{-02}	-0.075	1.60x10^{-03}	2.87x10^{-02}
OR2M3	0.106	2.91x10^{-02}	0.084	4.96x10^{-02}	0.101	1.61x10^{-03}	2.88x10^{-02}
PIGU	-0.162	5.62x10^{-03}	-0.140	3.51x10^{-02}	-0.136	1.62x10^{-03}	2.89x10^{-02}
SLC39A6	-0.081	4.62x10^{-02}	-0.098	1.61x10^{-02}	-0.088	1.62x10^{-03}	2.90x10^{-02}
CPT1A	0.217	2.66x10^{-02}	0.201	4.24x10^{-02}	0.213	1.67x10^{-03}	2.94x10^{-02}
MAP4	0.152	3.38x10^{-02}	0.205	1.18x10^{-02}	0.167	1.67x10^{-03}	2.94x10^{-02}
MMP28	-0.375	2.51x10^{-02}	-0.472	1.48x10^{-02}	-0.393	1.67x10^{-03}	2.94x10^{-02}
ABHD18	-0.101	9.24x10^{-03}	-0.097	3.36x10^{-02}	-0.093	1.68x10^{-03}	2.94x10^{-02}
RP4-714D9.5	-0.132	3.69x10^{-02}	-0.176	2.66x10^{-02}	-0.156	1.69x10^{-03}	2.95x10^{-02}
GPAM	-0.119	1.69x10^{-02}	-0.104	3.41x10^{-02}	-0.108	1.70x10^{-03}	2.96x10^{-02}
NEMF	-0.120	1.07x10^{-02}	-0.112	2.89x10^{-02}	-0.108	1.70x10^{-03}	2.97x10^{-02}
RP11-15H20.6	-0.105	4.88x10^{-02}	-0.120	4.50x10^{-02}	-0.123	1.72x10^{-03}	2.98x10^{-02}
ZNF382	-0.195	1.61x10^{-02}	-0.154	4.01x10^{-02}	-0.168	1.73x10^{-03}	3.00x10^{-02}
ZNF257	-0.418	2.45x10^{-02}	-0.419	3.12x10^{-02}	-0.421	1.74x10^{-03}	3.01x10^{-02}
TSR1	-0.116	1.79x10^{-02}	-0.087	4.44x10^{-02}	-0.100	1.76x10^{-03}	3.03x10^{-02}
POLE3	-0.081	3.37x10^{-02}	-0.109	1.22x10^{-02}	-0.088	1.77x10^{-03}	3.04x10^{-02}
SAR1A	-0.075	4.39x10^{-02}	-0.083	3.47x10^{-02}	-0.081	1.77x10^{-03}	3.04x10^{-02}
DGCR11	0.131	3.84x10^{-02}	0.141	2.93x10^{-02}	0.140	1.77x10^{-03}	3.04x10^{-02}
RP11-701H24.5	-0.220	2.50x10^{-02}	-0.208	4.67x10^{-02}	-0.219	1.77x10^{-03}	3.04x10^{-02}
CEP63	-0.135	1.59x10^{-02}	-0.132	1.76x10^{-02}	-0.121	1.78x10^{-03}	3.04x10^{-02}
MARK2	0.144	1.91x10^{-02}	0.138	3.84x10^{-02}	0.139	1.79x10^{-03}	3.05x10^{-02}
ZNF589	-0.114	2.34x10^{-02}	-0.103	4.93x10^{-02}	-0.110	1.79x10^{-03}	3.05x10^{-02}
RP11-419I17.1	0.138	1.39x10^{-02}	0.128	2.36x10^{-02}	0.124	1.84x10^{-03}	3.10x10^{-02}
RNF115	-0.065	3.14x10^{-02}	-0.082	1.18x10^{-02}	-0.067	1.84x10^{-03}	3.10x10^{-02}
EFCAB3	0.142	1.10x10^{-02}	0.112	3.91x10^{-02}	0.118	1.87x10^{-03}	3.13x10^{-02}
RP11-631M6.1	0.181	1.91x10^{-02}	0.164	4.64x10^{-02}	0.174	1.87x10^{-03}	3.13x10^{-02}
MAPK8	-0.126	3.21x10^{-02}	-0.134	4.88x10^{-02}	-0.136	1.90x10^{-03}	3.16x10^{-02}
PTPRE	-0.110	1.51x10^{-02}	-0.103	4.10x10^{-02}	-0.103	1.90x10^{-03}	3.17x10^{-02}
TRABD2A	-0.189	3.85x10^{-02}	-0.190	2.21x10^{-02}	-0.190	1.91x10^{-03}	3.17x10^{-02}
HDAC6	-0.092	2.96x10^{-02}	-0.092	3.12x10^{-02}	-0.090	1.93x10^{-03}	3.18x10^{-02}
CCDC18	-0.187	1.70x10^{-02}	-0.206	1.89x10^{-02}	-0.179	1.99x10^{-03}	3.24x10^{-02}
PLEKHA8	-0.115	3.43x10^{-02}	-0.113	2.13x10^{-02}	-0.110	2.01x10^{-03}	3.28x10^{-02}
RP11-574K11.28	0.121	2.47x10^{-02}	0.129	4.63x10^{-02}	0.124	2.02x10^{-03}	3.28x10^{-02}
TSHZ3	0.248	2.22x10^{-02}	0.263	1.97x10^{-02}	0.235	2.04x10^{-03}	3.30x10^{-02}
RP11-111K18.1	-0.153	2.71x10^{-02}	-0.176	2.00x10^{-02}	-0.153	2.06x10^{-03}	3.32x10^{-02}
SASH1	0.454	2.20x10^{-02}	0.440	3.43x10^{-02}	0.434	2.06x10^{-03}	3.32x10^{-02}
MAP2K4	-0.101	2.94x10^{-02}	-0.096	4.14x10^{-02}	-0.100	2.07x10^{-03}	3.33x10^{-02}
HFM1	-0.346	4.68x10^{-02}	-0.494	2.11x10^{-02}	-0.409	2.11x10^{-03}	3.36x10^{-02}
RP11-295D4.3	0.196	2.84x10^{-02}	0.193	3.43x10^{-02}	0.192	2.11x10^{-03}	3.36x10^{-02}
SLC22A16	-0.250	9.63x10^{-03}	-0.279	1.80x10^{-02}	-0.232	2.11x10^{-03}	3.36x10^{-02}
GIN1	-0.091	3.03x10^{-02}	-0.095	4.17x10^{-02}	-0.093	2.12x10^{-03}	3.37x10^{-02}
RP11-365P13.5	0.121	2.07x10^{-02}	0.100	4.99x10^{-02}	0.108	2.12x10^{-03}	3.37x10^{-02}
C22orf39	-0.086	2.99x10^{-02}	-0.085	4.47x10^{-02}	-0.086	2.15x10^{-03}	3.39x10^{-02}

TMX2	-0.103	5.64x10^{-03}	-0.091	3.05x10^{-02}	-0.084	2.15x10^{-03}	3.39x10^{-02}
XKR4	0.193	4.20x10^{-02}	0.282	2.32x10^{-02}	0.232	2.18x10^{-03}	3.42x10^{-02}
KIF5B	-0.098	1.63x10^{-02}	-0.094	3.54x10^{-02}	-0.089	2.20x10^{-03}	3.44x10^{-02}
ARHGAP17	0.175	3.25x10^{-02}	0.212	1.12x10^{-02}	0.175	2.21x10^{-03}	3.46x10^{-02}
ZNF273	-0.113	1.80x10^{-02}	-0.136	1.26x10^{-02}	-0.108	2.23x10^{-03}	3.48x10^{-02}
RP11-58D2.1	0.189	3.10x10^{-02}	0.190	3.22x10^{-02}	0.187	2.26x10^{-03}	3.50x10^{-02}
SERINC1	-0.117	3.39x10^{-02}	-0.112	4.46x10^{-02}	-0.117	2.26x10^{-03}	3.50x10^{-02}
CHERP	0.209	3.46x10^{-02}	0.299	1.71x10^{-03}	0.206	2.28x10^{-03}	3.51x10^{-02}
KRT23	-0.331	1.26x10^{-02}	-0.320	4.06x10^{-02}	-0.312	2.29x10^{-03}	3.51x10^{-02}
NONO	0.096	3.74x10^{-02}	0.109	2.11x10^{-02}	0.098	2.33x10^{-03}	3.54x10^{-02}
KB-1125A3.12	0.116	3.77x10^{-02}	0.122	2.47x10^{-02}	0.115	2.36x10^{-03}	3.56x10^{-02}
RP1-101G11.3	0.142	4.93x10^{-02}	0.158	1.80x10^{-02}	0.148	2.40x10^{-03}	3.59x10^{-02}
PCBP1	0.188	8.58x10^{-03}	0.164	2.90x10^{-02}	0.154	2.42x10^{-03}	3.61x10^{-02}
CBX1	-0.113	3.03x10^{-02}	-0.100	4.93x10^{-02}	-0.107	2.43x10^{-03}	3.63x10^{-02}
FAM20C	0.329	1.83x10^{-02}	0.300	3.59x10^{-02}	0.306	2.46x10^{-03}	3.66x10^{-02}
DAP	0.228	7.56x10^{-03}	0.202	3.99x10^{-02}	0.198	2.48x10^{-03}	3.67x10^{-02}
NDC1	-0.155	7.19x10^{-03}	-0.140	3.94x10^{-02}	-0.132	2.48x10^{-03}	3.67x10^{-02}
PRPF4	-0.080	3.20x10^{-02}	-0.073	3.64x10^{-02}	-0.075	2.49x10^{-03}	3.67x10^{-02}
RP11-523H20.5	0.107	4.41x10^{-02}	0.109	3.19x10^{-02}	0.110	2.49x10^{-03}	3.68x10^{-02}
EPHX2	-0.113	2.44x10^{-02}	-0.127	4.92x10^{-02}	-0.123	2.52x10^{-03}	3.70x10^{-02}
CTPS2	-0.100	4.02x10^{-02}	-0.106	1.92x10^{-02}	-0.098	2.52x10^{-03}	3.70x10^{-02}
RP11-815J21.3	0.183	3.39x10^{-02}	0.201	4.03x10^{-02}	0.191	2.53x10^{-03}	3.72x10^{-02}
FAM200B	-0.104	3.87x10^{-02}	-0.140	2.05x10^{-02}	-0.117	2.54x10^{-03}	3.72x10^{-02}
COPB1	-0.081	2.88x10^{-02}	-0.072	4.68x10^{-02}	-0.075	2.55x10^{-03}	3.72x10^{-02}
HCK	-0.161	1.66x10^{-02}	-0.159	3.53x10^{-02}	-0.149	2.55x10^{-03}	3.73x10^{-02}
ZNF577	-0.219	3.55x10^{-02}	-0.248	3.99x10^{-02}	-0.235	2.56x10^{-03}	3.73x10^{-02}
RP11-382B18.1	0.134	1.42x10^{-02}	0.090	3.79x10^{-02}	0.106	2.60x10^{-03}	3.76x10^{-02}
NR3C1	-0.080	3.40x10^{-02}	-0.064	4.15x10^{-02}	-0.071	2.61x10^{-03}	3.76x10^{-02}
CNOT7	-0.104	1.91x10^{-02}	-0.088	3.69x10^{-02}	-0.089	2.63x10^{-03}	3.77x10^{-02}
BNIP3L	-0.221	3.77x10^{-02}	-0.310	9.70x10^{-03}	-0.242	2.66x10^{-03}	3.79x10^{-02}
ANAPC5	-0.069	1.80x10^{-02}	-0.066	3.20x10^{-02}	-0.062	2.69x10^{-03}	3.80x10^{-02}
IL6ST	-0.145	3.37x10^{-02}	-0.169	2.43x10^{-02}	-0.148	2.68x10^{-03}	3.80x10^{-02}
LACE1	-0.144	8.22x10^{-03}	-0.115	4.78x10^{-02}	-0.117	2.68x10^{-03}	3.80x10^{-02}
NOM1	-0.113	2.21x10^{-02}	-0.105	3.27x10^{-02}	-0.102	2.72x10^{-03}	3.83x10^{-02}
RP11-20I23.5	0.175	4.57x10^{-02}	0.228	1.17x10^{-02}	0.182	2.74x10^{-03}	3.86x10^{-02}
CYP20A1	-0.091	3.22x10^{-02}	-0.076	3.31x10^{-02}	-0.081	2.75x10^{-03}	3.86x10^{-02}
GGNBP2	-0.074	2.60x10^{-02}	-0.061	4.59x10^{-02}	-0.066	2.76x10^{-03}	3.87x10^{-02}
SPATA5	-0.109	1.17x10^{-02}	-0.080	4.43x10^{-02}	-0.086	2.77x10^{-03}	3.88x10^{-02}
WRN	-0.110	4.43x10^{-02}	-0.165	9.49x10^{-03}	-0.124	2.78x10^{-03}	3.89x10^{-02}
RP11-558F24.4	0.244	1.47x10^{-02}	0.186	4.92x10^{-02}	0.202	2.79x10^{-03}	3.90x10^{-02}
SMIM8	-0.100	4.17x10^{-02}	-0.114	2.98x10^{-02}	-0.104	2.84x10^{-03}	3.93x10^{-02}
AC007743.1	0.186	1.08x10^{-02}	0.135	4.16x10^{-02}	0.147	2.86x10^{-03}	3.94x10^{-02}
AC017035.2	0.186	2.88x10^{-02}	0.194	3.07x10^{-02}	0.181	2.86x10^{-03}	3.94x10^{-02}
ARID1B	0.075	3.13x10^{-02}	0.083	4.66x10^{-02}	0.080	2.90x10^{-03}	3.97x10^{-02}
ZNF300	-0.286	2.06x10^{-02}	-0.255	2.61x10^{-02}	-0.251	3.02x10^{-03}	4.08x10^{-02}
SPX	-0.366	2.32x10^{-02}	-0.397	4.27x10^{-02}	-0.366	3.07x10^{-03}	4.13x10^{-02}

APPL2	0.105	2.11x10^{-02}	0.094	3.72x10^{-02}	0.094	3.09x10^{-03}	4.13x10^{-02}
FSTL1	-0.450	1.56x10^{-02}	-0.501	3.14x10^{-02}	-0.428	3.09x10^{-03}	4.13x10^{-02}
ALOX5	-0.130	3.14x10^{-02}	-0.140	3.50x10^{-02}	-0.129	3.12x10^{-03}	4.15x10^{-02}
OSTM1	-0.091	2.59x10^{-02}	-0.091	4.24x10^{-02}	-0.087	3.15x10^{-03}	4.17x10^{-02}
MIPOL1	0.098	4.26x10^{-02}	0.100	2.05x10^{-02}	0.094	3.23x10^{-03}	4.24x10^{-02}
PLA2G4B	-0.260	2.84x10^{-02}	-0.296	1.90x10^{-02}	-0.250	3.27x10^{-03}	4.28x10^{-02}
RP11-391L3.3	0.174	4.79x10^{-02}	0.194	1.64x10^{-02}	0.174	3.29x10^{-03}	4.29x10^{-02}
SLC9A4	0.266	2.35x10^{-02}	0.255	1.34x10^{-02}	0.234	3.33x10^{-03}	4.32x10^{-02}
EDEM1	0.172	6.04x10^{-03}	0.116	4.40x10^{-02}	0.125	3.37x10^{-03}	4.34x10^{-02}
ZNF350	-0.089	3.52x10^{-02}	-0.101	4.31x10^{-02}	-0.094	3.37x10^{-03}	4.34x10^{-02}
FAM132B	0.662	2.31x10^{-02}	0.656	3.01x10^{-02}	0.610	3.43x10^{-03}	4.38x10^{-02}
MFF	-0.100	1.63x10^{-02}	-0.077	4.44x10^{-02}	-0.080	3.46x10^{-03}	4.39x10^{-02}
MUS81	-0.123	4.33x10^{-02}	-0.124	3.93x10^{-02}	-0.123	3.48x10^{-03}	4.40x10^{-02}
HSPA9	-0.068	4.74x10^{-02}	-0.066	3.64x10^{-02}	-0.066	3.49x10^{-03}	4.41x10^{-02}
NDUFB10	0.072	4.71x10^{-02}	0.092	3.28x10^{-02}	0.079	3.50x10^{-03}	4.41x10^{-02}
MALT1	-0.080	3.97x10^{-02}	-0.073	4.36x10^{-02}	-0.075	3.51x10^{-03}	4.41x10^{-02}
TBC1D23	-0.072	4.59x10^{-02}	-0.093	3.60x10^{-02}	-0.081	3.62x10^{-03}	4.49x10^{-02}
GSR	-0.100	4.18x10^{-02}	-0.112	3.99x10^{-02}	-0.103	3.62x10^{-03}	4.49x10^{-02}
ATP6V1B2	-0.107	4.12x10^{-02}	-0.121	3.85x10^{-02}	-0.111	3.66x10^{-03}	4.52x10^{-02}
TMED7-TICAM2	-0.240	2.37x10^{-02}	-0.216	4.45x10^{-02}	-0.218	3.68x10^{-03}	4.53x10^{-02}
GTF2B	-0.092	3.88x10^{-02}	-0.092	4.12x10^{-02}	-0.090	3.73x10^{-03}	4.56x10^{-02}
RP3-398D13.3	-0.176	4.11x10^{-02}	-0.207	4.30x10^{-02}	-0.191	3.72x10^{-03}	4.56x10^{-02}
SLAIN2	-0.216	5.68x10^{-03}	-0.144	3.90x10^{-02}	-0.151	3.74x10^{-03}	4.56x10^{-02}
TAF6L	-0.134	2.10x10^{-02}	-0.128	4.70x10^{-02}	-0.123	3.80x10^{-03}	4.59x10^{-02}
PLCG1	-0.157	3.30x10^{-02}	-0.124	4.71x10^{-02}	-0.136	3.80x10^{-03}	4.59x10^{-02}
SNN	-0.143	4.93x10^{-02}	-0.221	1.08x10^{-02}	-0.162	3.86x10^{-03}	4.64x10^{-02}
RP11-17A4.2	0.136	2.20x10^{-02}	0.111	4.25x10^{-02}	0.114	3.92x10^{-03}	4.69x10^{-02}
FANCB	-0.221	9.12x10^{-03}	-0.210	4.35x10^{-02}	-0.191	3.93x10^{-03}	4.69x10^{-02}
SRSF8	-0.126	2.70x10^{-02}	-0.126	4.82x10^{-02}	-0.122	3.96x10^{-03}	4.70x10^{-02}
STRAP	0.151	2.68x10^{-02}	0.143	1.85x10^{-02}	0.129	3.95x10^{-03}	4.70x10^{-02}
GON4L	-0.119	3.12x10^{-02}	-0.124	4.77x10^{-02}	-0.117	4.06x10^{-03}	4.77x10^{-02}
RP11-575L7.4	0.139	3.53x10^{-02}	0.148	4.25x10^{-02}	0.138	4.15x10^{-03}	4.83x10^{-02}
DNAJC2	-0.112	1.12x10^{-02}	-0.089	4.84x10^{-02}	-0.089	4.18x10^{-03}	4.85x10^{-02}
RNF14	-0.159	3.80x10^{-02}	-0.202	4.10x10^{-02}	-0.179	4.20x10^{-03}	4.87x10^{-02}
TLR4	-0.154	3.01x10^{-02}	-0.177	3.66x10^{-02}	-0.155	4.26x10^{-03}	4.91x10^{-02}
AQR	-0.099	1.13x10^{-02}	-0.080	4.66x10^{-02}	-0.078	4.28x10^{-03}	4.91x10^{-02}
MYLK4	-0.263	4.95x10^{-02}	-0.340	1.42x10^{-02}	-0.276	4.29x10^{-03}	4.92x10^{-02}
CLSTN1	0.181	2.04x10^{-02}	0.180	3.26x10^{-02}	0.162	4.32x10^{-03}	4.93x10^{-02}
FBLN2	-0.356	3.08x10^{-02}	-0.368	3.60x10^{-02}	-0.346	4.41x10^{-03}	5.00x10^{-02}

Supplementary Table 9: Dysregulated RNAs in whole blood RNAseq comparing PAH patients and disease controls. List of 727 differentially expressed ($p< 0.05$), directionally consistent genes between PAH patients (PH Group I) and patients with other cardiovascular disorders from Discovery (2/3 samples) and Validation (1/3 samples) analyses which also met FDR corrected significance ($q< 0.05$) in combined Discovery and Validation analysis (all samples). Genes listed by significance (lowest FDR q first).

	RNA Discovery		RNA Validation		Combined Discovery and Validation		
Gene	**logFC**	**Sig**	**logFC**	**Sig**	**logFC**	**Sig**	**FDR**
NEUROD2	-0.734	2.39x10^{-09}	-1.023	1.80x10^{-11}	-0.830	2.92x10^{-17}	3.40x10^{-13}
FGF23	-0.793	9.82x10^{-09}	-0.813	1.53x10^{-11}	-0.832	1.81x10^{-15}	1.41x10^{-11}
PRRG3	-0.867	4.42x10^{-08}	-0.708	3.00x10^{-08}	-0.868	1.34x10^{-13}	7.82x10^{-10}
HEPACAM	-0.594	1.61x10^{-06}	-0.799	2.08x10^{-09}	-0.679	7.68x10^{-13}	3.58x10^{-09}
SLC25A48	-0.751	2.62x10^{-06}	-0.651	3.94x10^{-06}	-0.749	1.23x10^{-10}	4.77x10^{-07}
GPM6A	-1.008	1.77x10^{-06}	-0.637	2.36x10^{-05}	-0.972	2.37x10^{-10}	7.88x10^{-07}
GPT2	-0.183	9.22x10^{-03}	-1.182	1.84x10^{-05}	-0.684	4.39x10^{-10}	1.28x10^{-06}
SOX11	-0.442	2.58x10^{-06}	-0.381	5.30x10^{-04}	-0.435	8.46x10^{-10}	1.79x10^{-06}
RP11-69P2.1	-0.743	1.34x10^{-05}	-0.699	4.67x10^{-08}	-0.754	8.30x10^{-10}	1.79x10^{-06}
RP1-17K7.2	-0.712	3.38x10^{-06}	-0.714	3.13x10^{-05}	-0.715	9.42x10^{-10}	1.83x10^{-06}
RP11-217O12.1	-1.200	3.94x10^{-06}	-0.676	4.44x10^{-06}	-1.114	1.75x10^{-09}	2.92x10^{-06}
AC079779.4	-0.829	1.94x10^{-05}	-0.766	1.82x10^{-06}	-0.868	1.71x10^{-09}	2.92x10^{-06}
KCNJ3	-0.407	3.02x10^{-05}	-0.446	6.98x10^{-05}	-0.428	8.62x10^{-09}	9.56x10^{-06}
FAM184B	-0.330	9.23x10^{-05}	-0.409	1.37x10^{-05}	-0.363	9.78x10^{-09}	1.04x10^{-05}
CTB-129P6.7	-0.385	1.22x10^{-05}	-0.236	1.18x10^{-03}	-0.351	2.91x10^{-08}	2.82x10^{-05}
ZPR1	-0.223	2.19x10^{-04}	-0.311	9.93x10^{-06}	-0.254	3.26x10^{-08}	2.92x10^{-05}
DPPA4	-0.642	7.16x10^{-06}	-0.261	5.40x10^{-03}	-0.562	3.87x10^{-08}	3.33x10^{-05}
RP11-87N24.3	-0.250	2.77x10^{-03}	-0.626	2.33x10^{-06}	-0.379	7.04x10^{-08}	5.29x10^{-05}
RP11-113I24.1	-0.246	7.35x10^{-04}	-0.365	2.01x10^{-05}	-0.296	9.76x10^{-08}	7.10x10^{-05}
AP000339.4	0.260	5.10x10^{-05}	0.295	6.01x10^{-04}	0.273	1.12x10^{-07}	7.93x10^{-05}
RP11-38O23.4	-0.524	4.51x10^{-04}	-0.636	2.15x10^{-06}	-0.569	1.77x10^{-07}	1.15x10^{-04}
RP5-857K21.6	2.045	2.35x10^{-05}	1.618	1.87x10^{-02}	2.033	2.49x10^{-07}	1.52x10^{-04}
RNF168	-0.349	9.66x10^{-05}	-0.203	1.46x10^{-03}	-0.323	2.77x10^{-07}	1.65x10^{-04}
AC009404.2	-0.533	6.10x10^{-04}	-0.519	8.05x10^{-06}	-0.570	3.17x10^{-07}	1.85x10^{-04}
SNORA48	0.600	3.86x10^{-03}	1.156	1.81x10^{-05}	0.812	6.26x10^{-07}	3.42x10^{-04}
CTA-414D7.1	-0.291	3.99x10^{-04}	-0.282	1.36x10^{-04}	-0.295	6.53x10^{-07}	3.46x10^{-04}
RASSF6	-0.194	1.88x10^{-02}	-0.667	1.95x10^{-04}	-0.384	2.09x10^{-06}	1.02x10^{-03}
S1PR2	-0.231	5.61x10^{-04}	-0.214	1.11x10^{-03}	-0.231	2.45x10^{-06}	1.14x10^{-03}
SNORA70	0.764	4.86x10^{-03}	1.315	8.53x10^{-05}	0.972	3.12x10^{-06}	1.37x10^{-03}
TPH1	-0.386	4.38x10^{-04}	-0.309	3.71x10^{-03}	-0.369	3.96x10^{-06}	1.68x10^{-03}
PARD6B	-0.250	5.43x10^{-04}	-0.156	1.30x10^{-03}	-0.227	5.94x10^{-06}	2.43x10^{-03}
CENPP	0.452	1.39x10^{-04}	0.373	2.86x10^{-02}	0.427	6.46x10^{-06}	2.55x10^{-03}
MCM2	-0.377	4.89x10^{-04}	-0.470	6.00x10^{-03}	-0.400	7.55x10^{-06}	2.70x10^{-03}
RPS6KA6	-0.590	5.70x10^{-04}	-0.290	2.25x10^{-03}	-0.541	7.22x10^{-06}	2.70x10^{-03}
AC096655.2	-0.123	4.17x10^{-02}	-0.372	5.35x10^{-06}	-0.215	7.48x10^{-06}	2.70x10^{-03}
NTNG1	-0.432	2.13x10^{-03}	-0.559	3.23x10^{-03}	-0.495	8.72x10^{-06}	3.03x10^{-03}
SNORA67	0.736	7.28x10^{-03}	1.454	9.66x10^{-04}	1.012	1.00x10^{-05}	3.43x10^{-03}
ZNF395	-0.135	1.16x10^{-02}	-0.237	2.30x10^{-03}	-0.182	1.92x10^{-05}	5.98x10^{-03}
BICC1	-0.295	4.55x10^{-03}	-0.394	1.61x10^{-03}	-0.342	1.96x10^{-05}	6.00x10^{-03}
PTENP1	0.327	1.81x10^{-03}	0.294	3.36x10^{-02}	0.351	2.22x10^{-05}	6.64x10^{-03}
SNORA71A	0.515	7.49x10^{-03}	0.946	9.44x10^{-04}	0.659	2.47x10^{-05}	7.00x10^{-03}
CIAO1	-0.086	1.15x10^{-02}	-0.163	6.03x10^{-04}	-0.110	3.37x10^{-05}	9.01x10^{-03}
RP11-808N1.1	-0.335	4.48x10^{-04}	-0.235	4.78x10^{-02}	-0.302	3.75x10^{-05}	9.81x10^{-03}
SNORA2C	0.561	1.56x10^{-02}	1.129	1.69x10^{-03}	0.781	3.96x10^{-05}	1.02x10^{-02}

AC005614.3	0.166	5.59x10^{-04}	0.182	1.60x10^{-02}	0.163	4.40x10^{-05}	1.11x10^{-02}
RNY3	0.533	3.57x10^{-02}	1.340	9.02x10^{-03}	1.011	4.44x10^{-05}	1.11x10^{-02}
GREM1	-0.285	1.49x10^{-03}	-0.198	6.41x10^{-03}	-0.261	4.73x10^{-05}	1.17x10^{-02}
RP11-85F14.1	0.150	1.83x10^{-02}	0.366	9.19x10^{-04}	0.222	5.02x10^{-05}	1.19x10^{-02}
SNORA71D	0.781	7.41x10^{-03}	1.263	7.18x10^{-03}	0.990	5.39x10^{-05}	1.27x10^{-02}
RP11-434D9.2	0.165	3.57x10^{-02}	0.412	5.59x10^{-04}	0.261	5.98x10^{-05}	1.37x10^{-02}
SNORA84	0.456	2.23x10^{-02}	1.089	1.53x10^{-03}	0.681	6.11x10^{-05}	1.38x10^{-02}
TNS4	-0.200	7.08x10^{-04}	-0.195	4.17x10^{-02}	-0.196	6.28x10^{-05}	1.40x10^{-02}
SNORA10	0.510	3.96x10^{-02}	1.240	7.05x10^{-04}	0.801	6.32x10^{-05}	1.40x10^{-02}
AC002303.5	-0.109	3.51x10^{-02}	-0.260	1.86x10^{-04}	-0.161	6.61x10^{-05}	1.44x10^{-02}
NUCKS1	-0.224	3.27x10^{-03}	-0.305	7.30x10^{-03}	-0.242	6.95x10^{-05}	1.47x10^{-02}
KANK3	-0.148	1.38x10^{-02}	-0.282	1.25x10^{-03}	-0.190	6.95x10^{-05}	1.47x10^{-02}
RN7SK	0.676	2.99x10^{-03}	0.639	9.52x10^{-03}	0.659	8.13x10^{-05}	1.66x10^{-02}
VPS33A	-0.108	1.34x10^{-02}	-0.200	3.51x10^{-04}	-0.131	8.53x10^{-05}	1.73x10^{-02}
SNORA49	0.432	2.39x10^{-02}	0.834	2.02x10^{-04}	0.566	8.67x10^{-05}	1.73x10^{-02}
SNORA24	0.817	1.36x10^{-02}	1.469	4.68x10^{-03}	1.076	9.09x10^{-05}	1.79x10^{-02}
AC009196.1	0.256	1.84x10^{-03}	0.306	1.94x10^{-02}	0.265	9.18x10^{-05}	1.80x10^{-02}
SF3B2	-0.097	2.01x10^{-02}	-0.185	4.13x10^{-03}	-0.132	9.55x10^{-05}	1.84x10^{-02}
RP3-428A13.2	0.210	8.87x10^{-03}	0.262	1.09x10^{-02}	0.239	9.67x10^{-05}	1.85x10^{-02}
EDEM1	-0.083	2.95x10^{-02}	-0.208	2.81x10^{-03}	-0.128	1.09x10^{-04}	2.03x10^{-02}
SET	-0.110	2.57x10^{-02}	-0.219	1.87x10^{-03}	-0.151	1.16x10^{-04}	2.13x10^{-02}
AC006145.4	0.111	2.03x10^{-02}	0.201	1.05x10^{-03}	0.141	1.24x10^{-04}	2.23x10^{-02}
SNORD10	0.511	3.18x10^{-02}	1.129	1.33x10^{-03}	0.734	1.30x10^{-04}	2.33x10^{-02}
RP11-165N12.2	0.092	2.80x10^{-02}	0.146	6.44x10^{-03}	0.122	1.37x10^{-04}	2.43x10^{-02}
GPR85	-0.196	1.17x10^{-02}	-0.228	7.21x10^{-03}	-0.223	1.43x10^{-04}	2.52x10^{-02}
AC006129.4	-0.215	1.77x10^{-02}	-0.354	2.54x10^{-02}	-0.313	1.47x10^{-04}	2.53x10^{-02}
SNORA59B	0.455	1.11x10^{-02}	0.570	4.91x10^{-03}	0.500	1.49x10^{-04}	2.53x10^{-02}
BMPR1B	-0.332	1.35x10^{-02}	-0.436	2.19x10^{-03}	-0.379	1.53x10^{-04}	2.56x10^{-02}
DNAH12	0.167	2.39x10^{-02}	0.329	2.27x10^{-03}	0.222	1.59x10^{-04}	2.62x10^{-02}
CAPN14	-0.221	4.36x10^{-02}	-0.523	8.09x10^{-03}	-0.374	1.80x10^{-04}	2.90x10^{-02}
RAB12	-0.183	6.91x10^{-03}	-0.184	2.42x10^{-02}	-0.194	1.90x10^{-04}	3.03x10^{-02}
SNORA52	0.591	4.20x10^{-02}	1.499	1.33x10^{-03}	0.897	2.04x10^{-04}	3.16x10^{-02}
RP11-438L7.1	0.130	5.28x10^{-03}	0.149	3.81x10^{-02}	0.140	2.17x10^{-04}	3.30x10^{-02}
AC006509.7	-0.154	3.82x10^{-02}	-0.257	9.92x10^{-04}	-0.202	2.30x10^{-04}	3.40x10^{-02}
FER	0.084	4.00x10^{-02}	0.170	6.83x10^{-04}	0.111	2.78x10^{-04}	3.98x10^{-02}
RN7SL1	0.687	6.63x10^{-03}	0.642	4.32x10^{-02}	0.710	2.83x10^{-04}	4.00x10^{-02}
HNRNPU	-0.061	4.59x10^{-02}	-0.149	8.90x10^{-03}	-0.095	2.83x10^{-04}	4.00x10^{-02}
SNORA73B	0.662	2.06x10^{-02}	1.069	7.40x10^{-03}	0.805	2.97x10^{-04}	4.12x10^{-02}
SCARNA21	0.473	2.17x10^{-02}	0.742	2.71x10^{-03}	0.560	3.19x10^{-04}	4.30x10^{-02}
SNORA54	0.434	3.96x10^{-02}	0.916	2.53x10^{-03}	0.601	3.55x10^{-04}	4.67x10^{-02}
RP11-21M24.1	-0.100	3.30x10^{-02}	-0.204	2.49x10^{-03}	-0.134	3.63x10^{-04}	4.72x10^{-02}
SCARNA13	0.581	1.85x10^{-02}	0.859	7.58x10^{-03}	0.675	3.82x10^{-04}	4.89x10^{-02}
CCDC115	-0.149	1.00x10^{-02}	-0.170	2.72x10^{-02}	-0.160	3.87x10^{-04}	4.92x10^{-02}

Supplementary Table 10: Dysregulated RNAs in whole blood RNAseq comparing PH patients and disease controls. List of 87 differentially expressed ($p < 0.05$), directionally consistent genes between PH patients (PH Groups I-IV) and patients with other cardiovascular disorders from Discovery (2/3 samples) and Validation (1/3 samples) analyses which also met FDR corrected significance (q< 0.05) in combined Discovery and Validation analysis (all samples). Genes listed by significance (lowest FDR q first).